



Department of Organic
Chemistry



Palacký University
Olomouc

PALACKÝ UNIVERSITY

Olomouc

Faculty of Science
Department of Organic Chemistry

High-throughput conjugation of drug-like molecules for chemical biology

Ph.D. Thesis

Mgr. Soňa Krajčovičová

Supervisor: doc. RNDr. Miroslav Sural, Ph.D.

Academic Year: 2018/2019

Bibliographic entry

Author: Mgr. Soňa Krajčovičová
Faculty of Science, Palacký University
Department of Organic Chemistry

Title of Thesis: *High-throughput conjugation of drug-like molecules for chemical biology*

Degree program: Chemistry

Field of Study: Organic chemistry

Supervisor: Doc. RNDr. Miroslav Sural, Ph.D.

Academic Year: 2018/2019

Number of pages: 132 + 47 pages of appendices

Keywords: Solid-phase synthesis; conjugates; protein kinase inhibitors; CDK inhibitors; folic acid; triterpenes; BODIPY; PROTAC; preloaded resins

Bibliografický záznam

| | |
|--------------------------|--|
| Autor: | Mgr. Soňa Krajčovičová Přírodovědecká fakulta, Univerzita Palackého Katedra organické chemie |
| Název práce: | <i>Efektivní příprava konjugátů potenciálních léčiv pro molekulárně-biologické studie</i> |
| Studijní program: | Chemie |
| Studijní obor: | Organická chemie |
| Vedoucí práce: | Doc. RNDr. Miroslav Sural, Ph.D. |
| Akademický rok: | 2018/2019 |
| Počet stran: | 132 + 47 stran příloh |
| Klíčová slova: | Syntéza na pevné fázi; konjugáty; inhibitory proteinových kináz; CDK inhibitory; kyselina listová; triterpeny; BODIPY; PROTAC; přemodifikované pryskyřice |

I declare hereby with my signature, that this abovementioned thesis is my own original work. Furthermore, I confirm that I have clearly referenced in accordance with departmental requirements.

26.6.2019, Olomouc

.....

Mgr. Soňa Krajčovičová

Abstract

My Ph.D. thesis is generally devoted to syntheses of bioconjugates, which can serve as tools for chemical biology. The synthetic approaches are mainly focused on solid-phase organic synthesis, with proper pre-modification of intermediates in solution, if required. The general aspects of solid-phase synthesis were shortly described in the *Introduction* part, as well as biological background and brief overview of the two studied groups of therapeutically interested compounds – protein kinase inhibitors and triterpenes.

First project of the *Results and discussion* is dealing with synthesis of purine CDK inhibitors conjugated with folic acid. Purine CDK inhibitors are well-known compounds, mainly because of their potency to inhibit proliferation of cancer cells. However, one of the most serious problems of traditional chemotherapy nowadays is very little specificity for cancer cells over the healthy ones, which leads to systemic toxicity. Tumor targeted delivery system can serve as solution to increasing specificity, thus decreasing toxicity in healthy cells. It is based on overexpression of cell specific receptors, for example the folate receptor, in cancer cells. The folate receptors bind and transport folic acid into cells and are overexpressed in a wide range of human cancers. Thus, the aim of the project is synthesis of conjugates of purine CDK inhibitors with folic acid, followed by biological evaluation of their behavior in cells.

Second project is focused on preparation of thalidomide preloaded resin for rapid preparation of PROTAC conjugates. The proteolysis targeting chimeras (PROTAC) concept has gained wide attention over the past years. This small-molecule-induced protein degradation strategy represents a novel approach to specifically target proteins that are not currently therapeutically tractable and promote their proteasomal degradation via ubiquitylation. One such PROTAC family uses the phthalimides (thalidomide, pomalidomide, lenalidomide), potent immunomodulatory drugs capable of binding to the E3 ubiquitin ligase cereblon. Thus, the phthalimide family is often employed as a part of PROTACs to hijack cereblon to target proteins. Pharmacological targeting of protein kinases has been validated as an effective therapeutic strategy, and over 37 kinase inhibitor drugs have received approval for clinical use in certain cancers. However, specific resistance often reduces the sensitivity of targeted kinases to drugs during therapy, and therefore novel molecules or approaches are intensively sought. Kinase degradation induced by PROTACs thus provides an interesting alternative. The aim of the project is therefore synthesis of commercially available and yet pharmacologically proven protein kinases inhibitors with thalidomide preloaded linker and their subsequent biological evaluation in cell.

The last project is dealing with synthesis of conjugates of cytotoxic triterpenes with fluorescent dye. Triterpenes are naturally occurring compounds, which can be

found in almost all living organisms. They are possessed with promising biological activities; however, their mechanism of action remains uncovered. For a better understanding, how some very promising triterpenic molecules selectively kill cancer cells, we decided to study their behavior in cells. The aim of the project is, therefore, synthesis of conjugates of triterpenes with BODIPY, as a chromophore, subsequent study with fluorescent microscopy and study of conjugates potential interaction with proteins inside the cells.

Abstrakt

Moje doktorská práce se obecně věnuje syntéze biokonjugátů, které mohou sloužit jako nástroje v chemické biologii. Syntetické přístupy byly zaměřené hlavně na syntézu na pevné fázi, s případnou modifikací reagentů v roztoku.

Základní charakteristika syntézy na pevné fázi je stručně popsána v části *Úvod*, rovněž i s biologickým pozadím a krátkým souhrnem dvou studovaných oblastí – inhibitorů proteinových kináz a triterpenů.

První projekt v části *Výsledky a diskuze* se zabývá syntézou purinových CDK inhibitorů konjugovaných s kyselinou listovou. Purinové CDK inhibitory jsou známou skupinou terapeuticky významných látek, díky jejich schopnosti inhibovat proliferaci nádorových buněk. Nicméně jedním z nejvýznamnějších problémů současné chemoterapie je velmi malá specifita pro nádorové buňky v porovnání se zdravými, což vede k celkové systémové toxicitě. Cílený transport k nádorovým buňkám může proto sloužit jako řešení pro zajištění vyšší specifity a tím pádem snížení toxicity u zdravých buněk. Je založen na principu zvýšené exprese specifických buněčných receptorů, ku příkladu folátových, v nádorových buňkách. Folátové receptory vážou a přenášejí kyselinu listovou do buněk a mají zvýšenou expresi právě v celé řadě nádorových buněk. Cílem tohoto projektu je tedy syntéza konjugátů purinových CDK inhibitorů a kyseliny listové, s následnou biologickou evaluací a studiem jejich chování uvnitř buněk.

Druhý projekt je zaměřen na přípravu thalidomidem modifikované pryskyřice pro rychlou přípravu PROTAC konjugátů. Proteolýzu-zaměřující chiméry (z angl. PROTAC) představují koncept, který si získal značnou pozornost v posledních letech. Tyto malé molekuly, které jsou schopny degradovat proteiny, reprezentují nový přístup k specifickému cílení proteinů, které momentálně nejsou terapeuticky dosažitelné a mohou tak způsobit jejich degradaci díky procesu ubiquitinace. Jednu z PROTAC skupin představují thalidomidové deriváty (thalidomid, pomalidomid, lenalidomid), které se vážou na E3 ligázu cereblon. Jsou tedy často použity jako části PROTAC konjugátů, které jsou schopny dostat cereblon k cíleným proteinům. Farmakologické cílení proteinových kináz se ukázalo jako efektivní terapeutická strategie a přes 37 inhibitorů bylo schváleno pro klinické aplikace u určitých typů rakoviny. Nicméně specifická rezistence snižuje citlivost cílených kináz na léčiva během terapie, proto nové molekuly a přístupy jsou velmi žádoucí. Degradace kináz pomocí PROTAC molekul může v tomto případě představovat zajímavou alternativu. Cílem projektu je syntéza konjugátů komerčně dostupných a zároveň klinicky prověřených inhibitorů proteinových kináz s linkerem modifikovaným thalidomidem a jejich následná biologická evaluace uvnitř buněk.

Poslední projekt je zaměřen na syntézu konjugátů cytotoxických triterpenů s fluorescenční značkou. Triterpeny jsou přírodní látky, které můžeme najít téměř ve všech živých organismech. Jsou známé svojí biologickou účinností, ale přesný mechanismus jejich účinku není zcela prozkoumán. Pro lepší pochopení, jak některé velmi zajímavé triterpenoidní molekuly selektivně zabíjejí nádorové buňky, jsme se rozhodli studovat jejich chování uvnitř buněk. Cílem projektu je tedy syntéza konjugátů s BODIPY, jakožto chromoforem, pro následné studium uvnitř buněk pomocí fluorescenční mikroskopie a studium jejich cytotoxicity.

Acknowledgement

I have to admit that not only the last four months, but the last, almost four years, since I started my PhD, was very intense and soul-changing period. Thus, I am more than happy to appreciate here the most important people that I had the honor to meet and who were making this journey memorable.

First and foremost, I would like to sincerely thank to my advisor Mirek Soural for the opportunity to work in his research group and for his first-class supervision of my whole PhD journey. I consider myself extremely lucky to have supervisor, who was able to cheer up, advise and motivate me during the hard times, when I was struggling in the lab and the number of unsuccessful results was uncountable. I am humbly grateful for the freedom and independence with which I have been able to work all the time, thanks to him. And moreover, he figured out the perfect balance between being a supervisor and being a friend to me, which I appreciate very much.

I would like to mention Lukas Maier, prof. Petr Klan and Tomas Slanina, as the three persons who influenced me significantly as both, scientists and humans, and thanks to them I have had a very solid laboratory and knowledge background. I am thankful to have such inspiring people in my life.

I would like to mention also my colleague and one of my most favourite people in the world – Kristynka “Hviezdzicka” Burglova – and thank her for our friendship, internal jokes, coffee breaks and all the great memories we have shared together since my early beginnings in Olomouc. You know everything about me, so I probably have to be your friend forever. :) I appreciate your patience and exceptional support during the most difficult times (not necessarily due to chemistry), you know you can count on me anytime as well.

As being an NMR operator became a notable part of my PhD, I cannot forget to mention my another favourite person Michal. With his enormous help I was introduced to the magical world of advanced NMR measurements and I am deeply thankful for his support, love and persistence during these last few months. Thank you for keeping me sane, it’s hard to imagine my world without you in it.

I would like to emphasize my other beloved colleagues and very close friends – Pata Trapani, Michal Kriegelstein, David Vanda and Martin Porubsky, for the great times in and out of the lab, for the same sense of humor, fruitful chemistry discussions and tons of common memories. I am deeply grateful to have you in my life, guys. Similarly, I have to thank to my “ThunderFury” friends, mostly to Radek Flekal, Milos Hollan and Stanko Kucera for all the funny memories on PubQuizes, to Tomas Pospisil and Ondra Kovac for the unforgettable helium refilling sessions and to Jirka Pospisil for the superior chemistry discussions and help with my internship arrangement. You all were making my time in Olomouc very special!

I am also grateful to co-authors of our publications, mainly to Vladimir Krystof, Radek Jorda, Deniska Hendrychova and Jarka Stankova for excellent biological outputs, to Milan Urban for great co-operation and endless discussions about everything and to Martinka Drabikova for being the best undergraduate student I have had so far.

Finally, I would like to mention Steve Karreman and Adam Zielinski, who I met during my internship in Germany. Especially Steve, my true life-saver, when the nasty laboratory accident happened to me. I really, really appreciate your help and cannot explain by words my gratitude, even now, more than a year ago. Thank you both for making my stay in Göttingen as less painful as possible!

And last but not least, I am deeply thankful to my parents and family for providing me the opportunity to study what I love and for being there for me anytime I was in a trouble. *Lúbim vás!*

“Science, I had come to learn, is as political, competitive, and fierce career as you can find, full of the temptation to find easy paths.”

-Paul Kalanithi

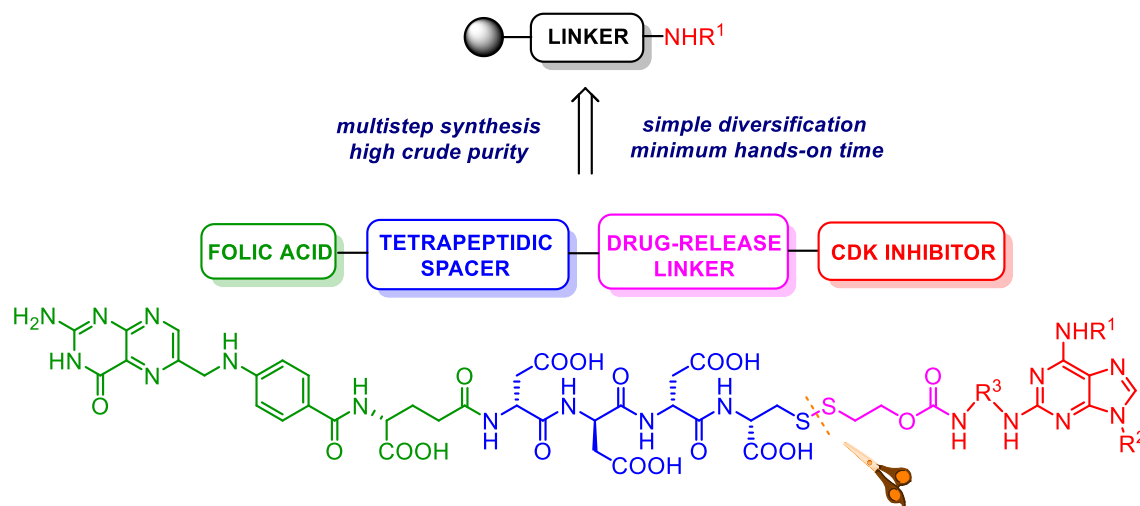
“People will forget what you said, what you wrote or what you created. But they never will forget how you made them feel.”

-Buca

Aims of the Thesis

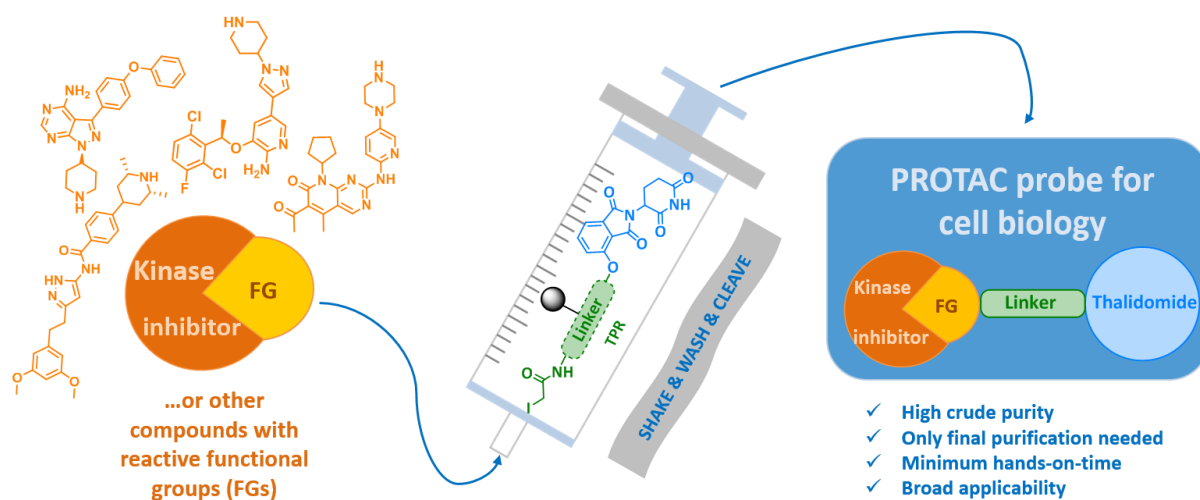
1) Tumor targeting delivery for purine CDK inhibitors

Stepwise synthesis of drug-delivery system, bearing four main components (CDK inhibitor, self-immolative linker, hydrophilic spacer and folic acid) on solid-support and study of their impact inside the cells overexpressing folate receptor.



2) Proteolysis-targeting chimera (PROTAC) for protein kinases targeted degradation

Development of thalidomide-preloaded resin for easy and rapid preparation of desired conjugates possessed with suitable functional groups – demonstrated on selected protein kinases inhibitors. Test applicability of the thalidomide conjugates on selected protein kinases.



3) BODIPY labeled triterpenes for visualization within cells

Development of BODIPY labeled resin, as another application of preloaded resins, for easy and rapid preparation of desired conjugates possessed with suitable functional groups – demonstrated on selected triterpenes. Following study of BODIPY-triterpene conjugates distribution within cells with fluorescent microscopy and examination of their cytotoxic activity against selected cancer cell lines.

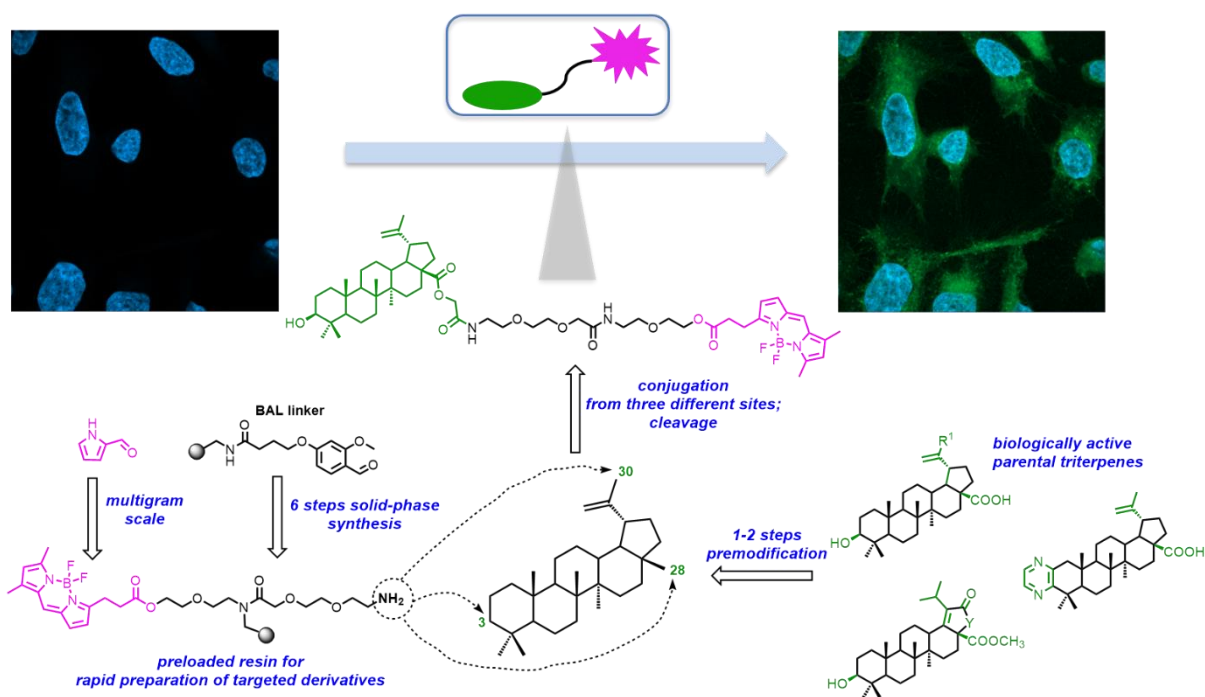


Table of contents

| | |
|---|------------|
| I. INTRODUCTION | |
| 1.1. General aspects of solid-phase organic synthesis | 18 |
| 1.1.1. Acid labile linkers immobilized <i>via</i> carboxylic acid | 20 |
| 1.1.2. Acid labile linkers immobilized <i>via</i> amino group | 21 |
| 1.1.3. Swelling properties of the resins | 22 |
| 1.1.4. Benefits and drawbacks of solid-phase method | 22 |
| 1.2. The short overview of protein kinase enzymes family | 23 |
| 1.2.1. Structure of the catalytic domain | 27 |
| 1.2.2. The basis of protein kinase inhibitors | 28 |
| 1.3. The short overview of the pentacyclic triterpenes | 33 |
| 1.3.1. The biological properties of the lupane group | 34 |
| II. RESULTS AND DISCUSSION | |
| 2.1. Tumor targeting delivery for purine CDK inhibitors | 40 |
| 2.1.1. Introduction | 40 |
| 2.1.2. Synthesis | 47 |
| 2.1.2.1. Synthesis of 2,6,9-trisubstituted purine intermediates | 49 |
| 2.1.2.2. Synthesis of the disulfide-containing linker | 54 |
| 2.1.2.3. Synthesis of the hydrophilic spacer and attachment of folic acid | 60 |
| 2.1.3. Biology | 64 |
| 2.1.4. Conclusion | 66 |
| 2.1.5. Authors' contributions | 67 |
| 2.2. Proteolysis-targeting chimera (PROTAC) for protein kinases targeted degradation | 68 |
| 2.2.1. Introduction | 68 |
| 2.2.2. Synthesis | 76 |
| 2.2.3. Biology | 83 |
| 2.2.4. Conclusion | 86 |
| 2.2.5. Authors' contributions | 86 |
| 2.3. BODIPY labeled triterpenes for visualization within cells | 87 |
| 2.3.1. Introduction | 87 |
| 2.3.2. Synthesis and photochemical properties | 98 |
| 2.3.2.1. Synthesis of BODIPY-FL propanoic acid | 100 |
| 2.3.2.2. Synthesis of pre-modified triterpenes | 102 |
| 2.3.2.3. Synthesis of preloaded resins | 105 |
| 2.3.2.4. Photochemical measurements | 118 |
| 2.3.3. Biology | 119 |
| 2.3.4. Conclusion | 122 |
| 2.3.5. Authors' contributions | 123 |
| 2.4. Summary | 124 |
| 2.5. Literature | 125 |
| III. APPENDICES | |
| Curriculum Vitae | 134 |
| List of publications | 137 |
| Appendix A | 138 |
| Appendix B | 150 |
| Appendix C | 154 |
| Appendix D | 164 |

List of abbreviations

| | | | |
|-----------------------|---|-------------------------------|---|
| AIP | Apoptosis inducing factor | DPT | 12-deoxyphorbol-13-tetradecanoate |
| ALK | Anaplastic lymphoma kinase | DPP | 12-deoxyphorbol-13-phenylacetate |
| AMEBA | Acid-sensitive methoxy benzaldehyde | DTT | Dithiothreitol |
| AR | Androgen receptor | DVB | Divinyl benzene |
| ATP | Adenosine triphosphate | ER | Endoplasmatic reticulum |
| BAL | Backbone amide linker <i>or</i> butane amide linker | ERRα | Oestrogen related receptor α |
| BHA | Benzhydryl amine | ERK | Extracellular-signal-regulated kinase |
| BODIPY | Boron dipyrin | FA | Folic acid |
| BRD4 | Bromodomain-containing protein 4 | FAEEAA | 1-(9 <i>H</i> -fluoren-9-yl)-3-oxo-2,7,10-trioxa-4-azadodecan-12-oic acid |
| BTK | Bruton's tyrosine kinase | FGFR | Fibroblast growth factor receptor |
| BTTP | <i>tert</i> -Butylimino tri(pyrrolidino)phosphorene | Fmoc | Fluorenylmethoxycarbonyl |
| ^tBu | <i>tert</i> -Butyl | FOLR1 | Folate receptor 1 |
| CA | Carbonic anhydrase | FTIR | Fourier-transform infrared spectroscopy |
| CAMK | Calmodulin-dependent protein kinase | Gag | Group-specific antigen |
| CDK | Cyclin-dependent kinase | GSH | Glutathione |
| cIAP | Calf intestinal alkaline phosphatase | GSK | Glycogen synthase kinase |
| CK1 | Casein kinase 1 | HAL | Hyper-acid labile resin |
| CLK | CDK-like kinase | HeLa | Henrietta Lacks |
| CRBN | cereblon | HER | Human epidermal growth factor |
| CRL | Cullin-ring ligase | HIV | Human immunodeficiency virus |
| Cy5 | Cyanine dye | HMDS | Hexamethyldisilazane |
| DBU | 1,8-Diazabicyclo(5.4.0)undec-7-ene | HOBt | Hydroxybenzotriazol |
| DCE | Dichloroethane | HPLC | High-performance liquid chromatography |
| DDQ | 2,3-Dichloro-5,6-dicyano-1,4-benzoquinone | HSV-1 | Herpes simplex virus-1 |
| DEGDE | Diethyleneglykol diethylether | ic | Internal conversion |
| DFG | Asp-Phe-Gly | IR | Infrared |
| DHFR | Dihydrofolate reductase | isc | Intersystem crossing |
| DIC | <i>N,N'</i> -Diisopropylcarbodiimide | LC-MS | Liquid chromatography-mass spectrometry |
| DIPEA | <i>N,N</i> -Diisopropylethylamine | | |
| DMAP | 4-Dimethylaminopyridine | | |
| DMF | Dimethylformamide | | |
| DMSO | Dimethyl sulfoxide | | |

| | | | |
|---------------|----------------------------------|-----------------|--|
| MAPK | Mitogen activated protein kinase | TFA | Trifluoroacetic acid |
| MEK | MAPK/ERK kinase | TFMSA | Trifluoromethane sulfonic acid |
| MDM2 | Mouse-double minute 2 | THF | Tetrahydrofuran |
| MLCK | Myosin light chain kinase | TK | Tyrosine kinase |
| MLK | Mixed-lineage kinase | TKL | Tyrosine kinase-like |
| MS | Mass spectrometry | TMP | Trimethoprim |
| Nek | Never in mitosis kinase | TPA | 12-O-Tetradecanoylphorbol-13-acetate |
| NMP | <i>N</i> -methyl pyrrolidone | TPR | Thalidomide preloaded resin |
| NMR | Nuclear magnetic resonance | βTRCP | β-Transducin repeat containing protein |
| OSu | Hydroxysuccinimide ester | TTBK | Tau tubulin kinase |
| PAL | Peptide amide linker | Ub | Ubiquitin |
| PDB | Protein Data Bank | UHPLC-MS | Ultra-high-performance liquid chromatography-mass spectrometry |
| PeT | Photo-induced electron transfer | UMP | Uracil monophosphate |
| PK | Protein kinase | VHL | von Hippel-Lindau |
| PKA | Protein kinase A | vr | Vibrational relaxation |
| PKC | Protein kinase C | VRK | Vaccinia-related kinase |
| PKG | Protein kinase G | XPhos | 2-Dicyclohexylphosphino-2',4',6'-triisopropylbiphenyl |
| POI | Protein of interest | | |
| PROTAC | Proteolysis targeting chimeras | | |
| PS | Polystyrene | | |
| RB | Retinoblastoma | | |
| RCG | Receptor guanylyl cyclase | | |
| RIPK | Receptor interacting PK | | |
| SAC | Spindle assembly checkpoint | | |
| SAR | Structure-activity relationship | | |
| SASRIN | Super acid sensitive resin | | |
| SMDC | Small molecule drug candidate | | |
| SPS | Solid-phase synthesis | | |
| STE | Sterile | | |
| SYK | Spleen tyrosine kinase | | |
| TBAF | Tetrabutylammonium fluoride | | |
| TBDPS | <i>tert</i> -Butyldiphenylsilyl | | |
| TBK1 | TANK binding kinase 1 | | |
| TEA | triethylamine | | |

Foreword

This thesis is written as a compilation of the projects, which have been published during my PhD studies. Since the title “*High-throughput conjugation of drug-like molecules for chemical biology*” covers a wide spectrum of synthetic and medicinal chemistry topics, it is above the scope of this thesis to deeply examine all of them. Thus, the general introductory part should not serve as an exhaustive review, but moreover as a guide for the reader to introduce our motivation for working on the selected research projects.

The next part, *Results and discussion*, is divided into chapters, which content correspond to the published papers. Each chapter should serve as an extended version of the publication, including short introduction to studied compounds and actual discussion about unsuccessful results during synthesis and pathways towards the final compounds. Summarization of authors’ contributions on the individual work is also included. The discussed manuscripts are attached as *Appendices* at the end of the thesis.

The *Supporting information* contain all relevant experimental data and is attached as an electronic file on CD. They can also be found on the web pages of the corresponding publisher.

Part
I

Introduction

1.1. General aspects of solid-phase organic synthesis

Since the famous pioneering work of Bruce Merrifield^[1] in the 1960's dealing with peptide synthesis, the concept of solid-phase synthesis has expanded into all fields of synthetic organic chemistry, along with preparation of oligonucleotides,^[2,3] peptide nucleic acids,^[4,5] oligosaccharides^[6-8] and to solid-phase synthesis of small organic molecules,^[9-11] including total synthesis of biologically relevant compounds.^[12-14]

The general idea of solid-phase synthesis is covalent binding of reactants on insoluble solid support, most commonly polystyrene resin cross-linked with divinylbenzene (PS-DVB), while keeping all other reactants in solution. By contrast to solution-phase synthesis, the high concentration of reagents is often used to force the reactions to as high conversion as possible. The resin is then thoroughly washed with proper solvents after each reaction step, to simply remove excess reagents and soluble byproducts. The examination of intermediates is performed by cleavage from the resin and with further use of common analytical techniques, such as HPLC, mass spectrometry or NMR spectrometry (Figure 1).

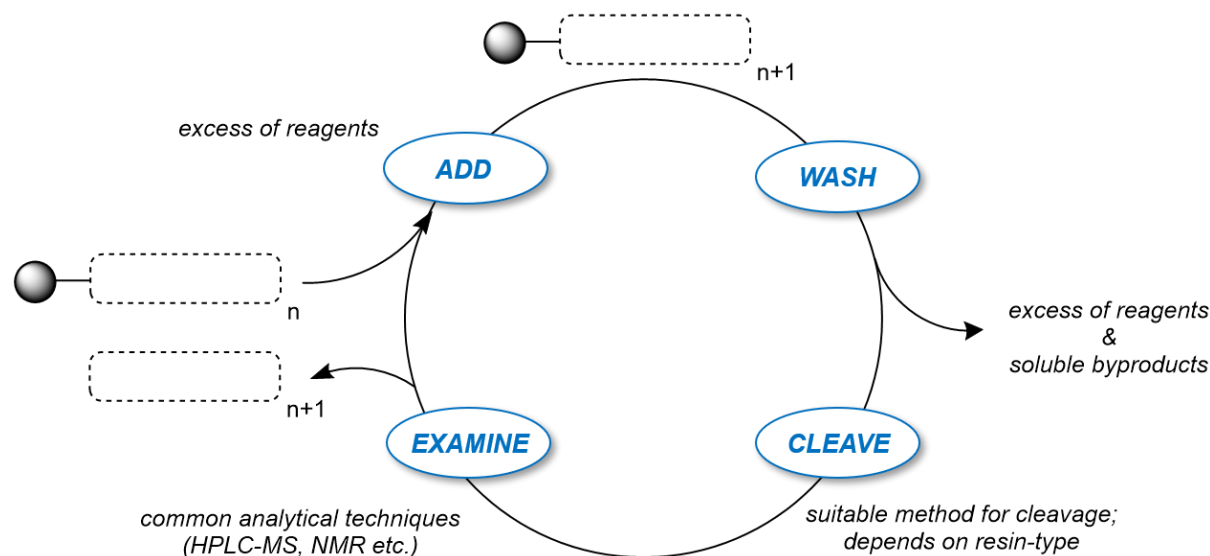


Figure 1. General concept of solid-phase synthesis.

To successfully apply solid-phase method in preparation of desired compounds, careful choice of suitable solid support should be made. This include choice of linker as well as insoluble resin beads, on which are linkers permanently attached (Figure 2.a). Linkers represent a key fragment of efficiency in anchoring and removing organic molecule from solid support, so the correct choice of the linker group is crucial. A general consensus seems to be made with polystyrene with 1-2% DVB cross-linking, possessing ideal swelling properties in polar aprotic solvents (Figure 2.b).^[15]

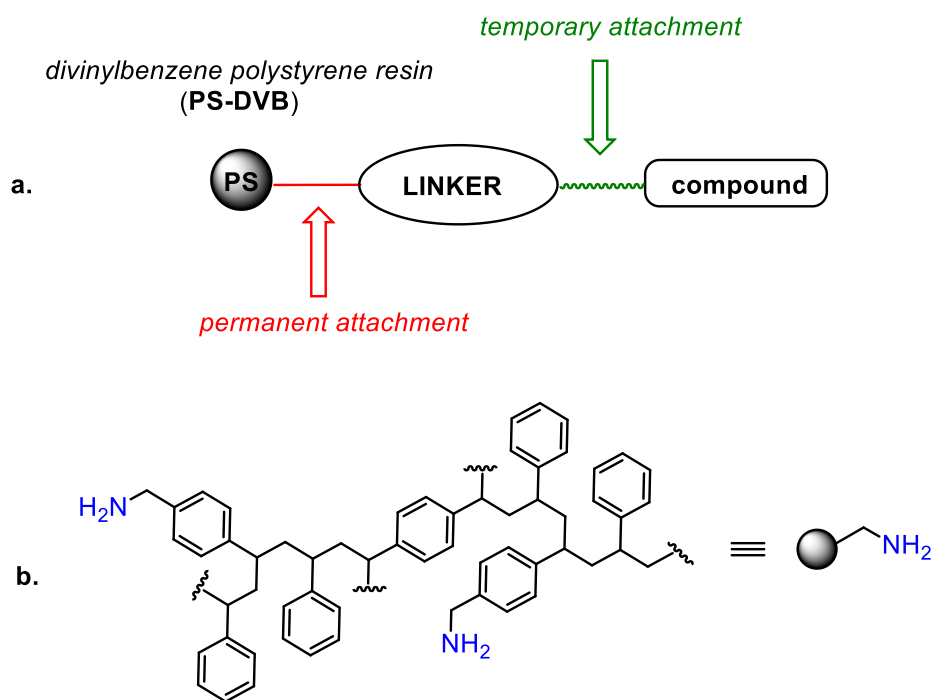


Figure 2. Attachment of the target compound to a solid-support.

Several requirements on linker choice should be met. Importantly, attachment of the first compound should be straightforward and provide good to high yields. The linker must be stable to all chemical transformations during synthesis, which means, that not all reaction conditions could be suitable for every kind of linker (e.g. acid labile linkers will not survive strong acidic conditions during synthesis). Moreover, it is also required to obtain compounds pure and clean after cleavage, without unwanted side reactions.^[16]

The suitable type of the linker also depends on immobilization strategy of the first component. In this regard, immobilization *via* carboxylic or amino group is distinguished (Figure 3).^[15,16] Since deep examination of all resin types and cleavage conditions is beyond the scope of this thesis, I would like to focus mostly on the acid labile linkers, with attachment via carboxylic or amine group immobilization.

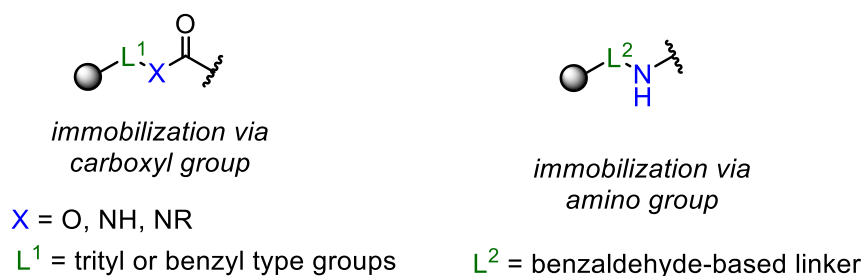


Figure 3. General immobilization strategies.

1.1.1. Acid labile linkers immobilized *via* carboxylic acid

Immobilization of the first compound on solid support as a carboxylate belongs to the most frequently used method. The selection of the linker depends also on desired derivatization of carboxylic function, as it could come as an acid or an amide after cleavage from the resin.^[15,16] Thus, carboxylic group could be attached to the solid-support as an ester, amide, hydrazide or *O*-substituted oxime (Figure 4).

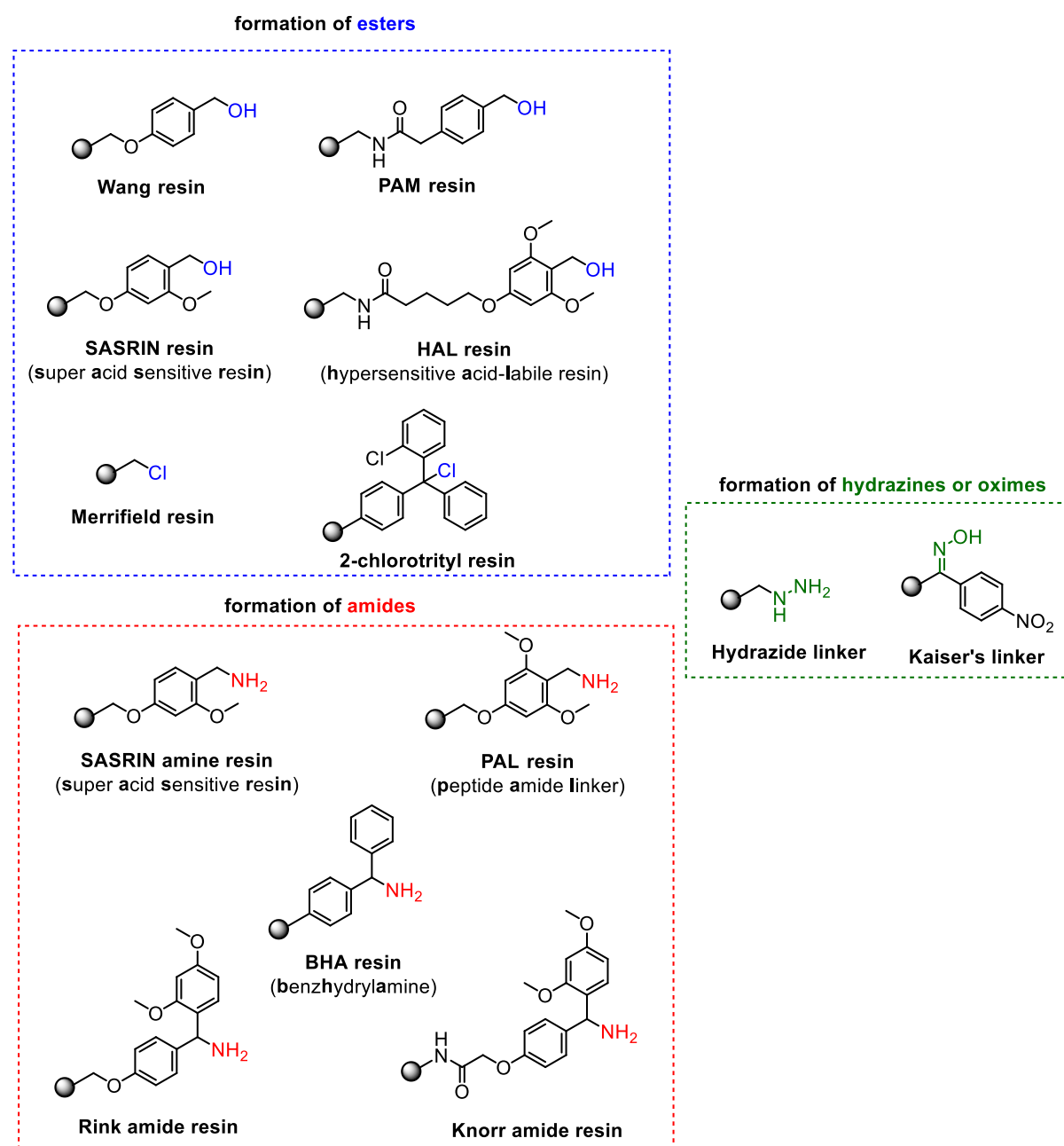
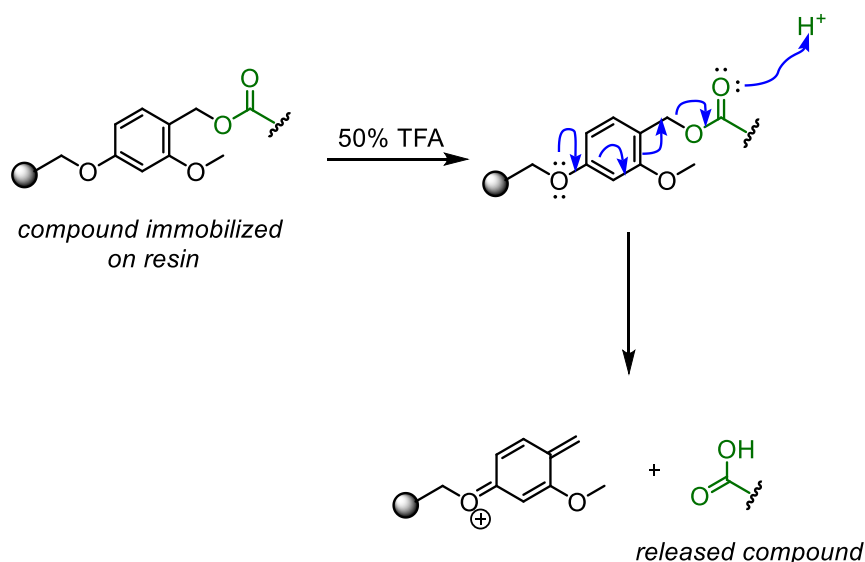


Figure 4. The most common linkers used for carboxylic acid attachment.

The commonly used acids for cleavage from the resin were hydrofluoric (HF) or hydrobromic (HBr) acids. However, such strong acidic conditions have been used for resins such as Merrifield, PAM or benzhydryl, which did not possess any stabilization

group, so compounds are strongly bonded to the solid support.^[15] In case of HF, low temperatures (0°C) and short reaction times (30 – 60 min) were advised in order to avoid side reactions and special glassware was required because of its ability to etching the glass. Hence, these strong acidolytic cleavage procedures were extremely hazardous and were not generally applicable to multiple parallel synthesis.^[15] Luckily, development of more acid labile linkers, possessing electrons-enriched benzyl function, enabled use of less harsh acidic conditions.^[17–19] One of the advantages of such immobilization are conveniently tunable release reaction conditions, which are dictated mostly by number of electron-donating groups (very often alkoxy) on benzyl core of the linker. Generally speaking, the more alkoxy groups are presented, the more labile is linker and the lower concentration of an acid is required for the cleavage, due to the better resonance stabilization of carbocation (Scheme 1). Frequently used acidic conditions for benzyl-type linkers are trifluoroacetic acid (TFA) or trifluoromethanesulfonic acid (TFMSA) on various concentrations.



Scheme 1. Mechanism of compound release from the resin.

1.1.2. Acid labile linkers immobilized *via* amino group

The use of benzaldehyde-based linkers is routine strategy for general preparation of immobilized secondary and tertiary amines. The most commonly used linkers of this type are **1**, AMEBA or BAL (Figure 5), on which amines are attached after reductive amination. The BAL linker was found to be also useful for the synthesis of peptides with carboxy terminal amino acid prone to racemization, as no activation of the carboxylic acid was needed.^[16] Moreover, the linker is also convenient for C-terminal dipeptides, that are liable to diketopiperazine formation, since no benzyl ester of a dipeptide is present during synthesis.^[16] Willingness to acidic cleavage of benzaldehyde-based linker from the resin is analogous to the electron-rich benzyl linkers mentioned above.

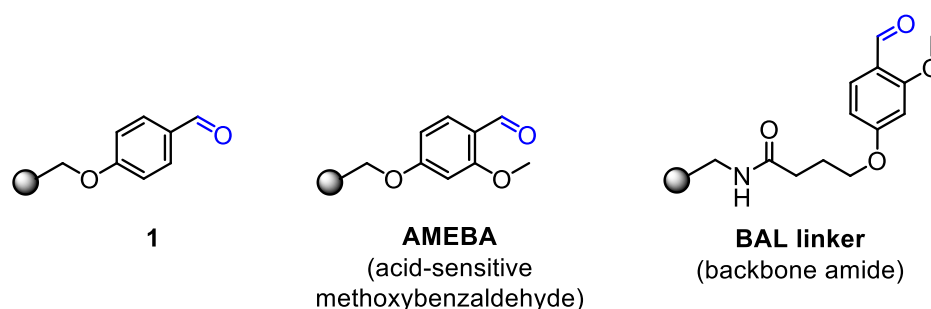


Figure 5. Benzaldehyde-based linker.

1.1.3. Swelling properties of the resins

The smooth contact between the solvent and the reagents during every reaction in solid-phase synthesis is crucial for successful outcome. Even though the PS-DVB resins are insoluble, in some solvents they swell strongly than in others. They can form a thick polymer gel, in which the polymer bound starting material act as in a solvent-like environment. Such behavior is highly dependent on various aspects, e.g. resin type, linkers, particle size, functional groups or on the attached reagents. Hence, in suitable solvents could be the swelling properties much higher, than in a polymer-shrinking, thus unsuitable solvents.^[20]

Commonly used solvents for polystyrene resins are DMF, NMP or dichloromethane, that swell the resin effectively. Other solvents, such as THF, 1,4-dioxane, chloroform or toluene are also generally used. Polar protic solvents (water, alcohols) and hydrocarbons (hexane, cyclohexane) or ethers (diethylether) are incompatible with polystyrene resins, due to the low solvating properties. However, they could be very beneficial in washing sequences, especially with polar by-products formed during the reactions. They allow the polymer network to be closed and reopened from various sites and therefore helped to remove the impurities.

1.1.4. Benefits and drawbacks of solid-phase method

Numerous organic reactions have been converted to solid-phase (including stereoselective synthetic transformations^[21–23] and air/moisture-sensitive reactions such as palladium catalyzed cross-couplings^[24,25] or metathesis^[26,27]) and very sophisticated automated parallel methods have been developed for the efficient production of compound libraries. Besides, nowadays are many suggestions for linkers, resins or cleavage techniques suitable for vast major of substrates, making solid-phase synthesis broadly applicable not only for peptide chemistry. In fact, solid-phase chemistry is often a choice for pharmaceutical companies for synthesis of large libraries of compounds for high-throughput screening.

One of the beauties of this concept is its simplicity. Compare to the traditional chemistry in solution, the reaction work-up is very effortless and often accomplished

in order of minutes. Since the separation from excess of reagents and soluble byproducts is done by filtering and washing, purification of intermediates with e.g. extraction or column chromatography is not necessary to obtain compounds with high crude purities. Also, high boiling solvents, such as DMF or DMSO could be use with apparent impunity due to the simple filtering off after the reaction. Moreover, handling of toxic, volatile, flammable or explosive compounds can be proceeded safely after immobilization on resins. Therefore, resins serve dual purposes: not only they bound increasingly elongated synthetic chain during the construction of the molecule but are also frequently used as protecting groups of otherwise reactive moieties.

However, despite the indisputable advantages mentioned above, the concept of solid-phase synthesis sometimes generates strong resistance among the scientific community. The traditional synthetic organic chemists often need full analytical characterization of all reaction intermediates, as a strong evidence to support the proposed chemical structure of the product, nonetheless that is often at the expense of time spent on each reaction step (so called *“hands-on-time”*). The optimization of reaction conditions also could be time-consumable, since monitoring of reaction progress is sluggish (requires cleavage from the resin, or methods such as solid-state NMR or FTIR) and excess of the reagents used could be, surely, quite expensive. Solid-phase synthesis is also usually limited to milligram quantities of final products, thus not very convenient for multi-gram industry purposes (except of automated peptide synthesis).

Anyhow, the previous advantages are still strong enough for considerable group of synthetic chemists to benefit from solid-phase concept. In fact, proper combination of both solution and solid-phase chemistry could be desirable to pursue satisfying results of chemical syntheses.

Since syntheses of conjugates of both protein kinase inhibitors or triterpenes were playing essential roles within my dissertation thesis, I consider appropriate to introduce reader to the world of these biologically important molecules.

1.2. The short overview of protein kinase enzymes family

Protein kinases represent the largest families of genes in eukaryotes^[28,29] and play a crucial roles in nearly every aspect of cellular function.^[30] A number of diseases, including diabetes, inflammation but mostly cancer, are linked to protein kinase-mediated cell signaling pathways.^[31] They control metabolism, cell division and movement, transcription, cytoskeletal rearrangement or programmed cell death and they participate in the immune response and nervous system function.^[30,32] For these reasons they made an attractive target for an initial in-depth analysis of the gene distribution in the draft of human genome.^[32]

The human genome encodes some 518 protein kinases that share catalytic domain conserved in sequence and structure. However, they are remarkably different in the mechanism of the catalysis regulation.^[31] In 2002, Manning *et al.*^[32] published a study describing the protein kinase complement of the human genome – the kinome. They divided the eukaryotic protein kinase component into 9 groups, according to their catalytic domain,^[32–34] as such:

- The **AGC group** consists of 63 members and contains *PKA* (*protein kinase A*), *PKG* (*protein kinase G*), *PKC* (*protein kinase C*). They are important in cellular growth and proliferation and are frequently dysregulated in various cancers.^[30,32]
- The **CMGC group** consists of 61 members and 4 families, including *CDK* (*cyclin-dependent protein kinases*, *CDK1-11*), *MAPK* (*mitogen-activated protein kinases*), *CLK* (*CDK-like kinases*) and *GSK* (*glycogen synthase kinases*). Their role is mostly in cell cycle progression and transcription regulation (CDKs), controlling intracellular signaling pathways (MAPKs) or in many other cellular processes, such as regulation of glycogen synthesis (GSKs).^[30]
- The **CAMK group** consists of 74 members and contains calcium/calmodulin-dependent protein kinases. The members of this group include *CaMK1/2/4*, *MAPKAPK2/3/5* (*mitogen-activated protein kinase activating protein kinases*), *Nek1-11* (*never in mitosis kinases*) or *MLCK* (*myosin light chain kinases*).^[30,32]
- The **RCG group** (receptor guanylyl cyclase) contains of 5 members and is similar in domain sequences to protein-tyrosine kinases.
- The **CK1 group** (also known as Casein Kinase 1) consists of 12 members and contains family of *CK1*, *TTBK1/2* (*tau tubulin kinase*) and the *VRK1/2/3* (*vaccinia-related kinase*).^[30] The essential role of this group of kinases is regulation of the circadian rhythm.^[35]
- The **TKL group** (tyrosine-kinase like) is a diverse family that mirrored both protein-tyrosine and protein-serine/threonine kinases. The group resides 43 members and consists of e.g. *MLK1-4* (*mixed-lineage kinases*), *LISK*, *IRAK* or *RIPK* (*receptor-interacting protein kinase*).
- The **TK group** (tyrosyl kinase) group consists of 90 members and is one of the most widely described and crucial kinase family in the field of cancer biology. It covers 58 receptor and 32 non-receptor TKs and catalyzes phosphorylation of tyrosine residues. Dysregulation in receptor TKs is a frequent issue of tumor initiation process. Non-receptor TKs are closely linked to signaling processes.^[34]
- The **STE group** consists of about 47 members and contains human homologs of the yeast *STE20*, *STE11* and *STE7* kinases. MEK1/2/5/7 of the STE7 family

are dual specificity protein kinases that catalyze phosphorylation of tyrosine and threonine residues of the target ERK/MAP kinases.[30,32]

The last group is named as **OTHERS** and includes 83 members.

The graphical representation is depicted on Figure 6.

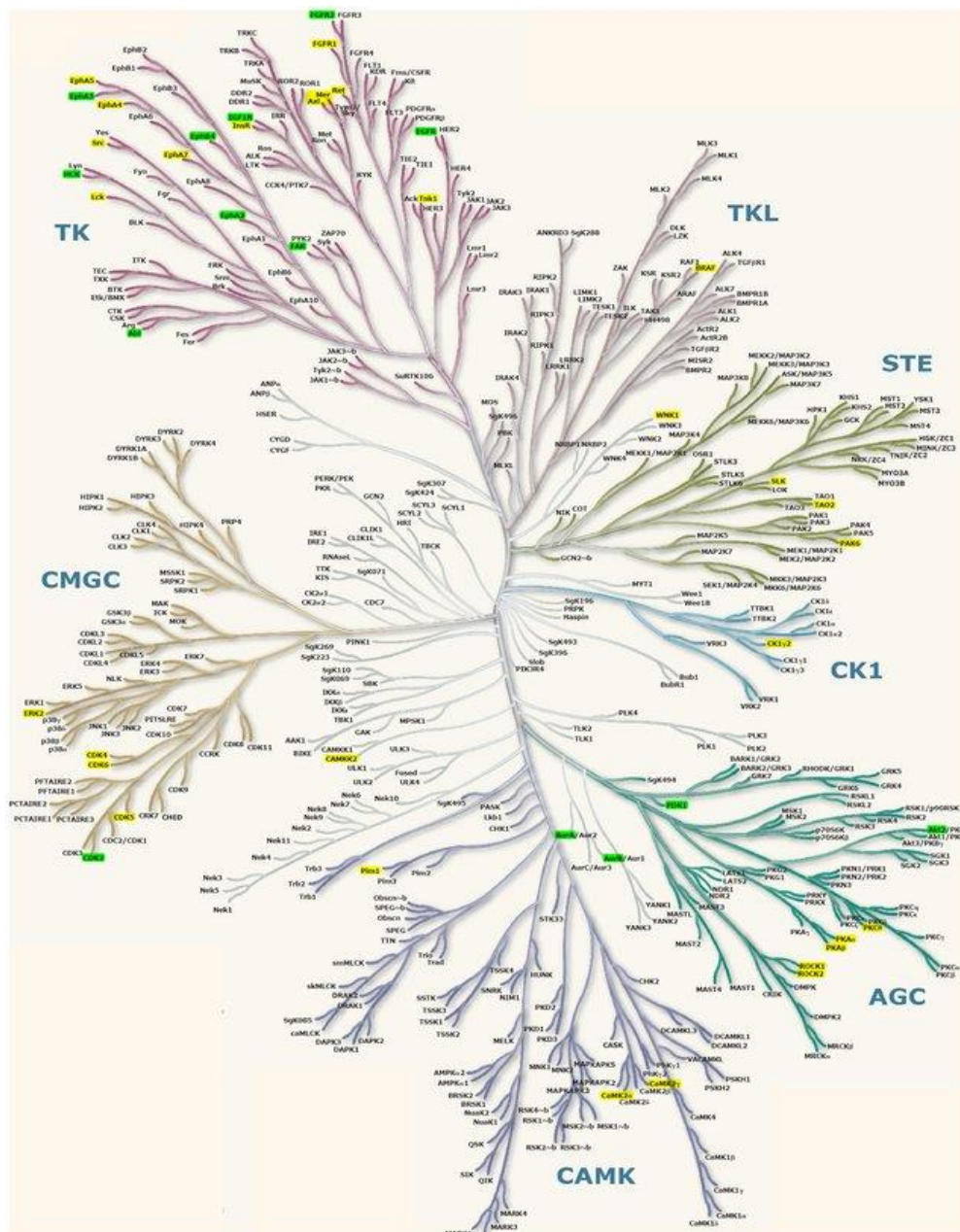
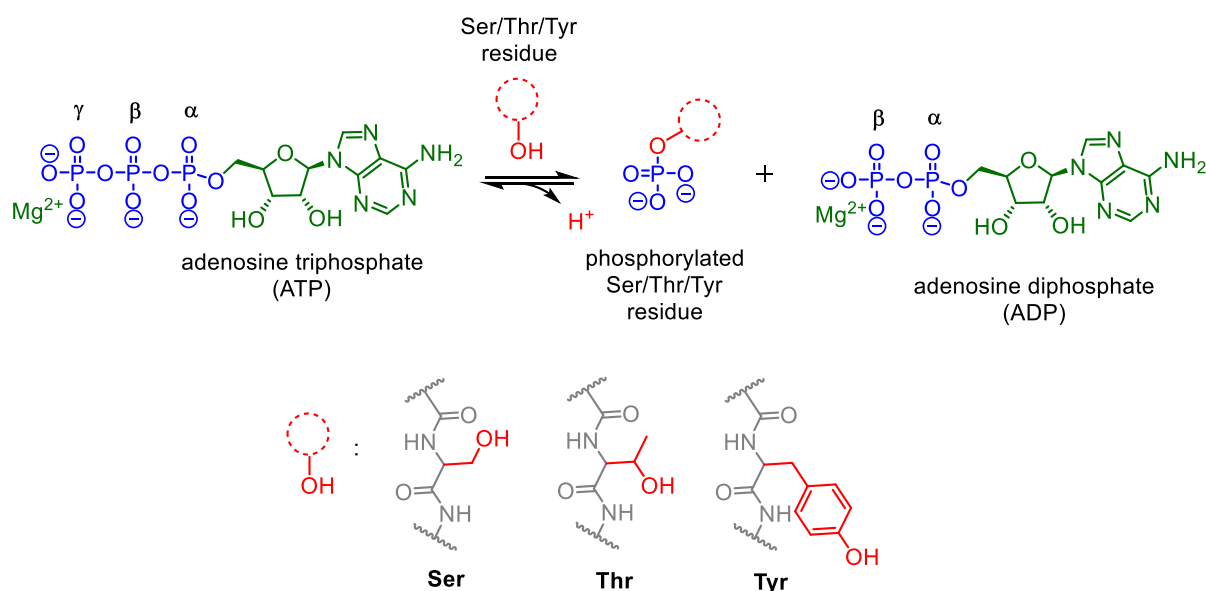


Figure 6. The main groups of protein kinases. Picture available from www.kinase.com/human/kinome.

The mechanism of how protein kinases participate in cell regulation processes is called *phosphorylation*, which is common posttranslational modification with 500 000 potential phosphorylation sites in the human proteome.[36–38] Hence, protein kinases are considered as ATP-dependent phosphotransferases, which catalyzed transfer of single phosphoryl group from the gamma position of ATP (adenosine triphosphate) to

the hydroxyl group of amino acid residues in protein substrates, particularly to serine (Ser), threonine (Thr) and tyrosine (Tyr), respectively (Scheme 2).^[37] These phosphorylated residues are asymmetrically distributed – 85% for serine, 11.8% for threonine and 1.8% for tyrosine residues.^[39] This specificity is dependent on many factors, e.g. the residue itself, the conformation of the phosphorylated motif or on the surrounding primary sequence. Protein phosphorylation could occur in both, ordered and disordered regions. Ordered regions are usually encoded for catalytic, structural or conformational interactions and are enriched in tyrosine residues, whereas disordered regions are enriched in serine or threonine residues and often mediated protein-protein interactions.^[38] Thus, the process of phosphorylation serves two primary roles: as a “connector”, which binds proteins to each other and as a molecular on-off switch to trigger a cascade of a cellular events.^[40]



Scheme 2. Mechanism of phosphorylation of protein residues.^[38]

The phosphate group has special properties that are utilized to regulate critical biological functions. Phosphates are salts of phosphoric acid, with three possible ionization states with pK_a 2.15, 7.2 and 12.3, respectively.^[38] The protein phosphorylation modification is stable at physiological pH, at which phosphate groups are predominantly dianionic. Notably, a divalent cation, such as Mg^{2+} is required for the reaction, so that the predominant physiological substrate is $MgATP^{1-}$.^[30,38]

When the phosphate group is incorporated into protein, it is immediately capable of making strong hydrogen bonds, thus affect other intra- as well as intermolecular interactions. It is well-suited for interaction with e.g. guanidine group of arginine residues.^[38]

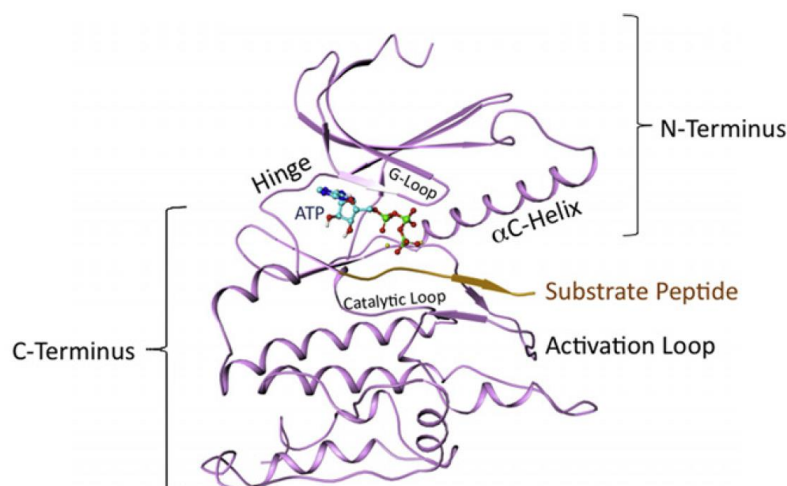
Interestingly, the N-phosphorylation of residues, containing amine group in their side-chains (histidine, lysine or arginine) appears as an edge of protein phosphorylation

research. Its role in humans is poorly understood, due to particular instability of the phosphoramidate bond. However, there have been reports of phosphorylated histidine residues on human proteins, whereas the nucleoside diphosphate kinase phosphorylation of potassium channel histidine residue is the best studied case.^[41]

1.2.1. Structure of the catalytic domain

The structure of the catalytic domain of protein kinases is very important for the deeper understanding of their activation, regulation and inhibition on molecular level.^[38] One of the first defined crystal structures of this kind was reported in 1991, when the structure of PKA was determined.^[42] Since this revelation, around 200 unique kinases have been described in the Protein Data Bank (PDB).^[43] The crystal structures stored in this database include typical examples of all major protein kinase families.^[44]

The catalytic domain has two major subdomains: a smaller N-terminal “lobe” consists of five β -strands with one critical α -helix (α C-helix) and a larger C-terminal “lobe” that is primarily α -helical.^[38] The two subdomains are joined by a peptide strand (the hinge) with the cleft formed between the subdomains constituting the active site (Figure 7). This cleft has a back hydrophobic pocket that supports regulatory functions and a front pocket containing the residues directly involved in catalysis or ATP binding.^[38,45] The so called “gatekeeper” residue, located in the hinge region between the N and C lobes, separates the adenine binding site from adjacent hydrophobic pocket and controls access to the hydrophobic pocket. Its mutations may convert the threonine gatekeeper residue to a larger hydrophobic residue have been related to drug resistance.^[46]



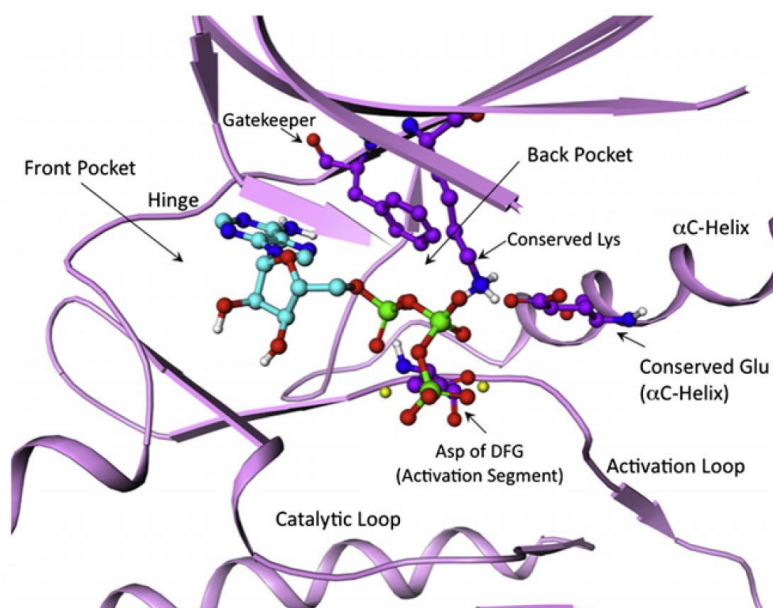


Figure 7. The catalytically active conformation of the protein kinase domain.^[38]

Close to the γ -phosphate of ATP is bonded the peptide substrate as an extended conformation across the front end of the nucleotide binding pocket. A centrally located loop known as the “activation loop,” typically 20–30 residues in length, provides a platform for the peptide substrate.^[45] In most kinases is this loop phosphorylated, when the kinase is active. Phosphorylation of the activation loop stabilizes it in an open and extended conformation that is lenient for substrate binding.^[45]

1.2.2. The basis of protein kinase inhibitors

Protein kinases could play an important role in the initiate stage of tumor growth, as they may contribute to the uncontrolled proliferation of cancer cells and the development of the metastatic disease. It is known, that cancer cells depend almost completely on signaling by protein kinases for their continued proliferation, whereas normal cells rarely invoke these pathways.^[40]

There are several examples in which specific kinases have become mutated in cancer cells. For instance, the cytoplasmic tyrosine kinase BCR-ABL is present in 15 – 30% of adult cases of acute lymphoblastic leukemia and virtually all cases of chronic myeloid leukemia. This mutation led to design and development of imatinib, which was approved as Gleevec™, and showed that the plasticity of kinase structure can enable the development of selective kinase inhibitors, despite the high sequence conservation in this extensive protein family. As another example could serve EGFR mutations with enhanced kinase activity, that have been detected in several human tumor types, e.g. breast cancer.^[40]

Nowadays, the significant research activity is put to the development of small molecule inhibitors of the various kinases, which are considered as crucial for the

initiation and growth of tumors. Because protein kinases use ATP as a source of phosphate, one of the main approaches aimed to design inhibitors that interact with the ATP-binding site of the protein. Such interaction makes phosphorylation of protein kinases inaccessible, hence blocking the signaling process.^[40]

The C-terminal domain contains a flexible activation loop. It is usually 20 - 30 amino acids long and marked by a conserved Asp-Phe-Gly (“DFG”) motif at the beginning. We can divide kinase inhibitors formally into two groups, according to their ability to adopt two main conformations:

- Those that inhibit the *active* form of the enzyme (*DFG-in*)
- Those that inhibit the *inactive* form of the enzyme (*DFG-out*)^[46,47]

In an active state conformation, the Asp group of the DFG motif points into the ATP-binding site and coordinates two Mg^{2+} ions,^[42,46] with the activation loop open. Moreover, the active conformation possesses the orientation of the α C helix, located on the N-terminal domain, rotated inward toward the active site. Such orientation also able the crucial ion pair interaction, between the conserved Glu of the α C helix and the Lys of the β -3 strand of the β -sheet in the N-lobe, responsible for the kinase activity.^[46]

The inactive conformation seen in kinases corresponds to a flipped conformation of the DFG motif, in which the Asp flips by 180°C relative to the active state. This led to Asp and Phe residues swapping their positions. The “*DFG-out*” state opens a new allosteric pocket directly adjacent to the ATP binding pocket (Figure 8).^[46]

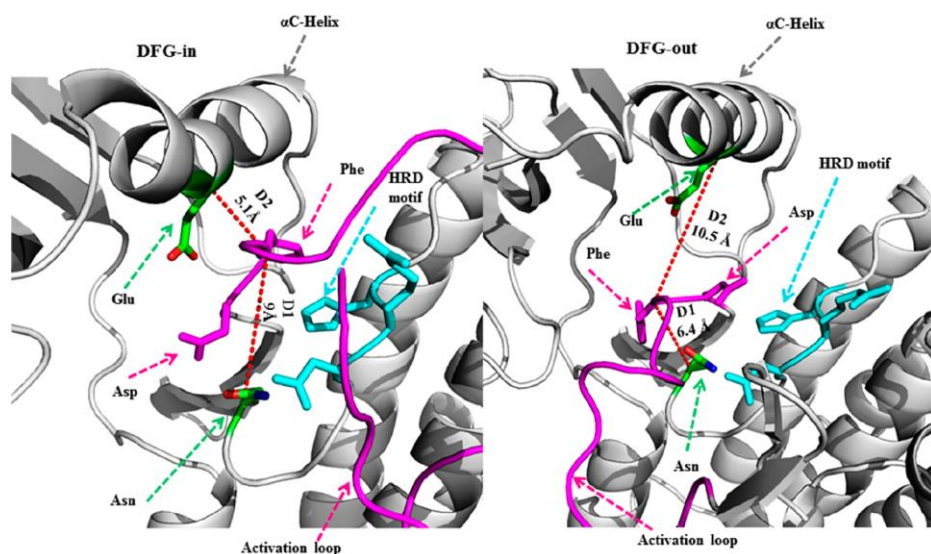
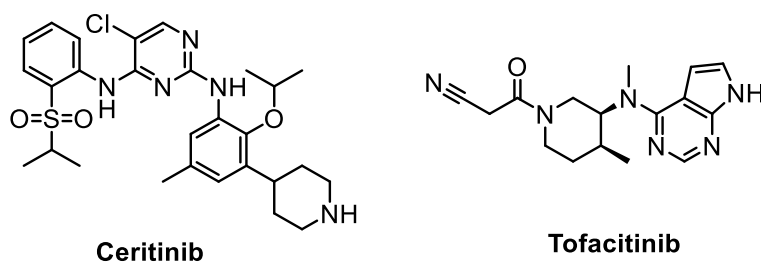


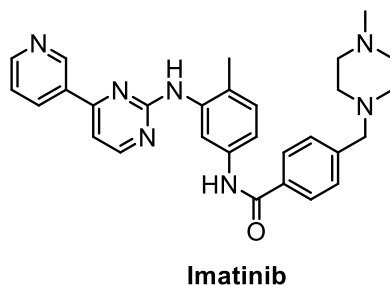
Figure 8. Schematic representation of the classifying conformations as DFG-in and DFG-out.

According to the binding mode, we can divide small molecule kinase inhibitors into four categories:^[48,49]

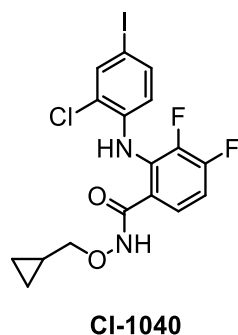
Type I – ATP-competitive inhibitors, recognized DFG-in conformation of the kinase. This type typically consists of a heterocyclic moiety that occupies the purine binding site, whereas the side chain occupied the adjacent hydrophobic pockets I and II (Figure 9), for instance ceritinib or tofacitinib.^[48,49]



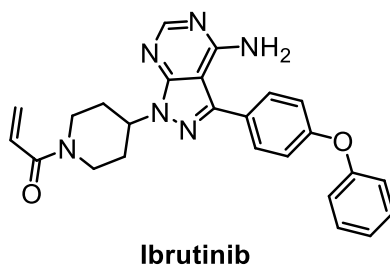
Type II – recognized DFG-out conformation. A twist of the activation loop to the DFG-out conformation exposes an additional hydrophobic binding site, directly next to the ATP binding site (Figure 9). A well-known example of this kind is imatinib, which serendipitous discovery revealed a common pharmacophore of all inhibitors of this kind – conserved set of hydrogen bonds.^[48]



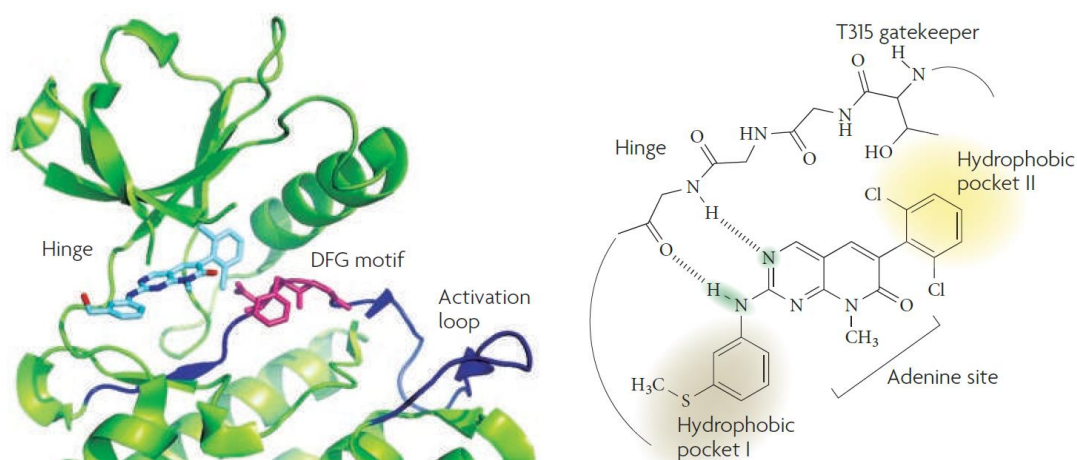
Type III – allosteric inhibitors, binds outside the ATP-binding site – the allosteric site. Kinases belonging to this group tend to express the highest degree of selectivity, because they exploit binding sites and regulatory mechanisms that are unique to the particular kinase (Figure 9). The most known example is CI-1040, which inhibits MEK1 and MEK2 by occupying a pocket adjacent to the ATP binding site.^[48,49]



Type IV – covalent inhibitors, are capable of forming a covalent bond to the kinase active site by reaction with nucleophilic cysteine side-chain. These inhibitors were designed as Michael acceptors, possessing electrophilic acrolein moiety, which may react with nucleophilic sulfur from cysteine residue.^[48] One example could serve a small molecule inhibitor ibrutinib that targets BTK (Figure 9).



Notably, the vast majority of the approved kinase inhibitors are Type I and are generally more selective, however, the reasons for such selectivity advantage are not known yet.^[46,47]



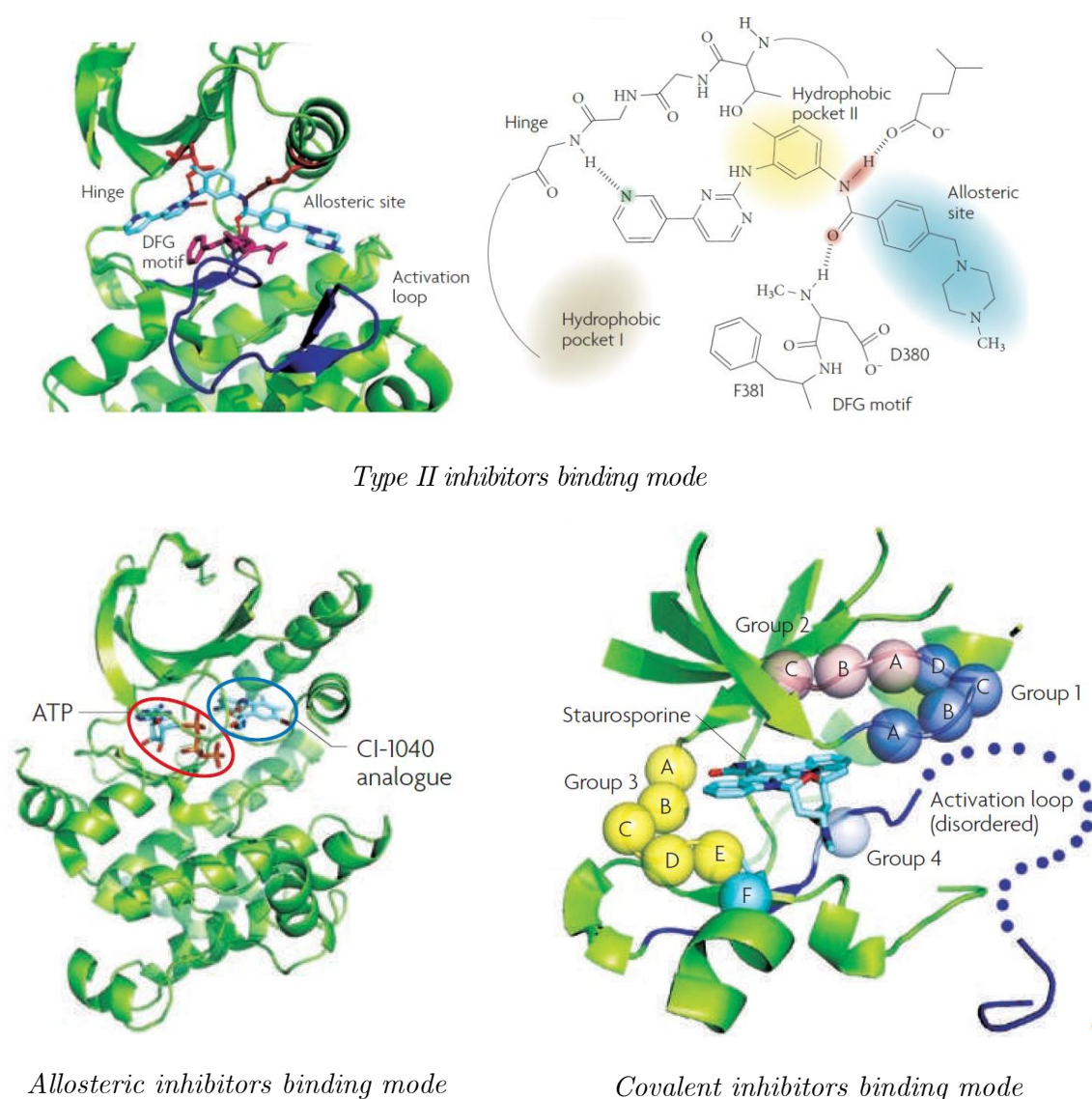


Figure 9. Graphical representation of kinase inhibitors binding modes.

Discovering the full range of intracellular targets for all kinase inhibitors seems like a challenging task. In addition to the 518 kinases encoded in the human genome, there exist over 2000 other nucleotide-dependent enzymes, polymerases, reductases or methyltransferases, that possess binding sites.^[48]

Despite the fact, that there has been a great deal of recent progress toward increasing the selectivity of *type-I* protein kinase inhibitors, they generally suffer for low selectivity, since their scaffolds are often based on adenine-like heterocycle moieties.^[50,51] Current efforts are usually limited to determining drug distribution to various organs and monitoring pharmacodynamics, such as particular phosphorylation site. Moreover, the rapid proliferation of cancer cells caused the acquisition of mutations conferring drug resistance, mostly at gatekeeper residue.^[48] Such lack of selectivity can lead to off-target kinase inhibition and undesired side effects. Thus, finding kinase inhibitors that will be able to successfully pass the clinical trials and become the drugs, is still very demanding. Some techniques, which could be beneficial

for improvement of selectivity of kinase inhibitors, will be discussed more deeply in *Results and discussion* part.

1.3. The short overview of the pentacyclic triterpenes

As was mentioned already, cancer is still the main cause of death in western civilization. Another essential group of compounds, that gained wide interest in treatment of cancer, are triterpenes and their semisynthetic derivatives.

These natural compounds may be found as secondary metabolites in plants,^[52] fungi^[53] or marine invertebrates^[54] and played a key role in the growth, development and reproduction of the organisms. They are found in bark, cork or in the wax covering leaves.^[55] Moreover, pentacyclic triterpenes covered an extensive spectrum of biological properties, not only as potential anticancer agents,^[56,57] but also as antimicrobial,^[58] antiviral,^[57] antibacterial^[59] or antimalarial^[60] compounds. All these features are making them attractive targets for biological screening and in the last decades the broad spectrum of biological activities of lupane, oleanane and ursane triterpenes (Figure 10) have been evaluated.

Lupeol, betulin and betulinic acid belong to the lupane type pentacyclic triterpenes, consisting of four cyclohexane (A – D) and one cyclopentane (E) rings. Erythrodiol with oleanolic acid exhibit an oleanan structure with five cyclohexane rings, which is similar structure motif also for ursane group, represented by ursolic acid (Figure 10). The oleanane and ursane group differs only in position of methyl group on E-ring.^[55] They could be extracted from natural plants in a relatively good yields,^[61,62] which is common strategy how to obtain them in enantiomerically pure form for further synthetic derivatization.^[63] However, the total syntheses of pentacyclic triterpenes have been also published.^[64,65]

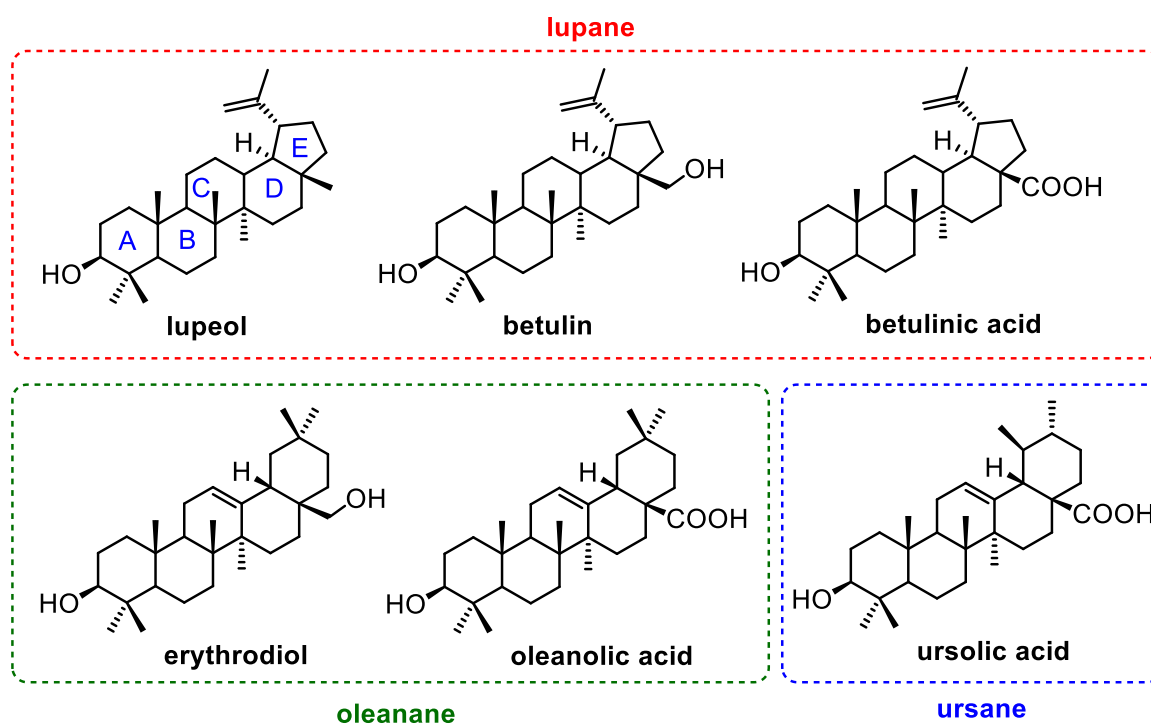


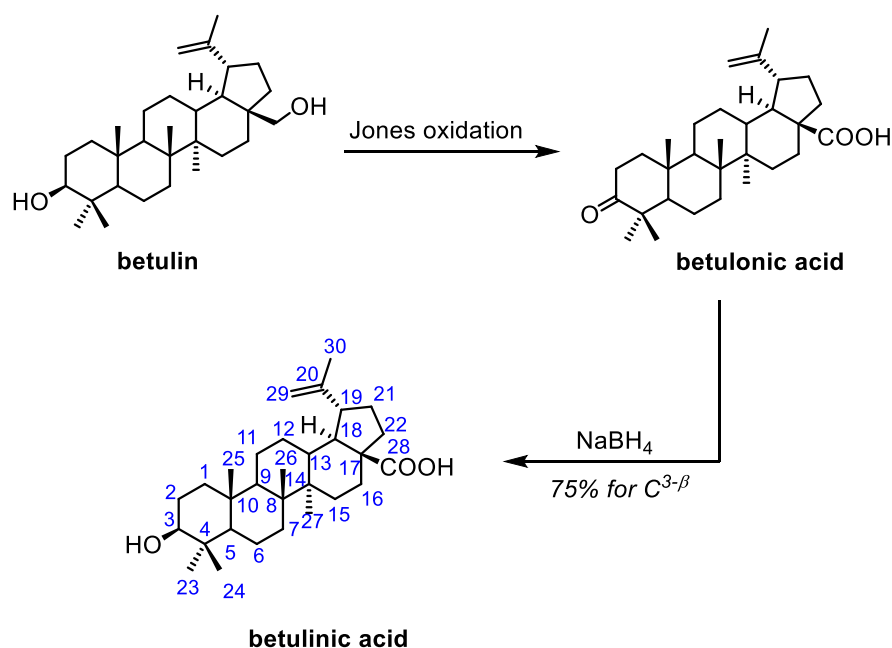
Figure 10. The chemical structure of the main representatives of pentacyclic triterpenes.

1.3.1. The biological properties of the lupane group

As was mentioned above, this group shows an interesting spectrum of biological properties, such as:

- **Antitumor**

The antitumor properties of lupane type triterpenes were first discovered more than 40 years ago, by extraction from the stem bark of various plants.^[66,67] This led to the isolation of betulinic acid, which subsequently became the most examined derivative from this group.^[68] One of the most widely reported sources of betulinic acid is the birch tree (*Betula*), where both betulinic acid and betulin can be obtained in substantial quantities.^[69] This white crystalline solid exhibits limited solubility in organic solvents such as methanol, chloroform, DMF or DMSO, however, it is highly soluble in pyridine and acetic acid.^[69] The semisynthetic preparation of betulinic acid from betulin is done by Jones oxidation to obtain betulonic acid and subsequent reduction with sodium borohydride provides a mixture of C^{3 α} and C^{3 β} hydroxyl products in a ratio 5:95, which upon crystallization in methanol affords the desired diastereomer in very good overall yields (Scheme 3).^[69,70] The modification of positions C³, C²⁸ and the allylic pattern at C²⁰, C²⁹ and C³⁰ are common approaches towards new betulinic acid derivatives.^[71]



Scheme 3. Semi-synthetic preparation of betulinic acid from betulin.

The antitumor activity of betulinic acid and its derivatives could be decisive for therapeutic application, since these compounds exhibit a high activity against several tumors and cancers.^[71] First reports showed a melanoma-specificity^[72] of betulinic acid, however, more recent evidence indicated a broader spectrum of activity against other cancer cell lines, such as neuroblastoma, malignant brain-tumor, prostate carcinoma, ovarian carcinoma or glioblastoma.^[71,73–75] Neuroblastoma cells resistant to CD95- or doxorubicin-triggered apoptosis remained sensitive to treatment with betulinic acid. It strongly and consistently suppressed the growth and colony forming ability of all human melanoma cell lines and in combination with ionizing radiation, the effect of betulinic acid on growth inhibition was additive.^[62] Moreover, the conjugates of amino acids with betulinic acid through C²⁸ carboxylic group showed promising toxicity profile against cultured human melanoma and human epidermal carcinoma of the mouth.^[76] In recent years, the numerous examples of other betulinic acid derivatives with strong cytotoxic effects have been evaluated (Figure 11).^[68,69,77]

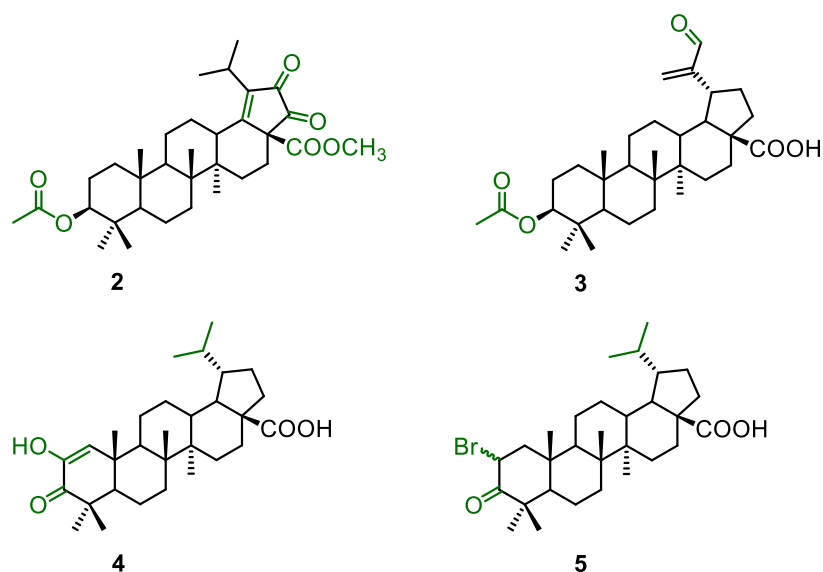
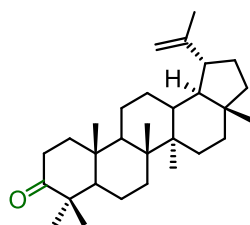


Figure 11. Derivates of betulinic acid with strong anticancer activity.^[68,69,77]

The antitumor mechanism of action of betulinic acid is through apoptosis and thus differs from other, more “classical” anticancer agents such as doxorubicin.^[62,78] It triggers apoptosis by a direct effect on mitochondria and induces loss of transmembrane potential of a benzyloxycarbonyl-Val-Ala-Asp-fluoromethyl ketone inhibitable caspase. Mitochondria undergo cleavage of caspase-8 and caspase-3, due to cytochrome C or AIF (apoptosis-inducing factor) released from betulinic acid.^[62]

Betulin itself remained inactive against several tested cancer cells (melanoma, epidermoid carcinoma, leukemia and neuroblastoma), presumably due to the overall poor solubility.^[71]

Lupenone, the oxo-derivative of lupeol, has significant inhibitory effect on PTP1B enzyme activity, which is closely related to the occurrence and development of various human cancers (e.g. breast cancer, prostate cancer or gastric cancer).^[79]



lupenone

- **Anti-HIV**

Anti-HIV triterpenes are classified into five different classes, according to their mechanism and their molecular targets as:

- *Entry inhibitors, that block HIV adsorption or membrane fusion*
- *Reverse transcriptase inhibitors*

- *Protease inhibitors*
- *Virus maturation inhibitors that do not inhibit HIV-1 protease*
- *Inhibitors with unknown mechanism of action*

Currently approved anti-HIV drugs are either HIV-1 reverse transcriptase or protease inhibitors.^[71] The potent anti-HIV compounds were **7** and its diastereomer **8** (Figure **12**), which act as entry inhibitors and block HIV adsorption or membrane fusion.^[80] The IC₅₀ value for **8** ranging between 40 and 100 nM in various *in vitro* cell-based assays against HIV-1.

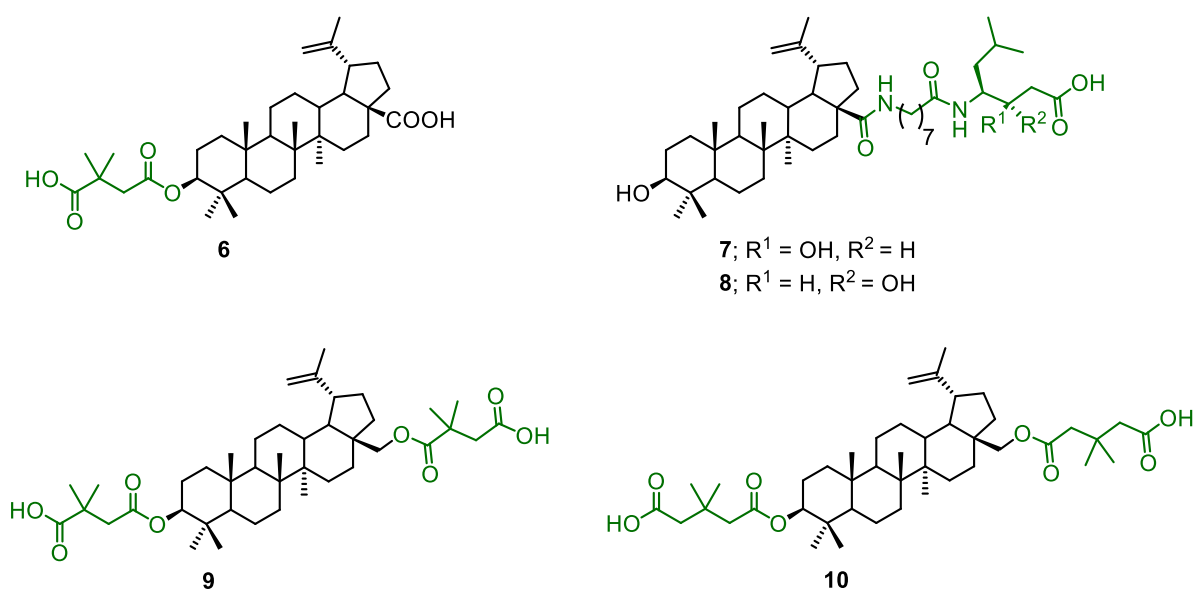


Figure 12. The potent anti-HIV triterpenes.

It was reported that betulin itself was inactive as anti-HIV agent, whereas betulinic acid exhibited IC₅₀ value of 1.4 μM inhibiting HIV-1 replication.^[69] Nevertheless, derivatization at C^{3-β} and C²⁸ was observed to be crucial for increasing anti-HIV activity. The derivatives **6**, **9** and **10** act as a virus maturation inhibitors (Figure **12**).^[71,81,82] Compared to betulinic acid, compound **6** had therapeutic index 2150-fold higher and was 4000-fold more active.^[81] It acts late in the HIV-1 life cycle and binds to the CA-p2 junction of Gag polyprotein by viral protease during HIV-1 particle assembly and sterically inhibits cleavage of this site. Incomplete processing of Gag polyprotein results in virions, which lack a functional core and hence are non-infectious.^[71]

• Other antiviral

The antiviral activity of betulin and betulinic acid and their derivatives have been examined against influenza A, HSV-1, influenza FPV/Rostock and ECHO-6 enterovirus.^[71] Introduction of ureides at C²⁸ of betulonic acid increased its antiviral activity against HSV-1 virus.^[83] Potent anti-HIV compound **6** mentioned above was inactive against HSV-1 and influenza virus.^[84] Betulinic acid and betulin caused

significant reduction of the ECHO-6 virus.^[85] Lupenone exhibit strong inhibitory effect against African swine fever virus (ASFV), HSV-1 and HSV-2.^[86]

- **Anti-inflammatory**

Betulin and betulinic acid showed to be the most effective compounds in skin inflammation and ear edema induced by mezerein, DPT, DPP or TPA in mice,^[71] whereas they seem to be inactive against inflammation induced by resiniferatoxin, xylene and arachidonic acid.^[87] Both have been found to inhibit activity of phospholipase A₂, which plays a crucial role in inflammation process, at 5 μ M conc. by 30% (betulin) and 40% (betulinic acid).^[88] Lupenone could reduce the nitric oxide and reactive oxygen species (ROS), which can be used to prevent inflammatory and oxidative stress-related diseases.^[79] However, mechanism of lupenone against inflammation still needs further elucidation for *in vitro* and *in vivo* studies.^[79]

Despite the fact, that mechanism of action of betulinic acid is widely known, there is a vast number of its derivatives with potent biological activities, which have their mechanisms uncovered. Therefore, it is important to find ways how to determine them, in order to find better therapeutic agents. One of the possibilities are conjugation with fluorescent dyes and tracking such conjugates *in vivo* with fluorescence microscopy. Another drawback, which limits the use of triterpenes as therapeutic drugs, are their low solubility in water. Both approaches, how to increase the potential of triterpenic derivatives, will be discussed deeper in the *Results and discussion* part of the thesis.

Part
II

Results and discussion

2.1. Tumor targeting delivery for purine CDK inhibitors

The results of this project were published in: Krajčovičová, S.; Gucký, T.; Hendrychová, D.; Kryštof, V.; Sural, M. *J. Org. Chem.* 2017, *82*, 13530.^[89] The manuscript is attached in Appendix A (p. 138 - 149). Supporting information is available at: <https://pubs.acs.org/doi/suppl/10.1021/acs.joc.7b02650> and is attached as an electronic file on CD.

2.1.1. Introduction

Cyclin-dependent kinases as targets for cancer treatment

As was mentioned in the previous chapters, cyclin-dependent protein kinases (CDK) belong to the ATP-competitive (*type I*) and serine/threonine kinase family.^[32,90] These critical regulatory enzymes driven all cell-cycle transitions and their activity is often associated with successful cell division.^[32,91] Different families of cyclins, which are crucial regulatory subunits necessary for the CDK activity, have been identified and their expression vary significantly through the phases of the cell cycle. Each CDK is selective for a limited number of cyclins and this, on the other hand, determines the selectivity towards its substrates during the cell cycle.^[90,92] The human genome encodes 21 CDKs, however, only seven (CDK1-4, 6, 10, 11) have been shown to participate directly in the cell cycle progression. The rest play an indirect role, such as activation of other CDKs (CDK3), regulation of transcription (CDK7-9) or neuronal function (CDK5).^[92] Thus, selective inhibition of CDKs may limit the progression of a tumor cell through the cell cycle and facilitate the induction of apoptotic pathways.^[91,93]

During the cell cycle progression through the first gap (G1) phase and initiation of the DNA synthesis (S) phase, the regulation is handled by several cyclins and their associated CDKs. At the beginning, after the cell enters the initial G0 phase, CDK4 and CDK6 form active complexes with D-type cyclins (D1-3) followed by phosphorylation of the retinoblastoma protein (RB1). In late G1, active CDK2-cyclin E heterodimers reinforce RB1 phosphorylation on additional sites to irreversibly initiate the gene expression of the S phase.^[93] At this stage, which is known as restriction point and is decisive in cancer as alternations in the key regulatory players in the G1 and S phase transition, the cells are able to proliferate independently of mitogenic stimuli. Beyond this restriction point, RB1 is maintained in a hyperphosphorylated state by the sequential activities of CDK2-cyclin A, CDK1-cyclin A and CDK1-cyclin B complexes. In a complex with cyclin A, CDK1 is suddenly activated at the transition from the second gap (G2) phase to the mitosis (M) phase to facilitate the beginning of mitosis through regulation of chromosome condensation and microtubule dynamics (Figure 13). An anaphase signal is activated when (even a single) chromosome is not properly attached to the mitotic spindle. The stop is

mediated by the spindle assembly checkpoint (SAC), which is a circuit of signaling proteins. Cell cycle checkpoints are series of surveillance pathways which ensure that cells pass accurate copies of their genome on to the next generations. Defects in the SAC can lead to premature separation of sister chromatids and could accelerate chromosomal instability, which is a typical feature of cancer cell lines.^[93] Complete inhibition of the SAC causes death in human tumor cells, suggesting that inactivation of the mitotic checkpoint kinases could be a reasonable strategy for cancer cells suppression.^[93,94]

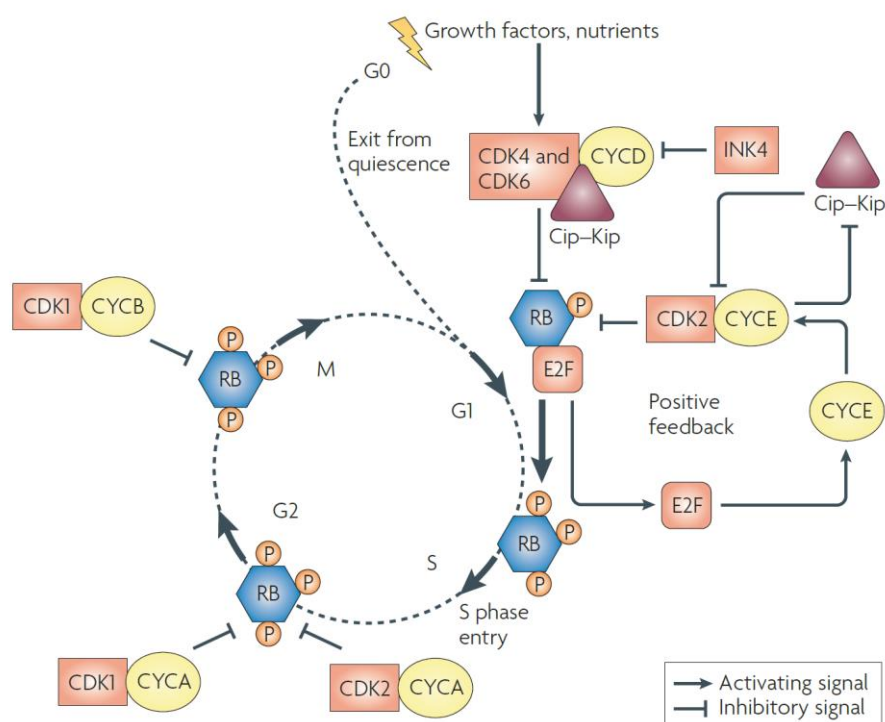


Figure 13. The cell cycle control by CDKs.^[93]

Mitogenic stimuli induce release of the CDK4 and CDK6 from the INK4 and initiate phosphorylation of RB. They also bind stoichiometrically to the CDK2 inhibitor of Cip-Kip enzyme family. Partially phosphorylated RB proteins release E2F transcription factors, enabling the expression of genes required for G1 to S phase transition of DNA synthesis. This includes the cyclin E gene, which allosterically regulates CDK2 activity in late G1, thus creating a stimulus that antagonizes Cip-Kip inhibitors and reinforces RB inactivation, leading to an irreversible switch to S phase. Cyclin A and B-dependent CDKs are activated at later phases of the cell cycle to maintain RB in a hyperphosphorylated form until the cell exits mitosis. (RB = retinoblastoma; E2F = family of transcription factors; INK4 = inhibitory proteins; P = phosphorylation).^[93]

Development of CDK inhibitors

Over the last two decades, several CDK inhibitors have been developed as potential anticancer drugs and tested in numerous trials and several tumor types.^[91] This first

generation of CDK inhibitors, so called *pan-CDK inhibitors*, were relatively non-specific and did not meet the expectations following preclinical studies, although some compounds, such as purine-like analogs Olomoucine^[95] and Roscovitine^[96] (as *R*-enantiomer) (Figure 14) showed relatively low selectivity towards CDK4 and CDK6.^[91,93,97] Purine scaffold was presented in both inhibitors as “starting point” for design of many other inhibitors, very likely due to the structural similarity with the ATP itself.^[90]

As pan-CDK inhibitors may act on many phases of the cell cycle, the drug must maintain a reasonable pharmacokinetic profile to be able to survive during sufficient exposure of the damaged tissue over the entire duration of the cell cycle.^[93] For instance, although one of the most extensively studied CDK inhibitors Flavopiridol can induce cell cycle arrest in G1 and G2 phases, it simultaneously induces cytotoxic response as a result of CDK7 and CDK9 inhibition that leads to transcription suppression. Thus, Flavopiridol may have clinical activity in hematological malignancies (chronic lymphocytic leukemia or mantle cell lymphoma), in which scheduling also seems to influence its efficacy.^[91,98,99] It was found out that a relatively short infusion time resulted in response rates of 41% in 22 assessable patients with chronic lymphocytic leukemia.^[91,93,100] Among with Flavopiridol, another well examined purine CDK inhibitor Roscovitine was evaluated in the clinics (also known as Seliciclib; developed by Cyclacel). Roscovitine made it to the randomized Phase II trial, in which it was administrated to patients with advanced non-small lung cancer, however, this study was terminated as Roscovitine did not seem to improve progression-free survival in this patient population.^[91] The third described inhibitor Olomoucine has never been evaluated in the clinics, although it was one of the first occurred CDK inhibitors.^[95]

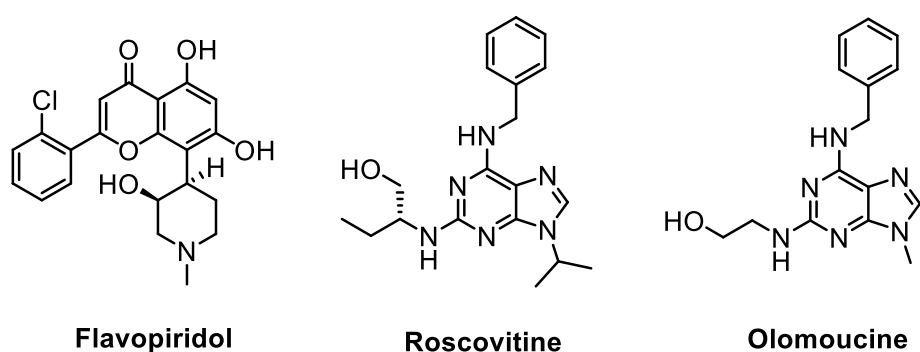


Figure 14. The most examined pan-CDK inhibitors.

The second generation, followed Flavopiridol and Roscovitine-like structures, was developed with the aim of increasing selectivity toward CDK1 and CDK2 and/or increasing overall potency. Numerous CDK inhibitors seemed to be promising in preclinical studies, however, only a few progressed Phase I clinical trials.^[91] Dinaciclib (Figure 15), the second-generation CDK inhibitors, was evaluated as highly potent

inhibitor of CDK1, CDK2, CDK5 and CDK9 (IC₅₀ values in single-digit nanomolar range), whereas activity towards CDK4, CDK6 and CDK7 was almost over an order higher.^[91] Despite the fact, that initial results from Phase I studies were promising (Dinaciclib induced stable disease in a range of malignancies and displayed tolerable toxicity), the following randomized Phase II trials were arrested because interim analysis showed that the time to disease progression was inferior with Dinaciclib treatment.^[91,101]

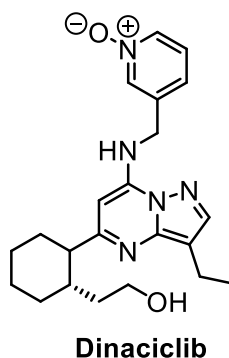


Figure 15.

The later studies revealed potency of 2,6,9-trisubstituted purine analogs (the next generations of Roscovitine) as highly potent CDK inhibitors.^[102,103] Their synthesis is rather straightforward and started usually from the 2,6-dihalogenated purine,^[102,104,105] 2-amino-6-chloropurine^[106] or by building the purine ring from the dichloropyrimidine precursor.^[107] Along with the solution-phase synthesis, the solid-phase approach is also applicable and widely used, as we described in the review in 2016.^[108]

Folate targeting

To minimize the exposition of healthy cells towards toxicities linked with application of potent, but not specific cytotoxic agents, the strategy for the selective delivery has been developed and a rapidly growing class of anticancer drugs use a targeting drug-delivery approach to malignant cells.^[109] In addition to antibodies, other tumor-selective ligands have been discovered to prepare novel drug conjugates. For instance, the vitamin folic acid (FA) showed high affinity for the folate receptor (FR), which represents a potentially useful biological target for the management of many human cancers, e.g. ovarian, endometrial or kidneys.^[110,111] This glycosylphosphatidylinositol-linked membrane protein binds extracellular folates with very high affinity and, through the nondestructive, recycling endosomal pathway, physically delivers inside the cell (Figure 16).^[110] Therefore, attachment of FA to potent chemotherapeutic compounds to form so called *small molecule drug conjugates* (SMDCs) is remarkably useful approach towards potent and simultaneously less toxic agents^[109] and several conjugates of this type have been evaluated or even entered the clinical trials, including taxol,^[112] vinca alkaloid vinblastine^[113] or thymidylate synthase inhibitor FdUMP.^[114]

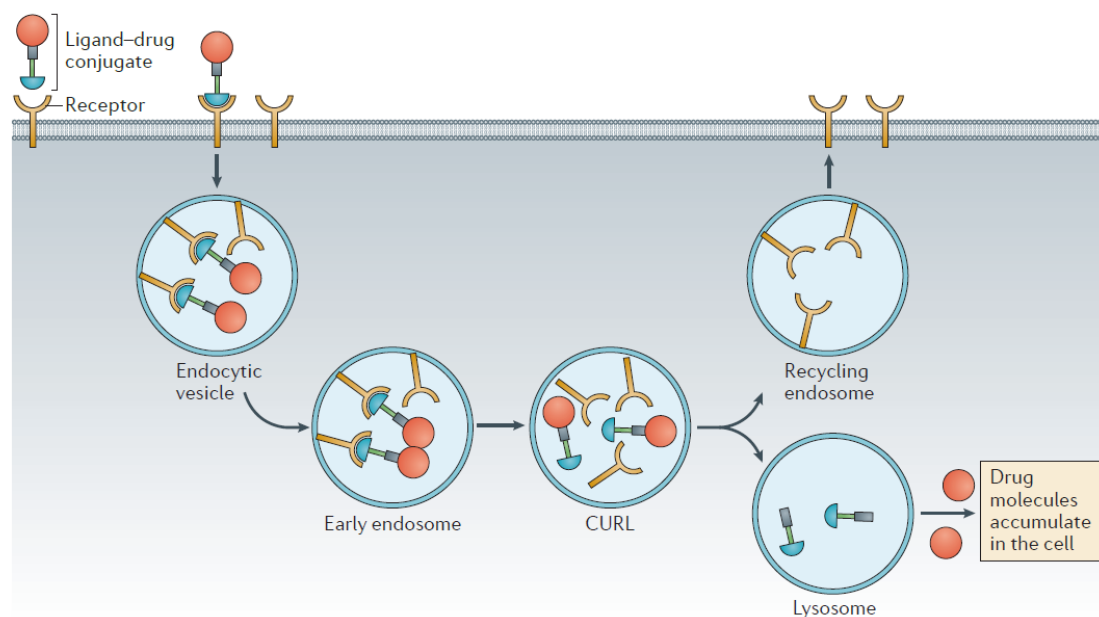


Figure 16. Schematic representation of the function of FA conjugates.^[109] (CURL = compartments for uncoupling of receptor and ligand)

The design of FA conjugates

In the early studies, the focus has been mostly paid on the actual ability of the FA-SMDCs to be delivered inside the tumor cells, hence ignoring the structure-activity relationships and importance of the fine-tuning the release properties of prepared conjugates, which inevitably led to results of limited success.^[110,115] Based on these ineffective attempts, some crucial properties of ideal FA conjugates ought to meet.

The development of releasable, self-immolative, disulfide-containing linkers, arranged between the FA ligand and a cytotoxic agent, yielded conjugates having superior activity against FR-positive cells, compare to the non-reducible counterparts.^[116] As examples should serve disulfide-containing SMDCs like maytansine,^[117] tubulysins^[118] or previously mentioned vinblastine.^[119] The novel thiophilic heterobifunctional linker **I-1** (Figure 17) was incorporated to the proposed SMDCs, as it was able to react with many *N*- and *O*-nucleophiles under mild conditions.^[110]

The second, somehow less popular approaches, conjugated *via* a releasable, pH-sensitive acyl hydrazine linkers **I-2** or *p*-alkoxybenzylidene acetal linkers **I-3** (Figure 17), were based on release of the active parent drug from its FA conjugate as the result of lowering pH in the endosome environment.^[120] The electron-donating effect of the *p*-alkoxy substituent in the aromatic ring increases acetal's sensitivity towards hydrolysis under mild acidic conditions, due to the resonance stabilization of carbocation.^[110] Herein, the maleimide moiety was designed for Michael addition with nucleophilic residues, instead of hydroxybenzotriazole.

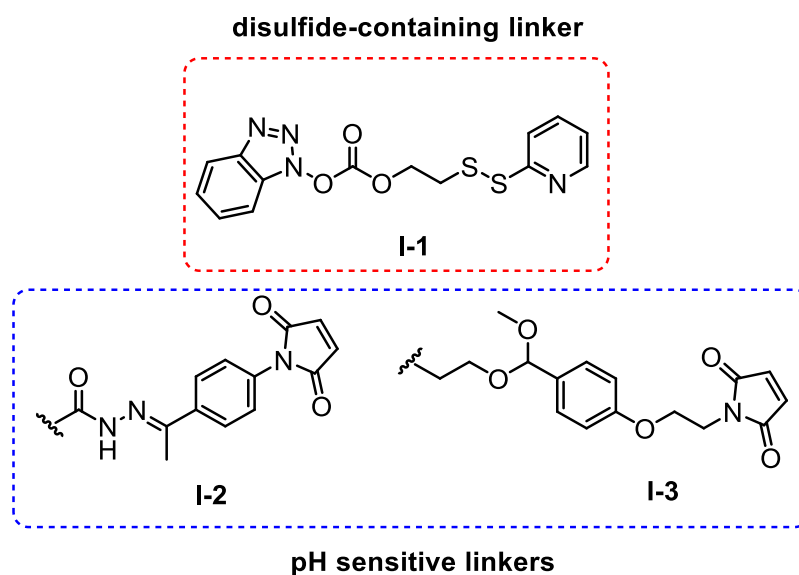
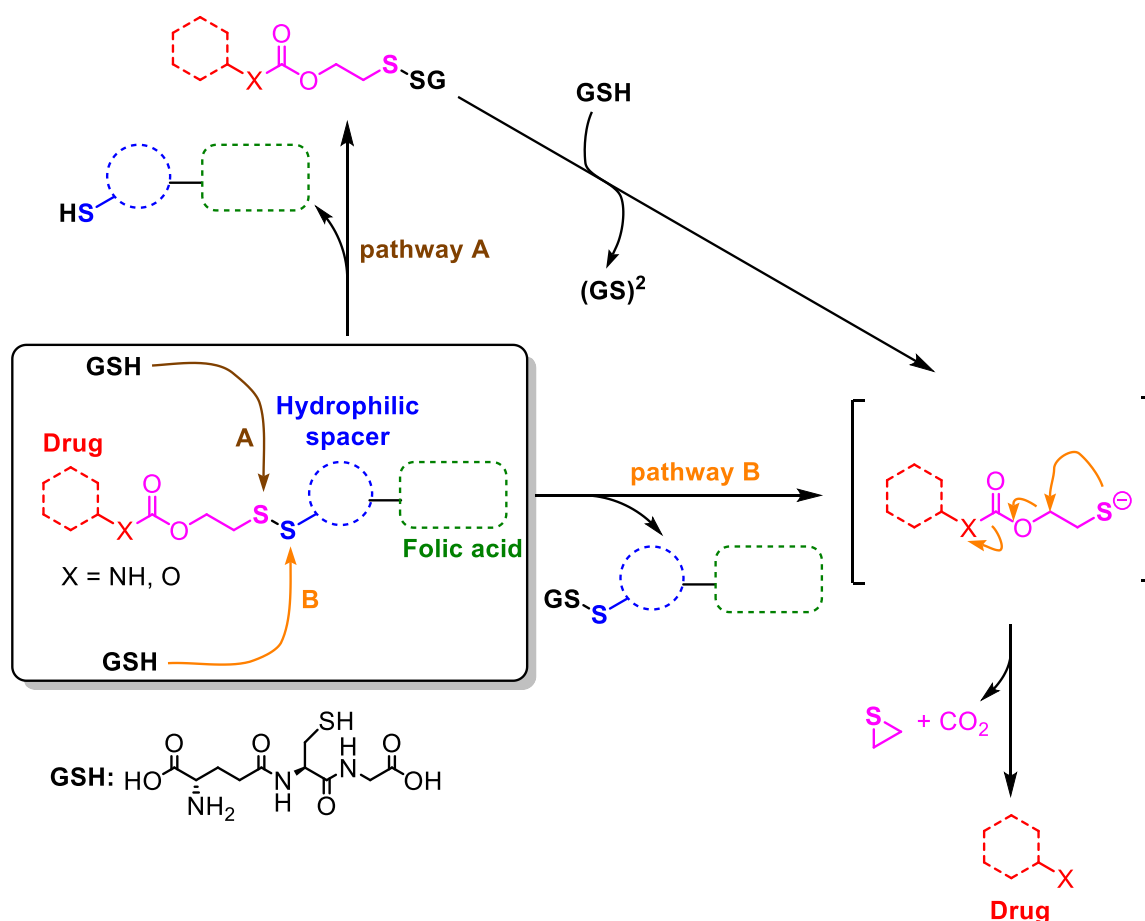


Figure 17. Design of the linkers.^[110]

Next issue that came upon evaluation of prepared conjugates was solubility, since vast majority of small-molecule chemotherapeutic compounds allows for their passive diffusion through cell membrane. FA-SMDCs with enhanced hydrophilicity (containing polar, charged amino acids residue spacer) will force these nonpolar molecules to enter FR-positive cells rather than indiscriminately into nontarget cells.^[110] The self-immolative cleavage of disulfide-based linker is depicted on Scheme 4.



Scheme 4. The self-immolative cleavage of disulfide-based linker and subsequent release of the drug in the endosomal environment. A thiol group of a reducing agent can attack either of the two sulfur atoms in the linker system, resulting in two distinguished pathways. (GSH = glutathione)

Bearing this concept in mind, we proposed a design of our final purine CDK inhibitors for conjugation with FA (Figure 18). The study of Roscovitine and Dinaciclib-like inhibitors, namely trisubstituted pyrazolo[1,5-*a*][1,3,5]triazines,^[121,122] pyrazolo[4,3-*d*]pyrimidines^[123] and pyrazolo[1,5-*a*]pyrimidines,^[124–126] revealed ideal substitution patterns on each position of purine moiety for single-digit-nanomolar activities.^[102,127] Moreover, the combination of 2-cyclohexanediamine, 9-cycloalkyl and 6-heterobiaryl methylamino substituents has been found out to significantly increase CDK activity and cytotoxic effects in cancer cell lines, compared to previously published compounds of this class, e.g. well known derivative CR8.^[102,128] Hence, these observations motivated us for preparation of selected purine CDK inhibitors **I-4a-g** for conjugation with FA *via* C² position (Figure 18), which should not interfere in terms of interaction of inhibitors within the CDK catalytic domain. Letters **a-g** represent substitutions on purine core and will be followed during the whole synthetic explanations below.

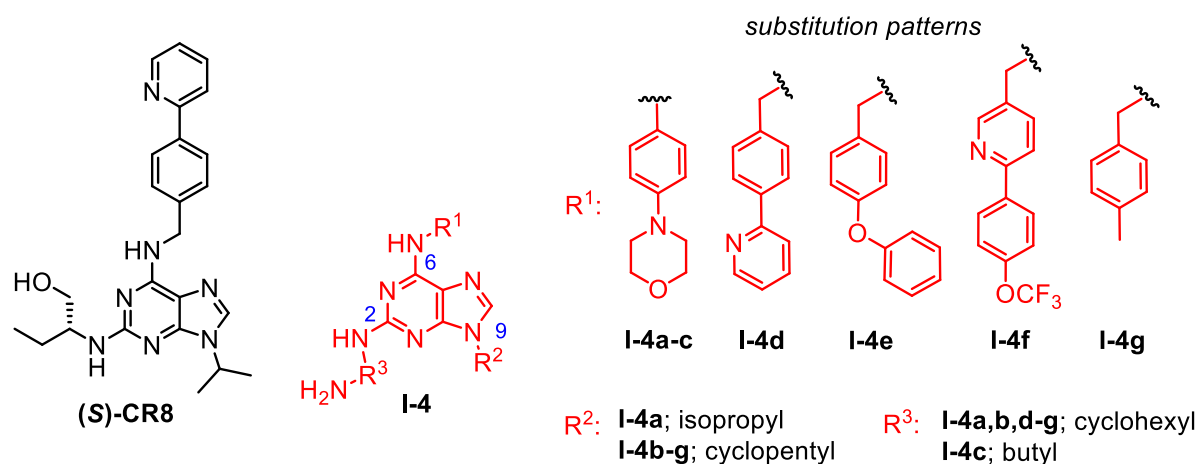
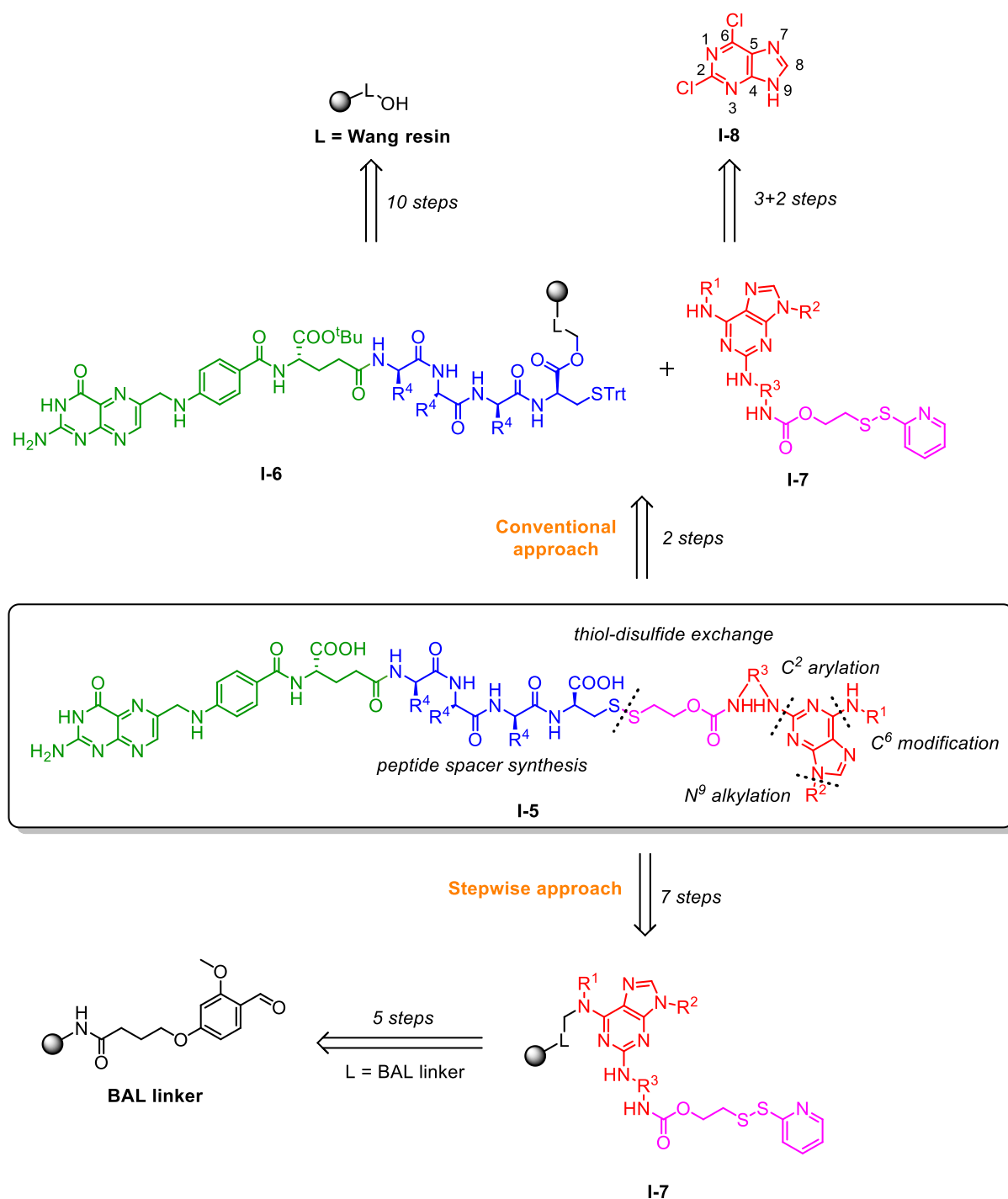


Figure 18. Potent CR8 purine CDK inhibitor and our selected substitution patterns based on previously reported molecules.

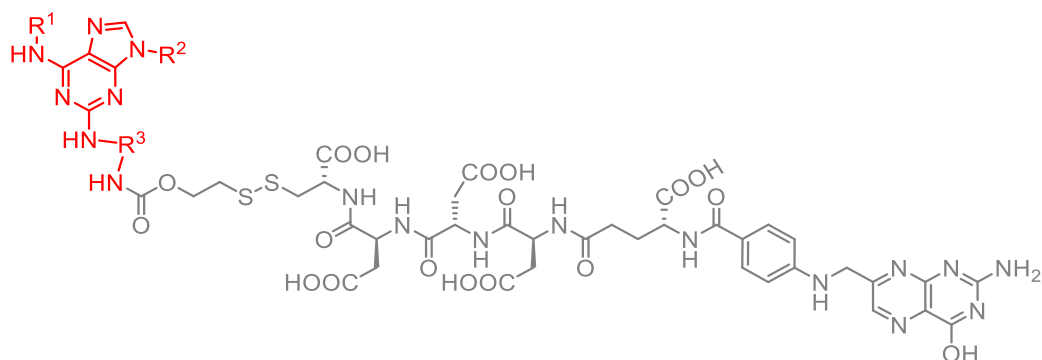
2.1.2. Synthesis

The preparation of target FA conjugates is generally^[129] applied in convergent synthetic fashion (for our purposes named as *conventional approach*). It relies on synthesis of hydrophilic, peptidic spacer with folic acid on solid support, whereas self-immolative linker with drug candidate are synthesized in solution. These two parts are then connected via thiol-disulfide exchange reaction to yield final compounds. However, this approach required tedious several step purifications during synthesis, which is inconvenient for high-throughput synthesis and subsequent biological screening. Moreover, according to our experience, handling with folic acid derivatives is rather problematic, due to its zwitterionic character, high polarity and poor solubility in organic solvents (except for DMSO).^[129]

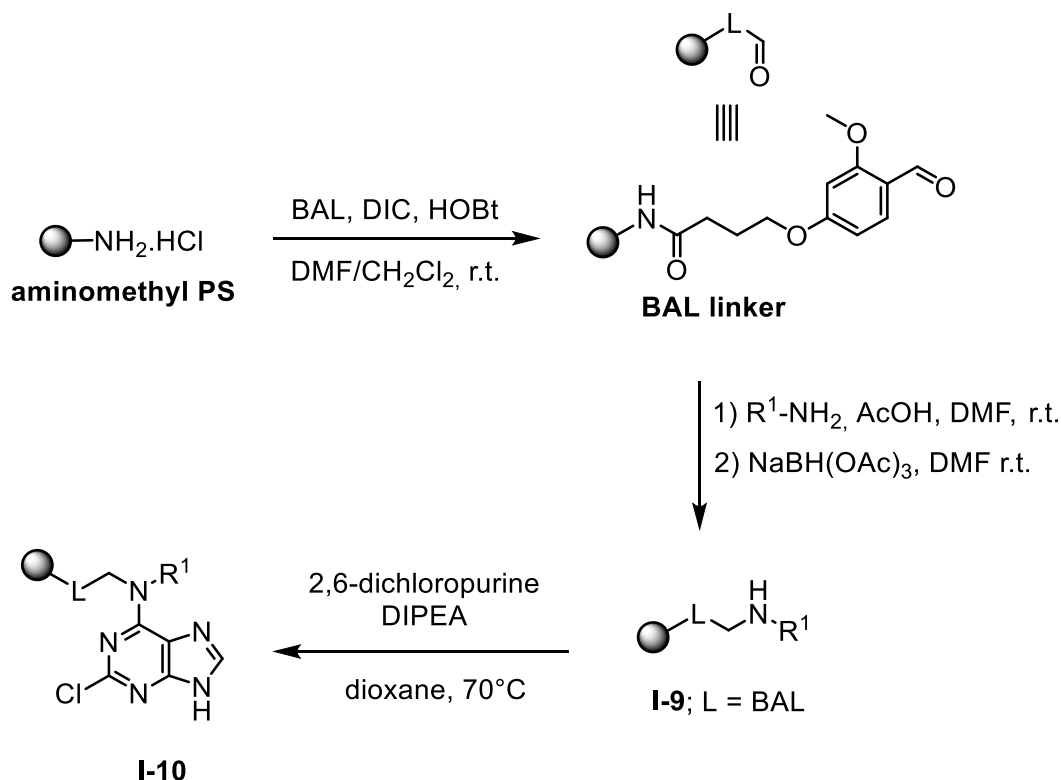
Hence, we envisioned a linear strategy (for our purposes named as *stepwise approach*), in which the drug candidate is built step-by-step on the solid-support started from a BAL linker, followed by the addition of pre-modified linker in solution, thiol-disulfide exchange to form disulfide bond directly on the resin and ending with the cleavage from the resin with only one final purification of the whole conjugate **I-5** (Scheme 5). The synthetic approach towards final conjugates is fully described in our published paper,^[89] however, I consider appropriate to summarize the optimization steps.

Scheme 5. Retrosynthetic analysis of the final FA conjugates **I-5**.

2.1.2.1. Synthesis of 2,6,9-trisubstituted purine intermediates



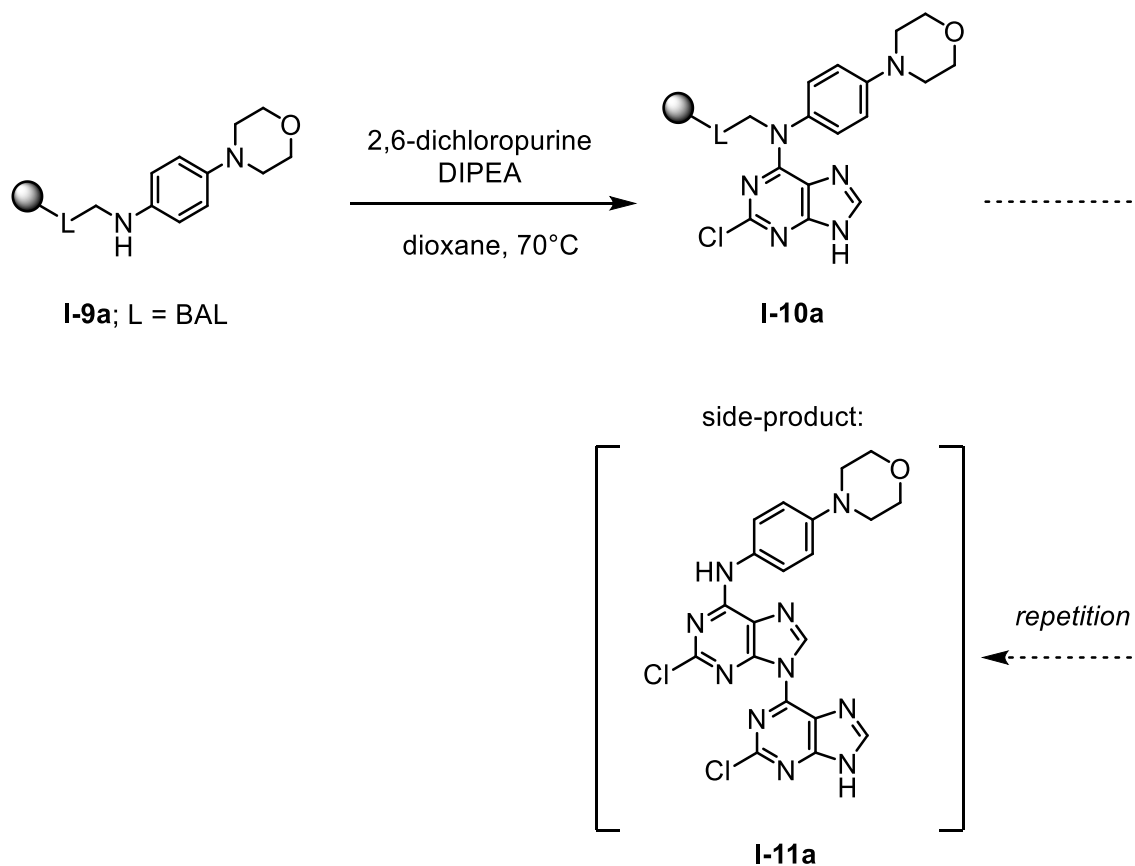
The synthesis started with immobilization of 4-(4-formyl-3-methoxyphenoxy)butanamide linker (BAL linker) to commercially available aminomethyl polystyrene resin. The following reductive amination with various benzylamines and anilines afforded intermediates **I-9**. Subsequent aromatic nucleophilic substitution (S_NAr) proceeded with excellent regioselectivity at C⁶ position and produced compounds **I-10** (Scheme 6).



Scheme 6. Preparation of immobilized purine intermediates.

However, it was necessary to optimize the reaction conditions for the aromatic nucleophilic substitution in case of 4-morpholinoaniline derivatives **I-9a**. In the published procedure^[130] authors used THF as a solvent with heating at 50°C. Under this condition the conversion was not complete and required repetition of this step, which subsequently led to formation of dimeric purine side-product **I-11a** (Scheme 7) due to the possible arylation on N⁹ in presence of base (DIPEA). It is worth mentioning

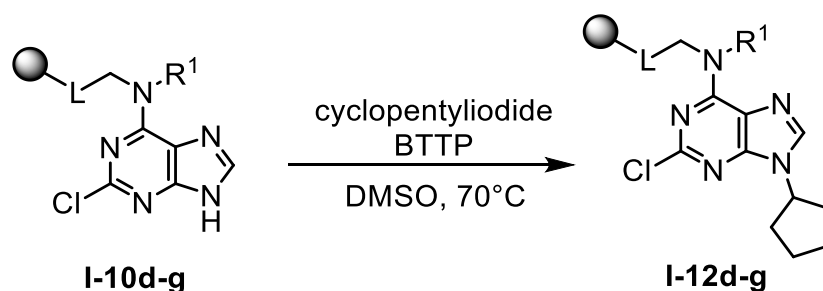
that observation of by-product **I-11a** was based on mass calculation from UHPLC-MS traces and was not isolated.



Scheme 7. Formation of dimeric purine by-product **I-11a**.

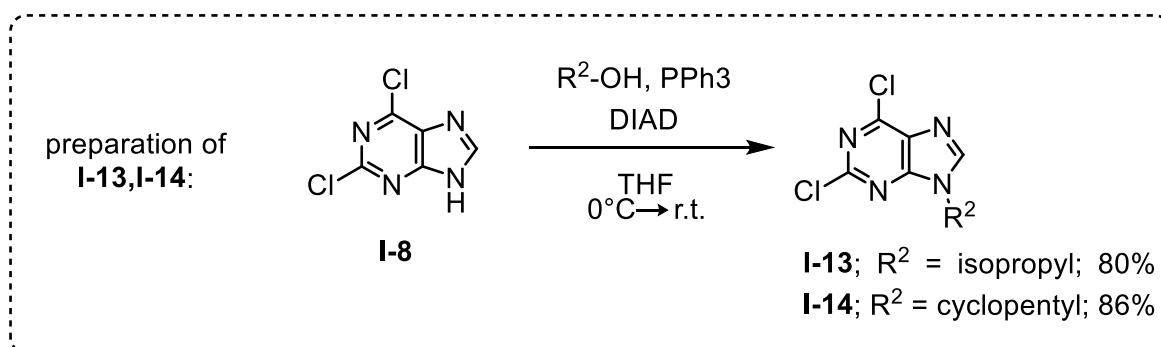
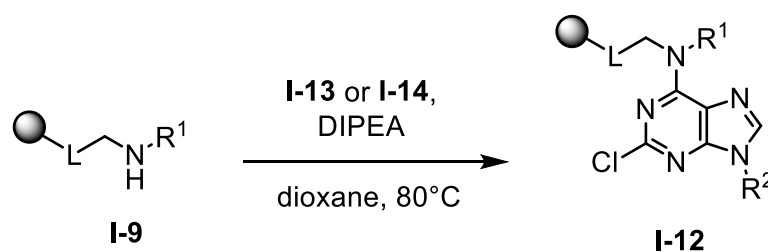
Due to this fact we tried to change a solvent as well as reaction temperature to force nucleophilic substitution towards full conversion, without necessity to repeat reaction. Unluckily, we had not been able to proceed this reaction quantitatively, without the presence of purine dimer and/or starting material on UHPLC-MS analysis.

The reaction sequence for benzylic amines **I-10d-g** continued with alkylation at the N⁹ position. The best results were obtained after reaction with *tert*-butylimino-tri(pyrrolidino)phosphorene (BTTP) in DMSO (Scheme 8), however, the crude purities were lowered.



Scheme 8. Alkylation on N⁹ position.

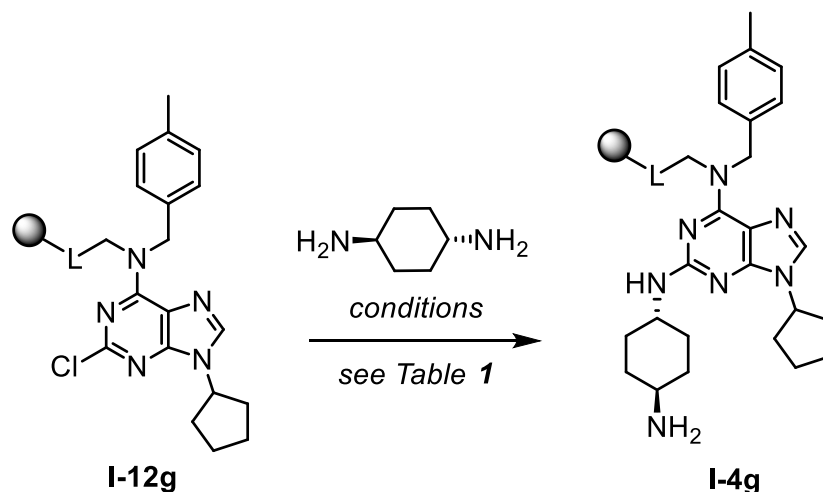
Thus, an alternative pathway with pre-modified N⁹ substituted purine *via* Mitsunobu reaction, was proposed. Prepared N⁹-alkylated 2,6-dichloropurines **I-13** and **I-14** in solution were reacted with the all immobilized amines **I-9** (benzylic as well as anilinic) to afford desired intermediates **I-12** in excellent crude purities (Scheme 9).



Scheme 9. Alternative pathway with N⁹ pre-modified purines.

The first challenging part of the synthesis seemed to be modification of position C² on purine scaffold (optimized on compound **I-12g**), since it generally suffers from lower reactivity than C⁶ position and much harsher conditions are needed.^[90] We put quite effort to optimizations and tested several conditions, including various high boiling solvents, temperatures, reaction times and/or even a microwave heating (Table 1). Unfortunately, according to the UHPLC-MS traces we detected presence of the starting material **I-12g** in most attempts, indicating incomplete conversion (cond. a, b, d, f – i, k), or the resin-bound compounds did not survive microwave irradiation under such harsh conditions and decomposed (cond. c, e, j). We observed that in the presence of a stronger base, the crude purity was somehow better, but still not satisfying enough (cond. i). Fortunately, we were able to push the reaction to the full conversion, although the conditions were still very harsh (cond. l; 48 hours heating at 160 °C in

diethylene glycol diethylether, with ruthless excess of *trans*-1,4-diaminocyclohexane), required extended reaction time and addition of the base and the amine to the reaction mixture after 24 hours of stirring. Moreover, time-to-time troubles with reproducibility were also observed. Therefore, another synthetic approach seemed to be requisite.

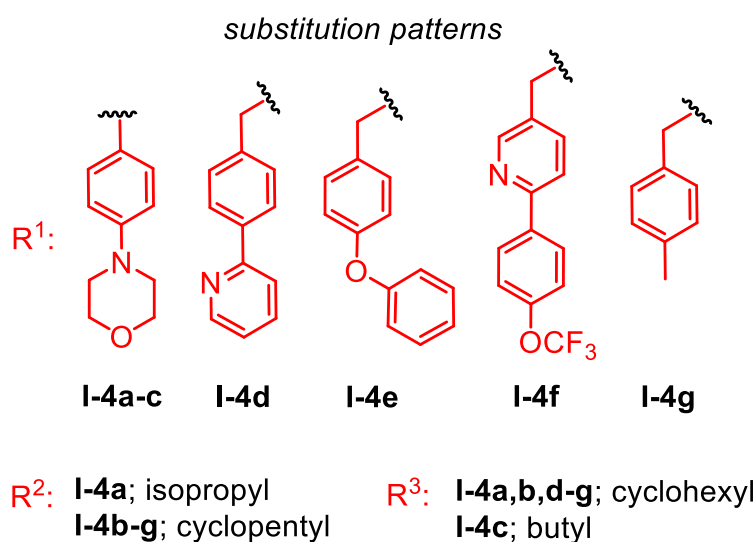
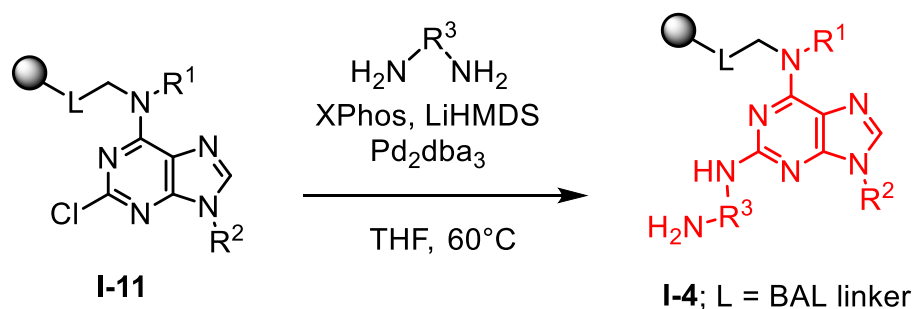


Scheme 10.

| # | Base | Conc. [M] | Amine conc.[M] | Solvent | Temp. [°C] | Reaction time | Observation |
|-----------|-------|-----------|----------------|---------|-------------------|---------------|------------------------------|
| a. | - | - | 4 | DMSO | 100 | 16 h | <i>Incomplete conversion</i> |
| b. | - | - | 4 | DEGDE | 130 | 24 h | <i>Incomplete conversion</i> |
| c. | - | - | 4 | DMSO | 120 ^{MW} | 2 h | <i>Resin decompose</i> |
| d. | - | - | 4 | NMP | 150 ^{MW} | 2 h | <i>Incomplete conversion</i> |
| e. | - | - | 4 | NMP | 180 ^{MW} | 4 h | <i>Resin decompose</i> |
| f. | DIPEA | 4 | 4 | NMP | 150 | 16 h | <i>Incomplete conversion</i> |
| g. | DIPEA | 4 | 4 | DEGDE | 160 | 16 h | <i>Incomplete conversion</i> |
| h. | DIPEA | 5 | 4 | DEGDE | 160 | 24 h | <i>Incomplete conversion</i> |
| i. | BTTP | 5 | 4 | DEGDE | 160 | 24 h | <i>Incomplete conversion</i> |
| j. | DABCO | 4 | 4 | DEGDE | 150 ^{MW} | 2 h | <i>Resin decompose</i> |
| k. | DABCO | 4 | 4 | DEGDE | 160 | 16 h | <i>Incomplete conversion</i> |
| l. | DIPEA | 5 | 5 | DEGDE | 160 | 48 h* | <i>Full conversion</i> |

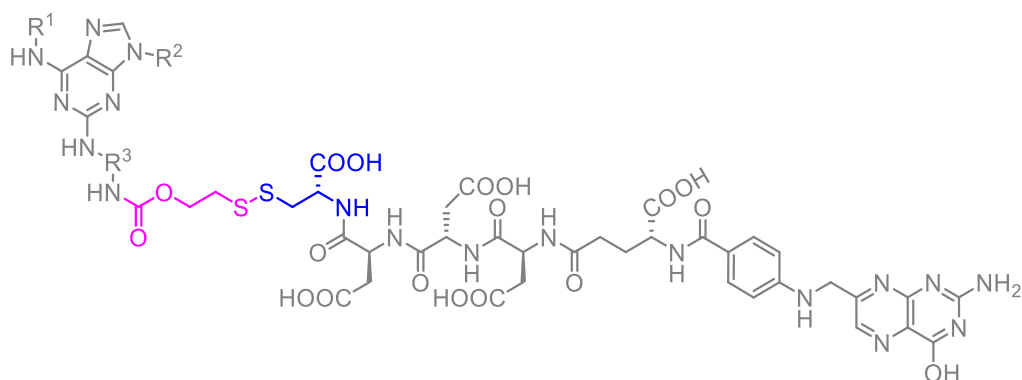
Table 1. Summarized procedures for aromatic nucleophilic substitution. * - reagents were added twice, after 24h. (DEGDE = diethylene glycol diethylether; Amine = *trans*-1,4-diaminocyclohexane; MW = microwave irradiation; decomp = decompose).

One of the common ways how to obtain C - N bonds is the Buchwald-Hartwig cross-coupling reaction. Under the reaction conditions depicted in the Scheme 11, we successfully obtained the intermediates **I-4** in excellent crude purity, regardless of the substitution at C⁶ (reaction works very well for both, benzylic amines as well as 4-morpholinoaniline) and with good reproducibility. Compared with the previous methodology (nucleophilic substitution) was Buchwald coupling much feasible and thus used as a standard protocol for all derivatives **I-4a-g** (Scheme 11).



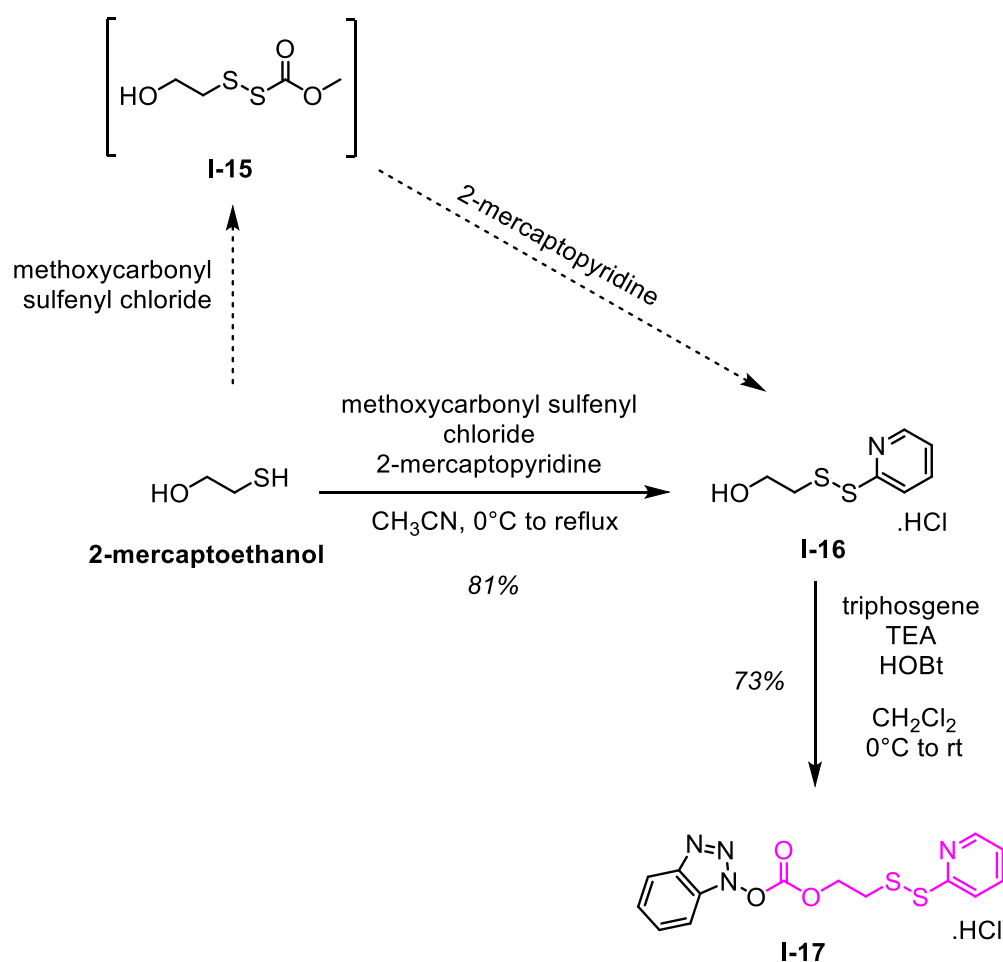
Scheme 11. Buchwald-Hartwig coupling in order to attach alkyldiamine moiety on position C².

2.1.2.2. Synthesis of the disulfide-containing linker



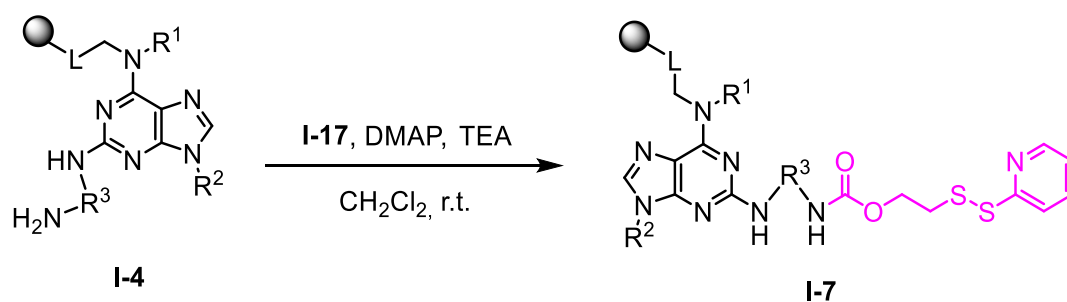
As was mentioned above, introduction of the disulfide moiety between the drug candidate (in our case the 2,6,9-trisubstituted purine derivatives) and the folic acid with oligopeptide chain seemed to be crucial for the overall activity of the compounds. The synthesis of the disulfide linker was accomplished by slightly optimized literature procedure^[131] after 2 steps (Scheme **12**). Alkoxy carbonyl sulfenyl chlorides are highly reactive electrophilic species and sources of RS^+ ^[132] that in first step reacted with nucleophilic 2-mercaptoethanol to form disulfide intermediate **I-15** *in situ*, which upon subsequent treatment with 2-mercaptopyridine yielded asymmetric disulfide **I-16** in excellent yields. It is worth mentioning, that the choice of leaving group in thiol-disulfide exchange is determined mostly by pK_a of the thiol and by pH of the solution.^[133]

The formation of carbonate **I-17** required presence of triphosgene as a milder, better-to-handle and less toxic reagent than phosgene. A very reactive diphosgene ester is formed *in situ* and upon treatment with hydroxybenzotriazole (HOBt) yielded desired carbonate **I-17** (Scheme **12**). According to our experience, the carbonate is air and bench stable for 3+ years.



Scheme 12.

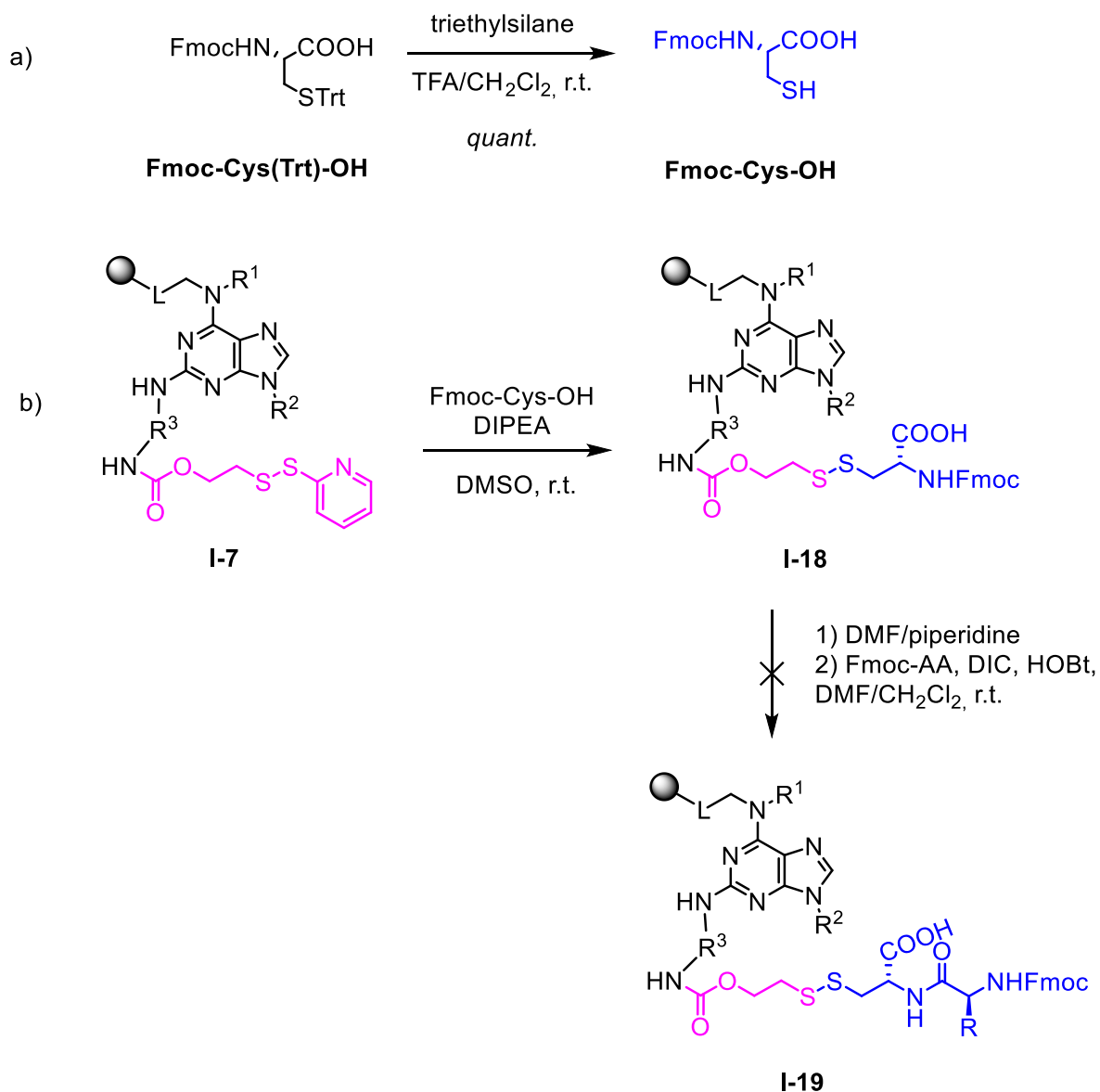
The installation of the carbonate linker to the polymer bounded intermediates proceeded smoothly and we obtained desired carbamates in quantitative conversion under mimicked conditions from literature^[131] (Scheme 13).



Scheme 13.

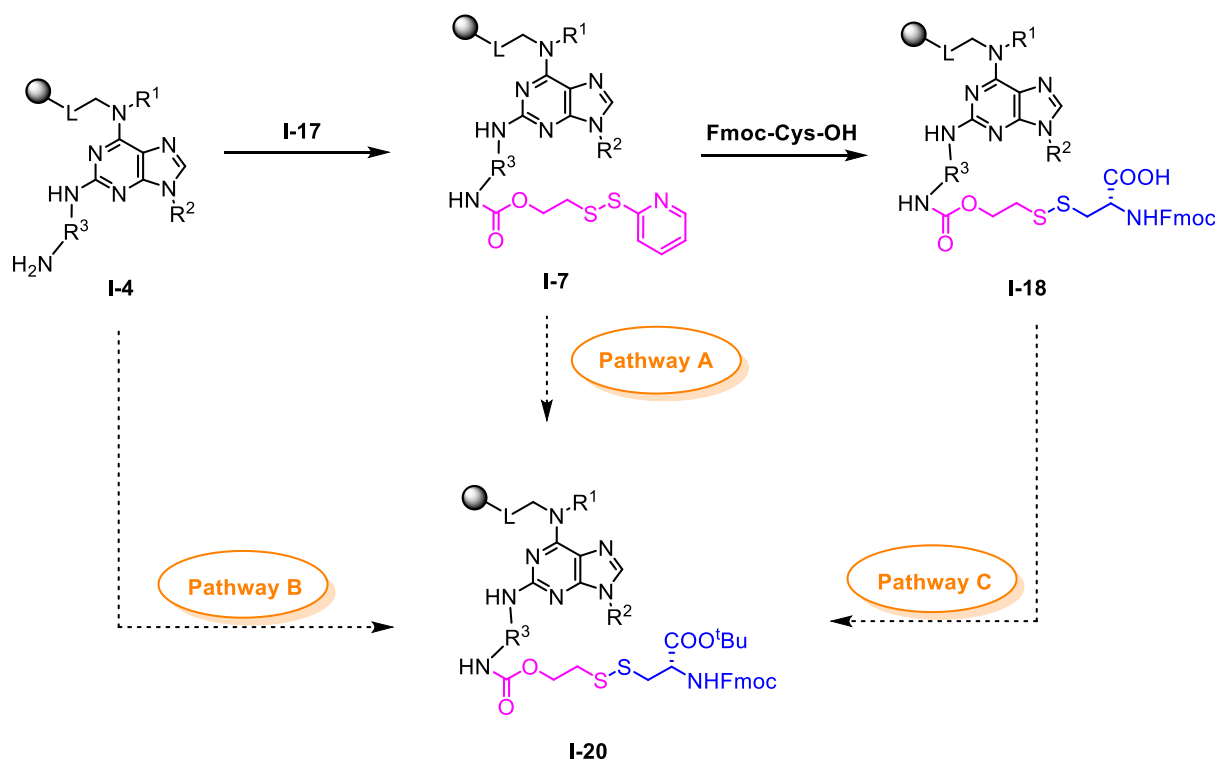
The following thiol-disulfide exchange of intermediate **I-7** on solid-phase (Scheme 14.b) was successfully accomplished with use of Fmoc-Cys-OH (which is not commercially available and has to be S-protected prior to use; Scheme 14.a). However, the further Fmoc-cleavage and acylation with Fmoc-amino acid (i.e. first step of a peptidic spacer synthesis) under standard DIC/HOBt protocol failed (Scheme

14.b). We believed that it could be caused by the presence of unprotected carboxylate. For this reason, alternative pathways were suggested.



Scheme 14. a) Preparation of Fmoc-Cys-OH; b) Thiol-disulfide exchange with Fmoc-Cys-OH and unsuccessful acylation with another Fmoc-amino acid.

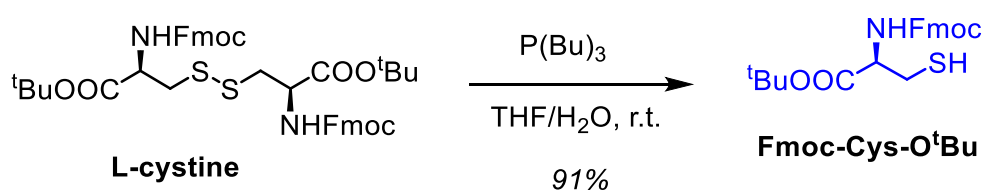
Generally, there could be 3 synthetic pathways how to synthesize the desired intermediate **I-20** with protected carboxylic function (Scheme 15).



Scheme 15. General pathways for preparation of intermediate **I-20**.

Pathway A: Thiol-disulfide exchange with protected cysteine

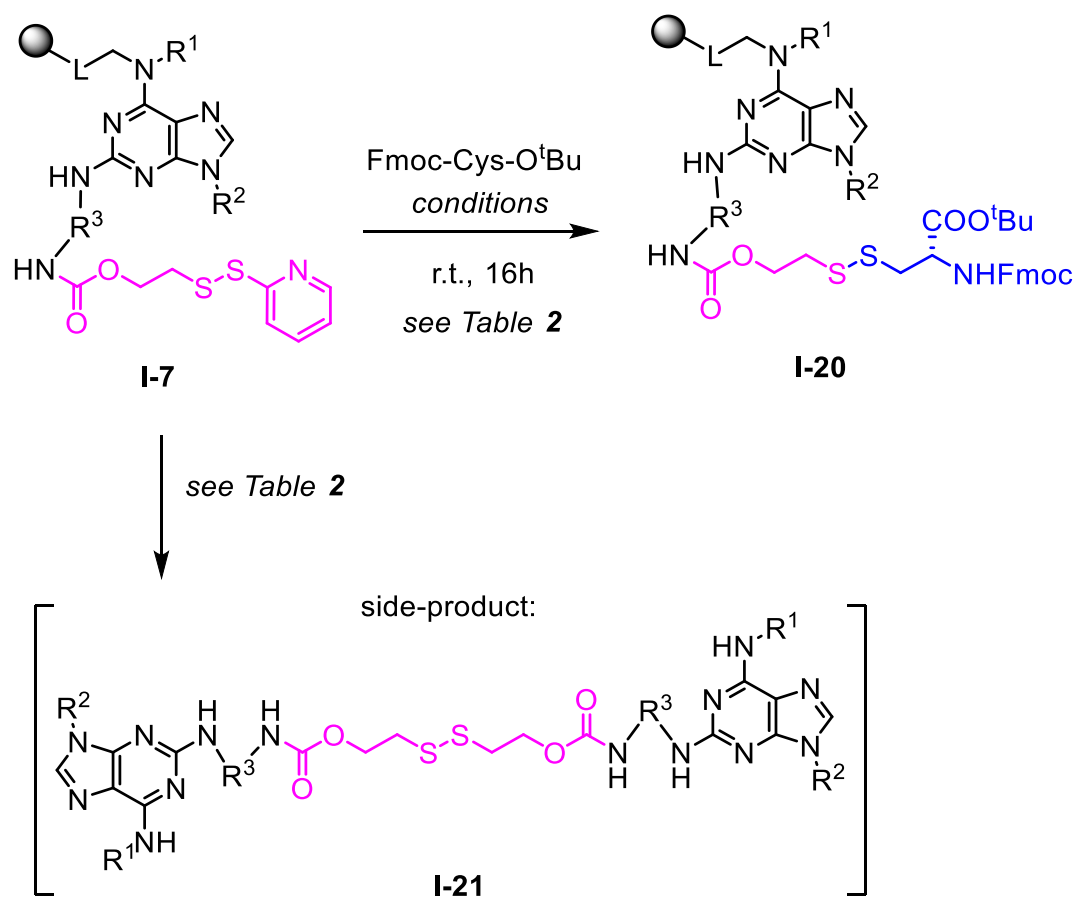
The first possible pathway is reduction of commercially available Fmoc protected L-cysteine to Fmoc-Cys- O^tBu (Scheme 16). Addition of just traces of water was crucial to process reaction successfully.^[134]



Scheme 16.

Following thiol-disulfide exchange seemed to be a challenging task, because several attempts were applied but with limited results (Table 2). The reaction in either THF or CH_2Cl_2 led to the symmetric disulfides **I-21** (cond. b, c, f; calculated from UHPLC-MS traces according to mass) or other by-products which were not identified (cond. e). The non-reactivity of the Fmoc-Cys- O^tBu was presumably caused by change in pH of solution and/or pK_a of the thiol functional group, which could dramatically influence the reaction outcome,^[133] or simply due to the steric reasons. Moreover, the thiol itself is less nucleophilic than thiolate and base is necessary for reactivity (cond. a, only starting material **I-7** was presented). The formation of the symmetric disulfides **I-21**

suggested cleavage of the asymmetrical disulfide bond in basic environment. The best results were observed with use of DIPEA in dichloromethane (cond. d), however, the crude purity was rather low, and we decided to try another synthetic pathway.



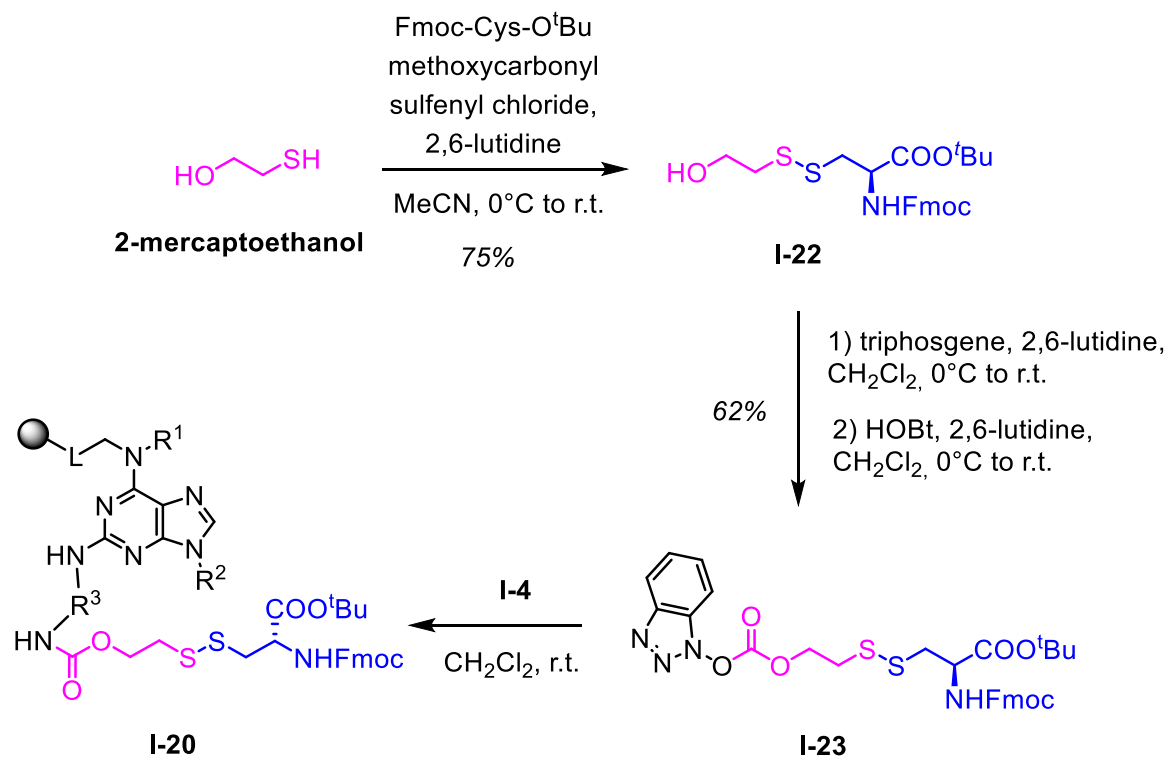
Scheme 17.

| # | Base | Conc. [M] | Conc. of X [M] | Solvent | Observation |
|----|-------|-----------|----------------|---------------------------------|---------------------------------|
| a. | - | - | 0.8 | THF | I-7 |
| b. | DIPEA | 0.5 | 1 | THF | I-21 |
| c. | DIPEA | 0.5 | 1 | CH ₂ Cl ₂ | I-21 |
| d. | DIPEA | 0.3 | 0.3 | CH ₂ Cl ₂ | I-20 ; <i>low purity</i> |
| e. | DIPEA | 0.5 | 1 | DMSO | <i>Unknown product</i> |
| f. | BTTP | 1 | 0.6 | THF | I-21 |

Table 2. Summarized attempts to afford intermediate **I-20**.

Pathway B: Direct preparation of linker with COOtBu

The first step was preparation of disulfide containing alcohol **I-22**, with 2-mercaptoethanol under previously mentioned conditions. Addition of base (2,6-lutidine) in huge excess maintained neutral pH during reaction, thus prevented cleavage of acid labile *tert*-butyl protecting group on carboxylic moiety. Although elevated temperatures were omitted due to the partial Fmoc deprotection in presence of base, the reaction proceeded smoothly and with excellent yields. Following formation of carbonate in presence of triphosgene provided desired intermediate **I-23** (Scheme 18). Again, addition of base during reaction was crucial to maintain protection on carboxylic moiety, however, the huge excess paid its price during the work-up. The purification of linker **I-23** seemed to be quite tricky, since it decomposed during column chromatography on silica gel and we had to avoid strong basic as well as acidic conditions for work-up, due to the presence of both acid (*tert*-butyl) and base (Fmoc) labile protecting groups. Moreover, the common extraction with copper sulfate (to get rid of amines) only led to decomposition of **I-23**, presumably due to the presence of other coordinating groups. Hence, we were forced to use semipreparative HPLC for purification to obtain **I-23** in sufficiently good yields (60 – 70%). Finally, the following nucleophilic substitution with intermediates **I-4** (Scheme 18) provided compounds **I-20** in excellent crude purities (up to 90 %).

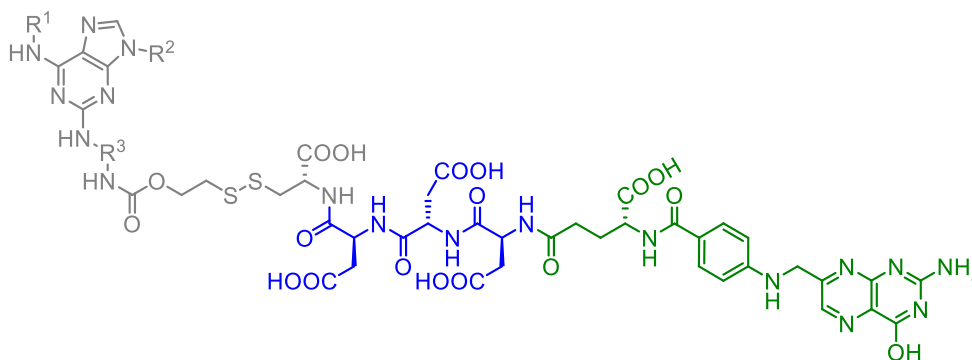


Scheme 18.

Pathway C: Protection of COOH on resin

This pathway was finally not tested, due to the successful optimization of the pathway B.

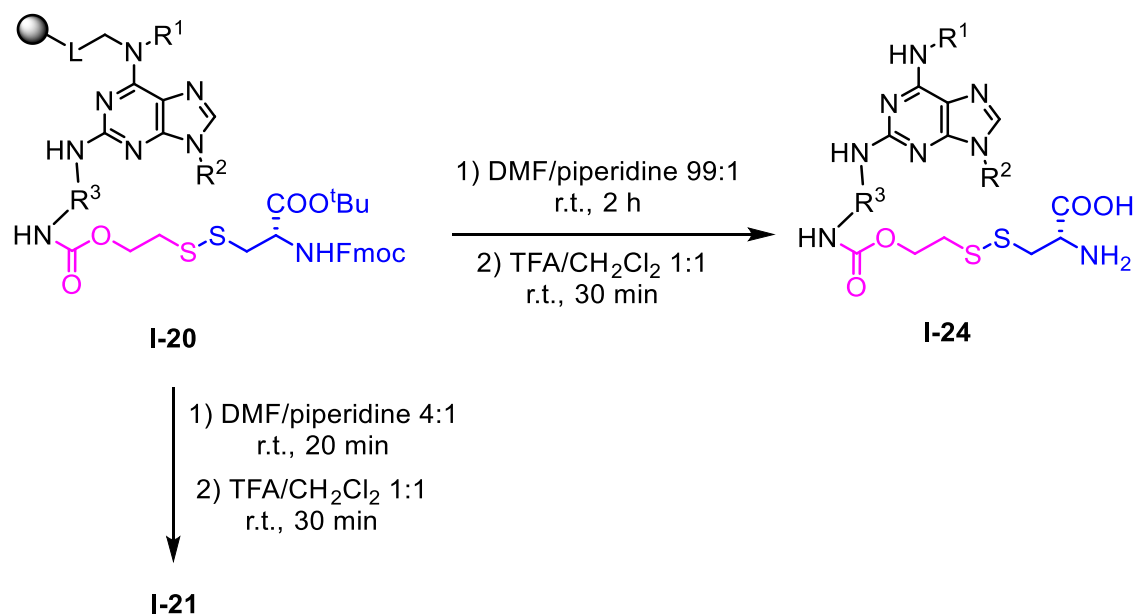
2.1.2.3. Synthesis of the hydrophilic spacer and attachment of folic acid



According to the published results, the spacer modification has a rather small impact on the targeted activities of folates and it basically consists of amino acids with side-chain hydrophilic groups.^[135] For our purposes we decided to use aspartic acid side chains to fulfill this requirement.

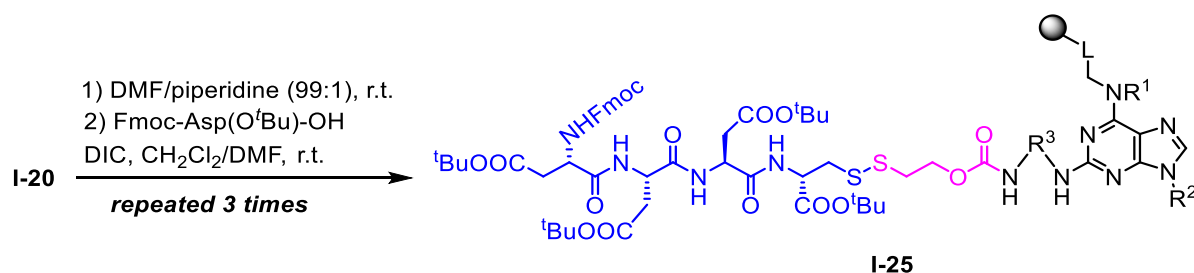
Synthesis of the peptidic spacer started with deprotection of Fmoc protecting group. Unfortunately, the standard cleavage conditions (DMF/piperidine 4:1) commonly used in peptide chemistry, yielded only a symmetric disulfide **I-21** (Scheme 19; structure suggested from UHPLC-MS traces). Its formation is probably caused by the nucleophilic nature of piperidine, which in higher concentration can cleave Fmoc protecting group and simultaneously participates in cleavage of disulfide bond, which subsequently formed the non-desired product.

Hence, a lower concentration to cleave Fmoc group had to be applied and the best results were obtained with use of DMF/piperidine 99:1 after 2 hours (Scheme 19), when the formation of a symmetric disulfide **I-21** was completely suppressed, indicating that pH during the reaction plays crucial role.^[133]



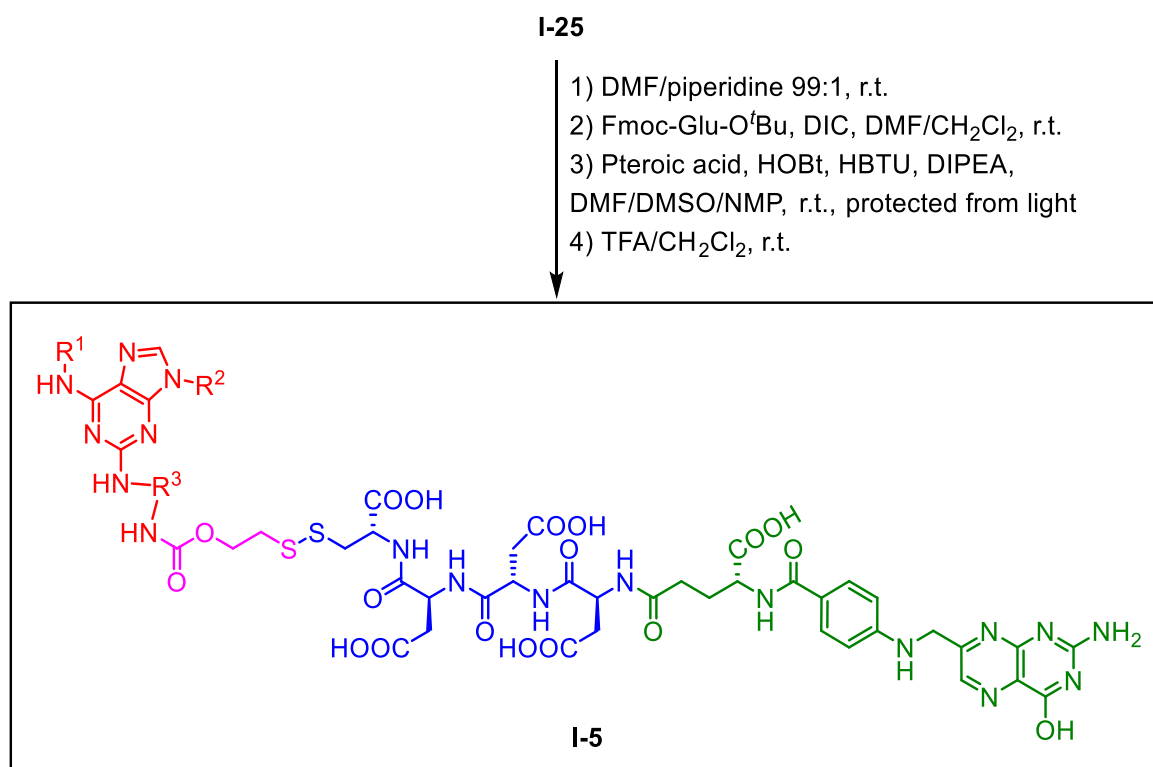
Scheme 19.

The reaction sequence continued from **I-20** with repeated steps of Fmoc cleavage and DIC promoted peptide couplings with use of commercially available Fmoc-Asp(O^tBu)-OH to afford peptidic spacer-linker-purine intermediates **I-25** (Scheme 20).



Scheme 20.

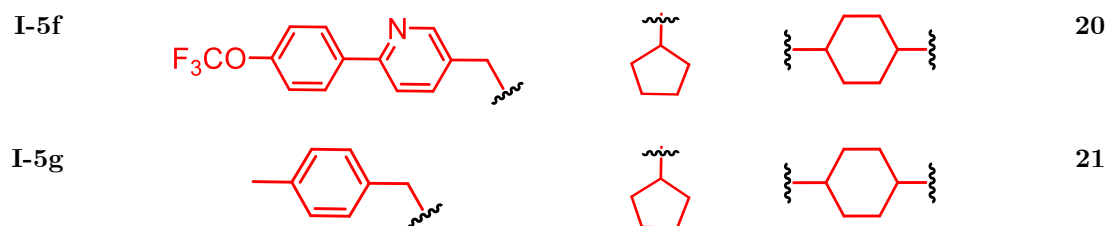
The following 2 steps acylation with Fmoc-Glu-O^tBu and pteronic acid yielded the final intermediates that upon cleavage from the polymer support and purification on semipreparative HPLC afforded final compounds **I-5** (Scheme 21).



Scheme 21. Final compounds preparation.

The reaction sequence was successfully tested using different building blocks, which were suggested from SAR studies (Table 3). Furthermore, Figure 19 displays the HPLC-UV traces of representative reaction intermediates after cleavage from the polymer support. This figure demonstrates that the optimized procedure furnished the corresponding compounds in excellent crude purities and good yields after 15 reaction steps and final reverse-phase purification.

| Cmpd | R ¹ | R ² | R ³ | Yield ^a [%] |
|------|----------------|----------------|----------------|------------------------|
| I-5a | | | | 27 |
| I-5b | | | | 22 |
| I-5c | | | | 25 |
| I-5d | | | | 23 |
| I-5e | | | | 19 |



^a - overall yield calculated from the loading of resin 2 after the entire reaction sequence and preparative HPLC purification

Table 3. Substitution on purine core.

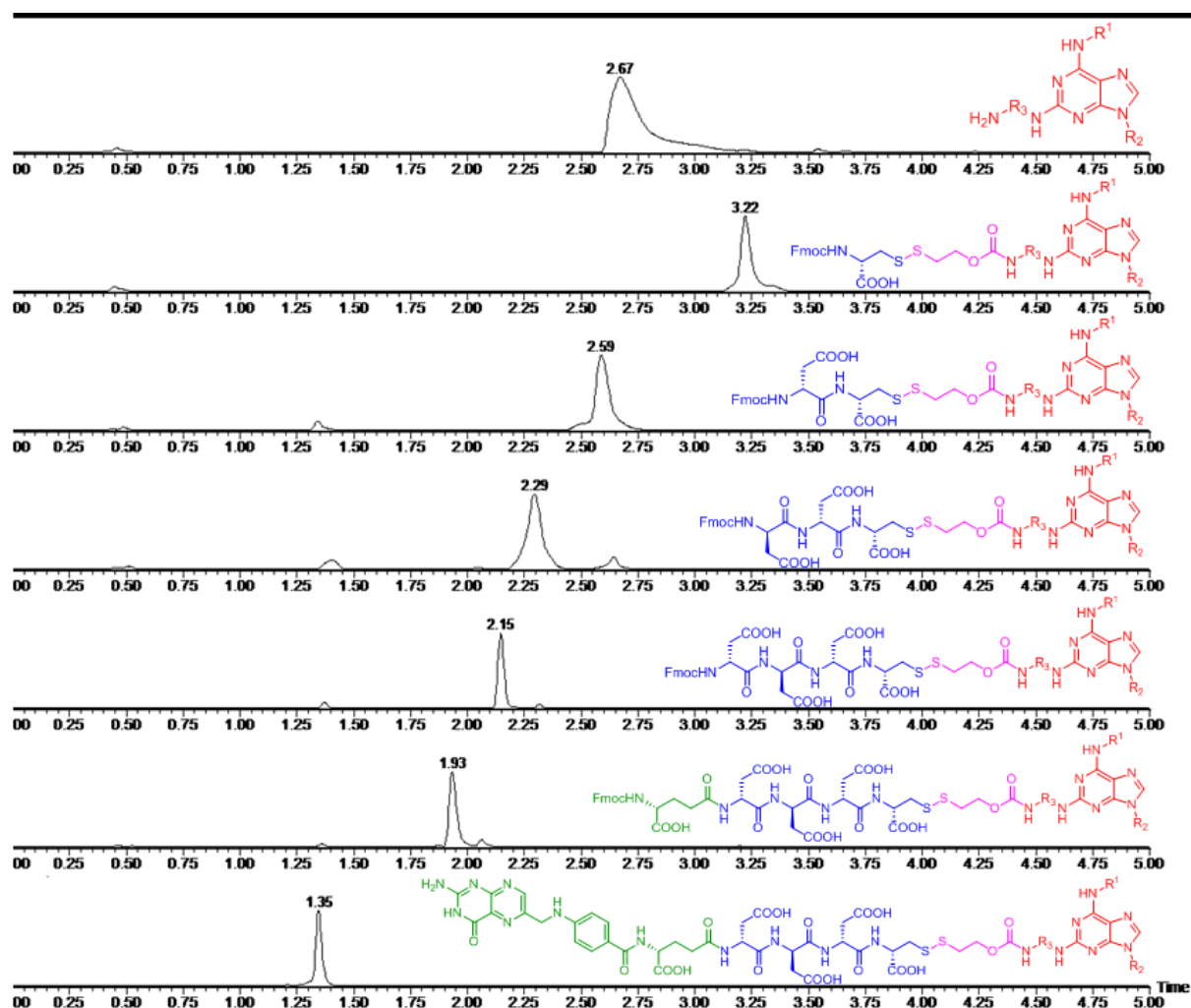


Figure 19. Final crude purities of intermediates. The substitution on purine ring did not influence the purity.

2.1.3. Biology

To test the applicability of our prepared compounds, we decided to mimic drug release *in vitro* on representative derivative **I-5d**. The mechanism of self-immolative cleavage of the linker is based on 1,2-elimination, as was suggested above (Scheme 4). The release of the compound **I-4d** was successfully accomplished by treating a 0.04 mM solution of conjugate **I-5d** (Figure 20.C) with 4 mM of the general reducing agent dithiothreitol (DTT) at 37 °C. The release was monitored by UHPLC-UV ($\lambda = 289$ nm) at pH 7 and 7.4. The disulfide bond was cleaved within 5 min and yielded the drug-spacer intermediate (Figure 20.B), followed by self-immolative cleavage and quantitative release the purine inhibitor **I-4d** after 20 h (Figure 20.A). It is important to mention that use of glutathione (GSH) instead of DTT led to cleavage of the conjugate **I-5d** after the same time.

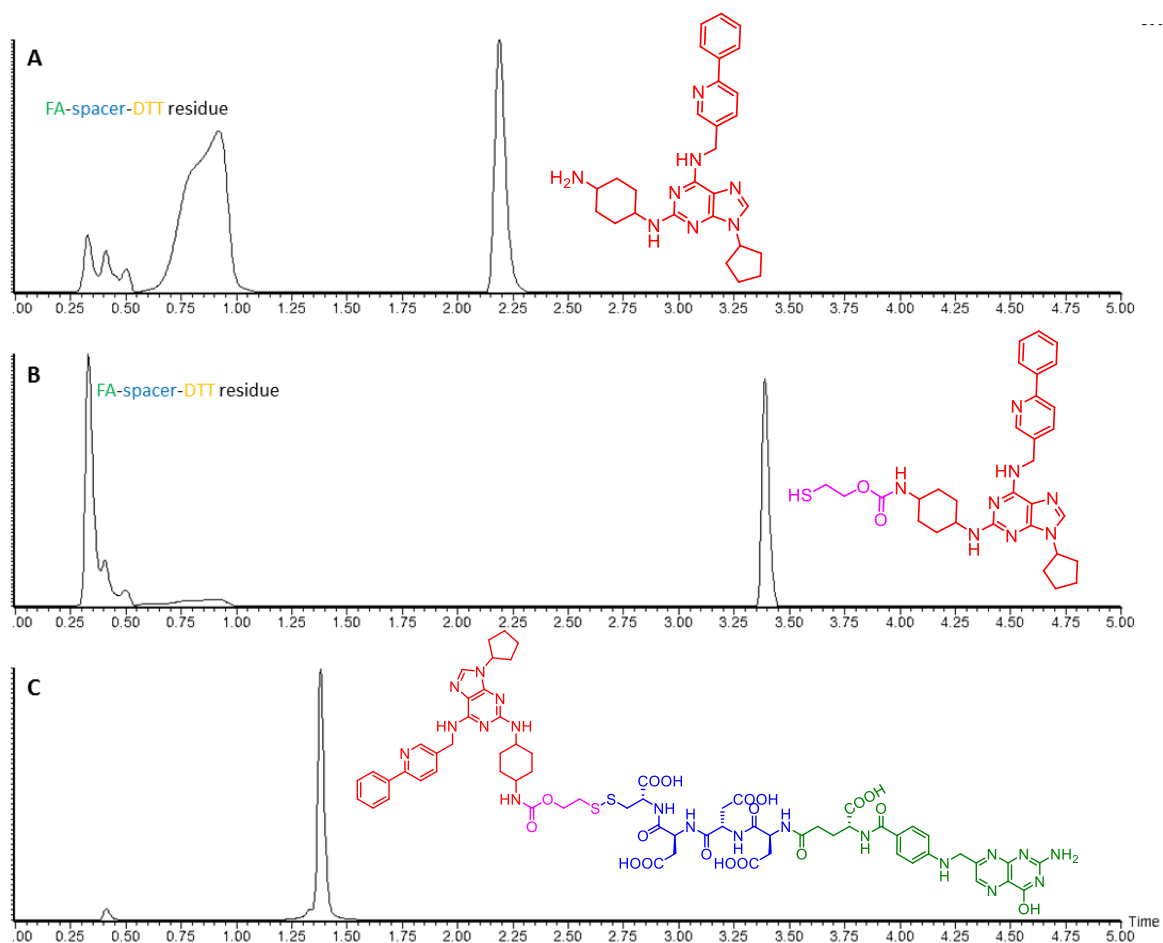


Figure 20. Mimicked disulfide bond reduction with subsequent self-immolative cleavage of the conjugate **I-5d**. (FA = folic acid; DTT = dithiothreitol)

As another proof of concept, conjugate **I-5d** was further tested for its binding to the HeLa cell line overexpressing FOLR1 by flow cytometry using the folate-receptor-targeted fluorescence probe FolateRSense 680 (PerkinElmer) as a competing agent

(Figure 21.A). This experiment was provided by V. Kryštof group. The HeLa cell line was used due to its overexpression of FOLR1 and significantly greater probe uptake over other cell lines.

The cells were stained with 1 μ M FolateRSense 680 in the absence or presence of conjugate **I-5d** (Figure 21.B,C). The probe was combined with either the unconjugated inhibitor or free folic acid (Figure 21.D,E) in control incubations. Quantification of cell-associated fluorescence was provided after 1 hour of incubation by flow cytometry. The presence of **I-5d** remarkably decreased the percentage of cells with bound FolateRSense 680 from 75.6% to 11.4% (Figure 21.C), as was suggested from the experiments. Free folate also reduced the percentage of positive cells and therefore confirmed the function of the probe (Figure 21.D). The specificity of cellular binding of conjugate was demonstrated in a control experiment in which an excess of unconjugated CDK inhibitor **I-4d** did not compete with the probe (Figure 21.E).^[89] Importantly, very similar results were obtained for all other tested conjugates, varying between 10.3 – 15.7% of probe positive cells in case of the competition between probe and the conjugates.

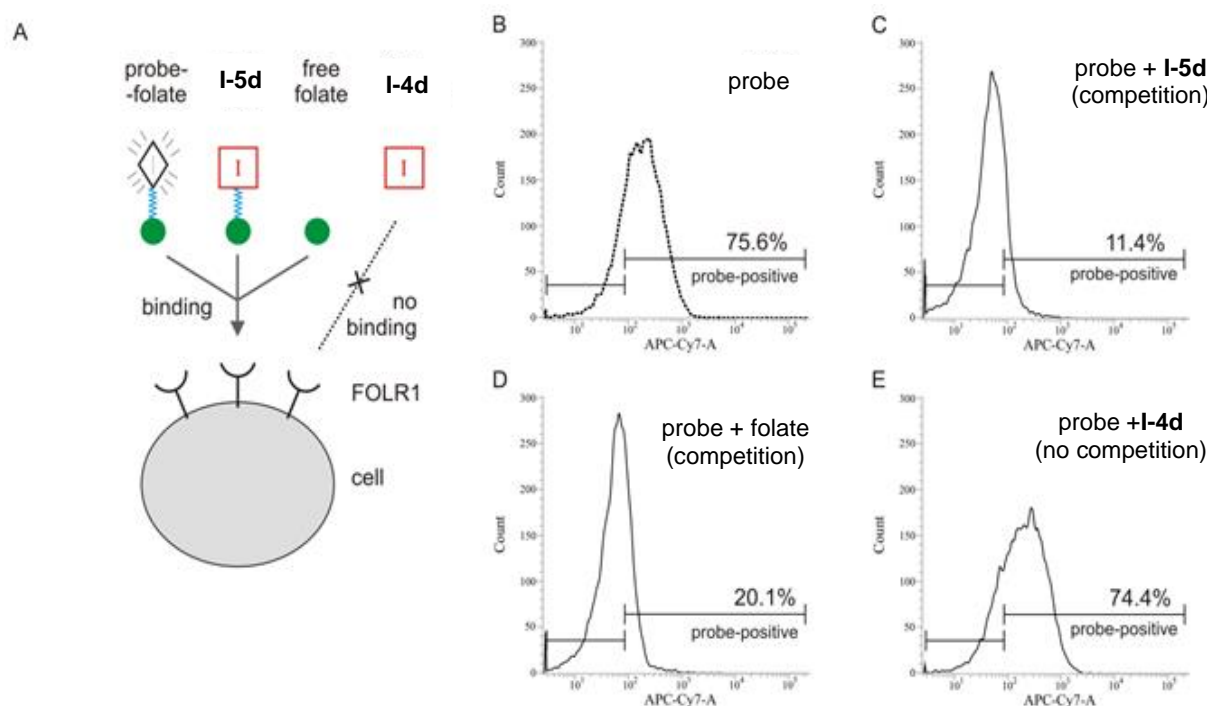


Figure 21. *In vitro* binding to folate receptor.^[89]

Finally, final compound **I-5d** was measured for its kinase inhibitory potency toward recombinant human CDK2/cyclin E according with the IC₅₀ value of 77 nM, which is comparable to the inhibition activities of related purine inhibitors.^[102,136–138] The high potency of **I-5d** could be considered as unexpected; nevertheless, it can be beneficial, since the inhibition of cellular CDKs is not necessarily limited by the speed of release of the free purine inhibitor from conjugate.

2.1.4. Conclusion

We successfully optimized and synthesized the route towards the final compounds, purified them by semipreparative HPLC and obtained in good to excellent overall yields (see Table 3), considering the number of steps leading to such results. Our prepared conjugates were then tested for their kinase inhibitory activity, provided by V. Kryštof group. The most potent conjugate was subjected to the *in vitro* simulation of disulfide reduction, to prove applicability of our system, which was provided and evaluated by me.

Eventhough we had not been able to perform all steps on solid-support, due to the problematic thiol-disulfide exchange, our stepwise hybrid concept still enables the rapid production of the desired compounds with minimum *hands-on-time*. Moreover, we also successfully overcame problem with folic acid solubility and high polarity, which represents potential drawback in the conventional approach, since it will definitely influence pH of the solution during thiol-disulfide exchange. The diversification of individual parts of the target conjugates can be easily accomplished by changing the building blocks in the reaction sequence (Figure 22). Thus, the method represents a general approach for the modification and study of folate conjugates of diverse drug-like heterocycles using parallel or combinatorial solid-phase synthesis.

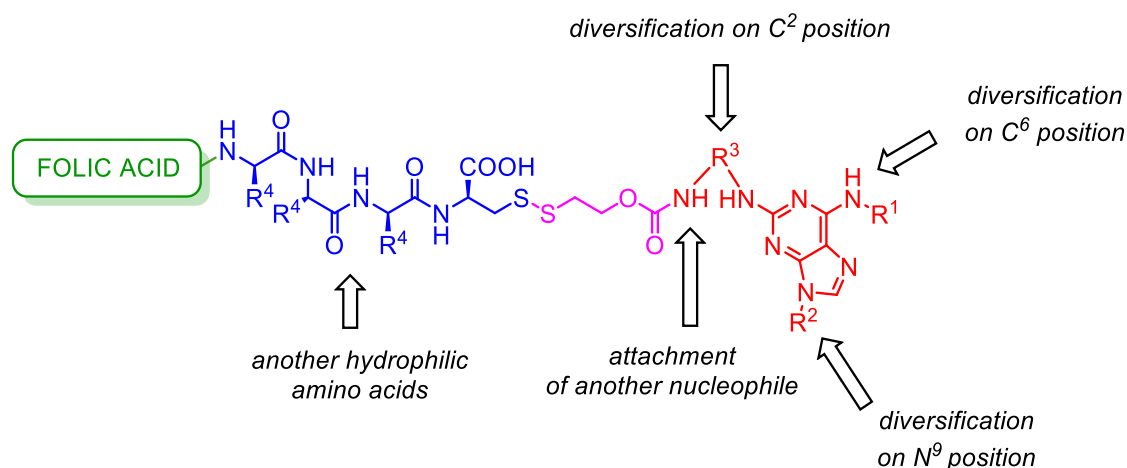


Figure 22. Possible diversification sides of the FA molecules.

Flow cytometric measurements demonstrated the ability of an example conjugate to bind to cancer cells overexpressing the folate receptor. Moreover, *in vitro* simulation of intracellular reducing of disulfide bond with subsequent self-immolative cleavage demonstrated the applicability of our conjugates to release the inhibitor. To conclude, we confirmed binding of CDK inhibitors-FA conjugates to FOLR1-overexpressing cells, suggesting that this concept is a possible route to the development of more selective anticancer drugs. And last, but not least, the proposed so-called *hybrid* approach is not

limited exclusively to purines but can furnish conjugates of any immobilized compound containing reactive nucleophilic moieties.

2.1.5. Authors' contributions

As main author of publication, I developed and optimized the synthetic route towards the final compounds, both in solution and on solid-phase, synthesized all compounds and intermediates, provided their full characterization (NMR, HRMS, UHPLC-MS, IR) and performed *in vitro* simulation of disulfide reduction. I wrote major part of the manuscript, except for the biological evaluation (provided by D.H. and written by V.K.) and purine CDK inhibitors introduction (written by T.G.).

2.2. Proteolysis-targeting chimera (PROTAC) for protein kinases targeted degradation

The results of this project were published in: Krajčovičová, S.; Jorda, R.; Hendrychová, D.; Kryštof, V.; Soural, M. *Chem. Commun.* 2019, 55, 929.^[139]

The manuscript is attached in Appendix B (p. 150 - 153). The Supporting information is available at: <http://www.rsc.org/suppdata/c8/cc/c8cc08716d/c8cc08716d1.pdf> and is attached as an electronic file on CD.

2.2.1. Introduction

The fundamental concept of PROTAC

The control of intracellular processes has long been a target for manipulation by small molecules in the chemical biology. However, not every protein has an enzymatic activity that can be inhibited and is therefore considered as “undruggable”, because many of these potential targets do not have suitable binding pockets that directly modulate protein function. Moreover, high systemic drug exposure may be needed to maintain sufficient target inhibition *in vivo*, which increases potential risk of undesired side effects.^[140,141]

One method of modulating intracellular protein concentrations is through nucleic acid-based agents. Even though these tools have been proven to be useful in research, their development as drug candidates has faced its limits, mostly for their high instability in serum^[142] or accumulation in kidneys,^[140,143,144] which failed to demonstrate a broader therapeutic applicability.^[145]

Targeted protein degradation with use of bifunctional small molecules to remove specific proteins from within cells offers a new strategy with therapeutic interventions, not achievable with existing approaches. Using small molecules emerged a high potential due to their ability to access a wide range of organs and sites of action and modulate multiple targets simultaneously.^[146] Inhibition of certain cellular pathways promotes feedback-mediated increased expression of the target protein, which leads to pharmacological insufficiency. Induced protein degradation not only reduces the number of active proteins that need to be inhibited but also counteracts compensatory protein overexpression.^[140]

PROTAC technology, pioneered recently by Crews et al.,^[147] combines the modularity of nucleic acid-based strategies with the *in vivo* pharmacology of small molecule therapeutics. It is based on event-driven, rather than occupancy-driven pharmacology model, and can potentially exploit binding anywhere on the protein of interest (POI) in order to achieve degradation.^[140]

Bifunctional PROTAC molecules bind noncovalently to the POI with one part whereas simultaneously binds to an E3 ligase to form a ternary complex. The recruited E3 ligase then mediates the transfer of ubiquitin from an E2 enzyme to the POI, the ternary complex dissociates and the ubiquitylated POI is removed by the proteasome and the PROTAC can bind to another POI (Figure 23). A variety of E3 ligases are utilized in this technology. Cereblon (CRBN), von Hippel-Lindau (VHL), MDM2, cIAP or β TRCP act as substrate recognition subunits in multiunit cullin-ring (CRL) E3 ligase complexes.^[148,149]

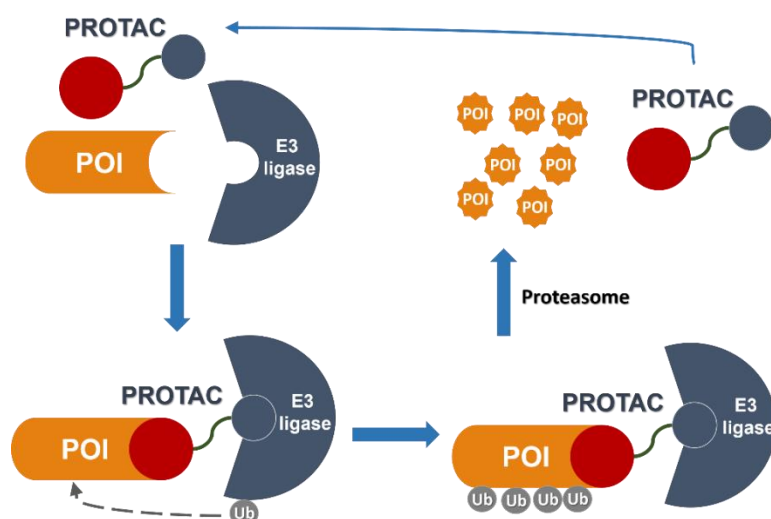


Figure 23. Mechanism of PROTACs. (POI = protein of interest; Ub = ubiquitin)

The ubiquitin-proteasome system is the primary mechanism for removing misfolded proteins from the cytosol and nucleus.^[140] Ubiquitin is a small protein consisting of 76 amino acids and is implicated in many cellular functions. Its attachment to lysine side chains is a common post-translational modification and can control cellular localization.^[141] Since ubiquitin possesses seven lysines, the chains linked through Lys448 have been associated with proteasomal degradation,^[150,151] whereas others (Lys63, Lys11) have been associated with subcellular localization, endocytosis and transcriptional regulation.^[152,153]

The ubiquitin degradation cascade begins with an E1 ubiquitin-activating enzyme which creates a thioester on ubiquitin in an ATP dependent manner, whereas E3 specifically binds to the target protein and catalyzes the proximity-induced transfer of the activated ubiquitin to the target protein.^[140] Thus, ubiquitination results in the degradation of the protein via the proteasome.^[141] This approach has proven to be therapeutically useful as cancer cells are often more reliant than healthy cells on the proteasome to clear misfolded proteins.^[141,154]

PROTAC molecules

One of the first published PROTACs (Figure 24) was based on peptide motifs and hence composed of a phosphopeptide portion of NF- κ B inhibitor- α to recruit β TRCP and the angiogenesis inhibitor ovalicin to covalently bind to the target protein MetAP2. The potential of the proposed system was further tested in a cellular environment. Although it was shown the degradation of the androgen receptor (AR) in living mammalian cells by injecting of β TRCP-based PROTAC into HEK293 cells, the potency of these PROTACs were in the micromolar range and cellular permeability was rather low.^[155]

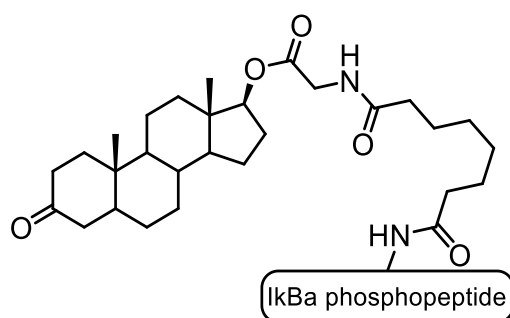


Figure 24. First published PROTAC.^[155]

The first improvement was a switch to a smaller E3 ligase recruiting peptide fragment, namely hydroxylated proline, which was recognized by the E3 ligase VHL.^[156,157] An AR-targeting PROTAC was developed using DHT conjugated to the HIF1 α peptide fragment with a poly-D-arginine tag, derived from an arginine-containing peptide fragment based on the HIV Tat peptide that facilitates cellular uptake of proteins suitable for cell penetration.^[158] Analogous PROTACs using estradiol demonstrated ER degradation, which led to reduced proliferation of ER-dependent breast cancer cell lines.^[159–161] Unfortunately, the potencies of these peptide PROTACs remained in micromolar range, presumably due to the poor cell penetration associated with peptide-based therapeutics and thus finding an alternative approach, bearing small-molecule PROTACs was desired.^[140]

Further efforts were put to identification of an appropriate small-molecule replacement for the HIF1 α peptide fragment to provide an alternative E3 ligase for all-small-molecule PROTACs.^[140] It was successfully accomplished with the discovery of small molecule ligands for E3 ubiquitin ligases (Figure 25), in which nonpeptidic ligand creates more druglike small-molecule degraders that possess physicochemical properties improving their therapeutic potential.^[145]

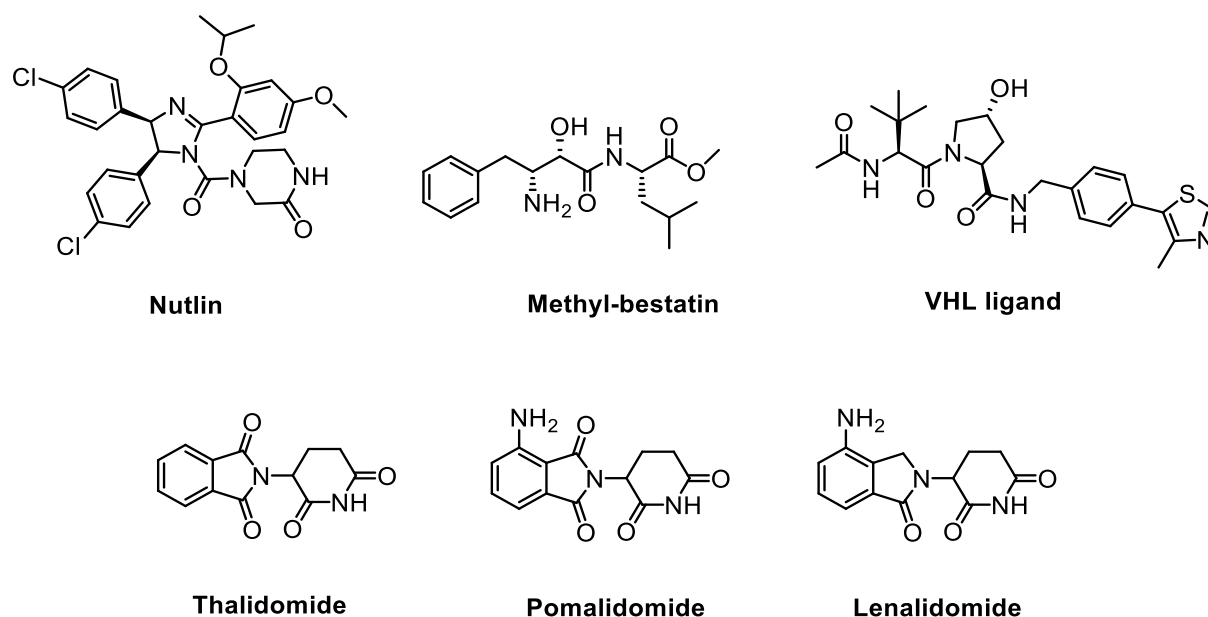


Figure 25. Small molecule ligands for E3 ubiquitin ligases.

Development of nutlin as an inhibitor of the p-53 Mouse Double Minute 2 (MDM2) E3 ubiquitin ligase yielded the first all-small molecule PROTAC (Figure 26).^[162,163] It was designed to degrade AR and consisted of a nonsteroidal AR ligand fused via a PEG linker to nutlin and the potency of this conjugate was demonstrated in HeLa cells at low micromolar concentrations, however, very similar that of peptide PROTACs.^[163]

Utilizing the first VHL-based small-molecule PROTAC (Figure 26) was described with nanomolar potency for nearly complete degradation of oestrogen-related receptor- α (ERR α) and receptor-interacting serine/threonine protein kinase 2 (RIPK2). *In vivo* degradation of ERR α -targeted PROTAC was achieved with 40% knockdown of the protein in heart, kidney and tumor xenografts.^[140,164]

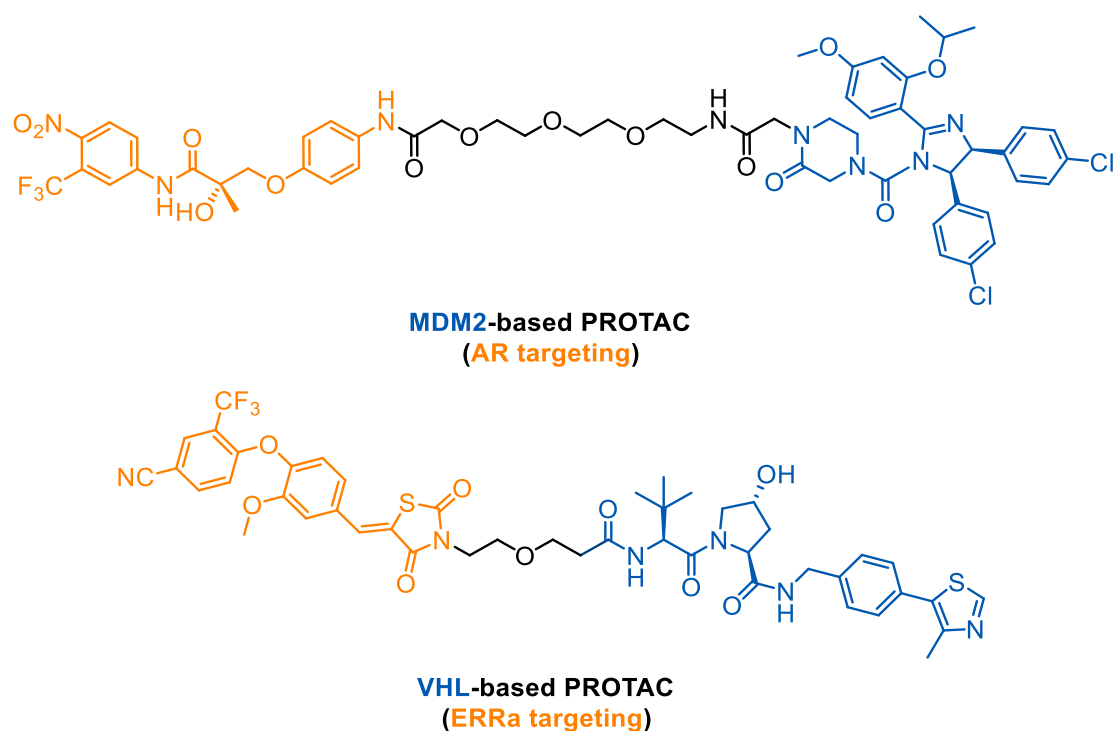


Figure 26. Small molecule PROTACs.^[163,164]

Lately, the E3 ligase cereblon (CRBN) was identified as a primary target for thalidomide, followed by a discovery of phthalimides-induced degradation of the lymphoid transcription factors IKZF1 and IKZF3 by binding to CRBN, thus able the E3 ligase to ubiquitylate them.^[165,166] However, further study revealed that not all of the phthalimides have the same substrate degradation spectrum and therefore are utilized in different clinical situations – lenalidomide induced the degradation of CKI α , whereas thalidomide and pomalidomide did not.^[167–169]

Conjugation of a small-molecule OTX015 to pomalidomide led to a PROTAC conjugate ARV-825 (Figure 27) capable of degrading the epigenetic regulator BRD4 at picomolar concentrations,^[170] suggested a superstoichiometric degradation of BRD4 due to the catalytic activity of this PROTAC.^[164] Compare to other BRD4 inhibitors (JQ1 or OTX015), the PROTAC conjugate provided a more sustained suppression of MYC levels.^[171] Further study, in which was JQ1 conjugated to thalidomide resulted to PROTAC dBET1 (Figure 27), induced BRD4 degradation at low nanomolar concentrations.^[172] BRD4 was also successfully targeted for degradation using PROTAC that hijack VHL. The PROTAC conjugate MZ1 (Figure 27), based on JQ1 inhibitor, with complete degradation of BRD4 after 3 h and sustained knockdown out to 24 h, appeared to be more stable than thalidomide-based dBET1.^[173]

Finally, the PROTAC generation capable of degradation oncogenic fusion protein BCR-ABL was reported and employed tyrosine kinase inhibitors (imatinib, bosutinib and dasatinib) to couple with either VHL or pomalidomide ligand.^[174] However, no

degradation by imatinib-based PROTACs was detected, despite observed kinase inhibition effects.

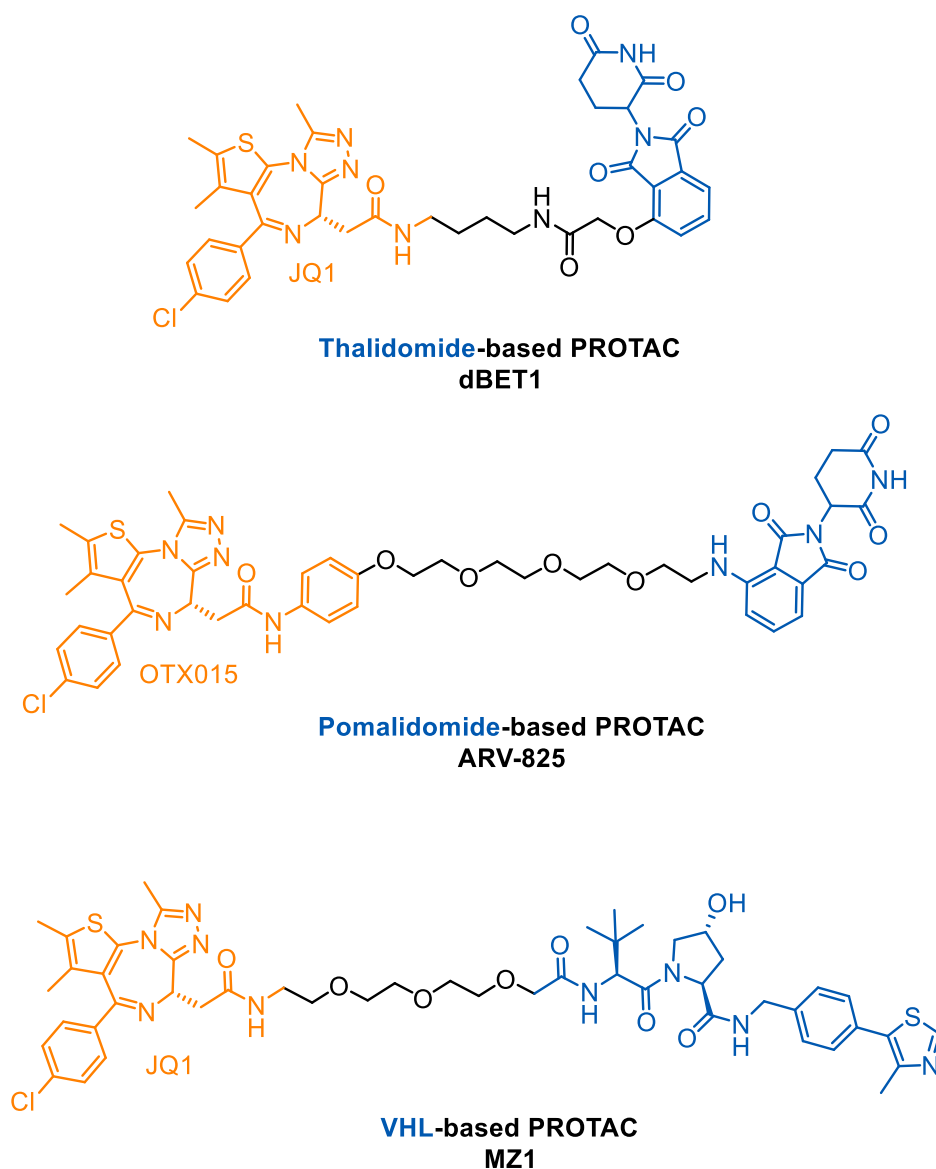


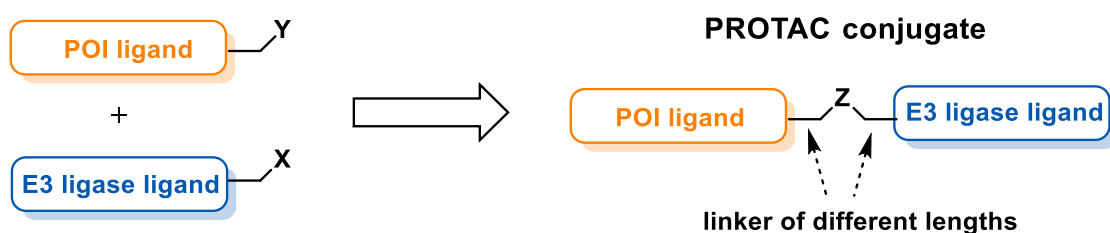
Figure 27. BRD4 targeted PROTAC conjugates.

A systematic survey towards the most suitable linker length was also studied.^[175] According to a study focusing on TANK-binding kinase 1 (TBK1), the flexible alkyl ether chemistry was applied between inhibitor of TBK1 and hydroxyproline derivative capable of binding VHL. The measured degradation potency (DC_{50}) suggested that PROTACs with 12 – 29 atoms linker lengths were identified to degrade TBK1 with submicromolar potency, despite the higher polar surface area and presumed lower cell penetrance.^[175] These observations were consistent with the idea of PROTAC, where is required to allow proteins to come together without incurring steric conflicts.^[175]

Synthetic strategies to obtain PROTAC conjugates

The synthetic strategies towards new PROTAC conjugates exclusively involved synthesis in solution, until our published work, dealing with the synthesis on polystyrene resin.

The most common approach by far, is either acylation of activated carboxylic acid or nucleophilic substitution of halogen alkane of one, pre-modified part of the conjugate with primary amine-containing part.^[170,172,176–178] Other possible approach is simple click reaction between azide-containing part with alkyne-containing part of the conjugate^[179] (Scheme 22).

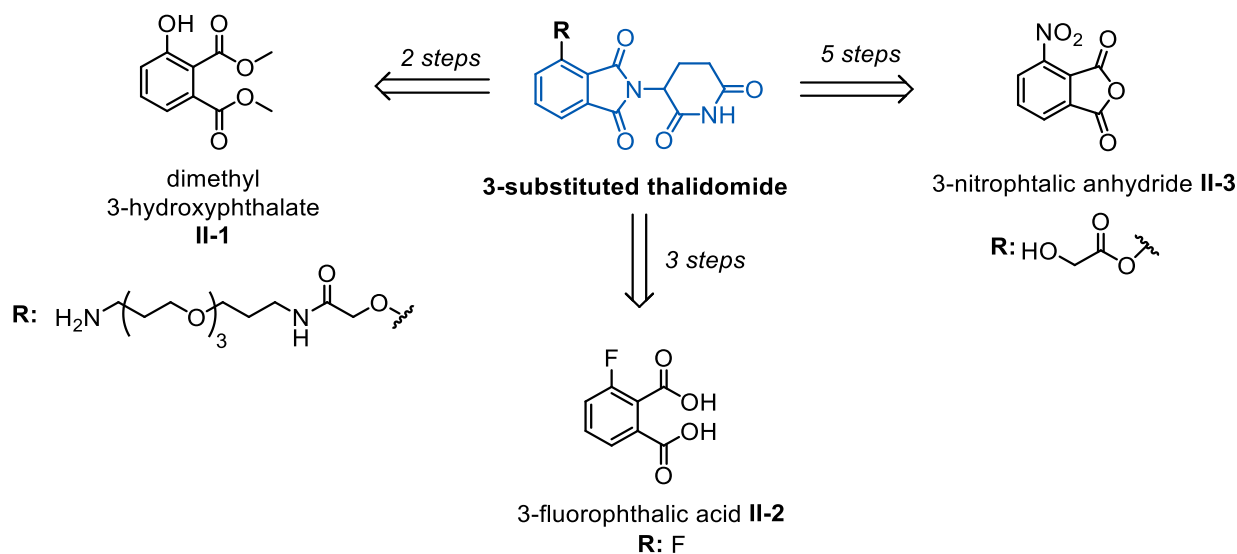


Y, X: COOH, halogene, alkyne, N₃, NH₂

Z: amide, ester, triazole, secondary/tertiary amine, ether

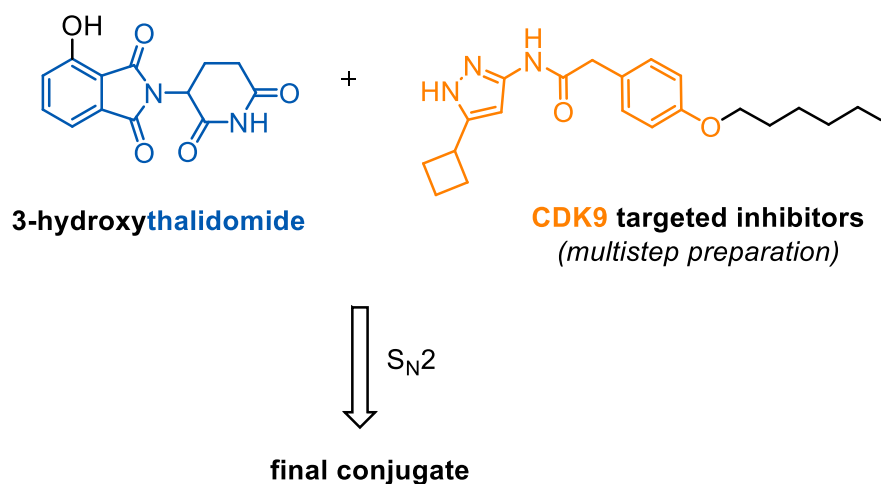
Scheme 22. General synthetic approach towards PROTAC derivatives. (POI = protein of interest)

The preparation of thalidomide precursors **II-1-3** is demonstrated on Scheme 23 from the 3-substituted starting materials which were in 2-5 steps converted to desired compounds.^[170,172,176] Variable synthesis of linker lengths was subsequently demonstrated with pre-modified intermediates suitable for further coupling with the POI ligand, containing reactive functional group, e.g. carboxylic acid, halogen alkane or aldehyde.^[176–178] Nevertheless, the main disadvantage of these pathways relies in unavoidable purification after each synthetic transformation which requires assistance of skilled synthetic chemist.



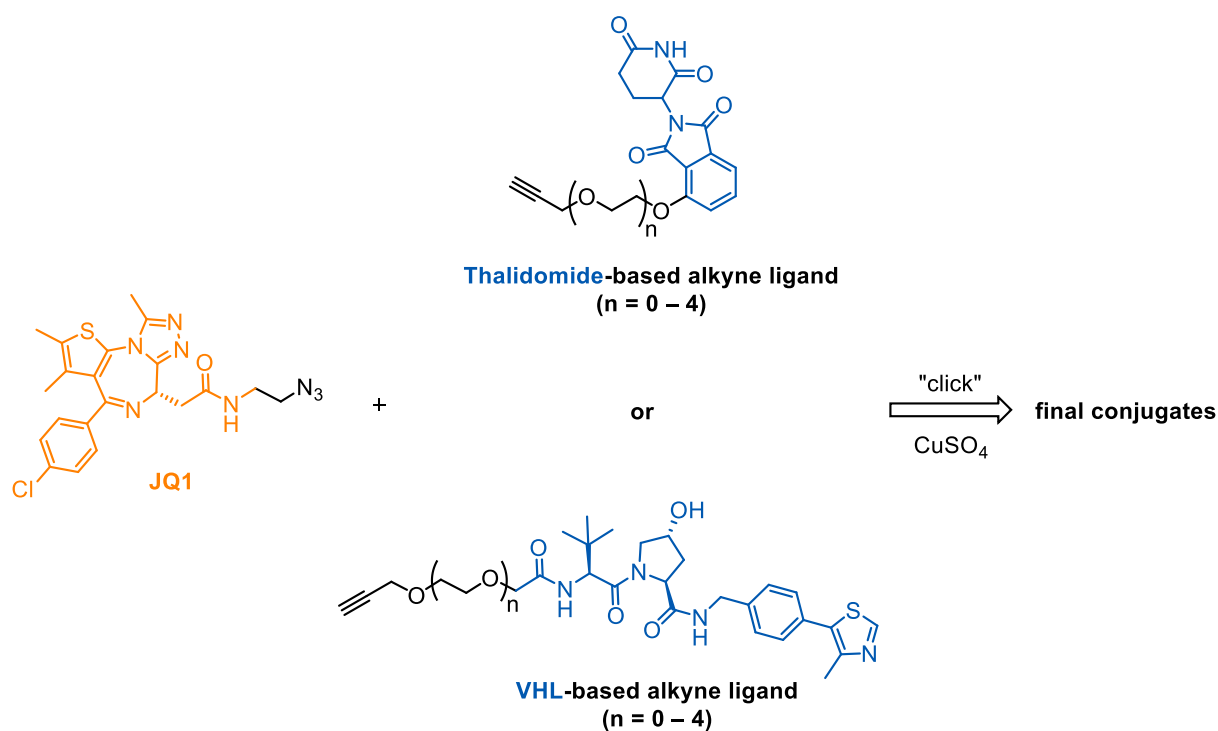
Scheme 23.

Robb *et al.* demonstrated their synthetic approach in synthesis of selective CDK9 targeted PROTAC conjugates, where the pre-modified part of the POI ligand contained electrophilic alkyl iodide (Scheme 24).^[177] Subsequent nucleophilic substitution with 3-hydroxythalidomide yielded final conjugates. The disadvantage of this approach relies in individual synthesis of the other POI ligands with defined linker lengths, which does not allow easy modification of their size.



Scheme 24.

The “click” chemistry approach was demonstrated with preparation of PROTAC with alkyne-containing thalidomide and VHL-targeted ligands, respectively, and azide modification of the POI ligand, specifically JQ-1 (Scheme 25).^[179] Five representative conjugates for each E3 ligase ligand were prepared with modified linker lengths, however, it can be quite tricky to get rid of copper salts from final compounds and tedious purification is required.



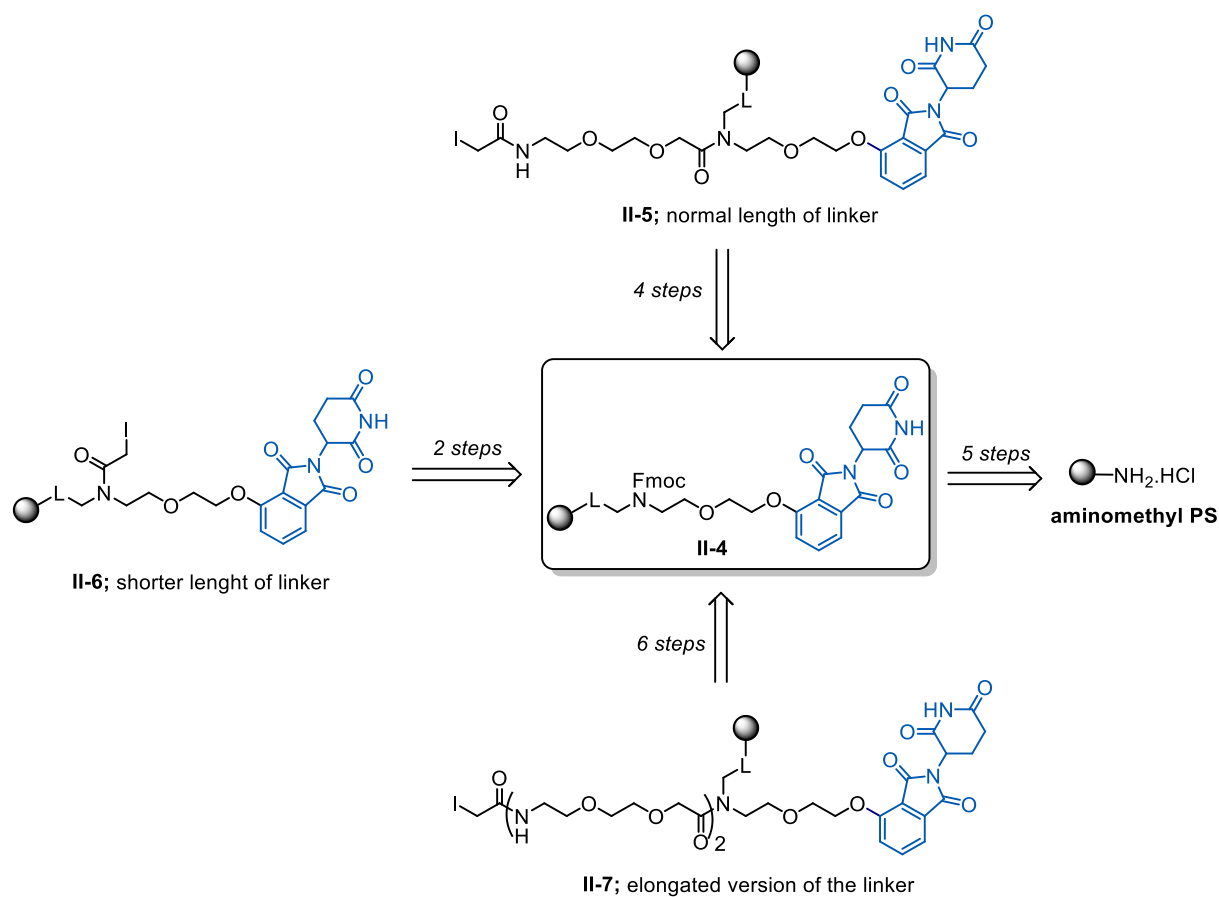
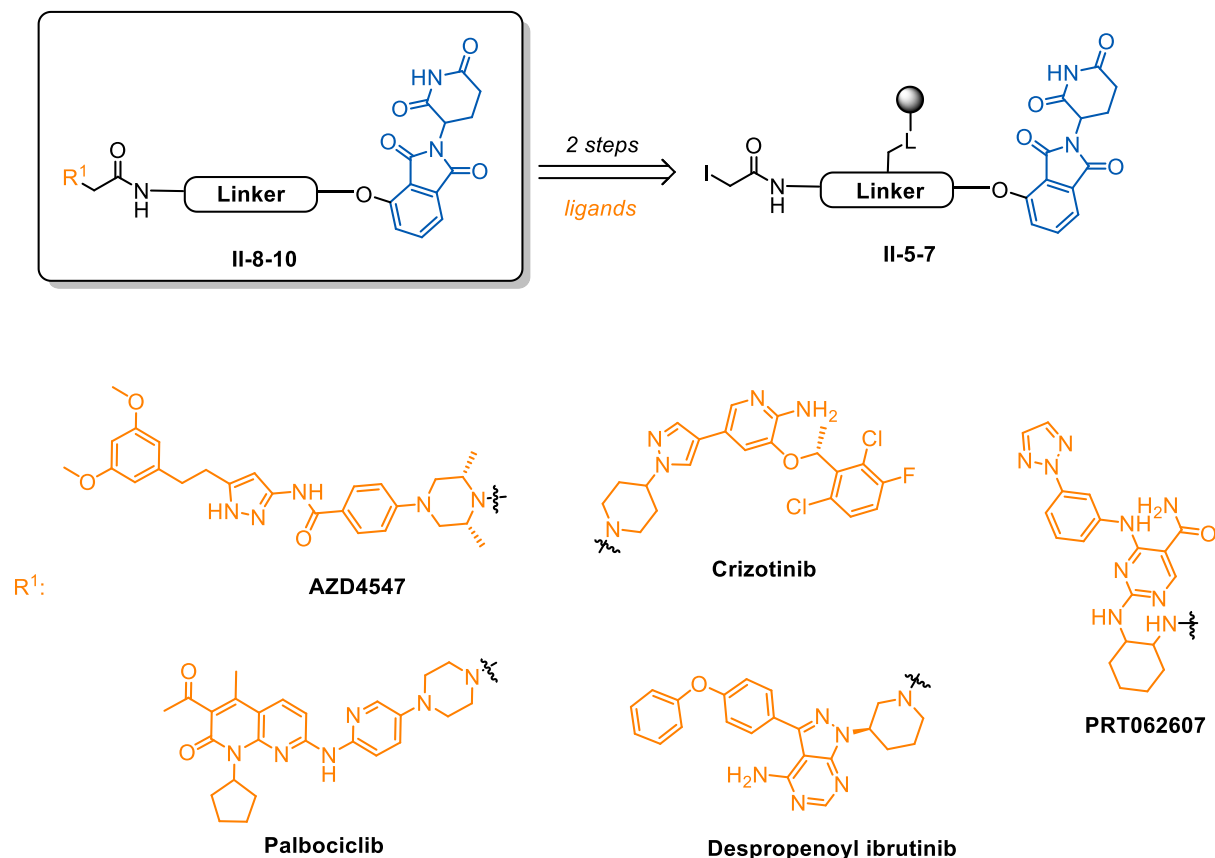
Scheme 25.

From all of the abovementioned examples it is obvious that although it is possible to prepare PROTAC conjugates in acceptable yields and purities, the concept of easy approachable and rapid synthesis of other potentially useful derivatives is still missing. In this regard, use of solid-phase synthesis should be highly advantageous, due to the possibility of application of high-throughput synthesis with simple laboratory equipment and no need of purification within the reaction sequence.

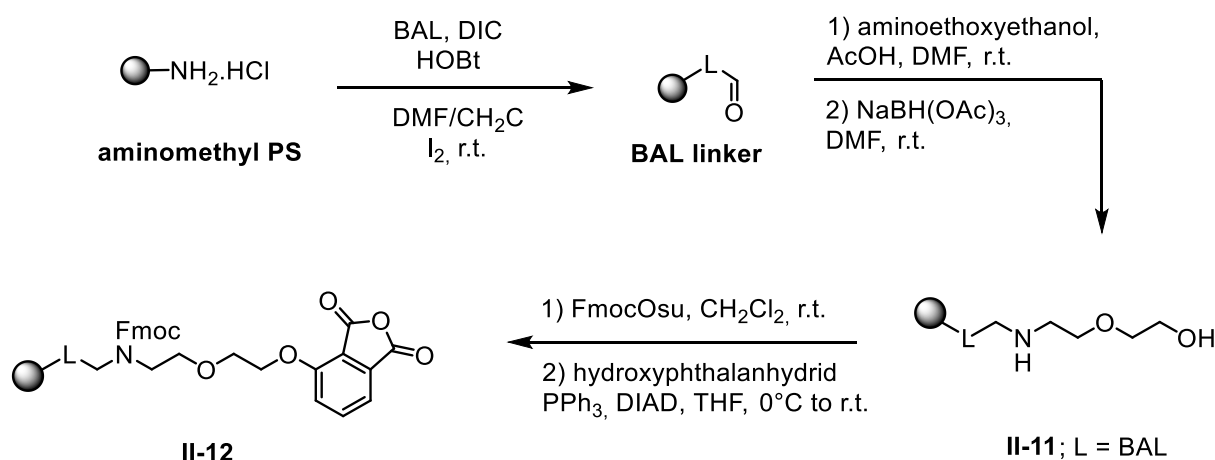
2.2.2. Synthesis

The synthetic approach towards final conjugates is described in our published paper,^[139] however, I consider appropriate to briefly summarize the optimization steps.

In general, the preparation of our thalidomide preloaded resins (TPRs) started from the commercially available aminomethyl polystyrene resin, which was in 5 steps converted to the key intermediate **II-4**. Following elongation of the spacer yielded three different TPRs **II-5-7** (Scheme **26**), which were subjected to the reaction with selected protein kinases inhibitors (palbociclib, crizotinib, AZD4547, despropenoylibrutinib and PRT062607) to afford final compounds **II-8-10** (Scheme **27**). These kinase inhibitors, which potently target CDK4, ALK, FGFR, BTK and SYK kinases, respectively, were selected due to presence of reactive amine functions oriented outside the kinases' active sites, hence available for conjugation without loss of inhibitory activity.

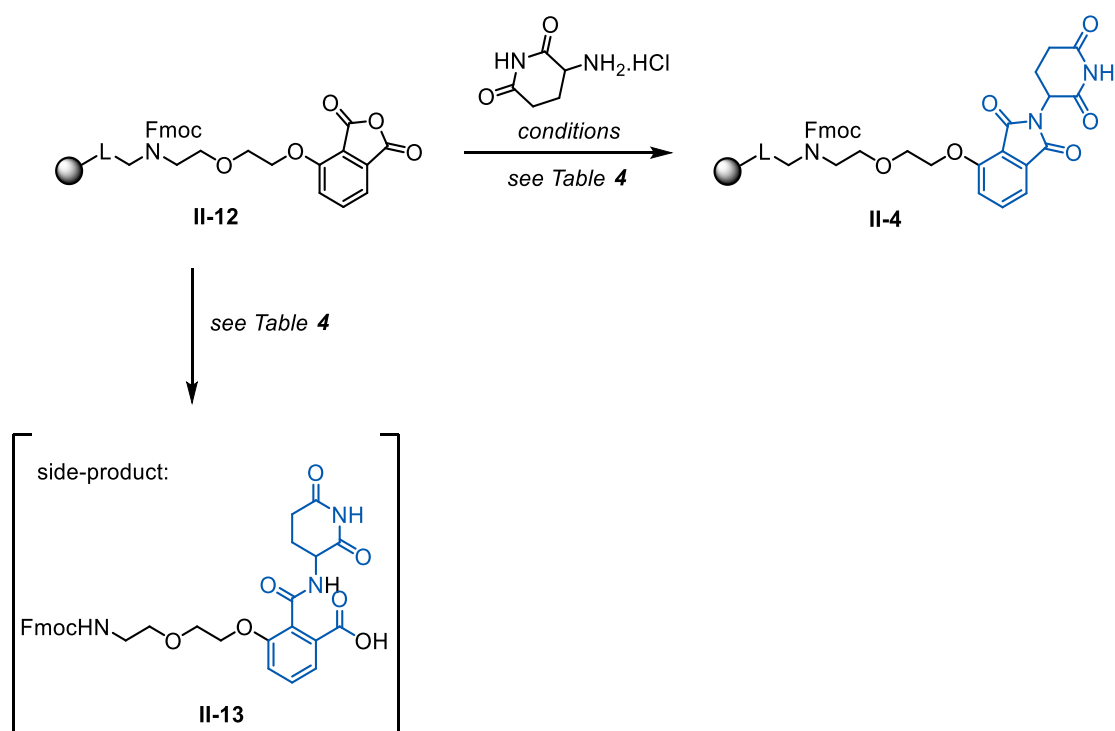
Scheme 26. General retrosynthetic analysis for TPRs II-5-7.^[139]Scheme 27. Retrosynthetic scheme towards final compounds.^[139]

The synthesis started with reductive amination of BAL resin with aminoethoxyethanol, followed by chemoselective protection with FmocOsu and Mitsunobu alkylation to obtain intermediate **II-12** (Scheme 28).



Scheme 28.

Following ring closure reaction to form thalidomide moiety seemed to be solvent and base dependent reaction that required careful optimization. Table 4 summarizes tested reaction conditions for the thalidomide scaffold formation. According to UV-LCMS analysis, the crude purity was lowered significantly with use of THF and DBU (cond. f and g) and we observed side-products related to phthalimide ring opening and phthalamide derivative **II-13** formation (cond. a – h, l, m; structure of **II-13** was proposed from MS traces). Additionally, the reaction conditions led to cleavage of intermediate from the resin and resulted in a dramatic drop of the loading after the reaction (cond. a – m, o), which was highly undesirable. The best results were obtained with use of dry toluene and DCE as solvents and TEA as a base, however, only with use of basically catalytic amount of a base and an amine (cond. n) was the loading of resin **II-4** approximately the same as for **II-12**. Notably, Fmoc protecting group was cleaved in presence of base at elevated temperature and reaction with FmocOsu prior to analysis was necessary (to make the compound **II-4** cleavable from the resin). We also tested the direct Mitsunobu reaction of N-Fmoc protected intermediate **II-11** with 3-hydroxy thalidomide, unfortunately, we observed only mixture of products, very likely due to the presence of another acidic proton.



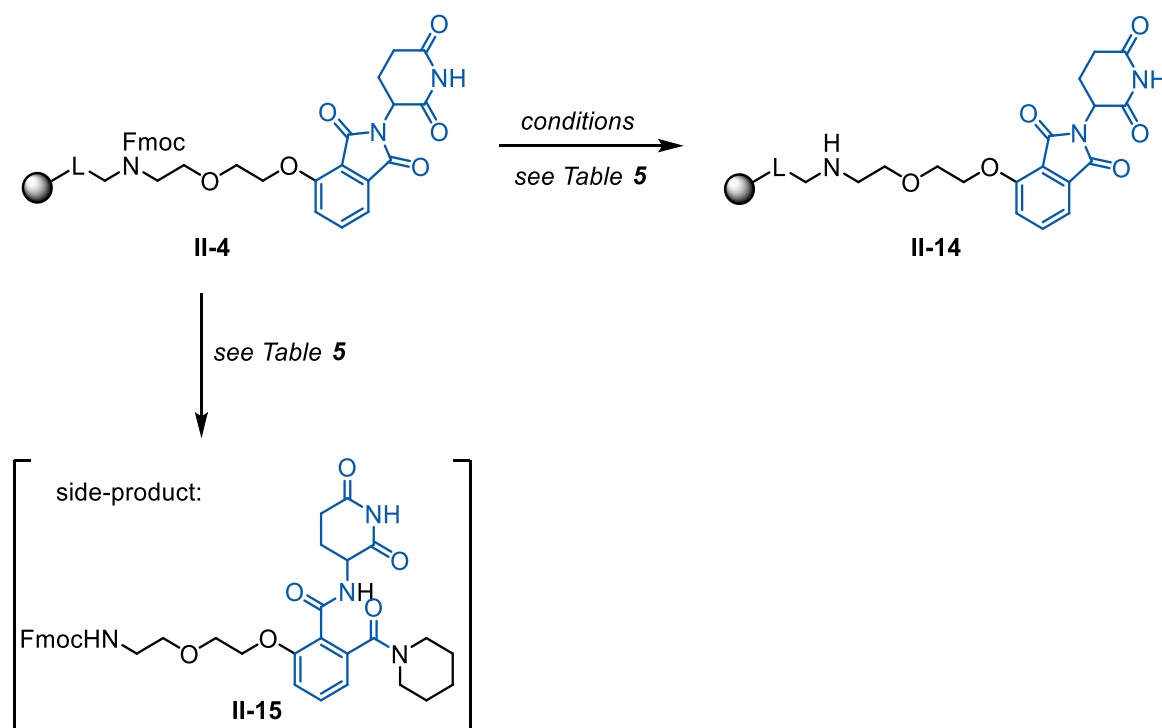
Scheme 29.

| # | Base | Conc. [M] | Amine conc.[M] | Solvent | Temp. | Reaction time | Observation |
|----|-------|-----------|----------------|---------------|--------|---------------|----------------------------------|
| a. | DIPEA | 0.8 | 0.2 | THF | reflux | 2 h | II-13 |
| b. | DIPEA | 0.8 | 0.2 | THF | reflux | 4 h | II-13 |
| c. | DIPEA | 0.8 | 0.2 | (dry) THF | reflux | 2 h | II-13 |
| d. | DIPEA | 0.8 | 0.2 | (dry) THF | reflux | 4 h | II-13 |
| e. | DIPEA | 2 | 0.4 | THF | reflux | 4 h | II-13 |
| f. | DBU | 0.8 | 0.2 | THF | reflux | 2 h | II-13 |
| g. | DBU | 2 | 0.4 | THF | reflux | 4 h | II-13 |
| h. | DIPEA | 0.4 | 0.2 | (dry) THF | reflux | 14 h | II-13 |
| i. | DIPEA | 0.4 | 0.2 | (dry) toluene | reflux | 14 h | <i>Low loading</i> |
| j. | DIPEA | 0.4 | 0.2 | (dry) DCE | reflux | 14 h | II-4 ; <i>Low loading</i> |
| k. | TEA | 0.4 | 0.2 | (dry) toluene | reflux | 14 h | <i>Low loading</i> |
| l. | TEA | 0.4 | 0.2 | (dry) THF | reflux | 14 h | II-13 |
| m. | TEA | 0.2 | 0.2 | (dry) THF | reflux | 14 h | II-13 |
| n. | TEA | 0.036 | 0.036 | (dry) toluene | reflux | 14 h | II-4 |

| | | | | | | | |
|-----------|---|---|-----|-----------|------|------|--------------------|
| o. | - | - | 0.2 | (dry) DMF | r.t. | 14 h | <i>Low loading</i> |
|-----------|---|---|-----|-----------|------|------|--------------------|

Table 4. Optimization conditions for thalidomide ring formation. (Amine = 3-aminopiperidine-2,6-dione hydrochloride).

The following deprotection of Fmoc under standard cleavage conditions (DMF/piperidine 4:1) led to partial-thalidomide-ring-opening and formation of side-product **II-15** (Scheme 30), due to the nucleophilic character of piperidine. The retention time (reverse-phase HPLC) of both compounds (**II-4** and **II-15**) overlapped, thus, finding suitable conditions for deprotection was required to allow the purification of final compounds. We observed either no conversion with use of inorganic base (Table 5, cond. a) or just partial conversion (cond. c) in case of weaker non-nucleophilic organic base. Luckily, the use of stronger non-nucleophilic base (DBU; cond b) had positive impact on reactivity, since we have been able to obtain pure product **II-14** in 10 minutes with no indication of side-product **II-15**. These conditions for deprotection were then used during the whole synthetic sequence.

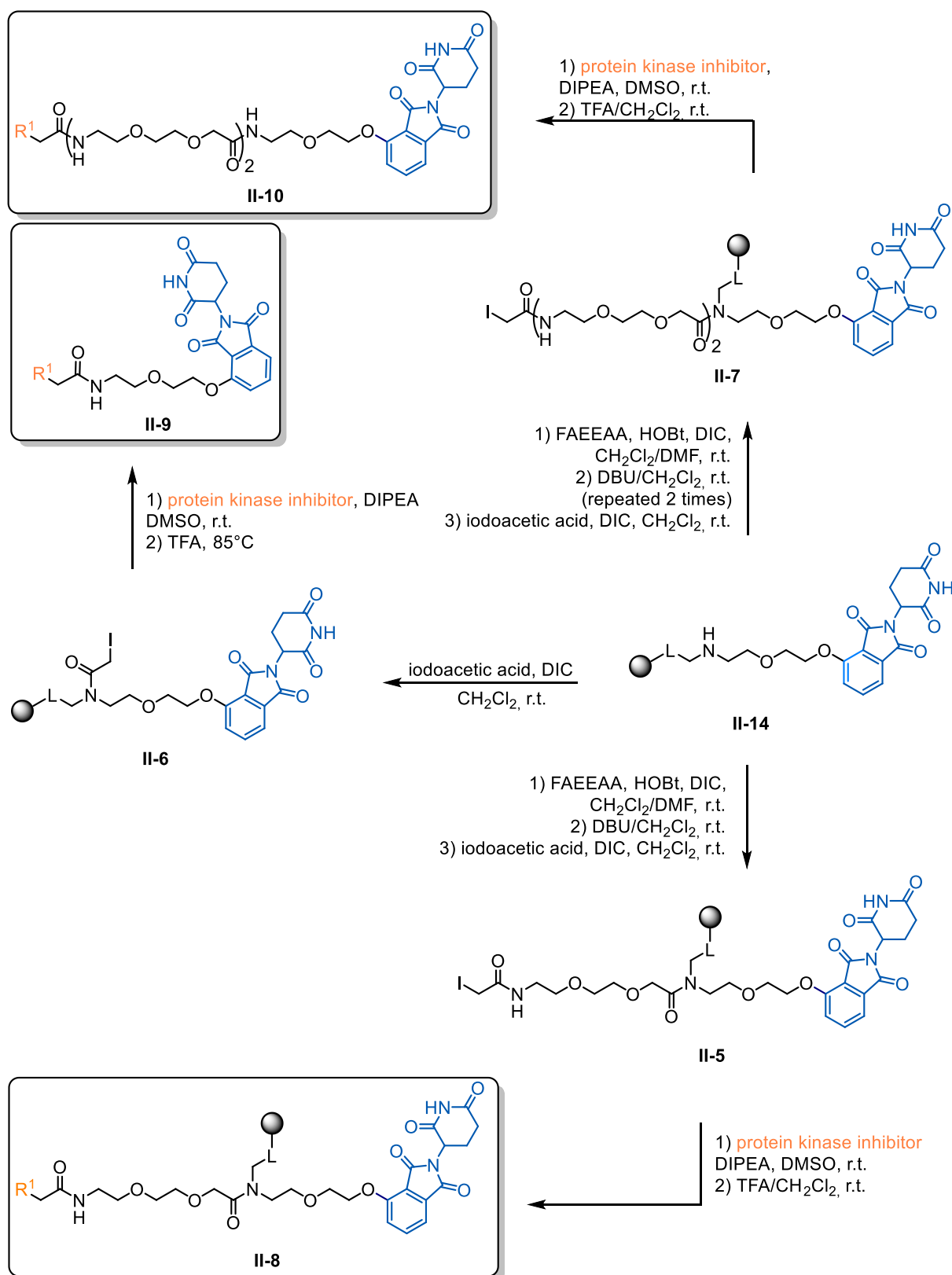


Scheme 30.

| # | Base | Conc. [M] | Solvent | Temp. | Reaction time | Observation |
|----|---------------------------------|-----------|---------------------------------|-------|---------------|--------------------------------|
| a. | Cs ₂ CO ₃ | 0.3 | DMF | r.t. | 20 min | II-4 only |
| b. | DBU | 3.4 | CH ₂ Cl ₂ | r.t. | 10 min | II-14 ; full conversion |
| c. | TEA | 1.4 | THF | 50 °C | 1 h | Partial conversion |

Table 5. Selective Fmoc deprotection.

Following steps, involving acylation with FAEEAA and iodoacetic acid to afford thalidomide-preloaded resins (TPRs) **II-5-7**, proceeded smoothly in excellent crude purities (above 90%). The iodoacetic functionality was installed on TPRs for reaction with primary/secondary amines of abovementioned kinase inhibitors, but the resin **II-14** (or its elongated version, after deprotection of Fmoc) could be used directly to couple various molecules bearing suitable reactive functional groups capable of reaction with amines, such as aldehyde, carboxylic acid or aryl/alkyl/arylhalogens, which make the strategy broadly applicable (Scheme **31**). Table **6** summarized final derivatives with specification of inhibitors for each PROTAC conjugate **II-8-10**, again in exceptionally great crude purities in high overall yields. The applicability of the method to produce preloaded resins with variable linker lengths was demonstrated by extremely simple preparation of compounds **II-9** and **II-10**, respectively, as was suggested. Notably, the cleavage from the resin was provided at room temperature in the standard cleavage cocktail (TFA/CH₂Cl₂ 1:1), except for compound **II-9** which demanded boiling trifluoroacetic acid to quantitative release. The lower overall yield of **II-8e** was probably caused by the steric hindrance of two methyl groups next to the amine moiety.

Scheme 31. Synthetic approach towards final conjugates **II-8-10**.

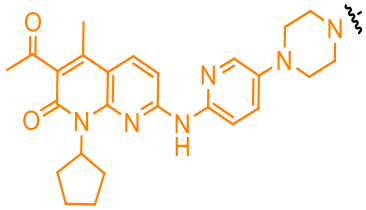
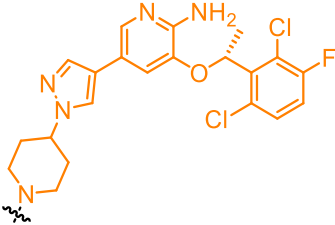
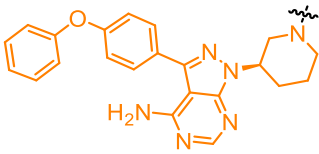
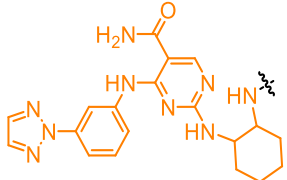
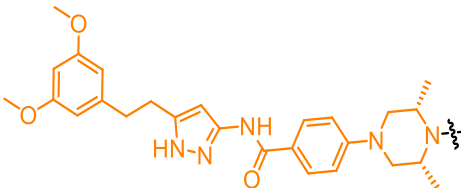
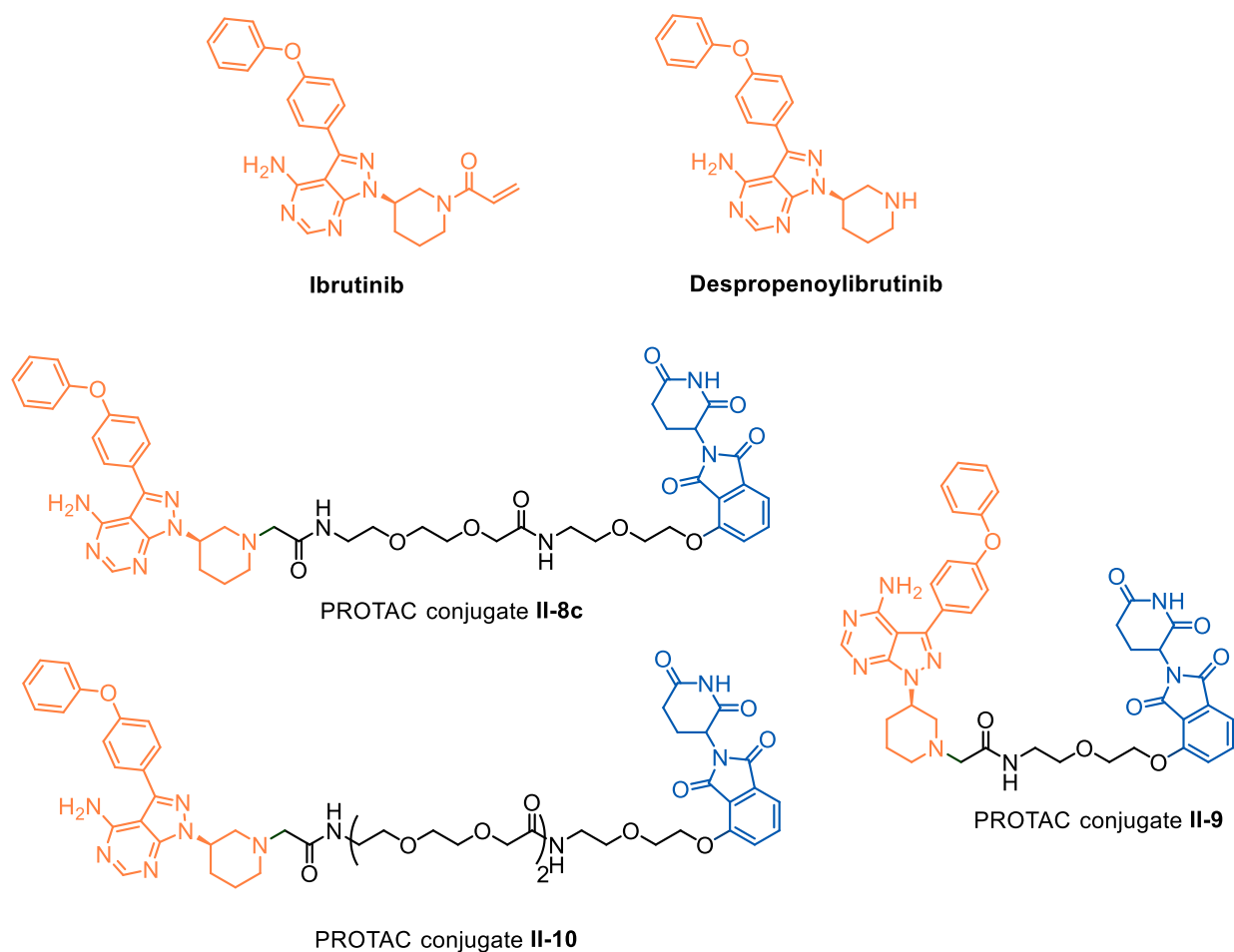
| Cmpd | R ¹ (Protein kinase inhibitor) | Commercial name | Targeted protein kinase | Yield [%] |
|--------------------------|---|------------------------|-------------------------|---------------|
| II-8a |  | Palbociclib | CDK4 | 50 |
| II-8b |  | Crizotinib | ALK | 85 |
| II-8c; II-9; II-10 |  | Despropenoyl ibrutinib | BTK | 83; 76; 70 |
| II-8d |  | PRT062607 | SYK | 49 |
| II-8e |  | AZD4547 | FGFR | 24 |

Table 6. Summarization of our prepared PROTAC conjugates.

2.2.3. Biology

The representative conjugates **II-8c**, **II-9** and **II-10** were then selected to verify the functionality of prepared PROTACs. They possessed despropenoyl ibrutinib, a derivative of a recently FDA-approved drug specifically inhibiting BTK kinase.^[180] In our initial characterization experiments, we compared the potencies of ibrutinib and despropenoyl ibrutinib (Figure 28) with that of PROTAC **II-8c** in a biochemical kinase assay. These experiments were provided by V. Kryštof group.

It was found out that our conjugate **II-8c** inhibited purified recombinant BTK with IC₅₀ like that of parental despropenoyl ibrutinib, which confirmed its biological functionality. Two other PROTACs **II-9** and **II-10** with shorter and longer linkers, respectively, were similarly potent on the kinase (Table 7).

**Figure 28.**

| Compound | BTK IC ₅₀ [μ M] |
|-----------------------|---------------------------------|
| Ibrutinib | <0.001 |
| Despropenoylibrutinib | 0.065 \pm 0.012 |
| PROTAC II-8c | 0.159 \pm 0.037 |
| PROTAC II-9 | 0.106 \pm 0.014 |
| PROTAC II-10 | 0.109 \pm 0.004 |

Table 7. BTK kinase inhibitory activity.

The induced BTK degradation in cells was also demonstrated. In the preliminary experiments with **II-8c**, we observed that the decrease in BTK is time-dependent with a considerable effect between 10 – 24 h, which is in agreement with recently published data.^[181] Ramos cells were treated with various doses of **II-8c** for 16 h and activated BTK by adding immunoglobulin M to culture media. Western blot analysis of lysed cells revealed that BTK degradation was dose-dependent, with a maximal knockdown achieved at a 2 mM concentration (Figure **29.A**). Moreover, in control experiments

neither ibrutinib nor despropenoylibrutinib were able to induce the degradation of BTK and only inhibited BTK activity, which agreed with general mechanism of action of PROTAC conjugates where E3 ligase recruited moiety is necessary for degradation of the protein of interest. SYK and SRC kinases were used in parallel to confirm the specificity of protein degradation induced by **II-8c**.

The effect of linker length on the resulting conjugate applicability is demonstrated on Figure 29.B which contains results of shorter and longer version **II-9** and **II-10**, respectively. The degradation activity strongly depended on linker length, with the best results achieved for original version of the linker (PROTAC **II-8c**). Conjugate with the extended version of linker (PROTAC **II-10**) also degraded the BTK, however, with lower potency than **II-8c**. Conjugate with the shorter version (PROTAC **II-9**) degraded the BTK on higher concentration than 2 mM. This indicates that linker with less than 12 linear atom sequence between the POI ligand (despropenoylibrutinib) and the E3 ligase ligand (thalidomide) is not capable to degrade the BTK efficiently, which acknowledged previous studies implied by Crews.^[175] Overall, the distance between POI ligand and E3 ligase ligand clearly has dramatic influence on the resulting degradation activity.

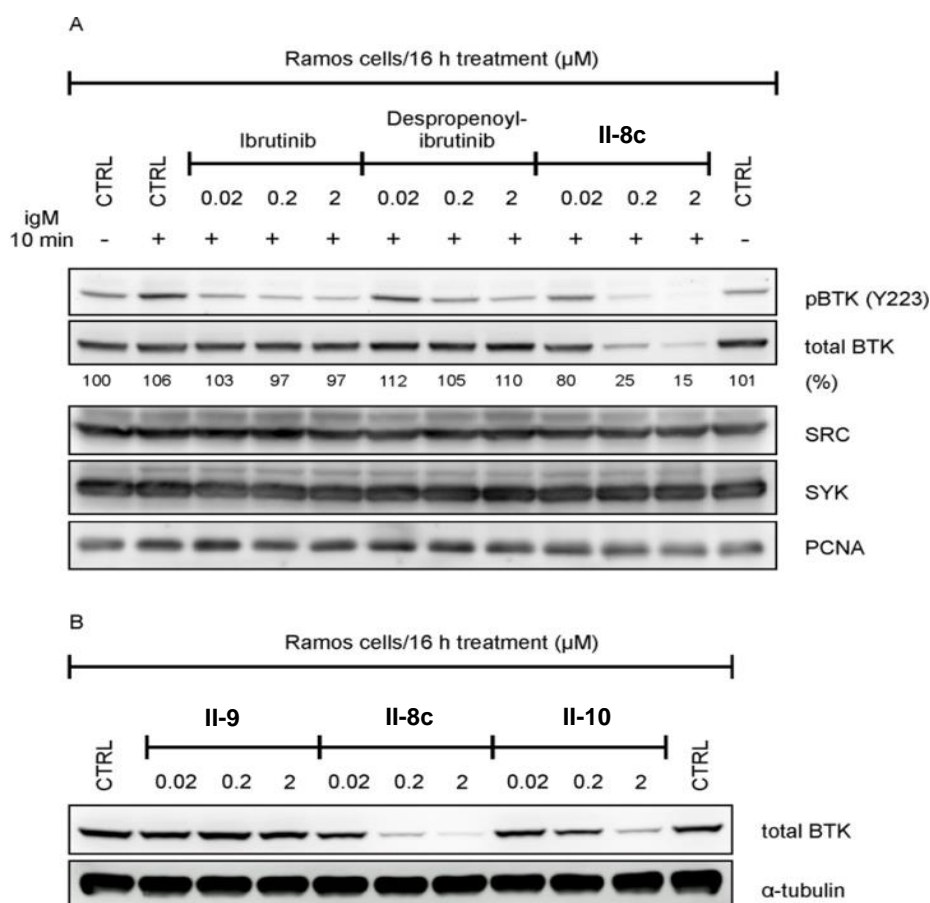


Figure 29. BTK degradation results of prepared conjugates **II-8c,9,10**.^[139]

2.2.4. Conclusion

We successfully optimized and synthesized *en route* towards thalidomide-preloaded resins **II-5-7**, which were subsequently conjugated with 6 protein kinases inhibitors with selective kinase targeting. The final compounds were purified by semipreparative HPLC and obtained in good yields. The kinase inhibitory activity and degradation study was provided on representative conjugates **II-8c,9,10** (provided by V. Kryštof group).

The developed TPRs can be used to easily and rapidly synthesize desired conjugates in excellent crude purities and to modify their individual parts for preliminary screening experiments focused on molecule optimization. With respect to obtained biological data, one of the most important features of the method is undoubtedly simple enlargement of the spacer and comfortable production of the corresponding TPRs that differ exactly in this parameter. The general simplicity of TPRs utilization consists in *shake-wash-cleave* procedure that can be performed by a person without synthetic experience or special laboratory equipment. In the best case, TPR could be used as a simple kit for routine preparation of PROTACs. Importantly, the synthetic approach is versatile and can also be applied to other proteins for which ligands suitable for conjugation are available (with reactive functional groups, such as carboxylic acid, aldehyde, primary/secondary amine etc.). Compared to the solution-phase methods described in Chapter 2.2.1., only single final purification is required, and modularity of the synthesis allows preparation of library of designed compounds using parallel synthesis.

2.2.5. Authors' contributions

As main author of the publication,^[139] I developed and optimized the synthetic route towards the final compounds, synthesized all compounds, provided their full characterization (NMR, HRMS, UHPLC-MS) and wrote major part of the manuscript (except for the biological evaluation, which was provided and written by R.J. and V.K.).

2.3. BODIPY labeled triterpenes for visualization within cells

The results of this project were published in: Krajčovičová, S.; Staňková, J.; Džubák, P.; Hajdúch, M.; Sural, M.; Urban, M. *Chem. Eur. J.* 2018, *24*, 4957.^[182]

The manuscript is attached in Appendix C (p. 154 - 163). The Supporting information is attached as an electronic file on CD.

2.3.1. Introduction

The fluorescence process begins when a molecule in a singlet electronic ground state (S_0) absorbs a photon of a suitable energy, followed by excitation to higher energy orbitals (S_2), which relax quickly to the first singlet excited state (S_1). The decay of the excited state can occur with photon emission (*fluorescence*) or in a nonradiative fashion. The excited state can also undergo forbidden *intersystem crossing* (ITC) to the triplet excited state (T_1) with subsequent relaxation by proton emission called *phosphorescence*. These processes are summarized in Jablonski diagram (Figure 30).^[183]

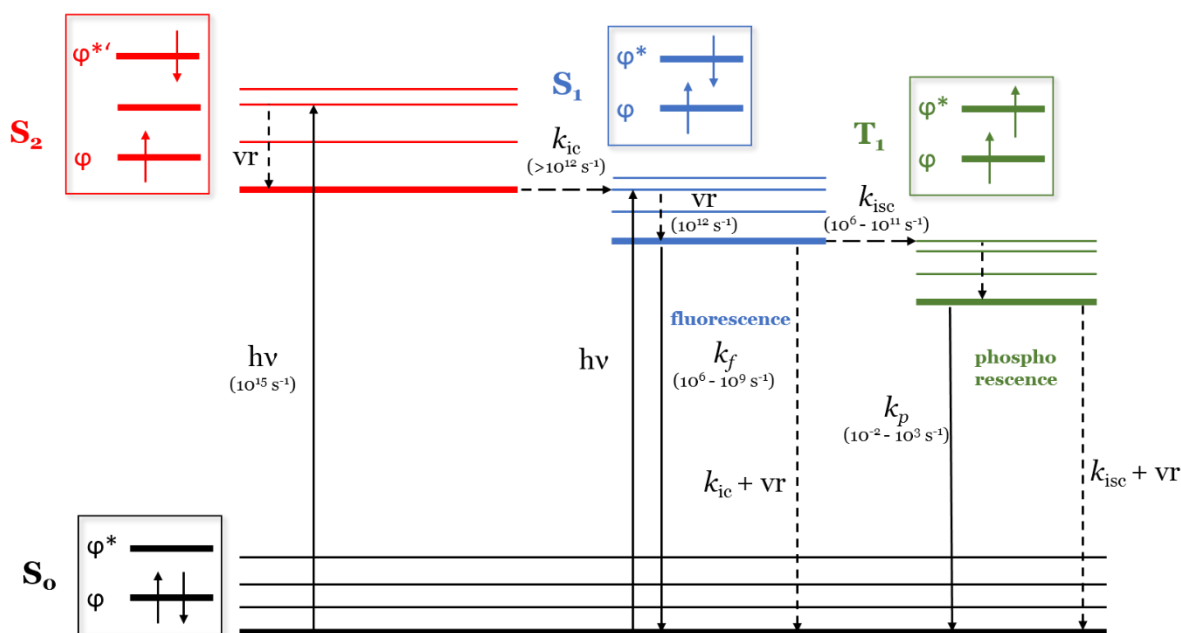


Figure 30. Jablonski diagram. (vr = vibrational relaxation; ic = internal conversion; isc = intersystem crossing)

In general, the maximal absorption (λ_{\max}) is related to the energy between the S_0 and the higher energy levels, whereas the absorptivity of a molecule at λ_{\max} is given by the extinction coefficient (ϵ), defined by the Lambert-Beer law. The maximal emission wavelength (λ_{em}) is lower in energy (and, therefore, longer) than λ_{\max} due to the energy losses by solvent reorganization or other processes.^[183,184] The difference between λ_{\max} and λ_{em} is termed as Stokes shift. Fluorophores with small Stokes shifts are prone to self-quenching *via* energy transfer and thus limiting the number of labels that can be

attached to a biomolecule.^[183] This phenomenon can be utilized to create useful protease substrates, because proteolysis of densely labeled proteins leads to an increase in fluorescence intensity. Another important feature of a fluorophore is its quantum yield or quantum efficiency which is simply the ratio of photons emitted to those absorbed.^[183]

Small molecules capable of fluorescence are incredible tools for chemical biology, serving as enzyme substrates, biomolecular labels, environmental indicators or cellular stains.^[183,185–189] Finding a suitable fluorophore to visualize biochemical processes can be daunting, since many molecules are available either commercially or through *de novo* design and synthesis. Probe selection and design can be simplified by understanding the properties of these fluorescent compounds.

The most representative and widely used fluorophores in biological assays are coumarin, fluorescein, boron difluoride dipyrromethene (BODIPY), rhodamine and cyanine dyes (Figure 31).^[183,190,191]

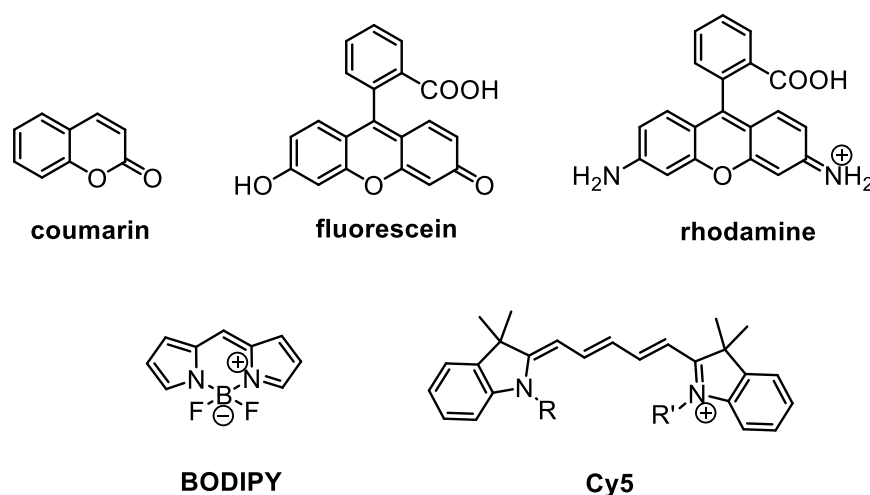


Figure 31. Commonly used dyes in chemical biology.^[190]

However, some of these fluorophores do not completely satisfy the required needs of probes, e.g. the negatively charged fluorescein often suffers for lack of cellular permeability but, on the other hand, showed non-specific binding to cellular compartments.^[190] In contrast, rhodamine as a cationic dye is often prone to localize in the mitochondria or adsorb nonspecifically to proteins or lipids, however, it is at the same time sufficiently hydrophobic, photostable and easily penetrate the cellular membrane.^[192] Among these, BODIPY dye is considered a potential scaffold for functional fluorescent probe development, since it shows high photostability, high fluorescence quantum yield, small Stokes shift and/or negative total charge.^[193–196] Moreover, BODIPY derivatives are readily soluble in most organic solvents and are characterized by a strong absorption and fluorescence spectral bands in the visible, green-yellow part of the spectrum.^[197]

There are many publications stated that BODIPY dyes can be used as fluorescence sensors, switches or probes,^[198–200] in light harvesting arrays,^[201–203] in photovoltaic devices,^[204–206] in biomedicine as fluorescence markers for bioimaging^[196,207–210] and as singlet-oxygen generators in photodynamic therapy.^[211,212] The key success lies in a fact, that the core (Figure 32) is reasonably versatile and can be modified on selected positions (α , β and/or *meso*) by electrophilic reactions (sulfonation, nitration, halogenation), nucleophilic reactions, Pd-mediated cross-coupling reactions, such as Suzuki and Sonogashira couplings, or with Knoevenagel reaction (Scheme 32).^[193,194,213]

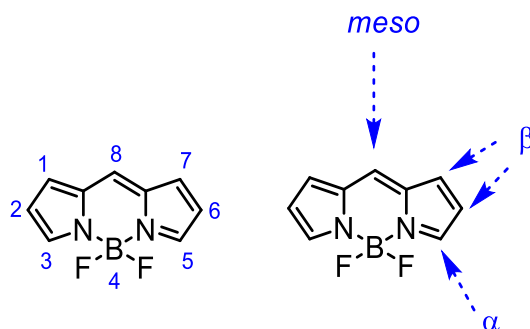


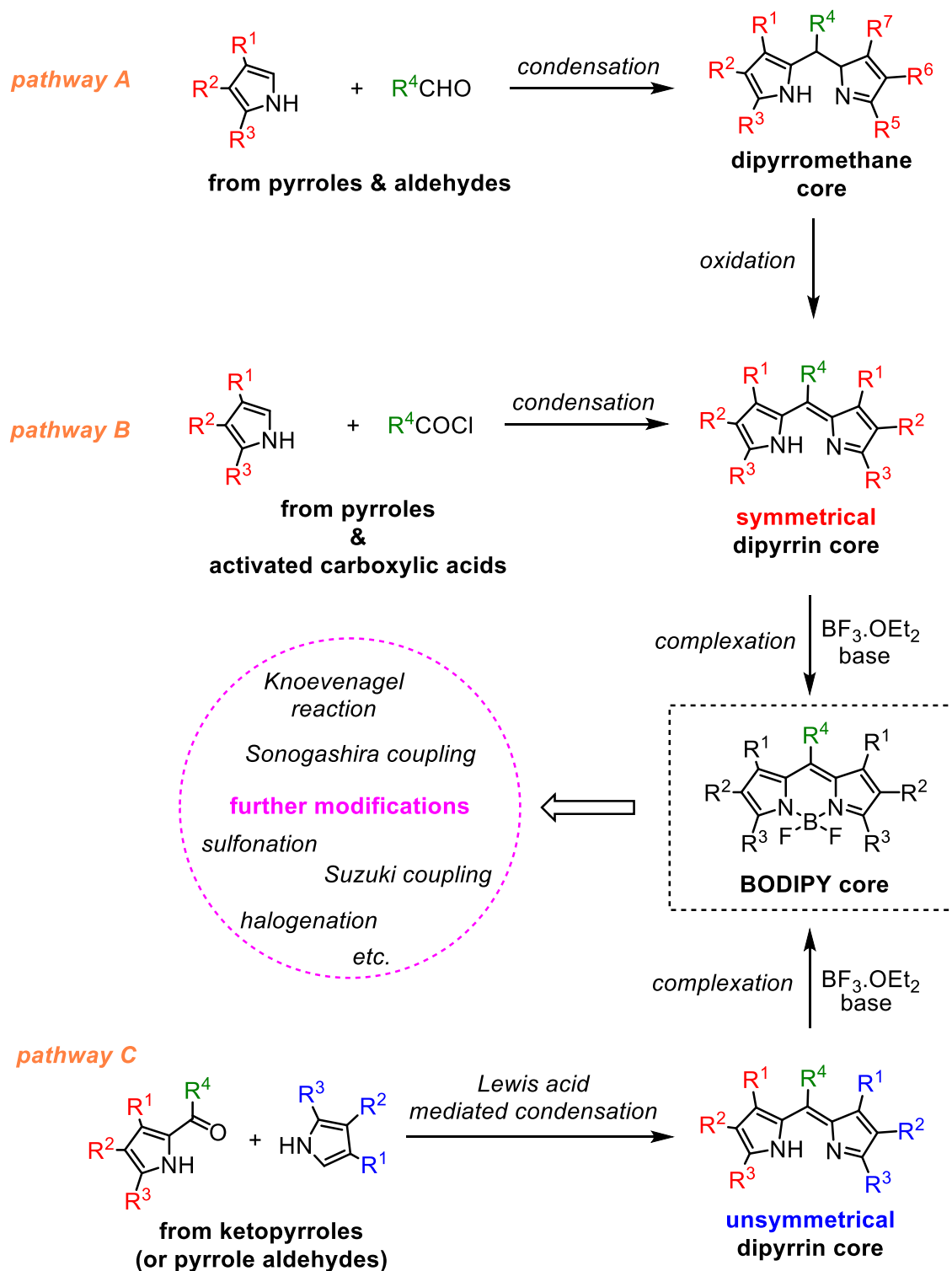
Figure 32. General numbering of positions on BODIPY core.^[193]

In general, the synthesis of BODIPY core can be distinguished in three distinct pathways, depending on what kind of dyes (symmetrical or unsymmetrical) are required.

For the syntheses of symmetrical dyes, the condensation reaction of excess of pyrrole with activated carboxylic acid (mostly acyl chlorides,^[214,215] but anhydrides are also acceptable^[216]) yields unstable, symmetrical dipyrin intermediate (Scheme 32, pathway **B**) which is subsequently converted to BODIPY core after complexation with boron trifluoride in basic environment. Another option is the condensation reaction with aromatic aldehydes and pyrroles (in excess) that also leads to formation of symmetrical products, however, oxidation step is necessary to form required dipyrin core (Scheme 32, pathway **A**).^[193] The oxidants used for this transformation are often *p*-chloranil or DDQ, which can introduce potential experimental complications, in case of oxidation-labile moieties on pyrrole scaffold.

The synthetic approach towards unsymmetrical BODIPY dyes is achieved *via* preparation of ketopyrrole (or pyrrole aldehyde) intermediates followed by a Lewis acid mediated condensation with another pyrrole fragment (Scheme 32, pathway **C**) that yields unsymmetrical dipyrin core, which is subsequently complexed with boron to form BODIPY.^[193] Notably, this method is particularly valuable for preparation of unsymmetrical BODIPY dyes, although the preparation of symmetric scaffolds is also possible.^[217] Further modification of resulting BODIPY dyes, particularly on *meso*

position, tend to be relatively easy and could be extraordinarily valuable, e.g. for study of photoinduced electron transfer (PeT) mechanisms.^[218–220]

Scheme 32.^[193]

Therefore, BODIPY with spectral bands tunable along the whole visible spectrum (even in the near-infrared region)^[193,195,210] can be synthesized or the intersystem

crossing probability can be enhanced and promote single-oxygen generation by so called *heavy atom effect*.^[211,212]

Since it is above the scope of this thesis to sufficiently cover the whole spectrum of BODIPY's applications, I will focus mainly on the most significant one for us – its use in chemical biology.

BODIPY dyes as a tool for chemical biology

To the most common applications of BODIPY dyes in field of chemical biology belong:

- **Targeted intracellular distribution**

Due to the high lipophilicity of BODIPY dyes, they prone to penetrate cells easily and have tendency to accumulate in subcellular membranes,^[190] if they not possess with any hydrophilic functionality (such as ethylene glycol or carboxylate). Noteworthy, BODIPYs containing a targeting group for the particular organelle will probably not target other cellular compartments.^[190] As examples of BODIPYs with localization in the ER, lysosomes or Golgi apparatus could serve compounds **III-1-9** (Figure **34**).^[190,221]

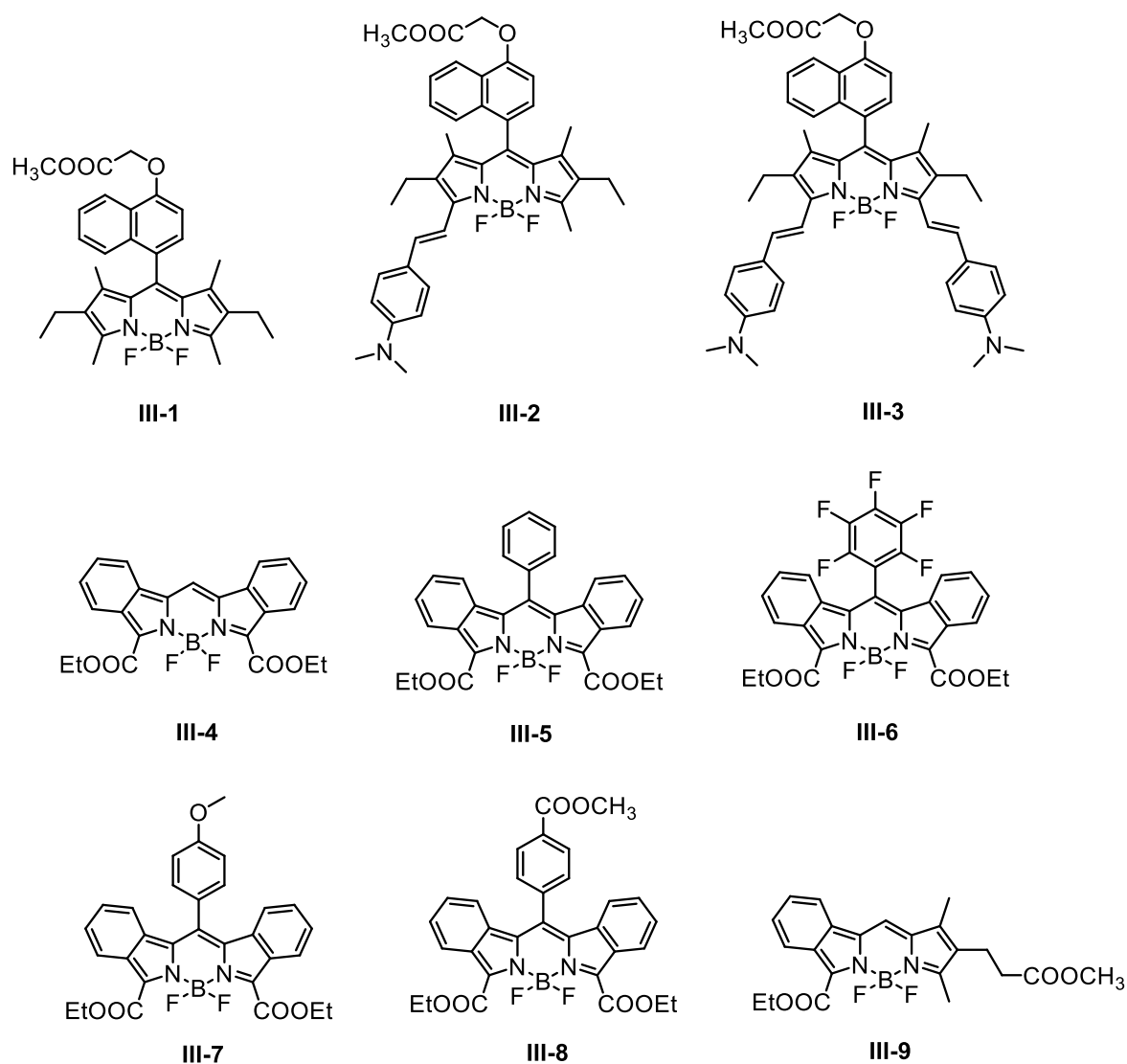


Figure 33.

Moreover, BODIPYs with selective targeting to the cytosol can also be prepared (Figure 34). The monoalkoxy containing BODIPYs **III-10,11** were developed to overcome the problems with water solubility without loss of cell permeability.^[222]

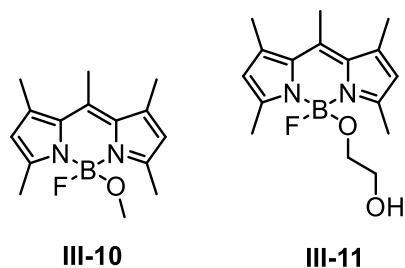


Figure 34.

Since mitochondria is negatively charged, localization of positively charged molecules is often observed. For such reason, the commercially available MitoTrackers usually include intrinsically cationic rhodamine dyes,^[192] as was mentioned above. In case of neutral BODIPY dye, the mitochondria localization can also be achieved by

introducing a cationic moiety, such as ammonium or phosphonium group (Figure 35) by straightforward conversion from their corresponding amine or phosphine.^[190,223,224]

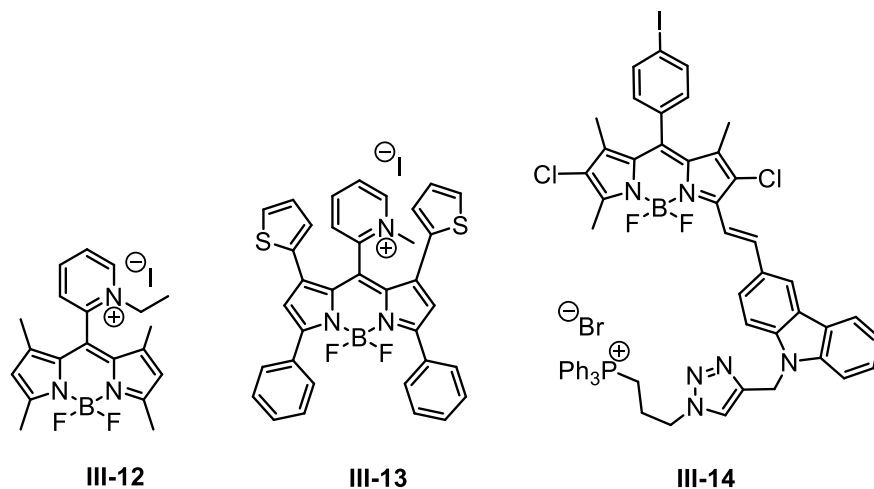


Figure 35.

- **Imaging probes for target proteins**

The visualization of target proteins seemed to be a difficult task for many research groups. The possible approaches could be labeling a target protein which is fused with a peptide or protein tag,^[225–227] conjugating an inhibitor for target receptor with a fluorophore or high-throughput screening of various fluorescent molecules.^[228]

For visualization of carbonic anhydrases (CAs), the tumor-associated enzymes, BODIPYs were conjugated with aromatic sulfonamides (**III-15**, **III-16**; Figure 36) and exhibited comparable inhibitory activities with known CA inhibitor acetazolamide as with several CA isozymes.^[229] The tyrosine kinase Src was labeled with Desatinib-BODIPY conjugate **III-17** (Figure 36) and although the IC_{50} for this conjugate was approximately 10-fold higher than was for Desatinib itself, it still possessed with sufficiently high affinity to bind Src.^[190,230]

Other examples were BODIPY conjugates **III-18** (with human serotonin receptor antagonist Granisteron)^[231] and **III-19** (with human progesterone receptor antagonist Mifepristone),^[232] respectively, exhibited comparably high affinity for their targeted receptors.

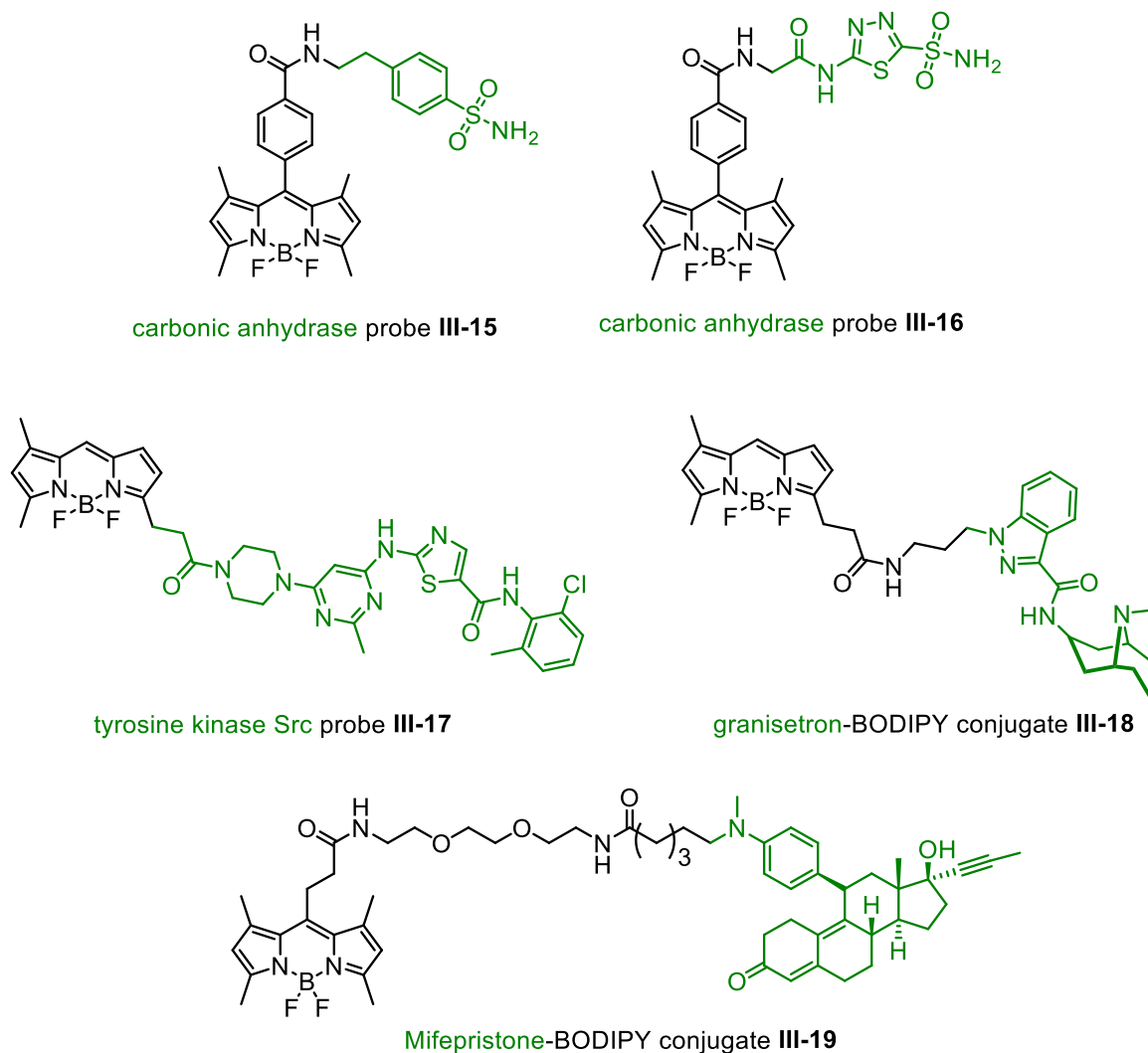


Figure 36.

To specifically label target proteins, various peptide tags with small-ligand molecules that can form covalent bonds or tight non-covalent complexes have been developed.^[225–227] For visualization of *Escherichia coli* dihydrofolate reductase (eDHFR), the trimethoprim (TMP) ligand, fused with BODIPY, has been used (**III-20**; Figure **37.a**)^[233] and showed specific labeling of expressed fusion proteins on the plasma membrane or in the nucleus.

For covalent bonding to the small peptide tag, containing two pairs of Arg-Cys (RC) residues, the BODIPY **III-21** with α,β -unsaturated ester moiety was used. After coupling reaction, where peptide tag bound strongly to **III-21** *via* Michael addition, the emission color of **III-22** changed from orange to green due to the shortening of the π -conjugated system (Figure **37.b**).^[234]

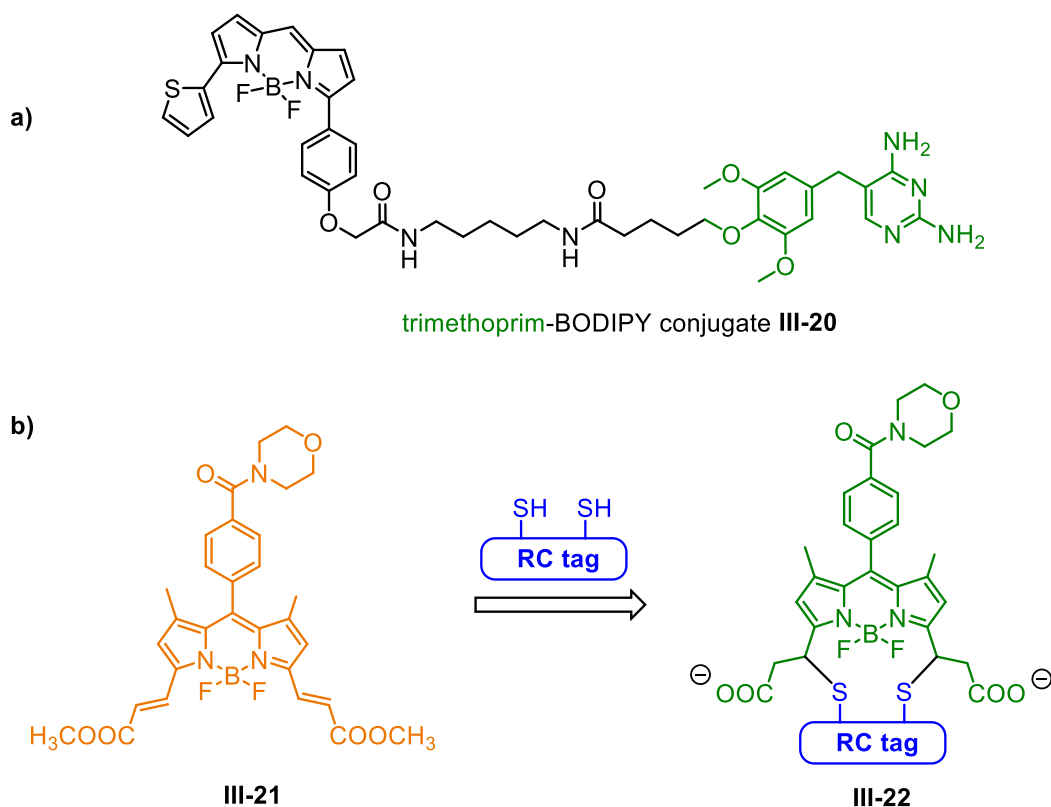


Figure 37.

- **pH sensors**

Since a decreased pH values are often observed in some types of tumour tissues or organelles (e.g. endosomes are around 5.5 – 6.3, whereas lysosomes 4.7), pH-sensitive fluorescent probes could be helpful.^[235] The photo-induced-electron transfer mechanism of such probes rely on fluorescence OFF-ON system, which depends on protonation of an amino group (Figure 38). As examples could serve trastuzumab, the monoclonal antibody for the human epidermal growth factor 2 (HER-2), conjugated with pH sensitive BODIPY **III-23** with pK_a 6.0 suitable for selective imaging in lysosomes.^[236] Another pH sensitive probe **III-24** (Figure 38) was developed to image bone-resorbing osteoclasts in live mice and showed almost identical pH as **III-23**, suggesting that bisphosphonate group had no harmful effect on this value. Intense fluorescence was observed due to acidic compartment during bone resorption.^[237,238]

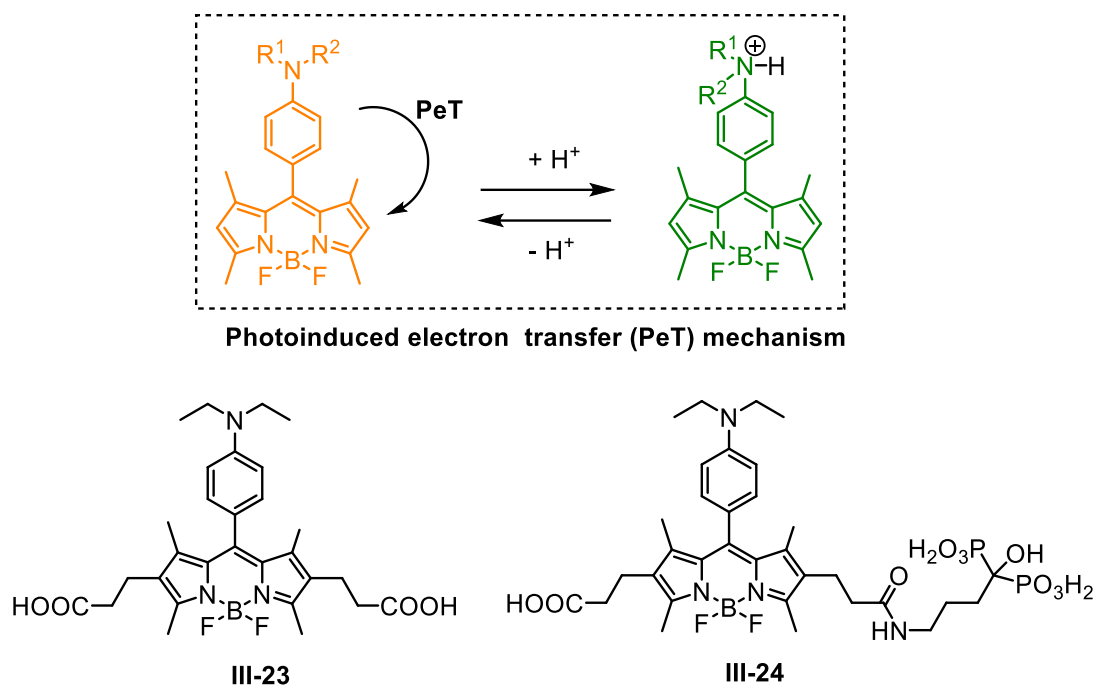
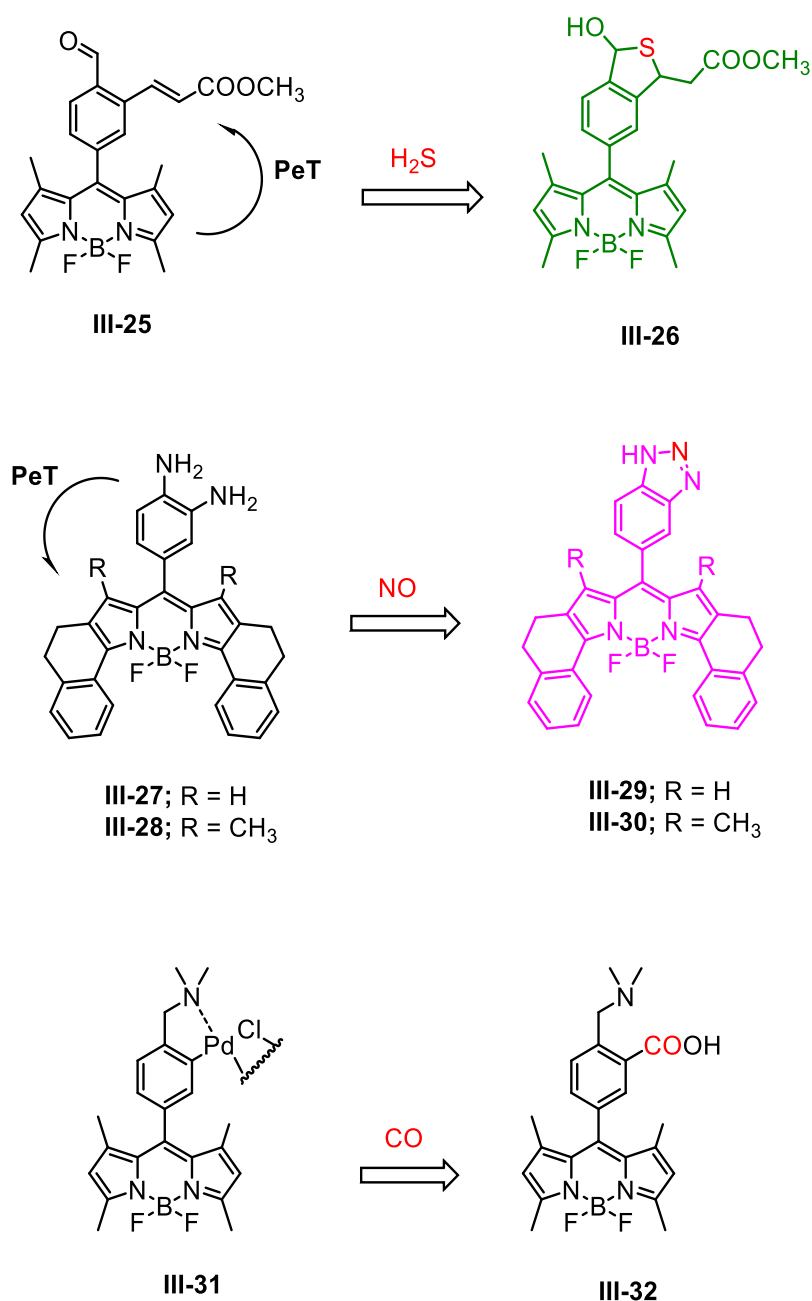


Figure 38.

- Gaseous signaling probes

Endogenous production of hydrogen sulfide (H₂S), nitric oxide (NO) and carbon monoxide (CO) can be visualized in cells if reactive moiety for their detection is presented.^[239–241] Compound **III-25** was able to selectively react with H₂S *via* double Michael addition and exhibit turn-ON fluorescence presumably due to the inhibition of PeT (Scheme **33**).^[220] For visualization of NO, the *o*-phenylenediamine moiety is frequently used, not only because it selectively reacts with NO but also as electron donor in PeT quenching.^[218] In this manner, BODIPY probes **III-27** and **III-28** (Scheme **33**) were prepared and showed over 400-fold fluorescence enhancement in response to reaction with NO.^[219] Interestingly, both NO-probes were membrane permeable and showed response to NO inside of cells without cytotoxicity. Lastly, to selective detection of CO in living cells the BODIPY-palladium complex **III-31** was developed (Scheme **33**).^[242] The fluorescence in this complex was quenched by the heavy atom effect of palladium, which was subsequently released after reaction with CO, followed by fluorescence recovery.

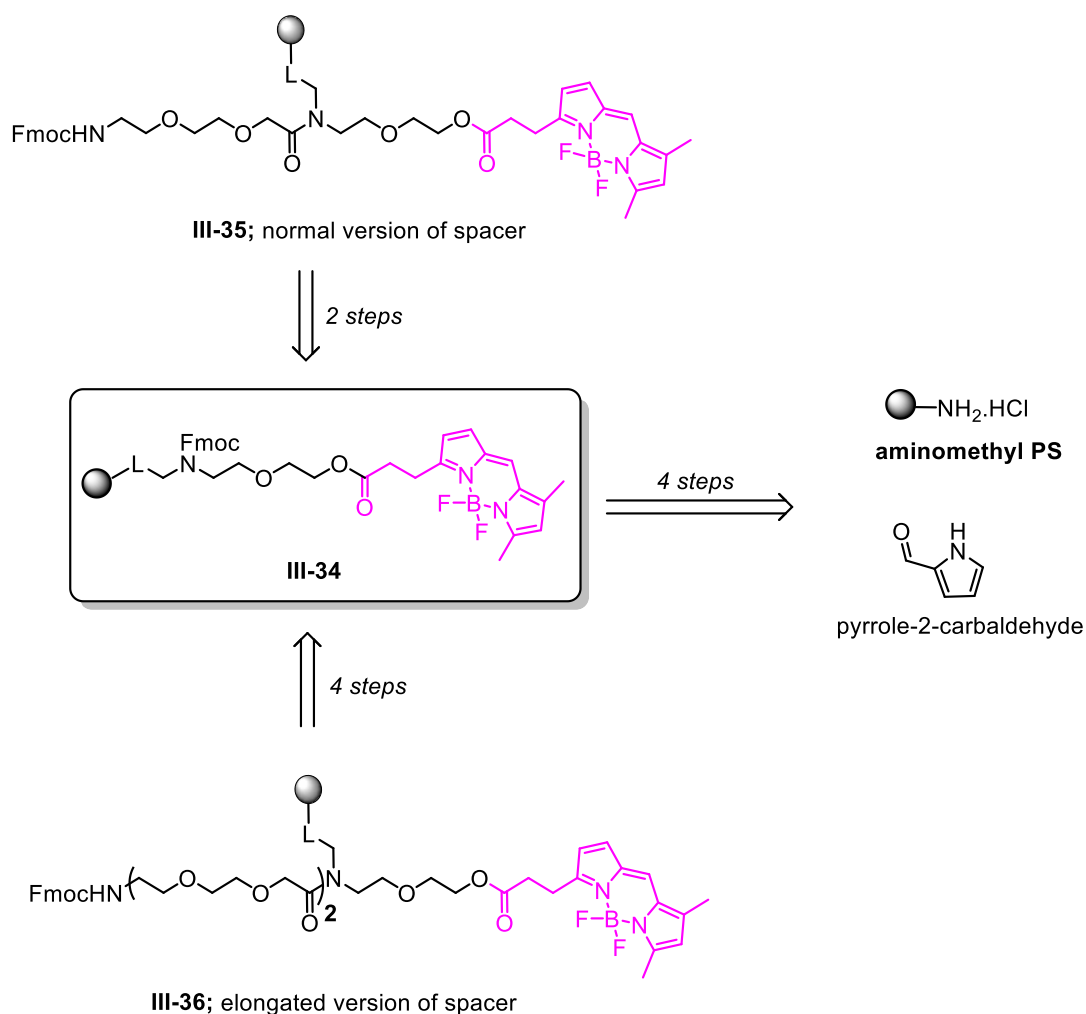
Scheme 33.^[218–220]

Although it seems like the BODIPY core has many advantages (and it is certainly truth), some undesirable features are also presented. For instance, the stability towards strong acidic or basic environment is limited, which questioned its use for solid-phase synthesis.^[183,243] Consequently, only one example of actual BODIPY synthesis using SPS was published to date,^[244] and moreover, in this particular case, authors used the solid support rather as a protecting group for amine functionality than a general tool for rapid preparation of fluorescently labelled compounds. In this regard, our aim was the preparation of preloaded resin containing BODIPY for further conjugation with molecules of interests.

2.3.2. Synthesis and photochemical properties

The synthetic approach towards the preloaded resin and final conjugates is described in our published paper,^[182] however, I consider appropriate to summarize the optimization steps.

The synthesis of BODIPY preloaded resin **III-34** started from the commercially available amino methyl polystyrene resin (Scheme 34). This BODIPY dye was selected due to its known spectroscopic properties, overall neutral charge and suitable functional group for conjugation. However, since its commercial price was above 80 000 CZK per gram, we decided to prepare it by ourselves in 4 steps from pyrrole-2-carbaldehyde. We modified and optimized the previously reported synthetic approaches^[245,246] and managed to synthesize this dye in an excellent overall yield of 40% and multigram scale quantities (up to 4 grams, calculated price 5000 CZK per gram). Following elongation of the spacer yielded two BODIPY preloaded resins **III-35** and **III-36** (Scheme 34).

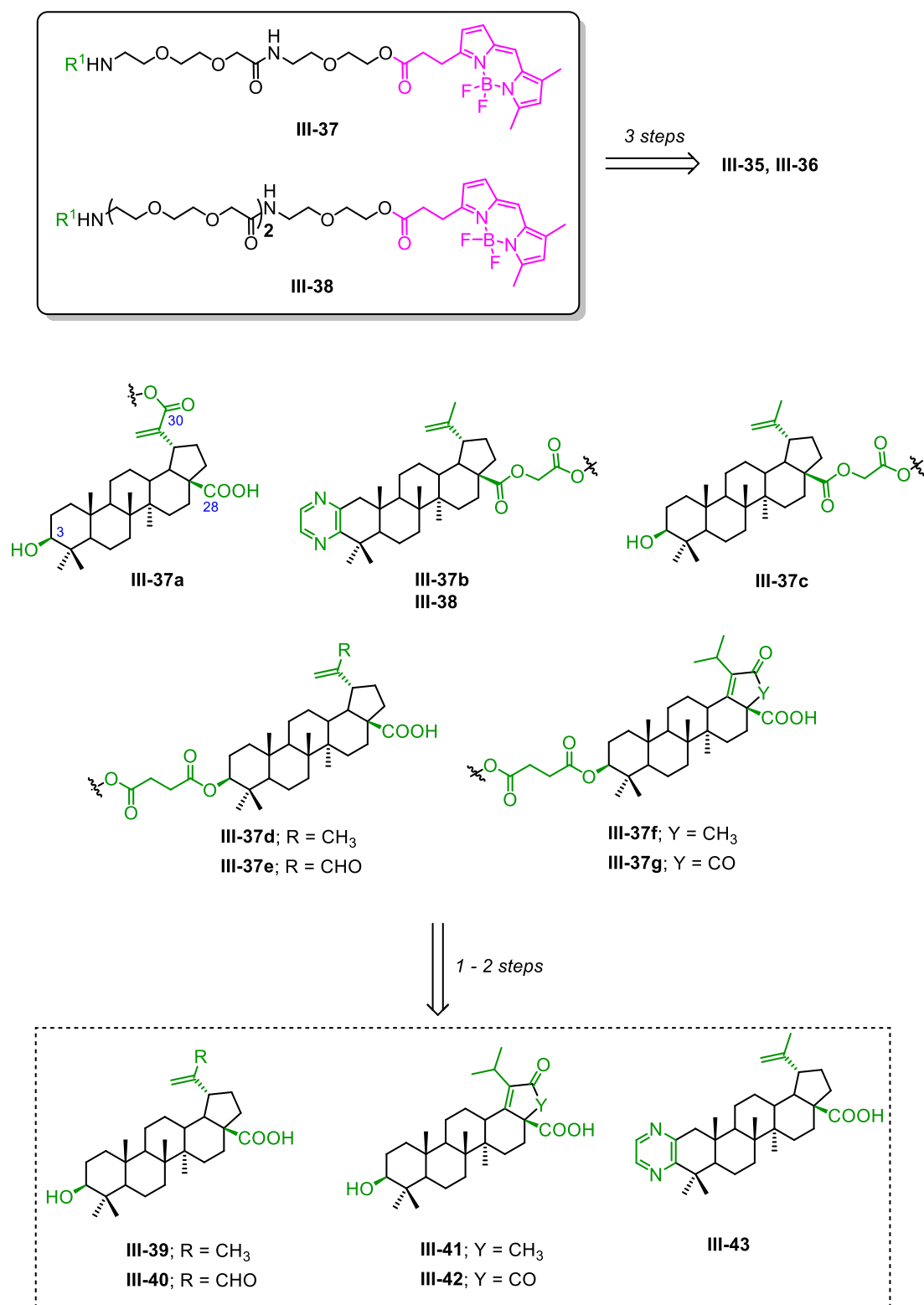


Scheme 34. Retrosynthetic analysis towards final compounds.

The selection of parental triterpene derivatives **III-39-43**, was based on their low micromolar cytotoxic profile towards various cancer cell lines and/or unknown

mechanism of action.^[68,247,248] Betulinic acid **III-39** was used as a standard, since it is the widely studied cytotoxic triterpene with already reported mode of action.^[249,250]

For the conjugation with the preloaded resins was necessary to equip parental triterpenes with the suitable functional group. The modification of the scaffold was performed at 3 different parts (C³, C²⁸, C³⁰) and yielded the corresponding hemisuccinates, glycolates or α,β -unsaturated carboxylic acid, respectively. These carboxylic acids were used to acylate the preloaded resins **III-35**, **III-36** (after cleavage of Fmoc protecting group) and the following acid-mediated cleavage from the resin provided final conjugates **III-37**, **III-38** (Scheme 35).

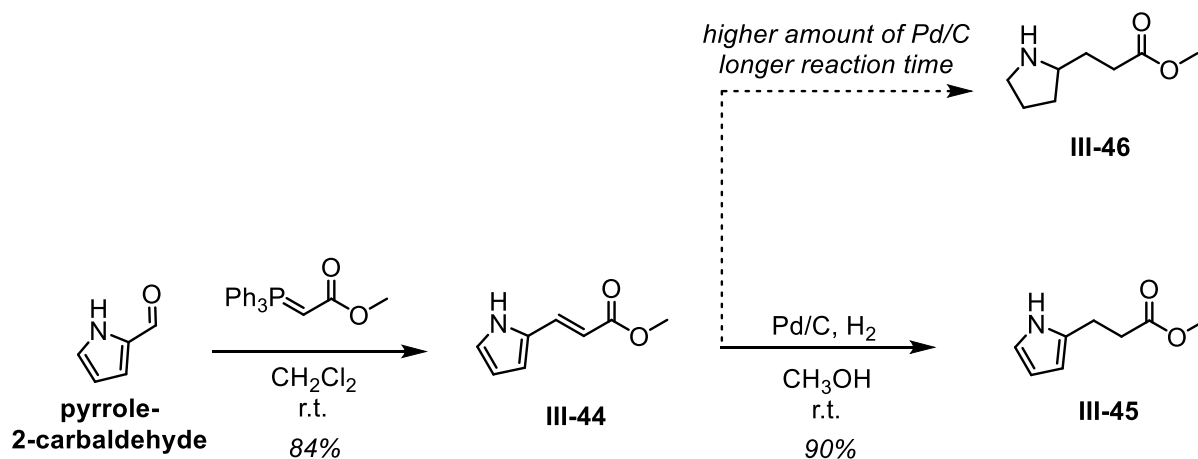


Scheme 35.

2.3.2.1. Synthesis of BODIPY-FL propanoic acid

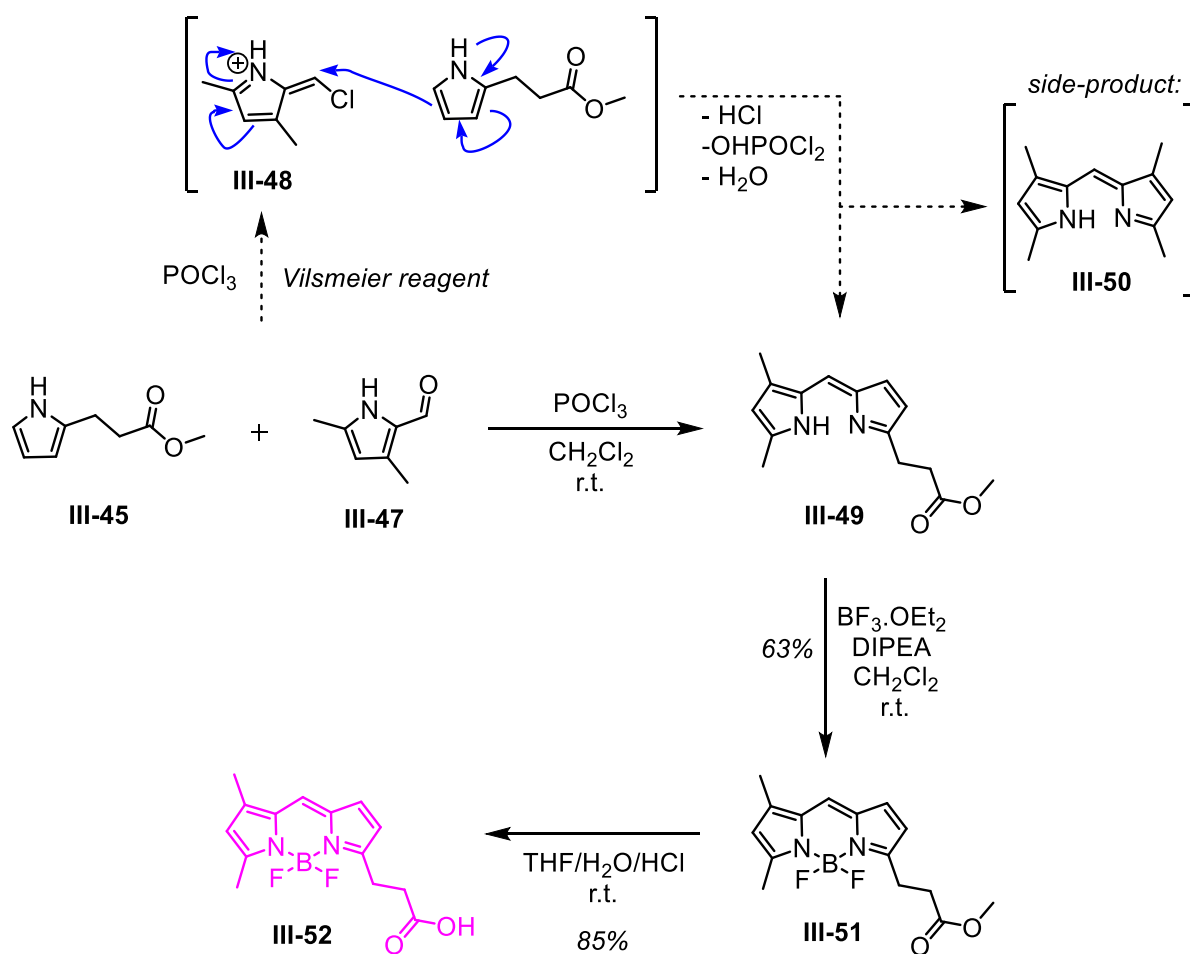
The synthetic pathway started from the commercially available pyrrole-2-carbaldehyde and triphenylphosphonium ylide acetate, which were converted to pyrrole α,β -unsaturated ester **III-44** *via* Horner-Wadsworth-Emmons reaction with excellent *E*-regioselectivity due to the formation of stabilized ylide. Following reduction of double

bond was achieved with palladium assisted hydrogenation to produce compound **III-45** (Scheme 36). It is worth mentioning, that prolongation of reaction time or higher loadings of palladium catalyst led to complete reduction of pyrrole to pyrrolidine scaffold **III-46** (elucidated from UHPLC/MS traces).



Scheme 36.

POCl_3 mediated condensation of **III-45** with 3,5-dimethylpyrrole-2-carbaldehyde **III-47** yielded unsymmetrical dipyrin core **III-49**. POCl_3 reacted with pyrrole aldehyde to form unstable Vilsmeier reagent **III-48** *in situ*, which was attacked by a second pyrrole **III-45** to form dipyrin. Notably, the formation of non-desired symmetrical dipyrin **III-50** was observed in less than 5% formation (according to UHPLC/MS traces) and was not isolated or characterized. Dipyrin **III-49** was then subjected without further isolation to complexation with $\text{BF}_3 \cdot \text{OEt}_2$ to provide BODIPY FL propanoic ester **III-51**. The isolation of this intermediate needed a quite tedious purification from inorganic by-products, especially after scale-up (more than 2 g), in order to obtain better yields. Finally, acidic hydrolysis of ester provided BODIPY FL propanoic acid **III-52** (Scheme 37) in high yield. Interestingly, BODIPY core was stable in aqueous hydrochloric acid for 48 hours, which indicated unusually long kinetic stability of BODIPY in acidic media.^[251]

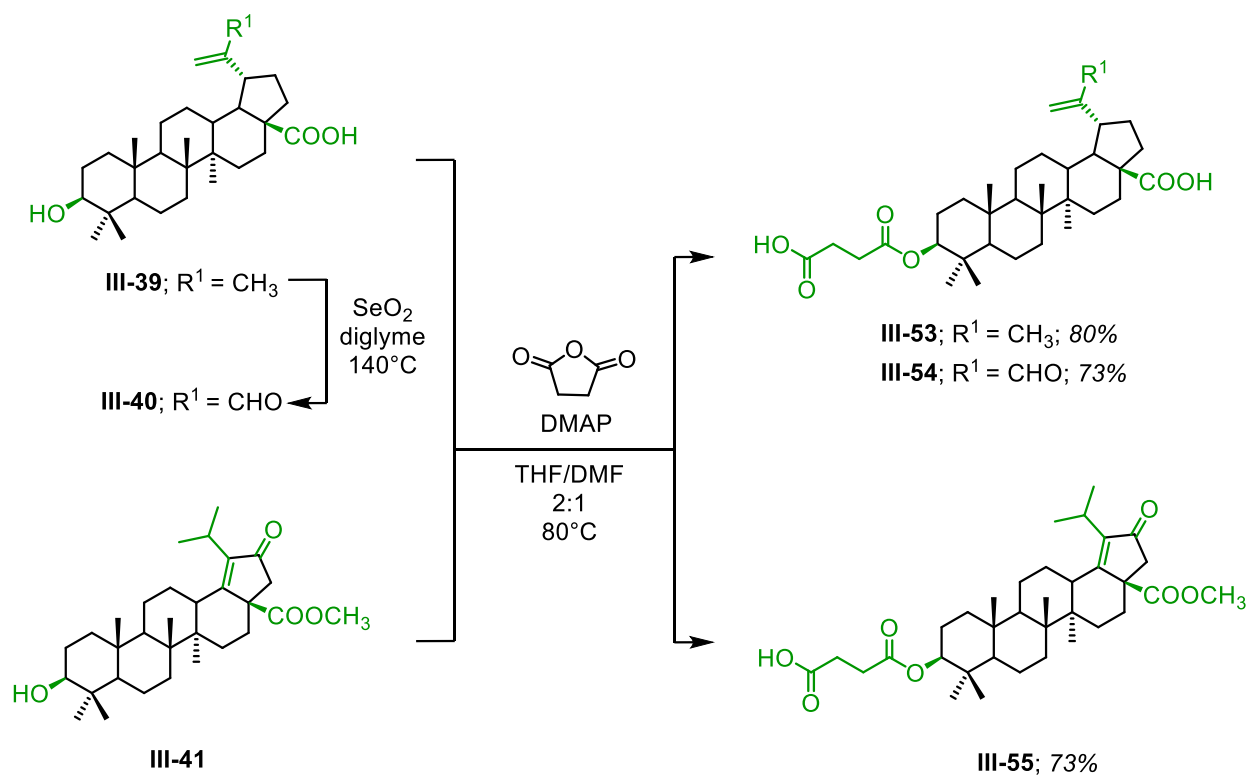


Scheme 37.

2.3.2.2. Synthesis of pre-modified triterpenes

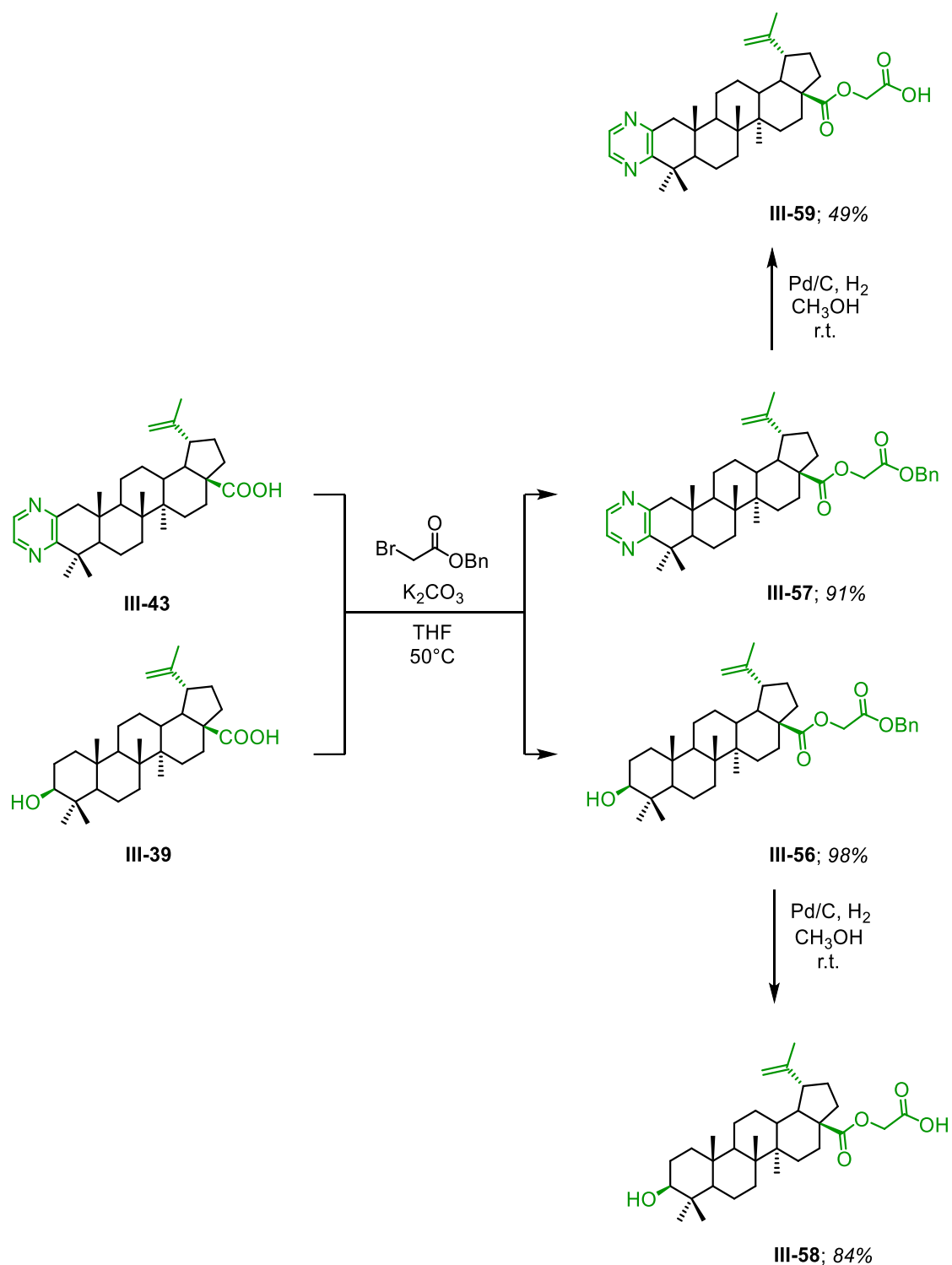
Modification of semisynthetic triterpenes **III-39-41**, **III-43** as hemisuccinates and glycolates, respectively, was inspired by our previous work on biotinylated conjugates.^[252]

Briefly, betulinic acid **III-39**, betulinic acid aldehyde **III-40** (prepared from **III-39** *via* SeO₂ mediated allylic oxidation) and monoketone **III-41** were treated with succinic anhydride in presence of DMAP (Scheme 38) to provide triterpenes **III-53-55** with carboxylic function ready for conjugation. Hemisuccinic diketone **III-42** was purchased commercially and used without modification.



Scheme 38.

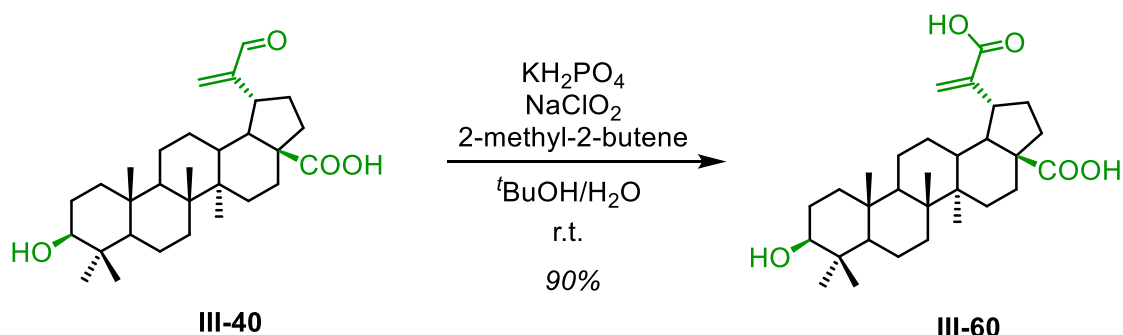
For modification of C²⁸ position was necessary to extend the neopentyl-type carboxylic function as it generally suffers from lower reactivity due to the steric hindrance. As such, we reacted betulinic acid **III-39** and pyridine triterpene derivative **III-43** with benzyl bromoacetate to yield compounds **III-56** and **III-57**, respectively. Following deprotection of benzyl moiety was achieved with palladium assisted catalytic hydrogenation and yielded pre-modified triterpenes **III-58**, **III-59** (Scheme 39).



Scheme 39.

For conjugation of betulinic acid **III-39** on C^{30} position, a different approach was used as was previously published.^[252] The betulinic acid aldehyde **III-40** was subjected to chemoselective Pinnick oxidation (Scheme 40) in order to produce carboxylic acid **III-60** for acylation with preloaded resins. This reaction represents a convenient way how to convert aldehydes to the corresponding carboxylic acids in a presence of unprotected

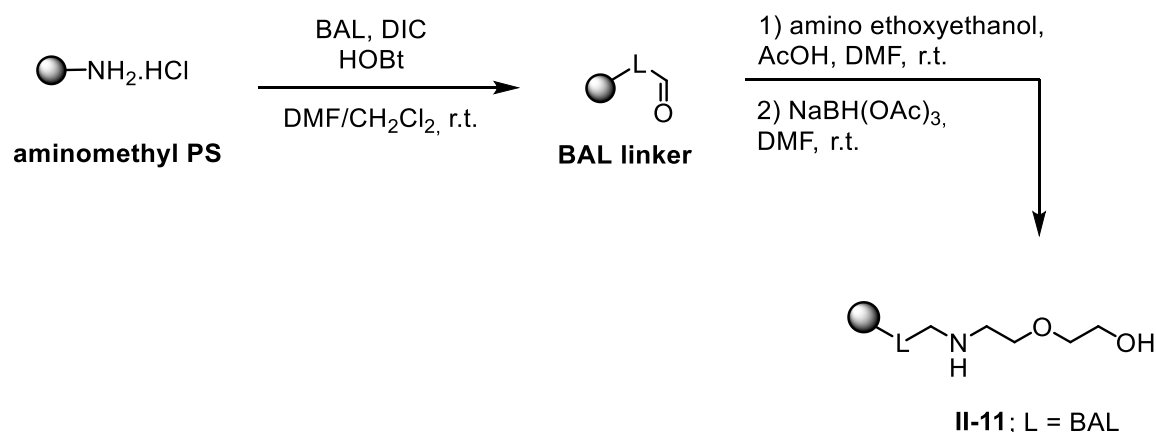
hydroxyl functions and double bonds.^[253] 2-methyl-2-butene is used as a scavenger of hypochlorous acid that is formed during the transformation.



Scheme 40.

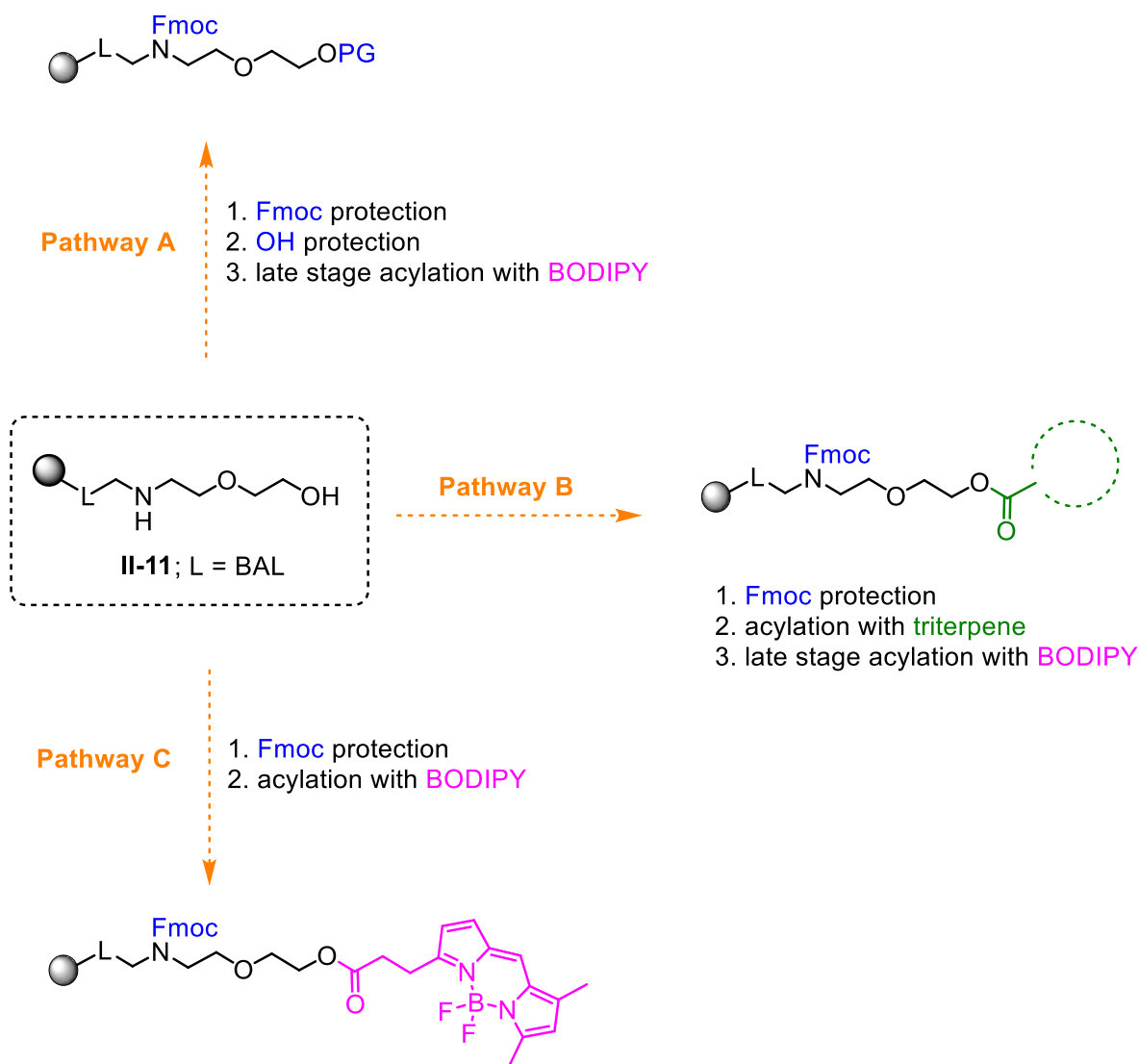
2.3.2.3. Synthesis of preloaded resins

The synthesis started similarly to previous project (thalidomide preloaded resin), from the commercially available amino methyl polystyrene resin, which was acylated with BAL linker. Following reductive amination with amino ethoxyethanol provided the same intermediate **II-11** (Scheme 41).



Scheme 41.

Generally, the preparation of preloaded resin, containing amino ethoxyethanol moiety, can be achieved in three distinct pathways, depicted on Scheme 42. Since we found out that BODIPY core is unstable under conditions commonly used in SPS, we envisioned at first pathways **A** and **B** where dye is installed at late stage of synthesis, to minimize contact with potentially harmful reagents.

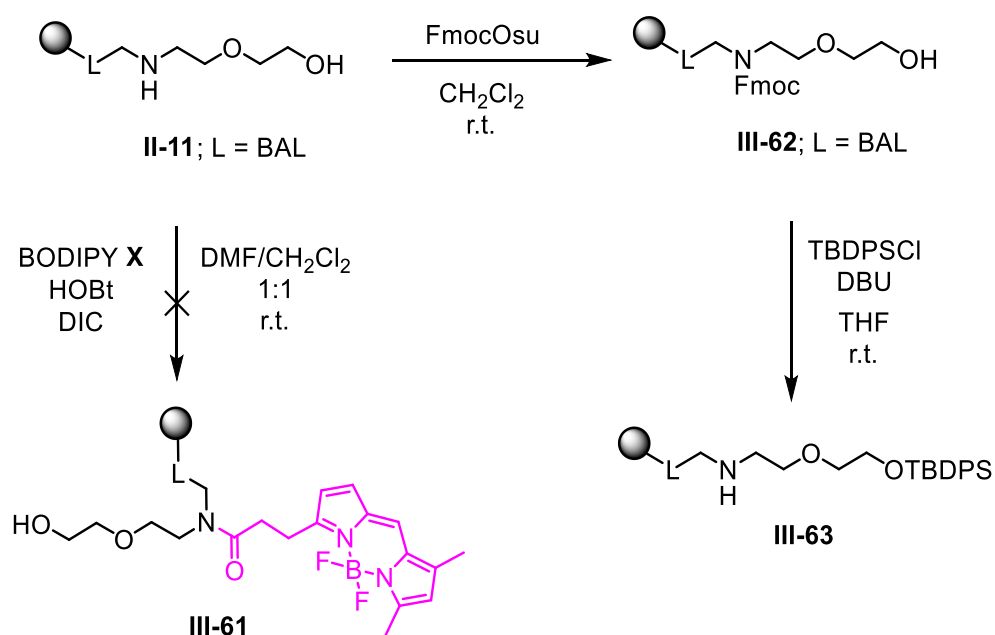


Scheme 42.

Pathway A

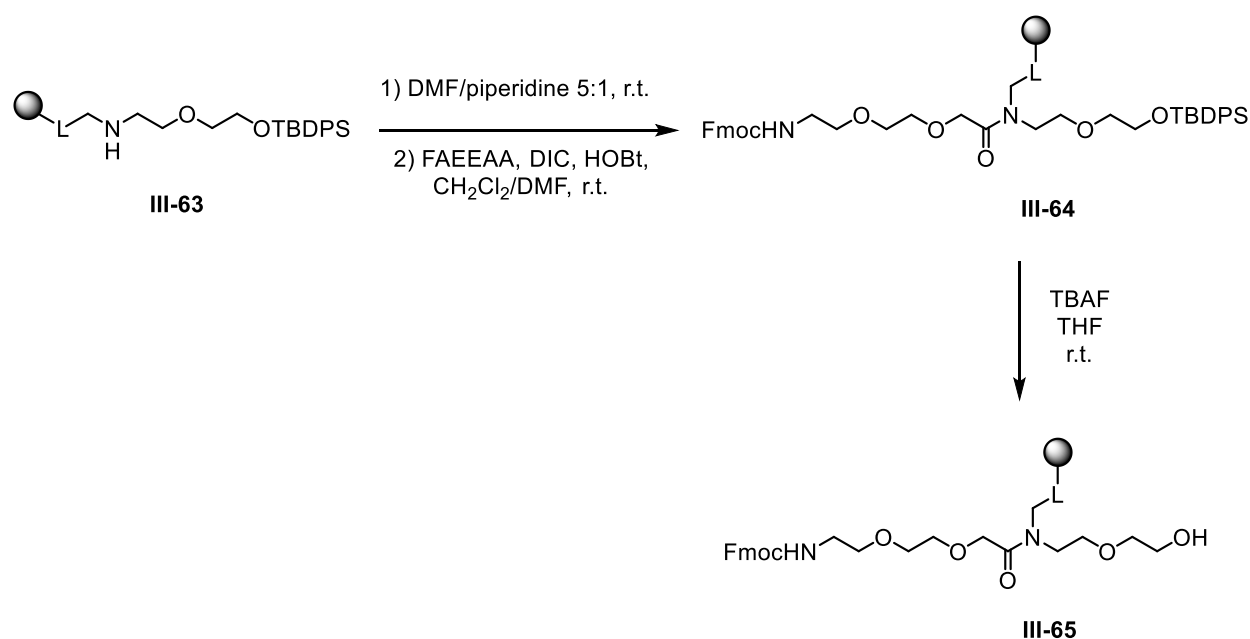
Since both functionalities can react under acylation conditions, we needed to protect them and for further independent manipulations the orthogonal protecting groups must have been chosen. It is important to mention, that we, at first, tried acylation reaction of **II-11** with BODIPY **III-52**, believed in chemoselective output **III-61** without protection of primary hydroxyl group, unfortunately, we observed no conversion to the desired product **III-61** (Scheme 43).

Thus, we decided to protect secondary amine functionality with FmocOsu and primary alcohol with silyl protecting group (*tert*-butyldiphenylsilyl, in our case), which can be orthogonally deprotected with source of fluoride anions, e.g. TBAF. The reaction was carried out in presence of DBU (instead of usually used imidazole or sodium hydride, which did not produce desired product) and provided **III-63**.



Scheme 43.

Following with FAEEAA for elongation of the linker yielded intermediate **III-64**, which upon treatment with TBAF led to deprotection of silyl protecting group (Scheme 44).



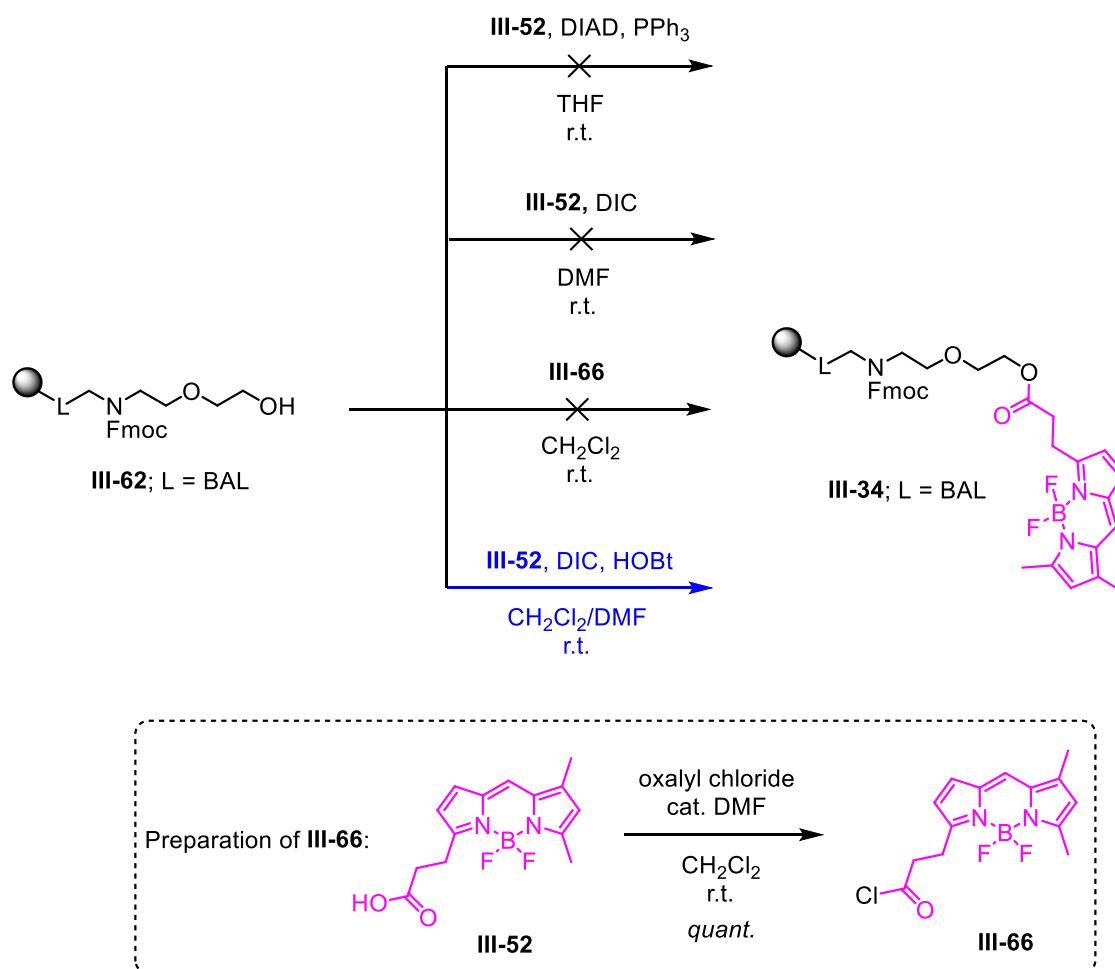
Scheme 44.

Acylation of primary hydroxyl moiety with prepared BODIPY **III-52** needed to be optimized, because it suffers from lower reactivity in general and we wanted to avoid elevated temperatures due to possible instability of BODIPY core.

The suitable reaction conditions were optimized on intermediate **III-62** (Scheme 45). First, we tried DIC technique for acylation, however, only with limited success.

Another possible option seemed to be Mitsunobu reaction, but again, our substrate did not react and only starting material was recovered. Thus, we decided to convert BODIPY FL propanoic acid **III-52** to its corresponding acyl chloride **III-66**, in presence of oxalyl chloride and catalytic amount of DMF (Scheme 45), and without isolation subjected it to reaction with immobilized Fmoc amino ethoxyethanol **III-62**. Unluckily, no desired product was detected at all, although we convinced ourselves about the full conversion of acid to acyl chloride *via* UHPLC-MS analysis in methanol that yielded BODIPY ester **III-51**.

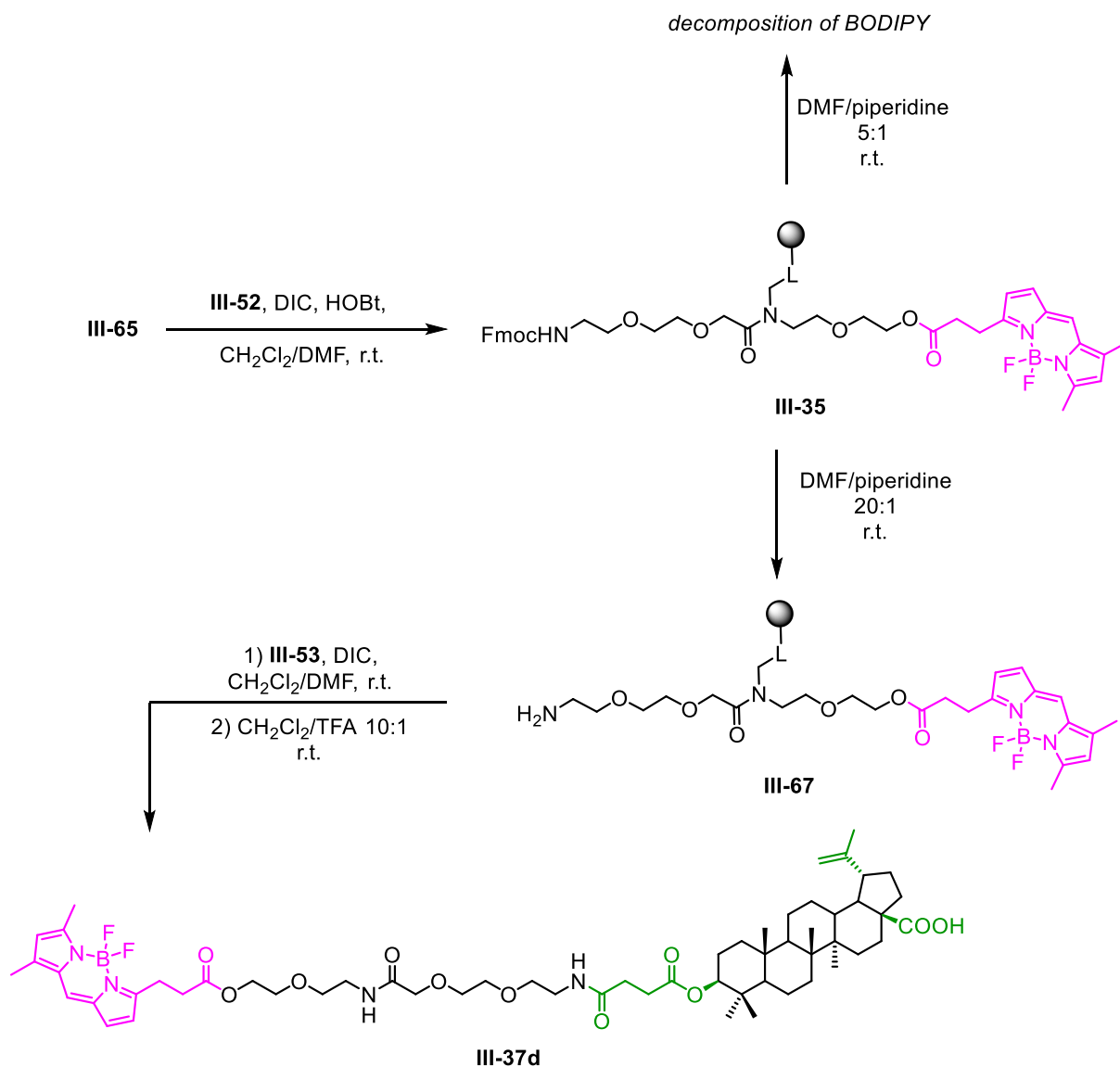
Fortunately, we have been able to obtain desired product **III-34** after reaction under DIC/HOBt conditions. Importantly, cleavage from the resin, prior to analysis of samples containing BODIPY, was carried out in less acidic cleavage cocktail, than is typically used for BAL linker ($\text{CH}_2\text{Cl}_2/\text{TFA}$ 10:1), since we observed a total decomposition of BODIPY core under standard cleavage conditions ($\text{CH}_2\text{Cl}_2/\text{TFA}$ 1:1).



Scheme 45.

Accordingly, BODIPY **III-52** successfully reacted with intermediate **III-65** as well. However, following deprotection of Fmoc under standard cleavage conditions used in SPS (DMF/piperidine 4:1, 30 minutes) led to total decomposition of the BODIPY core

with consequent diminish of fluorescence. Luckily, use of lower concentration of piperidine (DMF/piperidine 20:1, 30 minutes) was much more suitable and we observed full conversion to product **III-67**, with negligible loss of fluorescent activity. Subsequent acylation with pre-modified betulinic acid **III-53** yielded first final conjugate **III-37d** (Scheme 46).



Scheme 46.

Interestingly, omitted HOBt during this final step greatly improved the resulting crude purity. Further, 28-oxyallobetulin derivative **III-68** (Figure 39) arised as a consequence of Meerwein-Wagner carbocation 1,2-rearrangement^[254] during acidic cleavage of conjugate **III-37d** from the resin. Nevertheless, this compound was not subjected for further fluorescent microscopy study, since it showed no biological activity.

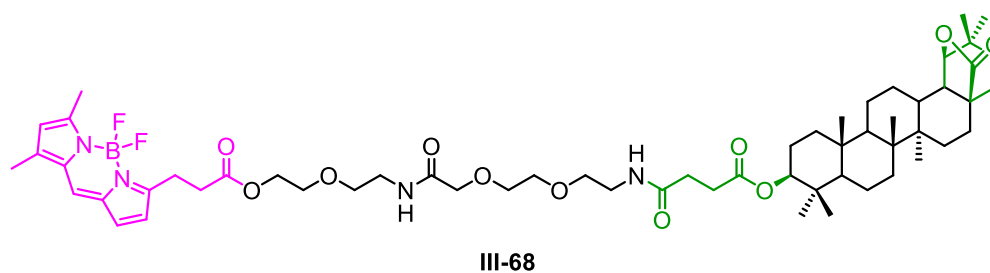
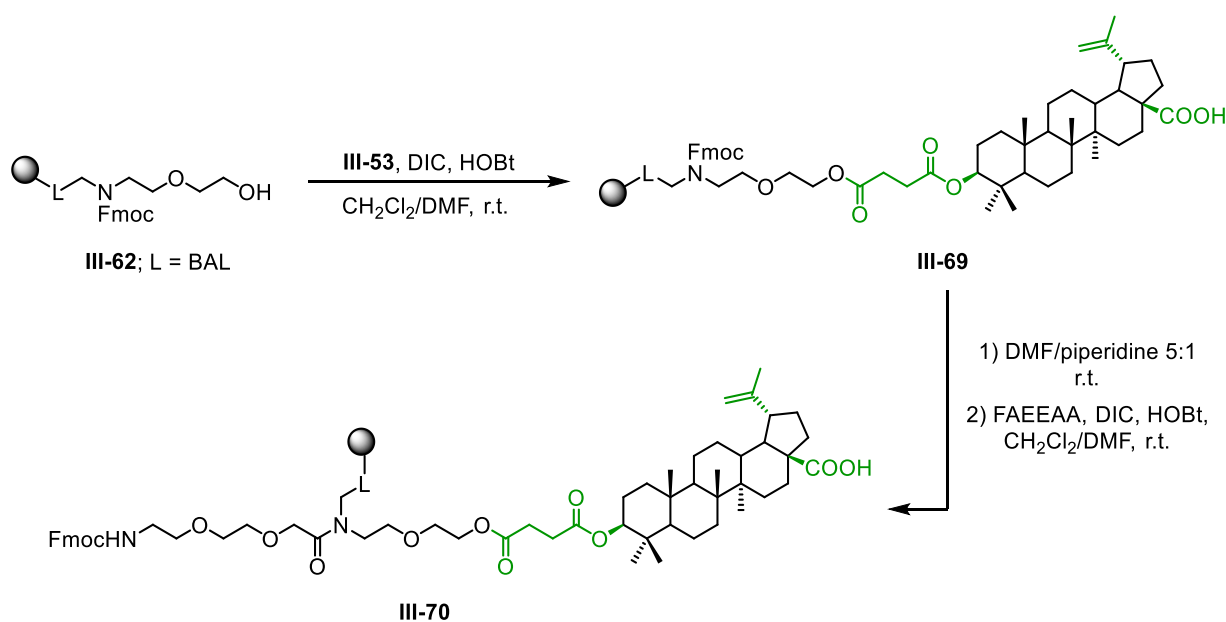


Figure 39.

Pathway B

Along with simultaneous optimization of pathway A, we have been also developing other possible synthetic approaches. Despite the fact, that we were able to attach triterpene moiety on Fmoc intermediate **III-62** (Scheme 47), the reaction was never quantitative (presumably due to the steric reasons) and it needed repetition. Moreover, after deprotection of Fmoc, the acylation reaction with FAEEAA also needed to be repeated to reach full conversion of **III-70**. For this reason, we chose to leave this approach and focus to more efficient alternatives.



Scheme 47.

Pathway C

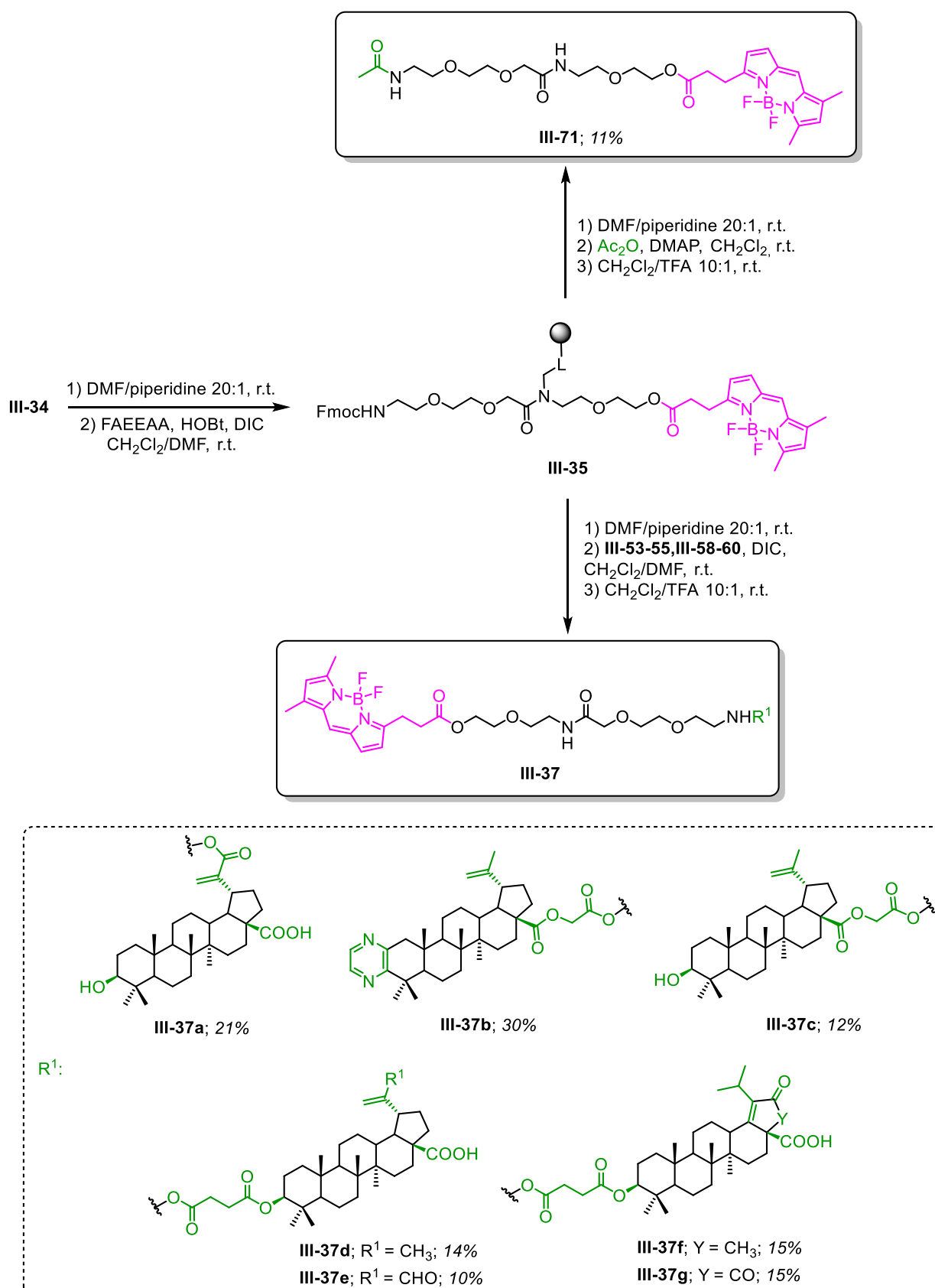
As we were able to optimize Fmoc deprotection conditions as well as attachment of BODIPY **III-52** during synthesis of final compound **III-37d** without loss of fluorescent activity or rapid decomposition of the BODIPY scaffold, we decided to shorten the reaction sequence. The modification consisted in elimination of the protection step with TBDPS and direct attachment of BODIPY dye in the beginning of the reaction

sequence. The greatest advantage of this pathway lied on fact that the synthesis was shorter by two steps.

Therefore, after acylation with BODIPY and deprotection of Fmoc under optimized conditions, we successfully attached FAEEAA linker to obtain preloaded resin **III-35** (Scheme 48). The following deprotection of Fmoc and DIC promoted coupling with premodified triterpenes **III-53-55**, **III-58-60** yielded final products **III-37** (Scheme 48), upon cleavage from the polymer support.

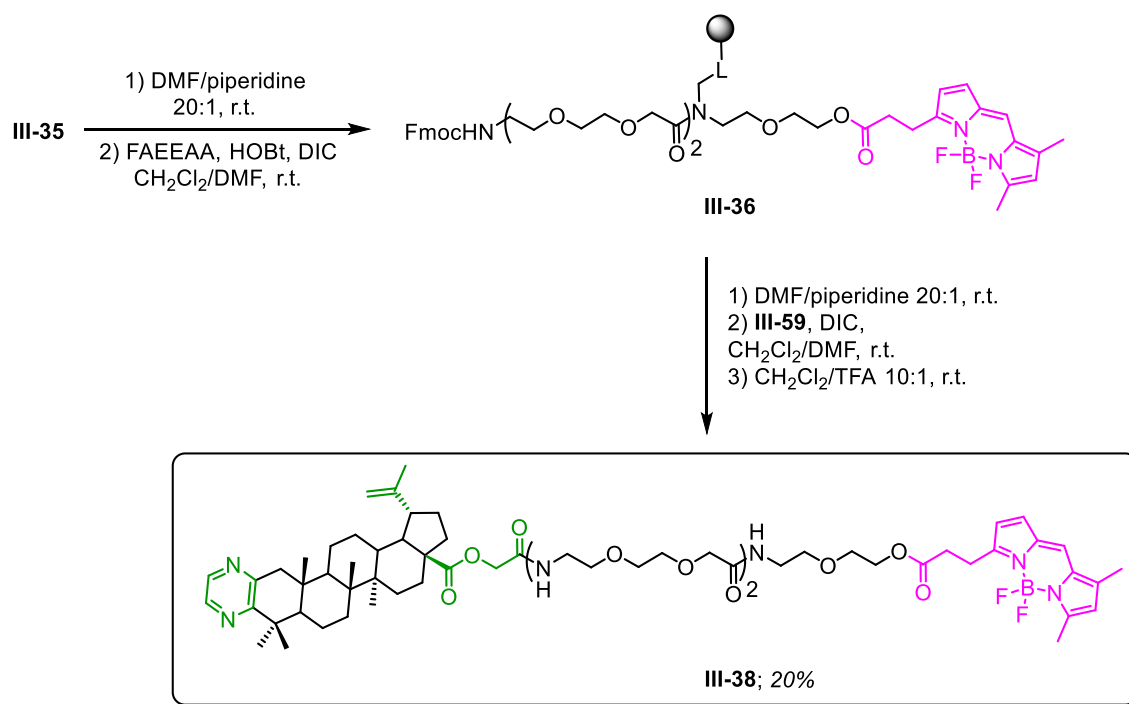
Final product **III-71** was prepared from **III-35** (Scheme 48) using acetic anhydride in presence of DMAP, as a negative control for biological tests. The purpose of this compound was to demonstrate that the cell penetration and targeting the organelles depended on the triterpene scaffold and not on the BODIPY core (for more information see Chapter 2.3.3.).

Compounds were prepared in good crude purities and overall yields (after semipreparative HPLC-purification), which were sufficiently enough for further biological evaluation.



Scheme 48. Scheme of final conjugates.

To determine the impact of linker's length on cell targeting, elongation of the spacer to **III-36** and subsequent acylation with pyrazine **III-59** (Scheme 49) to obtain final compound **III-38** was performed.

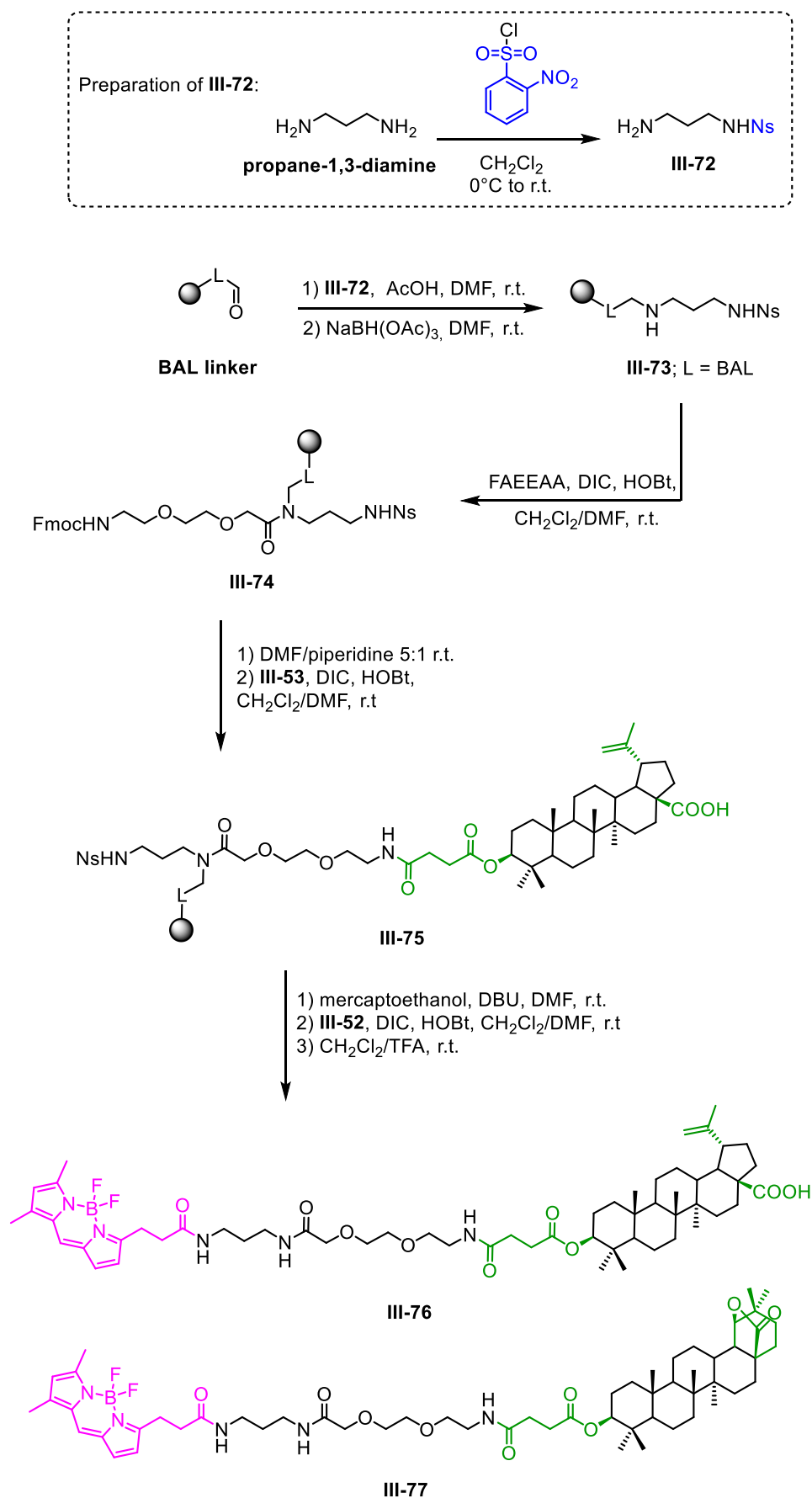


Scheme 49.

Different strategies to obtain the target conjugates

Because we wished to examine also other possibilities of linker preparation,^[255] we simultaneously investigated alternative route towards final compounds. Accordingly, the commercially available propane-1,3-diamine was reacted with 2-nitrobenzene sulfonyl chloride (nosyl chloride) and the product **III-72** was immobilized to BAL resin using reductive amination to **III-73** (Scheme 50). Nosyl group represents another suitable option of amine protection widely used in solid-phase synthesis. Following acylation with FAEEAA provided intermediate **III-74**.

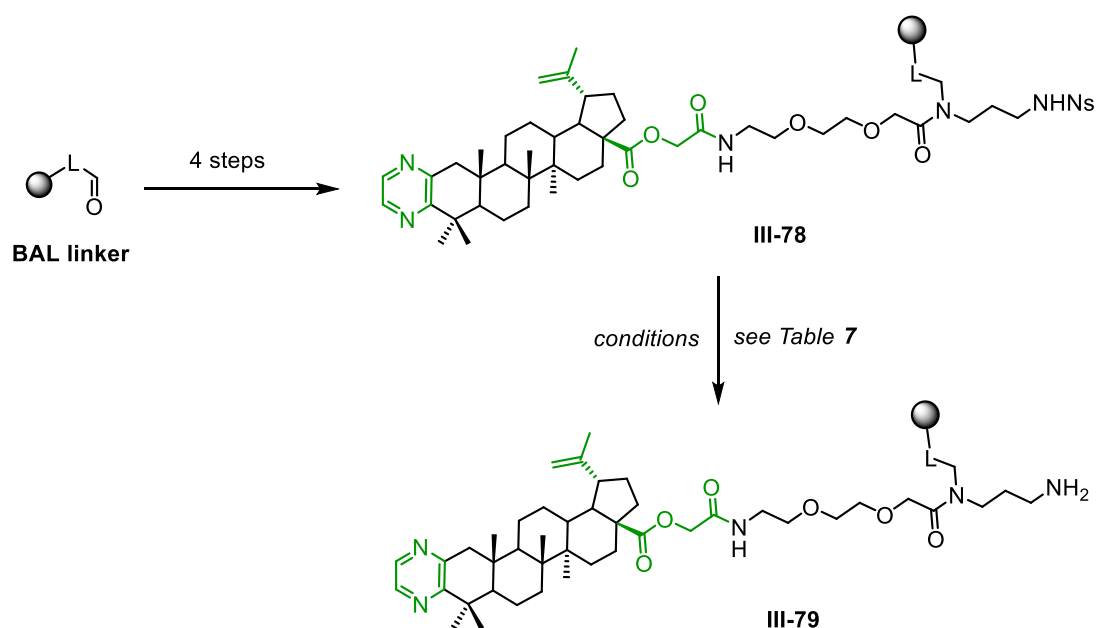
After chemoselective deprotection of Fmoc, the acylation with triterpene **III-53** was performed (Scheme 50). The decision to choose this strategy over the acylation reaction with BODIPY was based on our experience with instability of the core under nosyl deprotection conditions, which require higher concentration of base and nucleophile (thiolate). Following deprotection of nosyl group and attachment of BODIPY **III-52** yielded conjugate **III-76**. We again isolated product of rearrangement **III-77** mentioned above that arised after acid-mediated cleavage from the resin.



Scheme 50.

However, synthesis of the rest of desired conjugates seemed to be surprisingly difficult. When we used another immobilized triterpenes, particularly pyrazine **III-78** and diketone **III-80** that were prepared after 4 steps from BAL linker accordingly to the procedures above, we have not been able to cleave the nosyl group from.

In case of pyrazine derivative **III-78**, we often observed very low conversion to product (and majority of starting material; Table 8, cond. a – e, h, i). Luckily, use of more concentrated cocktail of thiophenol and DBU at elevated temperature (cond. f, g) yielded desired intermediate **III-79** (Scheme 51).

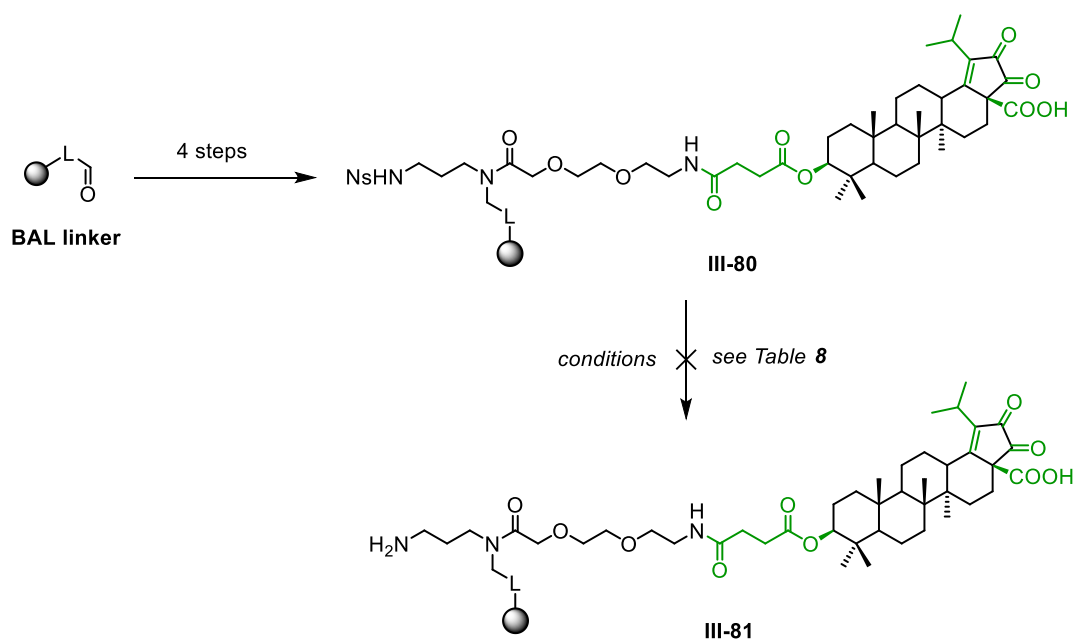


| # | Base | Conc.[M] | Thiol | Conc.[M] | Solvent | Temp. | React. time | Observation |
|----|------|----------|---------------------|----------|---------|-------|-------------|---------------|
| a. | DBU | 0.3 | mercaptoethano 1 | 0.6 | DMF | 50°C | 30 min | III-78 |
| b. | DBU | 0.3 | mercaptoethano 1 | 0.6 | DMF | 50°C | 90 min | III-78 |
| c. | DBU | 0.3 | mercaptoethano 1 | 0.6 | DMF | 50°C | 3 h | III-78 |
| d. | DBU | 0.3 | thiophenol | 0.6 | DMF | r.t. | 90 min | III-78 |
| e. | DBU | 0.6 | thiophenol | 0.6 | DMF | 50°C | 16 h | III-78 |
| f. | DBU | 1 | thiophenol | 1 | DMF | 75°C | 16 h | III-79 |

| | | | | | | | | |
|----|------|---|------------|---|--------------------|------|------|---------------|
| g. | DBU | 1 | thiophenol | 1 | CH ₃ CN | 75°C | 16 h | III-79 |
| h. | BTTP | 1 | thiophenol | 1 | DMF | r.t. | 16 h | III-78 |
| i. | DBU | 1 | thiophenol | 1 | CH ₃ CN | r.t. | 16 h | III-78 |

Table 8.

Unfortunately, deprotection of polymer bounded diketone **III-80**, which was prepared with same route as pyrazine before, was not successful whatsoever (Scheme 52). Various conditions (Table 9) led only to the formation of unknown side-products (cond. a, b) or full decomposition of starting material (cond. c, d, e). Further, analysis of this intermediate was complicated by missing chromophore in the structure **III-81**, thus we had to reckon its presence only by corresponding mass in UHPLC-MS traces.



Scheme 52.

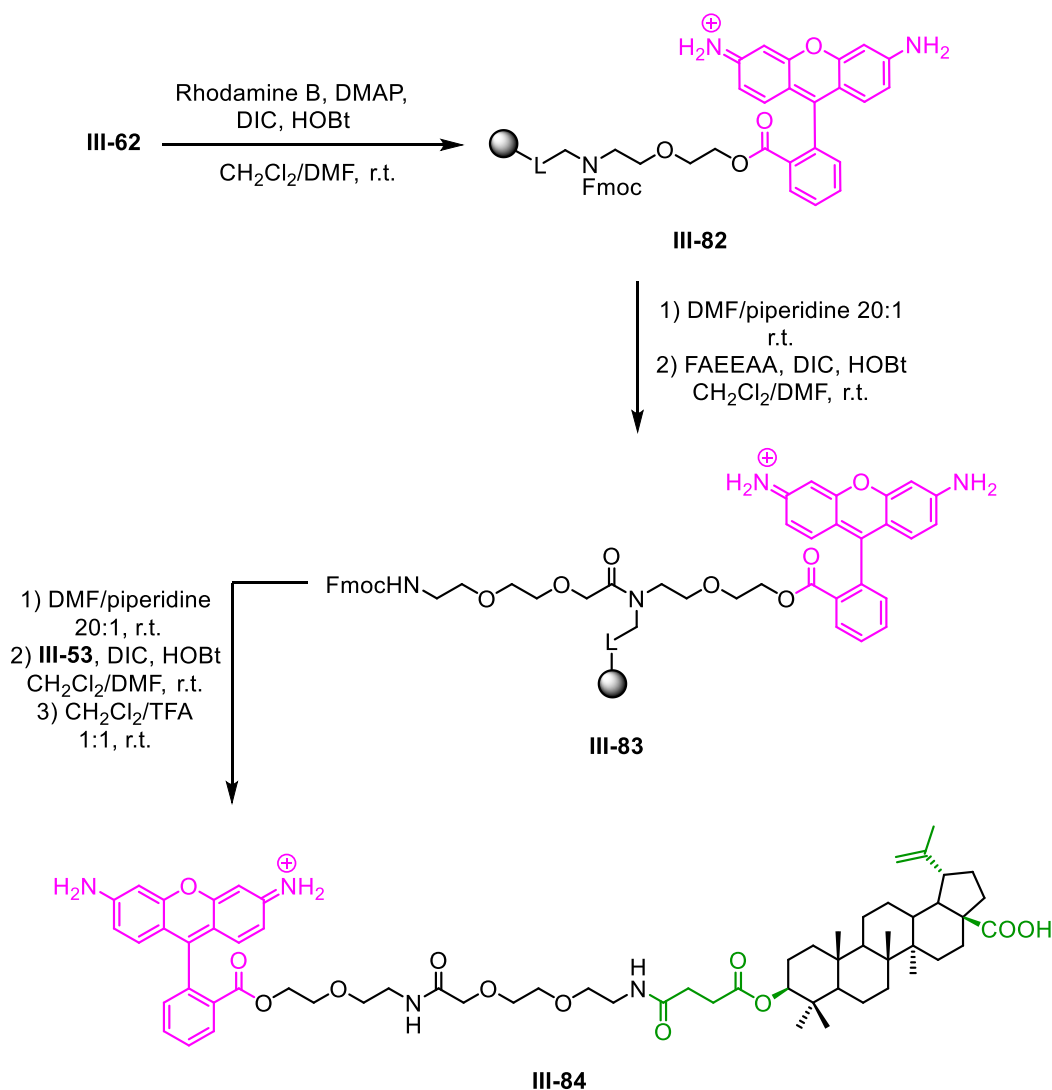
| # | Base | Conc.[M] | Thiol | Conc.[M] | Solvent | Temp. | React. time | Observation |
|----|------|----------|---------------------|----------|--------------------|-------|-------------|----------------------|
| a. | DBU | 0.3 | mercaptoethano l | 0.3 | DMF | 50°C | 90 min | <i>Side-products</i> |
| b. | DBU | 0.3 | thiophenol | 0.6 | DMF | r.t. | 90 min | <i>Side-products</i> |
| c. | DBU | 1 | thiophenol | 1 | DMF | 75°C | 16 h | <i>decomposition</i> |
| d. | DBU | 1 | thiophenol | 1 | CH ₃ CN | r.t. | 16 h | <i>decomposition</i> |
| e. | DBU | 1 | thiophenol | 1 | CH ₃ CN | 75°C | 16 h | <i>decomposition</i> |
| f. | BTTP | 1 | thiophenol | 1 | DMF | r.t. | 16 h | III-80 |

Table 9.

Although we have been able to prepare two final compounds **III-76** and **III-77**, the problem with smooth and easy deprotection of nosyl functionality was a major drawback and we decided to focus rather on the abovementioned pathway with amino ethoxyethanol.

Different choice of dye

Alternative fluorescent dye to be used as the label was also studied and one conjugate bearing triterpene **III-53** and Rhodamine B was prepared (Scheme 53). As in the previous case, the 28-oxyallobetulin product of rearrangement was observed as the by-product. However, due to high non-polarity of the compounds was almost impossible to successfully perform purification using both RP-HPLC and silica gel chromatography. From this reason, preparation of another conjugates containing Rhodamine B was discontinued.



Scheme 53.

2.3.2.4. Photochemical measurements

All the prepared final conjugates **III-37**, **III-38**, **III-71**, with amino ethoxyethanol linker, were subjected to measurements of their absorption and emission spectra and calculation of their quantum yields of fluorescence (Φ), in order to examine the impact of triterpene core on this phenomenon.

Surprisingly, we observed a quenching of fluorescence intensity by triterpene moiety, varying between 0.14 – 0.30 (Table 10), compare to BODIPY FL propanoic acid **III-52** itself ($\Phi = 0.98$). To support this theory, quantum yield of fluorescence of compound **III-71** was also calculated with value 0.71, indicating that the quenching is caused by triterpene scaffold. The graphical representations of conjugates **III-37b** and **III-71** are depicted on Figure 40.

| Compound | Φ | Compound | Φ |
|----------------|--------|----------------|--------|
| III-52 | 0.98 | III-37e | 0.14 |
| III-37a | 0.17 | III-37f | 0.25 |
| III-37b | 0.21 | III-37g | 0.26 |
| III-37c | 0.17 | III-38 | 0.30 |
| III-37d | 0.20 | III-71 | 0.71 |

Table 10.

Such observation could be explained by so called *static quenching* between BODIPY dye and triterpenes, presumably due to the hydrophobic effects, which was recently described in literature,^[256,257]. Noteworthy, this observation did not interfere with the subsequent fluorescent microscopy measurements.

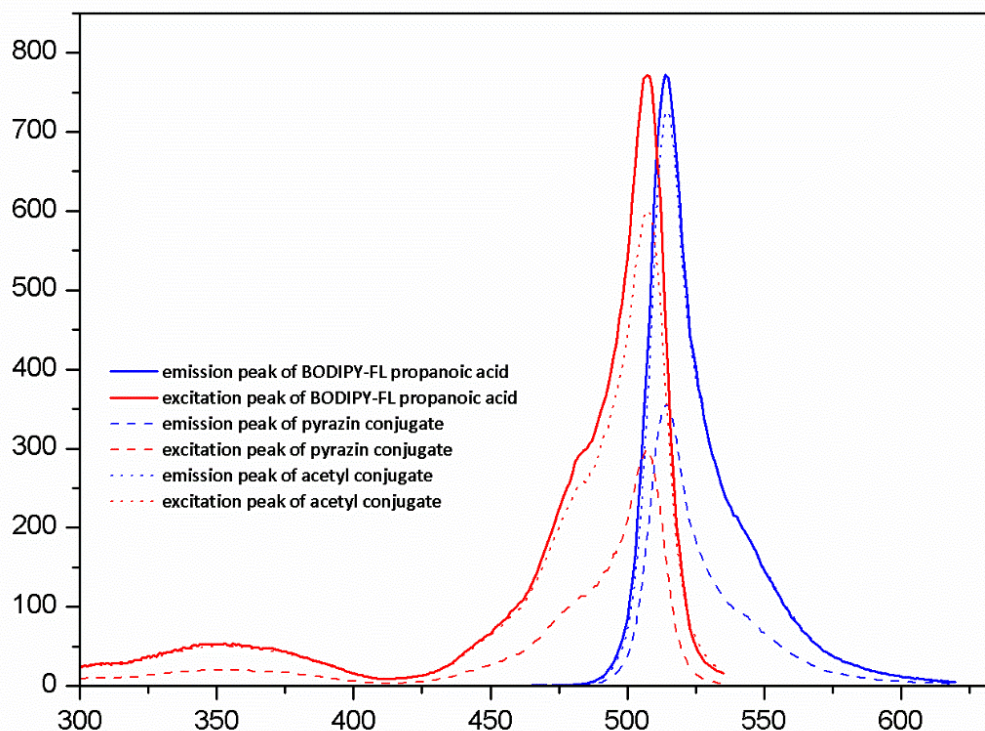


Figure 40.

2.3.3. Biology

The conjugates **III-37**, **III-38**, **III-71**, which were prepared by the most suitable, convenient and general pathway mentioned above, were subjected to measurements of their cytotoxic activity and to fluorescence microscopy, to investigate their distribution within cells. These measurements were provided by P. Džubák group.

The cytotoxic activity of the parent compounds **III-39-43** and fluorescent conjugates was investigated *in vitro* against eight human cancer cell lines and two non-tumor fibroblasts. The cancer cell lines were derived from T-lymphoblastic leukemia CCRF-CEM, leukemia K562 and their multiresistant counterparts (CEM-DNR, K562-TAX), solid tumors including lung (A549) and colon (HCT116, HCT116p53-/-) carcinomas, osteosarcoma cell line (U2OS), and, for comparison, on two human non-cancer fibroblast lines (BJ, MRC-5). In general, the CCRF-CEM cell line was the most sensitive cancer cell line to the prepared compounds, with only a few exceptions. Therefore, SARs assumptions were mostly based on the activities in CCRF-CEM cells.

Among the parental compounds, aldehyde of betulinic acid **III-40** and pyrazine **III-43** were cytotoxic against the CCRF-CEM line in the low micromolar range. The therapeutic index is rather low for aldehyde **III-40** but surprisingly high in the case of

pyrazine (Table 11). The synthesized fluorescent conjugate of aldehyde **III-37e** remained highly but unselectively cytotoxic, probably due to the presence of the reactive acrolein moiety.

Comparing two fluorescent conjugates of pyrazine (**III-37b** and **III-38**), with normal and elongated version of the spacer, respectively, the slight decrease of activity and selectivity in comparison with the parent compound **III-43** was observed. Therefore, the free carboxylic group plays an important role as a pharmacophore on triterpenic core. Interestingly, the length of the linker also affects the activity of the conjugates, where the longer derivative **III-38** was more active than the shorter one **III-37b**.

In case of diketone conjugate **III-37g**, only the cytotoxicity on CCRF-CEM cell line was observed, whereas the monoketone conjugate **III-37f** completely lost both its cytotoxic activity and selectivity.

The hemisuccinic modification of betulinic acid **III-37d** at the position C³ remained active, although its conjugates at positions C²⁸ and C³⁰ (compounds **III-37c** and **III-37a**, respectively) were almost inactive, which indicated importance of free carboxylic group and allylic motive as the pharmacophores. This was proved also when we tested 28-oxyallobetulin conjugate **III-68**, which showed no cytotoxic activity whatsoever.

| Comp. | IC ₅₀ (μM/L) ^a | | | | | | | | | | |
|---------------------------|--------------------------------------|---------|---------|--------------|-------|----------|-------|-------|-------|-------|-----------------|
| | CCRF-CEM | CEM-DNR | HCT 116 | HCT116p53-/- | K562 | K562-TAX | A549 | U2OS | BJ | MRC-5 | TI ^b |
| III-39^c | 8.09 | 14.04 | 4.29 | 14.09 | 9.43 | 15.78 | 15.96 | 20.75 | 24.23 | 28.18 | 3.24 |
| III-40^c | 1.53 | 7.66 | 8.83 | 12.43 | 9.68 | 7.73 | 7.23 | 7.51 | 11.99 | 2.39 | 4.70 |
| III-41^c | 15.16 | 20.16 | 27.25 | 34.67 | 21.01 | 24.25 | 27.12 | 40.06 | 44.28 | 42.67 | 2.87 |
| III-42^c | 35.58 | 35.98 | >50 | 43.11 | >50 | >50 | >50 | >50 | >50 | >50 | >1.41 |
| III-43^c | 0.53 | 0.63 | 11.54 | 11.6 | 31.84 | 34.41 | 47.3 | 32.43 | >50 | >50 | >94.34 |
| III-37d | 6.62 | >50 | >50 | >50 | >50 | >50 | >50 | 33.75 | 43.61 | 43.6 | 6.59 |
| III-37e | 0.76 | 6.06 | 1.65 | 10.52 | 1.96 | 1.6 | 1.45 | 1.46 | 1.87 | 1.62 | 2.30 |
| III-37f | >50 | >50 | >50 | >50 | >50 | >50 | >50 | >50 | >50 | >50 | N.A. |
| III-37g | 3.4 | >50 | 45.7 | >50 | >50 | >50 | >50 | >50 | 45.84 | 44.26 | 13.25 |
| III-37b | 18.09 | 20.28 | >50 | >50 | >50 | >50 | >50 | >50 | >50 | >50 | >2.76 |
| III-38 | 6.13 | 9.27 | 18.92 | 12.07 | 29.02 | 35.05 | 29.14 | 26.34 | 39.74 | 38.23 | 6.36 |
| III-37c | >50 | >50 | >50 | >50 | >50 | >50 | >50 | >50 | >50 | >50 | N.A. |

| | | | | | | | | | | | |
|----------------|-------|-------|-------|-----|-------|------|-------|-------|-------|-------|------|
| III-37a | 41.17 | 40.68 | 41.96 | >50 | 49.02 | 40.6 | 41.43 | 45.02 | 48.81 | 40.75 | 1.09 |
| III-68 | >50 | >50 | >50 | >50 | >50 | >50 | >50 | >50 | >50 | >50 | N.A. |
| III-71 | >50 | >50 | >50 | >50 | >50 | >50 | >50 | >50 | >50 | >50 | N.A. |

^aThe lowest concentration that kills 50 % of the cells. The standard deviation in cytotoxicity assays is typically up to 15 % of the average value. ^bTherapeutic index is calculated for IC₅₀ of CCRF-CEM line vs. an average of both fibroblasts (BJ and MRC-5). ^cParent compounds used as a standard. Compounds with IC₅₀ > 50 μ M are considered inactive.

Table 11. Cytotoxic activity of prepared conjugates compared to parental counterparts. (Red color = cancer cell lines; Green color = fibroblasts; Blue color = therapeutic index)

Following fluorescent microscopy experiments revealed that all the tested fluorescent conjugates stain living cells and pass through the cellular membrane into the cytoplasmic compartment (Figure 41). In addition, we used acetyl BODIPY conjugate **III-71** as a negative control to prove, that the triterpenoid part is responsible for the cellular uptake. This observation is in accordance with high lipophilicity of triterpenes.

In case of aldehyde conjugate **III-37e**, the very reactive acrolein moiety resulted in a different staining pattern labeling cellular cytoplasm homogenously, which is presumably caused by nonspecific covalent interaction with multiple intracellular proteins. Staining is distinct when compared to other tested compounds (**III-37a-d,f,g** and **III-38**), which labeled subtler cytoplasmic and membrane structures, likely mitochondria, endoplasmic reticulum (ER), and the nuclear membrane. Co-staining experiments are being performed to confirm this unambiguously. Such results are consistent with precedent studies on another lupane triterpenes that were found to interact with mitochondrion and ER.^[258,259]

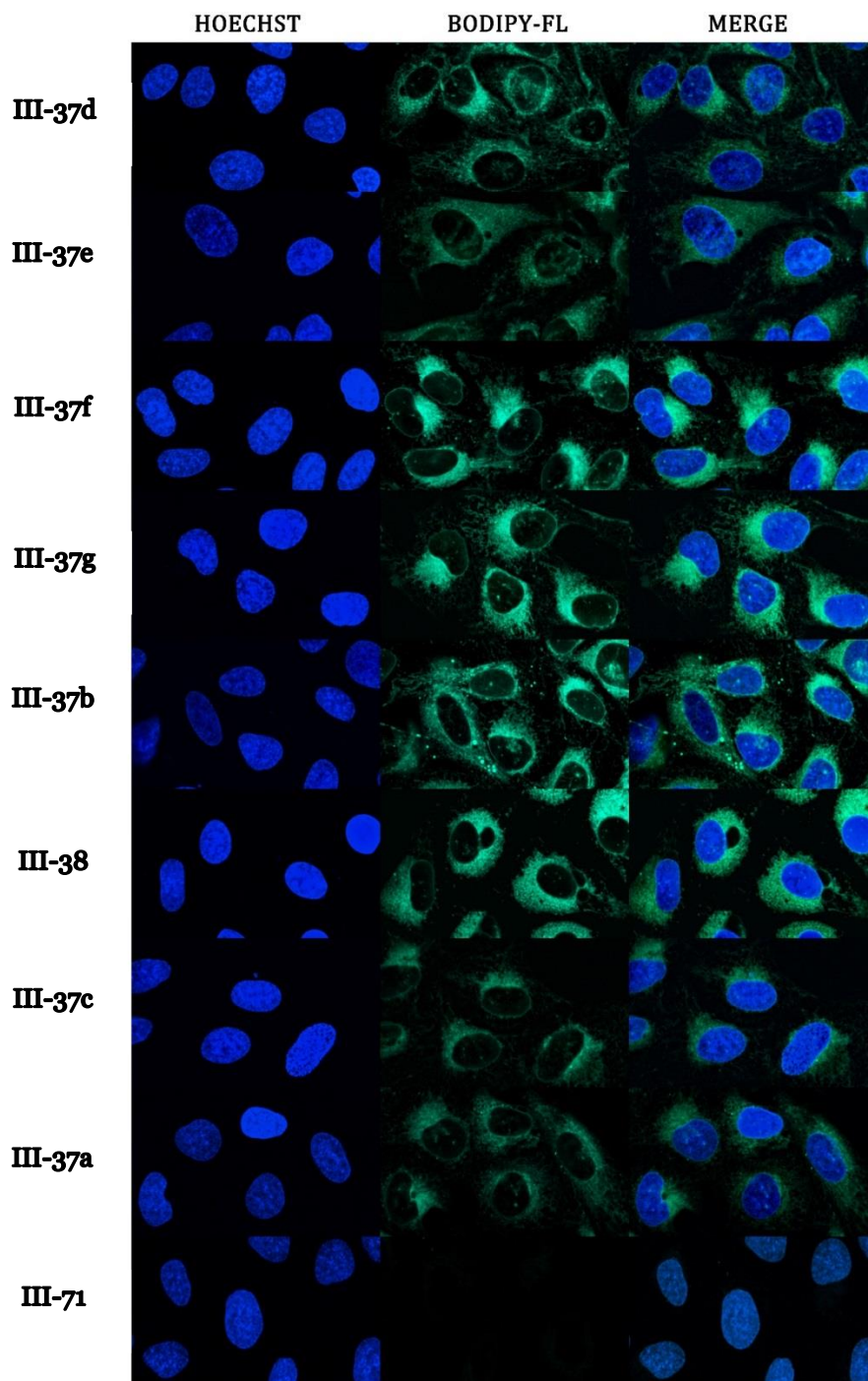


Figure 41.

2.3.4. Conclusion

We successfully optimized the route towards the fluorescently labeled preloaded resins **III-35** and **III-36**, followed by the synthesis of final compounds **III-37**, **III-38** with corresponding parental triterpenes. We also synthesized, yet commercially available but rather expensive, BODIPY-FL propanoic acid **III-52** with modified synthesis to give better yields and suitable also for multigram scale quantities.

The synthetic route towards preloaded resins had to be modified significantly. The choice of amino ethoxyethanol, as the most suitable linker, was based on its ability to orthogonal attachment of silyl based protecting groups, that required mild deprotection conditions. The whole sequence could also be approached with direct attachment of BODIPY dye. Despite previous reports on the limited applicability of BODIPYs in solid-phase synthesis,^[183,243,244] due to their low stability under both basic and acidic conditions, we developed and optimized synthetic protocols to overcome these problems.

The prepared preloaded resins allow for routine, rapid and simple conjugation of various compounds (not necessarily triterpenes) possessing suitable functional groups to the BODIPY label through an ethylene-oxy linker of various lengths. The preloaded resin can be applied using simple laboratory equipment, common coupling reagents and conditions, and minimum *hands-on-time*, and it can even be commercialized similarly to biotin-preloaded resin (Biotin NovaTagQ, Novabiochem).

Final conjugates of BODIPY and cytotoxic triterpenes, bearing amino ethoxyethanol linker, were synthesized and their spectroscopic and biological properties were evaluated. To prove that BODIPY with the linker do not interfere with the biological study, we prepared a conjugate in which the triterpenic part was replaced with acetate (conjugate **III-71**). Live cell studies focused on fluorescence conjugate uptake demonstrated nonspecific labeling in aldehyde **III-37e** and a more specific labeling pattern in the case of conjugates **III-37a-d,f,g** and **III-38**.

Ongoing research is now focused on a more specific determination of which organelles, proteins or protein complexes are targeted by our conjugates, and this will be the aim of further proteomic and molecular biology studies, for example, co-localization experiments.

2.3.5. Authors' contributions

As main author of the publication,^[182] I developed and optimized the synthetic route towards the final compounds, synthesized all compounds both in solution and on solid-phase, fully characterized (NMR, HRMS, UHPLC-MS, quantum yields of fluorescence) all of them, including pre-modified triterpenes and BODIPY dye. I also wrote major part of the manuscript (except for the biological evaluation, which was provided and written by J.S. and P.D.) and I also participated to the fluorescence microscopy measurements (which was provided by J.S.).

2.4. Summary

According to the results summarized in this thesis I can conclude that all aims defined at the beginning were satisfactorily fulfilled.

In the first project, dealing with synthesis of tumor targeted delivery system for purine CDK inhibitors, we successfully developed and optimized the high-throughput synthetic route towards the final compounds. The most potent conjugate was subjected to the *in vitro* simulation of disulfide reduction, which proved the linker can undergo self-immolative cleavage. This demonstrates the applicability of our conjugates to release the inhibitor. Flow cytometric measurements further demonstrated the ability of an example conjugate to bind to cancer cells overexpressing the folate receptor. Detailed studies of conjugates cellular selectivity are still in progress.

Second project also resulted in successful optimization of reaction pathway, this time towards thalidomide-preloaded resins applicable for general use in PROTACs area. We successfully synthesized 6 conjugates of thalidomide and protein kinases inhibitors, with selective kinase targeting. Also, two preloaded resins with longer and shorter version of the linker were successfully prepared. The kinase inhibitory activity and degradation study proved applicability of our proposed system.

In the last project, we developed BODIPY-preloaded resins applicable for rapid and simple preparation of fluorescently labelled conjugates using solid-phase synthesis, which required careful optimization since BODIPY core is rather unstable under strong acidic and basic conditions. After conjugation with set of representative triterpenes, selected according to their low micromolar cytotoxic activity and/or unknown mechanism of action, we provided their preliminary study inside cells with use of fluorescent microscopy. More detailed co-localization studies are currently underway.

For me personally, it was an absolute pleasure to work on such research projects. Although I had almost no previous experience with solid-phase synthesis when I started my PhD study, I adapted to this technique quickly, smoothly and with ease. Moreover, I surely improved my synthetic skills in way of solution-phase synthesis during the process as well. I also appreciate the opportunity to participate in fluorescent microscopy measurements and independently provided measurements of quantum yields of fluorescence. Also, my ability to understand biological aspects and backgrounds of the prepared compounds enhanced hugely during this past few years and I humbly appreciate all the fruitful discussions.

And last, but not least, I am immensely thankful for the opportunity to serve as an NMR operator at our department, which enabled me to understand much more deeply the aspects of this beautiful analytical technique.

2.5. Literature

- [1] R. B. Merrifield, *J. Am. Chem. Soc.* **1963**, *85*, 2149–2154.
- [2] S. L. Beaucage, M. H. Caruthers, *Tetrahedron Lett.* **1981**, *22*, 1859–1862.
- [3] B. C. Froehler, P. G. Ng, M. D. Matteucci, *Nucleic Acids Res.* **1986**, *14*, 5399–5407.
- [4] P. Nielsen, M. Egholm, R. Berg, O. Buchardt, *Science* **1991**, *254*, 1497–1500.
- [5] H. Challa, S. A. Woski, *Tetrahedron Lett.* **1999**, *40*, 8333–8336.
- [6] C. Schuerch, J. M. Frechet, *J. Am. Chem. Soc.* **1971**, *93*, 492–496.
- [7] S. Danishefsky, K. McClure, J. Randolph, R. Ruggeri, *Science* **1993**, *260*, 1307–1309.
- [8] O. J. Plante, *Science* **2001**, *291*, 1523–1527.
- [9] C. C. Leznoff, *Acc. Chem. Res.* **1978**, *11*, 327–333.
- [10] J. M. J. Fréchet, *Tetrahedron* **1981**, *37*, 663–683.
- [11] B. A. Bunin, J. A. Ellman, *J. Am. Chem. Soc.* **1992**, *114*, 10997–10998.
- [12] E. A. Couladouros, A. D. Magos, *Mol. Divers.* **2005**, *9*, 111–121.
- [13] A. Hayata, H. Itoh, M. Inoue, *J. Am. Chem. Soc.* **2018**, *140*, 10602–10611.
- [14] I. R. Marsh, M. Bradley, S. J. Teague, *J. Org. Chem.* **1997**, *62*, 6199–6203.
- [15] F. Guillier, D. Orain, M. Bradley, *Chem. Rev.* **2000**, *100*, 3859.
- [16] A. B. Hughes, Ed., *Amino Acids, Peptides and Proteins in Organic Chemistry*, Wiley-VCH, Weinheim, **2009**.
- [17] S.-Sun. Wang, *J. Am. Chem. Soc.* **1973**, *95*, 1328–1333.
- [18] M. Mergler, R. Tanner, J. Gosteli, P. Grogg, *Tetrahedron Lett.* **1988**, *29*, 4005–4008.
- [19] M. Mergler, R. Nyfeler, R. Tanner, J. Gosteli, P. Grogg, *Tetrahedron Lett.* **1988**, *29*, 4009–4012.
- [20] R. Santini, M. C. Griffith, M. Qi, *Tetrahedron Lett.* **1998**, *39*, 8951–8954.
- [21] R. P. Iyer, M.-J. Guo, D. Yu, S. Agrawal, *Tetrahedron Lett.* **1998**, *39*, 2491–2494.
- [22] P. Králová, V. Fülöpová, M. Maloň, T. Volná, I. Popa, M. Sural, *ACS Comb. Sci.* **2017**, *19*, 173–180.
- [23] C. M. L. Delpiccolo, M. A. Fraga, E. G. Mata, *J. Comb. Chem.* **2003**, *5*, 208–210.
- [24] S. Bräse, J. H. Kirchoff, J. Köbberling, *Tetrahedron* **2003**, *59*, 885–939.
- [25] A. Skogh, S. D. Friis, T. Skrydstrup, A. Sandström, *Org. Lett.* **2017**, *19*, 2873–2876.
- [26] R. G. Franzen, *Top. Catal.* **2016**, *59*, 1143–1150.
- [27] S. N. Khan, A. Kim, R. H. Grubbs, Y.-U. Kwon, *Org. Lett.* **2011**, *13*, 1582–1585.
- [28] International Human Genome Sequencing Consortium, *Nature* **2001**, *409*, 860–921.
- [29] G. M. Rubin, M. D. Yandell, J. R. Wortman, G. L. Gabor Miklos, C. R. Nelson, I. K. Hariharan, M. E. Fortini, P. W. Li, R. Apweiler, W. Fleischmann, et al., *Science* **2000**, *287*, 2204–2215.
- [30] R. Roskoski, *Pharmacol. Res.* **2015**, *100*, 1–23.
- [31] M. E. M. Noble, *Science* **2004**, *303*, 1800–1805.
- [32] G. Manning, *Science* **2002**, *298*, 1912–1934.
- [33] J. Martin, K. Anamika, N. Srinivasan, *PLoS ONE* **2010**, *5*, e12460.
- [34] G. Manning, G. D. Plowman, T. Hunter, S. Sudarsanam, *Trends Biochem. Sci.* **2002**, *27*, 514–520.
- [35] B. Kloss, J. L. Price, L. Saez, J. Blau, A. Rothenfluh, C. S. Wesley, M. W. Young, *Cell* **1998**, *94*, 97–107.
- [36] S. Lemeer, A. J. Heck, *Curr. Opin. Chem. Biol.* **2009**, *13*, 414–420.
- [37] J. A. Adams, *Chem. Rev.* **2001**, *101*, 2271–2290.
- [38] P. A. Schwartz, B. W. Murray, *Bioorganic Chem.* **2011**, *39*, 192–210.
- [39] J. V. Olsen, B. Blagoev, F. Gnad, B. Macek, C. Kumar, P. Mortensen, M. Mann, *Cell* **2006**, *127*, 635–648.
- [40] D. E. Thurston, *Chemistry and Pharmacology of Anticancer Drugs*, CRC Press/Taylor & Francis, Boca Raton, **2007**.
- [41] S. Srivastava, Z. Li, K. Ko, P. Choudhury, M. Albaqumi, A. K. Johnson, Y. Yan, J. M. Backer, D. Unutmaz, W. A. Coetzee, et al., *Mol. Cell* **2006**, *24*, 665–675.
- [42] D. R. Knighton, J. H. Zheng, L. F. Ten Eyck, V. A. Ashford, N. H. Xuong, S. S. Taylor, J. M. Sowadski, *Science* **1991**, *253*, 407–414.

- [43] H. M. Berman, J. Westbrook, Z. Feng, G. Gilliland, T. N. Bhat, H. Weissig, I. N. Shindyalov, P. E. Bourne, *Nucleic Acids Res.* **2000**, *28*, 235–242.
- [44] N.d.
- [45] M. Huse, J. Kuriyan, *Cell* **2002**, *109*, 275–282.
- [46] R. S. K. Vijayan, P. He, V. Modi, K. C. Duong-Ly, H. Ma, J. R. Peterson, R. L. Dunbrack, R. M. Levy, *J. Med. Chem.* **2015**, *58*, 466–479.
- [47] D. K. Treiber, N. P. Shah, *Chem. Biol.* **2013**, *20*, 745–746.
- [48] J. Zhang, P. L. Yang, N. S. Gray, *Nat. Rev. Cancer* **2009**, *9*, 28–39.
- [49] R. Roskoski, *Pharmacol. Res.* **2016**, *103*, 26–48.
- [50] M. I. Davis, J. P. Hunt, S. Herrgard, P. Ciceri, L. M. Wodicka, G. Pallares, M. Hocker, D. K. Treiber, P. P. Zarrinkar, *Nat. Biotechnol.* **2011**, *29*, 1046–1051.
- [51] S. Maddox, D. Hecht, J. L. Gustafson, *Future Med. Chem.* **2016**, *8*, 241–244.
- [52] J. Pollier, A. Goossens, *Phytochemistry* **2012**, *77*, 10–15.
- [53] J. S. Dahiya, *Phytochemistry* **1991**, *30*, 1235–1237.
- [54] Z. Wang, H. Zhang, W. Yuan, W. Gong, H. Tang, B. Liu, K. Krohn, L. Li, Y. Yi, W. Zhang, *Food Chem.* **2012**, *132*, 295–300.
- [55] M. Laszczyk, *Planta Med.* **2009**, *75*, 1549–1560.
- [56] J. J. Ramírez-Espinosa, M. Y. Rios, P. Paoli, V. Flores-Morales, G. Camici, V. de la Rosa-Lugo, S. Hidalgo-Figueroa, G. Navarrete-Vázquez, S. Estrada-Soto, *Eur. J. Med. Chem.* **2014**, *87*, 316–327.
- [57] R. Paduch, M. Kandefér-Szerszen, *Mini-Rev. Org. Chem.* **2014**, *11*, 262–268.
- [58] E. A. Mireku, A. Y. Mensah, I. K. Amponsah, C. A. Danquah, D. Anokwah, M. Kwesi Baah, *Nat. Prod. Res.* **2018**, 1–4.
- [59] C.-M. Wang, H.-T. Chen, Z.-Y. Wu, Y.-L. Jhan, C.-L. Shyu, C.-H. Chou, *Molecules* **2016**, *21*, 139.
- [60] C. Beaufay, M.-F. Hérent, J. Quetin-Leclercq, J. Bero, *Malar. J.* **2017**, *16*, DOI 10.1186/s12936-017-2054-y.
- [61] E.-Q. Xia, B.-W. Wang, X.-R. Xu, L. Zhu, Y. Song, H.-B. Li, *Int. J. Mol. Sci.* **2011**, *12*, 5319–5329.
- [62] P. Yogeewari, D. Sriram, *Curr. Med. Chem.* **2005**, *12*, 657–666.
- [63] P. Šiman, A. Filipová, A. Tichá, M. Niang, A. Bezrouk, R. Havelek, *PLoS One* **2016**, *11*, e0154933.
- [64] K. Surendra, E. J. Corey, *J. Am. Chem. Soc.* **2009**, *131*, 13928–13929.
- [65] S. Arseniyadis, R. Rodriguez, J. Camara, J. F. Gallard, E. Guittet, L. Toupet, G. Ourisson, *Tetrahedron* **1995**, *51*, 9947–9972.
- [66] M. Ogura, G. A. Cordell, R. Farnsworth, *Lloydia* **1977**, *40*, 157–168.
- [67] K. Sheth, S. Jolad, R. Wiedhopf, J. R. Cole, *J. Pharm. Sci.* **1972**, *61*, 1819.
- [68] J. Šarek, J. Klinot, P. Džubák, E. Klinotová, V. Nosková, V. Křeček, G. Kořínková, J. O. Thomson, A. Janošťáková, S. Wang, et al., *J. Med. Chem.* **2003**, *46*, 5402–5415.
- [69] R. H. Cichewicz, S. A. Kouzi, *Med. Res. Rev.* **2004**, *24*, 90–114.
- [70] D. S. H. L. Kim, Z. Chen, van T. Nguyen, J. M. Pezzuto, S. Qiu, Z.-Z. Lu, *Synth. Commun.* **1997**, *27*, 1607–1612.
- [71] S. Alakurtti, T. Mäkelä, S. Koskimies, J. Yli-Kauhaluoma, *Eur. J. Pharm. Sci.* **2006**, *29*, 1–13.
- [72] E. Pisha, H. Chai, I. S. Lee, T. E. Chagwedera, N. R. Farnsworth, G. A. Cordell, C. W. Beecher, H. H. Fong, A. D. Kinghorn, D. M. Brown, *Nat. Med.* **1995**, *1*, 1046–1051.
- [73] V. Zuco, R. Supino, S. C. Righetti, L. Cleris, E. Marchesi, C. Gambacorti-Passerini, F. Formelli, *Cancer Lett.* **2002**, *175*, 17–25.
- [74] M. L. Schmidt, K. L. Kuzmanoff, L. Ling-Indeck, J. M. Pezzuto, *Eur. J. Cancer Oxf. Engl.* **1990**, *33*, 2007–2010.
- [75] S. Fulda, I. Jeremias, H. H. Steiner, T. Pietsch, K. M. Debatin, *Int. J. Cancer* **1999**, *82*, 435–441.
- [76] H. J. Jeong, H. B. Chai, S. Y. Park, D. S. Kim, *Bioorg. Med. Chem. Lett.* **1999**, *9*, 1201–1204.
- [77] R. Mukherjee, V. Kumar, S. K. Srivastava, S. K. Agarwal, A. C. Burman, *Anticancer Agents Med. Chem.* **2006**, *6*, 271–279.

- [78] S. Fulda, C. Friesen, M. Los, C. Scaffidi, W. Mier, M. Benedict, G. Nuñez, P. H. Krammer, M. E. Peter, K. M. Debatin, *Cancer Res.* **1997**, *57*, 4956–4964.
- [79] F. Xu, X. Huang, H. Wu, X. Wang, *Biomed. Pharmacother.* **2018**, *103*, 198–203.
- [80] J. F. Mayaux, A. Bousseau, R. Pauwels, T. Huet, Y. Hénin, N. Dereu, M. Evers, F. Soler, C. Poujade, E. De Clercq, *Proc. Natl. Acad. Sci. U. S. A.* **1994**, *91*, 3564–3568.
- [81] Y. Kashiwada, F. Hashimoto, L. M. Cosentino, C.-H. Chen, P. E. Garrett, K.-H. Lee, *J. Med. Chem.* **1996**, *39*, 1016–1017.
- [82] Y. Kashiwada, J. Chiyo, Y. Ikeshiro, T. Nagao, H. Okabe, L. M. Cosentino, K. Fowke, K. H. Lee, *Bioorg. Med. Chem. Lett.* **2001**, *11*, 183–185.
- [83] O. B. Flekhter, E. I. Boreko, L. R. Nigmatullina, E. V. Tret'yakova, N. I. Pavlova, L. A. Baltina, S. N. Nikolaeva, O. V. Savinova, F. Z. Galin, G. A. Tolstikov, *Russ. J. Bioorganic Chem.* **2003**, *29*, 594–600.
- [84] T. Kanamoto, Y. Kashiwada, K. Kanbara, K. Gotoh, M. Yoshimori, T. Goto, K. Sano, H. Nakashima, *Antimicrob. Agents Chemother.* **2001**, *45*, 1225–1230.
- [85] N. I. Pavlova, O. V. Savinova, S. N. Nikolaeva, E. I. Boreko, O. B. Flekhter, *Fitoterapia* **2003**, *74*, 489–492.
- [86] A. M. Madureira, J. R. Ascenso, L. Valdeira, A. Duarte, J. P. Frade, G. Freitas, M. J. U. Ferreira, *Nat. Prod. Res.* **2003**, *17*, 375–380.
- [87] A. Huguet, M. del Carmen Recio, S. Máñez, R. Giner, J. Ríos, *Eur. J. Pharmacol.* **2000**, *410*, 69–81.
- [88] P. Bernard, T. Scior, B. Didier, M. Hibert, J. Y. Berthon, *Phytochemistry* **2001**, *58*, 865–874.
- [89] S. Krajčovičová, T. Gucký, D. Hendrychová, V. Kryštof, M. Soral, *J. Org. Chem.* **2017**, *82*, 13530–13541.
- [90] J.-L. Haesslein, N. Jullian, *Curr. Top. Med. Chem.* **2002**, *2*, 1037–1050.
- [91] U. Asghar, A. K. Witkiewicz, N. C. Turner, E. S. Knudsen, *Nat. Rev. Drug Discov.* **2015**, *14*, 130–146.
- [92] C. Sánchez-Martínez, L. M. Gelbert, M. J. Lallena, A. de Dios, *Bioorg. Med. Chem. Lett.* **2015**, *25*, 3420–3435.
- [93] S. Lapenna, A. Giordano, *Nat. Rev. Drug Discov.* **2009**, *8*, 547.
- [94] G. J. P. L. Kops, B. A. A. Weaver, D. W. Cleveland, *Nat. Rev. Cancer* **2005**, *5*, 773–785.
- [95] L. Havlíček, J. Hanuš, J. Veselý, S. Leclerc, L. Meijer, G. Shaw, M. Strnad, *J. Med. Chem.* **1997**, *40*, 408–412.
- [96] J. Cicenias, K. Kalyan, A. Sorokinas, E. Stankunas, J. Levy, I. Meskinyte, V. Stankevicius, A. Kaupinis, M. Valius, *Ann. Transl. Med.* **2015**, *3*, 135.
- [97] J. Vesely, L. Havlicek, M. Strnad, J. J. Blow, A. Donella-Deana, L. Pinna, D. S. Letham, J. Kato, L. Detivaud, S. Leclerc, et al., *Eur. J. Biochem.* **1994**, *224*, 771–786.
- [98] C. T. Kouroukis, A. Belch, M. Crump, E. Eisenhauer, R. D. Gascoyne, R. Meyer, R. Lohmann, P. Lopez, J. Powers, R. Turner, et al., *J. Clin. Oncol.* **2003**, *21*, 1740–1745.
- [99] T. S. Lin, K. A. Blum, D. B. Fischer, S. M. Mitchell, A. S. Ruppert, P. Porcu, E. H. Kraut, R. A. Baiocchi, M. E. Moran, A. J. Johnson, et al., *J. Clin. Oncol.* **2010**, *28*, 418–423.
- [100] J. C. Byrd, T. S. Lin, J. T. Dalton, D. Wu, M. A. Phelps, B. Fischer, M. Moran, K. A. Blum, B. Rovin, M. Brooker-McEldowney, et al., *Blood* **2007**, *109*, 399–404.
- [101] M. M. Mita, A. A. Joy, A. Mita, K. Sankhala, Y.-M. Jou, D. Zhang, P. Statkevich, Y. Zhu, S.-L. Yao, K. Small, et al., *Clin. Breast Cancer* **2014**, *14*, 169–176.
- [102] T. Gucký, R. Jorda, M. Zatloukal, V. Bazgier, K. Berka, E. Řezníčková, T. Béres, M. Strnad, V. Kryštof, *J. Med. Chem.* **2013**, *56*, 6234–6247.
- [103] M. Zatloukal, R. Jorda, T. Gucký, E. Řezníčková, J. Voller, T. Pospíšil, V. Malínková, H. Adamcová, V. Kryštof, M. Strnad, *Eur. J. Med. Chem.* **2013**, *61*, 61–72.
- [104] M. T. Fiorini, C. Abell, *Tetrahedron Lett.* **1998**, *39*, 1827–1830.
- [105] C. R. Coxon, E. Anscombe, S. J. Harnor, M. P. Martin, B. Carbain, B. T. Golding, I. R. Hardcastle, L. K. Harlow, S. Korolchuk, C. J. Matheson, et al., *J. Med. Chem.* **2017**, *60*, 1746–1767.

- [106] Y.-T. Chang, N. S. Gray, G. R. Rosania, D. P. Sutherlin, S. Kwon, T. C. Norman, R. Sarohia, M. Leost, L. Meijer, P. G. Schultz, *Chem. Biol.* **1999**, *6*, 361–375.
- [107] M. Legraverend, O. Ludwig, E. Bisagni, S. Leclerc, L. Meijer, N. Giocanti, R. Sadri, V. Favaudon, *Bioorg. Med. Chem.* **1999**, *7*, 1281–1293.
- [108] S. Krajčovičová, M. Soural, *ACS Comb. Sci.* **2016**, *18*, 371–386.
- [109] M. Srinivasarao, C. V. Galliford, P. S. Low, *Nat. Rev. Drug Discov.* **2015**, *14*, 203–219.
- [110] I. R. Vlahov, C. P. Leamon, *Bioconjug. Chem.* **2012**, *23*, 1357–1369.
- [111] H. Elnakat, *Adv. Drug Deliv. Rev.* **2004**, *56*, 1067–1084.
- [112] J. W. Lee, J. Y. Lu, P. S. Low, P. L. Fuchs, *Bioorg. Med. Chem.* **2002**, *10*, 2397–2414.
- [113] I. R. Vlahov, H. K. R. Santhapuram, P. J. Kleindl, S. J. Howard, K. M. Stanford, C. P. Leamon, *Bioorg. Med. Chem. Lett.* **2006**, *16*, 5093–5096.
- [114] J. Liu, C. Kolar, T. A. Lawson, W. H. Gmeiner, *J. Org. Chem.* **2001**, *66*, 5655–5663.
- [115] C. Leamon, *Adv. Drug Deliv. Rev.* **2004**, *56*, 1127–1141.
- [116] C. P. Leamon, I. Pastan, P. S. Low, *J. Biol. Chem.* **1993**, *268*, 24847–24854.
- [117] C. A. Ladino, R. V. Chari, L. A. Bourret, N. L. Kedersha, V. S. Goldmacher, *Int. J. Cancer* **1997**, *73*, 859–864.
- [118] C. P. Leamon, J. A. Reddy, M. Vetzal, R. Dorton, E. Westrick, N. Parker, Y. Wang, I. Vlahov, *Cancer Res.* **2008**, *68*, 9839–9844.
- [119] C. P. Leamon, J. A. Reddy, I. R. Vlahov, E. Westrick, N. Parker, J. S. Nicoson, M. Vetzal, *Int. J. Cancer* **2007**, *121*, 1585–1592.
- [120] R. J. Lee, S. Wang, P. S. Low, *Biochim. Biophys. Acta BBA - Mol. Cell Res.* **1996**, *1312*, 237–242.
- [121] K. Bettayeb, H. Sallam, Y. Ferandin, F. Popowycz, G. Fournet, M. Hassan, A. Echalié, P. Bernard, J. Endicott, B. Joseph, et al., *Mol. Cancer Ther.* **2008**, *7*, 2713–2724.
- [122] F. Popowycz, G. Fournet, C. Schneider, K. Bettayeb, Y. Ferandin, C. Lamigeon, O. M. Tirado, S. Mateo-Lozano, V. Notario, P. Colas, et al., *J. Med. Chem.* **2009**, *52*, 655–663.
- [123] R. Jorda, L. Havlíček, I. W. McNae, M. D. Walkinshaw, J. Voller, A. Šturc, J. Navrátilová, M. Kuzma, M. Mistrík, J. Bártek, et al., *J. Med. Chem.* **2011**, *54*, 2980–2993.
- [124] D. A. Heathcote, H. Patel, S. H. B. Kroll, P. Hazel, M. Periyasamy, M. Alikian, S. K. Kanneganti, A. S. Jogalekar, B. Scheiper, M. Barbazanges, et al., *J. Med. Chem.* **2010**, *53*, 8508–8522.
- [125] K. Paruch, M. P. Dwyer, C. Alvarez, C. Brown, T.-Y. Chan, R. J. Doll, K. Keertikar, C. Knutson, B. McKittrick, J. Rivera, et al., *Bioorg. Med. Chem. Lett.* **2007**, *17*, 6220–6223.
- [126] D. S. Williamson, M. J. Parratt, J. F. Bower, J. D. Moore, C. M. Richardson, P. Dokurno, A. D. Cansfield, G. L. Francis, R. J. Hebdon, R. Howes, et al., *Bioorg. Med. Chem. Lett.* **2005**, *15*, 863–867.
- [127] R. Jorda, K. Paruch, V. Krystof, *Curr. Pharm. Des.* **2012**, *18*, 2974–2980.
- [128] K. Bettayeb, N. Oumata, A. Echalié, Y. Ferandin, J. A. Endicott, H. Galons, L. Meijer, *Oncogene* **2008**, *27*, 5797–5807.
- [129] J. Roy, T. X. Nguyen, A. K. Kanduluru, C. Venkatesh, W. Lv, P. V. N. Reddy, P. S. Low, M. Cushman, *J. Med. Chem.* **2015**, *58*, 3094–3103.
- [130] B. Vaňková, J. Hlaváč, M. Soural, *J. Comb. Chem.* **2010**, *12*, 890–894.
- [131] J. Roy, T. X. Nguyen, A. K. Kanduluru, C. Venkatesh, W. Lv, P. V. N. Reddy, P. S. Low, M. Cushman, *J. Med. Chem.* **2015**, *58*, 3094–3103.
- [132] A. R. Katritzky, O. Meth-Cohn, C. W. Rees, Eds., *Comprehensive Organic Functional Group Transformations*, Pergamon, Oxford, OX; New York, **1995**.
- [133] S. Patai, Z. Rappoport, Eds., *Sulphur-Containing Functional Groups (1993)*, John Wiley & Sons, Inc., Chichester, UK, **1993**.
- [134] O. Dmitrenko, C. Thorpe, R. D. Bach, *J. Org. Chem.* **2007**, *72*, 8298–8307.
- [135] C. P. Leamon, I. R. Vlahov, J. A. Reddy, M. Vetzal, H. K. R. Santhapuram, F. You, A. Bloomfield, R. Dorton, M. Nelson, P. Kleindl, et al., *Bioconjug. Chem.* **2014**, *25*, 560–568.
- [136] M. P. Trova, K. D. Barnes, L. Alicea, T. Benanti, M. Bielaska, J. Bilotta, B. Bliss, T. N. Duong, S. Haydar, R. J. Herr, et al., *Bioorg. Med. Chem. Lett.* **2009**, *19*, 6613–6617.

- [137] M. P. Trova, K. D. Barnes, C. Barford, T. Benanti, M. Bielaska, L. Burry, J. M. Lehman, C. Murphy, H. O'Grady, D. Peace, et al., *Bioorg. Med. Chem. Lett.* **2009**, *19*, 6608–6612.
- [138] N. Oumata, K. Bettayeb, Y. Ferandin, L. Demange, A. Lopez-Giral, M.-L. Goddard, V. Myriantopoulos, E. Mikros, M. Flajolet, P. Greengard, et al., *J. Med. Chem.* **2008**, *51*, 5229–5242.
- [139] S. Krajcovicova, R. Jorda, D. Hendrychova, V. Krystof, M. Sural, *Chem. Commun.* **2019**, *55*, 929–932.
- [140] A. C. Lai, C. M. Crews, *Nat. Rev. Drug Discov.* **2017**, *16*, 101–114.
- [141] G. M. Burslem, C. M. Crews, *Chem. Rev.* **2017**, *117*, 11269–11301.
- [142] P. C. de Smidt, T. Le Doan, S. de Falco, T. J. van Berkel, *Nucleic Acids Res.* **1991**, *19*, 4695–4700.
- [143] R. S. Geary, T. A. Watanabe, L. Truong, S. Freier, E. A. Lesnik, N. B. Sioufi, H. Sasmor, M. Manoharan, A. A. Levin, *J. Pharmacol. Exp. Ther.* **2001**, *296*, 890–897.
- [144] B. M. McMahon, D. Mays, J. Lipsky, J. A. Stewart, A. Fauq, E. Richelson, *Antisense Nucleic Acid Drug Dev.* **2002**, *12*, 65–70.
- [145] P. Ottis, C. M. Crews, *ACS Chem. Biol.* **2017**, *12*, 892–898.
- [146] I. Churcher, *J. Med. Chem.* **2018**, *61*, 444–452.
- [147] G. M. Burslem, B. E. Smith, A. C. Lai, S. Jaime-Figueroa, D. C. McQuaid, D. P. Bondeson, M. Toure, H. Dong, Y. Qian, J. Wang, et al., *Cell Chem. Biol.* **2018**, *25*, 67–77.e3.
- [148] M. D. Petroski, R. J. Deshaies, *Nat. Rev. Mol. Cell Biol.* **2005**, *6*, 9–20.
- [149] R. J. Deshaies, C. A. P. Joazeiro, *Annu. Rev. Biochem.* **2009**, *78*, 399–434.
- [150] V. Chau, J. W. Tobias, A. Bachmair, D. Marriott, D. J. Ecker, D. K. Gonda, A. Varshavsky, *Science* **1989**, *243*, 1576–1583.
- [151] Y. Lu, B. -h. Lee, R. W. King, D. Finley, M. W. Kirschner, *Science* **2015**, *348*, 1250834–1250834.
- [152] D. Komander, M. Rape, *Annu. Rev. Biochem.* **2012**, *81*, 203–229.
- [153] K. Husnjak, I. Dikic, *Annu. Rev. Biochem.* **2012**, *81*, 291–322.
- [154] J. Adams, *Nat. Rev. Cancer* **2004**, *4*, 349–360.
- [155] K. M. Sakamoto, K. B. Kim, R. Verma, A. Ransick, B. Stein, C. M. Crews, R. J. Deshaies, *Mol. Cell. Proteomics* **2003**, *2*, 1350–1358.
- [156] W.-C. Hon, M. I. Wilson, K. Harlos, T. D. W. Claridge, C. J. Schofield, C. W. Pugh, P. H. Maxwell, P. J. Ratcliffe, D. I. Stuart, E. Y. Jones, *Nature* **2002**, *417*, 975–978.
- [157] J.-H. Min, *Science* **2002**, *296*, 1886–1889.
- [158] J. S. Schneekloth, F. N. Fonseca, M. Koldobskiy, A. Mandal, R. Deshaies, K. Sakamoto, C. M. Crews, *J. Am. Chem. Soc.* **2004**, *126*, 3748–3754.
- [159] P. Bargagna-Mohan, S.-H. Baek, H. Lee, K. Kim, R. Mohan, *Bioorg. Med. Chem. Lett.* **2005**, *15*, 2724–2727.
- [160] A. Rodriguez-Gonzalez, K. Cyrus, M. Salcius, K. Kim, C. M. Crews, R. J. Deshaies, K. M. Sakamoto, *Oncogene* **2008**, *27*, 7201–7211.
- [161] D. Zhang, S.-H. Baek, A. Ho, K. Kim, *Bioorg. Med. Chem. Lett.* **2004**, *14*, 645–648.
- [162] L. T. Vassilev, *Science* **2004**, *303*, 844–848.
- [163] A. R. Schneekloth, M. Pucheault, H. S. Tae, C. M. Crews, *Bioorg. Med. Chem. Lett.* **2008**, *18*, 5904–5908.
- [164] D. P. Bondeson, A. Mares, I. E. D. Smith, E. Ko, S. Campos, A. H. Miah, K. E. Mulholland, N. Routly, D. L. Buckley, J. L. Gustafson, et al., *Nat. Chem. Biol.* **2015**, *11*, 611–617.
- [165] T. Ito, H. Ando, T. Suzuki, T. Ogura, K. Hotta, Y. Imamura, Y. Yamaguchi, H. Handa, *Science* **2010**, *327*, 1345–1350.
- [166] E. S. Fischer, K. Böhm, J. R. Lydeard, H. Yang, M. B. Stadler, S. Cavadini, J. Nagel, F. Serluca, V. Acker, G. M. Lingaraju, et al., *Nature* **2014**, *512*, 49–53.
- [167] J. Krönke, E. C. Fink, P. W. Hollenbach, K. J. MacBeth, S. N. Hurst, N. D. Udeshi, P. P. Chamberlain, D. R. Mani, H. W. Man, A. K. Gandhi, et al., *Nature* **2015**, *523*, 183–188.
- [168] G. Petzold, E. S. Fischer, N. H. Thomä, *Nature* **2016**, *532*, 127–130.
- [169] L. Ades, P. Fenaux, *Hematology* 2011, *2011*, 556–560.

- [170] J. Lu, Y. Qian, M. Altieri, H. Dong, J. Wang, K. Raina, J. Hines, J. D. Winkler, A. P. Crew, K. Coleman, et al., *Chem. Biol.* **2015**, *22*, 755–763.
- [171] T. Shimamura, Z. Chen, M. Soucheray, J. Carretero, E. Kikuchi, J. H. Tchaicha, Y. Gao, K. A. Cheng, T. J. Cohoon, J. Qi, et al., *Clin. Cancer Res.* **2013**, *19*, 6183–6192.
- [172] G. E. Winter, D. L. Buckley, J. Paulk, J. M. Roberts, A. Souza, S. Dhe-Paganon, J. E. Bradner, *Science* **2015**, *348*, 1376–1381.
- [173] M. Zengerle, K.-H. Chan, A. Ciulli, *ACS Chem. Biol.* **2015**, *10*, 1770–1777.
- [174] A. C. Lai, M. Toure, D. Hellerschmied, J. Salami, S. Jaime-Figueroa, E. Ko, J. Hines, C. M. Crews, *Angew. Chem. Int. Ed.* **2016**, *55*, 807–810.
- [175] A. P. Crew, K. Raina, H. Dong, Y. Qian, J. Wang, D. Vigil, Y. V. Serebrenik, B. D. Hamman, A. Morgan, C. Ferraro, et al., *J. Med. Chem.* **2018**, *61*, 583–598.
- [176] J. Lohbeck, A. K. Miller, *Bioorg. Med. Chem. Lett.* **2016**, *26*, 5260–5262.
- [177] C. M. Robb, J. I. Contreras, S. Kour, M. A. Taylor, M. Abid, Y. A. Sonawane, M. Zahid, D. J. Murry, A. Natarajan, S. Rana, *Chem. Commun.* **2017**, *53*, 7577–7580.
- [178] J. Papatzimas, E. Gorobets, D. Brownsey, R. Maity, N. Bahlis, D. Derksen, *Synlett* **2017**, *28*, 2881–2885.
- [179] R. P. Wurz, K. Dellamaggiore, H. Dou, N. Javier, M.-C. Lo, J. D. McCarter, D. Mohl, C. Sastri, J. R. Lipford, V. J. Cee, *J. Med. Chem.* **2018**, *61*, 453–461.
- [180] F. Cameron, M. Sanford, *Drugs* **2014**, *74*, 263–271.
- [181] A. Zorba, C. Nguyen, Y. Xu, J. Starr, K. Borzilleri, J. Smith, H. Zhu, K. A. Farley, W. Ding, J. Schiemer, et al., *Proc. Natl. Acad. Sci.* **2018**, *115*, E7285–E7292.
- [182] S. Krajcovicova, J. Stankova, P. Dzubak, M. Hajduch, M. Soural, M. Urban, *Chem. - Eur. J.* **2018**, *24*, 4957–4966.
- [183] L. D. Lavis, R. T. Raines, *ACS Chem. Biol.* **2008**, *3*, 142–155.
- [184] B. Valeur, M. N. Berberan-Santos, *Molecular Fluorescence: Principles and Applications*, Wiley-VCH; Wiley-VCH Verlag GmbH & Co. KGaA, Weinheim, Germany: [Chichester, England], **2012**.
- [185] I. Johnson, *Histochem. J.* **1998**, *30*, 123–140.
- [186] J. Zhang, R. E. Campbell, A. Y. Ting, R. Y. Tsien, *Nat. Rev. Mol. Cell Biol.* **2002**, *3*, 906–918.
- [187] J. V. Frangioni, *Curr. Opin. Chem. Biol.* **2003**, *7*, 626–634.
- [188] J. Goddard, J. Reymond, *Curr. Opin. Biotechnol.* **2004**, *15*, 314–322.
- [189] N. Johnsson, K. Johnsson, *ACS Chem. Biol.* **2007**, *2*, 31–38.
- [190] T. Kowada, H. Maeda, K. Kikuchi, *Chem Soc Rev* **2015**, *44*, 4953–4972.
- [191] L. M. Wysocki, L. D. Lavis, *Curr. Opin. Chem. Biol.* **2011**, *15*, 752–759.
- [192] L. V. Johnson, M. L. Walsh, L. B. Chen, *Proc. Natl. Acad. Sci.* **1980**, *77*, 990–994.
- [193] A. Loudet, K. Burgess, *Chem. Rev.* **2007**, *107*, 4891–4932.
- [194] G. Ulrich, R. Ziessel, A. Harriman, *Angew. Chem. Int. Ed.* **2008**, *47*, 1184–1201.
- [195] H. Lu, J. Mack, Y. Yang, Z. Shen, *Chem Soc Rev* **2014**, *43*, 4778–4823.
- [196] Y. Ni, J. Wu, *Org. Biomol. Chem.* **2014**, *12*, 3774.
- [197] J. Bañuelos, *Chem. Rec.* **2016**, *16*, 335–348.
- [198] H. Sunahara, Y. Urano, H. Kojima, T. Nagano, *J. Am. Chem. Soc.* **2007**, *129*, 5597–5604.
- [199] X. Qian, Y. Xiao, Y. Xu, X. Guo, J. Qian, W. Zhu, *Chem. Commun.* **2010**, *46*, 6418.
- [200] N. Boens, V. Leen, W. Dehaen, *Chem Soc Rev* **2012**, *41*, 1130–1172.
- [201] C.-W. Wan, A. Burghart, J. Chen, F. Bergström, L. B.-Å. Johansson, M. F. Welford, T. G. Kim, M. R. Topp, R. M. Hochstrasser, K. Burgess, *Chem. - Eur. J.* **2003**, *9*, 4430–4441.
- [202] F. D’Souza, P. M. Smith, M. E. Zandler, A. L. McCarty, M. Itou, Y. Araki, O. Ito, *J. Am. Chem. Soc.* **2004**, *126*, 7898–7907.
- [203] J. Iehl, J.-F. Nierengarten, A. Harriman, T. Bura, R. Ziessel, *J. Am. Chem. Soc.* **2012**, *134*, 988–998.
- [204] J. Lu, H. Fu, Y. Zhang, Z. J. Jakubek, Y. Tao, S. Wang, *Angew. Chem. Int. Ed.* **2011**, *50*, 11658–11662.
- [205] H. Imahori, H. Norieda, H. Yamada, Y. Nishimura, I. Yamazaki, Y. Sakata, S. Fukuzumi, *J. Am. Chem. Soc.* **2001**, *123*, 100–110.

- [206] S. Kolemen, Y. Cakmak, S. Erten-Ela, Y. Altay, J. Brendel, M. Thelakkat, E. U. Akkaya, *Org. Lett.* **2010**, *12*, 3812–3815.
- [207] C. Sun, J. Yang, L. Li, X. Wu, Y. Liu, S. Liu, *J. Chromatogr. B* **2004**, *803*, 173–190.
- [208] J.-S. Lee, N. Kang, Y. K. Kim, A. Samanta, S. Feng, H. K. Kim, M. Vendrell, J. H. Park, Y.-T. Chang, *J. Am. Chem. Soc.* **2009**, *131*, 10077–10082.
- [209] J. O. Escobedo, O. Rusin, S. Lim, R. M. Strongin, *Curr. Opin. Chem. Biol.* **2010**, *14*, 64–70.
- [210] K. Umezawa, D. Citterio, K. Suzuki, *Anal. Sci. Int. J. Jpn. Soc. Anal. Chem.* **2014**, *30*, 327–349.
- [211] S. G. Awuah, Y. You, *RSC Adv.* **2012**, *2*, 11169.
- [212] A. Kamkaew, S. H. Lim, H. B. Lee, L. V. Kiew, L. Y. Chung, K. Burgess, *Chem Soc Rev* **2013**, *42*, 77–88.
- [213] R. Ziesel, G. Ulrich, A. Harriman, *New J. Chem.* **2007**, *31*, 496.
- [214] M. Shah, K. Thangaraj, M.-L. Soong, L. T. Wolford, J. H. Boyer, I. R. Politzer, T. G. Pavlopoulos, *Heteroat. Chem.* **1990**, *1*, 389–399.
- [215] J. H. Boyer, A. M. Haag, G. Sathyamoorthi, M.-L. Soong, K. Thangaraj, T. G. Pavlopoulos, *Heteroat. Chem.* **1993**, *4*, 39–49.
- [216] Z. Li, E. Mintzer, R. Bittman, *J. Org. Chem.* **2006**, *71*, 1718–1721.
- [217] C. Tahtaoui, C. Thomas, F. Rohmer, P. Klotz, G. Duportail, Y. Mély, D. Bonnet, M. Hibert, *J. Org. Chem.* **2007**, *72*, 269–272.
- [218] Y. Gabe, Y. Urano, K. Kikuchi, H. Kojima, T. Nagano, *J. Am. Chem. Soc.* **2004**, *126*, 3357–3367.
- [219] H.-X. Zhang, J.-B. Chen, X.-F. Guo, H. Wang, H.-S. Zhang, *Anal. Chem.* **2014**, *86*, 3115–3123.
- [220] Y. Qian, J. Karpus, O. Kabil, S.-Y. Zhang, H.-L. Zhu, R. Banerjee, J. Zhao, C. He, *Nat. Commun.* **2011**, *2*, 495.
- [221] T. Uppal, X. Hu, F. R. Fronczek, S. Maschek, P. Bobadova-Parvanova, M. G. H. Vicente, *Chem. - Eur. J.* **2012**, *18*, 3893–3905.
- [222] A. M. Curtis, S. A. Santos, Y. Guan, J. A. Hendricks, B. Ghosh, D. M. Szantai-Kis, S. A. Reis, J. V. Shah, R. Mazitschek, *Bioconjug. Chem.* **2014**, *25*, 1043–1051.
- [223] S. Zhang, T. Wu, J. Fan, Z. Li, N. Jiang, J. Wang, B. Dou, S. Sun, F. Song, X. Peng, *Org. Biomol. Chem.* **2013**, *11*, 555–558.
- [224] N. Jiang, J. Fan, T. Liu, J. Cao, B. Qiao, J. Wang, P. Gao, X. Peng, *Chem. Commun.* **2013**, *49*, 10620.
- [225] M. J. Hinner, K. Johnsson, *Curr. Opin. Biotechnol.* **2010**, *21*, 766–776.
- [226] T. Gronemeyer, G. Godin, K. Johnsson, *Curr. Opin. Biotechnol.* **2005**, *16*, 453–458.
- [227] S. Mizukami, Y. Hori, K. Kikuchi, *Acc. Chem. Res.* **2014**, *47*, 247–256.
- [228] M. Vendrell, D. Zhai, J. C. Er, Y.-T. Chang, *Chem. Rev.* **2012**, *112*, 4391–4420.
- [229] P. A. Waghorn, M. W. Jones, A. McIntyre, A. Innocenti, D. Vullo, A. L. Harris, C. T. Supuran, J. R. Dilworth, *Eur. J. Inorg. Chem.* **2012**, *2012*, 2898–2907.
- [230] M. L. Vetter, Z. Zhang, S. Liu, J. Wang, H. Cho, J. Zhang, W. Zhang, N. S. Gray, P. L. Yang, *ChemBioChem* **2014**, *15*, 1317–1324.
- [231] S. K. V. Vernekar, H. Y. Hallaq, G. Clarkson, A. J. Thompson, L. Silvestri, S. C. R. Lummis, M. Lochner, *J. Med. Chem.* **2010**, *53*, 2324–2328.
- [232] R. Weinstain, J. Kanter, B. Friedman, L. G. Ellies, M. E. Baker, R. Y. Tsien, *Bioconjug. Chem.* **2013**, *24*, 766–771.
- [233] L. W. Miller, Y. Cai, M. P. Sheetz, V. W. Cornish, *Nat. Methods* **2005**, *2*, 255–257.
- [234] J.-J. Lee, S.-C. Lee, D. Zhai, Y.-H. Ahn, H. Y. Yeo, Y. L. Tan, Y.-T. Chang, *Chem. Commun.* **2011**, *47*, 4508.
- [235] J. R. Casey, S. Grinstein, J. Orłowski, *Nat. Rev. Mol. Cell Biol.* **2010**, *11*, 50–61.
- [236] Y. Urano, D. Asanuma, Y. Hama, Y. Koyama, T. Barrett, M. Kamiya, T. Nagano, T. Watanabe, A. Hasegawa, P. L. Choyke, et al., *Nat. Med.* **2009**, *15*, 104–109.
- [237] T. Kowada, J. Kikuta, A. Kubo, M. Ishii, H. Maeda, S. Mizukami, K. Kikuchi, *J. Am. Chem. Soc.* **2011**, *133*, 17772–17776.
- [238] J. Kikuta, Y. Wada, T. Kowada, Z. Wang, G.-H. Sun-Wada, I. Nishiyama, S. Mizukami, N. Maiya, H. Yasuda, A. Kumanogoh, et al., *J. Clin. Invest.* **2013**, JCI65054.
- [239] J. S. Stamler, *Cell* **1994**, *78*, 931–936.

- [240] C. Szabó, *Nat. Rev. Drug Discov.* **2007**, *6*, 917–935.
- [241] A. K. Mustafa, M. M. Gadalla, S. H. Snyder, *Sci. Signal.* **2009**, *2*, re2–re2.
- [242] B. W. Michel, A. R. Lippert, C. J. Chang, *J. Am. Chem. Soc.* **2012**, *134*, 15668–15671.
- [243] M. Lumbierres, J. M. Palomo, G. Kragol, S. Roehrs, O. Müller, H. Waldmann, *Chem. - Eur. J.* **2005**, *11*, 7405–7415.
- [244] M. Vendrell, G. G. Krishna, K. K. Ghosh, D. Zhai, J.-S. Lee, Q. Zhu, Y. H. Yau, S. G. Shochat, H. Kim, J. Chung, et al., *Chem. Commun.* **2011**, *47*, 8424.
- [245] K. Gießler, H. Griesser, D. Göhringer, T. Sabirov, C. Richert, *Eur. J. Org. Chem.* **2010**, *2010*, 3611–3620.
- [246] A. M. Hansen, A. L. Sewell, R. H. Pedersen, D.-L. Long, N. Gadegaard, R. Marquez, *Tetrahedron* **2013**, *69*, 8527–8533.
- [247] J. Sarek, M. Kvasnica, M. Urban, J. Klinot, M. Hajduch, *Bioorg. Med. Chem. Lett.* **2005**, *15*, 4196–4200.
- [248] M. Urban, J. Sarek, M. Kvasnica, I. Tislerova, M. Hajduch, *J. Nat. Prod.* **2007**, *70*, 526–532.
- [249] L. Huo, X. Bai, Y. Wang, M. Wang, *Biomed. Pharmacother.* **2017**, *92*, 347–355.
- [250] R. Biswas, J. Chanda, A. Kar, P. K. Mukherjee, *Food Chem.* **2017**, *232*, 689–696.
- [251] E. V. Rumyantsev, S. N. Alyoshin, Y. S. Marfin, *Inorganica Chim. Acta* **2013**, *408*, 181–185.
- [252] M. Soural, J. Hodon, N. J. Dickinson, V. Sidova, S. Gurska, P. Dzubak, M. Hajduch, J. Sarek, M. Urban, *Bioconjug. Chem.* **2015**, *26*, 2563–2570.
- [253] L. Kürti, B. Czakó, *Strategic Applications of Named Reactions in Organic Synthesis: Background and Detailed Mechanisms*, Elsevier Academic Press, Amsterdam ; Boston, **2005**.
- [254] W. Dehaen, A. A. Mashentseva, T. S. Seitembetov, *Molecules* **2011**, *16*, 2443–2466.
- [255] N. Cankarova, P. Funk, J. Hlavac, M. Soural, *Tetrahedron Lett.* **2011**, *52*, 5782–5788.
- [256] C. Würth, M. Grabolle, J. Pauli, M. Spieles, U. Resch-Genger, *Nat. Protoc.* **2013**, *8*, 1535–1550.
- [257] W. Peng, F. Ding, Y.-T. Jiang, Y.-K. Peng, *J. Agric. Food Chem.* **2014**, *62*, 2271–2283.
- [258] Y. Ye, T. Zhang, H. Yuan, D. Li, H. Lou, P. Fan, *J. Med. Chem.* **2017**, *60*, 6353–6363.
- [259] S. Mitsuda, T. Yokomichi, J. Yokoigawa, T. Kataoka, *FEBS Open Bio* **2014**, *4*, 229–239.

Part
III

Appendices

Curriculum Vitae

Born **17.9.1991** in Bratislava, Slovakia

| | |
|---------|--|
| Address | Zeyerova 18 779 00, Olomouc-Hodolany Czech Republic |
| Phone | +420 720 598 302 +421 911 261 576 |
| E-mail | sonakrajcovic@gmail.com sona.krajcovicova@upol.cz |

EDUCATION

- from **2015 Ph.D. student** in Organic chemistry, Palacký University, Olomouc, under supervision of assoc. prof. RNDr. Miroslav Sural, Ph.D.
- **MSc. Degree** in Organic chemistry, **2015**, Masaryk University, Brno, under supervision of assoc. prof. Mgr. Kamil Paruch, Ph.D.
- **Bc. Degree** in Biochemistry, **2013**, Masaryk University, Brno, under supervision of assoc. prof. Mgr. Kamil Paruch, Ph.D.
- School leaving exam, 1st Independent High School Bajkalská, **2010**, Bratislava, Slovakia

INTERNSHIPS

- Georg-August Universität Göttingen, Germany, under supervision of prof. Manuel Alcarazo, PhD., **2018**, DAAD fellowship, *4 months*
- Internship in pharmaceutical company, APIGENEX s.r.o., Prague, **2014**, *1 month*

PROFESSIONAL & TEACHING SKILLS

- From **2017** NMR operator on JEOL ECX500, 500 MHz spectrometer, Palacký University, Olomouc
- Supervisor of Bachelor students (Iva Delichristovová, Andrea Danišková), **2019**, Palacký University, Olomouc, *ongoing*
- Teaching exercises in basic course of organic chemistry, **2019**, Palacký University, *3 months*
- Teaching exercises in advanced course of organic chemistry, **2017**, Palacký University, Olomouc, *3 months*
- Teaching laboratory course of organic synthesis, **2016**, Palacký University, Olomouc, *3 months*
- Main supervisor of Master student (Bc. Martina Drábiková), **2015–2017**, Palacký University, Olomouc, *2 years*
- Laboratory supervisor of Bachelor student within Erasmus programme, **2013**, Masaryk University, Brno, *3 months*

AWARDS AND APPRECIATIONS

- “*Best oral communication award*”, XVIII International Conference on Heterocycles in Bioorganic Chemistry, **2019**, Ghent (Belgium)
- “*Top 5 presentations in chemical sciences*”, XIX. Interdisciplinary meeting of young life scientists, **2019**, Milovy (Czech Republic)
- *Dean’s Award of Palacký University*, Faculty of Science, **2019** (1st place in PhD category, 1st place in category “Chemistry”)
- *Dean’s Award of Palacký University*, Faculty of Science, **2018** (1st place in PhD category, 1st place in category “Chemistry”, overall winner of the competition)
- *Deutscher Akademischer Austauschdienst (DAAD)*, **2018** (short-term research funding), *4 months*
- *Principal investigator of student’s grant IGA (IGA_LF_2017_028)*, Palacký University, **2017**, *1 year*

JOURNAL PUBLICATIONS

1. Krajčovičová, S.; Jorda, R.; Hendrychová, D.; Kryštof, V.; Soural, M. *Chem. Commun.* **2019**, *55*, 929.
2. Cankařová, N.; La Venia, A.; Krajčovičová, S.; Krchňák, V. *J. Org. Chem.* **2019**, *84*, 636.
3. Krajčovičová, S.; Stanková, J.; Džubák, P.; Hajdúch, M.; Soural, M.; Urban, M. *Chem. Eur. J.* **2018**, *24*, 4957.
4. Pokorný, J.; Krajčovičová, S.; Hajdúch, M.; Holoubek, M.; Gurská, S.; Džubák, P.; Volná, T.; Popa, I.; Urban, M. *Future Med. Chem.* **2018**, *10*, 483.
5. Krajčovičová, S.; Gucký, T.; Hendrychová, D.; Kryštof, V.; Soural, M. *J. Org. Chem.* **2017**, *82*, 13530.
6. Maier, L.; Khirsarya, P.K.; Hylse, O.; Adla, S.K.; Černová, L.; Poljak, M.; Krajčovičová, S.; Weis, E.; Drápela, S.; Souček, K.; Paruch, K. *J. Org. Chem.* **2017**, *82*, 3382.
7. Drábiková M.; Krajčovičová S.;^{*} Soural, M. *Tetrahedron* **2017**, *73*, 6296.
8. Krajčovičová, S.; Soural, M. *ACS Comb. Sci.* **2016**, *18*, 371.

^{*}equally contributed

OTHER SCIENTIFIC CONTRIBUTIONS

- Krajčovičová, S. XVIII International Conference on Heterocycles in Bioorganic Chemistry “*Bioheterocycles*”, **2019**, Ghent (Belgium), **oral communication**.
- Krajčovičová, S. XIX. Interdisciplinary meeting of young life scientists, **2019**, Milovy (Czech Republic), **oral communication**.
- Krajčovičová, S.; Jorda, R.; Hendrychová, D.; Kryštof, V.; Soural, M. *53rd Advances in Organic, Bioorganic and Pharmaceutical Chemistry “Liblice”*, **2018**, Lázně Bělohrad (Czech Republic), **poster**.

- Krajčovičová, S. *52nd Advances in Organic, Bioorganic and Pharmaceutical Chemistry "Liblice"*, **2017**, Lázně Bělohrad (Czech Republic), **oral communication**.
- Krajčovičová, S.; Sural, M.; Stanková, J.; Džubák, P.; Urban, M. *Blue Danube Symposium of Heterocyclic Chemistry*, **2017**, Linz (Austria), **poster**.
- Urban, M.; Borková, L.; Pokorný, J.; Džubák, P.; Hajdúch, M.; Sural, M.; Šarek, J. Krajčovičová, S.; Řehulka, J.; Hodoň, J. *Blue Danube Symposium of Heterocyclic Chemistry*, **2017**, Linz (Austria), **poster**.
- Krajčovičová, S.; Sural, M.; Urban, M. *51st Advances in Organic, Bioorganic and Pharmaceutical Chemistry "Liblice"*, **2016**, Lázně Bělohrad (Czech Republic), **poster**.

LANGUAGE PROFICIENCY

| | |
|----------------|---|
| English | International English Language Testing System (IELTS) Academic, 6.5/9, level B2/C1 (05/2015) Academic, 6.0/9, level B2 (02/2010) |
| German | A2 (06/2017) |
| Czech | C2 |
| Slovak | C2 (native speaker) |

List of publications

Appendix A

Krajčovičová, S.; Gucký, T.; Hendrychová, D.; Kryštof, V.; Sural, M. *J. Org. Chem.* **2017**, *82*, 13530.

Appendix B

Krajčovičová, S.; Jorda, R.; Hendrychová, D.; Kryštof, V.; Sural, M. *Chem. Commun.* **2019**, *55*, 929.

Appendix C

Krajčovičová, S.; Stanková, J.; Džubák, P.; Hajdúch, M.; Sural, M.; Urban, M. *Chem. Eur. J.* **2018**, *24*, 4957.

Appendix D

Krajčovičová, S.; Sural, M. *ACS Comb. Sci.* **2016**, *18*, 371.

A Stepwise Approach for the Synthesis of Folic Acid Conjugates with Protein Kinase Inhibitors

Soňa Krajčovičová,[†] Tomáš Gucký,[‡] Denisa Hendrychová,[§] Vladimír Kryštof,^{§,||} and Miroslav Soural^{*,||}

[†]Department of Organic Chemistry, Faculty of Science, Palacký University, Tr. 17. listopadu 12, 771 46 Olomouc, Czech Republic

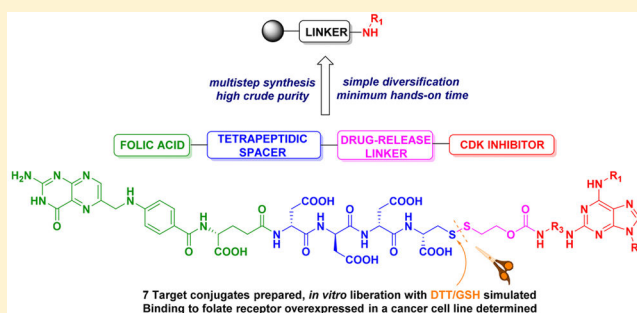
[‡]Department of Chemical Biology and Genetics, Centre of the Region Haná for Biotechnological and Agricultural Research, Palacký University and Institute of Experimental Botany AS CR, Šlechtitelů 27, 78371 Olomouc, Czech Republic

[§]Laboratory of Growth Regulators, Centre of the Region Haná for Biotechnological and Agricultural Research, Palacký University and Institute of Experimental Botany AS CR, Šlechtitelů 27, 78371 Olomouc, Czech Republic

^{||}Institute of Molecular and Translational Medicine, Faculty of Medicine and Dentistry, Palacký University, Hněvotínská 5, 779 00 Olomouc, Czech Republic

Supporting Information

ABSTRACT: Herein, we report an alternative synthetic approach for selected 2,6,9-trisubstituted purine CDK inhibitor conjugates with folic acid as a drug-delivery system targeting folate receptors. In contrast to the previously reported approaches, the desired conjugates were constructed stepwise using solid-phase synthesis starting from immobilized primary amines. The ability of the prepared conjugates to release the free drug was verified using dithiothreitol (DTT) and glutathione (GSH) as liberating agents. Finally, binding to the folate receptor (FOLR1) overexpressed in a cancer cell line was measured by flow cytometry using a fluorescent imaging probe.



INTRODUCTION

Little or no specificity toward cancer cells is one of the most serious problems of traditional cancer chemotherapy, as it leads to systemic toxicity. The systemic toxicity of conventional chemotherapy causes serious side effects and is also one of the limiting factors of treatment efficiency.¹ The use of small-molecule delivery systems that can decrease the systemic toxicity of cytotoxic drugs to normal cells is a promising approach. Tumor-targeting delivery systems have been studied intensively in the past three decades and represent a promising approach for both increasing chemotherapy selectivity and decreasing systemic toxicity. Selective drug delivery is based on the frequent overexpression of many receptors in tumor cells, which can serve as targets to deliver a cytotoxic agent selectively into a tumor. Relatively selective transport into tumor cells can be accomplished with the use of conjugates of a cytotoxic agent and tumor recognition moiety.²

One of the most recent and powerful approaches involves targeting the folate receptor (FOLR1).³ FOLR1 is a glycosylphosphatidylinositol-anchored cell-surface receptor that binds and transports folic acid into cells with high affinity ($K_d \approx 0.1$ – 1 nM). It is overexpressed in a wide range of human cancers.⁴ Folate-targeting technology has successfully been applied for the delivery of various chemotherapeutic agents to FOLR1-positive cancers.⁵ Because of its selective expression, FOLR1 is considered a “Trojan horse” that delivers molecules

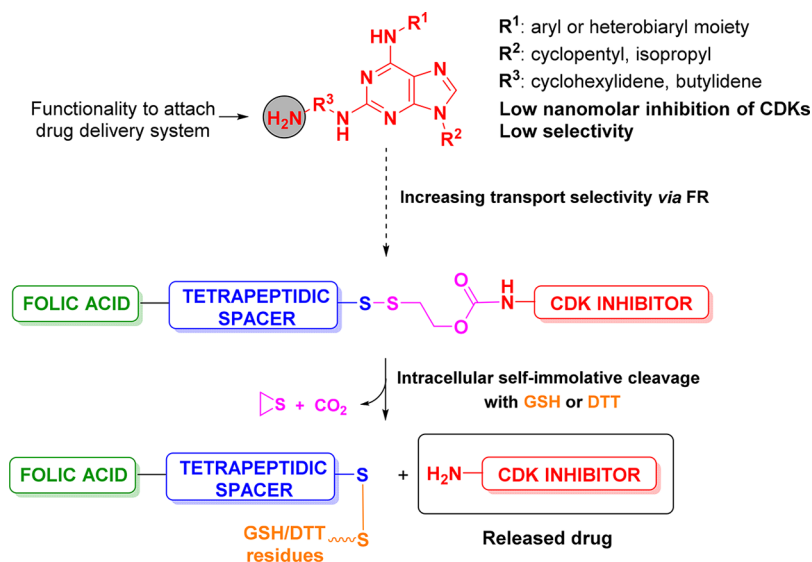
selectively to folate receptors.⁶ Specific drug delivery using FOLR1 has been studied intensively since the late 1980s. The crucial points for folic acid–drug conjugate design, namely, its optimal constitution for cell penetration and release of the free drug, have been reported.⁷ A suitable folic acid–drug conjugate consists of four parts: folic acid, a spacer, a cleavable self-immolative linker, and a cytotoxic agent. Determining a suitable spacer between folic acid and the cleavable drug-release linker, which is connected to the cytotoxic agent, has been studied with the aim of maintaining a high affinity of the final conjugate to the folate receptors. According to the published results, the spacer modification has a rather small impact on the targeted activities of folates, as it consists of hydrophilic groups.¹¹ One of the working classes of spacers for this purpose are oligopeptide chains, which have already been utilized in a number of conjugates with various cytotoxic agents. To date, four folate-based therapeutics are undergoing clinical testing.^{8–10}

Similarly, the potencies of bioreleasable self-immolative linkers have been extensively examined, and the choice of an appropriate candidate seems to be crucial.¹¹ These studies have resulted in the design of a disulfide linker that is most effectively cleaved within the cell, releasing the active drug. For

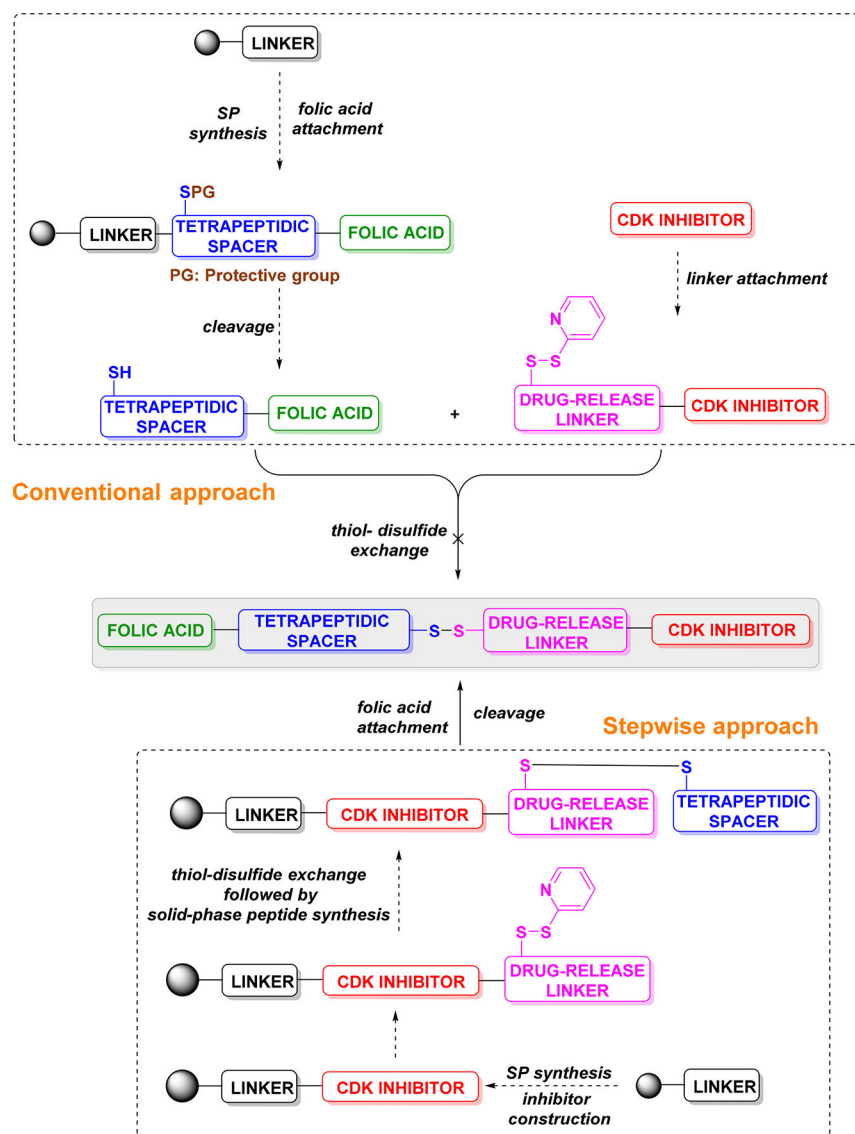
Received: October 18, 2017

Published: November 24, 2017

Scheme 1. Design and Potential Application of Target Conjugates



Scheme 2. Conventional and Suggested Stepwise Synthetic Approaches to Obtain the Target Conjugates



this reason, this type of linker has been successfully applied in a large number of folate–cytotoxic agent conjugates.¹¹ Among all others, the most successful conjugate, vintafolide, entered phase II clinical trials and phase III clinical trials for the treatment of platinum-resistant ovarian cancer. Although the clinical trials have been stopped, the strategy of FOLR1 targeting with small-molecule drug conjugates is promising.¹²

Cyclin-dependent kinases (CDKs) are specific serine/threonine protein kinases that play a key role in cell cycle regulation, especially in the progression of the cell cycle from the G1 to S phase and from the G2 to M phase.¹³ Therefore, CDKs are promising targets for the inhibition of cancer cell proliferation, and a large number of small-molecule CDK inhibitors have been synthesized and studied for their CDK inhibitory activities.¹³ To date, more than 20 of the most potent inhibitors have been registered for clinical trials on cancer diseases.^{14,15} The performed structure–activity relationship studies, together with proper knowledge of the binding sites for ATP in various CDKs, have enabled the synthesis of 2,6,9-trisubstituted purines that show potent biochemical, cellular, and *in vivo* activities. In particular, 2,6,9-trisubstituted purine derivatives bearing biarylmethylamino or biaryl amino substituents at the 6 position of the purine skeleton are the most active known CDK inhibitors.^{16–18} However, their possible clinical application is significantly limited by their low selectivity. Despite this fact, targeting of CDK inhibitors using conjugation with folic acid has not been reported to date.

We recently reported the syntheses and activities of highly potent purine CDK inhibitors bearing a 4-aminocyclohexyl moiety in the C² position.¹⁹ The terminal amino group of these compounds was found to be a suitable functionality to attach to the FOLR1-targeting system (Scheme 1). The preparation and preliminary evaluation of desired conjugates are summarized in this article.

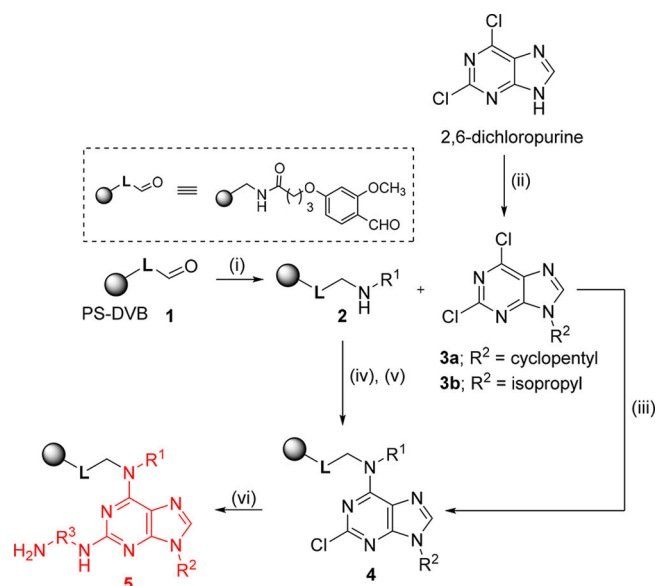
RESULTS AND DISCUSSION

Synthesis. First, we attempted to use the previously reported conventional synthetic approach.^{11,20,21} It consisted of the preparation of a folic-acid-oligopeptide-SH segment using solid-phase synthesis and its subsequent coupling with a premodified drug equipped with the self-immolative drug-release linker (Scheme 2, Conventional approach). However, despite the successful preparation of the corresponding intermediates, this strategy failed in the stage of the final thiol–disulfide exchange because of the low purity of the resulting products and irreproducibility on a preparative scale. Moreover, because of the zwitterionic structure and high polarity, the solubility of folic acid in organic solvents (except for DMSO) was limited, and the final products required at least two-step purification using reverse-phase chromatography.²²

For these reasons, we designed an alternative synthetic approach. It consisted of the sequential construction of the target conjugates in the following direction: purine → drug-release linker → tetrapeptide → folic acid (Scheme 2, Stepwise approach). Considering the well-known advantages of solid-phase synthesis in multistep reaction sequences (especially the fast and simple isolation of reaction intermediates without the need for tedious purification) and taking the previous knowledge in the area of polymer-supported synthesis of purines into account,²³ we designed the entire reaction sequence on the solid phase using a common aminomethyl polystyrene resin equipped with an acid-labile benzaldehyde linker (i.e., backbone amide linker, BAL).

The synthetic pathway was started by the immobilization of primary amines (resulting in purine C⁶ substitution) through the reductive amination of starting resin **1**. Intermediates **2** were regioselectively arylated with 2,6-dichloropurine and were then subjected to alkylation of the N⁹ position with alkyl halides to obtain intermediates **4** (Scheme 3, steps iv and v).

Scheme 3. Synthesis of Immobilized CDK Inhibitors^a



^aReagents and conditions: (i) R¹-amine, NaBH(OAc)₃, DMF/AcOH (10:1), room temperature; (ii) R²-OH, PPh₃, diisopropyl azodicarboxylate (DIAD), THF, room temperature (**3a**, 86%; **3b**, 80%); (iii) *N,N'*-diisopropylethylamine (DIPEA), dioxane, 80 °C; (iv) 2,6-dichloropurine, dioxane, DIPEA, 80 °C; (v) R²-I, *tert*-butylimino)-tris(pyrrolidino)phosphorane (BTTP), DMSO, 65 °C; (vi) H₂N-R³-NH₂, Pd₂dba₃ (dba = dibenzylideneacetone), 2-dicyclohexylphosphino-2',4',6'-triisopropylbiphenyl (XPhos), LiHMDS, THF, 60 °C.

Alternatively, we obtained such intermediates after the N⁹-alkylation of 2,6-dichloropurine in the solution phase using Mitsunobu conditions (yielding **3a** and **3b**), followed by their immobilization through the arylation of resin **2** (Scheme 3, step iii). The latter alternative procedure yielded the desired intermediates with higher crude purities. Subsequently, the C² position underwent replacement of the chlorine with diamines. Because of the low reactivities of intermediates **4**, the reaction of these intermediates with 1,4-diaminocyclohexane required very harsh conditions to yield intermediates **5** quantitatively. For this reason, we developed a more efficient Pd-catalyzed substitution using Buchwald–Hartwig C–N coupling conditions that was successfully tested for both 1,4-diaminocyclohexane and putrescine to yield intermediates **5** with excellent crude purities (for a representative example, see Figure 1).

As in the conventional synthetic approach, the key step of the stepwise solid-phase sequence was the formation of the disulfide bridge using thiol–disulfide exchange. First, we intended to mimic the solution-phase approach, and for this reason, intermediates **5** were reacted with reagent **7**, which had been presynthesized from mercaptoethanol according to a published procedure (Scheme 4).²⁴ The desired intermediates **8** were obtained in excellent crude purities, as detected by ultrahigh-performance liquid chromatography (UHPLC)-UV-MS analysis after trifluoroacetic-acid-mediated cleavage from

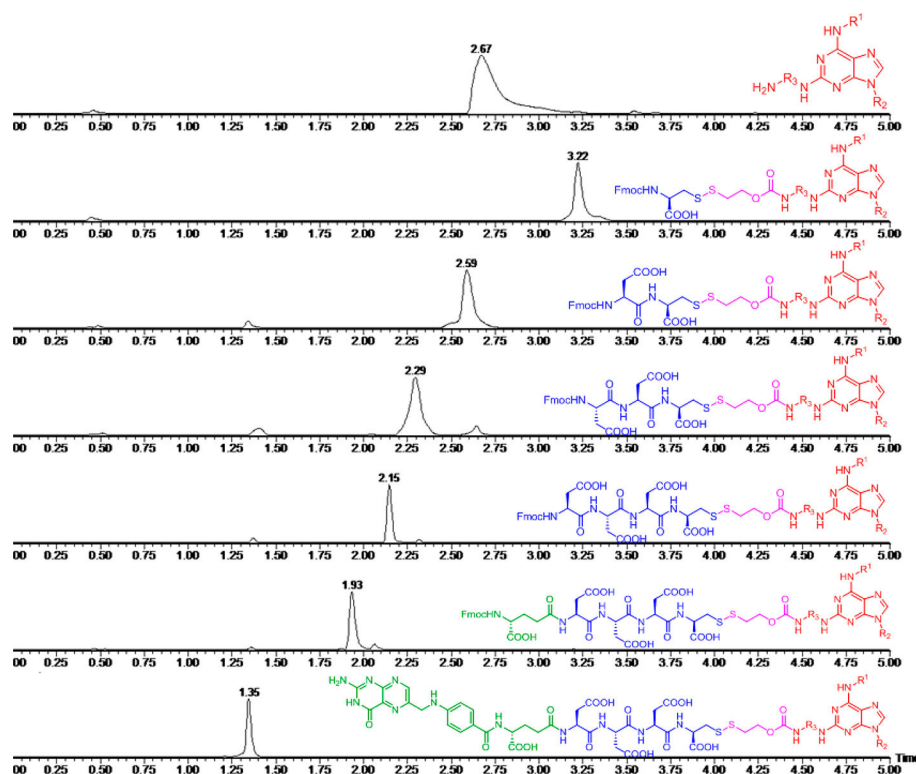
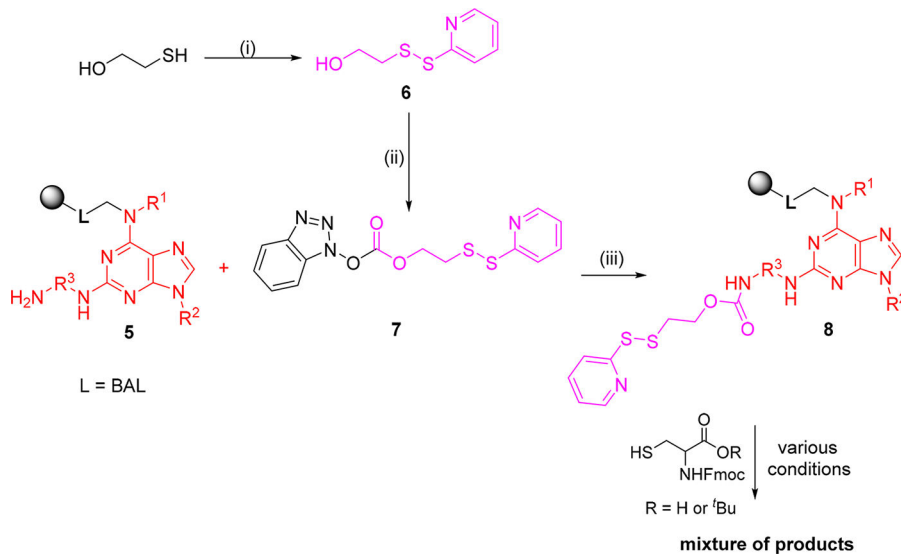


Figure 1. HPLC-UV traces of selected steps of the reaction sequence leading to compound 17c to demonstrate the crude purity of the corresponding intermediates after cleavage from the polymer support.

Scheme 4. Attempted Use of Intermediates 8 for Thiol–Disulfide Exchange^a



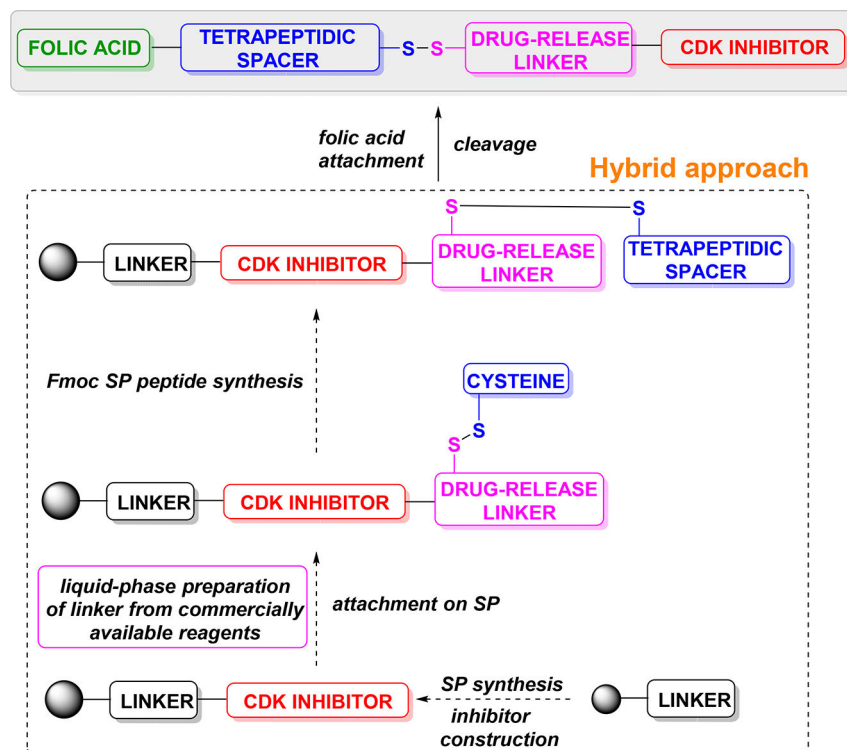
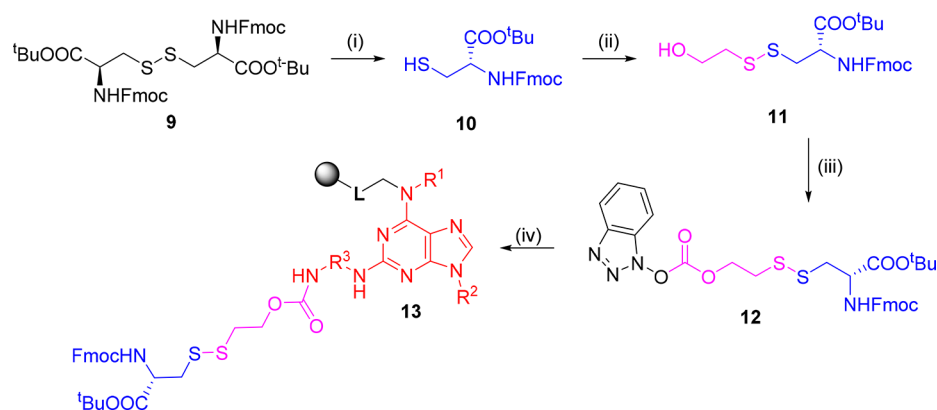
^aReagents and conditions: (i) methoxycarbonyl sulfonyl chloride, 2-mercaptopyridine, CH₃CN, 0 °C to reflux, (**6**: 81%); (ii) 1-hydroxybenzotriazole (HOBT), triphosgene, triethylamine (TEA), CH₂Cl₂, 0 °C to room temperature (**7**: 60%); (iii) DMAP, DIPEA, CH₂Cl₂, room temperature.

the resin. However, the subsequent reaction with Fmoc-Cys-OH or Fmoc-Cys-O^tBu provided results similar to those obtained in the case of the conventional approach: It was not possible to optimize the thiol–disulfide exchange to obtain the desired intermediates, even using various conditions (various pH values²⁵ and concentrations of reagents, solvents, and bases).

To overcome such problems, we switched to a hybrid approach consisting of the liquid-phase synthesis of the

problematic segment and its incorporation into the solid-phase synthesis sequence (Scheme 5). More specifically, intermediate **12** was prepared in three steps using commercially available L-cysteine derivative **9**. Compound **12** was then reacted with resin **5**, and the desired intermediate **13** was obtained in excellent crude purity, as determined from HPLC-UV traces after cleavage from the polymer support (see Scheme 6 and Figure 1).

Scheme 5. General Scheme for the Hybrid Approach to Overcome the Problematic Thiol–Disulfide Exchange

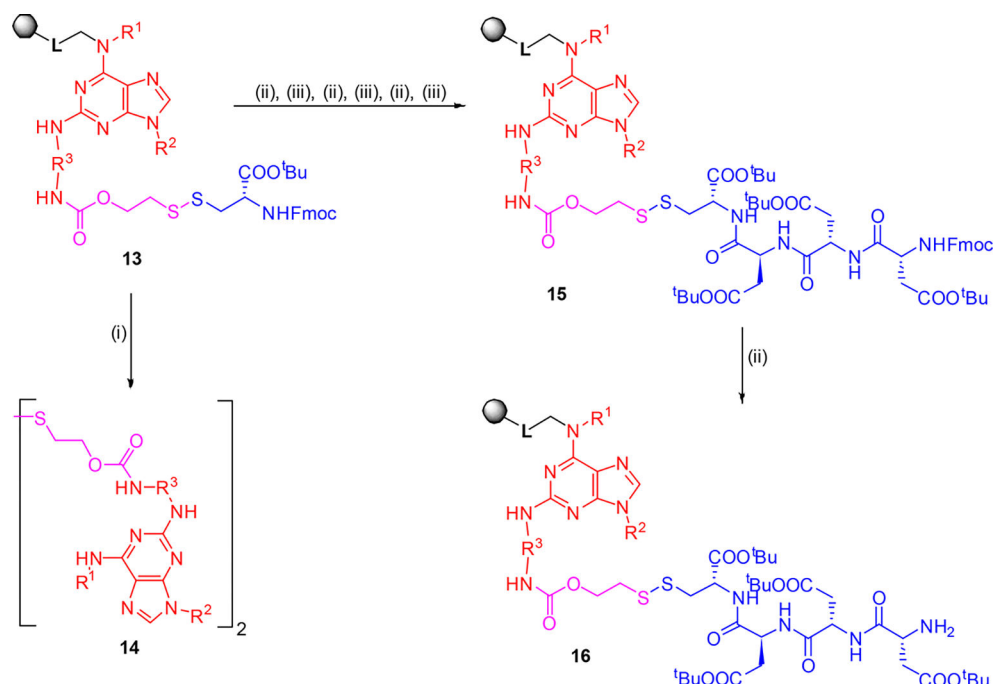
Scheme 6. Synthetic Sequence for the Proposed Hybrid Approach^a

^aReagents and conditions: (i) P(Bu)₃, THF/H₂O (40:1), room temperature (**10**, 91%); (ii) mercaptoethanol, methoxycarbonyl sulfonyl chloride, lutidine, CH₃CN, 0 °C to room temperature (**11**, 75%); (iii) HOBT, triphosgene, TEA, CH₂Cl₂, 0 °C to room temperature (**12**, 62%); (iv) CH₂Cl₂, room temperature.

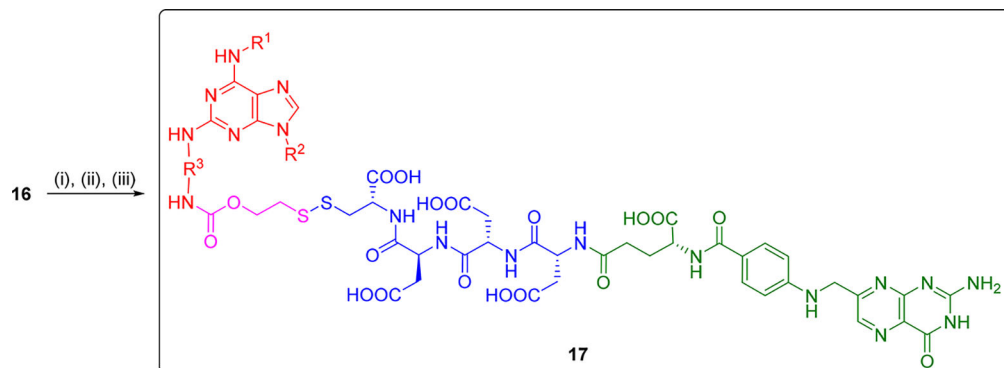
The subsequent task focused on the synthesis of the hydrophilic oligopeptide scaffold using repetitive coupling with Fmoc-Asp(O^tBu)-OH. Contrary to our expectations, this part of the reaction sequence also required careful optimization. Although the synthesis of a tetrapeptide from **13** using a standard Fmoc solid-phase peptide synthesis proceeded well and afforded intermediates **15** in high crude purity, cleavage of its Fmoc protective group using a common cocktail consisting of 20% piperidine in DMF caused the formation of unexpected major products. From the LC-MS traces, their structures were suggested to be the symmetrical disulfides **14** (Scheme 7). Fortunately, after further optimization, the formation of undesired byproducts **14** was fully suppressed using only 1% piperidine in DMF.

Finally, intermediates **16** were subjected to acylation with Fmoc-Glu(OH)-O^tBu, followed by cleavage of Fmoc protective group and acylation with pteric acid, which yielded the desired conjugates (Scheme 8). Products **17a–g** were cleaved from the polymer matrix using 50% TFA in CH₂Cl₂ and purified using semipreparative HPLC.

The reaction sequence was successfully tested using different building blocks, and the list of conjugates synthesized using the developed method is summarized in Table 1. Furthermore, Figure 1 displays the HPLC-UV traces of representative reaction intermediates. This figure demonstrates that the optimized procedure furnished the corresponding compounds in excellent crude purities and good yields after 15 reaction steps and reverse-phase purification.

Scheme 7. Undesired, Base-Catalyzed Redox Reaction Leading to Symmetrical Disulfides 14^a

^aReagents and conditions: (i) DMF/piperidine (4:1), room temperature; (ii) DMF/piperidine (99:1), room temperature; (iii) Fmoc-Asp(O^tBu)-OH, *N,N'*-diisopropylcarbodiimide (DIC), DMF/CH₂Cl₂ (1:1), room temperature.

Scheme 8. Finishing the Reaction Sequence^a

^aReagents and conditions: (i) Fmoc-Glu-O^tBu, DIC, DMF/CH₂Cl₂ (1:1), room temperature; (ii) pteric acid, HOBT, 2-(1*H*-benzotriazol-1-yl)-1,1,3,3-tetramethyluronium hexafluorophosphate (HBTU), DIPEA, DMF/DMSO/NMP (9:5:1), room temperature, protected from light; (iii) TFA/CH₂Cl₂ (1:1), room temperature.

In Vitro Disulfide Reduction Test. To test the applicability of our conjugates, we subsequently mimicked drug release *in vitro*. The mechanism of self-immolative cleavage of the linker is based on 1,2-elimination.²¹ Accordingly, the release of the CDK inhibitor was successfully accomplished by treating a 0.04 mM solution of representative conjugate 17d (Figure 2A) with 4 mM of the reducing agent dithiothreitol (DTT) at 37 °C. The release was monitored by UHPLC-UV ($\lambda = 289$ nm) at pH 7 and 7.4. The disulfide bond was cleaved within 5 min and yielded the drug-spacer intermediate (Figure 2B), which subsequently self-immolated and quantitatively released the purine inhibitor after 20 h (Figure 2C). Use of glutathione (GSH) instead of DTT led to cleavage of the conjugate 17d after the same time.

Cellular and Biochemical Assays. For a proof of concept, conjugate 17d was further tested for its binding to the HeLa

cell line overexpressing FOLR1 by flow cytometry using the folate-receptor-targeted fluorescence probe FolateRSense 680 (PerkinElmer) as a competing agent (Figure 3A). The HeLa cell line was used because of its overexpression of FOLR1 and significantly greater probe uptake over other cell lines; in addition, HeLa cells were also much more sensitive to the conjugate than other cell lines (see Supporting Information, Table S1). The cells were stained with 1 μ M FolateRSense 680 in the absence or presence of conjugate 17d (Figure 3B,C). In control incubations, the probe was combined with either the unconjugated inhibitor or free folic acid (Figure 3D,E). After 1 hour of incubation, cell-associated fluorescence was quantified by flow cytometry. Autofluorescence of the unstained cells was used for gating strategies, in which cells scattered outside the autofluorescence signal were considered probe-marked cells. The measurements confirmed that the presence of conjugated

Table 1. List of Synthesized Conjugates

| Compound | R ¹ | R ² | R ³ | Yield ^a ₁ |
|----------|----------------|----------------|----------------|---------------------------------|
| 17a | | | | 27% |
| 17b | | | | 22% |
| 17c | | | | 25% |
| 17d | | | | 23% |
| 17e | | | | 19% |
| 17f | | | | 20% |
| 17g | | | | 21% |

^aOverall yield calculated from the loading of resin 2 after the entire reaction sequence and preparative HPLC purification.

CDK inhibitor **17d** markedly decreased the percentage of cells with bound FolateRSense 680 from 75.6% to 11.4% (Figure 3C). Free folate also reduced the percentage of positive cells and thus confirmed the function of the probe (Figure 3D). The specificity of cellular binding of conjugate **17d** was demonstrated in a control experiment in which an excess of unconjugated CDK inhibitor (synthesized according to a previously published procedure)¹⁹ did not compete with the probe (Figure 3E). In a titration experiment, **17d** caused clear dose-dependent competition with the fluorescence probe (Figure 4), with half-maximal inhibitory concentration (IC₅₀) in the micromolar range.

Finally, conjugate **17d** was assayed to determine its kinase inhibitory potency toward recombinant human CDK2/cyclin E according to a published protocol.¹⁹ The IC₅₀ value for **17d** was 77 nM, which is comparable to the inhibition activities of related purine inhibitors.^{16–19} The high potency of **17d** was

rather surprising; however, it can be considered advantageous, because the inhibition of cellular CDKs is not necessarily limited by the speed of release of the free purine inhibitor from conjugate.

CONCLUSIONS

To conclude, we developed a synthetic method applicable for the preparation of purine CDK inhibitor conjugates targeted to the folate receptor. Compared to the conventional approach, a stepwise construction concept using solid-phase synthesis enabled the rapid production of the desired compounds. Furthermore, the diversification of individual parts of the target conjugates (oligopeptide, R¹–R³ substituents) can be easily accomplished by changing the building blocks in the reaction sequence. With respect to the numerous kinases as molecular targets of cytotoxic purines,²⁶ the strategy is not limited to CDK ligands, but can be used to produce the targeted conjugates of different inhibitors. The stepwise approach is not limited exclusively to purines but can furnish conjugates of any immobilized compound containing reactive nucleophilic moieties. Thus, the method reported herein represents a general approach for the modification and study of diverse drug-like heterocycles yielded by solid-phase synthesis. Flow cytometric measurements demonstrated the ability of an example conjugate to bind to cancer cells overexpressing the folate receptor. In addition, *in vitro* simulation of the intracellular liberation of the ligand from the drug-delivery handle demonstrated the applicability of our conjugates to release the inhibitor. In summary, we confirmed that CDK inhibitors conjugated to folate could bind FOLR1-overexpressing cells, suggesting that this concept is a possible route to the development of more selective anticancer drugs. Detailed biological experiments are in progress in our laboratories and will be reported in subsequent contributions.

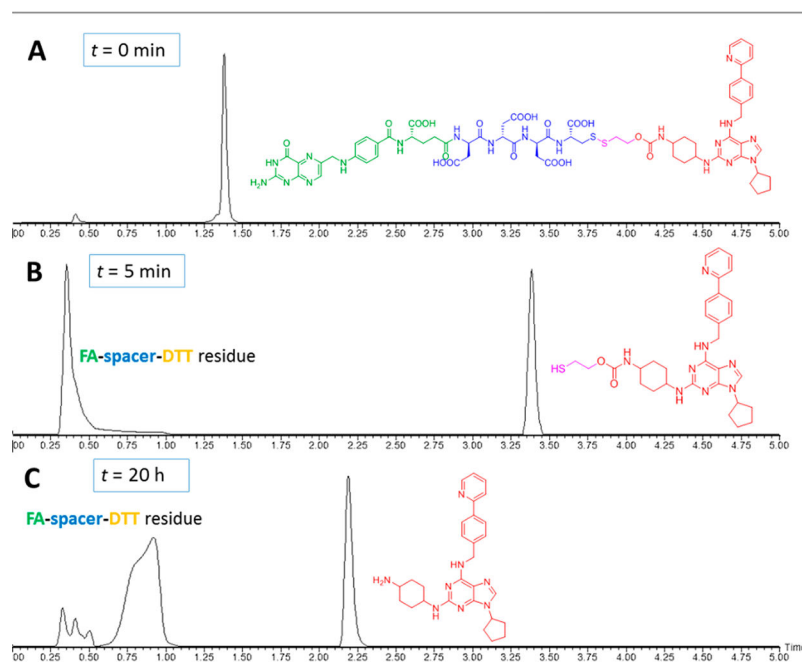


Figure 2. UHPLC-UV traces of the mimicked disulfide reduction test: (A) conjugate **17d**, (B) complete reduction of the disulfide bond in the presence of DTT after 5 min, (C) release of purine inhibitor after 20 h.

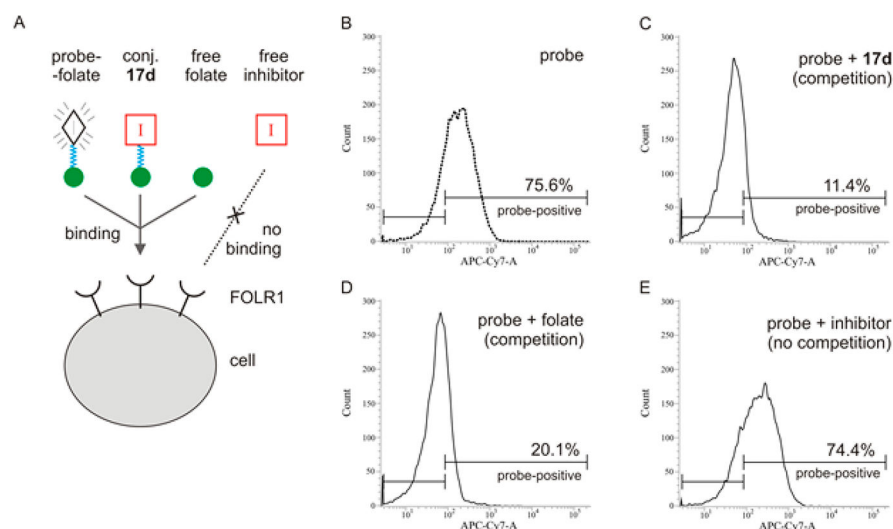


Figure 3. In vitro binding to the folate receptor: (A) Experimental design is shown for clarity. (B–E) HeLa cells were stained with 1 μM FolateRSense 680 probe (B) alone or in the presence of (C) conjugated CDK inhibitor 17d, (D) free folic acid, or (E) unconjugated CDK inhibitor in 50 μM concentrations. Segments mark probe-negative (left segment) and probe-positive (right segment) cells; numbers refer to the percentages of probe-positive cells.

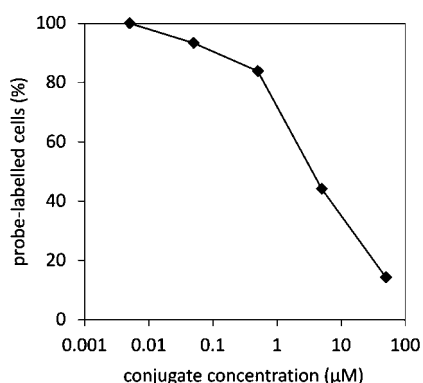


Figure 4. Dose-dependent competition of conjugate 17d with FolateRSense 680 probe for binding to the folate receptor in HeLa cells.

EXPERIMENTAL SECTION

General Information. All reagents were of reagent grade and were used without further purification. Solvents and chemicals were purchased from Sigma-Aldrich (Milwaukee, IL, www.sigmaaldrich.com) and Acros Organics (Geel, Belgium, www.acros.cz). Dry solvents were dried over 4 Å molecular sieves or stored as received from commercial suppliers. Aminomethyl resin [100–200 mesh, 1% divinylbenzene (DVB), 0.9 mmol/g] was obtained from AAPPTec (Louisville, KY, www.aapptec.com). The reactions were carried out in plastic reaction vessels (syringes, each equipped with a porous disk) using a manually operated synthesizer (Torviq, Niles, MI, www.torviq.com) or in dried glassware, unless stated otherwise. The volume of wash solvent was 10 mL per 1 g of resin. For washing, resin slurry was shaken with the fresh solvent for at least 1 min before the solvent was changed. Resin-bound intermediates were dried under a stream of nitrogen for prolonged storage and/or quantitative analysis. For the LC-MS analysis, a sample of resin (~5 mg) was treated with $\text{CH}_2\text{Cl}_2/\text{TFA}$ (1:1, 1 mL, v/v), the cleavage cocktail was evaporated under a stream of nitrogen, and the cleaved compounds were extracted into $\text{CH}_3\text{CN}/\text{H}_2\text{O}$ (1:1, 1 mL, v/v). The LC-MS analyses were carried out on a UHPLC-MS system consisting of a UHPLC chromatograph Acquity with a photodiode array detector and a single-quadrupole mass spectrometer (Waters), using an X-Select C18 column at 30 °C and a flow rate of 600 $\mu\text{L}/\text{min}$. Mobile phase consisted of (A) 0.01 M

ammonium acetate in H_2O and (B) CH_3CN , linearly programmed from 10% A to 80% B over 2.5 min and held at the latter composition for 1.5 min. The column was re-equilibrated with 10% of solution B for 1 min. The ESI ion source was operated at a discharge current of 5 μA , a vaporizer temperature of 350 °C, and a capillary temperature of 200 °C. Purification was carried out on a C18 reverse-phase column (YMC Pack ODS-A, 20 \times 100 mm, 5- μm particles), with a gradient formed from 10 mM aqueous ammonium acetate and CH_3CN at flow rate of 15 mL/min. Flash chromatography was carried out on silica gel (230–400 mesh). TLC plates were visualized under UV and/or with cerium ammonium molybdate (CAM) stain. For lyophilization of the residual solvents at –110 °C, a ScanVac Coolsafe 110-4 freeze dryer was used. NMR spectra were recorded on a JEOL ECX500 spectrometer at a magnetic field strength of 11.75 T (with operating frequencies of 500.16 MHz for ^1H and 125.77 MHz for ^{13}C). Chemical shifts (δ) are reported in parts per million (ppm), and coupling constants (J) are reported in Hertz (Hz). The ^1H and ^{13}C NMR chemical shifts (δ in ppm) were referenced to the residual signals of CDCl_3 [7.26 ppm (^1H) and 77.23 ppm (^{13}C)] and $\text{DMSO}-d_6$ [2.50 ppm (^1H) and 39.51 ppm (^{13}C)]. ^{19}F NMR chemical shifts (δ in ppm) were referenced to the signal of trifluoroacetic acid (–76.55 ppm). Structural assignment of resonances was performed with the help of 2D NMR gradient experiments (COSY, ^1H – ^{13}C HMQC, ROESY). Acetate salt (residual agent from the semipreparative HPLC purification) exhibited a singlet at 1.89–1.90 ppm in the ^1H NMR spectrum and two resonances at 21.1–21.3 ppm and 172.0–172.1 ppm in the ^{13}C NMR spectrum. Abbreviations in NMR spectra: app d, apparent doublet; app s, apparent singlet; app t, apparent triplet; br s, broad singlet; d, doublet; dd, doublet of doublets; m, multiplet; s, singlet; sp, septet; t, triplet. IR spectra (4000–400 cm^{-1}) were collected on a Nicolet Avatar 370 FTIR spectrometer. Solid samples were measured neat, and oily samples were measured as films. Abbreviations in IR spectra: s, strong; m, medium; w, weak. HRMS analysis was performed using an Orbitrap Elite LC-MS hybrid quadrupole mass spectrometer (Dionex UltiMate 3000, Thermo Exactive Plus, Waltham, MA) operating in positive full-scan mode (120000 fwhm) in the range of 100–1000 m/z . The settings for electrospray ionization were as follows: oven temperature, 150 °C; source voltage, 3.6 kV. The acquired data were internally calibrated with diisooctyl phthalate as a contaminant in CH_3OH . Samples were diluted to a final concentration of 0.1 mg/mL in H_2O and CH_3OH (50:50, v/v). Before HPLC separation (Phenomenex Gemini column, 50 \times 2.00 mm, 3- μm particles, C18), the samples were injected by direct infusion into the mass spectrometer using an autosampler. The mobile phase was isocratic $\text{CH}_3\text{CN}/\text{isopropanol}$

(IPA)/0.01 M ammonium acetate (40:5:55) at a flow rate of 0.3 mL/min.

Experimental Procedures. *2,6-Dichloro-9-cyclopentyl-9H-purine (3a)*. To a solution of 2,6-dichloropurine (2 g, 10.60 mmol) and PPh₃ (3.6 g, 13.76 mmol) in dry, degassed THF (20 mL) was added cyclopentanol (1.9 mL, 21.20 mmol), and the solution was cooled to 0 °C. At this temperature, DIAD (2.7 mL, 13.76 mmol) was slowly added, and the reaction mixture was stirred at ambient temperature under a nitrogen atmosphere. The reaction was monitored by UHPLC-MS, which indicated its completion after 18 h. The reaction mixture was concentrated, diluted with brine (100 mL), and extracted with EtOAc (5 × 70 mL). The organic extracts were combined, dried over MgSO₄, filtered, and evaporated under reduced pressure. The crude product was purified by flash chromatography (CH₂Cl₂/EtOAc = 1:1, v/v) to afford compound 3a as a bright yellow crystalline solid (2.3 g, 86% yield). ¹H NMR (500 MHz, CDCl₃): δ 8.15 (s, 1H), 2.37–2.32 (m, 2H), 2.07–1.94 (m, 4H), 1.90–1.80 (m, 2H) ppm. Other data were consistent with published results.²⁷

2,6-Dichloro-9-isopropyl-9H-purine (3b). To a solution of 2,6-dichloropurine (500 mg, 2.64 mmol) and PPh₃ (838 mg, 3.20 mmol) in dry, degassed THF (10 mL) was added isopropanol (400 μL, 5.30 mmol), and the solution was cooled to 0 °C. At this temperature, DIAD (630 μL, 3.20 mmol) was slowly added, and the reaction mixture was stirred at ambient temperature under a nitrogen atmosphere. The reaction was monitored by UHPLC-MS, which indicated its completion after 18 h. The reaction mixture was concentrated, diluted with brine (50 mL), and extracted with EtOAc (5 × 70 mL). The organic extracts were combined, dried over MgSO₄, filtered, and evaporated under reduced pressure. The crude product was purified by flash chromatography (CH₂Cl₂/EtOAc = 1:1, v/v) to afford compound 3b as a white crystalline solid (490 mg, 80% yield). ¹H NMR (500 MHz, CDCl₃): δ 8.17 (s, 1H), 4.91 (sp, J = 6.8 Hz, 1H), 1.65 (d, J = 6.8 Hz, 6H) ppm. Other data were consistent with published results.²⁸

2-(Pyridin-2-ylidinesulfanyl)ethan-1-ol (6). To a solution of methoxycarbonyl sulfonyl chloride (2.3 mL, 25.60 mmol) in CH₃CN (10 mL) at 0 °C was slowly added 2-mercaptoethanol (1.8 mL, 25.60 mmol) in CH₃CN (10 mL), and the solution was stirred for 30 min at 0 °C. To the clear solution was added 2-mercaptopyridine (2.5 g, 23.04 mmol) in CH₃CN (15 mL), and the yellow mixture was refluxed for 2 h until a white precipitate formed. The reaction mixture was cooled to ambient temperature and stirred for an additional 1 h at 0 °C. The precipitate was filtered and washed with CH₃CN (3 × 50 mL). The crude white solid product 6 was dried and used in the next step without further purification (3.9 g, 81% yield). Data were consistent with published results.²⁹

1H-Benzo[D][1,2,3]triazol-1-yl (2-(pyridin-2-ylidinesulfanyl)ethyl) Carbonate (7). To a solution of triphosgene (1.84 g, 6.20 mmol) in dry CH₂Cl₂ (15 mL) at 0 °C under a nitrogen atmosphere was slowly added a solution of compound 6 (3.9 g, 20.67 mmol) and TEA (2.9 mL, 20.67 mmol) in dry CH₂Cl₂ (15 mL). The reaction mixture was stirred at ambient temperature for 1 h. Then, a solution of HOBt (3.16 g, 20.67 mmol) and TEA (2.9 mL, 20.67 mmol) in dry CH₂Cl₂ (15 mL) was slowly added over a duration of 20 min at 0 °C. The reaction was monitored by UHPLC-MS, which indicated its completion after 12 h. The reaction mixture was concentrated, diluted with brine (50 mL), and extracted with CH₂Cl₂ (5 × 70 mL). The organic extracts were combined, dried over MgSO₄, filtered, and evaporated to dryness under reduced pressure. Product 7 was obtained as a white crystalline solid (2.86 g, 40% yield). ¹H NMR (500 MHz, CDCl₃): δ 8.46–8.45 (m, 1H), 8.22–8.20 (m, 1H), 8.04–7.97 (m, 1H), 7.79–7.76 (m, 1H), 7.70–7.62 (m, 2H), 7.57–7.53 (m, 1H), 7.10–7.08 (m, 1H), 4.81 (t, J = 6.4 Hz, 2H), 3.26 (t, J = 6.4 Hz, 2H) ppm. ¹³C NMR (126 MHz, CDCl₃): δ 159.0, 149.9, 147.1, 137.3, 133.4, 133.0, 126.5, 121.3, 120.4, 115.9, 115.2, 66.4, 36.7 ppm. HRMS (ESI) *m/z*: [M + H]⁺ calcd for C₁₄H₁₃N₄O₃S₂, 349.0424; found, 349.0425.

tert-Butyl ((9H-fluoren-9-yl)methoxy)carbonyl)cysteinate (10). To a solution of protected cystine 9 (700 mg, 0.87 mmol) in dry, degassed THF/H₂O (40:1, 12.5 mL, v/v) at 0 °C was slowly added

P(Bu)₃ (240 μL, 0.96 mmol), and the solution was stirred at ambient temperature. The reaction was monitored by TLC (hexane/EtOAc = 3:1, v/v), which indicated its completion after 6–12 h. The reaction mixture was diluted with 10% aqueous AcOH (50 mL) and extracted with EtOAc (5 × 70 mL). The organic extracts were combined, dried over MgSO₄, filtered, and evaporated under reduced pressure. The crude product was purified by flash chromatography (hexane/EtOAc = 3:1, v/v) to afford compound 10 as a pale yellow oil (639 mg, 92% yield). ¹H NMR (500 MHz, CDCl₃): δ 7.77 (d, J = 7.5 Hz, 2H), 7.61 (d, J = 7.4 Hz, 2H), 7.41 (app t, J = 7.4 Hz, 2H), 7.33 (app t, J = 7.4 Hz, 2H), 5.70 (d, J = 7.0 Hz, 1H), 4.57–4.53 (m, 1H), 4.46–4.37 (m, 2H), 4.24 (t, J = 6.9 Hz, 1H), 3.03–2.96 (m, 2H), 1.51 (s, 9H), 1.34 (t, J = 8.9 Hz, 1H) ppm. ¹³C NMR (126 MHz, CDCl₃): δ 169.0, 155.7, 143.9, 141.4, 127.8, 125.2, 125.1, 120.1, 83.1, 67.1, 55.4, 47.2, 28.1, 27.4 ppm. HRMS (ESI) *m/z*: [M – H][–] calcd for C₂₂H₂₄NO₄S, 398.1426; found, 398.1423.

tert-Butyl-N-(((9H-fluoren-9-yl)methoxy)carbonyl)-S-((2-hydroxyethyl)thio)cysteinate (11). To a solution of methoxycarbonyl sulfonyl chloride (200 μL, 2.22 mmol) in CH₃CN (2 mL) at 0 °C was slowly added 2-mercaptoethanol (155 μL, 2.22 mmol) in CH₃CN (2 mL), and the solution was stirred for 30 min. Then, a solution of compound 10 (800 mg, 2.00 mmol) and 2,6-lutidine (1.3 mL, 11.1 mL) in CH₃CN (5 mL) was slowly added to the reaction mixture. The reaction was monitored by UHPLC-MS, which indicated its completion after 1.5 h. The residual solvent was evaporated, and the reaction mixture was diluted with NH₄Cl (50 mL) and extracted with EtOAc (5 × 70 mL). The organic extracts were combined, dried over MgSO₄, filtered, and evaporated under reduced pressure. The crude product was purified by column chromatography (first, CH₂Cl₂/EtOAc = 1:1, v/v; second, hexane/EtOAc = 2:1, v/v) to afford compound 11 as a pale yellow oil (715 mg, 75% yield). ¹H NMR (500 MHz, CDCl₃): δ 7.77 (d, J = 7.6 Hz, 2H), 7.61 (d, J = 7.4 Hz, 2H), 7.41 (t, J = 7.4 Hz, 2H), 7.32 (t, J = 7.4 Hz, 2H), 5.67 (d, J = 7.3 Hz, 1H), 4.59 (dd, J = 12.5, 5.3 Hz, 1H), 4.46–4.36 (m, 2H), 4.24 (t, J = 7.0 Hz, 1H), 3.85 (app t, J = 5.6 Hz, 1H), 3.27 (dd, J = 14.1, 5.3 Hz, 1H), 3.15 (dd, J = 14.1, 5.3 Hz, 1H), 2.90–2.84 (m, 1H), 1.50 (s, 9H) ppm. ¹³C NMR (126 MHz, CDCl₃): δ 169.4, 155.9, 143.8, 141.4, 127.8, 127.2, 125.2, 120.1, 83.4, 67.3, 60.4, 54.3, 47.2, 42.2, 41.4, 28.1 ppm. HRMS (ESI) *m/z*: [M + H]⁺ calcd for C₂₄H₃₀NO₅S₂, 476.1565; found, 476.1562.

tert-Butyl-S-(((1H-benzo[d][1,2,3]triazol-1-yl)oxy)carbonyl)-oxyethylthio)-N-(((9H-fluoren-9-yl)methoxy)carbonyl)cysteinate (12). To a solution of triphosgene (310 mg, 1.05 mmol) in dry CH₂Cl₂ (8 mL) at 0 °C under a nitrogen atmosphere was slowly added a solution of compound 11 (715 mg, 1.50 mmol) and 2,6-lutidine (523 μL, 4.5 mmol) in dry CH₂Cl₂ (8 mL). The reaction mixture was stirred at ambient temperature for 3 h. Then, a solution of HOBt (230 mg, 1.50 mmol) and 2,6-lutidine (523 μL, 4.5 mmol) in dry CH₂Cl₂ (8 mL) was slowly added within 10 min at 0 °C, and the reaction mixture was stirred at ambient temperature. The reaction was monitored by UHPLC-MS, which indicated its completion after 12 h. The residual solvent was evaporated to dryness, and the crude reaction mixture was diluted with EtOAc (100 mL) and extracted with aqueous NH₄Cl (6 × 200 mL). The organic extract was dried over MgSO₄, filtered, and evaporated under reduced pressure. The crude product was used without further purification or was purified by semipreparative HPLC to afford compound 12 as a pale yellow solid (600 mg, 65% yield). ¹H NMR (500 MHz, CDCl₃): δ 8.16 (d, J = 8.4 Hz, 1H), 7.99 (d, J = 8.4 Hz, 1H), 7.74–7.72 (m, 3H), 7.59 (d, J = 7.4 Hz, 2H), 7.51 (t, J = 7.8 Hz, 1H), 7.42–7.27 (m, 5H), 5.66 (d, J = 7.3 Hz, 1H), 4.75 (t, J = 6.7 Hz, 2H), 4.59 (d, J = 6.6 Hz, 1H), 4.42 (dd, J = 10.2, 7.6 Hz, 1H), 4.37–4.31 (m, 1H), 4.22 (t, J = 6.9 Hz, 1H), 3.32 (dd, J = 13.8, 4.8 Hz, 1H), 3.20 (dd, J = 13.8, 4.8 Hz, 1H), 3.13–3.07 (m, 2H), 1.49 (s, 9H) ppm. ¹³C NMR (126 MHz, CDCl₃): δ 169.3, 160.8, 155.7, 147.2, 143.8, 141.4, 132.9, 127.8, 127.2, 126.5, 125.2, 120.1, 115.9, 115.2, 83.5, 67.2, 66.6, 54.2, 47.2, 42.1, 36.5, 28.1 ppm. HRMS (ESI) *m/z*: [M + H]⁺ calcd for C₃₁H₃₃N₄O₇S₂, 637.1791; found, 637.1790.

Preparation of BAL Resin 1. Aminomethyl polystyrene resin (1 g, loading of 0.98 mmol/g) was swollen in CH₂Cl₂ (10 mL) for 30 min, washed with DMF (3 × 10 mL), neutralized in DMF/piperidine (5:1,

10 mL) for an additional 30 min, and then again washed with DMF (5 × 10 mL). Backbone amide linker (700 mg, 2.94 mmol) and HOBT (450 mg, 2.94 mmol) were dissolved in DMF/CH₂Cl₂ (1:1, 10 mL, v/v), and DIC (460 μL, 2.94 mmol) was added. The resulting solution was added to a polypropylene fritted syringe with aminomethyl resin. The reaction slurry was shaken at ambient temperature overnight and then washed with DMF (3 × 10 mL) and CH₂Cl₂ (3 × 10 mL). A bromophenol blue test confirmed the quantitative acylation of amino groups.

General Procedure for Reductive Amination to Obtain Resin 2. BAL resin **1** was swollen in CH₂Cl₂ (10 mL) for 30 min and then washed with dry THF (3 × 10 mL) and dry DMF (3 × 10 mL). A solution of the corresponding amine (4.9 mmol) in DMF/AcOH (10:1, 10 mL, v/v) was added to the resin, and the mixture was shaken overnight at ambient temperature. Then, NaBH(OAc)₃ (210 mg, 2.94 mmol) in DMF/AcOH (20:1, 5 mL, v/v) was added portionwise to the reaction mixture during a period of 4 h, after which the mixture was washed with DMF (5 × 10 mL) and CH₂Cl₂ (3 × 10 mL) and neutralized with DMF/TEA (10:1, 10 mL, v/v) for an additional 30 min to obtain resin **2**. The loading was determined according to a published procedure.³⁰

General Procedure for the Preparation of Intermediates 4. Arylation with 2,6-Dichloropurine Followed by On-Resin N⁹-Alkylation. Resin **2** (500 mg) was swollen in CH₂Cl₂ (5 mL) for 30 min and then washed with CH₂Cl₂ (3 × 5 mL). 2,6-Dichloropurine (320 mg, 1.55 mmol) and DIPEA (256 μL, 1.55 mmol) were dissolved in dioxane (5 mL) and added to a sealed vial with resin **2**. The reaction slurry was shaken at 80 °C overnight and then washed with THF (5 × 5 mL) and CH₂Cl₂ (5 × 5 mL). The corresponding resin (500 mg) was swollen in CH₂Cl₂ (5 mL) for 30 min and then washed with CH₂Cl₂ (3 × 5 mL), DMF (3 × 5 mL), and DMSO (3 × 5 mL). Alkyl iodide (3.72 mmol), BTTP (1.13 mL, 3.72 mmol), and DMSO (5 mL) were added to the resin. The reaction slurry was shaken at 65 °C overnight and then washed with DMF (10 × 5 mL), DMSO (5 × 5 mL), THF (5 × 5 mL), and CH₂Cl₂ (10 × 5 mL).

Arylation with N⁹-Prealkylated Intermediates 3. Resin **2** (500 mg) was swollen in CH₂Cl₂ (5 mL) for 30 min and then washed with CH₂Cl₂ (3 × 5 mL). Intermediates **3** (3 mmol) and DIPEA (495 μL, 3 mmol) were dissolved in dioxane (5 mL) and added to a sealed vial with resin **2**. The reaction slurry was shaken at 80 °C overnight and then washed with THF (5 × 5 mL) and CH₂Cl₂ (5 × 5 mL).

General Procedure for the Preparation of Intermediates 5. Resin **4** (250 mg) was swollen in CH₂Cl₂ (5 mL) for 30 min and then washed with CH₂Cl₂ (3 × 5 mL) and dry THF (3 × 5 mL) that had been degassed prior to use. Amine (2 mmol), XPhos (96 mg, 0.2 mmol), Pd₂dba₃ (92 mg, 0.1 mmol) and LiHMDS (1 M solution in THF, 2 mL, 2 mmol) were dissolved in dry, degassed THF (5 mL) and added to a sealed vial with resin **4**. The reaction slurry was protected from light and shaken at 60 °C for 24 h, after which it was washed with DMF (10 × 5 mL), THF (5 × 5 mL), and CH₂Cl₂ (5 × 5 mL).

General Procedure for the Preparation of Intermediates 13. Resin **5** (250 mg) was swollen in CH₂Cl₂ (5 mL) for 30 min and then washed with CH₂Cl₂ (3 × 5 mL). Linker **12** (318 mg, 0.5 mmol) was dissolved in CH₂Cl₂ (2.5 mL) and added to a polypropylene fritted syringe with resin **5**. The reaction slurry was shaken at ambient temperature overnight and then washed with CH₂Cl₂ (5 × 3 mL).

General Procedure for the Preparation of Intermediates 15. To obtain intermediates **15**, the following procedures were repeated three times:

Step 1: Deprotection of Fmoc. Resin **13** (250 mg) was swollen in CH₂Cl₂ (5 mL) for 30 min and then washed with CH₂Cl₂ (3 × 5 mL). To the resin was added a solution of DMF/piperidine (99:1, 2.5 mL, v/v), and the slurry was shaken for 2 h at ambient temperature followed by wash with DMF (5 × 5 mL) and CH₂Cl₂ (5 × 5 mL).

Step 2: Acylation. Fmoc-Asp(O^tBu)-OH (308 mg, 0.75 mmol) was dissolved in DMF/CH₂Cl₂ (1:1, 2.5 mL, v/v), and DIC (58 μL, 0.37 mmol) was added. The reaction mixture was added to a propylene fritted syringe with deprotected resin **13**, and the reaction slurry was shaken overnight at ambient temperature. The resin was washed with CH₂Cl₂ (5 × 3 mL).

General Procedure for the Preparation of Intermediates 16. Resin **15** (250 mg) was swollen in CH₂Cl₂ (5 mL) for 30 min and then washed with CH₂Cl₂ (3 × 5 mL). To the resin was added a solution of DMF/piperidine (99:1, 2.5 mL, v/v), and the slurry was shaken for 2 h at ambient temperature. The resin was washed with CH₂Cl₂ (5 × 3 mL).

General Procedure for the Preparation of Final Compounds 17. Step 1: Acylation with Fmoc-Glu-O^tBu. Fmoc-Glu-O^tBu (317 mg, 0.75 mmol) was dissolved in DMF/CH₂Cl₂ (1:1, 2.5 mL, v/v), and DIC (58 μL, 0.37 mmol) was added. The reaction mixture was added to a propylene fritted syringe with resin **16**, and the reaction slurry was shaken overnight at ambient temperature. The resin was washed with CH₂Cl₂ (5 × 3 mL).

Step 2: Fmoc Cleavage and Acylation with Pteric Acid. The resin (250 mg) was swollen in CH₂Cl₂ (5 mL) for 30 min and then washed with CH₂Cl₂ (3 × 5 mL). To the resin was added a solution of DMF/piperidine (99:1, 2.5 mL, v/v), and the slurry was shaken for 2 h at ambient temperature and then washed with CH₂Cl₂ (5 × 3 mL).

Then, HBTU (112 mg, 0.3 mmol) and HOBT (46 mg, 0.3 mmol) were dissolved in DMF/DMSO/NMP (9:5:1, 7.5 mL, v/v), and pteric acid (250 mg, 0.64 mmol) was added. The reaction mixture was added to a propylene fritted syringe with the resin, and the reaction slurry was protected from light and shaken for 18 h at ambient temperature.

The resin was washed with DMF (10 × 5 mL), DMSO (10 × 5 mL), water (10 × 5 mL), DMSO (10 × 5 mL), DMF (10 × 5 mL), THF (10 × 5 mL), and CH₂Cl₂ (5 × 5 mL).

Step 3: Cleavage from the Resin. The resin (250 mg) was swollen in CH₂Cl₂ (5 mL) for 30 min and then washed with CH₂Cl₂ (3 × 5 mL). To the resin was added a solution of CH₂Cl₂/TFA (1:1, 5 mL, v/v), and the slurry was shaken for 2 h at ambient temperature, after which it was evaporated under a stream of nitrogen and extracted into CH₃CN/H₂O (1:1, 3 mL, v/v). The final conjugates **17a–g** were purified by semipreparative HPLC.

Conjugate 17a. Yellowish oil (60 mg, 27% yield). ¹H NMR (500 MHz, DMSO-*d*₆): δ 9.15 (br s, 1H), 8.63 (s, 1H), 8.25 (d, *J* = 6.9 Hz, 1H), 8.18 (d, *J* = 7.7 Hz, 1H), 8.05 (d, *J* = 6.6 Hz, 1H), 7.89 (s, 1H), 7.84 (d, *J* = 8.7 Hz, 2H), 7.73 (d, *J* = 6.4 Hz, 1H), 7.66–7.61 (m, 2H), 7.33 (br s, 1H), 7.28 (d, *J* = 8.0 Hz, 1H), 6.95 (t, *J* = 6.7 Hz, 1H), 6.87 (d, *J* = 9.1 Hz, 2H), 6.65–6.62 (m, 2H), 6.35 (br s, 1H), 4.55–4.47 (m, 7H), 4.29–4.20 (m, 3H), 4.16–4.14 (m, 3H), 3.76–3.72 (m, 5H), 3.22–3.13 (m, 2H), 3.06–3.02 (m, 4H), 2.98–2.94 (m, 5H), 2.74–2.55 (m, 4H), 2.03–1.95 (m, 4H), 1.86–1.81 (m, 2H), 1.48 (d, *J* = 6.6 Hz, 6H), 1.35–1.25 (m, 5H) ppm. ¹³C NMR (126 MHz, DMSO-*d*₆): δ 174.0, 172.3, 172.0, 171.1, 170.5, 170.1, 167.4, 161.9, 158.1, 155.2, 154.4, 154.1, 152.0, 150.6, 148.6, 148.4, 146.3, 135.5, 133.0, 131.1, 128.8, 127.8, 121.5, 115.4, 111.3, 66.2, 61.7, 56.8, 53.4, 52.5, 50.3, 49.9, 49.4, 49.3, 45.9, 43.6, 36.7, 31.6, 31.2, 26.8 ppm. IR ($\bar{\nu}_{\max}$) = 3270 (w), 3056 (w), 2919 (w), 2851 (w), 1632 (m), 1605 (m), 1511 (s), 1452–1411 (m), 1300 (m), 1263 (m), 1228 (s), 1178 (s), 1118 (m), 1005 (s), 951 (m), 924 (m), 822 (m), 765 (m), 719 (m) cm⁻¹. HRMS (ESI) *m/z*: [M + H]⁺ calcd for C₆₁H₇₆N₁₉O₁₉S₂, 1442.5001; found, 1442.5000.

Conjugate 17b. Yellowish oil (66 mg, 22% yield). ¹H NMR (500 MHz, DMSO-*d*₆): δ 8.62 (s, 1H), 8.24–8.23 (m, 1H), 8.19 (d, *J* = 7.1 Hz, 1H), 8.03 (d, *J* = 7.3 Hz, 1H), 7.84–7.83 (m, 3H), 7.73 (d, *J* = 7.6 Hz, 1H), 7.62 (d, *J* = 8.7 Hz, 2H), 7.39 (br s, 1H), 7.28 (d, *J* = 7.6 Hz, 1H), 6.94 (t, *J* = 5.2 Hz, 1H), 6.87 (d, *J* = 9.0 Hz, 2H), 6.63 (d, *J* = 8.7 Hz, 2H), 4.70–4.63 (m, 1H), 4.49–4.47 (m, 5H), 4.27–4.22 (m, 2H), 4.15 (t, *J* = 5.8 Hz, 2H), 3.76–3.68 (m, 5H), 3.60 (br s, 1H), 3.26 (br s, 1H), 3.21–3.15 (m, 1H), 3.05–3.02 (m, 4H), 3.00–2.88 (m, 4H), 2.74–2.53 (m, 4H), 2.24–1.99 (m, 11H), 1.85–1.83 (m, 4H), 1.67–1.64 (m, 2H), 1.31–1.26 (m, 4H) ppm. ¹³C NMR (126 MHz, DMSO-*d*₆): δ 174.1, 172.4, 172.4, 172.3, 172.1, 171.1, 170.6, 170.1, 166.1, 161.5, 158.1, 155.2, 154.5, 150.7, 148.6, 148.4, 146.3, 136.2, 132.9, 128.8, 127.8, 121.6, 121.1, 115.4, 111.3, 66.2, 61.7, 53.4, 52.6, 49.9, 49.4, 49.3, 45.9, 41.7, 37.3, 37.0, 36.7, 31.8, 31.6, 31.2, 26.9 ppm. IR ($\bar{\nu}_{\max}$) = 3304 (m), 2914 (w), 2849 (w), 1637 (s), 1604 (s), 1510 (s), 1450–1408 (m), 1264 (m), 1227 (m), 1183 (m), 1115 (m), 1002 (s),

950 (m), 924 (m), 820 (m), 766 (m) cm^{-1} . HRMS (ESI) m/z : $[\text{M} + \text{H}]^+$ calcd for $\text{C}_{63}\text{H}_{78}\text{N}_{19}\text{O}_{19}\text{S}_{22}$, 1468.5157; found, 1468.5165.

Conjugate 17c. Yellowish oil (60 mg, 25% yield). ^1H NMR (500 MHz, $\text{DMSO}-d_6$): δ 9.11 (br s, 1H), 8.62 (s, 1H), 8.25 (d, $J = 4.8$ Hz, 1H), 8.17 (d, $J = 7.2$ Hz, 1H), 8.02 (d, $J = 5.5$ Hz, 1H), 7.85–7.81 (m, 3H), 7.72 (d, $J = 7.0$ Hz, 1H), 7.61 (d, $J = 8.6$ Hz, 2H), 7.37–7.31 (m, 2H), 6.95 (t, $J = 6.1$ Hz, 1H), 6.87 (d, $J = 9.1$ Hz, 2H), 6.66–6.60 (m, 2H), 6.56–6.50 (m, 1H), 4.71–4.65 (m, 1H), 4.51–4.47 (m, 5H), 4.23–4.22 (m, 3H), 4.12 (t, $J = 6.2$ Hz, 2H), 3.75–3.70 (m, 6H), 3.27–3.23 (m, 3H), 3.20–3.14 (m, 2H), 3.05–3.02 (m, 4H), 3.02–2.87 (m, 8H), 2.72–2.56 (m, 4H), 2.22 (m, 1H), 2.16–2.06 (m, 3H), 2.04–1.92 (m, 4H), 1.70–1.60 (m, 3H), 1.55–1.44 (m, 5H) ppm. ^{13}C NMR (126 MHz, $\text{DMSO}-d_6$): δ 174.1, 172.4, 172.1, 171.1, 170.6, 170.1, 166.0, 161.2, 158.9, 155.9, 154.5, 152.0, 150.6, 148.6, 148.4, 146.3, 136.1, 132.8, 131.6, 128.7, 127.8, 121.1, 115.3, 111.3, 66.2, 61.7, 54.8, 53.5, 50.3, 50.2, 49.9, 49.2, 45.9, 43.6, 36.8, 31.8, 27.1, 23.7 ppm. IR ($\tilde{\nu}_{\text{max}}$) = 3282 (m), 2952 (w), 2916 (w), 2850 (w), 1639 (m), 1605 (m), 1511 (s), 1452–1411 (m), 1376 (m), 1228 (s), 1179 (m), 1121 (m), 1005 (s), 997 (m), 951 (m), 923 (m), 823 (m), 801 (m), 765 (s) cm^{-1} . HRMS (ESI) m/z : $[\text{M} + \text{H}]^+$ calcd for $\text{C}_{61}\text{H}_{76}\text{N}_{19}\text{O}_{19}\text{S}_{22}$, 1442.5001; found, 1442.5009.

Conjugate 17d. Yellowish oil (50 mg, 23% yield). ^1H NMR (500 MHz, $\text{DMSO}-d_6$): δ 8.64–8.58 (m, 2H), 8.37 (d, $J = 4.8$ Hz, 1H), 8.25 (d, $J = 5.7$ Hz, 1H), 8.16 (d, $J = 6.6$ Hz, 1H), 8.00 (d, $J = 8.3$ Hz, 2H), 7.90 (d, $J = 8.0$ Hz, 1H), 7.84 (td, $J = 7.9, 1.8$ Hz, 1H), 7.76–7.72 (m, 3H), 7.65 (d, $J = 8.8$ Hz, 1H), 7.59 (d, $J = 8.5$ Hz, 2H), 7.44 (d, $J = 8.2$ Hz, 2H), 7.34–7.27 (m, 2H), 6.94–6.90 (m, 1H), 6.64–6.61 (m, 2H), 6.07 (d, $J = 6.6$ Hz, 1H), 4.63 (br s, 3H), 4.49–4.41 (m, 4H), 4.38–4.36 (m, 1H), 4.16–4.13 (dd, $J = 12.8, 6.3$ Hz, 4H), 3.61–3.52 (m, 1H), 2.98–2.86 (m, 10H), 2.63–2.60 (m, 1H), 2.15–2.13 (m, 1H), 2.04–1.92 (m, 6H), 1.81–1.75 (m, 2H), 1.64–1.58 (m, 10H), 1.52–1.49 (m, 5H), 1.30–1.17 (m, 4H) ppm. ^{13}C NMR (126 MHz, $\text{DMSO}-d_6$): δ 174.8, 173.9, 173.6, 173.0, 172.4, 171.4, 171.1, 170.6, 165.6, 161.9, 158.3, 156.0, 155.2, 154.9, 150.5, 149.4, 148.3, 141.8, 137.2, 136.9, 128.5, 127.8, 127.6, 126.3, 122.4, 121.9, 120.0, 111.4, 61.7, 53.9, 53.4, 50.7, 50.4, 49.4, 49.2, 45.9, 43.5, 42.6, 38.5, 38.0, 37.4, 31.8, 31.6, 31.3, 27.7, 22.4 ppm. IR ($\tilde{\nu}_{\text{max}}$) = 3270 (w), 3054 (w), 2917 (w), 2850 (w), 1655 (m), 1604 (s), 1512 (s), 1394 (m), 1300 (m), 1263 (m), 1228 (s), 1178 (m), 1127 (m), 1046 (s), 999 (s), 949 (m), 902 (m), 822 (m), 768 (m), 719 (m) cm^{-1} . HRMS (ESI) m/z : $[\text{M} + \text{H}]^+$ calcd for $\text{C}_{65}\text{H}_{76}\text{N}_{19}\text{O}_{18}\text{S}_{22}$, 1474.5052; found, 1474.5055.

Conjugate 17e. Yellowish oil (24 mg, 19% yield). ^1H NMR (500 MHz, $\text{DMSO}-d_6$): δ 8.63 (s, 1H), 8.24 (br s, 2H), 8.18 (d, $J = 7.5$ Hz, 1H), 8.05 (d, $J = 7.1$ Hz, 1H), 7.72 (s, 2H), 7.62 (d, $J = 8.7$ Hz, 2H), 7.35–7.28 (m, 5H), 7.23 (d, $J = 6.8$ Hz, 1H), 7.10 (dd, $J = 14.3, 7.3$ Hz, 3H), 6.98 (s, 1H), 6.95–6.93 (m, 3H), 6.80 (dd, $J = 8.1, 1.9$ Hz, 1H), 6.64–6.62 (m, 2H), 6.05 (br s, 1H), 4.67–4.44 (m, 10H), 4.27–4.21 (m, 3H), 4.13 (t, $J = 6.0$ Hz, 3H), 3.22–3.15 (m, 3H), 2.99–2.91 (m, 6H), 2.70–2.55 (m, 5H), 2.27–1.92 (m, 10H), 1.85–1.63 (m, 11H), 1.23–1.22 (m, 4H) ppm. ^{13}C NMR (126 MHz, $\text{DMSO}-d_6$): δ 174.0, 172.2, 172.0, 171.0, 170.5, 170.0, 166.1, 158.2, 156.6, 156.4, 155.2, 154.4, 150.6, 150.1, 148.5, 143.3, 142.7, 135.5, 129.9, 129.68, 128.8, 127.8, 123.2, 122.4, 121.5, 118.3, 117.4, 116.6, 111.3, 61.7, 54.7, 53.3, 52.5, 50.3, 50.1, 49.8, 49.4, 49.2, 45.9, 43.6, 36.7, 31.8, 31.5, 31.2, 22.2, 21.7 ppm. IR ($\tilde{\nu}_{\text{max}}$) = 3269 (w), 3066 (w), 2947 (w), 2919 (w), 2851 (w), 1654 (m), 1605 (s), 1513 (s), 1487 (m), 1400 (m), 1376 (m), 1349 (m), 1246 (m), 1180 (m), 1128 (m), 1021 (s), 1002 (s), 950 (m), 901 (m), 820 (m), 768 (m), 719 (m), 691 (s) cm^{-1} . HRMS (ESI) m/z : $[\text{M} + \text{H}]^+$ calcd for $\text{C}_{66}\text{H}_{77}\text{N}_{18}\text{O}_{19}\text{S}_{22}$, 1489.5048; found, 1489.5049.

Conjugate 17f. Yellowish oil (45 mg, 20% yield). ^1H NMR (500 MHz, $\text{DMSO}-d_6$): δ 8.66 (br s, 1H), 8.62 (s, 1H), 8.25–8.18 (m, 3H), 8.17–8.15 (m, 3H), 7.98 (d, $J = 6.7$ Hz, 1H), 7.93 (d, $J = 8.2$ Hz, 2H), 7.85 (d, $J = 7.7$ Hz, 2H), 7.75–7.71 (m, 3H), 7.61 (d, $J = 8.8$ Hz, 2H), 7.45 (d, $J = 8.1$ Hz, 4H), 7.27 (d, $J = 7.6$ Hz, 1H), 6.96–6.93 (m, 1H), 6.66–6.62 (m, 2H), 6.14 (d, $J = 5.9$ Hz, 1H), 4.63 (br s, 3H), 4.51–4.47 (m, 6H), 4.23–4.18 (m, 3H), 4.13 (t, $J = 5.8$ Hz, 3H), 3.56 (br s, 1H), 3.20–3.17 (m, 2H), 2.997–2.88 (m, 4H), 2.73–2.60 (m, 3H), 2.22–1.94 (m, 10H), 1.88–1.63 (m, 11H), 1.27–1.23 (m, 5H) ppm. ^{13}C NMR (126 MHz, $\text{DMSO}-d_6$): δ 174.2, 172.5, 172.1, 171.1, 170.6,

170.1, 166.0, 161.6, 158.2, 155.2, 154.6, 152.9, 150.6, 149.0, 148.7, 148.4, 137.8, 136.4, 135.4, 128.7, 128.3, 127.8, 121.6, 121.2, 120.0, 119.1, 111.3, 61.7, 53.6, 52.7, 50.4, 50.2, 50.0, 49.4, 49.3, 45.9, 37.4, 37.2, 36.9, 31.8, 31.6, 31.2, 27.0, 23.7 ppm. ^{19}F $\{^1\text{H}\}$ NMR (471 MHz, $\text{DMSO}-d_6$): δ –59.69 (s, 3F) ppm. IR ($\tilde{\nu}_{\text{max}}$) = 3271 (m), 2936 (w), 1641 (m), 1604 (s), 1512 (m), 1480 (m), 1394 (m), 1337 (m), 1304 (m), 1254 (s), 1220 (s), 1170 (m), 1021 (s), 1002 (s), 998 (s), 952 (m), 901 (m), 823 (m), 764 (m) cm^{-1} . HRMS (ESI) m/z : $[\text{M} + \text{H}]^+$ calcd for $\text{C}_{66}\text{H}_{75}\text{F}_3\text{N}_{19}\text{O}_{19}\text{S}_{22}$, 1558.4875; found, 1558.4878.

$^1\text{J}_{\text{C-F}}$ was not determined because of poor signal-to-noise ratio.

Conjugate 17g. Yellowish oil (32 mg, 21% yield). ^1H NMR (500 MHz, $\text{DMSO}-d_6$): δ 8.63 (s, 1H), 8.21 (d, $J = 7.5$ Hz, 1H), 8.17 (d, $J = 7.4$ Hz, 2H), 8.09 (d, $J = 7.4$ Hz, 1H), 7.77 (d, $J = 7.2$ Hz, 1H), 7.71 (s, 1H), 7.64 (d, $J = 8.8$ Hz, 2H), 7.23–7.18 (m, 4H), 7.08 (d, $J = 7.8$ Hz, 2H), 6.92 (t, $J = 5.9$ Hz, 1H), 6.65–6.63 (m, 2H), 6.01 (d, $J = 7.1$ Hz, 1H), 4.64–4.60 (m, 1H), 4.56–4.47 (m, 7H), 4.36–4.23 (m, 3H), 4.14 (t, $J = 6.0$ Hz, 2H), 3.57 (br s, 2H), 3.25–3.14 (m, 3H), 3.01–2.91 (m, 4H), 2.74–2.62 (m, 4H), 2.25–2.24 (m, 5H), 2.18–2.03 (m, 9H), 1.85–1.78 (m, 6H), 1.67–1.62 (m, 2H), 1.27–1.21 (m, 5H) ppm. ^{13}C NMR (126 MHz, $\text{DMSO}-d_6$): δ 173.9, 172.2, 172.0, 171.9, 170.9, 170.4, 170.1, 168.3, 166.1, 158.2, 155.1, 154.1, 150.6, 148.6, 148.4, 137.7, 135.3, 129.3, 128.8, 128.5, 127.8, 127.2, 121.4, 111.2, 61.6, 52.9, 52.3, 50.0, 49.7, 49.3, 49.2, 45.9, 37.2, 36.6, 36.4, 31.7, 31.5, 31.2, 26.7, 23.7, 20.8 ppm. HRMS (ESI) m/z : $[\text{M} + \text{H}]^+$ calcd for $\text{C}_{66}\text{H}_{75}\text{F}_3\text{N}_{19}\text{O}_{19}\text{S}_{22}$, 1558.4875; found, 1558.4878.

■ ASSOCIATED CONTENT

● Supporting Information

The Supporting Information is available free of charge on the ACS Publications website at DOI: 10.1021/acs.joc.7b02650.

Spectroscopic data for the synthesized compounds and description of the folate uptake assay procedure (PDF)

■ AUTHOR INFORMATION

Corresponding Author

*E-mail: miroslav.soural@upol.cz.

ORCID

Vladimír Kryštof: 0000-0001-5838-2118

Miroslav Soural: 0000-0001-7288-8617

Notes

The authors declare no competing financial interest.

■ ACKNOWLEDGMENTS

The authors are grateful for Projects CZ.1.07/2.3.00/20.0009 from the European Social Fund; 15-15264S from the Czech Science Foundation; and IGA-LF-2017-028 and IGA_PrF_2017_014 from Palacky University, Olomouc, Czech Republic. The infrastructure of this project (Institute of Molecular and Translation Medicine) was supported by the National Program of Sustainability (Project LO1304). Eva Řezníčková is acknowledged for her assistance with biological experiments.

■ REFERENCES

- (1) Jaracz, S.; Chen, J.; Kuznetsova, L. V.; Ojima, I. *Bioorg. Med. Chem.* **2005**, *13*, 5043.
- (2) Casi, G.; Neri, D. *J. Med. Chem.* **2015**, *58* (22), 8751.
- (3) Assaraf, Y. G.; Leamon, C. P.; Reddy, J. A. *Drug Resist. Updates* **2014**, *17* (4-6), 89.
- (4) Weitman, S. D.; Lark, R. H.; Coney, L. R.; Fort, D. W.; Frasca, W.; Zurawski, V. R., Jr.; Kamen, B. A. *Cancer Res.* **1992**, *52*, 3396.
- (5) Leamon, C. P.; Reddy, J. A. *Adv. Drug Delivery Rev.* **2004**, *56*, 1127.
- (6) Low, P. S.; Henne, W. A.; Doorneweerd, D. D. *Acc. Chem. Res.* **2008**, *41* (1), 120.

- (7) Vlahov, I. R.; Leamon, C. P. *Bioconjugate Chem.* **2012**, *23*, 1357.
- (8) Leamon, C. P.; Reddy, J. A.; Klein, P. J.; Vlahov, I. R.; Dorton, R.; Bloomfield, A.; Nelson, M.; Westrick, E.; Parker, N.; Bruna, K.; Vetzal, M.; Gehrke, M.; Nicoson, J. S.; Messmann, R. A.; LoRusso, P. M.; Sausville, E. A. *J. Pharmacol. Exp. Ther.* **2011**, *336*, 336.
- (9) Vlahov, I. R.; Santhapuram, H. K. R.; Kleindl, P. J.; Howard, S. J.; Stanford, K. M.; Leamon, C. P. *Bioorg. Med. Chem. Lett.* **2006**, *16*, 5093.
- (10) Vlahov, I. R.; Vite, G. D.; Kleindl, P. J.; Wang, Y.; Santhapuram, H. K. R.; You, F.; Howard, S. J.; Kim, S. H.; Lee, F. F. Y.; Leamon, C. P. *Bioorg. Med. Chem. Lett.* **2010**, *20*, 4578.
- (11) Leamon, C. P.; Vlahov, I. R.; Reddy, J. A.; Vetzal, M.; Santhapuram, H. K. R.; You, F.; Bloomfield, A.; Dorton, R.; Nelson, M.; Kleindl, P.; Vaughn, J. F.; Westrick, E. *Bioconjugate Chem.* **2014**, *25*, 560.
- (12) Vergote, I.; Leamon, C. J. *Ther. Adv. Med. Oncol.* **2015**, *7* (4), 206.
- (13) Malumbres, M.; Barbacid, M. *Trends Biochem. Sci.* **2005**, *30*, 630.
- (14) Krystof, V.; Uldrijan, S. *Curr. Drug Targets* **2010**, *11*, 291.
- (15) Lapenna, S.; Giordano, A. *Nat. Rev. Drug Discovery* **2009**, *8*, 547.
- (16) Trova, M. P.; Barnes, K. D.; Barford, C.; Benanti, T.; Bielaska, M.; Burry, L.; Lehman, J. M.; Murphy, C.; O'Grady, H.; Peace, D.; Salamone, S.; Smith, J.; Snider, P.; Toporowski, J.; Tregay, S.; Wilson, A.; Wyle, M.; Zheng, X.; Friedrich, T. D. *Bioorg. Med. Chem. Lett.* **2009**, *19*, 6608.
- (17) Trova, M. P.; Barnes, K. D.; Alicea, L.; Benanti, T.; Bielaska, M.; Bilotta, J.; Bliss, B.; Duong, T. N.; Haydar, S.; Herr, R. J.; Hui, Y.; Johnson, M.; Lehman, J. M.; Peace, D.; Rainka, M.; Snider, P.; Salamone, S.; Tregay, S.; Zheng, X.; Friedrich, T. D. *Bioorg. Med. Chem. Lett.* **2009**, *19*, 6613.
- (18) Oumata, N.; Bettayeb, K.; Ferandin, Y.; Demange, L.; Lopez-Giral, A.; Goddard, M.-L.; Myrianthopoulos, V.; Mikros, E.; Flajolet; Greengard, P.; Meijer, L.; Galons, H. *J. Med. Chem.* **2008**, *51*, 5229.
- (19) Gucký, T.; Jorda, R.; Zatloukal, M.; Bazgier, V.; Berka, K.; Řezníčková, E.; Béres, E.; Strnad, M.; Kryštof, V. *J. Med. Chem.* **2013**, *56* (15), 6234.
- (20) Trindade, A. F.; Frade, R. F. M.; Maçôas, E. M. S.; Graça, C.; Rodrigues, C. A. B.; Martinho, J. M. G.; Afonso, C. A. M. *Org. Biomol. Chem.* **2014**, *12*, 3181.
- (21) Vlahov, I. R.; Leamon, C. P. *Bioconjugate Chem.* **2012**, *23*, 1357.
- (22) Roy, J.; Nguyen, T. X.; Kanduluru, A. K.; Venkatesh, C.; Lv, W.; Reddy, P. V. N.; Low, P. S.; Cushman, M. *J. Med. Chem.* **2015**, *58*, 3094.
- (23) Krajčovičová, S.; Soural, M. *ACS Comb. Sci.* **2016**, *18* (7), 371.
- (24) Roy, J.; Nguyen, T. X.; Kanduluru, A. K.; Venkatesh, C.; Lv, W.; Reddy, P. V. N.; Low, P. S.; Cushman, M. *J. Med. Chem.* **2015**, *58*, 3094.
- (25) Singh, R.; Whitesides, G. M. In *Sulphur-Containing Functional Groups*; Eds.: Patai, S., Rappoport, Z., Eds.; John Wiley & Sons Ltd.: Chichester, U.K., 1993; Chapter 13, pp 633–658.
- (26) Sharma, S.; Singh, J.; Ojha, R.; Singh, H.; Kaur, M.; Bedi, P. M. S.; Nepali, K. *Eur. J. Med. Chem.* **2016**, *112*, 298.
- (27) Gucký, T.; Jorda, R.; Zatloukal, M.; Krystof, V.; Rarová, L.; Řezníčková, E.; Mikulits, W.; Strnad, M. International Patent WO2014121764 A3, 2014.
- (28) Dwyer, M. P.; Guzi, T. J.; Paruch, K.; Doll, R. J.; Keertikar, K. M.; Girijavallabhan, V. M. European Patent EP1539756 B1, 2007.
- (29) Roy, J.; Nguyen, T. X.; Kanduluru, A. K.; Venkatesh, C.; Lv, W.; Reddy, P. V. N.; Low, P. S.; Cushman, M. *J. Med. Chem.* **2015**, *58*, 3094–3103.
- (30) Králová, P.; Fülöpová, V.; Maloň, M.; Volná, T.; Popa, I.; Soural, M. *ACS Comb. Sci.* **2017**, *19*, 173–180.



Cite this: *Chem. Commun.*, 2019, 55, 929

Received 1st November 2018,
Accepted 17th December 2018

DOI: 10.1039/c8cc08716d

rsc.li/chemcomm

Solid-phase synthesis for thalidomide-based proteolysis-targeting chimeras (PROTAC)[†]

S. Krajcovicova,^a R. Jorda,^b D. Hendrychova,^b V. Krystof^{b,*} and M. Soural^{b,*c}

A preloaded resin consisting of a thalidomide moiety and an ethylene-oxy linker allows the simple and fast formation of PROTACs. The feasibility of the procedure was illustrated by conjugating different protein kinase inhibitors. The biological functionality of an ibrutinib-like conjugate was then confirmed by a cellular experiment.

The PROTAC concept is based on the preparation of conjugates consisting of two main parts connected through a suitable linker, which is typically an ethylene-oxy-based aliphatic chain.^{1–5} One part of the conjugate interacts with the protein of interest (POI), whereas the other binds to a component of E3 ubiquitin ligase (Fig. 1).⁶ These bifunctional conjugates follow an event-driven pharmacological paradigm and can act catalytically to degrade superstoichiometric amounts of the target protein.⁶

A recently reported PROTAC family uses the phthalimides (thalidomide, pomalidomide, lenalidomide), potent immunomodulatory drugs capable of binding to the E3 ubiquitin ligase cereblon (CRBN).^{7–9} Thus, the phthalimide family is often employed as a part of PROTACs to hijack CRBN to target proteins.² To date, there are numerous methods^{10–13} for traditional solution-phase synthesis to obtain the desired conjugates by stepwise modification of appropriate inhibitors. However, a frequent feature of solution-phase synthesis is the tedious isolation and purification of intermediates, which requires the assistance of experienced synthetic chemists. For this reason, we suggested an alternative approach based on the use of polymer-supported chemistry. Solid-phase organic synthesis (SPOS) is well known for significant advantages as it allows for fast and easy isolation of synthetic intermediates/target compounds by

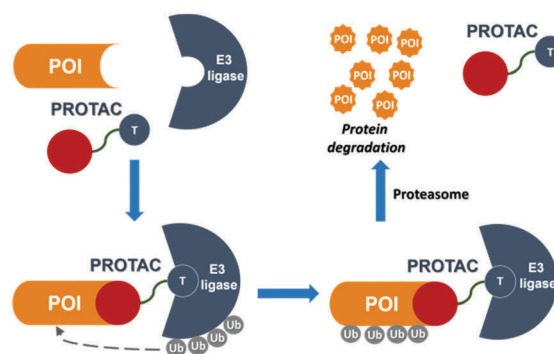


Fig. 1 Mechanism of action of PROTAC conjugates (POI = protein of interest; Ub = ubiquitin, T = thalidomide).

simple filtration of resin-bound substances from the reaction mixture. Compared to conventional methods, this feature significantly accelerates production of desired compounds and in the case of conjugates, the quick modification of their individual parts is possible. Furthermore, solid-phase synthesis requires only simple laboratory equipment and is easily applicable in a parallel synthesis. Recently, we successfully used the SPOS concept to prepare preloaded resins applicable for synthesis of biotinylated^{14,15} or fluorescently labeled¹⁶ molecules.

Pharmacological targeting of protein kinases has been validated as an effective therapeutic strategy, and over 37 kinase inhibitor drugs have received approval for clinical use in certain cancers.^{17,18} However, specific resistance often reduces the sensitivity of targeted kinases to drugs during therapy, and therefore novel molecules or approaches are intensively sought. In addition, some kinases also possess nonenzymatic (scaffolding) functions linked to cancer phenotypes, which are hardly modulated by pharmacological approaches.¹⁹ Kinase degradation induced by PROTACs thus provides an interesting alternative not only for mechanistic studies or therapy but also for kinases with kinase-independent functions.¹⁸ Indeed, PROTACs have been already applied to target several kinases, including for example AKT,²⁰ BCR-ABL,²¹ CDK9²² or BTK,²³ demonstrating the viability of this

^a Department of Organic Chemistry, Faculty of Science, Palacky University, 17. listopadu 12, 771 46 Olomouc, Czech Republic

^b Laboratory of Growth Regulators, Palacky University & Institute of Experimental Botany, the Czech Academy of Sciences, Slechtitelu 27, 78371 Olomouc, Czech Republic. E-mail: vladimir.krystof@upol.cz

^c Institute of Molecular and Translational Medicine, Faculty of Medicine and Dentistry, Palacky University, Hnevotinska 5, 779 00, Olomouc, Czech Republic. E-mail: miroslav.soural@upol.cz

[†] Electronic supplementary information (ESI) available. See DOI: 10.1039/c8cc08716d

approach. For this work we selected established kinase inhibitors or their close derivatives with a reactive amino function available for conjugation and prepared thalidomide PROTACs for several protein kinases.

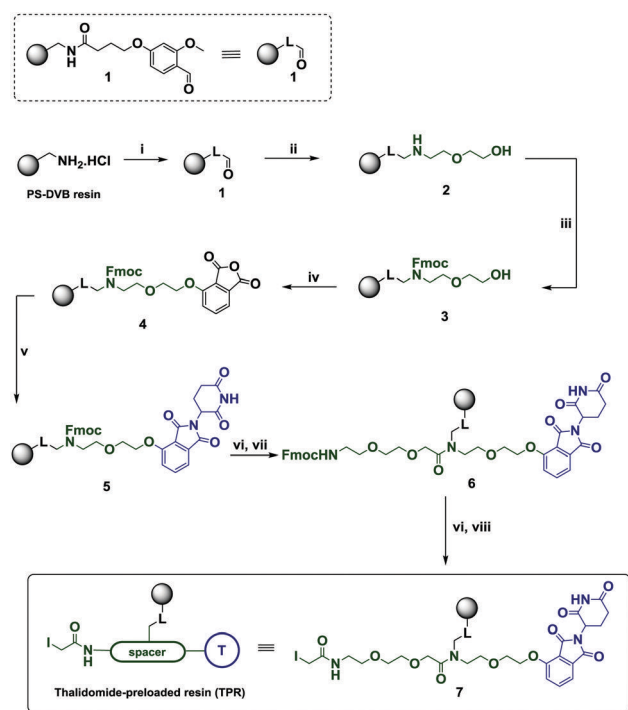
The preparation of the thalidomide-preloaded resin (TPR) began with aminomethyl polystyrene-divinylbenzene (PS-DVB) resin, which was acylated with 4-(4-formyl-3-methoxyphenoxy)butanoic acid. The resulting aldehyde resin **1** was reductively aminated with 2-(2-aminoethoxy)ethan-1-ol followed by the regioselective *N*-protection using Fmoc *N*-hydroxysuccinimide ester (Fmoc-OSu), producing the resin **3**. The reaction with 4-hydroxyisobenzofuran-1,3-dione under Mitsunobu alkylation conditions yielded resin **4**, which was subjected to thalidomide scaffold ring-closure using 3-aminopiperidine-2,6-dione hydrochloride in a presence of triethylamine (TEA). Similarly to the published solution-phase synthetic protocol,²⁵ we observed full ring closure to the desired thalidomide containing linker **5** after reaction in boiling toluene (Scheme 1). Interestingly, it seems that thalidomide ring closure is solvent-dependent reaction since we detected non-desired by-products when the reaction was carried out in THF instead of toluene.

Noteworthy, we also tested the direct Mitsunobu reaction of intermediate **3** with 4-hydroxythalidomide, however, we observed

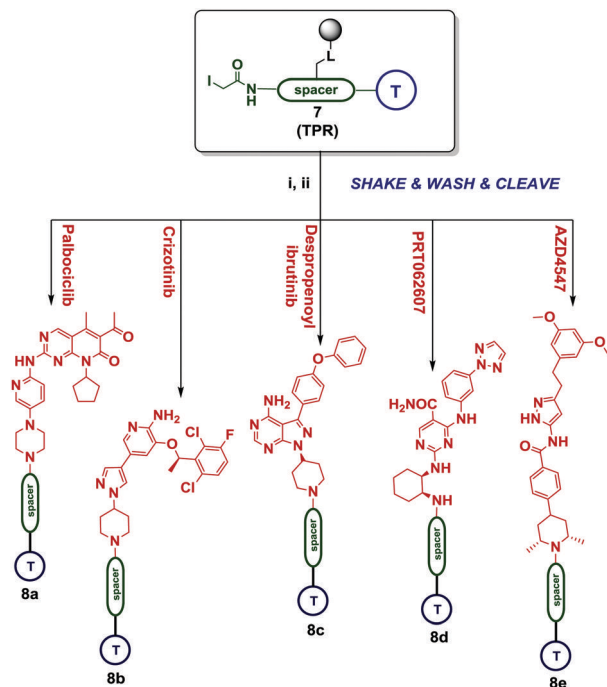
only mixture of products, very likely due to the presence of another acidic proton. Deprotection of the Fmoc protecting group and subsequent acylation with 1-(9*H*-fluoren-9-yl)-3-oxo-2,7,10-trioxo-4-azadodecan-12-oic acid (FAEEAA) yielded an intermediate **6**. The standard cleavage conditions (DMF/piperidine 4:1 to 1:1) were not applicable, since piperidine-promoted phthalimide scaffold opening was detected and since the piperidine-amide side product shared similar retention times on reverse HPLC, it was necessary to avoid its formation. We tested different bases and conditions and the best results were achieved with 1,8-diazabicyclo(5.4.0)undec-7-ene (DBU) in dichloromethane (1:1), leading to complete Fmoc removal in 15 minutes with the phthalimide scaffold being unaffected. It is important to mention that the resin **6** itself could be (after Fmoc deprotection) used directly to couple diverse molecules bearing suitable functionalities capable of reaction with primary amines, such as aldehyde, carboxylic acid or aryl/alkylhalogens *etc.* However, to make the strategy broadly applicable for derivatization of protein kinase inhibitors, which frequently contain the reactive aliphatic amines, the intermediate **6** was additionally deprotected and acylated with iodoacetic acid to yield the final thalidomide-preloaded resin (TPR) **7** (Scheme 1). Using the conditions reported in Scheme 1 (see ESI† for more details), we managed to obtain TPR in an excellent crude purity (above 90%), as calculated from LC-UV traces after TFA-mediated cleavage from the polymer support. The loading of TPR was calculated to 0.2 mmol g⁻¹ using the method of external standard. The applicability of TPR for conjugation was tested using a representative set of commercially available protein kinase inhibitors: palbociclib, crizotinib, AZD4547, despropenoylibrutinib and PRT062607 (BIIB057), which potently target CDK4, ALK, FGFR, BTK and SYK kinases, respectively (Scheme 2).

These kinase inhibitors were selected according to presence of primary or secondary non-aromatic amine functions oriented outside the kinases' active sites (confirmed by visual inspections of their co-crystal structures available from the Protein Data Bank), which are available for conjugation without loss of inhibitory activity. In accordance with the suggested simplicity, the inhibitors were dissolved in DMSO and after addition of *N,N*-diisopropylethylamine (DIPEA), the corresponding solution was shaken with the TPR for between 6–16 h, followed by a quick wash of the resin with fresh solvent. LC-UV traces of cleaved conjugates (see ESI†) demonstrate mostly high purity of target compounds. It is worth mentioning that the lower purity and, consequently, the overall yield of conjugate **8c** was probably caused by the steric hindrance of the reacting secondary amine moiety. We also successfully prepared both shortened and extended alternatives of TPR (intermediates **9** or **11**, respectively, Scheme 3) which were applied for conjugation with despropenoylibrutinib. For better distinction of final conjugates **10** and **12**, we report the full structure of linker in Scheme 3.

To verify the functionality of prepared PROTACs, we selected the representative conjugate **8c** consisting of a despropenoylibrutinib bait, a derivative of a recently FDA-approved drug specifically inhibiting BTK kinase.²⁴ Similarly to a recent study, we did not incorporate the electrophilic acrylamide moiety of ibrutinib into the PROTAC.¹² In our initial characterization



Scheme 1 Preparation of the thalidomide-preloaded resin (TPR). *Reagents and conditions:* (i) 4-(4-formyl-3-methoxyphenoxy)butanoic acid, 1-hydroxybenzotriazole (HOBT), *N,N'*-diisopropylcarbodiimide (DIC), DMF/CH₂Cl₂ (1:1), r.t., 16 h; (ii) 2-(2-aminoethoxy)ethan-1-ol, DMF/AcOH (9:1), r.t., 16 h then NaBH(OAc)₃, DMF/AcOH (11:1), r.t., 4 h; (iii) Fmoc-OSu, CH₂Cl₂, r.t., 16 h; (iv) 4-hydroxyisobenzofuran-1,3-dione, PPh₃, diisopropyl azodicarboxylate (DIAD), THF, -20 °C to r.t., 16 h; (v) 3-aminopiperidine-2,6-dione hydrochloride, TEA, toluene, reflux, 16 to 22 h; (vi) DBU/CH₂Cl₂ (1:1), r.t., 15 min; (vii) FAEEAA, HOBT, DIC, DMF/CH₂Cl₂, r.t., 16 h; (viii) iodoacetic acid, DIC, CH₂Cl₂, r.t., 90 min.



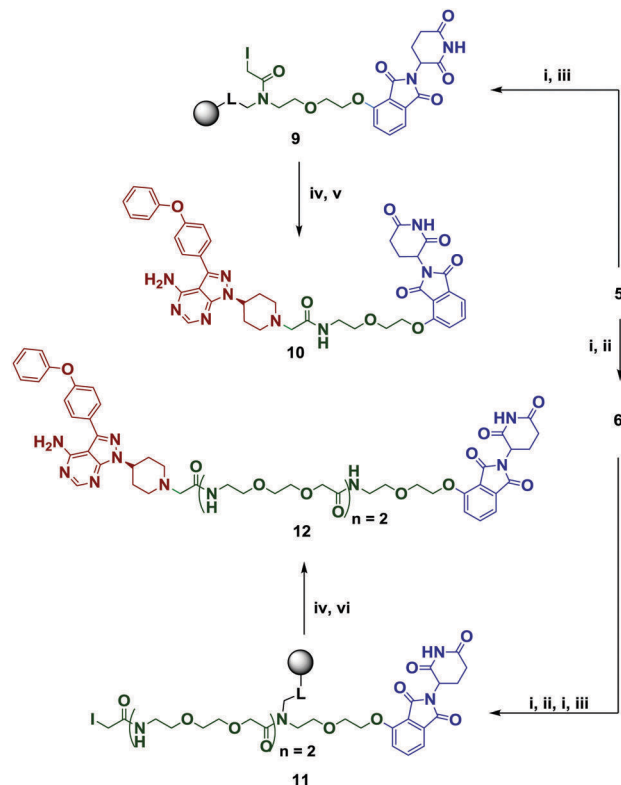
Scheme 2 Application of TPR for protein kinase inhibitor conjugation. *Reagents and conditions:* (i) DIPEA, DMSO, r.t. 6–16 h; (ii) TFA/CH₂Cl₂ (1:1), r.t. 2 h. (calculated yields from intermediate **6**: 50%, **8a**; 85%, **8b**; 83%, **8c**; 49%, **8d**; 24%, **8e**).

experiments, we compared the potencies of ibrutinib and despropenoylibrutinib with that of PROTAC **8c** in a biochemical kinase assay. Conjugate **8c** was also found to inhibit purified recombinant BTK with IC₅₀ like that of parental despropenoyl-ibrutinib (Table 1), which confirmed the biological functionality of **8c**. Two other PROTACs **10** and **12** with shorter and longer linkers, respectively, were similarly potent on the kinase.

Next, we wanted to demonstrate that PROTAC **8c** is able to induce BTK degradation in cells. In the preliminary experiments with **8c**, we observed that the decrease in BTK is time-dependent with a considerable effect between 10–24 h, which is in agreement with recently published data.²⁶ We therefore treated Ramos cells with various doses of **8c** for 16 h and activated BTK by adding immunoglobulin M to culture media. Western blot analysis of lysed cells revealed that BTK degradation was dose-dependent, with a maximal knockdown achieved at a 2 μM concentration; the levels of BTK decreased to 15% in comparison with untreated cells (Fig. 2).

As expected, in control experiments neither ibrutinib nor despropenoylibrutinib was able to induce the degradation of BTK; they only inhibited BTK activity, which was demonstrated by decreased levels of phospho-BTK (tyrosine 223) as a result of blocked autophosphorylation. SYK and SRC probed in parallel were not altered at all, further confirming the specificity of protein degradation induced by **8c**.

In conclusion, we report a novel chemical tool for the preparation of PROTAC conjugates. The developed thalidomide-preloaded resin (TPR) can be used to rapidly synthesize desired conjugates and to modify individual parts (*e.g.* spacer length)



Scheme 3 Preparation of shortened and extended versions of the thalidomide-preloaded resin. *Reagents and conditions:* (i) DBU/CH₂Cl₂ (1:1), r.t., 15 min; (ii) FAEEA, HOBT, DIC, DMF/CH₂Cl₂, r.t., 16 h; (iii) iodicetic acid, DIC, CH₂Cl₂, r.t., 90 min; (iv) despropenoylibrutinib, DIPEA, DMSO, r.t., 12 h; (v) neat TFA, reflux, 2 h; (vi) TFA/CH₂Cl₂ (1:1), r.t., 2 h. (calculated yield from intermediate **5**: 76%, **10**; or from intermediate **6**: 70%, **12**).

Table 1 Biochemical activities of parental compounds and the corresponding PROTAC conjugates

| Compound | BTK IC ₅₀ ^a (μM) |
|-----------------------|--|
| Ibrutinib | < 0.001 |
| Despropenoylibrutinib | 0.065 ± 0.012 |
| PROTAC 8c | 0.159 ± 0.037 |
| PROTAC 10 | 0.102 ± 0.012 |
| PROTAC 12 | 0.108 ± 0.011 |

^a Measured in tetraplicate.

for preliminary screening experiments focused on molecule optimization. Importantly, thalidomide preloaded resin can be easily prepared from readily available starting materials and used by a person without extensive synthetic experience or special laboratory equipment. We demonstrated the applicability of TPR by the derivatization of a set of protein kinase inhibitors, which afforded the desired conjugates mostly in high purities. We would like to emphasize that although our PROTACs were prepared to target protein kinases, the method is highly versatile and can also be applied to all other proteins for which inhibitors/modulators/ligands suitable for conjugation are available. TPR can be applied to modify inhibitors of choice, which contain

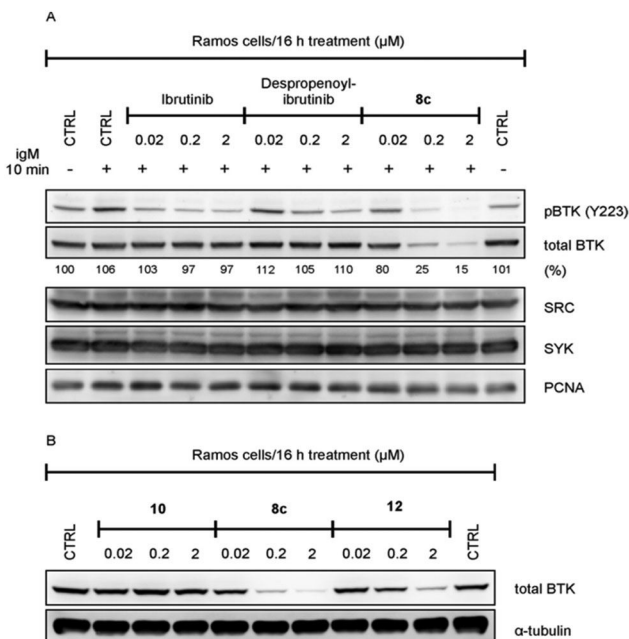


Fig. 2 PROTAC **8c** induces BTK degradation in cultured cells. (A) Protein levels in response to dose escalation of free ibrutinib, free despropenoyl-ibrutinib and despropenoyl-ibrutinib-PROTAC **8c** in Ramos cells. (B) Linker length contributes to PROTAC effectivity. The cells were treated with vehicle or inhibitors for 16 hours and then stimulated or not with anti-IgM ($5 \mu\text{g ml}^{-1}$) for 10 min before the harvest. Proteins were then detected by immunoblotting in lysed cells. SRC, SYK, PCNA and α -tubulin were probed for equal protein loading and degradation specificity. The BTK level was quantified using Multi Gauge software (version 3.2) and normalized to the IgM-untreated control.

sufficiently reactive functional groups (e.g. carboxylic acid, aldehyde, primary/secondary amine), which are exposed to the solvent in the active site of the target enzyme. This makes the resin broadly applicable for a large number of commercially available compounds without the need for their structural modification.

The authors are grateful to the National Program of Sustainability (project LO1304), Palacký University (IGA_LF_2018_032, IGA_PRF_2018_006) and the Ministry of Health of the Czech Republic (17-31834A). Tomáš Pospíšil is acknowledged for measurement of some NMR spectra.

Conflicts of interest

There are no conflicts of interest to declare.

Notes and references

- 1 T. W. Corson, N. Aberle and C. M. Crews, *ACS Chem. Biol.*, 2008, **3**, 677–692.

- 2 M. Toure and C. M. Crews, *Angew. Chem., Int. Ed.*, 2016, **55**, 1966–1973.
- 3 A. C. Lai and C. M. Crews, *Nat. Rev. Drug Discovery*, 2017, **16**, 101–114.
- 4 I. Churcher, *J. Med. Chem.*, 2018, **61**, 444–452.
- 5 K. C. Carmony and K.-B. Kim, in *Ubiquitin Family Modifiers and the Proteasome*, ed. R. J. Dohmen and M. Scheffner, Humana Press, Totowa, NJ, 2012, vol. 832, pp. 627–638.
- 6 C. M. Robb, J. I. Contreras, S. Kour, M. A. Taylor, M. Abid, Y. A. Sonawane, M. Zahid, D. J. Murry, A. Natarajan and S. Rana, *Chem. Commun.*, 2017, **53**, 7577–7580.
- 7 T. Ito, H. Ando, T. Suzuki, T. Ogura, K. Hotta, Y. Imamura, Y. Yamaguchi and H. Handa, *Science*, 2010, **327**, 1345–1350.
- 8 G. Lu, R. E. Middleton, H. Sun, M. Naniang, C. J. Ott, C. S. Mitsiades, K.-K. Wong, J. E. Bradner and W. G. Kaelin, *Science*, 2014, **343**, 305–309.
- 9 E. S. Fischer, K. Böhm, J. R. Lydeard, H. Yang, M. B. Stadler, S. Cavadini, J. Nagel, F. Serluca, V. Acker, G. M. Lingaraju, R. B. Tichkule, M. Schebesta, W. C. Forrester, M. Schirle, U. Hassiepen, J. Ottl, M. Hild, R. E. J. Beckwith, J. W. Harper, J. L. Jenkins and N. H. Thomä, *Nature*, 2014, **512**, 49–53.
- 10 R. P. Wurz, K. Dellamaggiore, H. Dou, N. Javier, M.-C. Lo, J. D. McCarter, D. Mohl, C. Sastri, J. R. Lipford and V. J. Cee, *J. Med. Chem.*, 2018, **61**, 453–461.
- 11 J. Papatzimas, E. Gorobets, D. Brownsey, R. Maity, N. Bahlis and D. Derksen, *Synlett*, 2017, 2881–2885.
- 12 A. D. Buhimschi, H. A. Armstrong, M. Toure, S. Jaime-Figueroa, T. L. Chen, A. M. Lehman, J. A. Woyach, A. J. Johnson, J. C. Byrd and C. M. Crews, *Biochemistry*, 2018, **57**, 3564–3575.
- 13 K. Yang, Y. Song, H. Xie, H. Wu, Y.-T. Wu, E. D. Leisten and W. Tang, *Bioorg. Med. Chem. Lett.*, 2018, **28**, 2493–2497.
- 14 M. Soral, J. Hodon, N. J. Dickinson, V. Sidova, S. Gurska, P. Dzubak, M. Hajduch, J. Sarek and M. Urban, *Bioconjugate Chem.*, 2015, **26**, 2563–2570.
- 15 N. Cankarova, P. Funk, J. Hlavac and M. Soral, *Tetrahedron Lett.*, 2011, **52**, 5782–5788.
- 16 S. Krajcovicova, J. Stankova, P. Dzubak, M. Hajduch, M. Soral and M. Urban, *Chem. – Eur. J.*, 2018, **24**, 4957–4966.
- 17 P. M. Fischer, *Med. Res. Rev.*, 2017, **37**, 314–367.
- 18 F. M. Ferguson and N. S. Gray, *Nat. Rev. Drug Discovery*, 2018, **17**, 353–377.
- 19 P. Hydrbring, M. Malumbres and P. Sicinski, *Nat. Rev. Mol. Cell Biol.*, 2016, **17**, 280–292.
- 20 R. K. Henning, J. O. Varghese, S. Das, A. Nag, G. Tang, K. Tang, A. M. Sutherland and J. R. Heath, *J. Pept. Sci.*, 2016, **22**, 196–200.
- 21 A. C. Lai, M. Toure, D. Hellerschmied, J. Salami, S. Jaime-Figueroa, E. Ko, J. Hines and C. M. Crews, *Angew. Chem., Int. Ed.*, 2016, **55**, 807–810.
- 22 C. M. Olson, B. Jiang, M. A. Erb, Y. Liang, Z. M. Doctor, Z. Zhang, T. Zhang, N. Kwiatkowski, M. Boukhali, J. L. Green, W. Haas, T. Nomanbhoy, E. S. Fischer, R. A. Young, J. E. Bradner, G. E. Winter and N. S. Gray, *Nat. Chem. Biol.*, 2017, **14**, 163–170.
- 23 Y. Sun, X. Zhao, N. Ding, H. Gao, Y. Wu, Y. Yang, M. Zhao, J. Hwang, Y. Song, W. Liu and Y. Rao, *Cell Res.*, 2018, **28**, 779–781.
- 24 F. Cameron and M. Sanford, *Drugs*, 2014, **74**, 263–271.
- 25 B. Zhou, J. Hu, F. Xu, Z. Chen, L. Bai, E. Fernandez-Salas, M. Lin, L. Liu, C.-Y. Yang, Y. Zhao, D. McEachern, S. Przybranowski, B. Wen, D. Sun and S. Wang, *J. Med. Chem.*, 2018, **61**, 462–481.
- 26 A. Zorba, C. Nguyen, Y. Xu, J. Starr, K. Borzilleri, J. Smith, H. Zhu, K. A. Farley, W. Ding, J. Schiemer, X. Feng, J. S. Chang, D. P. Uccello, J. A. Young, C. N. Garcia-Irrizary, L. Czabaniuk, B. Schuff, R. Oliver, J. Montgomery, M. M. Hayward, J. Coe, J. Chen, M. Niosi, S. Luthra, J. C. Shah, A. El-Kattan, X. Qiu, G. M. West, M. C. Noe, V. Shanmugasundaram, A. M. Gilbert, M. F. Brown and M. F. Calabrese, *Proc. Natl. Acad. Sci. U. S. A.*, 2018, **115**, E7285–E7292.

Cancer Cell Staining

A Synthetic Approach for the Rapid Preparation of BODIPY Conjugates and their use in Imaging of Cellular Drug Uptake and Distribution

Sona Krajcovicova,^[b] Jarmila Stankova,^[a] Petr Dzubak,^[a] Marian Hajduch,^[a] Miroslav Soural,^{*,[b]} and Milan Urban^{*,[a]}

Abstract: A solid-phase synthetic (SPS) method was developed for the preparation of BODIPY-labeled bioactive compounds that allows for fast and simple synthesis of conju-

gates for use in fluorescent microscopy. The approach was used to visualize cellular uptake and distribution of cytotoxic triterpenes in cancer cells.

Introduction

The visualization of small molecules in cells has become an essential tool in drug discovery. The most commonly used method is fluorescent microscopy, in which the studied molecule is equipped with a fluorescent label that allows direct visualization of the cellular uptake and distribution of the drug within the cell. A number of various conjugates of small molecules with a variety of fluorescent tags have been reported to date, with application as probes,^[1] photosensitizers,^[2] and luminescence switches and sensors.^[3] Among them, BODIPY dyes^[2,4] are commonly used fluorophores because of their superior physicochemical properties such as high photostability, high quantum yield of fluorescence, total neutral charge, and low polarity.^[4] In contrast to other dyes, the wavelengths of absorption and emission can be tuned easily by various substitutions on the BODIPY core.^[4] The simplest BODIPY derivatives show fluorescein-like parameters; however, unlike fluoresceins or rhodamines, they are prone to cellular permeability and lack nonspecific binding to proteins or lipids.^[5] In this work, we designed a versatile solid-phase synthetic (SPS) method for the synthesis of fluorescent conjugates of biologically active molecules. The solid-phase synthesis allows for fast and simple production of libraries of desired compounds with only minimum effort and hands-on-time because it saves many isolation and purification steps of the intermediates. Surprisingly, to our knowledge, there is only one report^[6] that describes the use of

SPS for adding substituents to the BODIPY core. However, there is no precedent for using SPS in the synthesis of conjugates of BODIPY and other molecules. In agreement with this, there are a number of articles stating that BODIPY is incompatible with the SPS concept because of the lack of stability under the standard SPS reaction conditions.^[3,6,7] Regardless of this potential issue, we have been able to develop a versatile procedure for the preparation of such conjugates by using a common backbone amide linker and standard coupling reagents and careful optimization of the reaction time and concentration of harsh reagents such as piperidine and trifluoroacetic acid. BODIPY-FL propanoic acid was selected as the most appropriate fluorescent label in this project. To prove the concept, we have synthesized a small set of BODIPY-labeled cytotoxic triterpenes in which we expected different mechanisms of action and differences in cellular uptake and distribution. The selected compounds (Figure 1) have low micromolar cytotoxicity on various cancer cell lines, whereas some were supposed to have a unique mechanism of action: aldehyde **2**,^[8] monoketone **3**,^[9] diketone **4**,^[9] and pyrazine **5**^[10] (Figure 1). Betulinic acid **1** was used as a standard because it is the most commonly studied cytotoxic triterpene and its mechanism of action has been well-studied.^[11,12]

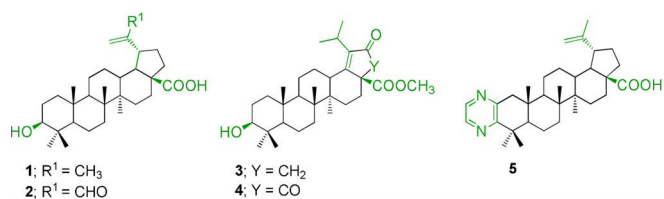


Figure 1. The selected triterpenoid structures.

[a] J. Stankova, Dr. P. Dzubak, Prof. M. Hajduch, Prof. M. Urban
Institute of Molecular and Translational Medicine
Palacky University in Olomouc, Faculty of Medicine and Dentistry
Hnevotinska 5, 77900, Olomouc (Czech Republic)
E-mail: milan.urban@upol.cz

[b] S. Krajcovicova, Prof. M. Soural
Department of Organic Chemistry
Palacky University in Olomouc, Faculty of Science
17. Listopadu 12, 77100, Olomouc (Czech Republic)
E-mail: miroslav.soural@upol.cz

Results and Discussion

Given that the pharmacophores of the selected triterpenes are suggested but yet unproven, chemical modification of some parts of the molecule may negatively influence their biological behavior. Therefore, we decided to attach the fluorescent dye at three different sites and to compare the results. Triterpenes 1–5 were modified in positions C³, C²⁸, or C³⁰ (Figure 2).

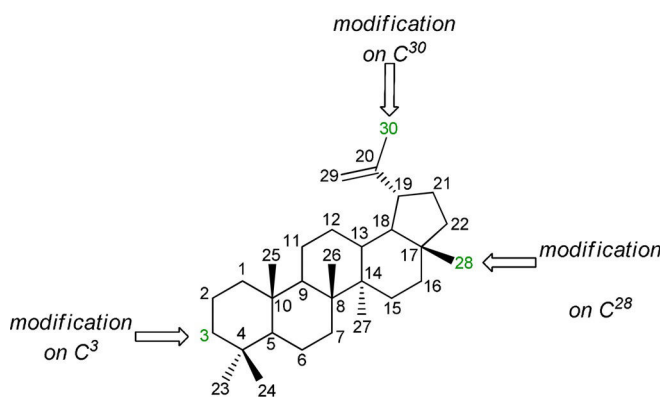
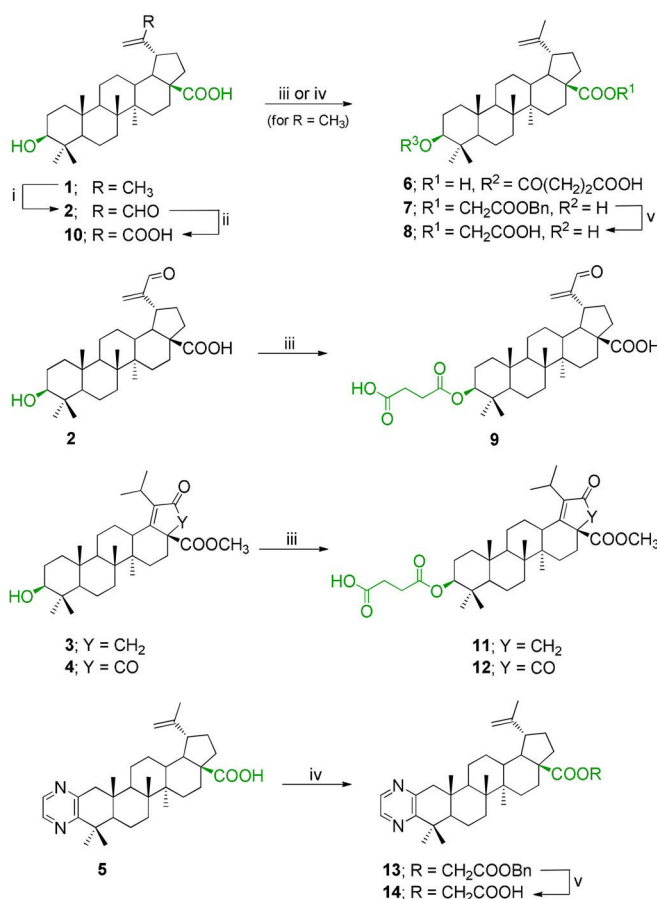


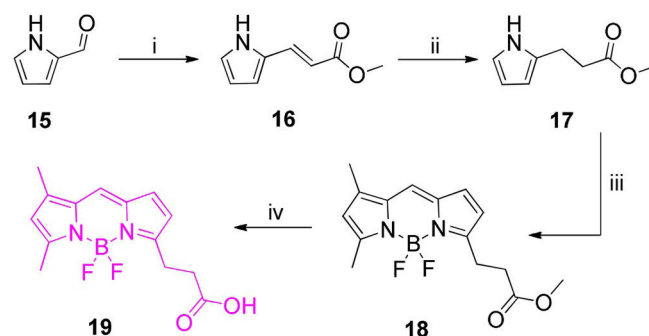
Figure 2. Three sites to attach the fluorescent dye.

The steric hindrance at some of the selected positions required that the original triterpenes had to be premodified by hemisuccinate at C³-OH, glycolate at C²⁸OOH, or oxidized to carboxylate at C³⁰ (Scheme 1, see the experimental part [EP] and the Supporting Information). Briefly, the C³ modified hemisuccinates **6**, **11**, and **12** were obtained after the reaction of betulinic acid **1**, monoketone **3**, or diketone **4**, with succinic anhydride in the presence of a base. C³ modified hemisuccinic aldehyde **9** was obtained after two-stage oxidation of betulinic acid **1** with selenium dioxide, followed by reaction of aldehyde **2** with succinic anhydride as noted above. C²⁸ modification of compounds **1** and **5** yielded protected glyoxalates **7** and **13**, which, upon catalytic hydrogenation in the presence of Pd/C, afforded the desired modified triterpenes **8** and **14**, respectively. Finally, compound **10** was obtained after facile and chemoselective Pinnick oxidation of aldehyde **2**, which generated the carboxyl at the C³⁰ position.

The synthesis of BODIPY-FL propanoic acid had to be optimized (Scheme 2, see the EP and the Supporting Information) to obtain better yields than those previously reported.^[13,14] Although BODIPY-FL propanoic acid **19** (Scheme 2) is commercially available, its extremely high price led us to synthesize the dye by ourselves. The reported syntheses^[13,14] had to be slightly modified and optimized to increase the overall yield. It started from commercially available pyrrole-2-carbaldehyde **15**, which was first converted into α,β -unsaturated ester **16** through Horner–Wadsworth–Emmons reaction with excellent selectivity, yielding only (*E*)-alkene. Such high selectivity was achieved because of the formation of a stabilized ylide. The following reduction provided intermediate **17**, which was then subjected to POCl₃-promoted coupling with commercially available 3,5-dimethyl-1*H*-pyrrole-2-carbaldehyde. Final treat-

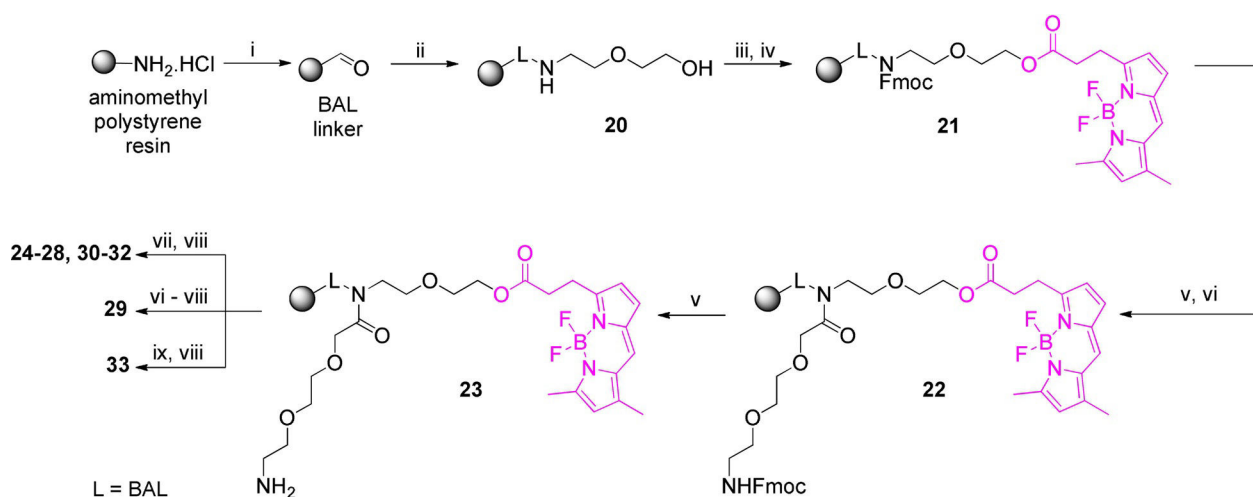


Scheme 1. Synthesis of premodified triterpenes. Reagents and conditions: i) SeO₂, diglyme, 140 °C; ii) KH₂PO₄, NaClO₂, *t*BuOH/2-methyl-2-butene (1:1), RT (**10**; 90%); iii) succinic anhydride, DMAP, THF/DMF (2:1), 80 °C (**6**; 80%; **9**; 73%; **11**; 73%); iv) benzylbromoacetate, K₂CO₃, THF, 50 °C (**7**; 98%, **13**; 91%); v) Pd/C, H₂, CH₃OH, RT (**8**; 84%, **14**; 49%).



Scheme 2. The synthetic route for the preparation of BODIPY-FL propanoic acid **19**. Reagents and conditions: i) methyl(triphenylphosphoranylidene)acetate, CH₂Cl₂, RT, 84%; ii) Pd/C, H₂, CH₃OH, RT, 90%; iii) a) 3,5-dimethylpyrrole-2-carbaldehyde, POCl₃, CH₂Cl₂, 0 °C to RT, b) BF₃·OEt₂, DIPEA, CH₂Cl₂, 0 °C to RT, 63%; iv) THF/H₂O/conc. HCl (3:2:1), 0 °C to RT, 85%.

ment with BF₃·OEt₂ yielded BODIPY-FL propanoate **18** in a one-pot reaction sequence (Scheme 2). Subsequent acidic hydrolysis of the ester yielded the final BODIPY-FL propanoic acid **19** in excellent overall yield of 40% (Scheme 2), indicating an unusually long kinetic stability of BODIPY dye in acidic media.^[15] Importantly, the improved synthesis of BODIPY-FL propanoic



Scheme 3. Synthesis of BODIPY-preloaded resin and its use for conjugation with triterpenes. Reagents and conditions: i) BAL, HOBT, DIC, DMF/CH₂Cl₂ (1:1), RT; ii) 2-(2-aminoethoxy)ethanol, NaBH(OAc)₃, DMF/AcOH (10:1), RT; iii) FmocOsU, CH₂Cl₂, RT; iv) **19**, HOBT, DIC, DMF/CH₂Cl₂ (1:1); v) DMF/piperidine (20:1), RT; vi) FAEEAA, DIC, HOBT, DMF/CH₂Cl₂ (1:1), RT; vii) **6**, **8–12**, **14**, DIC, DMF/CH₂Cl₂ (1:1), RT; viii) CH₂Cl₂/TFA (10:1), RT; ix) Ac₂O, DMAP, CH₂Cl₂, RT

acid is scalable up to gram-scale quantities, which addresses the most common problem in the synthesis of BODIPY dyes.

In contrast to the synthesis of biotin-preloaded resins,^[16,17] the procedure for the preparation of BODIPY-preloaded resin **23** had to be carefully optimized because of the limited chemical stability of BODIPY-FL. The aminomethyl resin was equipped with a backbone amide linker (BAL) and subjected to reductive amination with 2-(2-aminoethoxy)ethanol to obtain immobilized secondary amine **20** (Scheme 3). Chemoselective protection of the secondary amine with Fmoc was followed by acylation of the hydroxy group with prepared BODIPY-FL propanoic acid **19** to afford resin **21**. Cleavage of the Fmoc-protective group and acylation with [2-[2-(Fmoc-amino)ethoxy]ethoxy]acetic (FAEEAA) acid by using the standard DIC/HOBT (1,3-diisopropylcarbodiimide/1-hydroxybenzotriazole) technique yielded Fmoc-protected resin **22**, which, upon deprotection with low concentration of piperidine in DMF, yielded the desired preloaded resin **23** in very good crude purity (82%; calculated from UHPLC-MS traces). Subsequent acylation with the premodified triterpenes **6**, **8–12**, and **14** afforded the final conjugates **24–28**, **30**, and **31** (Scheme 3).

Compound **29**, containing an extended linker, was prepared to investigate the influence of the length of the linker on the cellular uptake and distribution, and compound **33** was designed to show the properties of the BODIPY-FL connected to linker without a triterpene. In contrast to the construction of intermediate **23**, omitting HOBT in the final acylation with triterpenes (Scheme 3, step vii) increased the final crude purities of all conjugates significantly. Additionally, TFA-mediated cleavage of conjugate **24** from the resin led to the formation of by-product **32** in equimolar ratio (calculated from UHPLC-MS traces) as a result of Wagner–Meerwein rearrangement.^[18] It is important to mention that the concentration of both piperidine and TFA had to be considerably lowered compared with standard cleavage conditions (20–50% piperidine in DMF; 25–50% TFA in CH₂Cl₂) to maintain good crude purities of all inter-

mediates as well as final conjugates and to prevent decomposition of the BODIPY scaffold (see the Supporting Information for details).

The excitation and emission spectra of BODIPY-FL propanoic acid **19** were measured and compared to BODIPY conjugates **24–33** (Figure 3). All of the conjugates **24–33** had the same absorption/emission wavelengths and Stokes shifts as the parent BODIPY-FL propanoic acid (see the Supporting Information for details). The quantum yields of fluorescence of the conjugates are lower than those of BODIPY-FL propanoic acid ($\Phi = 98$ for **19** vs. $\Phi = 0.14–0.30$ for compounds **24–32**). The diminished fluorescence is probably caused by the static quenching between BODIPY dye and triterpenes, which is consistent with recently published data.^[19,20]

The cytotoxic activity of the parent compounds and fluorescent conjugates was investigated in vitro against eight human cancer cell lines and two non-tumor fibroblasts by using the standard MTS test (Table 1). The cancer cell lines were derived from T-lymphoblastic leukemia CCRF-CEM, leukemia K562 and their multiresistant counterparts (CEM-DNR, K562-TAX), solid tumors including lung (A549) and colon (HCT116, HCT116p53-/-) carcinomas, osteosarcoma cell line (U2OS), and, for comparison, on two human non-cancer fibroblast lines (BJ, MRC-5). In general, the CCRF-CEM cell line was the most sensitive cancer cell line to the prepared compounds, with only a few exceptions. Therefore, SARs assumptions were mostly based on the activities in CCRF-CEM cells.

Among the unmodified studied molecules **1–5**, aldehyde **2** and pyrazine **5** were cytotoxic against the CCRF-CEM line in the low micromolar range of 1.53 and 0.53 μM , respectively. The therapeutic index is rather low for aldehyde **2** (4.7) but surprisingly high in the case of pyrazine (more than 94). The synthesized fluorescent conjugate of aldehyde **25** remained highly but unselectively cytotoxic, probably due to the presence of the reactive acrolein moiety. On the other hand, fluorescent conjugates of pyrazine (**28** and **29**) had slightly de-

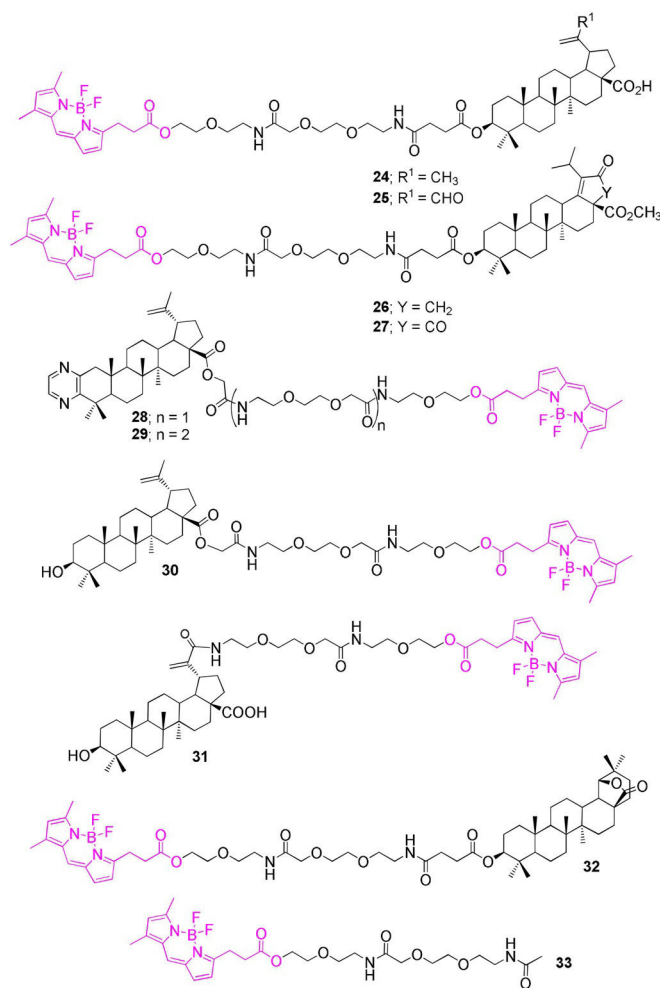


Figure 3. Structures of prepared conjugates **24–33**. Compound **32** formed as a byproduct and was not further studied because it lacked cytotoxic activity.

creased activity and selectivity in comparison with the parent compound **5**, which indicates an important role of the free carboxyl group as a pharmacophore. Interestingly, the length of the linker also affects the activity of the conjugates. This may be indicated by the comparison of conjugates **28** and **29** from which the longer derivative (**29**) was more active than the shorter one (**28**). Lastly, the conjugate of diketone **27** was cytotoxic only on CCRF-CEM cell line, whereas the monoketone conjugate **26** completely lost both its cytotoxic activity and selectivity. The conjugate of betulinic acid **24** at the position C³ remained active, although its conjugates at positions C²⁸ and C³⁰ (compounds **30** and **31**) were almost inactive.

In fluorescent microscopy experiments (which were performed in early intervals before the cytotoxic effect took place), we observed that all the tested fluorescent conjugates of triterpenes stain living cells and pass through the cellular membrane into the cytoplasmic compartment (Figure 4, full resolution image is in the Supporting Information). In addition, we used BODIPY conjugate **33** (which has the active triterpenic scaffold replaced by acetate) as a negative control. According to the results, this compound does not penetrate the cellular membrane, indicating that it is the triterpenoid part that is responsible for the cellular uptake. This is likely because of the high lipophilicity of triterpenes. Conjugate **25**, containing a Michael acceptor (acrolein moiety in this case), resulted in a different staining pattern—labeling cellular cytoplasm homogeneously, which is presumably caused by nonspecific covalent interaction with multiple intracellular proteins. Staining is distinct when compared to other tested compounds (**24**, **26**, **27**, **28**, **29**, **30**, **31**), which labeled more subtle cytoplasmic and membrane structures, likely mitochondria, endoplasmic reticulum (ER), and the nuclear membrane. Co-staining experiments are being performed to confirm this unambiguously. Such results are in agreement with precedent studies on another lupane triterpenes that were found to interact with mitochondrion and ER.^[21,22]

Table 1. Cytotoxic activity of the prepared compounds.

| Comp. | IC ₅₀ [μmol L ⁻¹] ^[a] | | | | IC ₅₀ [μmol L ⁻¹] ^[a] | | | | | | TI ^[b] |
|-------------------------|---|---------|--------|-------------|---|----------|-------|-------|-------|-------|-------------------|
| | CCRF-CEM | CEM-DNR | HCT116 | HCT116p53/- | K562 | K562-TAX | A549 | U2OS | BJ | MRC-5 | |
| 1 ^[c] | 8.09 | 14.04 | 4.29 | 14.09 | 9.43 | 15.78 | 15.96 | 20.75 | 24.23 | 28.18 | 3.24 |
| 2 ^[c] | 1.53 | 7.66 | 8.83 | 12.43 | 9.68 | 7.73 | 7.23 | 7.51 | 11.99 | 2.39 | 4.70 |
| 3 ^[c] | 15.16 | 20.16 | 27.25 | 34.67 | 21.01 | 24.25 | 27.12 | 40.06 | 44.28 | 42.67 | 2.87 |
| 4 ^[c] | 35.58 | 35.98 | > 50 | 43.11 | > 50 | > 50 | > 50 | > 50 | > 50 | > 50 | > 1.41 |
| 5 ^[c] | 0.53 | 0.63 | 11.54 | 11.6 | 31.84 | 34.41 | 47.3 | 32.43 | > 50 | > 50 | > 94.34 |
| 24 | 6.62 | > 50 | > 50 | > 50 | > 50 | > 50 | > 50 | 33.75 | 43.61 | 43.6 | 6.59 |
| 25 | 0.76 | 6.06 | 1.65 | 10.52 | 1.96 | 1.6 | 1.45 | 1.46 | 1.87 | 1.62 | 2.30 |
| 26 | > 50 | > 50 | > 50 | > 50 | > 50 | > 50 | > 50 | > 50 | > 50 | > 50 | N.A. |
| 27 | 3.4 | > 50 | 45.7 | > 50 | > 50 | > 50 | > 50 | > 50 | 45.84 | 44.26 | 13.25 |
| 28 | 18.09 | 20.28 | > 50 | > 50 | > 50 | > 50 | > 50 | > 50 | > 50 | > 50 | > 2.76 |
| 29 | 6.13 | 9.27 | 18.92 | 12.07 | 29.02 | 35.05 | 29.14 | 26.34 | 39.74 | 38.23 | 6.36 |
| 30 | > 50 | > 50 | > 50 | > 50 | > 50 | > 50 | > 50 | > 50 | > 50 | > 50 | N.A. |
| 31 | 41.17 | 40.68 | 41.96 | > 50 | 49.02 | 40.6 | 41.43 | 45.02 | 48.81 | 40.75 | 1.09 |
| 32 | > 50 | > 50 | > 50 | > 50 | > 50 | > 50 | > 50 | > 50 | > 50 | > 50 | N.A. |
| 33 | > 50 | > 50 | > 50 | > 50 | > 50 | > 50 | > 50 | > 50 | > 50 | > 50 | N.A. |

[a] The lowest concentration that kills 50% of the cells. The standard deviation in cytotoxicity assays is typically up to 15% of the average value. [b] Therapeutic index is calculated for IC₅₀ of CCRF-CEM line vs. an average of both fibroblasts (BJ and MRC-5). [c] Parent compounds used as a standard. Compounds with IC₅₀ > 50 μM are considered inactive.

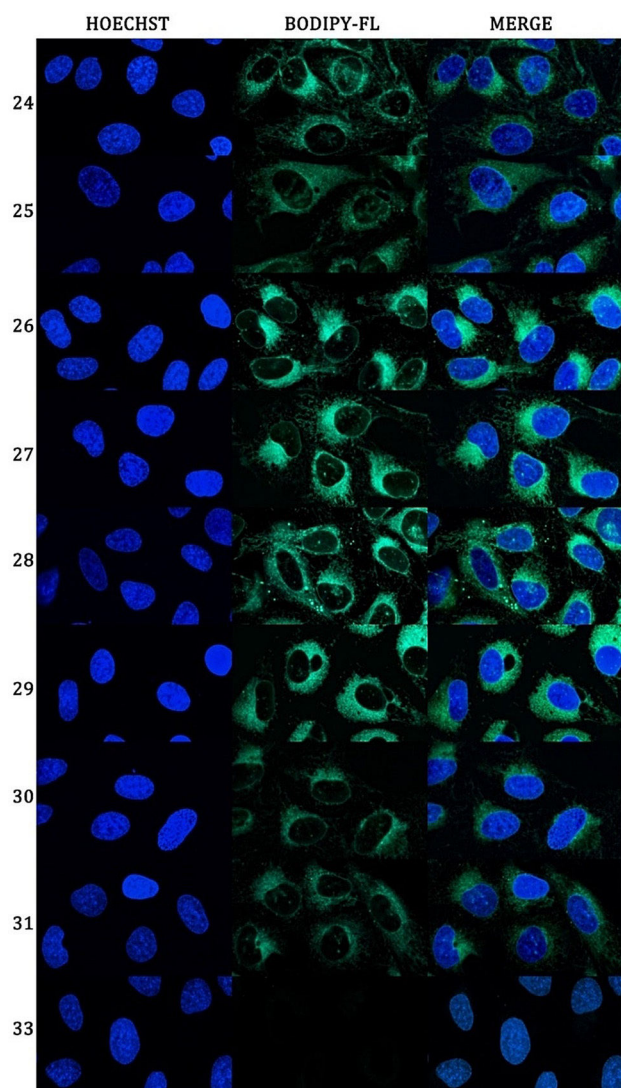


Figure 4. Fluorescence imaging of U2OS cells stained by BODIPY-triterpene conjugates (for full resolution see the Supporting Information).

Conclusion

We optimized the synthesis of BODIPY-FL propanoic acid **19** to give better yields than procedures reported by other authors, and the synthesis is suitable for multigram scale quantities. We prepared BODIPY-preloaded resin and applied it to attach the fluorescent dye to cytotoxic triterpene derivatives. Despite previous reports on the limited applicability of BODIPYs in solid-phase synthesis, because of their low stability under both basic and acidic conditions,^[3,6,7] we developed and optimized synthetic protocols to overcome these problems. The reported preloaded resin allows for routine and simple connection of various compounds to BODIPY label through a linker of choice using simple laboratory equipment, common coupling reagents and conditions, and minimum hands-on-time, and it can even be commercialized similar to biotin-preloaded resin (Biotin NovaTag™, Novabiochem). Nine conjugates of BODIPY with cytotoxic triterpenes were synthesized using resin **23** and their spectroscopic and biological properties were evaluated.

To prove that BODIPY with the linker do not interfere with the biological study, we prepared a conjugate in which the triterpene part was replaced with acetate. Live cell studies focused on fluorescence conjugate uptake demonstrated nonspecific labeling in aldehyde **25** and a more specific labeling pattern in the case of conjugates **24** and **26–31**. Ongoing research is now focused on a more specific determination of which organelles, proteins or protein complexes are targeted by our conjugates, and this will be the aim of further proteomic and molecular biology studies, for example, co-localization experiments.

Experimental Section

General technical information is available in the Supporting Information and is analogous to our previous publications.^[23,24] Note that the yields of the final conjugates (**24–33**, usually between 10–30%) are calculated as overall yields of the entire synthetic procedure between compound **20** and the final product in Scheme 3.

General procedure for the preparation of benzyl glyoxalates: To a stirred solution of starting material in THF were added benzyl bromoacetate (3 equiv) and K_2CO_3 (3 equiv). The reaction mixture was stirred at 50 °C and the progress of the reaction was monitored by TLC (hexane/EtOAc = 3:1, v/v) which indicated its completion after overnight stirring. The reaction mixture was concentrated, diluted with water (100 mL/1.32 mmol) and extracted with EtOAc (5 × 100 mL/1.32 mmol). The organic extracts were combined, dried over $MgSO_4$, filtered, and evaporated under reduced pressure. The crude products were purified by flash chromatography (hexane/EtOAc = 3:1 to 1:1, v/v) to give the desired compounds.

2-(Benzoyloxy)-2-oxoethyl betulinate (7): Compound **7** was prepared by following General Procedure A with **1** (600 mg, 1.32 mmol), benzyl bromoacetate (633 μ L, 4 mmol), and K_2CO_3 (552 mg, 4 mmol) in THF (20 mL); Yield: 783 mg (98%); white solid; 1H NMR (500 MHz, $CDCl_3$): δ = 7.38–7.35 (m, 5H; Ph), 5.22 (d, J = 6.5 Hz, 1H; OCH_2Ph), 5.18 (d, J = 12.3 Hz, 1H; OCH_2Ph), 4.73 (d, J = 2.0 Hz, 1H; $H^{29\text{ pro-Z}}$), 4.65 (d, J = 2.3 Hz, 2H; OCH_2CO), 4.61–4.60 (m, 1H; $H^{29\text{ pro-E}}$), 3.21–3.17 (dd, J = 11.0, 4.8 Hz, 1H; $H^{3\alpha}$), 2.97 (td, J = 11.3, 10.9, 4.7 Hz, 1H; $H^{19\beta}$), 2.30 (dt, J = 12.6, 2.7 Hz, 1H), 2.27 (td, J = 13.5, 13.4, 3.6 Hz, 1H), 2.06–1.99 (m, 1H), 1.96–1.86 (m, 1H), 1.72–1.13 (m, 24H; overlap with solvent), 0.97 (s, 6H; $2 \times CH_3$), 0.92 (s, 3H; CH_3), 0.83 (s, 3H; CH_3), 0.77 ppm (s, 3H; CH_3); ^{13}C NMR (126 MHz, $CDCl_3$): δ = 175.6, 168.1, 150.7, 135.4, 128.8, 128.6, 109.8, 79.2, 67.2, 60.4, 56.7, 55.6, 50.8, 49.6, 47.0, 42.6, 40.9, 39.0, 38.9, 38.3, 37.4, 37.1, 34.5, 32.1, 30.6, 29.8, 28.2, 27.6, 25.8, 21.1, 19.6, 18.5, 16.3, 16.1, 15.5, 14.9 ppm; HRMS (ESI): m/z calcd for $C_{39}H_{56}O_5$ 605.4201 [$M+H$]⁺; found: 605.4207.

Benzyl glyoxalate of betulinic acid pyrazine (13): Compound **13** was prepared by following General Procedure A with **5** (100 mg, 0.2 mmol), benzyl bromoacetate (96 μ L, 0.61 mmol), and K_2CO_3 (84 mg, 0.61 mmol) in THF (8 mL). Yield: 116 mg (91%); yellowish oil; 1H NMR (500 MHz, $CDCl_3$): δ = 8.30 (d, J = 2.1 Hz, 1H; pyrazine), 8.17 (d, J = 2.4 Hz, 1H; pyrazine), 7.33–7.24 (m, 5H; Ph, overlap with solvent), 5.14–5.06 (m, 2H; OCH_2Ph), 4.66–4.54 (m, 4H), 2.96–2.86 (m, 3H), 2.37–2.21 (m, 4H), 1.96–1.91 (m, 1H), 1.86–1.80 (m, 1H), 1.70–1.22 (m, 17H; overlap with solvent), 1.20 (s, 3H; CH_3), 1.18 (s, 3H; CH_3), 0.92–0.90 (m, 6H; $2 \times CH_3$), 0.70 ppm (s, 3H; CH_3); ^{13}C NMR (126 MHz, $CDCl_3$): δ = 175.5, 168.1, 159.8, 151.0, 150.5, 142.4, 141.6, 135.3, 128.8, 128.7, 128.6, 109.9, 67.2, 60.4, 56.7, 53.2, 49.5, 49.0, 48.9, 46.9, 42.6, 40.7, 39.6, 38.3, 37.1, 36.9, 33.4, 32.0, 31.7, 30.6, 29.7, 25.7, 24.2, 21.6, 20.2, 19.6, 16.3, 15.7, 14.8 ppm;

HRMS (ESI): m/z calcd for $C_{41}H_{54}N_2O_4$: 639.4156 $[M+H]^+$; found: 639.4155.

3 β -Hydroxylup-20(29)-ene-28,30-dioic acid (10): To a stirred solution of aldehyde **2** (100 mg, 0.21 mmol) in *t*BuOH/2-methyl-2-butene (1:1, 10 mL, v/v) was added NaClO₂ (96 mg, 1.06 mmol) and a solution of KH₂PO₄ (550 mg, 4.04 mmol) in H₂O (5 mL). The reaction mixture was stirred vigorously at ambient temperature and the progress of the reaction was monitored by TLC (CH₂Cl₂/CH₃OH=10:1, v/v), which indicated its completion after 5 h. The reaction mixture was concentrated, diluted with NH₄Cl (50 mL), and extracted with EtOAc (5×50 mL). Organic extracts were combined, dried over MgSO₄, filtered and evaporated under reduced pressure. The crude product was purified by flash chromatography (CH₂Cl₂/CH₃OH=5:1, v/v) to afford compound **10**. Yield: 90 mg (90%); white crystalline solid; ¹H NMR (500 MHz, [D₆]DMSO): δ = 12.17 (br s, 2H; 2×COOH), 5.96 (s, 1H; H^{29 pro-Z}), 5.60 (s, 1H; H^{29 pro-E}),

4.25 (d, J = 5.1 Hz, 1H), 4.08–4.07 (m, 1H), 2.98–2.94 (m, 1H), 2.22–2.07 (m, 3H), 1.99–1.91 (m, 1H), 1.82–1.75 (m, 2H), 1.62–1.52 (m, 2H), 1.43–1.24 (m, 16H), 0.90 (s, 3H; CH₃), 0.87 (s, 3H; CH₃), 0.86 (s, 3H; CH₃), 0.76 (s, 3H; CH₃), 0.65 ppm (s, 3H; CH₃); ¹³C NMR (126 MHz, [D₆]DMSO): δ = 177.2, 168.4, 147.7, 122.5, 76.7, 55.5, 54.8, 51.05, 49.8, 48.6, 41.9, 38.5, 38.2, 37.3, 36.7, 36.0, 33.9, 32.7, 31.6, 29.2, 28.1, 27.1, 26.8, 20.5, 17.9, 15.9, 15.8, 15.7, 14.3 ppm; HRMS (ESI): m/z calcd for $C_{30}H_{46}O_5$: 485.3262 $[M-H]^-$; found: 485.3252.

General procedure B for preparation of hemisuccinates: To a stirred solution of starting material in THF/DMF (2:1) was added succinic anhydride (6 equiv) and 4-dimethylaminopyridine (DMAP, 6 equiv). The reaction mixture was stirred at 80 °C and the progress of the reaction was monitored by TLC (CH₂Cl₂/CH₃OH = 10:1, v/v), which indicated its completion after 36 to 48 h. The reaction mixture was concentrated, diluted with NH₄Cl (150 mL/2.2 mmol) and extracted with EtOAc (5×100 mL/2.2 mmol). Organic extracts were combined, dried over MgSO₄, filtered, and evaporated under reduced pressure. The crude products were purified by flash chromatography (CH₂Cl₂/CH₃OH = 10:1, v/v) to afford the desired compounds.

Betulinic acid 3-hemisuccinate (6): Compound **6** was prepared by following General Procedure B with **1** (1 g, 2.2 mmol), succinic anhydride (1.32 g, 13.1 mmol), and DMAP (1.6 g, 13.1 mmol) in THF/DMF (2:1, 60 mL) for 36 h. Yield: 980 mg (80%); white solid; ¹H NMR (500 MHz, [D₆]DMSO): δ = 12.14 (br s, 2H; 2×COOH), 4.69 (s, 1H; H^{29 pro-Z}), 4.56 (s, 1H; H^{29 pro-E}), 4.37 (dd, J = 11.7, 4.6 Hz, 1H; H^{3 α}), 2.97–2.92 (m, 1H; H^{19 β}), 2.54–2.46 (m, 4H; overlap with solvent), 2.25–2.18 (m, 1H), 2.11 (m, 1H), 1.79 (m, 1H), 1.64 (s, 3H; CH₃), 1.62–1.07 (m, 12H), 0.94 (s, 3H; CH₃), 0.87 (s, 3H; CH₃), 0.80 (s, 3H; CH₃), 0.78 ppm (s, 6H; 2×CH₃). All other data were consistent with published results.^[6]

30-Aldehyde 3-hemisuccinate of betulinic acid (9): Compound **9** was prepared by following General Procedure B with **2** (1.5 g, 3.13 mmol), succinic anhydride (1.88 g, 18.78 mmol), and DMAP (2.3 g, 18.78 mmol) in THF/DMF (2:1, 30 mL) for 48 h. Yield: 1.3 g (73%); white solid; ¹H NMR (500 MHz, [D₆]DMSO): δ = 12.14 (br s, 2H; 2×COOH), 9.49 (s, 1H; CHO), 6.47 (s, 1H; H^{29 pro-Z}), 6.09 (s, 1H; H^{29 pro-E}), 4.37 (dd, J = 11.3, 4.6 Hz, 1H; H^{3 α}), 3.25 (dd, J = 11.1, 4.8 Hz, 1H), 3.19 (d, J = 21.6 Hz, 2H), 2.52–2.46 (m, 4H), 2.20–2.12 (m, 2H), 1.97–1.89 (m, 1H), 1.81–1.77 (m, 2H), 1.58–1.11 (m, 17H), 0.91 (d, J = 7.2 Hz, 3H; CH₃), 0.86 (s, 3H; CH₃), 0.78 ppm (d, J = 3.6 Hz, 9H; 3×CH₃); ¹³C NMR (126 MHz, [D₆]DMSO): δ = 195.6, 177.1, 175.0, 173.4, 171.6, 170.3, 156.3, 134.8, 79.9, 55.5, 54.6, 49.4, 41.9, 37.7, 37.4, 36.6, 36.1, 33.7, 31.6, 31.4, 29.2, 28.8, 27.6, 26.8, 23.3, 20.7, 20.5, 17.7, 16.4, 15.8, 15.6, 14.3, 14.1 ppm; HRMS (ESI): m/z calcd for $C_{34}H_{50}O_7$: 569.3473 $[M-H]^-$; found: 569.3456.

Hemisuccinate of 21-oxoacid (11): Compound **11** was prepared by following General Procedure B with **3** (700 mg, 1.45 mmol), succinic anhydride (867 mg, 8.68 mmol), and DMAP (1.05 g, 8.68 mmol) in THF/DMF (2:1, 15 mL) for 40 h. Yield: 1.3 g (73%); white solid; ¹H NMR (500 MHz, CDCl₃): δ = 4.51 (dd, J = 11.0, 5.5 Hz, 1H; H^{3 α}), 3.69 (s, 3H; COOCH₃), 3.22–3.16 (m, 1H), 2.70–2.60 (m, 4H), 2.49–2.43 (m, 2H), 2.13 (d, J = 18.6 Hz, 1H), 2.00 (dd, J = 12.5, 3.0 Hz, 1H), 1.92–1.23 (m, 9H; overlap with solvent), 1.21 (app s, 3H; CH₃), 1.20 (app s, 3H; CH₃), 1.02 (s, 3H; CH₃), 0.93 (s, 3H; CH₃), 0.90 (s, 3H; CH₃), 0.84 (s, 3H; CH₃), 0.83 ppm (s, 3H; CH₃); ¹³C NMR (126 MHz, CDCl₃): δ = 207.5, 177.7, 175.1, 172.1, 172.0, 145.9, 81.5, 55.6, 53.3, 52.7, 51.2, 47.8, 45.4, 41.5, 38.7, 38.0, 37.3, 35.0, 33.9, 29.5, 29.3, 29.2, 28.1, 27.8, 25.3, 23.7, 21.4, 20.3, 20.2, 18.3, 17.0, 16.8, 16.7, 16.1 ppm; HRMS (ESI): m/z calcd $C_{35}H_{52}O_7$: 585.3786 $[M+H]^+$; found: 585.3796.

Hemisuccinate of 21,22-dioxoacid (12): Compound **12** was prepared by following a previously published procedure.^[7] ¹H NMR (500 MHz, [D₆]DMSO): δ = 12.20 (br s, 1H; COOH), 4.40 (dd, J = 11.6, 4.7 Hz, 1H; H^{3 α}), 3.66 (s, 3H; COOCH₃), 3.37–3.30 (m, 1H; overlap with solvent), 2.72–2.69 (m, 1H), 2.52–2.44 (m, 4H; overlap with solvent), 2.25–2.22 (m, 1H), 1.97–1.87 (m, 3H), 1.74–1.31 (m, 14H), 1.19 (d, J = 3.5 Hz, 3H; CH₃), 1.18 (d, J = 3.5 Hz, 3H; CH₃), 1.00 (s, 3H; CH₃), 0.95 (s, 3H; CH₃), 0.86 (s, 3H; CH₃), 0.80 (s, 3H; CH₃), 0.79 ppm (s, 3H; CH₃); ¹³C NMR (126 MHz, [D₆]DMSO): δ = 194.4, 189.0, 173.4, 171.6, 170.5, 168.0, 149.2, 79.9, 58.1, 54.5, 53.5, 49.8, 45.6, 45.3, 41.0, 37.7, 37.4, 36.6, 33.9, 29.1, 28.7, 27.8, 27.5, 27.3, 26.4, 25.2, 23.3, 20.5, 19.9, 19.4, 17.7, 16.5, 16.4, 16.3, 15.6 ppm; HRMS (ESI): m/z calcd for $C_{35}H_{50}O_8$: 597.3422 $[M-H]^-$; found: 597.3408.

General procedure C for preparation of glyoxalates: To a freshly degassed solution of starting material in CH₂Cl₂/CH₃OH (2:1) was added Pd/C (10%, 3.5 mol%) and H₂ was bubbled through the resulting reaction mixture for 20 min. The reaction was monitored by TLC (CH₂Cl₂/CH₃OH/AcOH = 10:1:0.1, v/v), which indicated its completion after 1 h. The reaction mixture was diluted with CH₃OH (20 mL/0.83 mmol) and filtered through a bed of Celite. The residual solvent was evaporated under reduced pressure and the crude product was purified by flash chromatography (CH₂Cl₂/CH₃OH/AcOH 10:1:0.1, v/v).

Betulinic acid glyoxalate (8): Compound **8** was prepared by following General Procedure C with **7** (500 mg, 0.83 mmol), Pd/C (30 mg) in CH₂Cl₂/CH₃OH (2:1, 7.5 mL). Yield: 357 mg (84%); white solid; ¹H NMR (500 MHz, [D₆]DMSO): δ = 12.91 (br s, 1H; COOH), 4.65 (d, J = 2.0 Hz, 1H; H^{29 pro-Z}), 4.53 (s, 1H; H^{29 pro-E}), 4.50 (app s, 2H, OCH₂CO), 4.21 (br s, 1H; H^{3 α}), 2.94 (m, 1H), 2.90–2.84 (m, 1H), 2.18–2.13 (m, 2H), 1.92–1.86 (m, 1H), 1.83–1.75 (m, 1H), 1.62 (s, 3H; CH₃), 1.58–1.01 (m, 20H), 0.90 (s, 3H; CH₃), 0.84 (s, 3H; CH₃), 0.82 (s, 3H; CH₃), 0.72 (s, 3H; CH₃), 0.62 ppm (s, 3H; CH₃); ¹³C NMR (101 MHz, [D₆]DMSO): δ = 174.6, 169.3, 150.1, 109.7, 76.7, 60.3, 55.7, 54.8, 49.9, 48.6, 46.5, 42.0, 38.5, 38.2, 37.4, 36.7, 36.2, 33.9, 31.3, 29.8, 28.9, 28.1, 27.1, 25.0, 20.4, 18.9, 17.9, 15.9, 15.8, 15.7, 14.3 ppm. HRMS (ESI): m/z calcd for $C_{32}H_{50}O_5$: 513.3575 $[M-H]^-$; found: 513.3567.

Glyoxalate of pyrazine of betulinic acid (14): Compound **14** was prepared by following General Procedure C with **13** (500 mg, 0.78 mmol) and Pd/C (27 mg) in CH₂Cl₂/CH₃OH (2:1, 7.5 mL). Yield: 210 mg (49%); white solid; ¹H NMR (500 MHz, [D₆]DMSO): δ = 8.45 (d, J = 2.3 Hz, 1H; pyrazine), 8.32 (d, J = 2.4 Hz, 1H; pyrazine), 4.71 (d, J = 1.9 Hz, 1H; H^{29 pro-Z}), 4.59 (app s, 1H; H^{29 pro-E}), 4.55 (app s, 2H; OCH₂CO), 2.92 (td, J = 11.2, 10.9, 4.7 Hz, 1H; H^{19 β}), 2.88 (d, J = 16.6 Hz, 1H; H^{1 α}), 2.46 (d, J = 16.6 Hz, 1H; H^{1 β}), 2.28–2.20 (m, 2H), 1.93 (dd, J = 11.9, 8.1 Hz, 1H), 1.87–1.79 (m, 1H), 1.67 (s, 3H; CH₃), 1.67–1.28 (m, 15H), 1.24 (s, 3H; CH₃), 1.20 (s, 3H; CH₃), 1.17–1.05

(m, 2H), 1.00 (s, 3H; CH₃), 0.93 (s, 3H; CH₃), 0.72 ppm (s, 3H; CH₃); ¹³C NMR (126 MHz, [D₆]DMSO): δ = 174.7, 169.3, 158.5, 150.2, 150.1, 142.3, 141.7, 109.8, 60.2, 55.8, 52.0, 48.1, 47.8, 46.5, 42.1, 37.5, 36.2, 32.8, 31.3, 29.8, 29.0, 25.1, 24.0, 21.0, 19.5, 18.9, 15.8, 15.2, 14.4 ppm. HRMS (ESI): *m/z* calcd for C₃₄H₄₈N₂O₄: 547.3530 [M-H]⁻; found: 547.3527.

Methyl (E)-3-(1H-pyrrol-2-yl)acrylate (16): To a stirred solution of pyrrole-2-carbaldehyde **15** (1.5 g, 15.78 mmol) in CH₂Cl₂ (30 mL) was added methyl (triphenylphosphoranylidene)acetate (10.5 g, 31.57 mmol) in CH₂Cl₂ (50 mL). The resulting mixture was stirred at room temperature overnight. The residual solvent was evaporated and the crude oily product was purified by flash chromatography (hexane/EtOAc = 2:1, v/v) to afford compound **16**. Yield: 2 g (84%); pale-pink solid; ¹H NMR (500 MHz, CDCl₃): δ = 8.65 (br s, 1H), 7.56 (d, *J* = 16.0 Hz, 1H), 6.94–6.93 (m, 1H), 6.58–6.57 (m, 1H), 6.31–6.28 (m, 1H), 6.00 (d, *J* = 16.0 Hz, 1H), 3.78 ppm (s, 3H); ¹³C NMR (126 MHz, CDCl₃): δ = 168.2, 134.5, 128.5, 122.6, 114.7, 111.2, 111.0, 51.8 ppm; HRMS (ESI): *m/z* calcd for C₈H₉NO₂: 152.0706 [M+H]⁺; found: 152.0705.

Methyl 3-(1H-pyrrol-2-yl)propanoate (17): To a freshly degassed solution of **16** (2 g, 13.25 mmol) in CH₃OH (20 mL) was added Pd/C (10% loading, 3.5 mol%, 500 mg) and H₂ was bubbled through the resulting reaction mixture for 20 min. The reaction was monitored with UHPLC-MS, which indicated its completion after 1 h. The reaction mixture was diluted with CH₃OH (20 mL) and filtered through a bed of Celite. The residual solvent was evaporated and the crude product was purified by flash chromatography (hexane/EtOAc = 2:1, v/v) to afford **17**. Yield: 1.67 g (90%); pale-yellow oil; ¹H NMR (500 MHz, CDCl₃): δ = 8.51 (br s, 1H), 6.69–6.67 (m, 1H), 6.11 (dd, *J* = 5.7, 2.8 Hz, 1H), 5.92–5.91 (m, 1H), 3.71 (s, 3H), 2.92 (t, *J* = 6.8 Hz, 2H), 2.65 ppm (t, *J* = 6.8 Hz, 2H); ¹³C NMR (101 MHz, CDCl₃): δ = 174.7, 131.1, 117.0, 108.2, 105.7, 52.0, 34.5, 22.7 ppm; HRMS (ESI): *m/z* calcd for C₈H₁₁NO₂: 154.0863 [M+H]⁺; found: 154.0863.

BODIPY-FL-methyl propanoate (18): To a stirred solution of **17** (1.67 g, 10.92 mmol) and 3,5-dimethylpyrrole-2-carboxaldehyde (1.54 g, 12.01 mmol) in CH₂Cl₂ (80 mL) was added dropwise POCl₃ (1.12 mL, 12.01 mmol) at 0 °C and the reaction mixture was allowed to warm to ambient temperature. The reaction was monitored with UHPLC-MS, which indicated formation of dipyrromethane intermediate after 3 h. The reaction mixture was then cooled to 0 °C and *N,N*-diisopropylethylamine (DIPEA, 8.1 mL, 49.14 mmol) was added dropwise, followed by stirring for 20 min at 0 °C. BF₃·OEt₂ (5.4 mL, 43.68 mmol) was added subsequently and the reaction was stirred overnight at ambient temperature. The mixture was diluted with CH₂Cl₂ (50 mL) and brine (100 mL), filtered through a bed of Celite, again diluted with brine (100 mL) and extracted with CH₂Cl₂ (5 × 200 mL). Organic extracts were combined, dried over MgSO₄, filtered and evaporated under reduced pressure. The crude product was purified by flash chromatography (100% CH₂Cl₂) to give **18**. Yield: 2.13 g (63%); dark-green crystalline solid; ¹H NMR (500 MHz, CDCl₃): δ = 7.09 (s, 1H), 6.89 (d, *J* = 3.9 Hz, 1H), 6.27 (d, *J* = 4.0 Hz, 1H), 6.12 (s, 1H), 3.70 (s, 3H), 3.31 (t, *J* = 7.6 Hz, 2H), 2.78 (t, *J* = 7.5 Hz, 2H), 2.58 (s, 3H), 2.26 ppm (s, 3H); ¹³C NMR (126 MHz, CDCl₃): δ = 173.2, 160.8, 144.1, 135.5, 133.5, 128.3, 124.1, 120.7, 116.9, 52.0, 33.5, 30.0, 24.3, 15.2, 11.5 ppm; ¹⁹F {¹H} NMR (471 MHz, CDCl₃): δ = -145.23 (d, *J* = 31.4 Hz), -145.37 ppm (d, *J* = 31.4 Hz); HRMS (ESI): *m/z* calcd for C₁₅H₁₇BF₂N₂O₂: 305.1267 [M-H]⁻; found: 305.1266. Other spectral data were consistent with literature precedences.^[3]

BODIPY-FL-propanoic acid (19): To a stirred solution of **18** (1.43 g, 4.67 mmol) in THF (30 mL) was added water (20 mL) and conc. HCl (10 mL) at 0 °C. The reaction mixture was stirred at ambient temperature and monitored by UHPLC-MS, which indicated its comple-

tion after 52 h. The reaction mixture was diluted with water (100 mL) and extracted with CH₂Cl₂ (3 × 150 mL). Organic extracts were combined, dried over MgSO₄, filtered and evaporated under reduced pressure. Purification of the crude product by flash chromatography (CH₂Cl₂/AcOH 100:1, v/v) afforded **19**. Yield: 1.15 g (85%); dark-red crystalline solid; ¹H NMR (500 MHz, [D₆]DMSO): δ = 12.30 (s, 1H), 7.70 (s, 1H), 7.09 (d, *J* = 4.0 Hz, 1H), 6.38 (d, *J* = 4.0 Hz, 1H), 6.31 (s, 1H), 3.10–3.05 (t, *J* = 7.1 Hz, 2H), 2.64 (t, *J* = 8.5 Hz, 2H), 2.47 (s, 3H), 2.26 ppm (s, 3H); ¹³C NMR (126 MHz, [D₆]DMSO): δ = 173.4, 159.5, 156.9, 144.3, 134.5, 133.0, 128.8, 125.4, 120.4, 116.5, 32.3, 23.5, 14.5, 11.0 ppm; ¹⁹F {¹H} NMR (471 MHz, CDCl₃): δ = -145.21 (d, *J* = 31.8 Hz), -145.36 ppm (d, *J* = 31.8 Hz); HRMS (ESI): *m/z* calcd for C₁₄H₁₅BF₂N₂O₂: 291.1111 [M-H]⁻; found: 291.1105. Other spectral data were consistent with published results.^[3]

Preparation of BAL resin: Aminomethyl polystyrene resin (1 g, loading 0.98 mmol/g) was swollen in CH₂Cl₂ (10 mL) for 30 min, washed with DMF (3 × 10 mL), neutralized in DMF/piperidine (5:1, 10 mL) for additional 30 min and again washed with DMF (5 × 10 mL). Backbone amide linker (700 mg, 2.94 mmol) and HOBt (450 mg, 2.9 mmol) were dissolved in DMF/CH₂Cl₂ (1:1, 10 mL, v/v) and DIC (460 mg, 2.94 mmol) was added. The resulting solution was added to a polypropylene fritted syringe with aminomethyl resin. The reaction slurry was shaken at ambient temperature overnight, followed by washing with DMF (3 × 10 mL) and CH₂Cl₂ (3 × 10 mL). Bromphenol blue test confirmed quantitative acylation of the amino groups.

Procedure for reductive amination: BAL resin (1 g, loading 0.98 mmol/g) was swollen in CH₂Cl₂ (10 mL) for 30 min, then washed with anhydrous THF (3 × 10 mL) and anhydrous DMF (3 × 10 mL). The solution of 2-(2-aminoethoxy)ethanol (490 μL, 4.9 mmol) in DMF/AcOH (10:1, 10 mL, v/v) was added to a polypropylene fritted syringe with BAL resin and it was shaken overnight at ambient temperature. NaBH(OAc)₃ (210 mg, 2.94 mmol) in DMF/AcOH (20:1, 5 mL, v/v) was then added portionwise to the reaction mixture a during period of 4 h, followed by washing with DMF (5 × 10 mL) and CH₂Cl₂ (3 × 10 mL) and neutralization with DMF/TEA (10:1, 10 mL, v/v) for an additional 30 min to obtain resin **20**. The loading was determined according to a published procedure^[8] (0.4–0.6 mmol/g).

Procedure for protection with Fmoc: Resin **20** (250 mg) was swollen in CH₂Cl₂ (3 mL) for 30 min and then washed with CH₂Cl₂ (3 × 5 mL). Fmoc-OSu (505 mg, 1.5 mmol) was dissolved in CH₂Cl₂ (3 mL) and added to a polypropylene fritted syringe with the resin. The reaction slurry was shaken at ambient temperature overnight, followed by washing with CH₂Cl₂ (5 × 5 mL). An analytical sample was cleaved from the resin and UHPLC-MS analysis confirmed the presence of desired product. MS (ESI): *m/z* 328 [M+H]⁺.

Procedure for acylation with BODIPY-FL propanoic acid: Resin **20** equipped with Fmoc (250 mg) was swollen in CH₂Cl₂ (3 mL) for 30 min and then washed with DMF (3 × 3 mL) and CH₂Cl₂ (3 × 3 mL). BODIPY-FL propanoic acid **19** (220 mg, 0.75 mmol), HOBt (115 mg, 0.75 mmol) and DMAP (92 mg, 0.75 mmol) were dissolved in DMF/CH₂Cl₂ (1:1, 2.5 mL, v/v) and DIC (117 μL, 0.75 mmol) was added. The resulting solution was added to a polypropylene fritted syringe with the resin. The reaction slurry was shaken at ambient temperature overnight, followed by washing with DMF (10 × 3 mL) and CH₂Cl₂ (10 × 3 mL) to give resin **21**. An analytical sample was cleaved from the resin and UHPLC-MS analysis confirmed the presence of desired product. MS (ESI): *m/z* 600 [M-H]⁻.

General procedure D for deprotection of Fmoc: Resin **21** (250 mg) was swollen in CH₂Cl₂ (3 mL) for 30 min and then washed with DMF (3 × 3 mL). The freshly prepared solution of DMF/piperi-

dine (20:1, 2.5 mL, v/v) was added to polypropylene fritted syringe with the resin. The reaction slurry was shaken at ambient temperature for 30 min, followed by washing with CH₂Cl₂ (3×3 mL), THF (3×3 mL), DMF (3×3 mL), THF (3×3 mL), and CH₂Cl₂ (3×3 mL).

Procedure for acylation with FAEEAA: Fmoc deprotected resin **21** (250 mg) was swollen in CH₂Cl₂ (3 mL) for 30 min and then washed with DMF (3×3 mL) and CH₂Cl₂ (3×3 mL). [2-[2-(Fmoc-amino)ethoxy]ethoxy]acetic acid (334 mg, 0.9 mmol) and HOBt (137 mg, 0.9 mmol) were dissolved in DMF/CH₂Cl₂ (1:1, 3 mL, v/v) and DIC (140 μL, 0.9 mmol) was added. The resulting solution was added to polypropylene fritted syringe with the resin. The reaction slurry was shaken at ambient temperature overnight, followed by washing with DMF (10×3 mL) and CH₂Cl₂ (10×3 mL), which gave resin **22**. An analytical sample was cleaved from the resin and UHPLC-MS analysis confirmed the presence of desired product. MS (ESI): *m/z* 745 [M-H]⁻. The Fmoc was deprotected from resin **22** by the general procedure to give resin **23**.

Procedure for acylation with acetic anhydride: Resin **23** (200 mg) was swollen in CH₂Cl₂ (2 mL) for 30 min and then washed with DMF (3×2 mL) and CH₂Cl₂ (3×2 mL). DMAP (92 mg, 0.75 mmol) was dissolved in CH₂Cl₂ (2.5 mL) and acetic anhydride (71 μL, 0.75 mmol) was added. The resulting solution was added to polypropylene fritted syringe with the resin. The reaction slurry was shaken at ambient temperature overnight, followed by washing with CH₂Cl₂ (5×3 mL). Subsequent cleavage from the resin and UHPLC-MS analysis confirmed the presence of the desired product **33**.

General procedure E for acylation with triterpene derivatives: Resin **23** (250 mg) was swollen in CH₂Cl₂ (3 mL) for 30 min and then washed with DMF (3×3 mL) and CH₂Cl₂ (3×3 mL). To each solution of premodified triterpenes **6**, **8–12**, **14** (0.9 mmol) in DMF/CH₂Cl₂ (1:1, 3 mL, v/v) was added DIC (70 μL, 0.45 mmol) and the resulting mixture was added to a polypropylene fritted syringe with starting material. The reaction slurry was shaken at ambient temperature overnight, followed by washing with CH₂Cl₂ (10×3 mL). The final compounds were cleaved according to General Procedure F.

General procedure F for cleavage from the resin: Cleavage of intermediates **24–31** and **33** in analytical scale (ca. 5 mg) prior to analysis was carried out in CH₂Cl₂/TFA (10:1, 1 mL, v/v) for 30 min according to the General Information.

Cleavage of intermediates 24–31 and 33 in preparative scale (ca. 250 mg): The corresponding resin was swollen in CH₂Cl₂ (3 mL) for 30 min and then washed with CH₂Cl₂ (5×3 mL). A solution of CH₂Cl₂/TFA (10:1, 3 mL, v/v) was added to each polypropylene fritted syringe with resin. The reaction slurry was shaken at ambient temperature for 90 min (**28–30**) or 2 h (**24–27**, **31**, **33**) and then washed with CH₂Cl₂/TFA (10:1, 3×3 mL, v/v) and CH₂Cl₂ (3×3 mL). The cleavage cocktail with combined washes was evaporated under a stream of nitrogen, the crude products were dissolved in CH₃CN (3 mL) and purified by RP-HPLC to afford final compounds **24–33**.

BODIPY-FL-triterpene conjugate 24: Yield: 11.4 mg (14% overall yield); dark-red crystalline solid; ¹H NMR (500 MHz, CDCl₃): δ = 7.19 (t, *J* = 5.6 Hz, 1H), 7.09 (s, 1H), 6.87 (d, *J* = 4.0 Hz, 1H), 6.37 (t, *J* = 5.5 Hz, 1H), 6.27 (d, *J* = 4.0 Hz, 1H), 6.11 (s, 1H), 4.73 (d, *J* = 1.5 Hz, 1H; H^{29 *pro-Z*}), 4.60 (s, 1H; H^{29 *pro-E*}), 4.48–4.44 (m, 1H), 4.26–4.24 (m, 2H), 4.01 (s, 2H), 3.69–3.65 (m, 5H), 3.60–3.56 (m, 5H), 3.52–3.47 (m, 5H), 3.43 (t, *J* = 5.6 Hz, 2H), 3.28 (t, *J* = 7.6 Hz, 2H), 3.02–2.97 (m, 1H; H^{19b}), 2.79 (t, *J* = 7.6 Hz, 2H), 2.55 (s, 3H), 2.48 (t, *J* = 6.9 Hz, 2H), 2.25 (s, 3H), 1.68 (s, 3H; CH₃), 1.64–1.15 (m, 23H; overlap with solvent), 0.96 (s, 3H; CH₃), 0.92 (s, 3H; CH₃), 0.83 (s, 3H; CH₃), 0.82

(s, 3H; CH₃), 0.81 ppm (s, 3H; CH₃); ¹³C NMR (101 MHz, CDCl₃): δ = 181.0, 172.9, 172.7, 171.9, 170.5, 160.8, 156.9, 150.6, 144.2, 135.5, 133.4, 128.2, 124.1, 120.8, 116.8, 109.9, 81.4, 71.1, 70.8, 70.4, 70.2, 70.1, 69.1, 63.7, 56.5, 55.6, 50.6, 49.4, 47.1, 42.6, 41.0, 40.9, 39.5, 38.8, 38.5, 38.0, 37.3, 34.4, 33.4, 32.3, 31.1, 30.7, 30.0, 29.9, 28.2, 25.6, 24.1, 23.9, 21.1, 19.6, 18.4, 16.7, 16.4, 16.2, 15.2, 14.9, 11.5 ppm; ¹⁹F {¹H} NMR (471 MHz, CDCl₃): δ = -145.82 (d, *J* = 31.5 Hz), -145.96 ppm (d, *J* = 31.5 Hz); HRMS (ESI): *m/z* calcd for C₅₈H₈₅BF₂N₄O₁₁: 1061.6276 [M-H]⁻; found: 1061.6275; UV/Vis (CH₂Cl₂): λ_{max} = 507 nm; λ_{em} = 513 nm; Φ = 0.20.

BODIPY-FL-triterpene conjugate 25: Yield: 10.0 mg (10% overall yield); dark-red oil; ¹H NMR (500 MHz, CDCl₃): δ = 9.52 (s, 1H; CHO), 7.17 (t, *J* = 5.2 Hz, 1H), 7.09 (s, 1H), 6.88 (d, *J* = 3.9 Hz, 1H), 6.36 (t, *J* = 5.4 Hz, 1H), 6.29–6.26 (m, 2H), 6.12 (s, 1H; H^{29 *pro-Z*}), 5.91 (s, 1H; H^{29 *pro-E*}), 4.47–4.43 (m, 1H), 4.27–4.24 (m, 2H), 4.01 (s, 2H), 3.69–3.64 (m, 5H), 3.61–3.55 (m, 5H), 3.52–3.47 (m, 5H), 3.45–3.43 (m, 2H), 3.29 (t, *J* = 7.6 Hz, 2H), 2.79 (t, *J* = 7.6 Hz, 2H), 2.64 (t, *J* = 6.9 Hz, 2H), 2.55 (s, 3H), 2.48 (t, *J* = 7.0 Hz, 2H), 2.25 (s, 3H), 2.21–2.09 (m, 2H), 2.00–1.95 (m, 2H), 1.73–1.16 (m, 19H; overlap with solvent), 0.93 (s, 3H; CH₃), 0.91 (s, 3H; CH₃), 0.82 (s, 6H, 2×CH₃), 0.81 ppm (s, 3H; CH₃); ¹³C NMR (101 MHz, CDCl₃): δ = 195.2, 180.7, 172.9, 172.7, 171.9, 170.5, 160.8, 156.9, 144.3, 135.5, 133.4, 128.2, 124.1, 120.8, 116.8, 81.4, 71.1, 70.8, 70.4, 70.2, 70.1, 69.1, 63.7, 56.6, 55.6, 50.4, 42.5, 40.8, 39.5, 38.9, 38.4, 38.0, 37.3, 37.1, 34.4, 33.5, 32.1, 31.1, 30.1, 29.8, 28.2, 27.4, 24.1, 23.8, 21.0, 18.3, 16.7, 16.3, 16.2, 15.2, 14.8, 11.5 ppm; ¹⁹F {¹H} NMR (471 MHz, CDCl₃): δ = -145.85 (d, *J* = 31.8 Hz), -145.99 ppm (d, *J* = 31.8 Hz); HRMS (ESI): *m/z* calcd for C₅₈H₈₃BF₂N₄O₁₂: 1075.6069 [M-H]⁻; found: 1075.5985; UV/Vis (CH₂Cl₂): λ_{max} = 507 nm; λ_{em} = 513 nm; Φ = 0.14.

BODIPY-FL-triterpene conjugate 26: Yield: 10.7 mg (15% overall yield); dark-red solid; ¹H NMR (500 MHz, CDCl₃): δ = 7.15 (t, *J* = 4.7 Hz, 1H), 7.09 (s, 1H), 6.88 (d, *J* = 3.9 Hz, 1H), 6.32 (t, *J* = 5.2 Hz, 1H), 6.27 (d, *J* = 4.0 Hz, 1H), 6.12 (s, 1H), 4.50–4.47 (m, 1H), 4.27–4.24 (m, 2H), 4.00 (s, 2H), 3.70–3.65 (m, 5H), 3.69 (s, 3H, COOCH₃), 3.61–3.56 (m, 5H), 3.52–3.48 (m, 5H), 3.45–3.42 (m, 2H), 3.29 (t, *J* = 7.6 Hz, 2H), 3.21–3.17 (m, 1H), 2.79 (t, *J* = 7.6 Hz, 2H), 2.67–2.62 (m, 3H), 2.55 (s, 3H), 2.51–2.46 (m, 3H), 2.25 (s, 3H), 2.14–1.23 (m, 15H; overlap with solvent), 1.21 (d, *J* = 1.2 Hz, 3H; CH₃), 1.20 (d, *J* = 1.3 Hz, 3H; CH₃), 1.02 (s, 3H; CH₃), 0.93 (s, 3H; CH₃), 0.89 (s, 3H; CH₃), 0.83 (s, 3H; CH₃), 0.82 ppm (s, 3H; CH₃); ¹³C NMR (101 MHz, CDCl₃): δ = 207.4, 175.1, 172.9, 172.7, 171.9, 171.8, 170.4, 160.8, 156.9, 145.9, 144.2, 135.5, 133.4, 128.2, 124.1, 120.8, 116.8, 81.2, 71.1, 70.8, 70.4, 70.2, 70.1, 69.1, 63.7, 55.6, 53.2, 52.7, 51.2, 47.8, 45.4, 41.5, 39.5, 38.8, 38.7, 38.0, 37.3, 35.0, 33.9, 33.5, 31.0, 29.9, 29.6, 28.1, 27.8, 25.3, 24.1, 23.8, 21.4, 20.3, 20.2, 18.3, 17.0, 16.8, 16.7, 16.1, 15.2, 14.3, 11.5 ppm; ¹⁹F {¹H} NMR (471 MHz, CDCl₃): δ = -145.71 (d, *J* = 34.5 Hz), -145.85 ppm (d, *J* = 34.5 Hz); HRMS (ESI): *m/z* calcd for C₅₉H₈₅BF₂N₄O₁₂: 1089.6225 [M-H]⁻; found: 1089.6141; UV/Vis (CH₂Cl₂): λ_{max} = 507 nm; λ_{em} = 513 nm; Φ = 0.25.

BODIPY-FL-triterpene conjugate 27: Yield: 10.0 mg (15% overall yield); dark-red solid; ¹H NMR (500 MHz, CDCl₃): δ = 7.17 (t, *J* = 5.3 Hz, 1H), 7.09 (s, 1H), 6.88 (d, *J* = 3.9 Hz, 1H), 6.34 (t, *J* = 5.3 Hz, 1H), 6.27 (d, *J* = 4.0 Hz, 1H), 6.12 (s, 1H), 4.50–4.47 (m, 1H), 4.27–4.24 (m, 2H), 4.01 (s, 2H), 3.72 (s, 3H; COOCH₃), 3.69–3.65 (m, 4H), 3.61–3.56 (m, 4H), 3.53–3.48 (m, 4H), 3.46–3.42 (m, 2H), 3.39–3.33 (m, 1H), 3.31–3.28 (m, 2H), 2.81–2.76 (m, 2H), 2.67–2.64 (m, 2H), 2.56 (s, 3H), 2.51–2.48 (m, 2H), 2.25 (s, 3H), 2.11–1.91 (m, 6H), 1.76–1.32 (m, 14H; overlap with solvent), 1.28 (d, *J* = 6.9 Hz, 3H; CH₃), 1.25 (d, *J* = 6.9 Hz, 3H; CH₃), 1.06 (s, 3H; CH₃), 0.97 (s, 3H; CH₃), 0.91 (s, 3H; CH₃), 0.84 (s, 3H; CH₃), 0.83 ppm (s, 3H; CH₃); ¹³C NMR (101 MHz, CDCl₃): δ = 194.5, 189.5, 176.3, 172.9, 172.1, 171.9, 171.2, 170.6, 168.3, 160.8, 156.8, 150.8, 144.3, 135.5, 133.4, 128.1, 124.1, 120.7, 116.7, 81.3, 81.1, 71.1, 70.8, 70.4, 70.2, 70.0,

69.1, 63.7, 58.6, 55.6, 53.6, 51.0, 46.3, 45.7, 41.7, 39.5, 38.7, 38.0, 37.3, 34.7, 33.4, 31.0, 29.9, 29.5, 29.0, 28.6, 28.1, 27.6, 26.1, 24.0, 23.7, 21.2, 20.0, 18.2, 17.0, 16.9, 16.7, 16.3, 15.1, 11.5 ppm; ^{19}F $\{^1\text{H}\}$ NMR (471 MHz, CDCl_3): $\delta = -145.04$ (d, $J = 34.4$ Hz), -145.18 ppm (d, $J = 34.4$ Hz); HRMS (ESI): m/z calcd for $\text{C}_{59}\text{H}_{83}\text{BF}_2\text{N}_4\text{O}_{13}$: 1103.6018 $[\text{M}-\text{H}]^-$; found: 1103.5925; UV/Vis (CH_2Cl_2): $\lambda_{\text{max}} = 507$ nm; $\lambda_{\text{em}} = 513$ nm; $\Phi = 0.26$.

BODIPY-FL-triterpene conjugate 28: Yield: 21.7 mg (30% overall yield); dark-red solid; ^1H NMR (500 MHz, CDCl_3): $\delta = 8.41$ (d, $J = 2.3$ Hz, 1H; pyrazine), 8.27 (d, $J = 2.4$ Hz, 1H; pyrazine), 7.08 (s, 1H), 7.07–7.04 (m, 1H), 6.87 (d, $J = 4.0$ Hz, 1H), 6.52–6.51 (m, 1H), 6.27 (d, $J = 4.0$ Hz, 1H), 6.11 (s, 1H), 4.75 (d, $J = 1.6$ Hz, 1H; $\text{H}^{29\text{ pro-Z}}$), 4.64 (d, $J = 1.3$ Hz, 1H; $\text{H}^{29\text{ pro-E}}$), 4.59 (d, $J = 15.1$ Hz, 1H; OCH_2CO), 4.53 (d, $J = 15.1$ Hz, 1H; OCH_2CO), 4.26–4.24 (m, 2H), 3.99 (s, 3H), 3.68–3.64 (m, 4H), 3.62–3.61 (m, 2H), 3.58–3.54 (m, 4H), 3.52–3.47 (m, 4H), 3.29 (t, $J = 7.6$ Hz, 2H), 3.09 (d, $J = 16.6$ Hz, 1H; $\text{H}^{1\alpha}$), 2.97 (dd, $J = 11.0, 4.7$ Hz, 1H), 2.79 (t, $J = 7.4$ Hz, 2H), 2.55 (s, 3H), 2.44 (d, $J = 16.6$ Hz, 1H; $\text{H}^{1\beta}$), 2.31–2.26 (m, 2H), 2.25 (s, 3H), 2.00–1.96 (m, 1H), 1.93–1.89 (m, 1H), 1.79–1.74 (m, 1H), 1.70 (s, 3H; CH_3), 1.68–1.32 (m, 13H; overlap with solvent), 1.29 (s, 3H; CH_3), 1.27 (s, 3H; CH_3), 1.01 (s, 3H; CH_3), 0.98 (s, 3H; CH_3), 0.79 ppm (s, 3H; CH_3); ^{13}C NMR (101 MHz, CDCl_3): $\delta = 174.8, 172.6, 170.1, 167.7, 160.8, 159.9, 156.9, 150.9, 150.7, 150.2, 144.2, 142.5, 141.5, 135.5, 133.4, 128.1, 124.0, 120.7, 116.7, 110.2, 71.1, 70.9, 70.4, 70.0, 69.9, 69.1, 63.7, 62.6, 56.8, 53.2, 49.5, 49.0, 48.8, 46.9, 42.7, 40.7, 39.7, 39.0, 38.8, 38.3, 37.1, 37.0, 33.5, 32.1, 31.7, 30.6, 29.9, 25.6, 24.2, 24.1, 21.6, 20.2, 19.6, 16.3, 15.8, 15.1, 14.8, 11.5$ ppm; ^{19}F $\{^1\text{H}\}$ NMR (471 MHz, CDCl_3): $\delta = -145.04$ (d, $J = 31.8$ Hz), -145.18 ppm (d, $J = 31.8$ Hz); HRMS (ESI): m/z calcd for $\text{C}_{58}\text{H}_{81}\text{BF}_2\text{N}_6\text{O}_9$: 1053.6126 $[\text{M}-\text{H}]^-$; found: 1053.6134; UV/Vis (CH_2Cl_2): $\lambda_{\text{max}} = 507$ nm; $\lambda_{\text{em}} = 513$ nm; $\Phi = 0.21$.

BODIPY-FL-triterpene conjugate 29: Yield: 16.7 mg (20% overall yield); dark-red solid; ^1H NMR (500 MHz, CDCl_3): $\delta = 8.46$ (app s, 1H; pyrazine), 8.28 (d, $J = 2.4$ Hz, 1H; pyrazine), 7.08 (s, 1H), 7.07–7.06 (m, 1H), 6.87 (d, $J = 3.9$ Hz, 1H), 6.57 (t, $J = 5.1$ Hz, 1H), 6.27 (d, $J = 4.0$ Hz, 1H), 6.11 (s, 1H), 4.75 (app s, 1H; $\text{H}^{29\text{ pro-Z}}$), 4.64 (app s, 1H; $\text{H}^{29\text{ pro-E}}$), 4.60 (d, $J = 15.1$ Hz, 1H; OCH_2CO), 4.53 (d, $J = 15.1$ Hz, 1H; OCH_2CO), 4.26–4.23 (m, 2H), 4.00 (s, 4H), 3.68–3.46 (m, 24H), 3.28 (t, $J = 7.6$ Hz, 2H), 3.09 (d, $J = 16.7$ Hz, 1H), 3.01–2.96 (m, 1H), 2.79 (t, $J = 7.6$ Hz, 2H), 2.55 (s, 3H), 2.46 (d, $J = 16.7$ Hz, 1H), 2.30–2.27 (m, 2H), 2.25 (s, 3H), 2.00–1.93 (m, 2H), 1.77 (d, $J = 11.5$ Hz, 1H), 1.70 (s, 3H; CH_3), 1.68–1.34 (m, 14H; overlap with solvent), 1.30 (s, 3H; CH_3), 1.28 (s, 3H; CH_3), 1.01 (s, 3H; CH_3), 0.98 (s, 3H; CH_3), 0.80 ppm (s, 3H; CH_3); ^{13}C NMR (101 MHz, CDCl_3): $\delta = 174.8, 172.6, 170.1, 167.7, 160.8, 160.4, 157.1, 156.9, 151.0, 150.2, 144.2, 142.7, 135.5, 133.4, 128.2, 124.1, 120.7, 116.8, 110.2, 71.0, 70.9, 70.4, 70.1, 70.0, 69.0, 63.7, 62.6, 56.8, 53.1, 49.5, 48.9, 48.4, 46.9, 42.7, 40.7, 39.7, 39.0, 38.8, 38.3, 37.1, 37.0, 33.5, 32.2, 31.7, 30.6, 29.9, 25.6, 24.2, 24.1, 22.9, 21.6, 20.2, 19.6, 16.3, 15.8, 15.2, 14.8, 14.3, 11.5$ ppm; ^{19}F $\{^1\text{H}\}$ NMR (471 MHz, CDCl_3): $\delta = -145.85$ (d, $J = 34.2$ Hz), -145.99 ppm (d, $J = 34.2$ Hz); HRMS (ESI): m/z calcd for $\text{C}_{64}\text{H}_{92}\text{BF}_2\text{N}_7\text{O}_{12}$: 1200.6865 $[\text{M}+\text{H}]^+$; found: 1200.6848; UV/Vis (CH_2Cl_2): $\lambda_{\text{max}} = 507$ nm; $\lambda_{\text{em}} = 513$ nm; $\Phi = 0.30$.

BODIPY-FL-triterpene conjugate 30: Yield: 8.5 mg (12% overall yield); dark-red solid; ^1H NMR (500 MHz, CDCl_3): $\delta = 7.09$ (s, 1H), 7.07–7.06 (m, 1H), 6.88 (d, $J = 3.9$ Hz, 1H), 6.50–6.48 (m, 1H), 6.27 (d, $J = 4.0$ Hz, 1H), 6.12 (s, 1H), 4.73 (app s, 1H; $\text{H}^{29\text{ pro-Z}}$), 4.60 (d, $J = 2.0$ Hz, 1H; $\text{H}^{29\text{ pro-E}}$), 4.59 (d, $J = 15.5$ Hz; OCH_2CO), 4.52 (d, $J = 15.1$ Hz, 1H; OCH_2CO), 4.27–4.24 (m, 2H), 3.99 (s, 2H), 3.68–3.63 (m, 4H), 3.62–3.60 (m, 2H), 3.58–3.53 (m, 4H), 3.52–3.47 (m, 4H), 3.29 (t, $J = 7.6$ Hz, 2H), 3.18 (dd, $J = 11.4, 4.8$ Hz, 1H), 2.99–2.94 (m, 1H), 2.79 (t, $J = 7.6$ Hz, 2H), 2.56 (s, 3H), 2.25 (s, 3H), 2.25–2.20 (m, 2H), 1.98–1.86 (m, 3H), 1.68 (s, 3H; CH_3), 1.65–1.15 (m, 19H; overlap with solvent), 0.96 (s, 3H; CH_3), 0.96 (s, 3H; CH_3), 0.90 (s, 3H;

CH_3), 0.81 (s, 3H; CH_3), 0.75 ppm (s, 3H; CH_3); ^{13}C NMR (101 MHz, CDCl_3): $\delta = 174.8, 172.6, 170.1, 167.7, 156.9, 150.3, 144.3, 128.1, 124.1, 120.8, 116.8, 110.1, 79.2, 71.1, 70.9, 70.4, 69.9, 69.1, 63.7, 62.6, 56.8, 55.5, 50.7, 49.6, 47.0, 42.6, 40.9, 39.0, 38.9, 38.8, 38.3, 37.4, 37.1, 34.5, 33.5, 32.2, 30.6, 29.9, 28.2, 27.6, 25.7, 24.1, 21.0, 19.5, 18.5, 16.3, 16.2, 15.5, 15.2, 14.9, 11.5$ ppm; ^{19}F $\{^1\text{H}\}$ NMR (471 MHz, CDCl_3): $\delta = -145.76$ (d, $J = 30.5$ Hz), -145.90 ppm (d, $J = 30.5$ Hz); HRMS (ESI): m/z calcd for $\text{C}_{56}\text{H}_{83}\text{BF}_2\text{N}_4\text{O}_{10}$: 1019.6170 $[\text{M}-\text{H}]^-$; found: 1019.6171; UV/Vis (CH_2Cl_2): $\lambda_{\text{max}} = 507$ nm; $\lambda_{\text{em}} = 513$ nm; $\Phi = 0.17$.

BODIPY-FL-triterpene conjugate 31: Yield: 15.2 mg (21% overall yield); dark-red solid; ^1H NMR (500 MHz, CDCl_3): $\delta = 7.19$ (t, $J = 5.5$ Hz, 1H), 7.09 (s, 1H), 6.88 (d, $J = 4.0$ Hz, 1H), 6.40 (t, $J = 5.2$ Hz, 1H), 6.27 (d, $J = 4.0$ Hz, 1H), 6.12 (s, 1H), 5.67 (app s, 1H; $\text{H}^{29\text{ pro-Z}}$), 5.29 (app s, 1H; $\text{H}^{29\text{ pro-E}}$), 4.27–4.24 (m, 2H), 4.03 (s, 2H), 3.71–3.66 (m, 4H), 3.64–3.50 (m, 10H), 3.29 (t, $J = 7.6$ Hz, 2H), 3.17 (dd, $J = 11.0, 5.1$ Hz, 2H), 2.79 (t, $J = 7.6$ Hz, 2H), 2.55 (s, 3H), 2.25 (s, 3H), 2.22–2.13 (m, 2H), 1.96–1.84 (m, 3H), 1.67–1.34 (m, 15H), 1.25–1.16 (m, 4H), 0.95 (s, 6H; $2 \times \text{CH}_3$), 0.91 (s, 3H; CH_3), 0.80 (s, 3H; CH_3), 0.74 ppm (s, 3H; CH_3); ^{13}C NMR (101 MHz, CDCl_3): $\delta = 179.8, 172.6, 170.7, 169.1, 160.8, 156.9, 150.7, 144.3, 135.5, 133.4, 128.2, 127.9, 127.2, 125.1, 124.1, 120.8, 116.8, 79.1, 71.3, 70.8, 70.7, 70.3, 70.0, 69.1, 63.6, 56.5, 55.5, 50.9, 50.6, 42.6, 40.9, 39.4, 39.0, 38.9, 38.4, 37.4, 36.8, 34.5, 33.5, 32.9, 32.0, 29.8, 28.2, 27.5, 24.1, 21.1, 18.4, 16.3, 16.2, 15.6, 15.2, 14.9, 11.5$ ppm; ^{19}F $\{^1\text{H}\}$ NMR (471 MHz, CDCl_3): $\delta = -145.75$ (d, $J = 35.6$ Hz), -145.97 ppm (d, $J = 35.6$ Hz); HRMS (ESI): m/z calcd for $\text{C}_{54}\text{H}_{79}\text{BF}_2\text{N}_4\text{O}_{10}$: 991.5857 $[\text{M}-\text{H}]^-$; found: 991.5852; UV/Vis (CH_2Cl_2): $\lambda_{\text{max}} = 507$ nm; $\lambda_{\text{em}} = 513$ nm; $\Phi = 0.17$.

BODIPY-FL-triterpene conjugate 32: Yield: 4.5 mg (7% overall yield); dark-red oil; ^1H NMR (500 MHz, CDCl_3): $\delta = 7.17$ (t, $J = 5.3$ Hz, 1H), 7.09 (s, 1H), 6.88 (d, $J = 3.8$ Hz, 1H), 6.33 (t, $J = 5.2$ Hz, 1H), 6.27 (d, $J = 3.8$ Hz, 1H), 6.12 (s, 1H), 4.49–4.45 (m, 1H), 4.27–4.24 (m, 2H), 4.01 (s, 2H), 3.93 (s, 1H), 3.67 (dd, $J = 9.2, 5.3$ Hz, 4H), 3.61–3.56 (m, 4H), 3.53–3.48 (m, 4H), 3.46–3.42 (m, 2H), 3.29 (t, $J = 7.5$ Hz, 2H), 2.79 (t, $J = 7.6$ Hz, 2H), 2.66–2.62 (m, 2H), 2.55 (s, 3H), 2.50–2.47 (m, 2H), 2.25 (s, 3H), 1.85 (d, $J = 13.4$ Hz, 1H), 1.79 (d, $J = 11.1$ Hz, 1H), 1.72–1.18 (m, 24H; overlap with solvent), 1.02 (s, 3H; CH_3), 0.95 (s, 3H; CH_3), 0.90 (s, 3H; CH_3), 0.86 (s, 3H; CH_3), 0.85 (s, 3H; CH_3), 0.83 (s, 3H; CH_3), 0.82 ppm (s, 3H; CH_3); ^{13}C NMR (126 MHz, CDCl_3): $\delta = 180.1, 172.9, 172.6, 171.8, 170.4, 160.8, 156.9, 144.2, 135.5, 133.5, 128.2, 124.1, 120.8, 116.8, 109.9, 86.2, 81.3, 71.1, 70.8, 70.4, 70.2, 70.1, 69.1, 63.7, 55.8, 51.4, 46.9, 46.3, 40.8, 40.1, 39.5, 38.9, 38.8, 38.1, 37.4, 36.2, 33.9, 33.8, 33.5, 32.5, 32.1, 31.1, 30.1, 28.9, 28.1, 28.1, 26.7, 24.2, 24.1, 23.8, 21.1, 18.2, 16.8, 16.7, 15.7, 15.2, 13.8, 11.5$ ppm; ^{19}F $\{^1\text{H}\}$ NMR (471 MHz, CDCl_3): $\delta = -145.31$ (d, $J = 31.8$ Hz), -145.45 ppm (d, $J = 31.8$ Hz); HRMS (ESI): m/z calcd for $\text{C}_{58}\text{H}_{85}\text{BF}_2\text{N}_4\text{O}_{11}$: 1061.6276 $[\text{M}-\text{H}]^-$; found: 1061.6278; UV/Vis (CH_2Cl_2): $\lambda_{\text{max}} = 507$ nm; $\lambda_{\text{em}} = 513$ nm; $\Phi = 0.20$.

BODIPY-FL–2,11-dioxo-6,9,15-trioxa-3,12-diazaheptadecan-17-yl propionate 33: Yield: 2.49 mg (11% overall yield); dark-red crystalline solid; ^1H NMR (500 MHz, CDCl_3): $\delta = 7.18$ (t, $J = 5.5$ Hz, 1H), 7.09 (s, 1H), 6.88 (d, $J = 4.0$ Hz, 1H), 6.29–6.27 (m, 2H), 6.12 (s, 1H), 4.27–4.24 (m, 2H), 4.01 (s, 2H), 3.69–3.66 (m, 4H), 3.61–3.57 (m, 4H), 3.53–3.47 (m, 4H), 3.45–3.41 (m, 2H), 3.29 (t, $J = 7.6$ Hz, 2H), 2.79 (t, $J = 7.4$ Hz, 2H), 2.56 (s, 3H), 2.25 (s, 3H), 1.98 ppm (s, 3H); ^{13}C NMR (126 MHz, CDCl_3): $\delta = 172.7, 170.6, 170.5, 160.9, 156.9, 144.3, 135.5, 133.5, 128.2, 124.1, 120.1, 116.8, 71.2, 70.9, 70.5, 70.3, 70.1, 69.1, 63.7, 39.5, 38.8, 33.5, 24.1, 23.3, 15.2, 11.5$ ppm; ^{19}F $\{^1\text{H}\}$ NMR (471 MHz, CDCl_3): $\delta = -145.64$ (d, $J = 35.6$ Hz), -145.79 ppm (d, $J = 35.6$ Hz); HRMS (ESI): m/z calcd for $\text{C}_{26}\text{H}_{37}\text{BF}_2\text{N}_4\text{O}_9$: 565.2723 $[\text{M}-\text{H}]^-$; found: 565.2736; UV/Vis (CH_2Cl_2): $\lambda_{\text{max}} = 507$ nm; $\lambda_{\text{em}} = 513$ nm; $\Phi = 0.71$.

Acknowledgements

This work was mainly supported by the Czech Science Foundation (15–05620S), microscopy and part of the salaries were paid from the Technology Agency of the Czech Republic (TE01020028), the Czech Ministry of Education, Youth and Sports (Grant Numbers: LO1304, LM2015063) and internal grant of Palacky University IGA_PrF_2017_009, IGA_LF_2017_026, IGA_LF_2017_028.

Keywords: cytotoxicity · dyes/pigments · fluorescence microscopy · solid-phase synthesis · terpenoids

- [1] T. Ueno, T. Nagano, *Nat. Methods* **2011**, *8*, 642–645.
 [2] J. Bañuelos, *Chem. Rec.* **2016**, *16*, 335–348.
 [3] L. D. Lavis, R. T. Raines, *ACS Chem. Biol.* **2008**, *3*, 142–155.
 [4] A. Loudet, K. Burgess, *Chem. Rev.* **2007**, *107*, 4891–4932.
 [5] T. Kowada, H. Maeda, K. Kikuchi, *Chem. Soc. Rev.* **2015**, *44*, 4953–4972.
 [6] M. Vendrell, G. G. Krishna, K. K. Ghosh, D. Zhai, J.-S. Lee, Q. Zhu, Y. H. Yau, S. G. Shochat, H. Kim, J. Chung, Y.-T. Chang, *Chem. Commun.* **2011**, *47*, 8424–8426.
 [7] M. Lumbierres, J. M. Palomo, G. Kragol, S. Roehrs, O. Müller, H. Waldmann, *Chem. Eur. J.* **2005**, *11*, 7405–7415.
 [8] J. Šarek, J. Klinot, P. Džubák, E. Klinotová, V. Nosková, V. Křeček, G. Kořínková, J. O. Thomson, A. Janošťáková, S. Wang, S. Parsons, P. M. Fischer, N. Z. Zhelev, M. Hajdúch, *J. Med. Chem.* **2003**, *46*, 5402–5415.
 [9] J. Sarek, M. Kvasnica, M. Urban, J. Klinot, M. Hajdúch, *Bioorg. Med. Chem. Lett.* **2005**, *15*, 4196–4200.
 [10] M. Urban, J. Sarek, M. Kvasnica, I. Tislerova, M. Hajdúch, *J. Nat. Prod.* **2007**, *70*, 526–532.
 [11] L. Huo, X. Bai, Y. Wang, M. Wang, *Biomed. Pharmacother.* **2017**, *92*, 347–355.
 [12] R. Biswas, J. Chanda, A. Kar, P. K. Mukherjee, *Food Chem.* **2017**, *232*, 689–696.
 [13] A. M. Hansen, A. L. Sewell, R. H. Pedersen, D.-L. Long, N. Gadegaard, R. Marquez, *Tetrahedron* **2013**, *69*, 8527–8533.
 [14] K. Gießler, H. Griesser, D. Göhringer, T. Sabirov, C. Richert, *Eur. J. Org. Chem.* **2010**, 3611–3620.
 [15] E. V. Rumyantsev, S. N. Alyoshin, Y. S. Marfin, *Inorg. Chim. Acta* **2013**, *408*, 181–185.
 [16] M. Soral, J. Hodon, N. J. Dickinson, V. Sidova, S. Gurska, P. Dzubak, M. Hajdúch, J. Sarek, M. Urban, *Bioconjugate Chem.* **2015**, *26*, 2563–2570.
 [17] N. Cankarova, P. Funk, J. Hlavac, M. Soral, *Tetrahedron Lett.* **2011**, *52*, 5782–5788.
 [18] W. Dehaen, A. A. Mashentseva, T. S. Seitembetov, *Molecules* **2011**, *16*, 2443–2466.
 [19] C. Würth, M. Grabolle, J. Pauli, M. Spieles, U. Resch-Genger, *Nat. Protoc.* **2013**, *8*, 1535–1550.
 [20] W. Peng, F. Ding, Y.-T. Jiang, Y.-K. Peng, *J. Agric. Food Chem.* **2014**, *62*, 2271–2283.
 [21] Y. Ye, T. Zhang, H. Yuan, D. Li, H. Lou, P. Fan, *J. Med. Chem.* **2017**, *60*, 6353–6363.
 [22] S. Mitsuda, T. Yokomichi, J. Yokoigawa, T. Kataoka, *FEBS Open Bio* **2014**, *4*, 229–2239.
 [23] L. Borkova, R. Adamek, P. Kalina, P. Drasar, P. Dzubak, S. Gurska, J. Rehulka, M. Hajdúch, M. Urban, J. Sarek, *ChemMedChem* **2017**, *12*, 390–398.
 [24] B. Eignerova, M. Tichy, J. Krasulova, M. Kvasnica, L. Rarova, R. Christova, M. Urban, B. Bednarczyk-Cwynar, M. Hajdúch, J. Sarek, *Eur. J. Med. Chem.* **2017**, *140*, 403–420.

Manuscript received: December 22, 2017

Accepted manuscript online: February 7, 2018

Version of record online: March 12, 2018

Solid-Phase Synthetic Strategies for the Preparation of Purine Derivatives

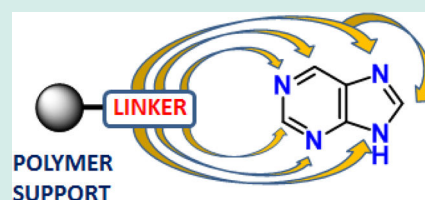
Soňa Krajčovičová[†] and Miroslav Soral^{*,†,‡}

[†]Department of Organic Chemistry, Faculty of Science, Palacký University, 771 46 Olomouc, Czech Republic

[‡]Institute of Molecular and Translation Medicine, Faculty of Medicine and Dentistry, Palacký University, Hněvotínská 5, 779 00, Olomouc, Czech Republic

ABSTRACT: This Review summarizes all of the currently described strategies applicable for the solid-phase synthesis of purine derivatives. The individual approaches are classified according to the immobilization procedure used resulting in a linkage of the final scaffold at various positions.

KEYWORDS: solid-phase synthesis, immobilization, purine, xanthine, combinatorial chemistry



INTRODUCTION

Purine-scaffold-containing compounds belong to the most studied heterocycles in medicinal chemistry and chemical biology. The presence of the purine moiety in the structure of nucleic acids has triggered tremendous amounts of research in the field of modified nucleosides and peptide nucleic acids (PNAs), which have been developed to modify the stability of DNA or RNA duplexes. Except for efforts to incorporate the purine derivatives into the structure of natural biomolecules, the heterocycle was frequently used as the main scaffold for the development of small synthetic molecules to inhibit various targets. In this context, the significance of 2,6,9-trisubstituted purines as the key ligands of numerous kinases should be highlighted.^{1–3} Recently, the research in this area resulted in the discovery of novel, highly potent, and selective anticancer agents.^{3–7}

In the late nineties, Merrifield's polymer-supported chemistry⁸ was fully expanded from the field of peptides and oligonucleotides to the area of small molecules. With respect to its significant advantages, particularly the simple isolation of reaction intermediates and quick production of chemical libraries, the solid-phase synthesis (SPS) of heterocycles was extensively studied. Unsurprisingly, among the diverse heterocycles, the SPS of purine derivatives was also of interest to organic chemists. In the first decade of the new millennium, numerous methods for the preparation/modification of the purine scaffold immobilized on a solid-phase were developed. It was demonstrated that depending on the type of the immobilization strategy, the target purines could be simply diversified at positions 2, 6, 8, and 9 using readily available starting materials. This fact led to the application of combinatorial solid-phase synthesis to produce and study collections of desired compounds, with CDK inhibitor libraries being the well-known examples.^{9–11}

To systematically cover the entire field, this Review summarizes all of the current synthetic strategies for the solid-phase synthesis of purine derivatives. The individual approaches are classified according to the scaffold position in which the target

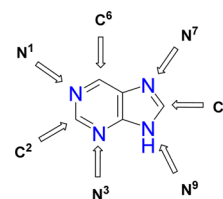


Figure 1. Purine molecular framework and individual positions available for linkage to a solid-phase.

purines were linked to the polymer support (Figure 1). The method of immobilization is the key aspect of solid-phase synthesis because it typically limits the resulting diversification possibilities. Although positions C⁶ and N⁹ have been identified as the most suitable for this purpose,^{10–13} a detailed literature survey revealed that the strategies for immobilization via any other position are available, except for the quaternary carbon atoms C⁴ and C⁵.

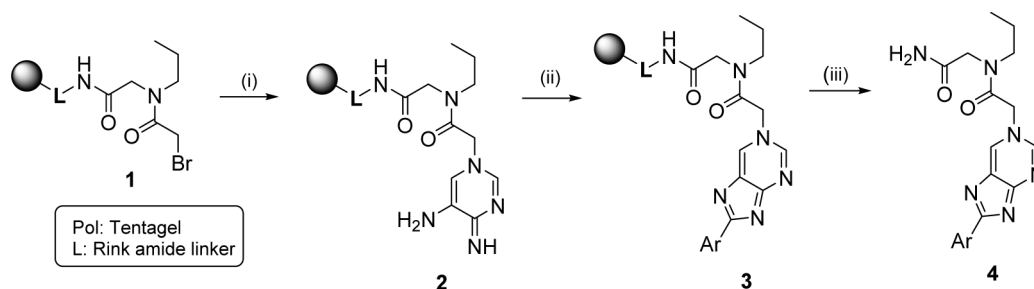
IMMOBILIZATION VIA THE N¹ POSITION

The single contribution dedicated to this area was from Fukase.¹⁴ Although his work was generally targeted to the solid-phase synthesis of benzimidazole libraries from *o*-phenylenediamines, he also reported the application of the method to prepare representative 1,8-disubstituted purines from 2,3-diaminopyrimidine as the key building block (Scheme 1). After selective pyrimidine N¹ alkylation (resin 2), the purine intermediate 3 was obtained by thermal cyclization with aldehydes followed by trifluoroacetic acid (TFA) cleavage to yield the products 4. Except for purines and benzimidazoles, this method was successfully tested to prepare 1/3-deazapurines from the corresponding diaminopyridines. Interestingly, it was reported that

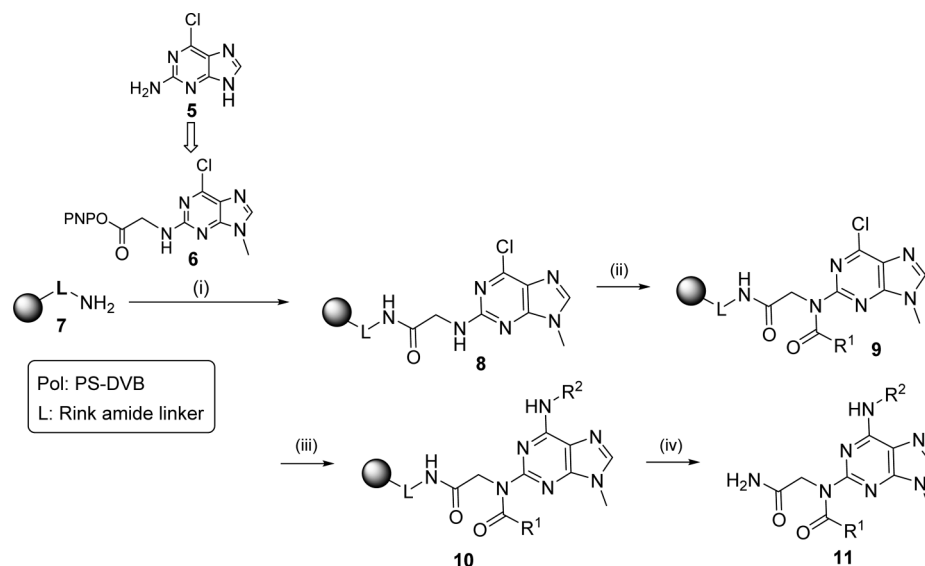
Received: April 27, 2016

Revised: May 24, 2016

Published: June 1, 2016

Scheme 1. Solid-Phase Synthesis of 1,8-Disubstituted Purines^a

^aReagents: (i) 2,3-diaminopyridine, dimethyl sulfoxide (DMSO), rt, 3 h; (ii) ArCHO, pyridine, 50 °C, overnight; (iii) TFA, 30 min, rt.

Scheme 2. Glycinamide-Based Synthesis of 2-(Acylamino)-6-aminopurines^a

^aReagents: (i) *N,N*-diisopropylethylamine (DIEA), *N,N*-dimethylformamide (DMF), 37 °C, 12 h; (ii) R¹COCl, 4-methyl-2,6-di-*tert*-butylpyridine, dichloromethane (DCM), 37 °C, 12 h; (iii) R²NH₂, DMF/DMSO, 4 °C, 16 h; (iv) DCM/TFA/Me₂S, rt, 2 h.

the presence of the peptoid spacer (see resin **1**) was crucial to perform the cyclization step only in the case of purines.

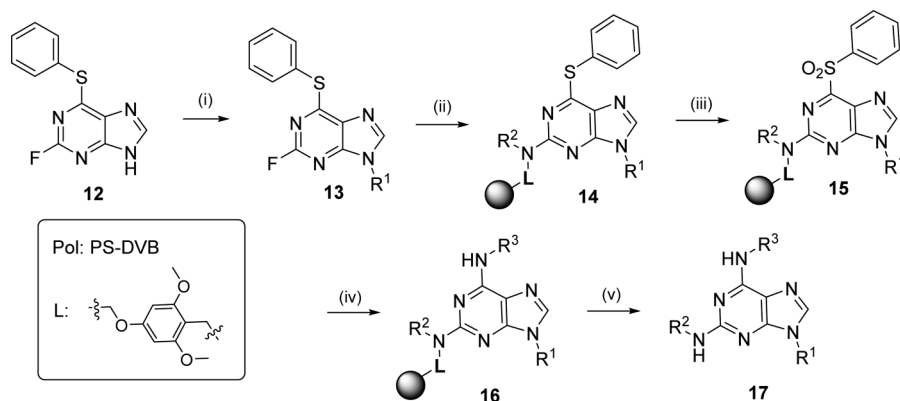
■ IMMOBILIZATION VIA THE C² POSITION

The oldest strategy of this type was developed by Schultz in 1996,¹⁵ and it was based on the solution-phase conversion of 2-amino-6-chloropurine **5** to the purine building block **6** (Scheme 2). After its immobilization on Rink amide resin **7**, the acylation of the intermediate **8** was accomplished followed by the C⁶ amination. The reaction had to be performed at a low temperature to avoid R¹ deacylation. The final acid-mediated cleavage afforded the target derivatives **11**. Compared with synthetic strategies that were introduced later, the disadvantage of this method is the requirement of the solution-phase premodification. Further, the spacer (–CH₂–CONH₂ moiety) becomes the inherent part of the target molecule. However, Schultz's concept was successfully used to synthesize a chemical library of more than 300 chemical entities.

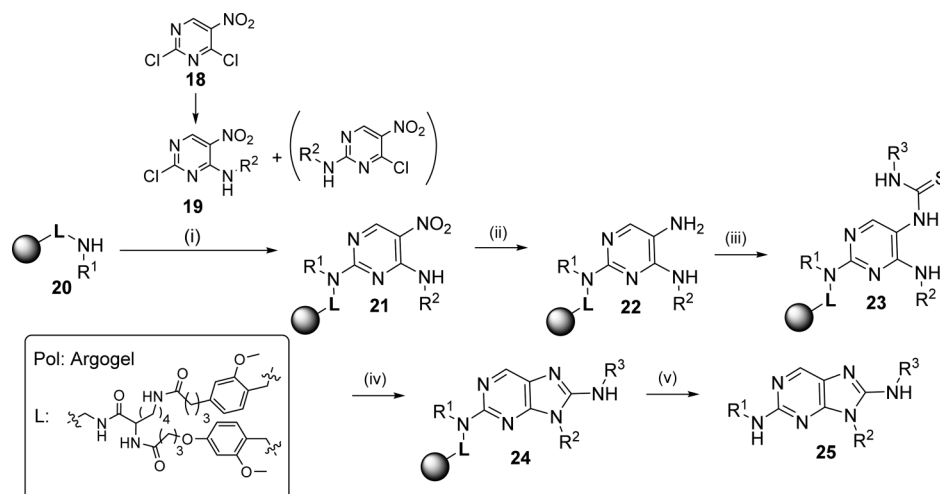
Later, Schultz improved his strategy to prepare 2,6,9-trisubstituted purines in a traceless manner.¹⁶ This approach was based on the amination of the purine C² with polymer-supported amines immobilized on the aldehyde linker (Scheme 3). In solution-phase purine chemistry, 2,6,9-trisubstituted derivatives are typically accessible from 2,6-dihalogenpurines. Similarly, dihalogenpurines were frequently used to prepare 2,6,9-trisubstituted

purines immobilized in the purine C⁶ position (see the Immobilization via C⁶ Position section). However, considering the significantly different reactivities between C² and C⁶, the reaction of 2,6-dihalogenpurines with nucleophiles is always preferentially targeted to the C⁶ position, which makes the strategy unavailable for the purine C² immobilization. Schultz overcame this issue by using N⁹-methyl-2-fluoro-6-phenylsulfenyl purine **12**. Its reaction with polymer-supported amines provided the purine C² immobilized intermediates **14**. The subsequent C⁶ substitution with amines to yield resin **16** was accomplished after the oxidation of sulfide **14** to the sulfone **15**. In this particular case, purine N⁹ modification was performed in the solution phase by the Mitsunobu reaction of **12** with alcohols; the crude purine intermediate **13** was then captured by the resin. In the strategies reported later, the Mitsunobu N⁹ alkylation was typically performed on-resin to avoid the requirement of the solution-phase step.

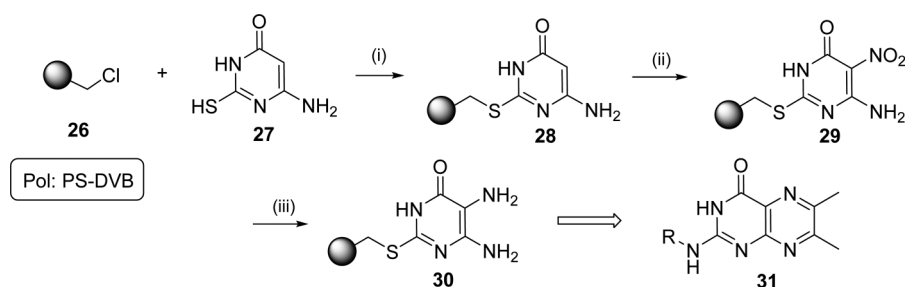
C² immobilization was also described to prepare the purine scaffold by the cyclization of solid-supported pyrimidine derivatives.¹⁷ The nonregioselective amination of the starting 2,4-dichloro-5-nitropyrimidine **18** also required the solution-phase premodification and the separation of the key building block **19** from the mixture of two isomers (Scheme 4). After compound **19** was immobilized on the resin, the reduction of the nitro group was performed using sodium dithionite. It should be

Scheme 3. Traceless Synthesis of 2,6,9-Trisubstituted Purines by Schultz^a

^aReagents: (i) $R^1\text{OH}$, diisopropyl azodicarboxylate (DIAD), PPh_3 , anh. tetrahydrofuran (THF), rt, overnight; (ii) Pol-L-NHR², DIEA, *n*-BuOH, 80 °C, 12 h; (iii) *m*-chloroperbenzoic acid (*m*-CPBA)/NaOH, dioxane/ H_2O , rt, overnight; (iv) $R^3\text{NH}_2$, anh. dioxane, 80 °C, overnight; (v) DCM/TFA/ $\text{Me}_2\text{S}/\text{H}_2\text{O}$ 45:45:5:5.

Scheme 4. Synthesis of 2,8,9-Trisubstituted Purines by Cole^a

^aReagents: (i) DIEA, DMF, 25 °C; (ii) $\text{Na}_2\text{S}_2\text{O}_4$, NH_4OH , *p*-dioxane, H_2O , 25 °C; (iii) R^3NCS , DMF or DCM, 80 °C (conventional heating/MW); (iv) DIC, DMF or EtOH, rt or 80 °C; (v) TFA/MeCN.

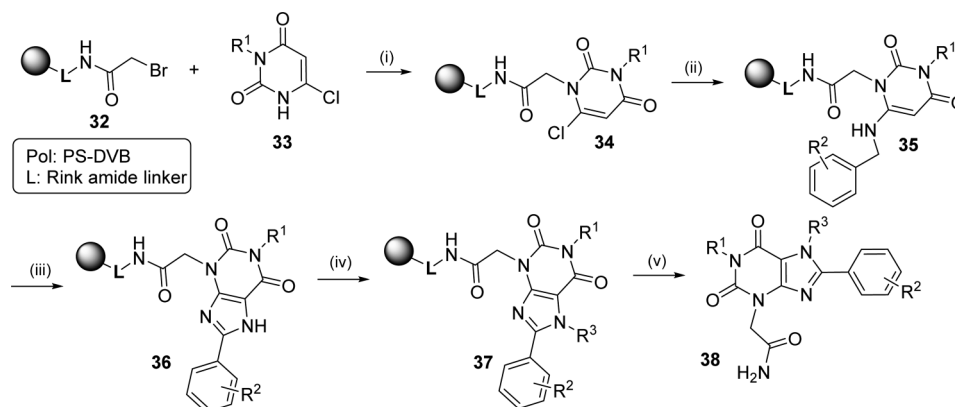
Scheme 5. Strategy for the Possible Preparation of C² Immobilized Purines via a Sulfidic Linkage^a

^aReagents: (i) KI, KOH, DMSO, 80 °C, 2 days; (ii) NaNO_2 , DMF, AcOH, H_2O , rt, 24 h; (iii) NaSH, DMF, H_2O , 40 °C, 20 h.

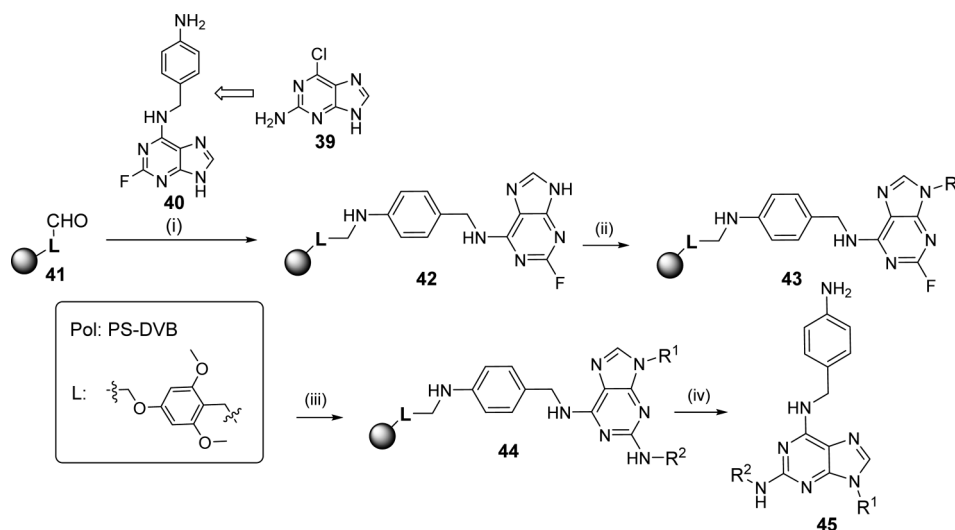
noted that the solid-phase reduction with $\text{Na}_2\text{S}_2\text{O}_4$ is typically performed in a biphasic system of DCM/ H_2O with a phase transfer catalyst;^{18–20} in this particular case, the use of Argogel resin enabled the use of aqueous dioxane. Finally, the purine scaffold was cyclized via the corresponding thioureas **23** to obtain the 8-alkyl/aryl amino substituted purines **25**.

Suckling suggested the solid-phase synthesis of purines and pteridines immobilized via a C² sulfanyl ether linker.²¹ This strategy

was based on the immobilization of 6-amino-2-sulfanylpuridin-4(3H)-one **27** on the chloromethyl resin **26**. The intermediate **28** was then reacted with sodium nitrite followed by reduction with sodium hydrosulfide to obtain the key intermediate **30**. Although authors stated that the method was applicable to the synthesis of purine derivatives, they synthesized these compounds only in the solution-phase by cyclization with orthoformate or cyanogen bromide. Therefore, the sequence depicted in Scheme 5 does not

Scheme 6. Method for N³ Immobilization Applied to the Preparation of Xanthine Derivatives⁴

^aReagents: (i) DMF, trimethylamine (TEA), 60 °C, 2 h; (ii) benzyl amines, DMF, 60 °C, 2 h; (iii) isopentyl nitrite, AcOH, 40 °C, 4 h; (iv) alkyl halogen, TEA, 60 °C, 2.5 h; (v) 95% TFA/DCM, rt, 30 min.

Scheme 7. Solid-Phase Synthesis of 2,9-Disubstituted Purines by Schultz⁴

^aReagents: (i) NaBH(OAc)₃, AcOH, DMF, rt, 12 h; (ii) R¹OH, diethyl azodicarboxylate (DEAD), PPh₃, DCM/THF, rt, 48 h (iii) R²NH₂, *n*-BuOH, DMSO, 100 °C, 48 h; (v) TFA/H₂O/Me₂S 95:5:5, rt, 1 h.

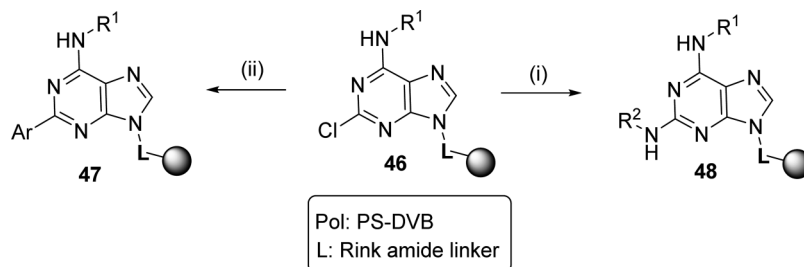
finish with the formation of the purine scaffold, but only pteridine derivative **31** was displayed. After the heterocyclization of intermediate **30**, the products were released from the resin by oxidation with DDQ and the subsequent treatment of the resulting sulfones with primary amines.

■ IMMOBILIZATION VIA THE N³ POSITION

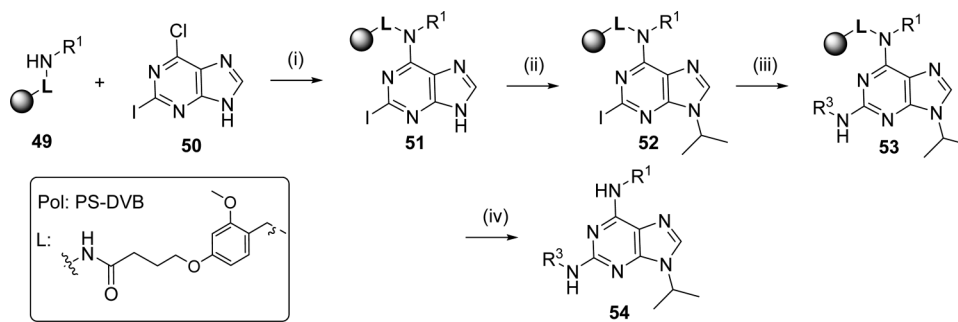
This strategy was initially introduced for 1,3,7,8-tetrasubstituted xanthines.²² Similar to the previously discussed methods, the key building block (6-chloropyrimidine-2,4(1*H*,3*H*)-dione) required premodification prior to its immobilization. After solution-phase N³-alkylation was performed, the intermediate **33** was appended to the Rink amide resin equipped with the bromoacetyl spacer **32** (Scheme 6). The resin **34** was then subjected to nucleophilic substitution with benzyl amines, and after nitrosation of the C⁵ position, the xanthine derivatives **36** were formed spontaneously. The third position of diversity was created via the N⁷ alkylation with alkyl halides. Authors reported the successful application of this method for the preparation of the xanthine library consisting of 90 chemical entities **38**.

■ IMMOBILIZATION VIA THE C⁶ POSITION

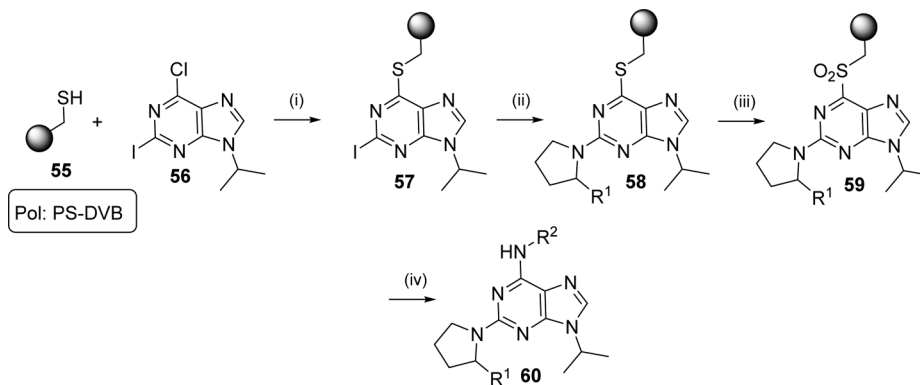
The first solid-phase synthesis of C⁶ immobilized purines was described in 1997 by Schultz.²³ This approach was targeted for the preparation of 2,9-disubstituted purines as potential CDK inhibitors; therefore, benzyl amine was locked in the C⁶ position to mimic the structure of Olomoucine.²⁴ As the key building block, *N*-(4-aminobenzyl)-2-fluoro-9*H*-purin-6-amine **40** was synthesized in solution-phase from 6-chloro-9*H*-purin-2-amine **39** and was reductively alkylated with PAL resin **41** (Scheme 7). The intermediate **42** was then successfully N⁹-alkylated with both primary and secondary alcohols based on the solid-phase Mitsunobu procedure. Then, C² was substituted with various primary amines. Due to the presence of the fluorine atom, the reaction required relatively mild reaction conditions compared to the chloro analogues (see the next paragraph). Subsequent TFA-mediated cleavage afforded the final purine derivatives **45**. Later, Garigipati used a very similar strategy to diversify the C⁶ position. He applied 6-chloro-2-fluoro-9*H*-purine to immobilize the compound via C⁶ based on the reaction with polymer-supported amines. Following the Schultz procedure, he obtained 2,6,9-trisubstituted purines.²⁵

Scheme 8. C² Palladium-Mediated Couplings on Immobilized Purines^a

^aReagents: (i) amine, Pd₂dba₃, P(*t*-Bu)₃, K₃PO₄, DMF, NMP, 100 °C, 48 h; (ii) aryl boronic acid, Pd₂dba₃, P(*t*-Bu)₃, K₃PO₄, DMF, N-methylpyrrolidone (NMP), 100 °C, 48 h.

Scheme 9. Use of 2-Iodopurine Derivative to Perform the C² Substitution^a

^aReagents: (i) DIEA, NMP, 60 °C, 7 h; (ii) isopropanol, DIAD, PPh₃, THF, rt, 24 h; (iii) diethanolamine or propanolamine, 200 °C, MW, NMP, 30 min; (iv) TFA/H₂O 98:2, 60 °C, rt.

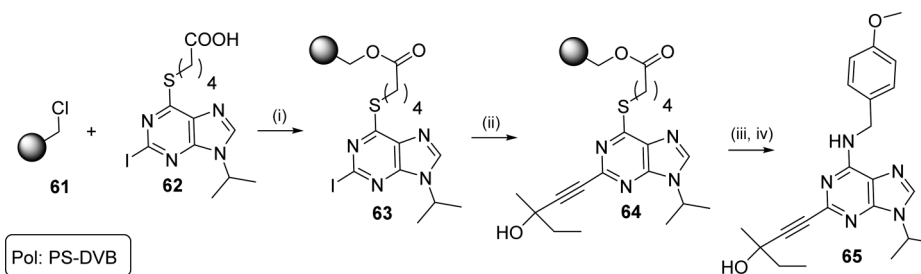
Scheme 10. Purine C⁶ Immobilization by Legerverend Using the Merrifield-SH Resin^a

^aReagents: (i) DMF, KO^tBu, 70 °C; (ii) pyrrolidine or pyrrolidin-2-methanol, tripropylamine (TPA), *N,N*-dimethylacetamide (DMA), 80 °C, 24 h; (iii) *m*-CIPBA, DCM, rt, 24 h; (iv) R²NH₂, THF, 60 °C, 24 h.

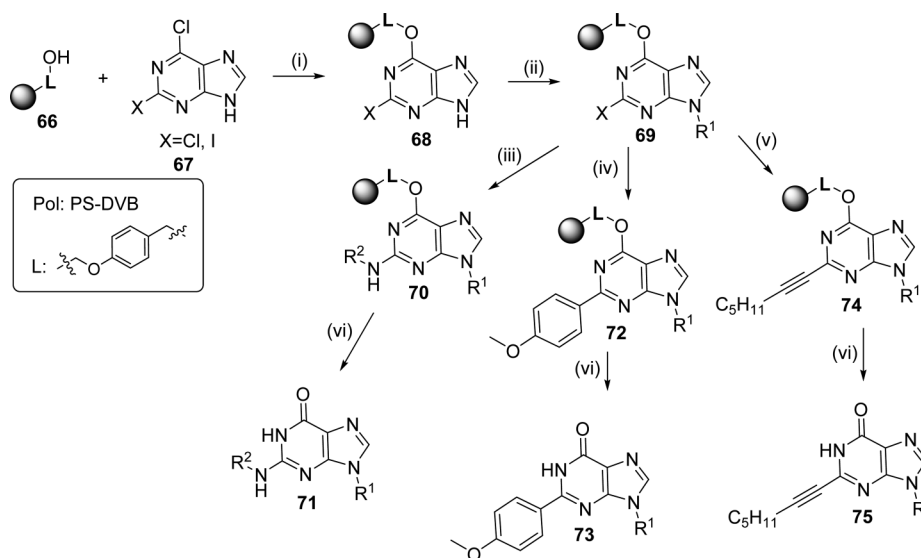
As previously mentioned, the most common starting material for the preparation of 2,6,9-trisubstituted purines is 2,6-dichloropurine. This compound is readily commercially available, and its reactivity in the C⁶ position allows for the regioselective nucleophilic substitution with various reagents, including polymer-supported amines (reaction temperature is typically up to 70 °C). In contrast, it is difficult to accomplish the subsequent substitution of the chlorine in the purine C² position. In the case of reactive nucleophiles (primary aliphatic amines, piperidines, or piperazines), the solid-phase amination can be accomplished using high boiling solvents, for example, DMSO, NMP, or diethylene glycol diethyl ether, at 150–200 °C.^{26,27} To avoid these harsh conditions, an alternative approach was introduced by Brill who studied the possible C² substitution under Pd catalysis.²⁸ He reported that the use of Pd₂dba₃ as the

promoter, P(*t*-Bu)₃ as the coligand and K₃PO₄ as a base furnished the desired products 48 in high yields (70–97%) at temperatures up to 100 °C. The same conditions were tested for Suzuki coupling to introduce an aryl ligand to the C² purine position (purines 47) (Scheme 8). However, both alternatives required relatively long reaction times (≥40 h). The study was performed with both the C⁶ and N⁹ immobilized purines.

To accelerate the C² substitution with amines, Al-Obeidi used the more reactive 6-chloro-2-iodo-9H-purine 50.²⁹ Its immobilization based on the C⁶ substitution with polymer-supported amines 49 and the subsequent Mitsunobu N⁹-alkylation followed by the amination of the C² position under microwave irradiation was studied. Two representative amines were tested (propanolamine and diethanolamine); in both cases, the reaction was completed within 30 min to yield the immobilized products 53.

Scheme 11. Purine C⁶ Solid-Phase Sonogashira Coupling by Legraverend^a

^aReagents: (i) Cs₂CO₃, KI, DMF; (ii) Pd(dppe)Cl₂, CuI, DIEA, 3-methyl-1-pentyn-3-ol, or Herrmann's catalyst, DIEA, 3-methyl-1-pentyn-3-ol, rt, 24 h; (iii) *m*-CPBA, DCM, rt, 24 h; (iv) 4-methoxybenzylamine, THF, 65 °C, 24 h.

Scheme 12. Solid-Phase Synthesis of 6-Oxopurines Reported by Tan^a

^aReagents: (i) DABCO, DMF, rt, 4 h; (ii) R¹OH, DIAD, PPh₃, THF, rt, overnight; (iii) amine, DMA, TPA, 80 °C, 24 h; (iv) alkyne, Pd(dppe)Cl₂, CuI, DIEA, DMA, rt, 48 h; (v) 4-methoxyphenylboronic acid, Pd-PPh₃, K₂CO₃, DMF, 80 °C, 48 h; (vi) 30% TFA/DCM, rt, 5 h.

Authors reported the use of the method for the preparation of a large purine library with crude purities of the compounds greater than 75%.

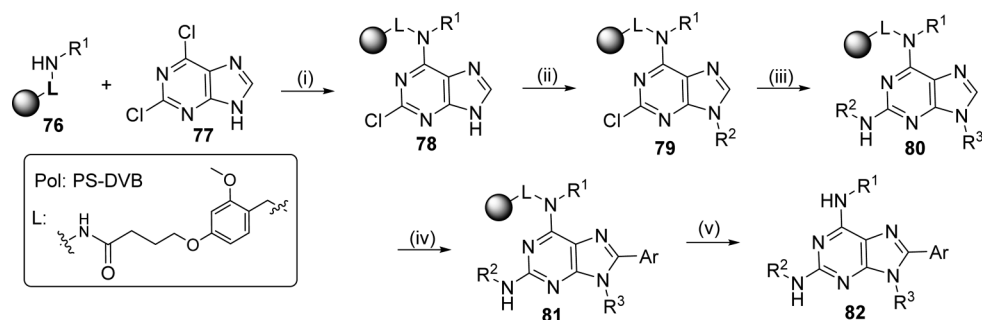
The use of a similar building block but with a different immobilization/cleavage strategy was developed by Legraverend, also in a project aimed at the preparation of a chemical library of new potential kinase inhibitors (Scheme 10).^{30,31} 6-Chloro-2-iodo-9-isopropyl-9H-purine **56** was reacted with Merrifield-SH **55** resin to yield the resin-bound compound **57**. Alternatively, 6-sulfanyl-2-iodo-9-isopropyl-9H-purine was immobilized on Merrifield-Cl resin. Iodine in the C² position was then replaced by the two representative amines (pyrrolidine and pyrrolidin-2-methanol) under conventional heating. Analogous to the Schultz's procedure, the sulfide **58** was oxidized to the corresponding sulfone **59**. The final reaction with amines led to the release of the products **60** from the polymer support.

Later, Legraverend extended his solid-phase purine chemistry to the area of C–C coupling. Similar to Schultz's concept, he managed to introduce aryls to the C² position based on the Suzuki reaction. Further, he accomplished the incorporation of an alkyne moiety via the Sonogashira coupling (Scheme 11).³² The reaction conditions were carefully optimized using 3-methyl-1-pentyn-3-ol as the representative building block. Interestingly, the reaction conditions revealed a strong dependence on the linkage to the resin. In contrast to the previous resin **57**, use of the

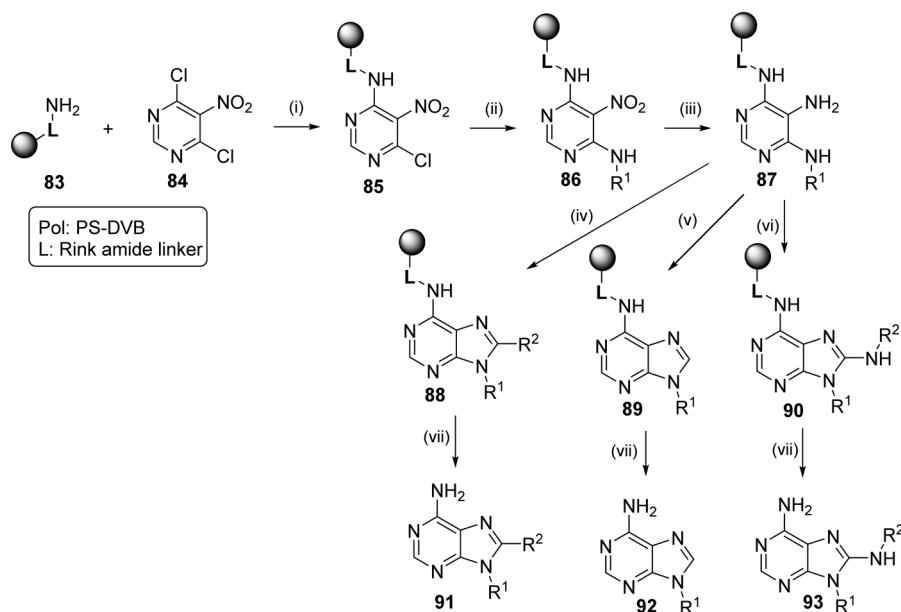
5-thiovaleric spacer (see intermediate **63**) was significantly more beneficial. Two different approaches to perform the Sonogashira coupling were developed based on the use of either Pd(dppe)Cl₂ or Herrmann's catalyst.³³

Amination and Suzuki coupling at the purine C² position were also reported by Tan for the solid-phase synthesis of 6-oxopurines (Scheme 12). Using 1,4-diazabicyclo[2.2.2]octane (DABCO), 6-chloro-2-halogen-9H-purine **67** was immobilized on Wang resin **66** via an ether linkage.³⁴ The subsequent N⁹ regioselective alkylation was performed via the Mitsunobu procedure. In contrast, the alternative alkylation with 1-bromobutane and sodium hydride as a base afforded a mixture of 7- and 9-butyl isomers in a 1:1 ratio. The key intermediates **69** were subjected to Suzuki coupling, Sonogashira coupling or C² amination, and after they were cleaved from the polymer support, the corresponding 6-oxopurines **71**, **73**, and **75** were obtained in a traceless manner.

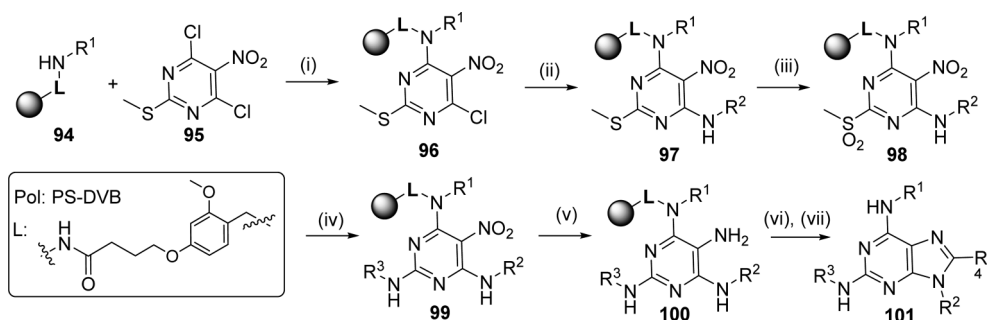
In addition to the C–C coupling in the C² position, modification of the C⁸ position was also described recently.²⁶ The purine scaffold was immobilized via C⁶ by the reaction of 2,6-dichloropurine **77** with polymer-supported secondary amines **76**. Subsequently, the N⁹ position was alkylated using alkyl halide and 1,8-diazabicyclo[5.4.0]undec-7-ene (DBU) (Scheme 13). In contrast to the previously reported N⁷/N⁹ nonregioselective alkylation,³⁴ the pure N⁹ isomers **80** were obtained in this case. After C² amination with piperidine or propanolamine, the direct

Scheme 13. C⁸ Direct Arylation of C⁶ Immobilized Purines^a

^aReagents: (i) DIEA, THF, 50 °C, 14 h; (ii) R²I, DBU, DMSO, 50 °C, 16 h; (iii) amine, diethylene glycol diethyl ether, 150 °C, 14 h; (iv) aryl iodide or aryl bromide, CuI, Pd(OAc)₂, piperidine, anh. DMF, 115 °C, 24 h (aryl iodide) or 48 h (aryl bromide); (v) 50% TFA/DCM, 1 h.

Scheme 14. 6,8,9-Trisubstituted Purines Synthesized by Gilbert from Immobilized Pyrimidines^a

^aReagents: (i) DIEA, DMF, rt, 2 h; (ii) amine, DIEA, DMF, rt, 2 h; (iii) LiAlH₄, AlCl₃, THF, rt, overnight; (iv) aldehyde, DDQ, DMF, rt, 5 h; (v) formamide, 160 °C, overnight; (vi) alkyl isothiocyanate, benzene, reflux then DCC, 80 °C, overnight; (vii) 30% TFA/DCM, rt, 20 min.

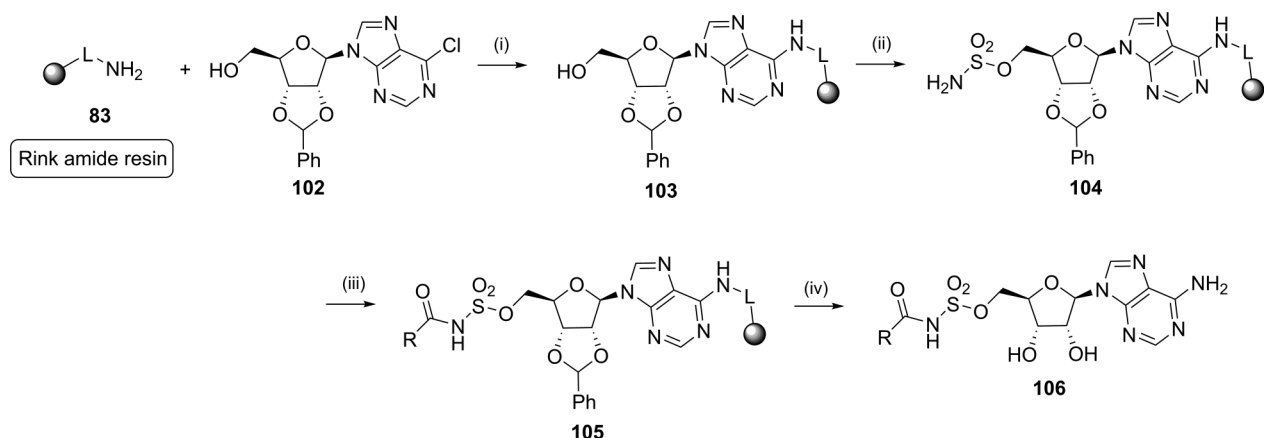
Scheme 15. Solid-Phase Synthesis of 2,6,8,9-Tetrasubstituted Purines by Smith^a

^aReagents: (i) DIEA, THF, rt, 1 h; (ii) R²NH₂, DIEA, THF, rt, 1 h; (iii) oxone, NaHCO₃, MeOH/DCM/H₂O 20:10:1, rt, 24 h; (iv) R³NH₂, DIEA, THF, rt, 1 h; (v) CrCl₂ (15 equiv), 20:1 DMF/MeOH, rt, 4 h; (vi) orthoester, MeSO₃H, 80 °C, 48 h; (vii) 90% TFA/H₂O, rt, 3 h.

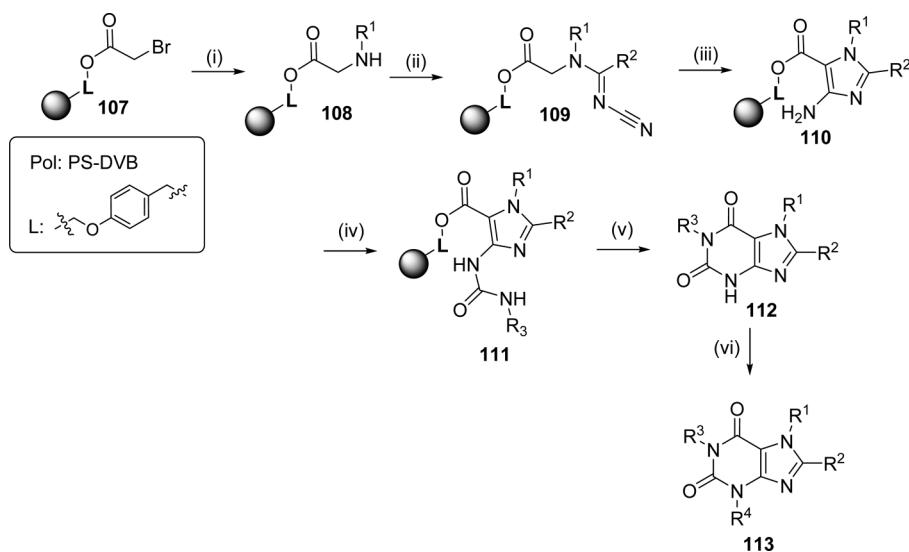
C⁸ arylation with aryl bromides or aryl iodides was tested. In both cases, the desired resin-bound products **81** were obtained under catalysis with CuI and Pd(OAc)₂, with piperidine as the most suitable base. This method was tested for a variety of building blocks and afforded the target compounds **82** in high yields and crude purity. Note that the arylation was generally applicable only

for N⁹-substituted intermediates, whereas 9H-purine analogues displayed a very low conversion.

The incorporation of the new substituent at the purine C⁸ position can be alternatively performed by the cyclization reaction of suitable pyrimidine intermediates. In the case of C⁶ immobilized purines, this strategy was initially described by

Scheme 16. Solid-Phase Synthesis of 5-*O*-[*N*-(Acyl)-sulfamoyl]adenosines^a

^aReagents: (i) DBU, BuOH/DMSO 1:1, MW, 80 °C, 2.5 h; (ii) sulfamoyl chloride, DMAP, DMF, rt, 3 h; (iii) carboxylic acid, DIC, DMAP, DCM, rt, 16 h; (iv) 5% TFA/DCM, rt, 1.5 h, then ammonium formate, 10% Pd/C, MeOH, 60 °C, 16 h.

Scheme 17. Solid-Phase Synthesis of Tetrasubstituted Xanthines by Lam^a

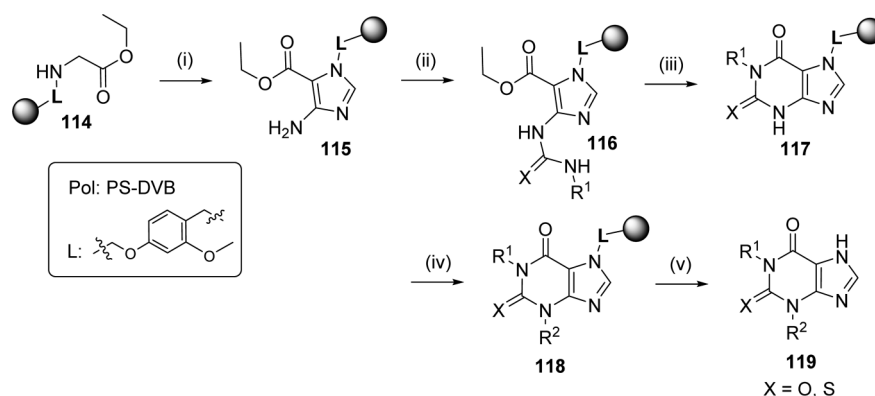
^aReagents: (i) R¹NH₂, THF, rt, 12 h; (ii) NC—N=CR²OEt, DBU, THF, rt, 12 h; (iii) *t*BuOK, *t*BuOH, DMF, rt, 2 h; (iv) R³NCO, xylene, rt, 24 h; (v) NaOEt, THF, MeOH, 90 °C, 2 h; (vi) R⁴X, DIEA, THF, rt, 12 h.

Gilbert,³⁵ who immobilized 4,6-dichloro-5-nitropyrimidine **84** on the Rink amide resin (Scheme 14). After amination of the pyrimidine C⁶ position with the primary amine, the nitro group was reduced with LiAlH₄–AlCl₃. The heterocyclization with aldehydes in the presence of 2,3-dichloro-5,6-dicyano-1,4-benzoquinone (DDQ) was followed by cleavage from the resin to afford C^{8,9}-substituted adenines **91**. Alternatively, C⁸-alkylamino derivatives **93** were obtained via the corresponding thioureas. To access C⁸-unsubstituted purines **92**, the cyclization with formamide was also performed; however, the final compound was obtained in limited yield (7%).

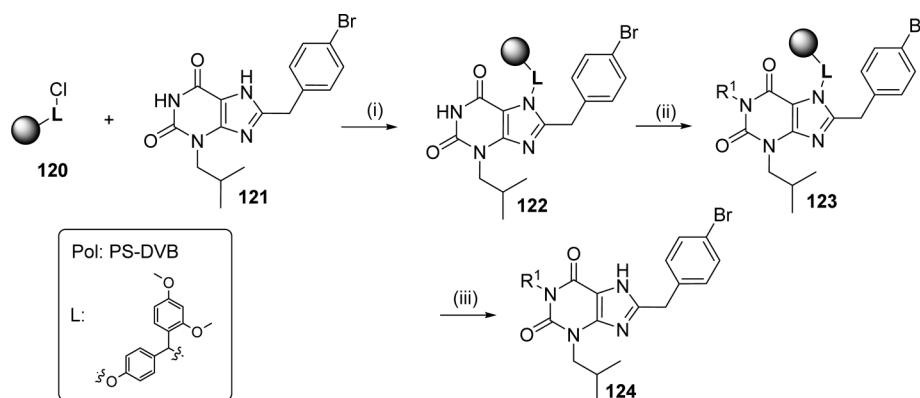
Later, the use of the pyrimidine cyclization approach was significantly improved by Smith who reported a suitable method for the full diversification of the purine scaffold at positions 2, 6, 8, and 9 (Scheme 15).³⁶ The key building block was 4,6-dichloro-2-(methylthio)-5-nitropyrimidine **95**. After its immobilization with polymer-supported amines **94**, the C⁴ amination gave intermediates **97**. To perform the C² amination, sulfidic derivatives were transformed to the corresponding sulfones **98**. In this

case, the previously described method with *m*-chloroperbenzoic acid was not applicable because of the undesired cleavage of the intermediates **98** from the polymer support, but NaHCO₃-buffered oxone was found to be a suitably mild reagent. In the case of the nitro group reduction to yield the pyrimidines **99**, a variety of traditional solid-phase reduction methods failed, presumably due to the presence of three electron-donating alkyl amino groups. However, the intermediates **99** were successfully obtained using the modified Miller's method.³⁷ Then, the purine scaffold **101** was cyclized with various orthoesters under acidic catalysis with methansulfonic acid (MSA).

Purine C⁶ immobilization was also reported in the chemistry of modified nucleosides (Scheme 16).³⁸ 2,3-*O*-Benzylidene-6-chloropurine riboside **102** was attached to the Rink amide resin, and the intermediate **103** was subjected to the sulfamoylation of the hydroxy group. After subsequent acylation of the resulting amino group, the intermediate **105** was cleaved from the resin and was deprotected by the catalytic reduction. The developed solid-phase protocol enabled the parallel, rapid and efficient

Scheme 18. Solid-Phase Synthesis of Disubstituted (Thio)Xanthines by Lam^a

^aReagents: (i) NC—N=CHOEt, DBU, THF 0 °C – rt, 24 h then NaOEt, DMF/EtOH, rt, 24 h; (ii) R³NCO or R³NCS, xylene; rt or 140 °C (for isothiocyanates), 24 h; (iii) NaOEt, reflux, THF, MeOH, 12 h; (iv) R²X, DIEA, DMF, rt, 24 h; (v) 90% TFA/DCM (for xanthines) or 90% TFA/DCM followed by AcOH, reflux (for thioxanthines), 12 h.

Scheme 19. N¹-Diversification of N⁷ Immobilized Xanthine Derivatives^a

^aReagents: (i) DMF, DIEA, rt, 6 h; (ii) R¹OH, dibutyl azodicarboxylate (DBAD), PPh₃, THF, rt, 1 h; (iii) 5% TFA/DCM, rt, 30 min.

synthesis of structurally diverse 5-O-[N-(acyl-sulfamoyl)]-adenosines.

In 2006, Lam reported the solid-phase synthesis of fully substituted xanthines **113** (Scheme 17).³⁹ This method was based on the 3-step synthesis of the imidazole intermediate **110** and its conversion to xanthine products. Prior to the cyclative cleavage, the linear intermediate **111** is attached to the resin via the final xanthine C⁶ position. For this reason, the strategy is included in this chapter, although the xanthine derivative itself is not resin-bound. The last substituent R⁴ was introduced by the alkylation of derivatives **112** after the cleavage step.

■ IMMOBILIZATION VIA THE N⁷ POSITION

A similar approach as that used in the previous case was employed to synthesize disubstituted (thio)xanthines immobilized at the scaffold C⁷ position (Scheme 18).⁴⁰ Instead of a Wang resin, the starting material was attached to a benzaldehyde linker by the reductive amination to give resin **114**. In the case of thioxanthine formation, the lower reactivity of isothiocyanates required harsh conditions and repeating of the reaction to obtain the thioureas **116**. In addition, a double cleavage procedure was required to obtain the final compounds **119** (X = S) in sufficient purity.

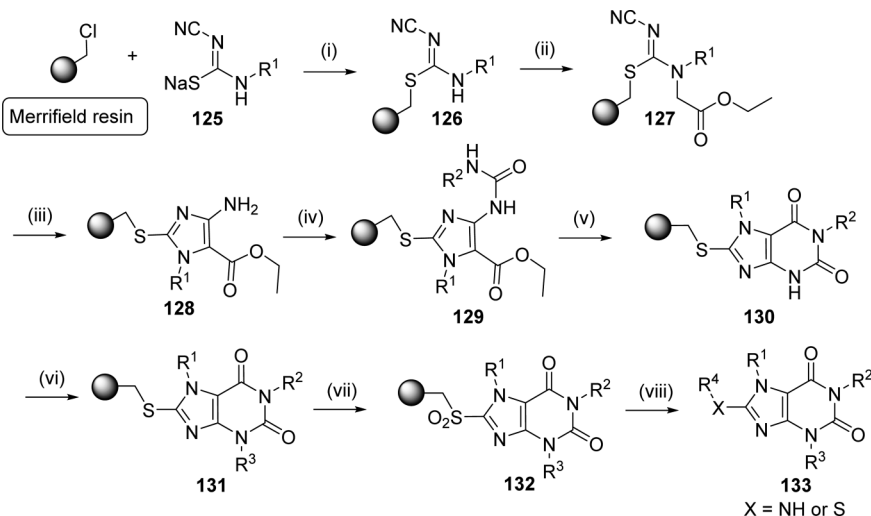
Alternative xanthine N⁷ immobilization was described by Bhalay (Scheme 19).⁴¹ In this case, the xanthine derivatives **121** were immobilized on Rink chloride resin **120**. The goal of the work was diversification of the intermediate at the N¹ position to

produce a chemical library of potential PDE5 inhibitors **124**. The N¹ alkylation was regioselectively performed with a broad range of alcohols by the Mitsunobu reaction without the formation of undesired O-alkylated byproducts.

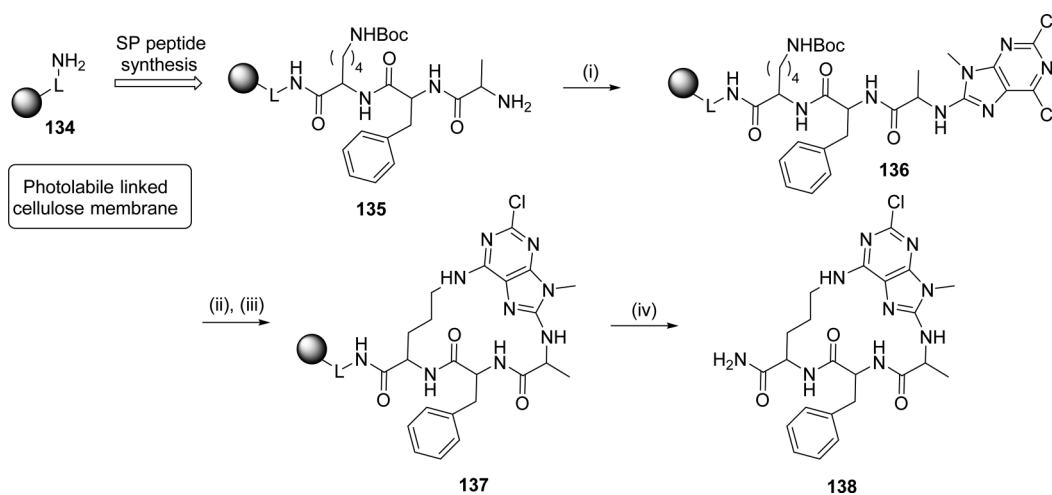
■ IMMOBILIZATION VIA THE C⁸ POSITION

The synthetic method reported earlier for the immobilization of xanthines at the C⁶ and N⁷ positions was applied to prepare derivatives linked to the polymer support at C⁸.⁴² The key imidazole intermediate **126** was attached to the Merrifield resin via the sulfidic linker (Scheme 20). After the xanthine scaffold has been formed, the sulfide **131** was oxidized to sulfone **132**, and the subsequent treatment of the resin with nucleophiles led to the release of the final compounds **133** from the polymer support. In addition to the reaction with amines leading to 8-alkylamino xanthine derivatives, the reaction with thiols was applied to prepare 8-alkylthio analogues. The methodology was successfully tested for 36 diverse products.

Further, C⁸ purine immobilization was applied in the synthesis of cyclic peptidomimetics. 2,6,8-Trichloro-7-methylpurine was used as the ring-closure scaffold to give the cyclic modified peptides of various ring sizes.⁴³ In Scheme 21, an illustrative example is given for the cyclization of tripeptide Lys-Phe-Ala. Note that the arylation of the polymer-supported peptide **135** with 2,6,8-trichloro-7-methylpurine was not regioselective, and the byproduct of the C⁶ substitution was also observed. After the

Scheme 20. Traceless Solid-Phase Synthesis of Tetrasubstituted Xanthenes Immobilized at the C⁸ Position^a

^aReagents: (i) DMF, 60 °C, overnight; (ii) bromo ethyl acetate, K₂CO₃, DMF, 45 °C, overnight; (iii) DBU, acetone, rt, overnight; (iv) R²-NCO, SnCl₂·2H₂O, toluene, 60 °C, overnight; (v) NaOEt, DMF, 60 °C, overnight; (vi) K₂CO₃, DMF, 60 °C, overnight; (vii) *m*-CPBA, DCM, 0 °C–rt, overnight; (viii) R⁴-NH₂, DMSO, MW, 120 °C, 30 min or R⁴-SH, TEA, DCE, 60 °C, overnight.

Scheme 21. SPOT Synthesis of Cyclic Peptidomimetics with the Purine Scaffold^a

^aReagents: (i) 2,6,8-trichloro-7-methylpurine, DCM, rt, 20 min; (ii) 80% TFA/DCM, rt, 1 h; (iii) 20% DIEA/NMP, 3 × 3 min MW; (iv) UV table ($\lambda_{\text{max}} = 365 \text{ nm}$, 7 mW/cm²), 2 h.

protecting group was cleaved, the linear intermediate **136** was intramolecularly C⁶ aminated with the lysine side chain amino group. The ring closure was significantly accelerated by MW heating.

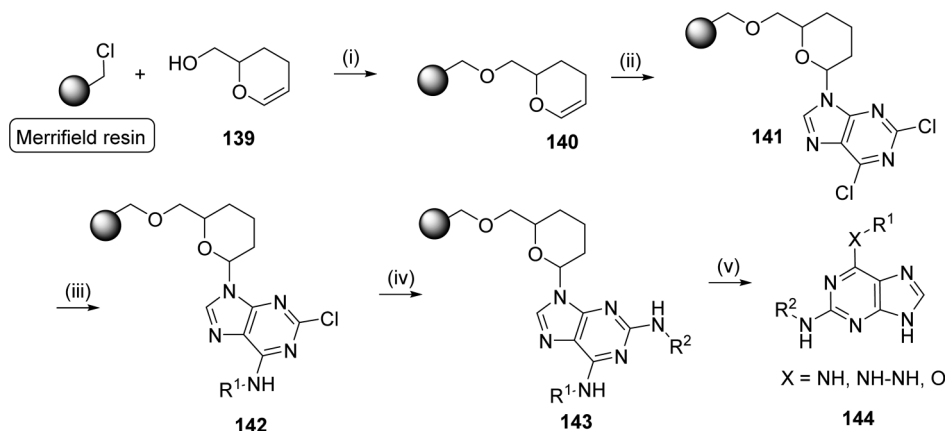
■ IMMOBILIZATION VIA THE N⁹ POSITION

Together with the C⁶ immobilization, the linkage of purine derivatives at the N⁹ position belongs to the most common solid-phase strategies. The purine intermediate can be appended either directly to form the linker-N⁹ bond or another chemical entity can be included as a spacer. One of the oldest concepts was introduced by Nugiel in 1997 based on the application of 2,6-dichloropurine and the tetrahydropyran (THP) resin **140**.⁴⁴ The immobilized 2,6-dichloropurine **141** was then subjected to the sequential C⁶ and C² aminolysis. In the case of C⁶ substitution, the introduction of an alkoxy and an alkylhydrazine substituent was described (Scheme 22). However, the method was limited to the solid-phase synthesis of 2,6-disubstituted

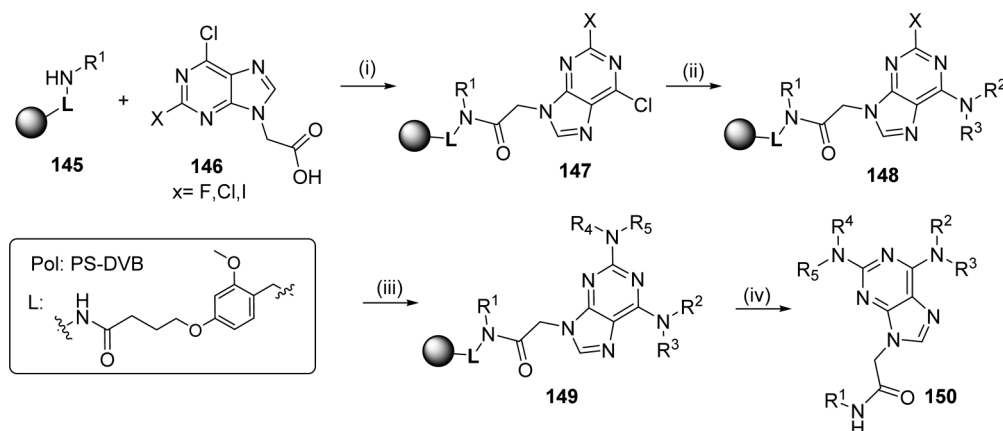
purines **144**, N⁹ alkylation was accessible only after the acid-mediated cleavage from the polymer support. More than seven years after Nugiel's contribution, the same approach was published by Chang.⁴⁵ Later, an alternative vinyl ether linker was introduced by Kim et al.⁴⁶

To diversify the N⁹ position, Al-Obeidi used the modified purine building block, 2-halogen-6-chloropurin-9-yl acetic acid **146**.⁴⁷ After the acylation of polymer-supported amines **145** with the purine building block **146**, both halogens were replaced with amines (Scheme 23). Similar to Schultz's observation, the preferential use of 2-Cl or 2-F derivatives was reported regarding their significantly higher reactivity towards nucleophilic substitution.

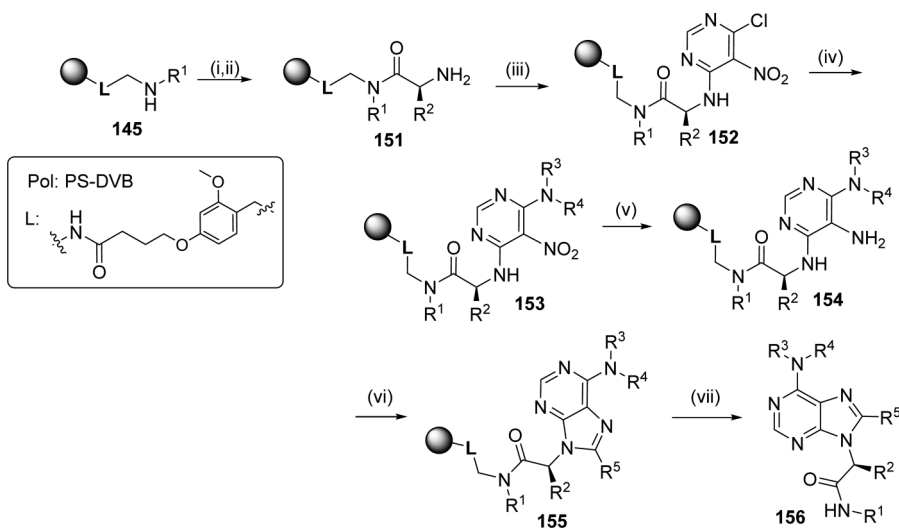
Recently, the method for the preparation of similar derivatives was developed using the pyrimidine intermediates. Polymer-supported α -amino acids **151** were used as the starting material.⁴⁸ The purine scaffold was accessed by the pyrimidine intermediates **154** cyclization with aldehydes (Scheme 24). The cyclization step was significantly accelerated by microwave heating

Scheme 22. Solid-Phase Synthesis of 2,6-Disubstituted Purines Using a THP Linker^a

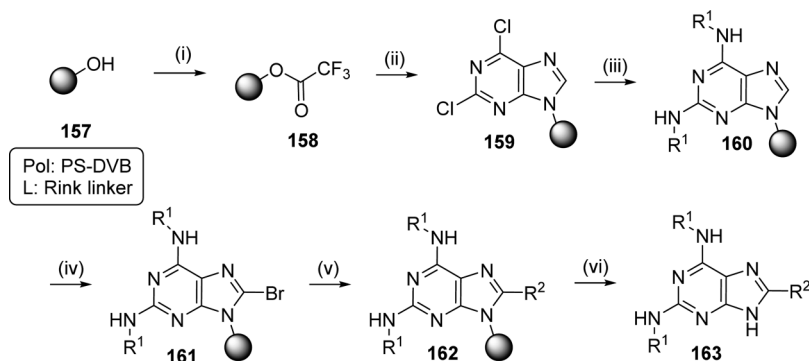
^aReagents: (i) NaH, DMF, 16 h; (ii) 2,6-dichloropurine, CSA, dichloroethane (DCE), 60 °C, 16 h; (iii) R¹NH₂, *n*-BuOH, TEA, 80 °C, 3 h; (iv) R²NH₂, neat, 150 °C, 2.5 h; (v) 20% TFA/DCM, 10 min.

Scheme 23. Solid-Phase Synthesis of 2,6,9-Trisubstituted Purines by Al-Obeidi^a

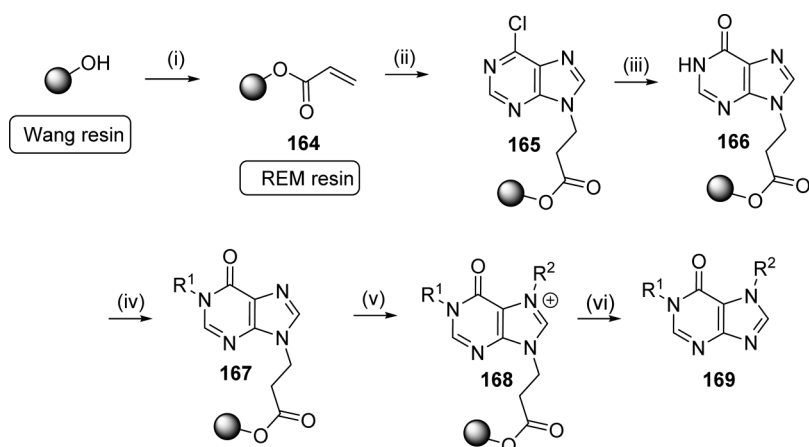
^aReagents: (i) DIC, 1-hydroxy-7-azabenzotriazole (HOAt), DCM, DMF; (ii) R²NHR³, DIEA, NMP, 60 °C or ArNH₂, 120 °C; (iii) R⁴NHR⁵, DIEA, NMP, MW, 150 °C, 1 h; (iv) 95% TFA/H₂O.

Scheme 24. Solid-Phase Synthesis of Purines from Polymer-Supported α -Amino Acids^a

^aReagents: (i) Fmoc-amino acid, HOBT, DIC, DMF, DCM, rt, 16 h; (ii) piperidine, DMF, rt, 30 min; (iii) 4,6-dichloro-5-nitropyrimidine, DIEA, dry DMF, rt, 16 h; (iv) 10% secondary amine in dry DMF, 60 °C, rt, 16 h; (v) Na₂S₂O₄, K₂CO₃, TBAHS, DCM, H₂O, rt, 16 h; (vi) aldehyde, DMSO, 100 °C, conventional heating (72 h) or MW heating (30 min); (vii) 50% TFA/DCM, rt, 2 h.

Scheme 25. C⁸ Pd-Mediated Couplings of N⁹ Immobilized Purines^a

^aReagents: (i) trifluoroacetic acid anhydride (TFAA), 2,6-lutidine; (ii) 2,6-dichloropurine, NMP, 2,6-lutidine; (iii) R¹NH₂, NMP, 125 °C, 60 h; (iv) bromine-2,6-lutidine complex, NMP, 3 h; (v) R²-SnBu₃ or R²-SnMe₃, Pd(OAc)₂, Cu₂O, dppp, NMP, 20 h; (vi) 20% TFA/DCM.

Scheme 26. Solid-Phase Synthesis of N¹,N⁷-Disubstituted Purines^a

^aReagents: (i) acryloyl chloride, DIEA, DCM, rt, 4 h; (ii) 6-chloropurine, DIEA, DMF, rt, 48 h; (iii) formic acid, DMF, 70 °C, 4 h; (iv) R¹Br, DBU, DMF, overnight; (v) alkyl halide, DMF, 50 °C, 24 h; (vi) NH₃, MeOH, DCM, rt, 24 h.

(30 min vs 72 h for conventional heating). In comparison to Al-Obeidi's strategy, two additional diversity positions were obtained (C⁸ substitution and ligand R² originating from the side chain of the natural amino acids). The method was successfully tested for diverse building blocks, and it can be applied to prepare sizable collections of target purines **156**. Additionally, the synthesis proceeded with the full retention of the stereocenter configuration.

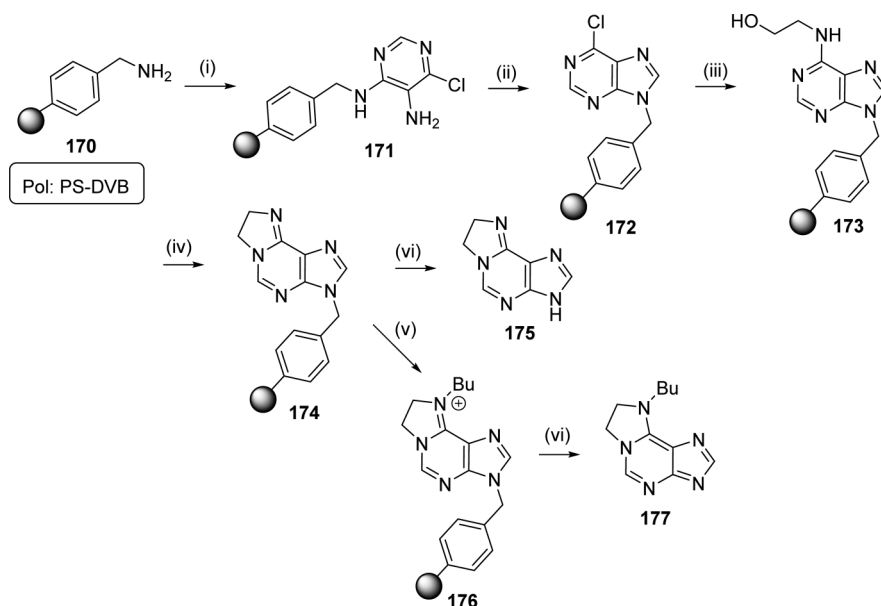
An alternative modification of the C⁸ position at the N⁹ immobilized purines was introduced by Brill. Similar to the direct C⁸ arylation reported earlier in the text (see the chapter devoted to C⁶ immobilization), Brill's method was based on the C–C coupling reaction. For this purpose, he developed a new method for the C⁸ bromination of immobilized purine intermediates **160** using a charge-transfer complex of bromine with lutidine in NMP (Scheme 25).⁴⁸ For the subsequent Suzuki or Stille coupling of the bromoderivative **161**, application of Pd(OAc)₂ and Cu₂O catalysis was identified as the most suitable procedure.⁴⁹ Purines with primary alkylamino substituents at their C² and C⁶ positions gave better coupling results than those bearing secondary amino functions.⁵⁰ Vinyl and alkynyl stannanes gave better results than some aromatic functions, especially pyridyl.

In 2005, Lam described the purine N⁹ immobilization using acrylic REM resin **164**. The goal was to develop the method

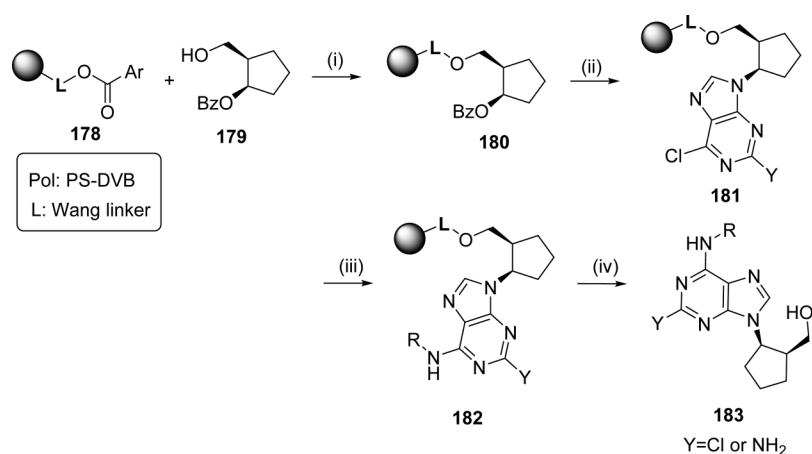
for the alkylation of the purine N⁷ position.⁵¹ In contrast to the frequently reported N⁹ alkylation, the regioselective N⁷ substitution of solid-supported purines was out of the spotlight for a long time. Typically, it was only reported as the side reaction during N⁹ alkylation with alkyl halides. Lam's strategy was based on Michael's addition of 6-chloropurine to REM resin **164** and hydrolysis of the intermediate **165** with formic acid. After subsequent N¹ and N⁷ alkylation, the final intermediate **168** was treated with ammonia to give the purine products **169** in a traceless manner.

Two years later, Lam extended the method to prepare 8-azapurines.⁵² The synthetic strategy applicable for the solid-phase synthesis of condensed purine derivatives (Scheme 27). In this case, the N⁹ immobilized 6-chloropurine intermediate was achieved by the cyclization of the pyrimidine intermediate **171**. After C⁶ substitution with ethanolamine, the alcohol **173** was turned to chloro derivative followed by the intramolecular cyclization to give **174**. Solid-phase synthesis of similar tricyclic purines was later reported by Karskela.⁵³

In the area of solid-phase synthesis of modified nucleosides, the purine N⁹ position is typically attached to the resin via the furanose moiety or its cyclic/uncyclic analog. Crimmins reported the preparation of the purine C⁶-modified carbocyclic nucleosides (Scheme 28).⁵⁴ This approach involves palladium-catalyzed coupling of the resin-bound carbocyclic pseudosugar

Scheme 27. Solid-Phase Synthesis of Condensed Purines^a

^aReagents: (i) 5-amino-4,6-dichloropyrimidine, *n*-BuOH, DMA, DIEA, 140 °C, 24 h; (ii) HC(OCH₃)₃, HCl, DMF, rt, 24 h; (iii) ethanolamine, THF, 60 °C, 4 h; (iv) thionyl chloride, DMF, MW, 180 °C, 20 min; (v) BuI, DMF, 60 °C, 36 h; (vi) toluene, H₂SO₄, rt, 4 h.

Scheme 28. Solid-Phase Synthesis of Carbocyclic Nucleosides^a

^aReagents: (i) DIEA, DMAP, DCM, 40 °C, overnight; (ii) 2,6-dihalogenpurine or 2-amino-6-chloropurine, Pd₂(dba)₃, PPh₃, pempidine (1,2,2,6,6-pentamethylpiperidine), 45 °C, 16 h; (iii) amine, DIEA, *n*-BuOH, 80 °C, 4 h; (iv) 5% TFA/DCM, 1.5 h.

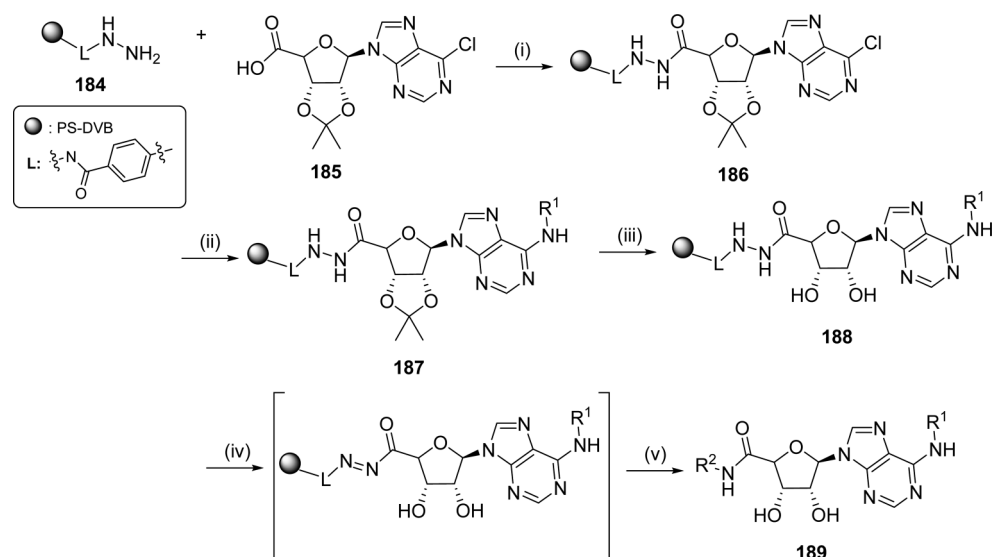
180 with a purine derivative to form the nucleoside resin **181**; this was followed by further functionalization of the purine to afford resin **182**, which upon cleavage from the resin, yielded purine-substituted carbocyclic nucleosides **183**. Alternatively, the purine nucleoside can be linked to the polymer support via the ribose secondary hydroxy groups and subjected to the chemical modification on the solid-phase.⁵⁵

Immobilization of the purine nucleoside **185** via the modified ribose scaffold was also described by Koomen using Kenner's linker or safety-catch arylhydrazide linker **184** (Scheme 29).⁵⁶ The safety-catch concept relies on the fact that the linker is acid and base stable and can be activated under oxidative conditions to generate the reactive acyldiazene. Subsequent attack by a nucleophile releases nitrogen gas and produces carboxylic acids, esters or amides, when water, alcohols or amines are used as nucleophiles. In this case, after C⁶ amination and isopropylidene group removal, the hydrazide linkage of the intermediate **188** was

oxidized to acyldiazene by the method of Lowe and co-workers using copper(II) acetate in the presence of a primary amine. Products **189** were released from the resin as the corresponding carboxamides.

CONCLUSION

The solid-phase synthesis concept offers many different approaches applicable for the preparation of diverse purines from readily available starting materials. As demonstrated, various strategies are available to append the purine scaffold (or its intermediate) at different positions to the resin. Synthetic robustness and variability of the polymer-supported purine chemistry led to the introduction of methodologies applicable for combinatorial solid-phase synthesis of desired compounds.^{56,57} In addition, the described approaches are not limited to the field of purine derivatives. They have been also successfully used for the solid-phase syntheses of purine analogues, such as

Scheme 29. Solid-Phase Synthesis of Modified Purine Nucleosides Using a Safety-Catch Arylhydrazide Linker^a

^aReagents: (i) DIC, DMF, rt, 16 h; (ii) R¹NH₂, NMP, 50 °C, 24 h; (iii) TFA–HO(CH₂)₂OH–DCM, rt, 18 h; (iv) Cu(OAc)₂, R²NH₂, THF, rt, 22 h.

1/3-deazapurines,^{58–60} 7-deazapurines,^{61–63} 9-deazapurines,^{64,65} or thiazolopyrimidines.⁶⁶ With respect to the large biological potential of purine isosters to inhibit various targets,⁶⁷ the development of novel solid-phase strategies for their preparation represents an important aspect for finding new, pharmacologically promising compounds.

AUTHOR INFORMATION

Corresponding Author

*E-mail: soural@orgchem.upol.cz. Phone: +420 5856342196. Fax: +420 585634465.

Notes

The authors declare no competing financial interest.

ACKNOWLEDGMENTS

This project was supported by the Ministry of Education, Youth and Sport of the Czech Republic, by the European Social Fund (project CZ.1.07/2.3.00/20.0009), and internal project of Palacky University Olomouc (IGA-PrF-2016-020). The infrastructure of this project (Institute of Molecular and Translation Medicine) was supported by the National Program of Sustainability (project LO1304).

ABBREVIATIONS

| | |
|-------|---|
| CDK | cyclin-dependent kinase |
| CSA | camphorsulfonic acid |
| DABCO | 1,4-diazabicyclo[2.2.2]octane |
| DBAD | dibutyl azodicarboxylate |
| DBU | 1,8-diazabicyclo[5.4.0]undec-7-ene |
| DCC | <i>N,N'</i> -dicyklohexylcarbodiimide |
| DCE | dichloroethane |
| DCM | dichloromethane |
| DDQ | 2,3-dichloro-5,6-dicyano-1,4-benzoquinone |
| DEAD | diethyl azodicarboxylate |
| DIAD | diisopropyl azodicarboxylate |
| DIC | <i>N,N'</i> -diisopropylcarbodiimide |
| DIEA | <i>N,N</i> -diisopropylethylamine |
| DMAP | 4-dimethylaminopyridine |

| | |
|----------------|------------------------------------|
| DMA | <i>N,N</i> -dimethylacetamide |
| DMF | <i>N,N</i> -dimethylformamide |
| DMSO | dimethyl sulfoxide |
| HOAt | 1-hydroxy-7-azabenzotriazole |
| HOBt | 1-hydroxybenzotriazole |
| <i>m</i> -CPBA | <i>m</i> -chloroperbenzoic acid |
| NMP | <i>N</i> -methylpyrrolidone |
| MSA | methansulfonic acid |
| PNP | <i>p</i> -nitrophenol |
| PS-DVB | polystyrene-divinylbenzene |
| TBAHS | tetrabutylammonium hydrogensulfate |
| TEA | triethylamine |
| TFA | trifluoroacetic acid |
| TFAA | trifluoroacetic acid anhydride |
| THF | tetrahydrofuran |
| THP | tetrahydropyran |
| TPA | tripropylamine |

REFERENCES

- (1) Sharma, S.; Singh, J.; Ojha, R.; Singh, H.; Kaur, M.; Bedi, P. M. S.; Nepali, K. Design strategies, structure activity relationship and mechanistic insights for purines as kinase inhibitors. *Eur. J. Med. Chem.* **2016**, *112*, 298–346.
- (2) Azevedo, W. F.; Leclerc, S.; Meijer, L.; Havlicek, L.; Strnad, M.; Kim, S. H. Inhibition of cyclic-dependent kinases by purine analogues: crystal structure of human cdk2 complexed with roscovitine. *Eur. J. Biochem.* **1997**, *243* (1–2), 518–26.
- (3) Meijer, L.; Borgne, A.; Mulner, O.; Chong, J. P. J.; Blow, J. J.; Inagaki, N.; Inagaki, M.; Delcros, J. G.; Moulinoux, J. P. Biochemical and cellular effects of roscovitine, a potent and selective inhibitor of the cyclin-dependent kinases cdc2, cdk2, and cdk5. *Eur. J. Biochem.* **1997**, *243* (1–2), 527–536.
- (4) Gucky, T.; Jorda, R.; Zatloukal, M.; Bazgier, V.; Berka, K.; Reznickova, E.; Beres, T.; Strnad, M.; Krystof, V. A Novel Series of Highly Potent 2,6,9-Trisubstituted Purine Cyclin-Dependent Kinase Inhibitors. *J. Med. Chem.* **2013**, *56* (15), 6234–6247.
- (5) Haider, Ch.; Grubinger, M.; Reznickova, E.; Weiss, T. S.; Rotheneder, H.; Miklos, W.; Berger, W.; Jorda, R.; Zatloukal, M.; Gucky, T.; Strnad, M.; Krystof, V.; Mikulits, W. Novel Inhibitors of Cyclin-Dependent Kinases Combat Hepatocellular Carcinoma without

Inducing Chemoresistance. *Mol. Cancer Ther.* **2013**, *12* (10), 1947–1957.

(6) Reznickova, E.; Popa, A.; Gucky, T.; Zatloukal, M.; Havlicek, L.; Bazgier, V.; Berka, K.; Jorda, R.; Popa, I.; Nasereddin, A.; Jaffe, Ch. L.; Krystof, V.; Strnad, M. 2,6,9-Trisubstituted purines as CRK3 kinase inhibitors with antileishmanial activity in vitro. *Bioorg. Med. Chem. Lett.* **2015**, *25* (11), 2298–2301.

(7) Zatloukal, M.; Jorda, R.; Gucky, T.; Reznickova, E.; Voller, J.; Pospisil, T.; Malinkova, V.; Adamcova, H.; Krystof, V.; Strnad, M. Synthesis and in vitro biological evaluation of 2,6,9-trisubstituted purines targeting multiple cyclin-dependent kinases. *Eur. J. Med. Chem.* **2013**, *61*, 61–72.

(8) Merrifield, R. B. Solid phase peptide synthesis. I. The synthesis of a tetrapeptide. *J. Am. Chem. Soc.* **1963**, *85* (14), 2149–54.

(9) Lai, J. Y. Q.; Langston, S.; Adams, R.; Beevers, R. E.; Boyce, R.; Burckhardt, S.; Cobb, J.; Ferguson, Y.; Figueroa, E.; Grimster, N.; Henry, A. H.; Khan, N.; Jenkins, K.; Jones, M. W.; Judkins, R.; Major, J.; Masood, A.; Nally, J.; Payne, H.; Payne, L.; Raphy, G.; Raynham, T.; Reader, J.; Reader, V.; Reid, A.; Ruprah, P.; Shaw, M.; Sore, H.; Stirling, M.; Talbot, A.; Taylor, J.; Thompson, S.; Wada, H.; Walker, D. Preparation of kinase-biased compounds in the search for lead inhibitors of kinase targets. *Med. Res. Rev.* **2005**, *25* (3), 310–330.

(10) Chang, Y. T.; Gray, N. S.; Rosania, G. R.; Sutherland, D. P.; Kwon, S.; Norman, T. C.; Sarohia, R.; Leost, M.; Meijer, L.; Schultz, P. G. Synthesis and application of functionally diverse 2,6,9-trisubstituted purine libraries as CDK inhibitors. *Chem. Biol.* **1999**, *6* (6), 361–375.

(11) Brun, V.; Legraverend, M.; Grierson, D. S. Traceless solid-phase synthesis of 2,6,9-trisubstituted purines from resin bound 6-thiopurines. *Tetrahedron* **2002**, *58* (39), 7911–7923.

(12) Gelens, E.; Koot, W. J.; Menge, W. M. P. B.; Ottenheijm, H. C. J.; Timmerman, H. Solid-Phase Synthesis of Heterocyclic Aromates: Applicability towards Combinatorial Chemistry, a Review. *Comb. Chem. High Throughput Screening* **2003**, *6* (1), 79–99.

(13) Bork, J. T.; Lee, J. W.; Chang, Y. T. The Combinatorial Synthesis of Purine, Pyrimidine and Triazine based Libraries. *QSAR Comb. Sci.* **2004**, *23* (4), 245–260.

(14) Akamatsu, H.; Fukase, K.; Kusumoto, S. New Efficient Route for Solid-Phase Synthesis of Benzimidazole Derivatives. *J. Comb. Chem.* **2002**, *4* (5), 475–483.

(15) Norman, T. C.; Gray, N. S.; Koh, J. T.; Schultz, P. G. A Structure-Based Library Approach to Kinase Inhibitors. *J. Am. Chem. Soc.* **1996**, *118* (31), 7430–7431.

(16) Ding, S.; Gray, N. S.; Ding, Q.; Schultz, P. G. A Concise and Traceless Linker Strategy toward Combinatorial Libraries of 2,6,9-Substituted Purines. *J. Org. Chem.* **2001**, *66*, 8273–8276.

(17) Cole, A. G.; Metzger, A.; Ahmed, G.; Brescia, M. R.; Chan, R. J.; Wen, J.; O'Brien, J.; Qin, L. Y.; Henderson, I. Solid-phase synthesis of N-9-substituted 2,8-diaminopurines. *Tetrahedron Lett.* **2006**, *47*, 8897–8900.

(18) Kaplánek, R.; Krchňák, V. Fast and effective reduction of nitroarenes by sodium dithionite under PTC conditions: application in solid-phase synthesis. *Tetrahedron Lett.* **2013**, *54* (21), 2600–2603.

(19) Messina, I.; Popa, I.; Maier, V.; Soral, M. Solid-Phase Synthesis of 5-Noranagrelide derivatives. *ACS Comb. Sci.* **2014**, *16* (1), 33–38.

(20) McMaster, C.; Fülöpová, V.; Popa, I.; Grepl, M.; Soral, M. Solid-Phase Synthesis of Anagrelide Sulfonyl Analogues. *ACS Comb. Sci.* **2014**, *16* (5), 221–224.

(21) Gibson, C. L.; La Rosa, S.; Suckling, C. J. A prototype solid phase synthesis of pteridines and related heterocyclic compounds. *Org. Biomol. Chem.* **2003**, *1*, 1909–1918.

(22) Heizmann, G.; Eberle, A. N. Xanthines as scaffold for molecular diversity. *Mol. Diversity* **1997**, *2* (3), 171–174.

(23) Gray, N. S.; Kwon, S.; Schultz, P. G. Combinatorial synthesis of 2,9-substituted purines. *Tetrahedron Lett.* **1997**, *38* (7), 1161–1164.

(24) Glab, N.; Labidi, B.; Qin, L. X.; Trehin, C.; Bergounioux, C.; Meijer, L. Olomoucine, an inhibitor of the cdc2/cdk2 kinases activity, blocks plant cells at the G1 to S and G2 to M cell cycle transitions. *FEBS Lett.* **1994**, *353* (2), 207–211.

(25) Dorff, P. H.; Garigipati, R. S. Novel solid-phase preparation of 2,6,9-trisubstituted purines for combinatorial library generation. *Tetrahedron Lett.* **2001**, *42* (15), 2771–2773.

(26) Vankova, B.; Krchnak, V.; Soral, M.; Hlavac, J. Direct C-H Arylation of Purine on Solid Phase and Its Use for Chemical Libraries Synthesis. *ACS Comb. Sci.* **2011**, *13* (5), 496–500.

(27) Vankova, B.; Hlavac, J.; Soral, M. Solid-phase Synthesis of Highly Diverse Purine-Hydroxyquinolinone Bisheterocycles. *J. Comb. Chem.* **2010**, *12* (6), 890–894.

(28) Brill, W. K.; Riva-Toniolo, C.; Müller, S. Catalysis of 2- and 6-Substitution Reactions of Purines on Solid Phase. *Synlett* **2001**, *2001* (7), 1097–1100.

(29) Austin, R. E.; Waldraff, Ch.; Al-Obeidi, F. Microwave assisted solid-phase synthesis of trisubstituted 2-(2,6-purin-9-yl)acetamides. *Tetrahedron Lett.* **2005**, *46* (16), 2873–2875.

(30) Brun, V.; Legraverend, M.; Grierson, D. S. Cyclin-dependent kinase (CDK) inhibitors: development of a general strategy for the construction of 2,6,9-trisubstituted purine libraries. Part 2. *Tetrahedron Lett.* **2001**, *42* (46), 8165–8167.

(31) Brun, V.; Legraverend, M.; Grierson, D. S. Cyclin-dependent kinase (CDK) inhibitors: development of a general strategy for the construction of 2,6,9-trisubstituted purine libraries. Part 1. *Tetrahedron Lett.* **2001**, *42* (46), 8161–8164.

(32) Brun, V.; Legraverend, M.; Grierson, D. S. Cyclin-dependent kinase (CDK) inhibitors: development of a general strategy for the construction of 2,6,9-trisubstituted purine libraries. Part 3. *Tetrahedron Lett.* **2001**, *42* (46), 8169–8171.

(33) Herrmann, W. A.; Brossmer, C.; Öfele, K.; Reisinger, C. P.; Priermeier, T.; Beller, M.; Fischer, H. Palladacycles as Structurally Defined Catalysts for the Heck Olefination of Chloro- and Bromoarenes. *Angew. Chem., Int. Ed. Engl.* **1995**, *34*, 1844–1848.

(34) Tan, T.M.Ch.; Yang, F.; Fu, H.; Raghavendra, M. S.; Lam, Y. Traceless Solid-Phase Synthesis and Biological Evaluation of Purine Analogs as Inhibitors of Multidrug Resistance Protein 4. *J. Comb. Chem.* **2007**, *9* (2), 210–218.

(35) Di Lucrezia, R.; Gilbert, I. H.; Floyd, Ch. D. Solid Phase Synthesis of Purines from Pyrimidines. *J. Comb. Chem.* **2000**, *2* (3), 249–253.

(36) Hammarstroem, L. G. J.; Smith, D. B.; Talamas, F. X. Utility of 4,6-dichloro-2-(methylthio)-5-nitropyrimidine. Part 3: Regioselective solid-phase synthesis of a 2,6,8,9-tetrasubstituted purine library. *Tetrahedron Lett.* **2007**, *48* (16), 2823–2827.

(37) Hari, A.; Miller, B. L. A new method for the mild and selective reduction of aryl nitro groups on solid support. *Tetrahedron Lett.* **1999**, *40*, 245.

(38) Redwan, I. N.; Ingemyr, H. J.; Ljungdahl, T.; Lawson, Ch. P.; Grotli, M. Solid-Phase Synthesis of 5'-O-[N-(Acyl)sulfamoyl]-adenosine Derivatives. *Eur. J. Org. Chem.* **2012**, *2012* (19), 3665–3669.

(39) He, R.; Ching, S. M.; Lam, Y. Traceless Solid-Phase Synthesis of Substituted Xanthines. *J. Comb. Chem.* **2006**, *8* (6), 923–928.

(40) He, R.; Lam, Y. A Highly Efficient Solid-Phase Synthesis of 1,3-Substituted Xanthines. *J. Comb. Chem.* **2005**, *7* (6), 916–920.

(41) Beer, D.; Bhalay, G.; Dunstan, A.; Glen, A.; Habertuer, S.; Moser, H. A Solid-Phase Approach Towards the Synthesis of PDES Inhibitors. *Bioorg. Med. Chem. Lett.* **2002**, *12* (15), 1973–1976.

(42) Lee, D.; Lee, S.; Liu, K.-H.; Bae, J.-S.; Baek, D. J.; Lee, T. Solid-Phase Synthesis of 1,3,7,8-Tetrasubstituted Xanthine Derivatives on Traceless Solid Support. *ACS Comb. Sci.* **2016**, *18* (1), 70–74.

(43) Scharn, D.; Germeroth, L.; Schneider-Mergener, J.; Wenschuh, H. Sequential Nucleophilic Substitution on Halogenated Triazines, Pyrimidines, and Purines: A Novel Approach to Cyclic Peptidomimetics. *J. Org. Chem.* **2001**, *66* (2), 507–513.

(44) Nugiel, D. A.; Cornelius, L. A. M.; Corbett, J. W. Facile Preparation of 2,6-Disubstituted Purines Using Solid-Phase Chemistry. *J. Org. Chem.* **1997**, *62* (1), 201–203.

(45) Chang, J.; Dong, Ch.; Guo, X.; Hu, W.; Cheng, S.; Wang, Q.; Chen, R. A solid-phase approach to novel purine and nucleoside analogs. *Bioorg. Med. Chem.* **2005**, *13* (15), 4760–4766.

- (46) Yoo, S.; Gong, Y. D.; Choi, M. Y.; Seo, J.; Yang Yi, K. A new vinyl ether type linker for solid-phase synthesis. *Tetrahedron Lett.* **2000**, *41* (33), 6415–6418.
- (47) Al-Obeidi, F.; Austin, R. E.; Okonya, J. F.; Bond, D. R. S. Microwave-assisted solid-phase synthesis (MASS) of 2,6,9-trisubstituted purines. *Mini-Rev. Med. Chem.* **2003**, *3* (5), 449–460.
- (48) Vanda, D.; Jorda, R.; Lemrová, B.; Volná, T.; Kryštof, V.; McMaster, C.; Soural, M. Synthesis of novel N⁹-substituted purine derivatives from polymer supported α -amino acids. *ACS Comb. Sci.* **2015**, *17* (7), 426–432.
- (49) Brill, W. K.D.; Riva-Toniolo, C. The bromination of purines with a charge transfer complex between bromine and lutidine. *Tetrahedron Lett.* **2001**, *42* (36), 6279–6282.
- (50) Brill, W. K.D.; Riva-Toniolo, C. Solid-phase synthesis of 2,6,8-trisubstituted purines. *Tetrahedron Lett.* **2001**, *42* (37), 6515–6518.
- (51) Fu, H.; Tan, M. K. Ch.; Lam, Y. Regiospecific Solid-Phase Strategy to N7-Substituted Purines and Its Application to 8-Azapurines and [i]-Condensed Purines. *J. Comb. Chem.* **2007**, *9* (5), 804–810.
- (52) Fu, H.; Lam, Y. Traceless Solid-Phase Synthesis of N1,N7-Disubstituted Purines. *J. Comb. Chem.* **2005**, *7*, 734–738.
- (53) Karskela, T.; Loennberg, H. Solid-phase synthesis of 7-substituted 3*H*-imidazo[2,1-*i*]purines. *Org. Biomol. Chem.* **2006**, *4* (24), 4506–4513.
- (54) Crimmins, M. T.; Zuercher, W. J. Solid-Phase Synthesis of Carbocyclic Nucleosides. *Org. Lett.* **2000**, *2* (8), 1065–1067.
- (55) Epple, R.; Kudirka, R.; Greenberg, W. A. Solid-Phase Synthesis of Nucleoside Analogues. *J. Comb. Chem.* **2003**, *5*, 292–310.
- (56) Rodenko, B.; Detz, R. J.; Pinas, V. A.; Lambertucci, C.; Brun, R.; Wanner, M. J.; Koomen, G.-J. Solid phase synthesis and antiprotozoal evaluation of di- and trisubstituted 50-carboxamidoadenosine analogues. *Bioorg. Med. Chem.* **2006**, *14* (5), 1618–1629.
- (57) Ding, S.; Gray, N. S.; Wu, Xu; Ding, Q.; Schultz, P. G. A Combinatorial Scaffold Approach toward Kinase-Directed Heterocycle Libraries. *J. Am. Chem. Soc.* **2002**, *124* (8), 1594–1596.
- (58) Lemrová, B.; Smyslová, P.; Popa, I.; Oždian, T.; Zajdel, P.; Soural, M. Directed Solid-Phase Synthesis of Trisubstituted Imidazopyridines and Imidazopyridines. *ACS Comb. Sci.* **2014**, *16* (10), 558–565.
- (59) Ermann, M.; Simkovsky, N. M.; Roberts, S. M.; Parry, D. M.; Baxter, A. D. Solid-Phase Synthesis of Imidazo[4,5-*b*]pyridin-2-ones and Related Urea Derivatives by Cyclative Cleavage of a Carbamate Linkage. *J. Comb. Chem.* **2002**, *4* (4), 352–358.
- (60) Cheng, C. C.; Shipps, G. W.; Yang, Z.; Sun, B.; Kawahata, N.; Soucy, K. A.; Soriano, A.; Orth, P.; Xiao, L.; Mann, P.; Black, T. Discovery and optimization of antibacterial AccC inhibitors. *Bioorg. Med. Chem. Lett.* **2009**, *19* (23), 6507–6514.
- (61) Seela, F.; Sirivolu, V. R. Pyrrolo-dC oligonucleotides bearing alkynyl side chains with terminal triple bonds: synthesis, base pairing and fluorescent dye conjugates prepared by the azide–alkyne “click” reaction. *Org. Biomol. Chem.* **2008**, *6* (9), 1674–1687.
- (62) Lee, J. H.; Lim, H.-S. Solid-phase synthesis of tetrasubstituted pyrrolo[2,3-*d*]pyrimidines. *Org. Biomol. Chem.* **2012**, *10* (21), 4229–4235.
- (63) Lee, J. H.; Zhang, Q.; Jo, S.; Chai, S. C.; Oh, M.; Im, W.; Lu, H.; Lim, H.-S. Novel Pyrrolopyrimidine-Based α -Helix Mimetics: Cell-Permeable Inhibitors of Protein-Protein Interactions. *J. Am. Chem. Soc.* **2011**, *133* (4), 676–679.
- (64) Rombouts, F. J. R.; Fridkin, G.; Lubell, W. D. Deazapurine Solid-Phase Synthesis: Construction of 3-Substituted Pyrrolo[3,2-*d*]pyrimidine-6-carboxylates on Cross-Linked Polystyrene Bearing a Cysteamine Linker. *J. Comb. Chem.* **2005**, *7* (4), 589–598.
- (65) Fridkin, G.; Lubell, W. D. Deazapurine Solid-Phase Synthesis: Combinatorial Synthesis of a Library of N3,N5,C6-Trisubstituted Pyrrolo[3,2-*d*]pyrimidine Derivatives on Cross-Linked Polystyrene Bearing a Cysteamine Linker. *J. Comb. Chem.* **2005**, *7* (6), 977–986.
- (66) Lee, T.; Park, J.-H.; Lee, D.-H.; Gong, Y.-D. Traceless Solid-Phase Synthesis of 2,4,6-Trisubstituted Thiazolo[4,5-*d*]pyrimidine-5,7-dione Derivatives. *J. Comb. Chem.* **2009**, *11* (3), 495–499.
- (67) Jorda, R.; Paruch, K.; Krystof, V. Cyclin-dependent kinase inhibitors inspired by roscovitine: purine bioisosteres. *Curr. Pharm. Des.* **2012**, *18* (20), 2974–2980.



Department of Organic
Chemistry



Palacký University
Olomouc

PALACKÝ UNIVERSITY

Olomouc

Faculty of Science
Department of Organic Chemistry

High-throughput conjugation of drug-like molecules for chemical biology

Summary of the Ph.D. Thesis

Mgr. Soňa Krajčovičová

Supervisor: doc. RNDr. Miroslav Sural, PhD.

Academic Year: 2018/2019

This Ph.D. thesis was elaborated within the framework of the Ph.D. within the framework of the Ph.D. study program P1417 Chemistry, field of study Organic Chemistry, guaranteed by the Department of Organic Chemistry, Faculty of Science, Palacký University, Olomouc in the years 2015 – 2019.

Author: Mgr. Soňa Krajčovičová
Faculty of Science, Palacký University
Department of Organic Chemistry
Olomouc

Supervisor: Doc. RNDr. Miroslav Sural, PhD.
Faculty of Science, Palacký University
Department of Organic Chemistry
Olomouc

Referees: Mgr. Jakub Švenda, Ph.D.
Faculty of Science, Masaryk University
Department of Chemistry
Brno

RNDr. Radim Nencka, Ph.D.
Institute of Organic Chemistry and Biochemistry
Prague

The oral defense will take place on in front of the committee for defense of the doctoral thesis at the Department of Organic Chemistry, Faculty of Science, Palacký University, Olomouc. At the same place is the thesis available since 26.6.2019.

I declare hereby with my signature, that this abovementioned thesis is my own original work. Furthermore, I confirm that I have clearly referenced in accordance with departmental requirements.

26.6.2019, Olomouc

.....

Mgr. Soňa Krajčovičová

Abstract

Chemical biology is considered to be one of the most progressive interdisciplinary fields in modern science, since it combines the application of chemical and biological techniques to prepare (or structurally modify) small molecules and determine their behavior in various biological systems. However, it is questionable, if synthesis of small, potentially interesting compounds, is the only way how to find suitable biologically useful probes. In this regard, conjugation can significantly improve pharmacological properties of small drug-like molecules to obtain more selective ligands of certain biological targets. As examples of biologically useful probes could be considered:

- small molecule drug candidates conjugated with vitamin folic acid whose folate receptor is overexpressed in various cancer cells and thus is used as a “Trojan horse” for selective delivery of potent compounds
- heterobifunctional proteolysis-targeting chimeras (PROTAC) conjugates with thalidomide moiety that can bind two specific proteins with subsequent targeted degradation
- conjugates of compounds of interests with fluorescent dye for further visualization of molecules in cells using a fluorescent microscopy

My thesis is therefore devoted to the synthetic strategy and consecutive applicability of our recently developed high-throughput concept of preloaded resins for preparation of probes for chemical biology with minimum *hands-on-time*, applied in the field of cytotoxic triterpenes (as fluorescently labeled conjugates) and protein kinases inhibitors (as PROTAC conjugates) and to the applicability of the stepwise synthetic approach in the preparation of target purine CDK inhibitors conjugated with folic acid.

Abstrakt

Chemická biologie je považována za jednu z nejvíce progresivních, mezioborových oblastí moderní vědy, protože kombinuje chemické a biologické principy a techniky na přípravu a modifikaci malých molekul pro aplikaci v biologických systémech. Nicméně zůstává otázkou, jestli syntéza malých organických molekul s potenciální biologickou aktivitou je jedinou cestou, jak najít nové a medicínálně využitelné sondy. Z tohoto důvodu může být spojení vícero malých, aktivních molekul výhodou a může vést k přípravě více selektivních ligandů se zlepšenými farmakologickým profilem. Jako příklad těchto sond můžeme považovat:

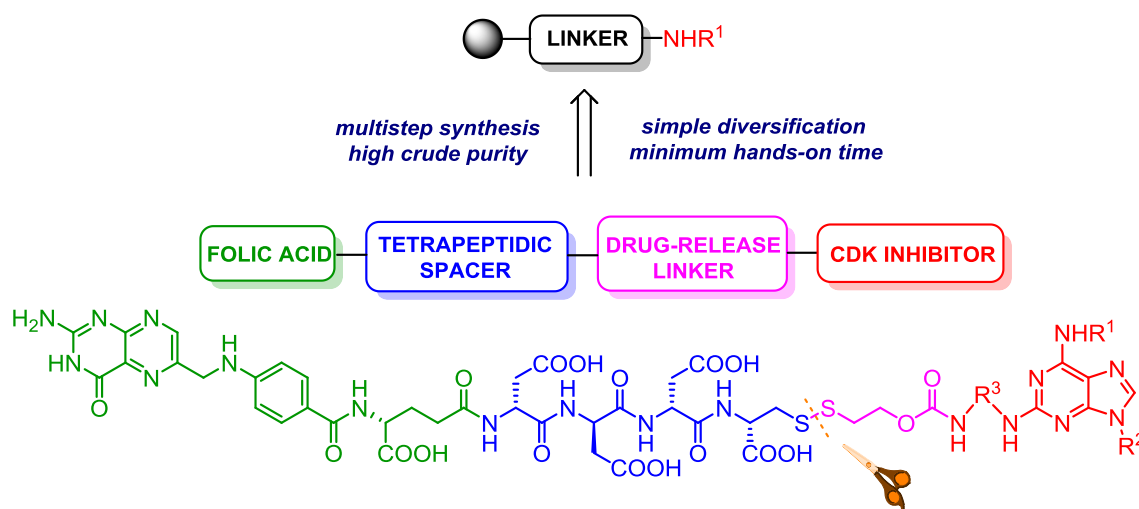
- konjugáty malých molekul sloužících jako potenciální léčiva s kyselinou listovou, jelikož se její receptor nadměrně vyskytuje v nádorových buňkách, a tedy tyto konjugáty mohou sloužit jako selektivní přenašeče („Trojské koně“) účinných molekul
- konjugáty heterobifunkčních, proteolýzu-zaměřujících chimér (z angl. PROTAC) s thalidomidovým zbytkem, které mohou vázat současně dva specifické proteiny s cílenou degradací
- konjugáty účinných látek a fluorescenční značky pro další vizualizaci v buňkách pomocí fluorescenční mikroskopie

Moje doktorská práce je tedy zaměřena na syntetickou strategii a následnou aplikaci našeho nedávně vyvinutého konceptu předpřipravených pryskyřic k přípravě sond pro chemickou biologii, v oblasti protinádorových triterpenů (jako fluorescenčně značené konjugáty) a proteinových kinázových inhibitorů (jako PROTAC konjugáty) a na přípravu a aplikaci syntetického přístupu k přípravě purinových CDK inhibitorů v konjugaci s kyselinou listovou.

Aims of the Thesis

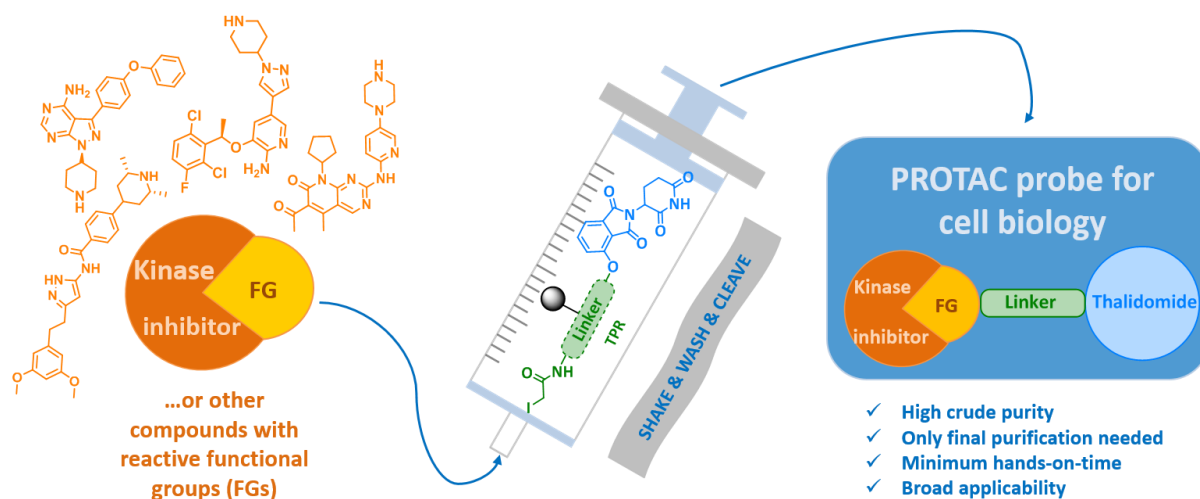
1) Tumor targeting delivery for purine CDK inhibitors

Stepwise synthesis of drug-delivery system, bearing four main components (CDK inhibitor, self-immolative linker, hydrophilic spacer and folic acid) on solid-support and study of their impact inside the cells overexpressing folate receptor.



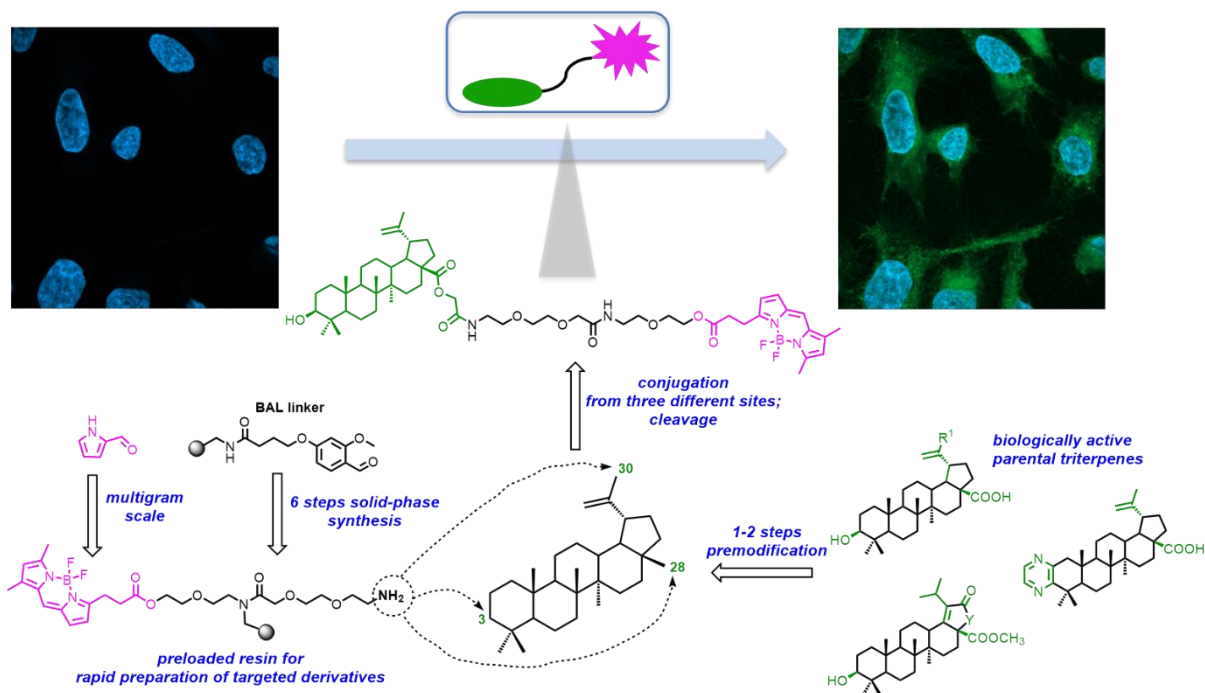
2) Proteolysis-targeting chimera (PROTAC) for protein kinases targeted degradation

Development of thalidomide-preloaded resin for easy and rapid preparation of desired conjugates possessed with suitable functional groups – demonstrated on selected protein kinases inhibitors. Test applicability of the thalidomide conjugates on selected protein kinases.



3) BODIPY labeled triterpenes for visualization within cells

Development of BODIPY labeled resin, as another application of preloaded resins, for easy and rapid preparation of desired conjugates possessed with suitable functional groups – demonstrated on selected triterpenes. Following study of BODIPY-triterpene conjugates distribution within cells with fluorescent microscopy and examination of their cytotoxic activity against selected cancer cell lines.



1. Tumor targeting delivery for purine CDK inhibitors

1.1. Introduction

Cyclin-dependent protein kinases (CDK) belong to the ATP-competitive (*type I*) and serine/threonine kinase family.^[1,2] These critical regulatory enzymes driven all cell-cycle transitions and their activity is often associated with successful cell division.^[1,3] Different families of cyclins, which are crucial regulatory subunits necessary for the CDK activity, have been identified and their expression vary significantly through the phases of the cell cycle. Each CDK is selective for a limited number of cyclins and this, on the other hand, determines the selectivity towards its substrates during the cell cycle.^[2,4] The human genome encodes 21 CDKs, however, only seven (CDK1-4, 6, 10, 11) have been shown to participate directly in the cell cycle progression. The rest play an indirect role, such as activation of other CDKs (CDK3), regulation of transcription (CDK7-9) or neuronal function (CDK5).^[4] Thus, selective inhibition of CDKs may limit the progression of a tumor cell through the cell cycle and facilitate the induction of apoptotic pathways.^[3,5]

Over the last two decades, several CDK inhibitors have been developed as potential anticancer drugs and tested in numerous trials and several tumor types.^[3] This first generation of CDK inhibitors, so called *pan-CDK inhibitors*, were relatively non-specific and did not meet the expectations following preclinical studies, although some compounds, such as purine-like analogs Olomoucine^[6] and Roscovitine^[7] (as *R*-enantiomer) (Figure 1) showed relatively low selectivity towards CDK4 and CDK6.^[3,5,8] Purine scaffold was presented in both inhibitors as “starting point” for design of many other inhibitors, very likely due to the structural similarity with the ATP itself.^[2]

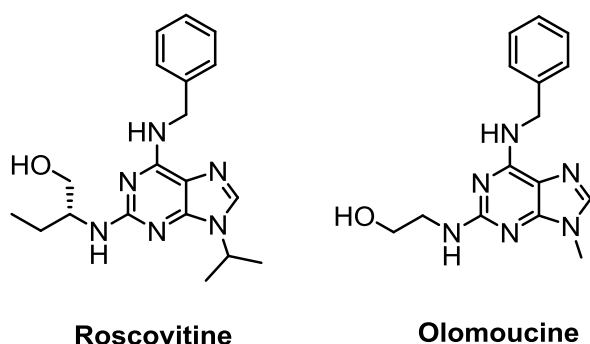


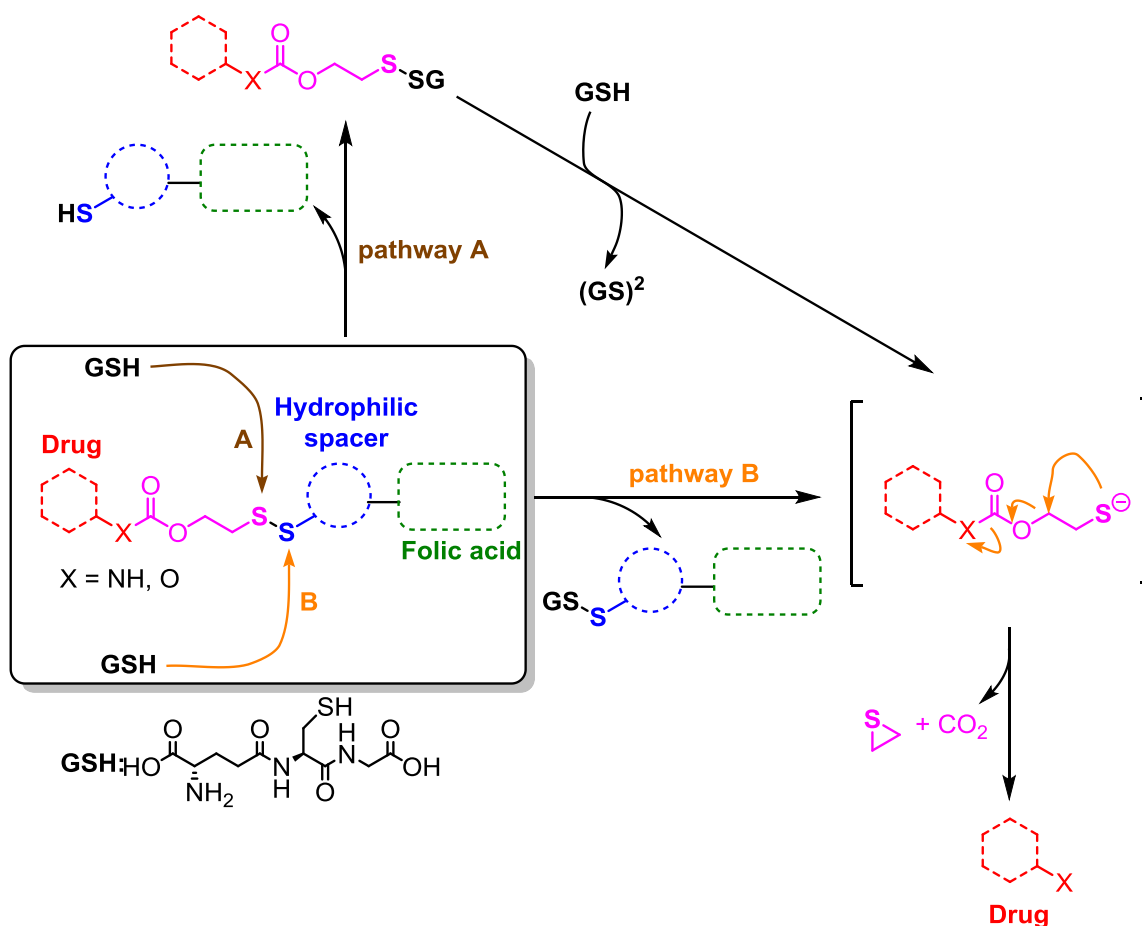
Figure 1. The most examined pan-CDK inhibitors.

The later studies revealed potency of 2,6,9-trisubstituted purine analogs (the next generations of Roscovitine) as highly potent CDK inhibitors.^[9,10] Their synthesis is rather straightforward and started usually from the 2,6-dihalogenated purine,^[9,11,12] 2-amino-6-chloropurine^[13] or by building the purine ring from the dichloropyrimidine precursor.^[14]

To minimize the exposition of healthy cells towards toxicities linked with application of potent, but not specific cytotoxic agents, the strategy for the selective delivery has been developed and a rapidly growing class of anticancer drugs use a targeting drug-delivery approach to malignant cells.^[15]

In addition to antibodies, other tumor-selective ligands have been discovered to prepare novel drug conjugates. For instance, the vitamin folic acid (FA) showed high affinity for the folate receptor (FR), which represents a potentially useful biological target for the management of many human cancers, e.g. ovarian, endometrial or kidneys.^[16,17] Therefore, attachment of FA to potent chemotherapeutic compounds to form so called *small molecule drug conjugates* (SMDCs) is remarkably useful approach towards potent and simultaneously less toxic agents.^[15] Several conjugates of this type have been evaluated or even entered the clinical trials, including taxol,^[18] vinca alkaloid vinblastine.^[19]

The development of releasable, self-immolative, disulfide-containing linker, arranged between the FA ligand and a cytotoxic agent, yielded conjugates having superior activity against FR-positive cells, compare to the non-reducible counterparts.^[20] Next issue that came upon evaluation of prepared conjugates was solubility, since vast majority of small-molecule chemotherapeutic compounds allows for their passive diffusion through cell membrane. FA-SMDCs with enhanced hydrophilicity (containing polar, charged amino acids residue spacer) will force these nonpolar molecules to enter FR-positive cells rather than indiscriminately into nontarget cells.^[16] The mechanism of self-immolative cleavage with subsequent release of drug is depicted on Scheme 1.



Scheme 1. The self-immolative cleavage of disulfide-based linker and subsequent release of the drug in the endosomal environment. A thiol group of a reducing agent can attack either of the two sulfur atoms in the linker system, resulting in two distinguished pathways. (GSH = glutathione)

Bearing this concept in mind, we proposed a design of our final purine CDK inhibitors for conjugation with FA (Figure 2). The study of Roscovitine-like inhibitors revealed ideal substitution patterns on each position of purine moiety for single-digit-nanomolar activities.^[9,21] Moreover, the combination of 2-cyclohexanediamine, 9-cycloalkyl and 6-heterobiaryl methylamino substituents has been found out to significantly increase CDK activity and cytotoxic effects in cancer cell lines, compared to previously published compounds of this class, e.g. well known derivative CR8.^[9,22] Hence, these observations motivated us for preparation of selected purine CDK inhibitors **I-1a-g** for conjugation with FA *via* C² position (Figure 2), which should not interfere in terms of interaction of inhibitors within the CDK catalytical domain.

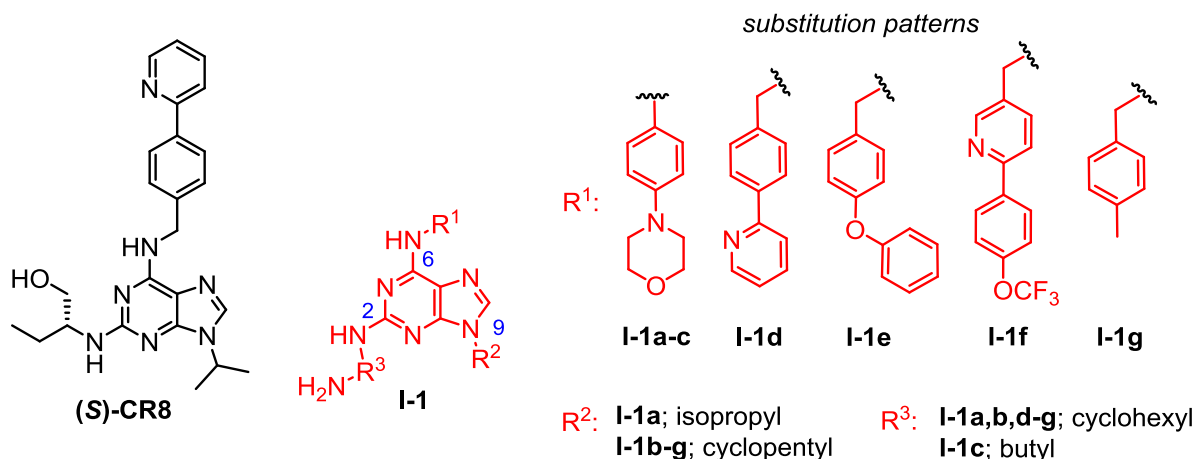
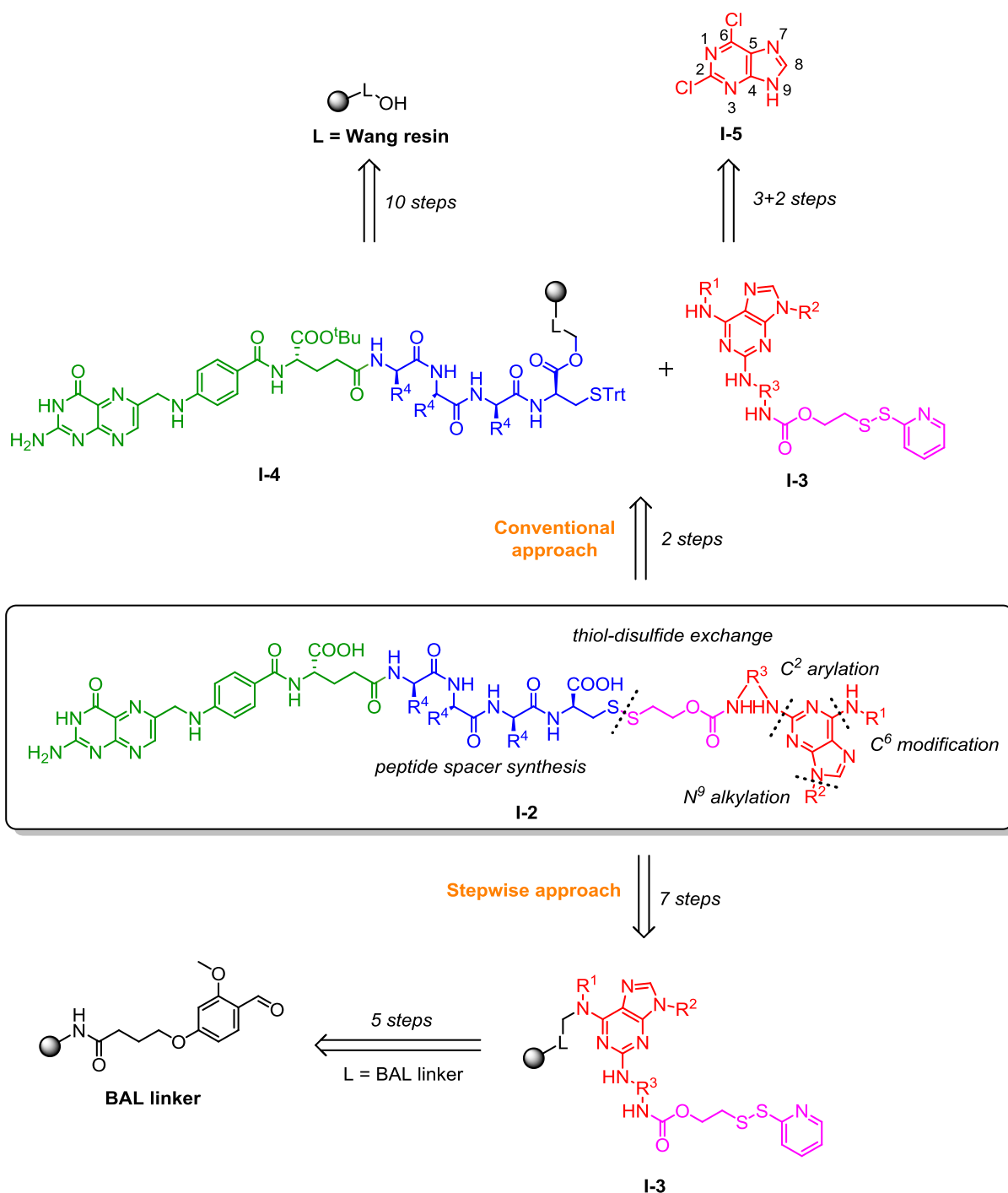


Figure 2. Potent CR8 purine CDK inhibitor and our selected substitution patterns based on previously reported molecules.

1.2. Synthesis

First, we attempted to use the previously reported conventional synthetic approach.^[16,23] It consisted of the preparation of a folic-acid-oligopeptide-SH segment using solid-phase synthesis and its subsequent coupling with a premodified drug equipped with the self-immolative drug-release linker (Scheme 2, Conventional approach). However, despite the successful preparation of corresponding intermediates, this strategy failed in the stage of the final thiol-disulfide exchange due to the low purity of the resulting products and irreproducibility on a preparative scale. Moreover, due to the zwitterionic structure and high polarity, the solubility of folic acid in organic solvents was limited (except for DMSO), and the final products required at least two-step purification using reverse-phase chromatography.^[16]

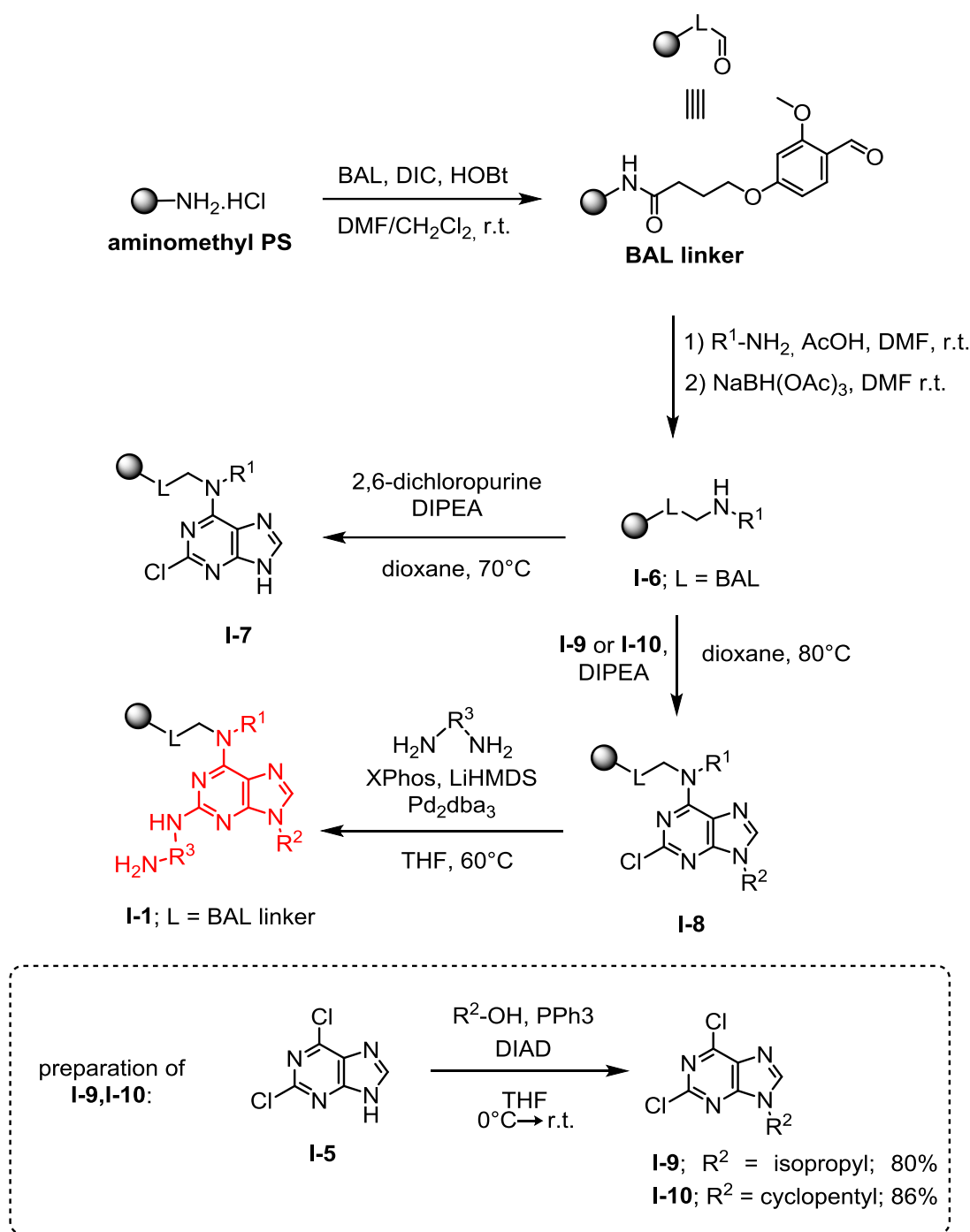


Scheme 2. Retrosynthetic analysis of the approaches towards final FA conjugates.

For these reasons, we designed an alternative synthetic approach. It consisted of the sequential construction of the target conjugates in the following direction: purine \rightarrow drug-release linker \rightarrow tetrapeptide \rightarrow folic acid (Scheme 2, Stepwise approach). With respect to the well-known advantages of solid-phase synthesis in multistep reaction sequences (especially the fast and simple isolation of reaction intermediates without the need for tedious purification) the entire reaction sequence was designed.

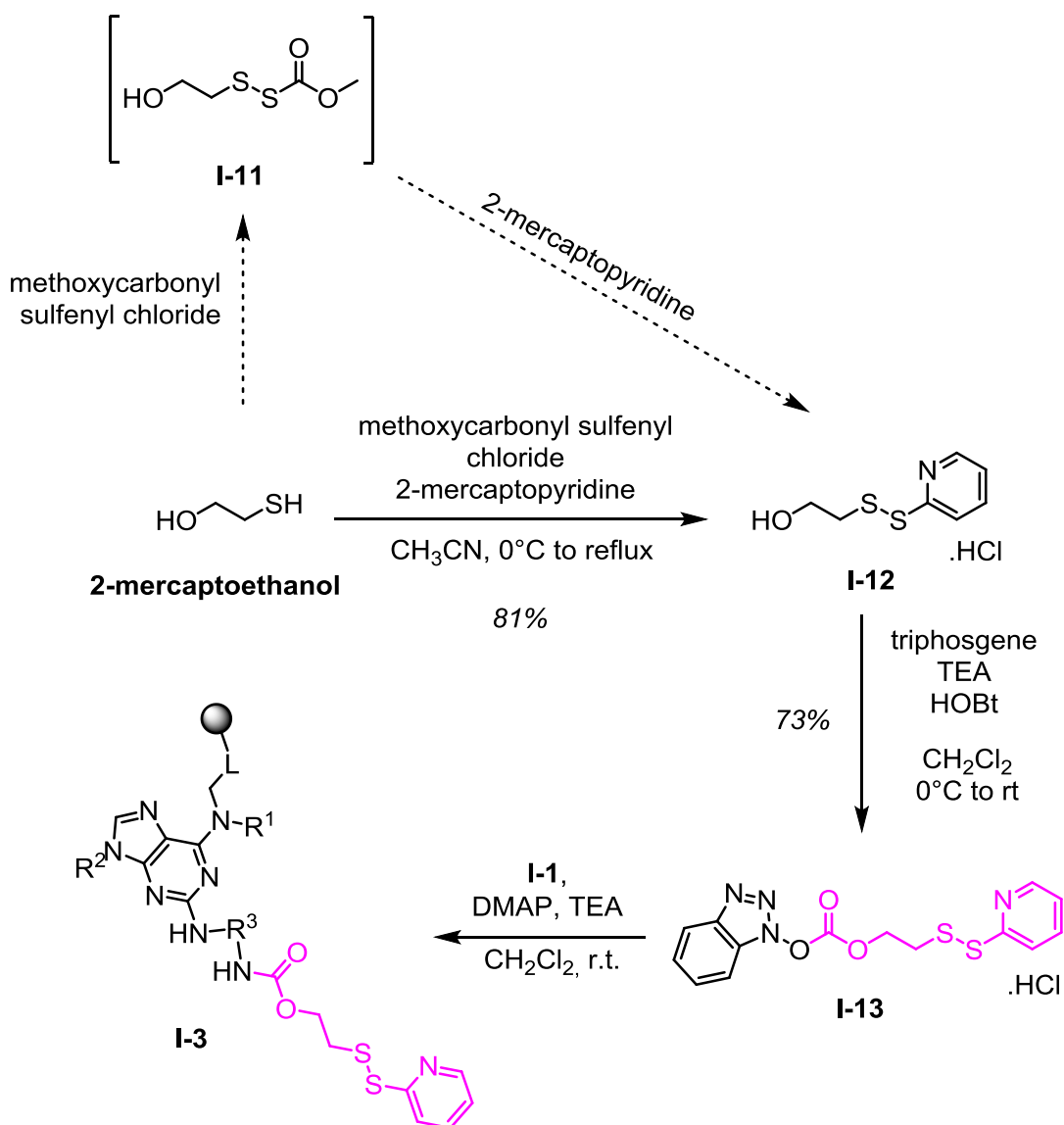
The synthesis started with immobilization of BAL linker to commercially available aminomethyl polystyrene resin. The following reductive amination with various benzylamines and anilines afforded intermediates **I-6**. Subsequent aromatic nucleophilic substitution (S_NAr) proceeded with excellent regioselectivity at C⁶ position (Scheme **3**). Alternatively, we obtained intermediates after the N⁹-alkylation of 2,6-dichloropurine in the solution phase using Mitsunobu conditions (yielding **I-9** and **I-10**), followed by their immobilization *via* the arylation of resin **I-6** (Scheme **3**). The latter alternative procedure yielded the desired intermediates **I-8** with higher crude purities.

The first challenging part of the synthesis seemed to be modification of position C² on purine scaffold, since it generally suffers from lower reactivity than C⁶ position and much harsher conditions are needed.^[2] We put quite effort to optimizations and tested several conditions, including various high boiling solvents, temperatures, reaction times and/or even a microwave heating, unfortunately, according to the UHPLC-MS traces we detected presence of the starting material **I-8** in most attempts. For this reason, we developed a more efficient Pd-catalyzed substitution using Buchwald-Hartwig C-N coupling conditions, which was successfully tested for both 1,4-diaminocyclohexane and putrescine to yield intermediates **I-1** (Scheme **3**) with excellent crude purities.



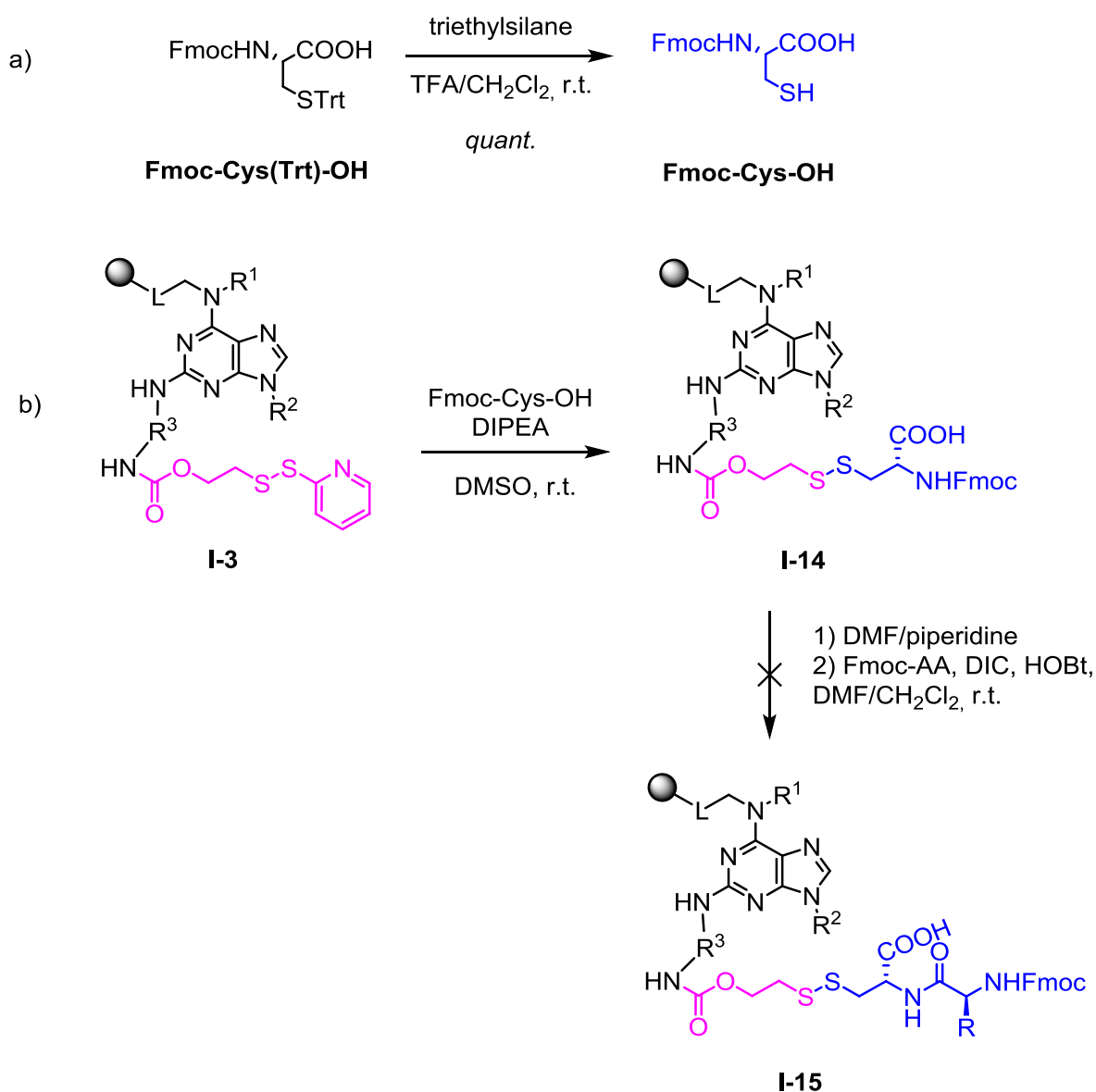
Scheme 3.

As was mentioned above, introduction of the disulfide moiety between the drug candidate (in our case the 2,6,9-trisubstituted purine derivatives) and the folic acid with oligopeptide chain seemed to be crucial for the overall activity of the compounds. The synthesis of the disulfide linker **I-3** was accomplished by slightly optimized literature procedure^[24] after 2 steps (Scheme 4).



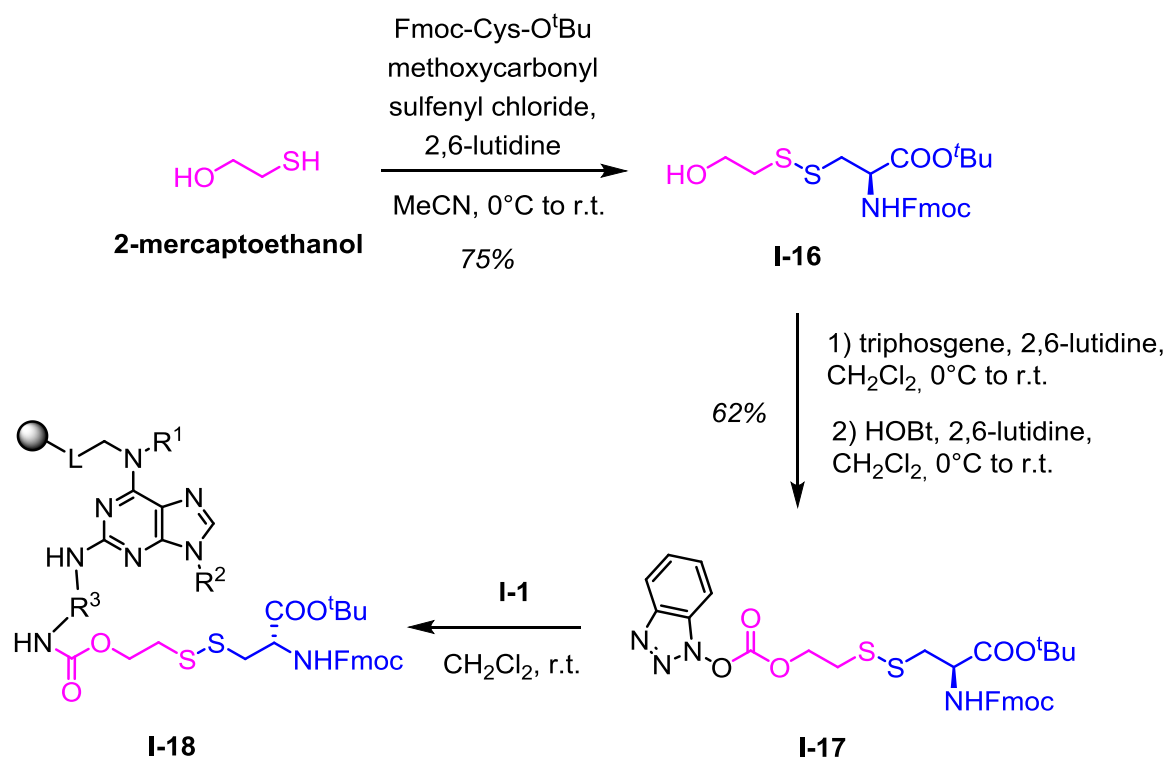
Scheme 4.

The prepared linker **I-13** was then reacted with immobilized amines **I-1** to provide **I-3** (Scheme 4). The following thiol-disulfide exchange on solid-phase was successfully accomplished with use of Fmoc-Cys-OH (Scheme 5.a) or Fmoc-Cys-O^tBu. However, the further Fmoc-cleavage and acylation with Fmoc-amino acid (i.e. first step of a peptidic spacer synthesis) under standard DIC/HOBt protocol failed (Scheme 5.b) and only provided mixture of products. Unfortunately, we have not been able to optimize this reaction pathway, despite the numerous optimizations and were forced to use another approach.



Scheme 5. a) Preparation of Fmoc-Cys-OH; b) Thiol-disulfide exchange with Fmoc-Cys-OH and unsuccessful acylation with another Fmoc-amino acid.

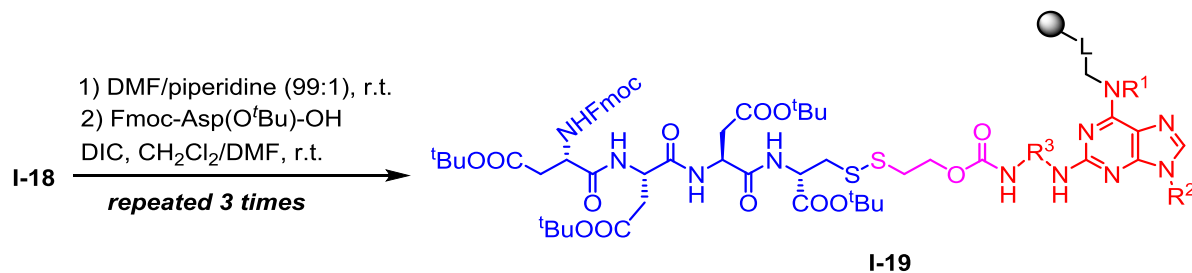
In this regard, we decided to prepare disulfide linker containing cysteine in solution, to overcome problematic thiol-disulfide exchange on solid-phase. The first step was preparation of disulfide containing alcohol **I-16**, where addition of base (2,6-lutidine) in huge excess maintained neutral pH during reaction, thus prevented cleavage of acid labile *tert*-butyl protecting group on carboxylic moiety. Following formation of carbonate in presence of triphosgene provided desired intermediate **I-17** (Scheme 6). Finally, the following nucleophilic substitution with amines **I-1** (Scheme 6) provided desired intermediates **I-18** in excellent crude purities (up to 90 %).



Scheme 6.

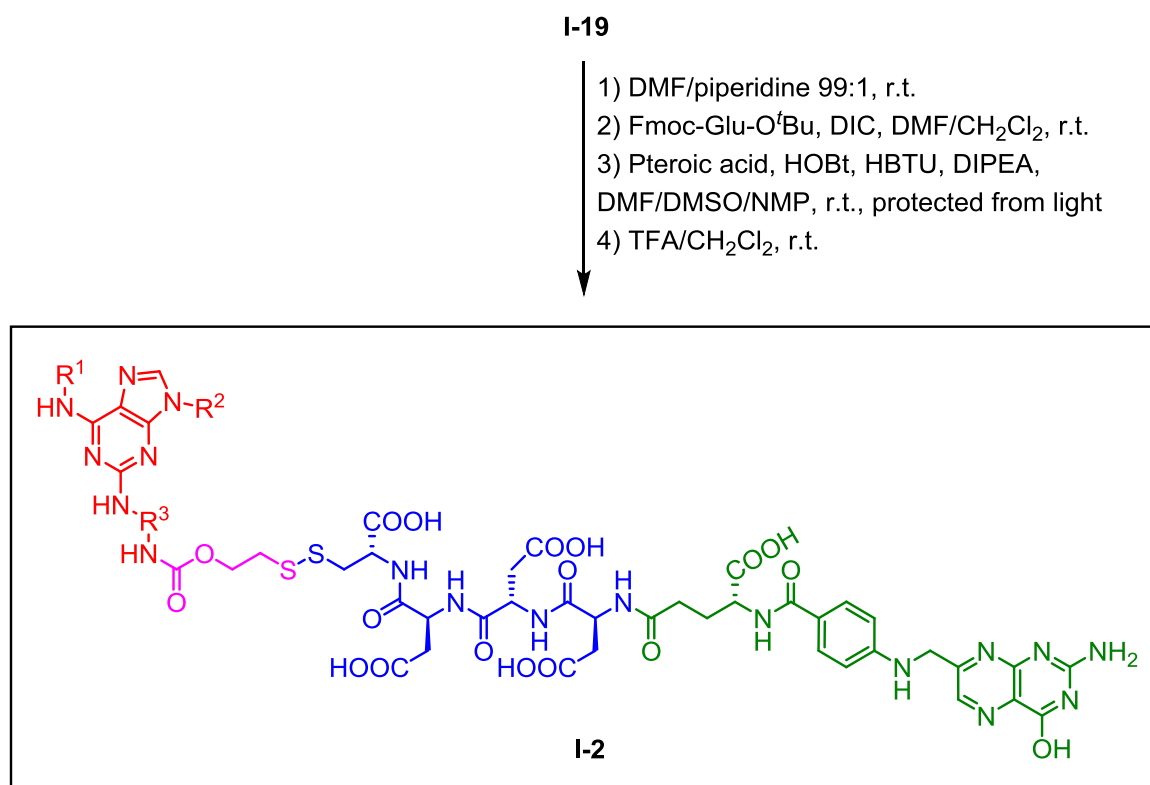
Synthesis of the peptidic spacer started with deprotection of Fmoc protecting group. Unfortunately, the standard cleavage conditions (DMF/piperidine 4:1) commonly used in peptide chemistry, yielded only symmetric disulfides. Their formation is probably caused by the nucleophilic nature of piperidine, which in higher concentration can cleave Fmoc protecting group and simultaneously participates in cleavage of disulfide bond. Hence, a lower concentration to cleave Fmoc group had to be applied and the best results were obtained with use of DMF/piperidine 99:1 after 2 hours (Scheme 7), when the formation of disulfides was completely suppressed, indicating that pH during the reaction plays crucial role.^[25]

The reaction sequence continued therefore from I-18 with repeated steps of Fmoc cleavage and DIC promoted peptide couplings with use of commercially available Fmoc-Asp(O^tBu)-OH to afford peptidic spacer-linker-purine intermediates I-19 (Scheme 7).



Scheme 7.

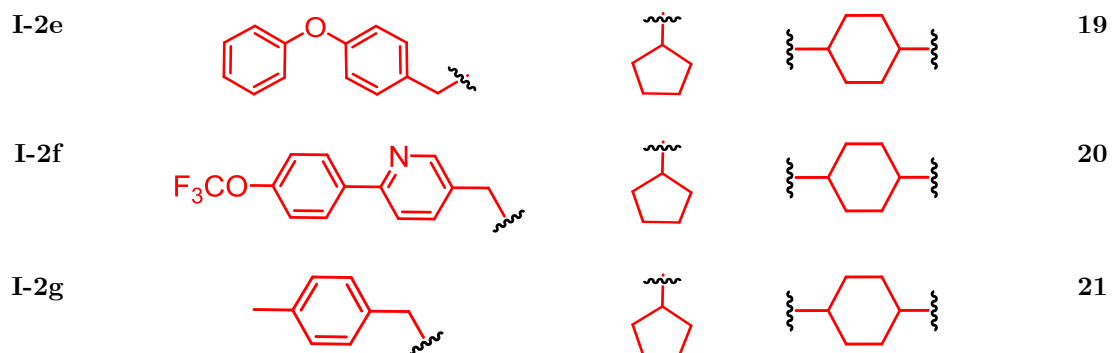
The following 2 steps acylation with Fmoc-Glu-O^tBu and pteronic acid yielded the final intermediates that upon cleavage from the polymer support and purification on semipreparative HPLC afforded final compounds **I-2** (Scheme 8).



Scheme 8. Final compounds preparation.

The reaction sequence was successfully tested using different building blocks, which were suggested from SAR studies (Table 1). Furthermore, Figure 3 displays the HPLC-UV traces of representative reaction intermediates after cleavage from the polymer support. This figure demonstrates that the optimized procedure furnished the corresponding compounds in excellent crude purities and good yields after 15 reaction steps and final reverse-phase purification.

| Cmpd | R ¹ | R ² | R ³ | Yield ^a [%] |
|------|----------------|----------------|----------------|------------------------|
| I-2a | | | | 27 |
| I-2b | | | | 22 |
| I-2c | | | | 25 |
| I-2d | | | | 23 |



^a - overall yield calculated from the loading of resin 2 after the entire reaction sequence and preparative HPLC purification

Table 1. Substitution on purine core.

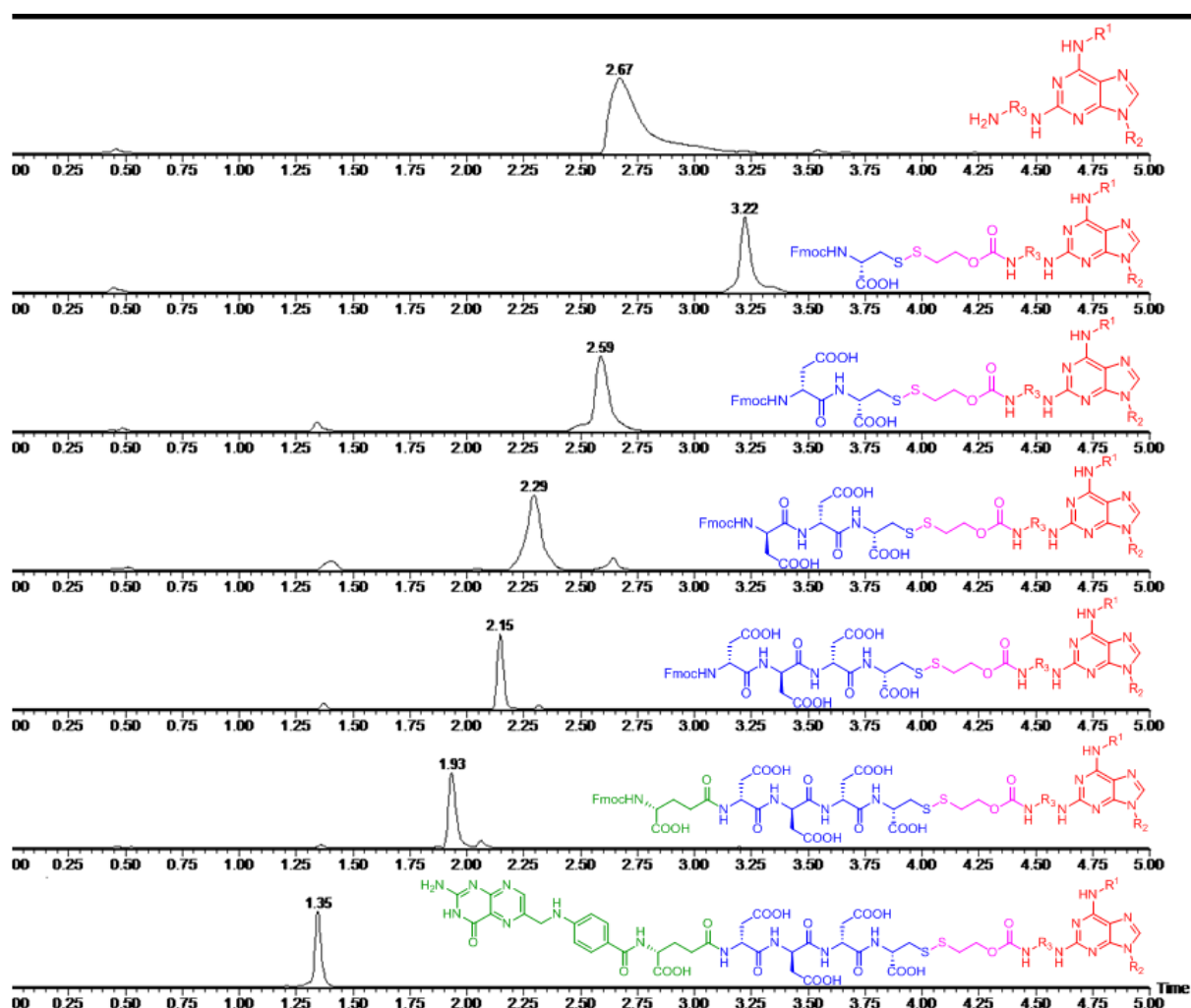


Figure 3. Final crude purities of intermediates. The substitution on purine ring did not influence the purity.

1.3. Biology

To test the applicability of our prepared compounds, we decided to mimic drug release *in vitro* on representative derivative **I-2d**. The release of the free inhibitor was successfully accomplished by treating a 0.04 mM solution of conjugate **I-2d** (Figure 4.C) with 4 mM of the general reducing agent dithiothreitol (DTT) at 37 °C. The release was monitored by UHPLC-UV ($\lambda = 289$ nm) at pH 7 and 7.4. The disulfide bond was cleaved within 5 min and yielded the drug-spacer intermediate (Figure 4.B), followed by self-immolative cleavage and quantitative release the purine inhibitor after 20 h (Figure 4.A).

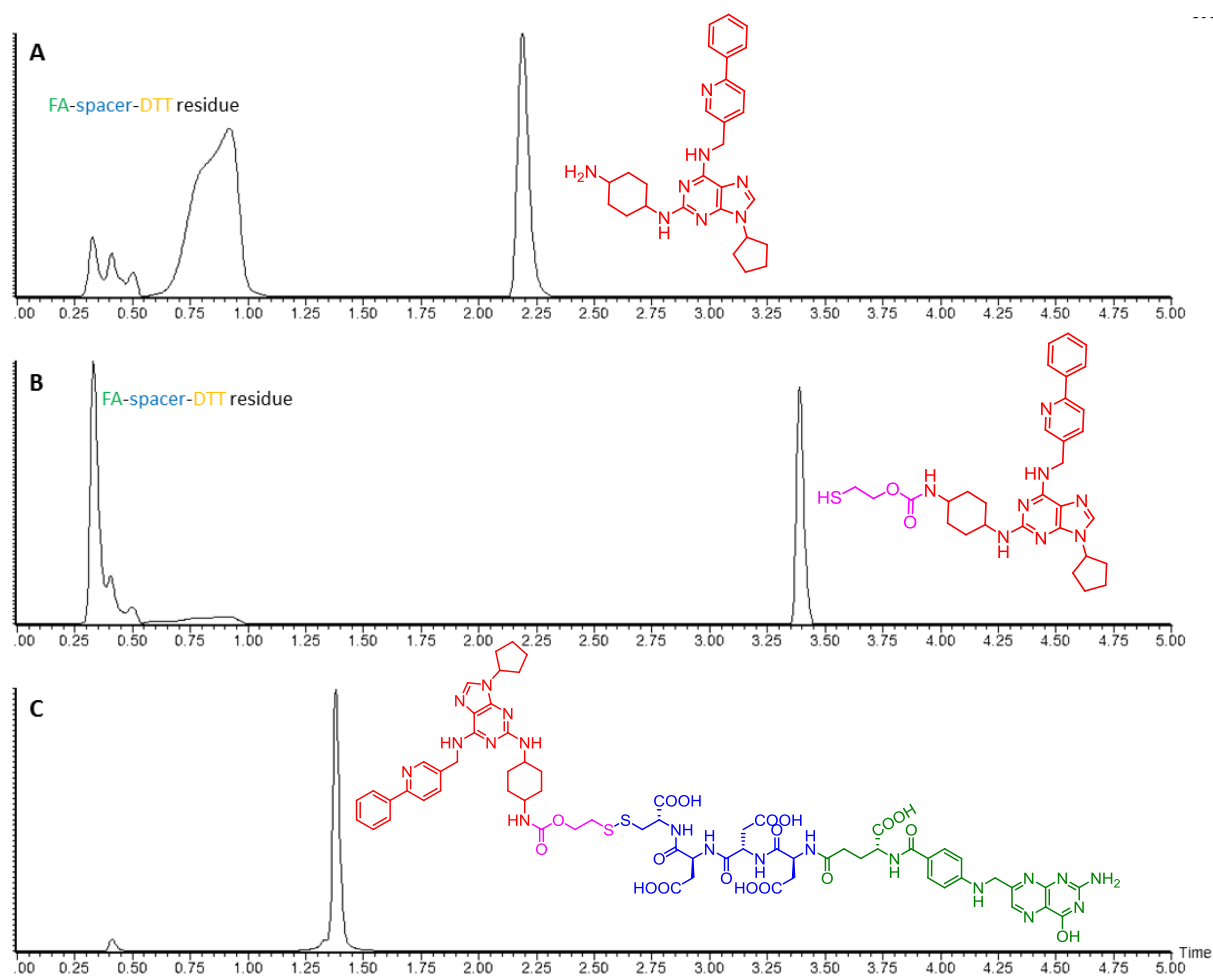


Figure 4. Mimicked disulfide bond reduction with subsequent self-immolative cleavage of the conjugate **I-2d**. (FA = folic acid; DTT = dithiothreitol)

As another proof of concept, conjugate **I-2d** was further tested for its binding to the HeLa cell line overexpressing FOLR1 by flow cytometry using the folate-receptor-targeted fluorescence probe FolateRSense 680 (PerkinElmer) as a competing agent (Figure Xa). This experiment was provided by V. Krystof group. The HeLa cell line was used due to its overexpression of FOLR1 and significantly greater probe uptake over other cell lines.

The cells were stained with 1 μ M FolateRSense 680 in the absence or presence of conjugate **I-2d** (Figure 5.B,C). The probe was combined with either the unconjugated inhibitor or free folic acid (Figure 5.D,E) in control incubations. Quantification of cell-associated fluorescence was provided after 1 hour of incubation by flow cytometry. The presence of conjugated CDK inhibitor **I-2d** remarkably decreased the percentage of cells with bound FolateRSense 680 from 75.6% to 11.4% (Figure 5.C), as was suggested from the experiments. Free folate also reduced the percentage of positive cells and therefore confirmed the function of the probe (Figure 5.D). The specificity of cellular binding of conjugate **I-2d** was demonstrated in a control experiment in which an excess of unconjugated CDK inhibitor **I-1d** did not compete with the probe (Figure 5.E).^[26]

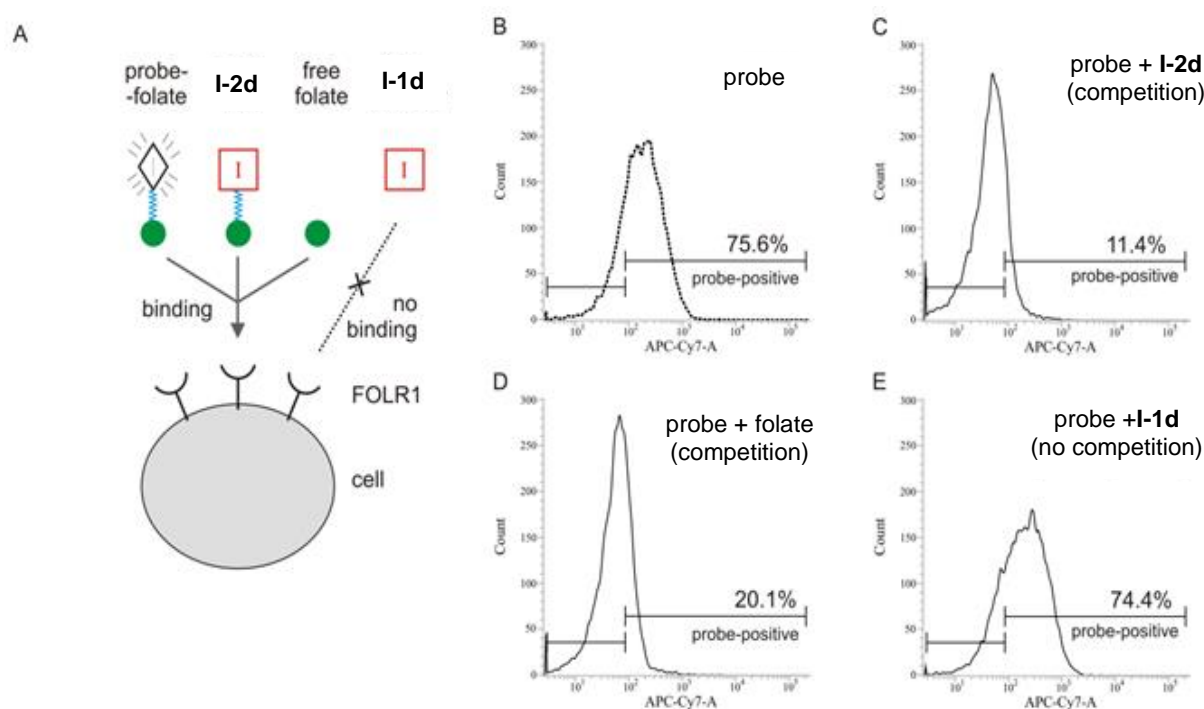


Figure 5. In vitro binding to folate receptor.^[26]

1.4. Conclusion

We successfully optimized and synthesized the route towards the final compounds, purified them by semipreparative HPLC and obtained in good to excellent overall yields (see Table 1), considering the number of steps leading to such results. Our prepared conjugates were then tested for their kinase inhibitory activity, provided by V. Kryštof group. The most potent conjugate was subjected to the *in vitro* simulation of disulfide reduction, to prove applicability of our system, which was provided and evaluated by me.

Eventhough we had not been able to perform all steps on solid-support, due to the problematic thiol-disulfide exchange, our stepwise hybrid concept still enables the rapid production of the desired compounds with minimum *hands-on-time*. The method

represents a general approach for the modification and study of folate conjugates of diverse drug-like heterocycles using parallel or combinatorial solid-phase synthesis.

Flow cytometric measurements demonstrated the ability of an example conjugate to bind to cancer cells overexpressing the folate receptor. Moreover, *in vitro* simulation of intracellular reducing of disulfide bond with subsequent self-immolative cleavage demonstrated the applicability of our conjugates to release the inhibitor. To conclude, we confirmed binding of CDK inhibitors-FA conjugates to FOLR1-overexpressing cells, suggesting that this concept is a possible route to the development of more selective anticancer drugs.

2. Proteolysis-targeting chimera (PROTAC) for protein kinases targeted degradation

2.1. Introduction

The control of intracellular processes has long been a target for manipulation by small molecules in the chemical biology. However, not every protein has an enzymatic activity that can be inhibited and is therefore considered as “undruggable”, because many of these potential targets do not have suitable binding pockets that directly modulate protein function. Moreover, high systemic drug exposure may be needed to maintain sufficient target inhibition *in vivo*, which increases potential risk of undesired side effects.^[27,28]

Targeted protein degradation with use of bifunctional small molecules to remove specific proteins from within cells offers a new strategy with therapeutic interventions, not achievable with existing approaches. Using small molecules emerged a high potential due to their ability to access a wide range of organs and sites of action and modulate multiple targets simultaneously.^[29]

PROTAC technology, pioneered recently by Crews et al.,^[30] combines the modularity of nucleic acid-based strategies with the *in vivo* pharmacology of small molecule therapeutics. It is based on event-driven, rather than occupancy-driven pharmacology model, and can potentially exploit binding anywhere on the protein of interest (POI) in order to achieve degradation.^[27]

Bifunctional PROTAC molecules bind noncovalently to the POI with one part whereas simultaneously binds to an E3 ligase to form a ternary complex. The recruited E3 ligase then mediates the transfer of ubiquitin from an E2 enzyme to the POI, the ternary complex dissociates and the ubiquitylated POI is removed by the proteasome and the PROTAC can bind to another POI (Figure 6).

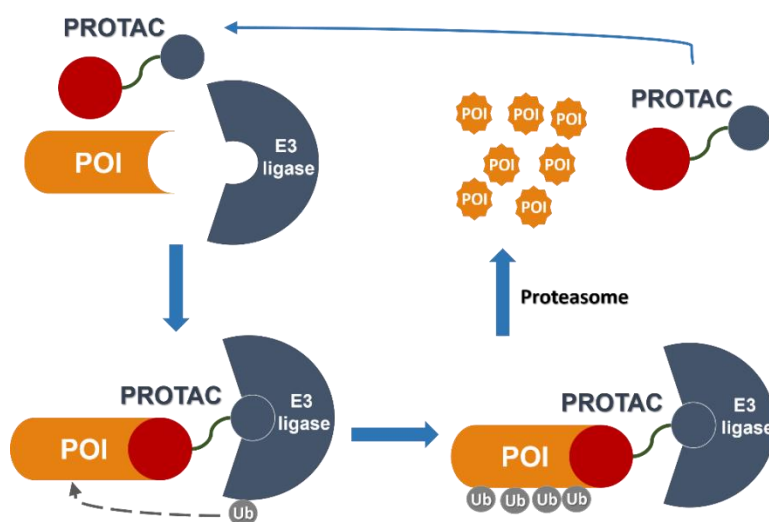
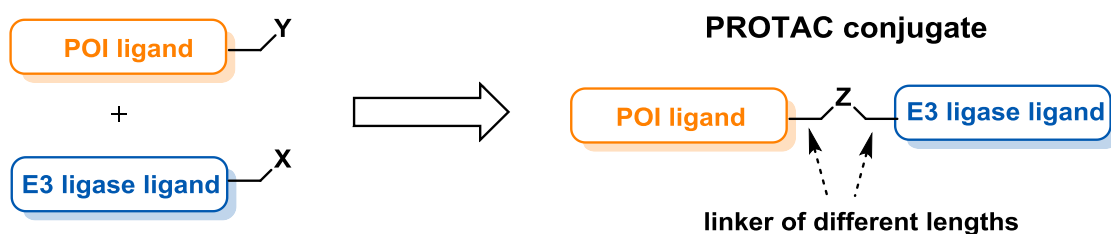


Figure 6. Mechanism of PROTACs. (POI = protein of interest; Ub = ubiquitin)

Lately, the E3 ligase cereblon (CRBN) was identified as a primary target for thalidomide, followed by a discovery of phthalimides-induced degradation of the lymphoid transcription factors IKZF1 and IKZF3 by binding to CRBN, thus able the E3 ligase to ubiquitylate them.^[31,32]

The synthetic strategies towards new PROTAC conjugates exclusively involved synthesis in solution, until our published work, dealing with the synthesis on polystyrene resin.

The most common approach by far, is either acylation of activated carboxylic acid or nucleophilic substitution of halogen alkane of one, pre-modified part of the conjugate with primary amine-containing part.^[33-37] Other possible approach is simple click reaction between azide-containing part with alkyne-containing part of the conjugate^[38] (Scheme 9). Nevertheless, the main disadvantage of these pathways relies in unavoidable purification after each synthetic transformation which requires assistance of skilled synthetic chemist. In this regard, use of solid-phase synthesis should be highly advantageous, due to the possibility of application of high-throughput synthesis with simple laboratory equipment and no need of purification within the reaction sequence.



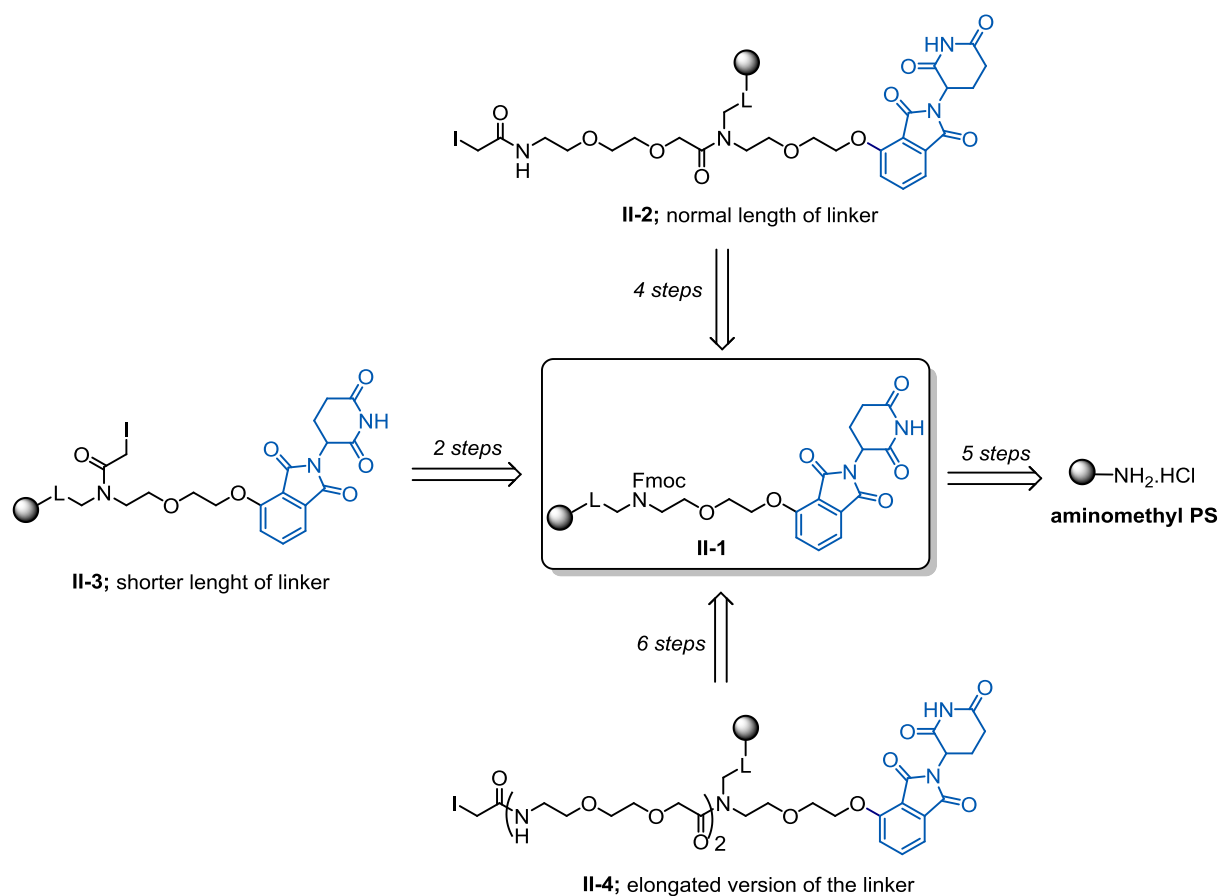
Y, X: COOH, halogene, alkyne, N₃, NH₂

Z: amide, ester, triazole, secondary/tertiary amine, ether

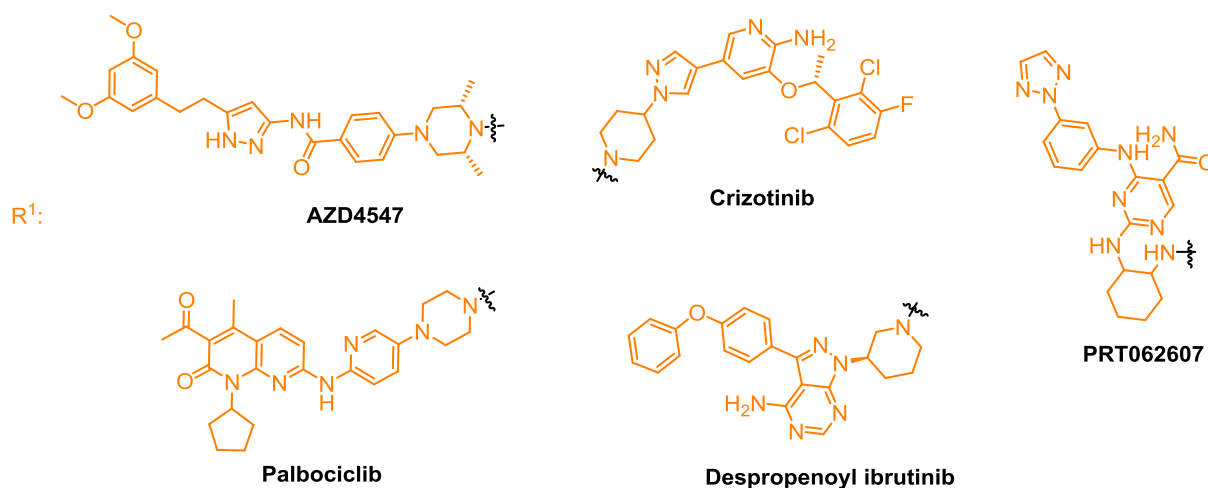
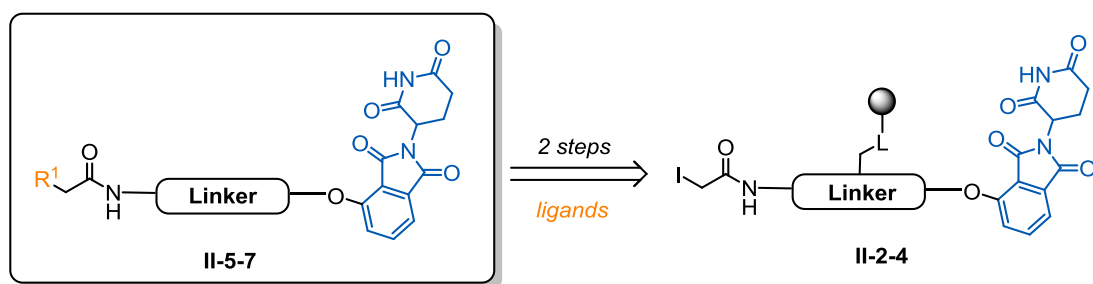
Scheme 9. General synthetic approach towards PROTAC derivatives. (POI = protein of interest)

2.2. Synthesis

In general, the preparation of our thalidomide preloaded resins (TPRs) started from the commercially available aminomethyl polystyrene resin, which was in 5 steps converted to the key intermediate **II-1**. Following elongation of the spacer yielded three different TPRs **II-2-4** (Scheme 10), which were subjected to the reaction with selected protein kinases inhibitors (palbociclib, crizotinib, AZD4547, despropenoylibrutinib and PRT062607) to afford final compounds **II-5-7** (Scheme 11). These kinase inhibitors, which potently target CDK4, ALK, FGFR, BTK and SYK kinases, respectively, were selected due to presence of reactive amine functions oriented outside the kinases' active sites, hence available for conjugation without loss of inhibitory activity.

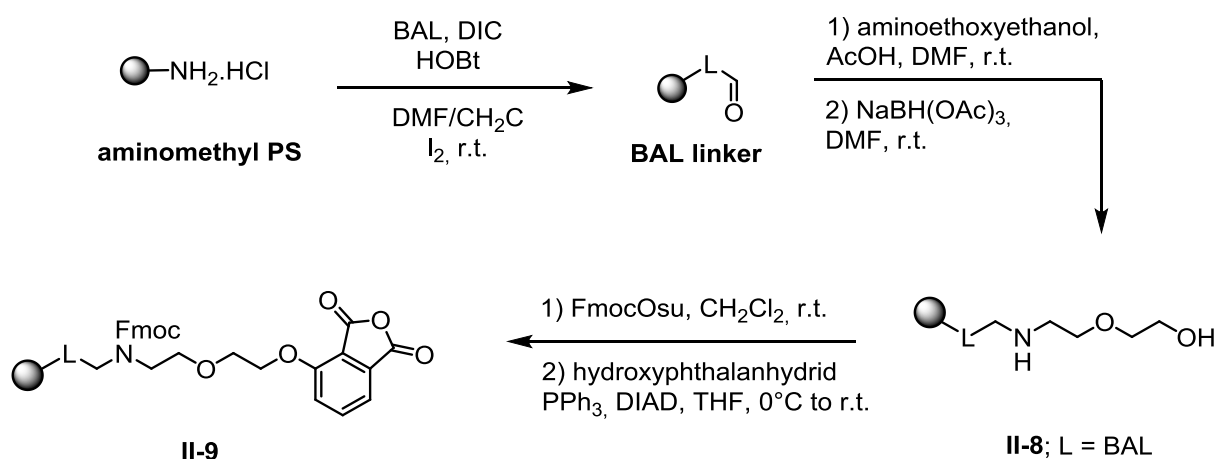


Scheme 10. General retrosynthetic analysis for TPRs **II-2-4**.^[39]



Scheme 11. Retrosynthetic scheme towards final compounds.^[39]

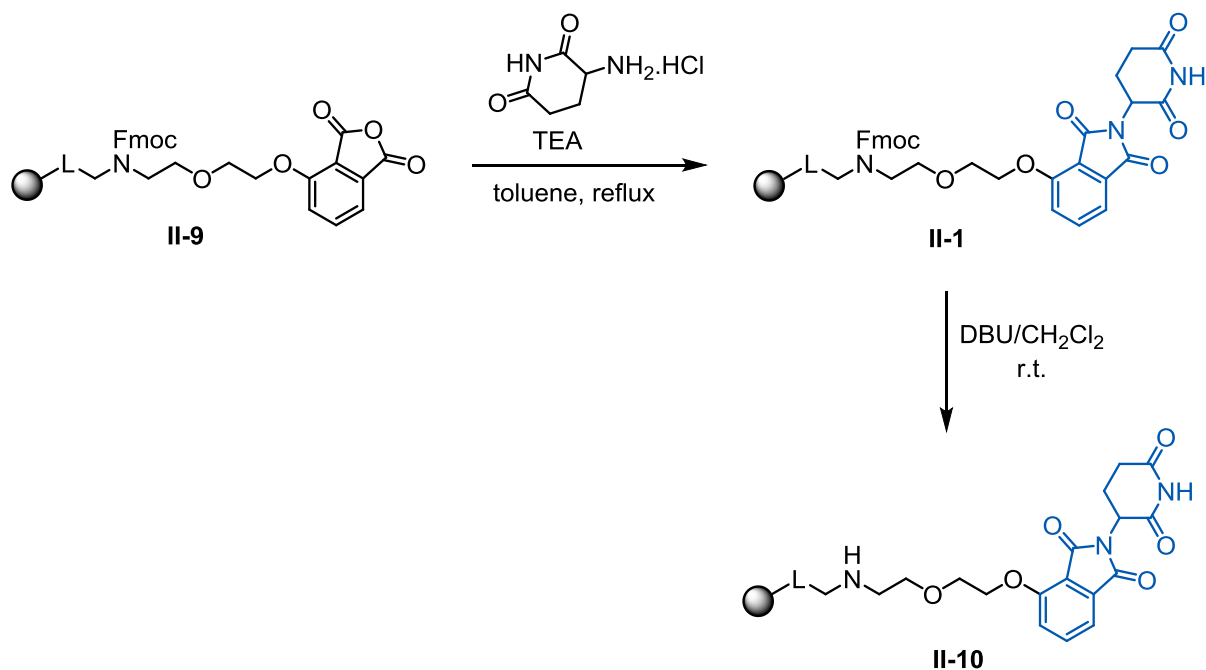
The synthesis started with reductive amination of BAL resin with aminoethoxyethanol, followed by chemoselective protection with FmocOsu and Mitsunobu alkylation to obtain intermediate **II-9** (Scheme 12).



Scheme 12.

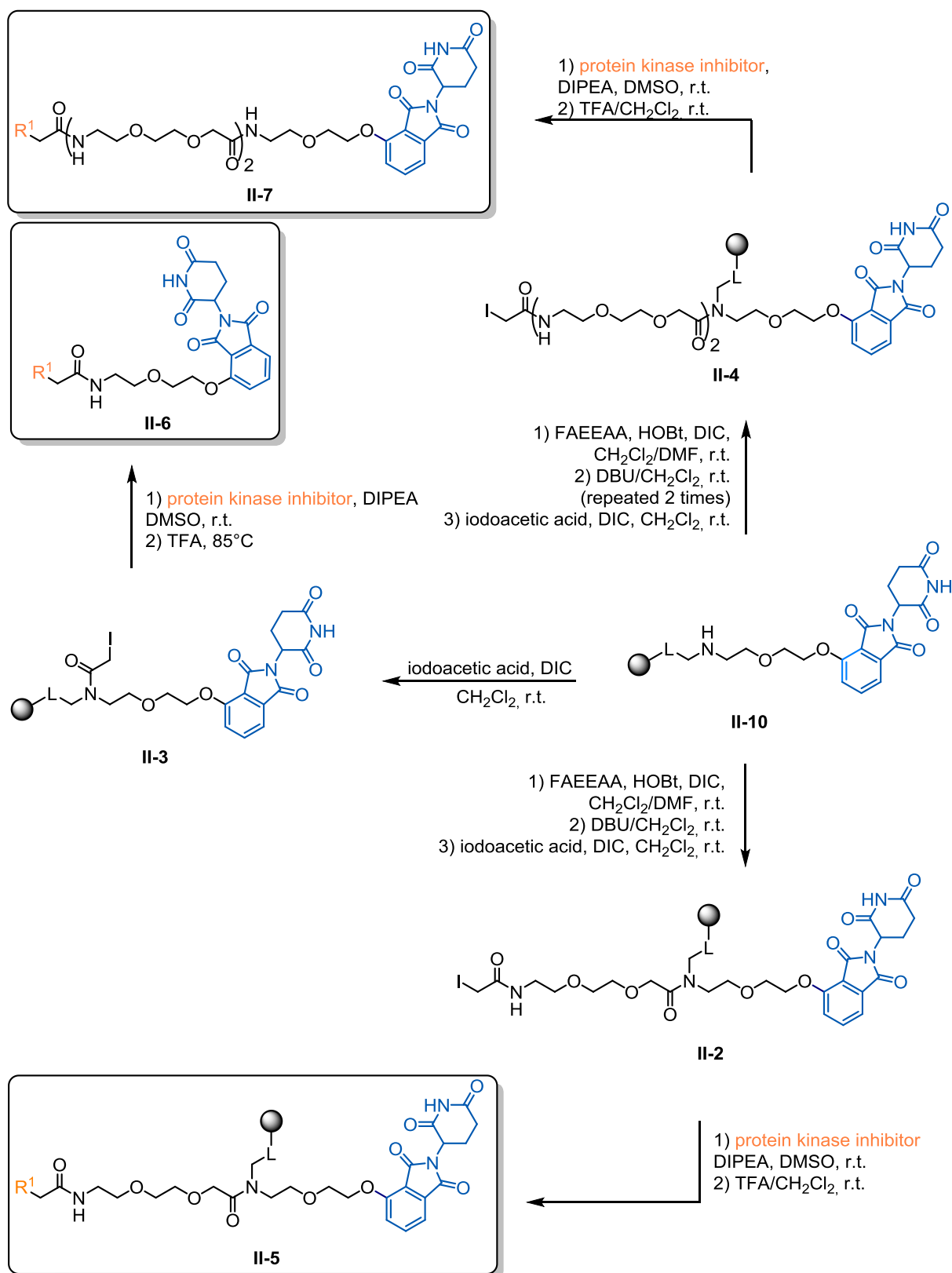
Following ring closure reaction to form thalidomide in **II-1** seemed to be solvent and base dependent reaction that required careful optimization. The best results were obtained with use of dry toluene as solvent and TEA as a base. The following deprotection of Fmoc under standard cleavage conditions (DMF/piperidine 4:1) led to

partial-thalidomide-ring-opening, due to the nucleophilic character of piperidine. Luckily, the use of stronger non-nucleophilic base (DBU) had positive impact on reactivity, since we have been able to obtain pure product **II-10** in 10 minutes (Scheme **13**) with no indication of ring-opening by-product.



Scheme 13.

Following steps, involving acylation with FAEEAA and iodoacetic acid to afford thalidomide-preloaded resins (TPRs) **II-2-4**, proceeded smoothly in excellent crude purities (above 90%). The iodoacetic functionality was installed on TPRs for reaction with primary/secondary amines of abovementioned kinase inhibitors, but the resin **II-10** (or its elongated version, after deprotection of Fmoc) could be used directly to couple various molecules bearing suitable reactive functional groups capable of reaction with amines, such as aldehyde, carboxylic acid or aryl/alkyl/arylhalogens, which make the strategy broadly applicable. Table **2** summarized final derivatives with specification of inhibitors for each PROTAC conjugate **II-5-7**.



Scheme 14. Synthetic approach towards final conjugates **II-5-7**.

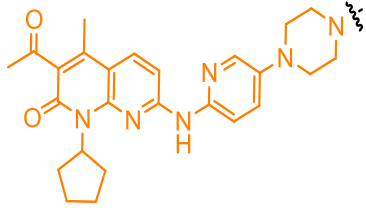
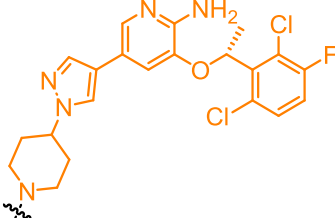
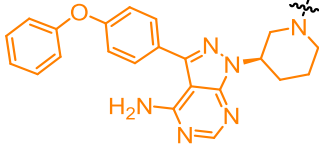
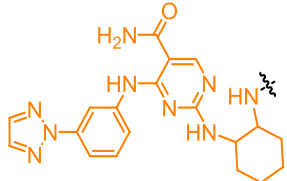
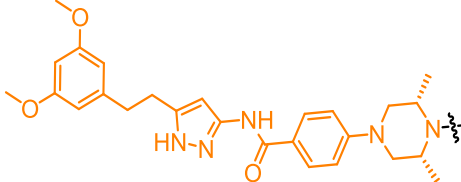
| Cmpd | R ¹ (Protein kinase inhibitor) | Commercial name | Targeted protein kinase | Yield [%] |
|--|---|------------------------|-------------------------|-----------------------------|
| II-5a |  | Palbociclib | CDK4 | 50 |
| II-5b |  | Crizotinib | ALK | 85 |
| II-5c; II-6; II-7 |  | Despropenoyl ibrutinib | BTK | 83; 76; 70 |
| II-5d |  | PRT062607 | SYK | 49 |
| II-5e |  | AZD4547 | FGFR | 24 |

Table 2. Summarization of our prepared PROTAC conjugates.

2.3. Biology

The representative conjugates **II-5c**, **II-6** and **II-7** were then selected to verify the functionality of prepared PROTACs. They possessed despropenoyl ibrutinib, a derivative of a recently FDA-approved drug specifically inhibiting BTK kinase.^[40] In our initial characterization experiments, we compared the potencies of ibrutinib and despropenoyl ibrutinib with that of PROTAC **II-5c** in a biochemical kinase assay. These experiments were provided by V. Kryštof group.

It was found out that our conjugate **II-5c** inhibited purified recombinant BTK with IC₅₀ like that of parental despropenoyl ibrutinib, which confirmed its biological

functionality. Two other PROTACs **II-6** and **II-7** (Figure 7) with shorter and longer linkers, respectively, were similarly potent on the kinase.

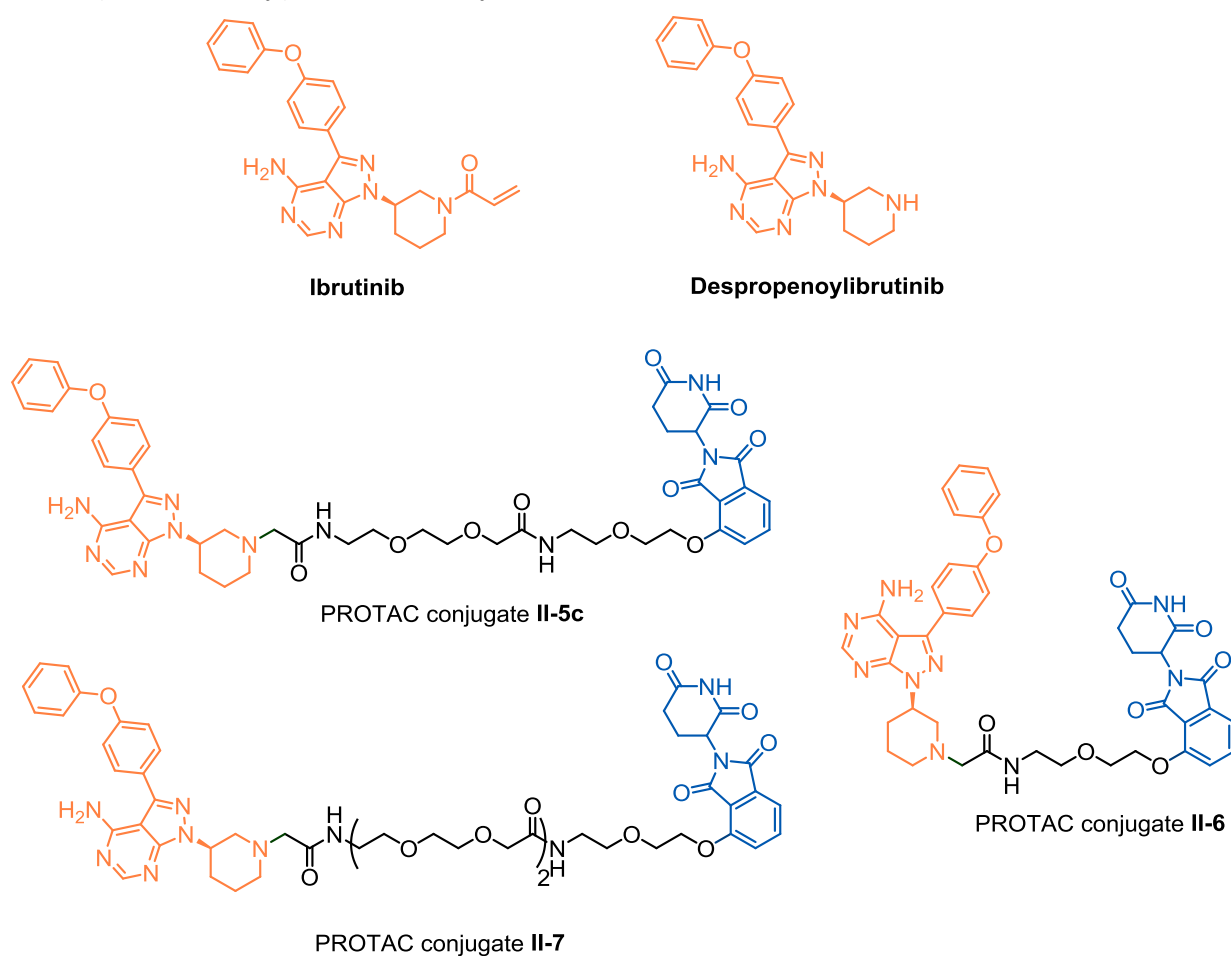


Figure 7.

The induced BTK degradation in cells was also demonstrated. In the preliminary experiments with **II-5c**, we observed that the decrease in BTK is time-dependent. Western blot analysis of lysed cells revealed that BTK degradation was dose-dependent, with a maximal knockdown achieved at a 2 mM concentration (Figure 8.A). Moreover, in control experiments neither ibrutinib nor despropenoylibrutinib were able to induce the degradation of BTK and only inhibited BTK activity, which agreed with general mechanism of action of PROTAC conjugates where E3 ligase recruited moiety is necessary for degradation of the protein of interest. SYK and SRC kinases were used in parallel to confirm the specificity of protein degradation induced by **II-5c**. The effect of linker length on the resulting conjugate applicability is demonstrated on Figure 8.B which contains results of shorter and longer version **II-6** and **II-7**, respectively. The degradation activity strongly depended on linker length, with the best results achieved for original version of the linker (PROTAC **II-5c**).

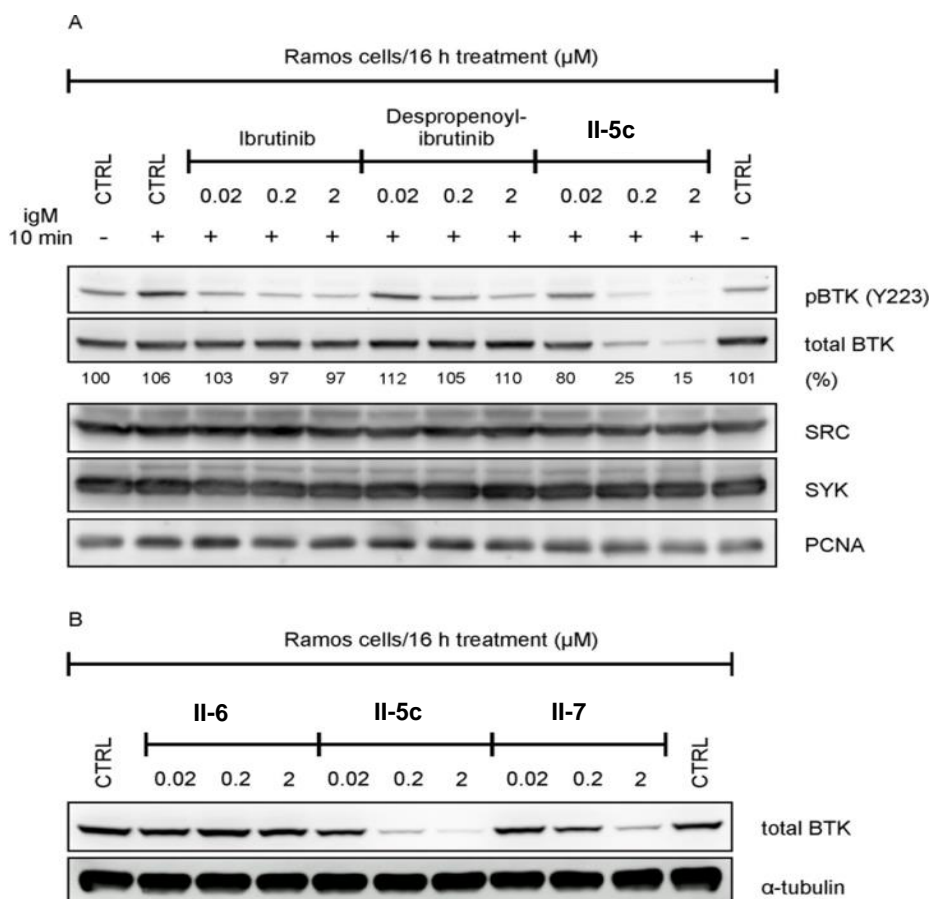


Figure 8. BTK degradation results of prepared conjugates II-5c, II-6, II-7.^[39]

2.4. Conclusion

We successfully optimized and synthesized *en route* towards thalidomide-preloaded resins **II-2-4**, which were subsequently conjugated with 6 protein kinases inhibitors with selective kinase targeting. The final compounds were purified by semipreparative HPLC and obtained in good yields. The kinase inhibitory activity and degradation study was provided on representative conjugates **II-5c**, **II-6** and **II-7** (provided by V. Kryštof group).

With respect to obtained biological data, one of the most important features of the method is undoubtedly simple enlargement of the spacer and comfortable production of the corresponding TPRs that differ exactly in this parameter. The general simplicity of TPRs utilization consists in *shake-wash-cleave* procedure that can be performed by a person without synthetic experience or special laboratory equipment. In the best case, TPR could be used as a simple kit for routine preparation of PROTACs. Importantly, the synthetic approach is versatile and can also be applied to other proteins for which ligands suitable for conjugation are available (with reactive functional groups, such as carboxylic acid, aldehyde, primary/secondary amine etc.). Compared to the solution-phase methods, only single final purification is required, and modularity of the synthesis allows preparation of library of designed compounds using parallel synthesis.

3. BODIPY labeled triterpenes for visualization within cells

3.1. Introduction

Small molecules capable of fluorescence are incredible tools for chemical biology, serving as enzyme substrates, biomolecular labels, environmental indicators or cellular stains.^[41–46] Finding a suitable fluorophore to visualize biochemical processes can be daunting, since many molecules are available either commercially or through *de novo* design and synthesis. Probe selection and design can be simplified by understanding the properties of these fluorescent compounds.

The most representative and widely used fluorophores in biological assays are coumarin, fluorescein, boron difluoride dipyrromethene (BODIPY), rhodamine and cyanine dyes (Figure 9).^[41,47,48]

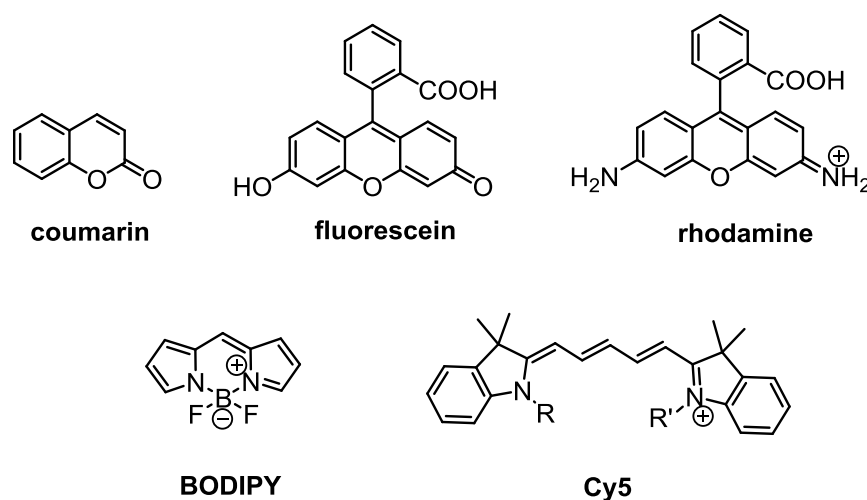


Figure 9. Commonly used dyes in chemical biology.^[47]

Among these, BODIPY dye is considered a potential scaffold for functional fluorescent probe development, since it shows high photostability, high fluorescence quantum yield, small Stokes shift and/or negative total charge.^[49–52] Moreover, BODIPY moiety is readily soluble in most organic solvents and is characterized by a strong absorption and fluorescence spectral bands in the visible, green-yellow part of the spectrum.^[53]

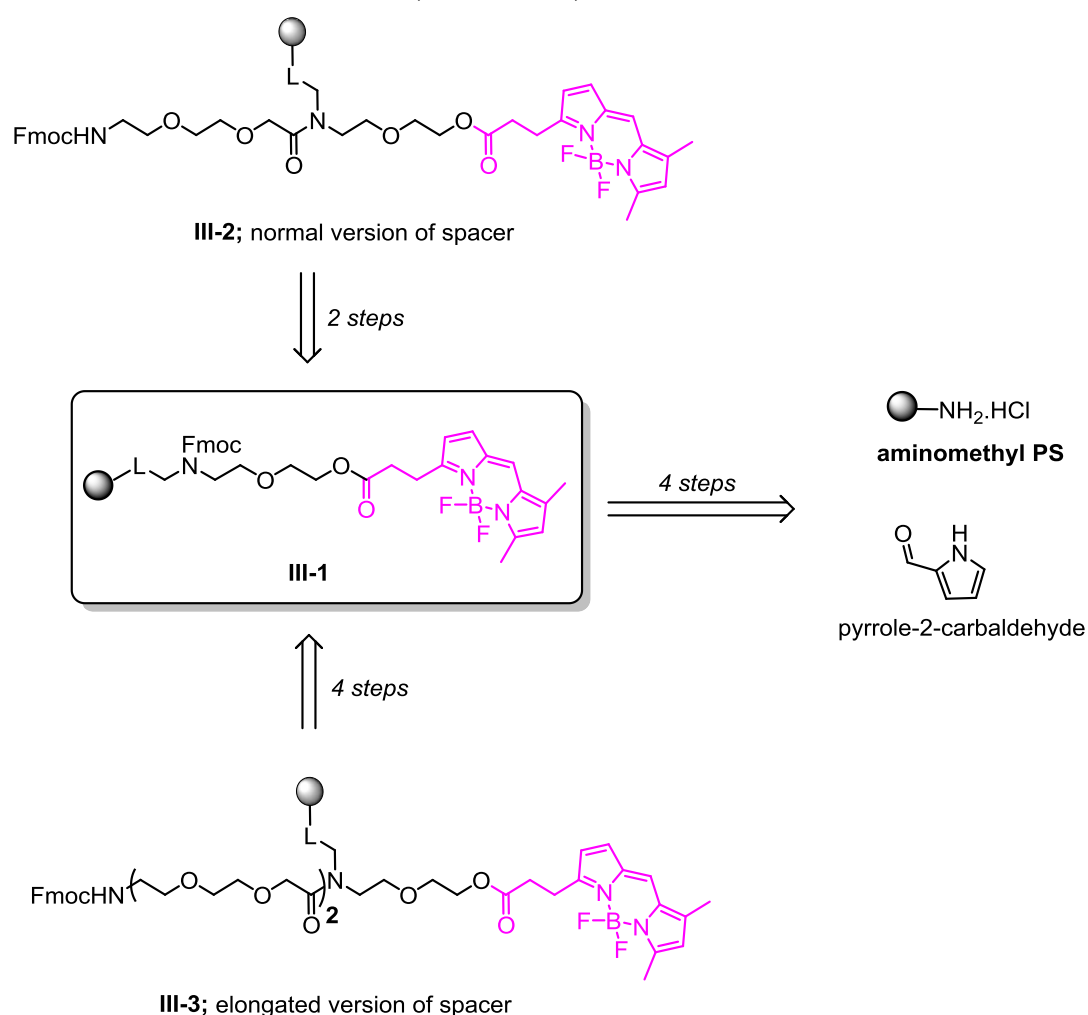
Triterpenes are natural compounds that may be found as secondary metabolites in plants,^[54] fungi^[55] or marine invertebrates^[56] and played a key role in the growth, development and reproduction of the organisms. They are found in bark, cork or in the wax covering leaves.^[57] Moreover, pentacyclic triterpenes covered an extensive spectrum of biological properties, not only as potential anticancer agents,^[58,59] but also

as antimicrobial,^[60] antiviral,^[59] antibacterial^[61] or antimalarial^[62] compounds. All these features are making them attractive targets for biological screening.

Despite the fact, that mechanism of action of betulinic acid, as one of the widely described triterpene, is known there is a vast number of its derivatives with potent biological activities, which have their mechanisms uncovered. Therefore, it is important to find ways how to determine them, in order to find better therapeutic agents. One of the possibilities are conjugation with fluorescent dyes and tracking such conjugates *in vivo* with fluorescence microscopy.

3.2. Synthesis

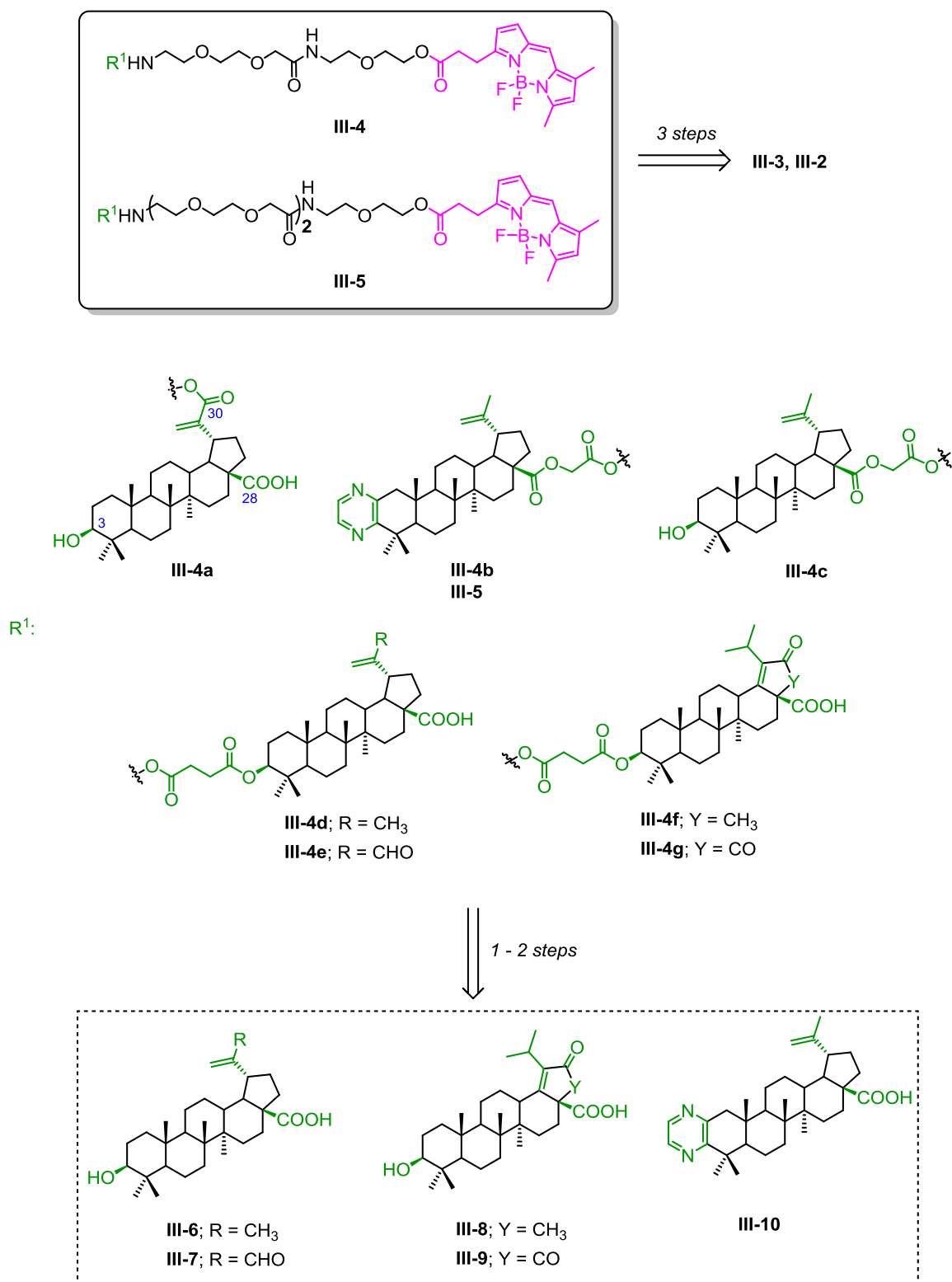
The synthesis of BODIPY preloaded resin **III-1** started from the commercially available amino methyl polystyrene resin (Scheme 15). This BODIPY dye was selected due to its known spectroscopic properties, overall neutral charge and suitable functional group for conjugation. Following elongation of the spacer yielded two BODIPY preloaded resins **III-2** and **III-3** (Scheme 15).



Scheme 15. Retrosynthetic analysis towards final compounds.

The selection of parental triterpene derivatives **III-6-10**, was based on their low micromolar cytotoxic profile towards various cancer cell lines and/or unknown mechanism of action.^[63-65] Betulinic acid **III-6** was used as a standard, since it is the widely studied cytotoxic triterpene with already reported mode of action.^[66,67]

For the conjugation with the preloaded resins was necessary to equip parental triterpenes with the suitable functional group. The modification of the scaffold was performed at 3 different parts (C³, C²⁸, C³⁰) and yielded the corresponding hemisuccinates, glycolates or α,β -unsaturated carboxylic acid, respectively. These carboxylic acids were used to acylate the preloaded resins **III-2**, **III-3** (after cleavage of Fmoc protecting group) and the following acid-mediated cleavage from the resin provided final conjugates **III-4**, **III-5** (Scheme 16).

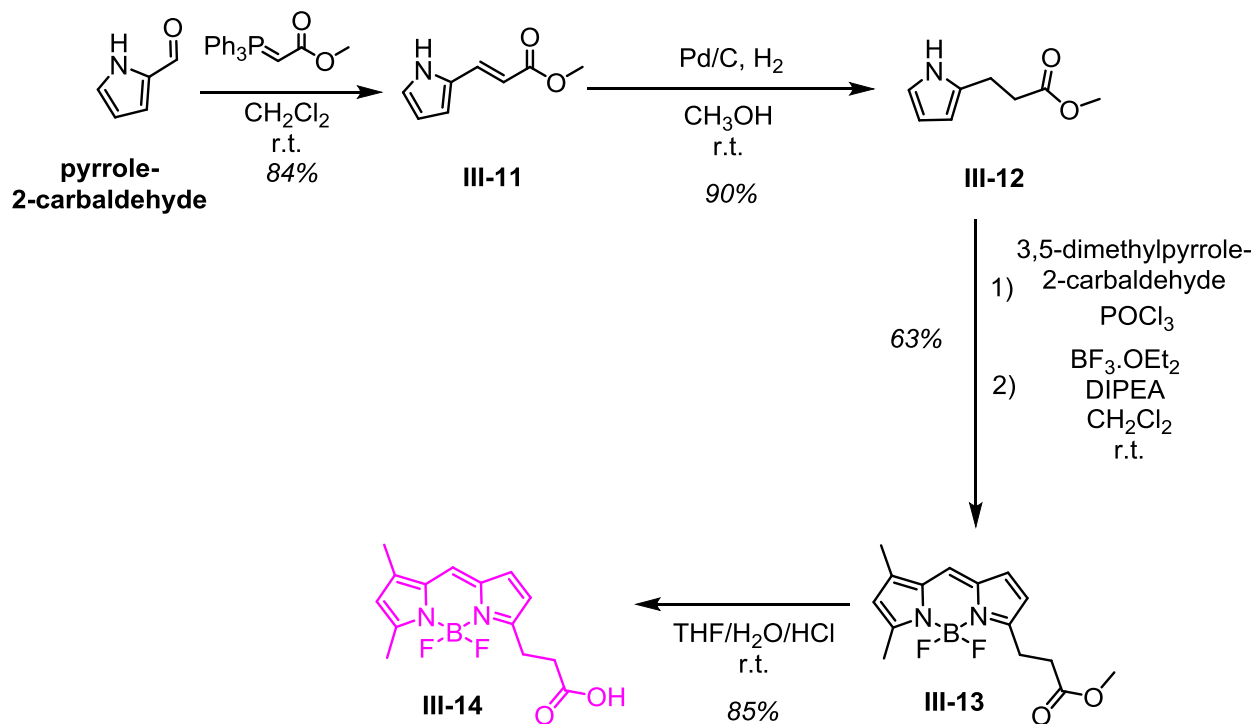


Scheme 16.

3.2.1. Synthesis of BODIPY-FL propanoic acid

The synthetic pathway started from the commercially available pyrrole-2-carbaldehyde and triphenylphosphonium ylide acetate, which were converted to pyrrole α,β -unsaturated ester **III-11** *via* Horner-Wadsworth-Emmons reaction with excellent *E*-regioselectivity due to the formation of stabilized ylide. Following reduction of double

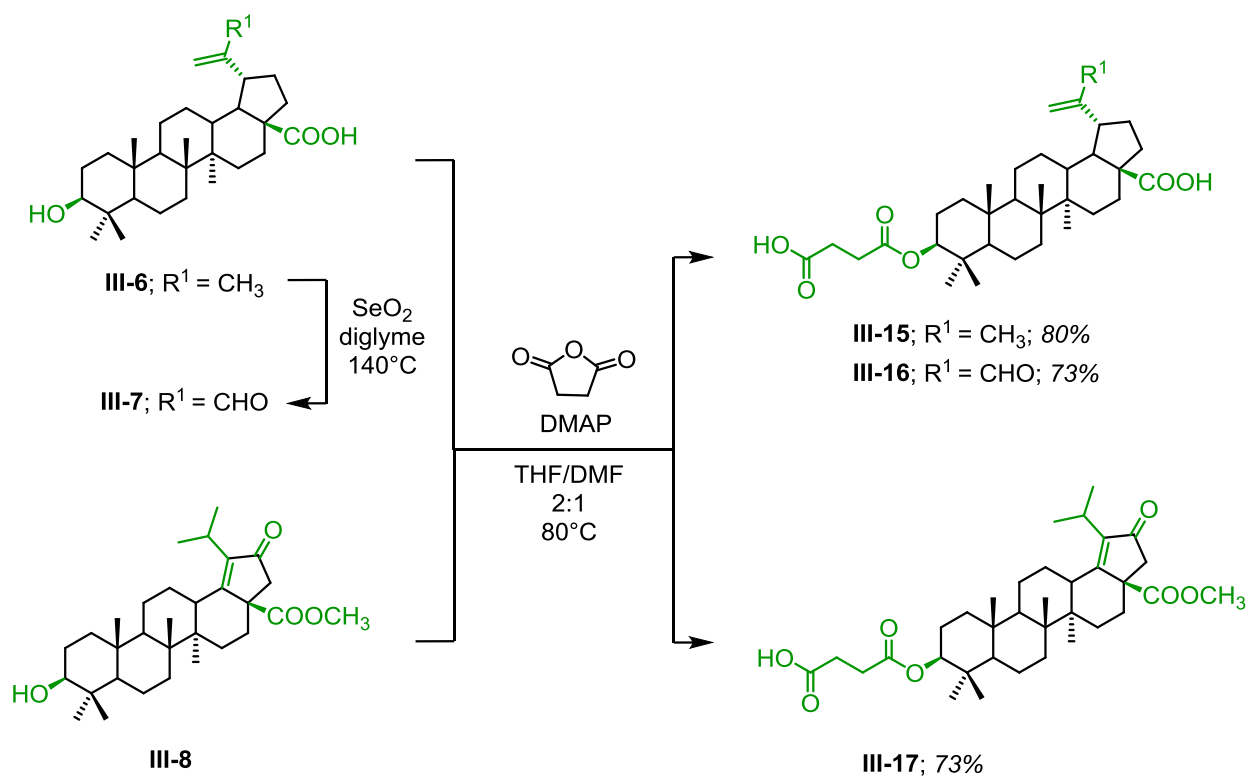
bond to **III-12** was achieved with palladium assisted hydrogenation. POCl₃ mediated condensation with commercially available 3,5-dimethylpyrrole-2-carbaldehyde yielded unsymmetrical dipyrin, which upon complexation with BF₃.OEt₂ provided BODIPY FL propanoic ester **III-13**. Finally, acidic hydrolysis of ester provided BODIPY FL propanoic acid **III-14** (Scheme 17) in high yield.



Scheme 17.

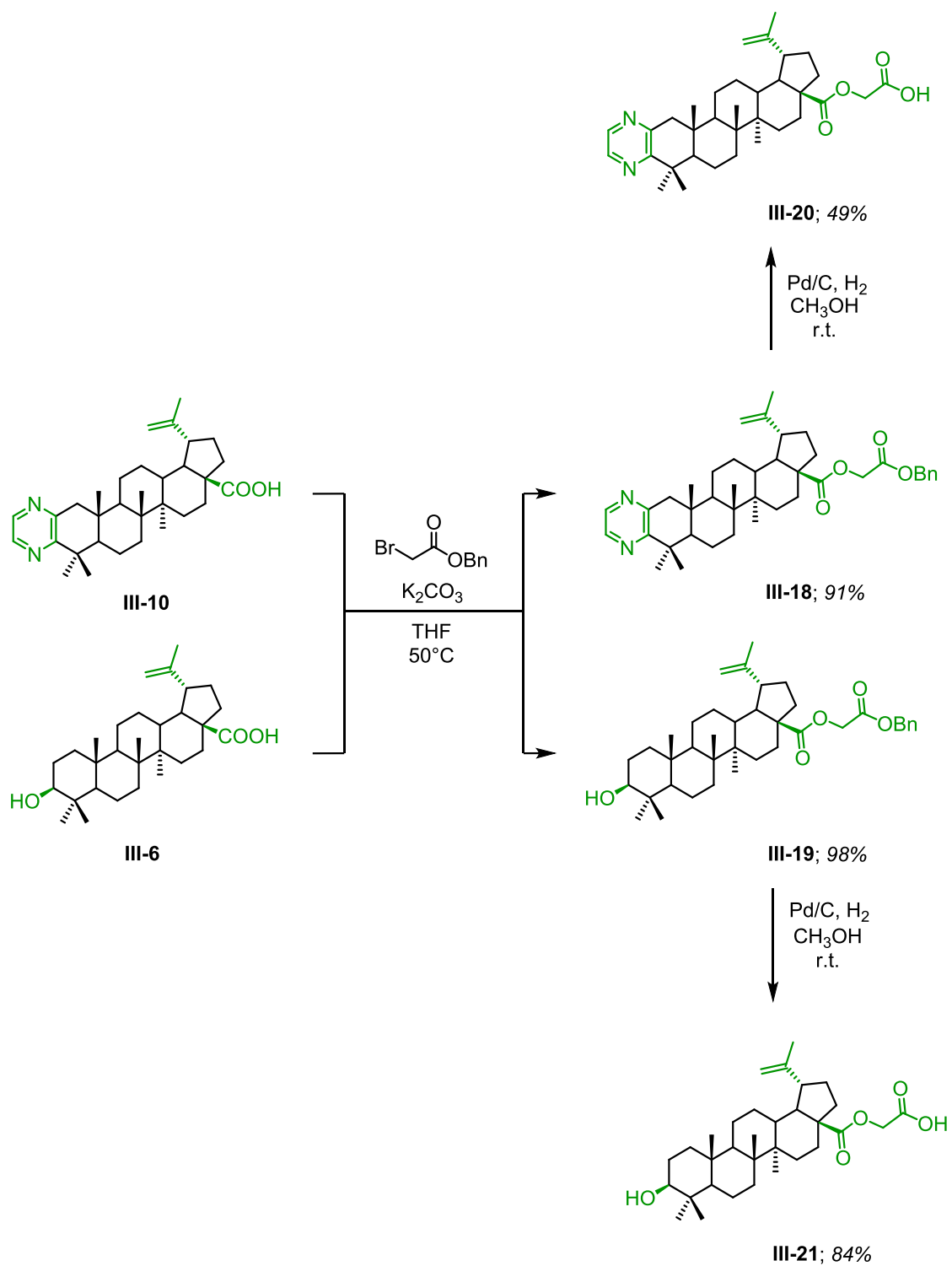
3.2.2. Synthesis of pre-modified triterpenes

Modification of semisynthetic triterpenes **III-6-8** as hemisuccinates and glycolates, respectively, was inspired by our previous work on biotinylated conjugates.^[68] Briefly, betulinic acid **III-6**, betulinic acid aldehyde **III-7** (prepared as a one-step modification from **III-6**) and monoketone **III-8** were treated with succinic anhydride in presence of DMAP (Scheme 18) to provide triterpenes **III-15-17** with carboxylic function ready for conjugation.



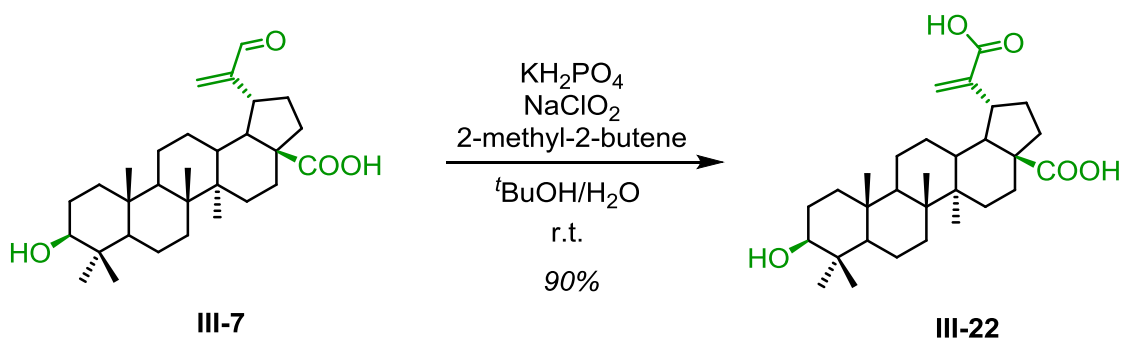
Scheme 18.

For modification of C²⁸ position was necessary to extend the neopentyl-type carboxylic function as it generally suffers from lower reactivity due to the steric hindrance. As such, we reacted betulinic acid **III-6** and pyridine triterpene derivative **III-10** with benzyl bromoacetate to yield compounds **III-19** and **III-18**, respectively. Following deprotection of benzyl moiety was achieved with palladium assisted catalytic hydrogenation and yielded pre-modified triterpenes **III-20**, **III-21** (Scheme 19) for further conjugation with preloaded resins.



Scheme 19.

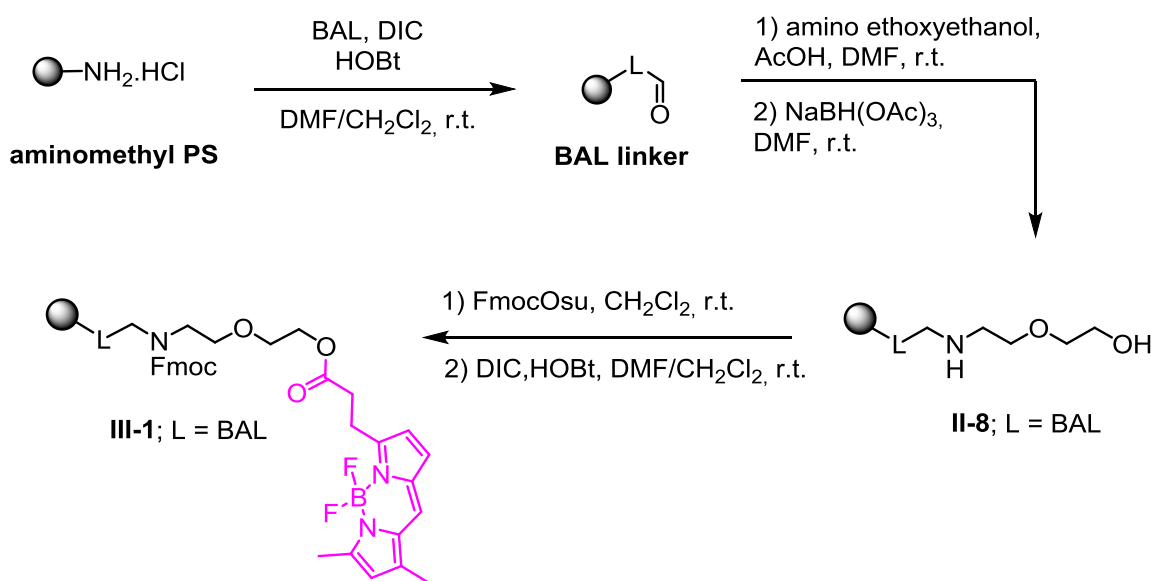
For conjugation of betulinic acid **III-6** on C³⁰ position, a different approach was used as was previously published.^[68] The betulinic acid aldehyde **III-7** was subjected to chemoselective Pinnick oxidation (Scheme 20) in order to produce carboxylic acid **III-22** for acylation with preloaded resin.



Scheme 20.

3.2.3. Synthesis of preloaded resins

The synthesis started similarly to previous project (thalidomide preloaded resin), from the commercially available amino methyl polystyrene resin, which was acylated with BAL linker. Following reductive amination with amino ethoxyethanol provided intermediate **II-8** (Scheme 21). Selective Fmoc protection and acylation with BODIPY **III-14**, provided under DIC/HOBt conditions, yielded key intermediate **III-1**.

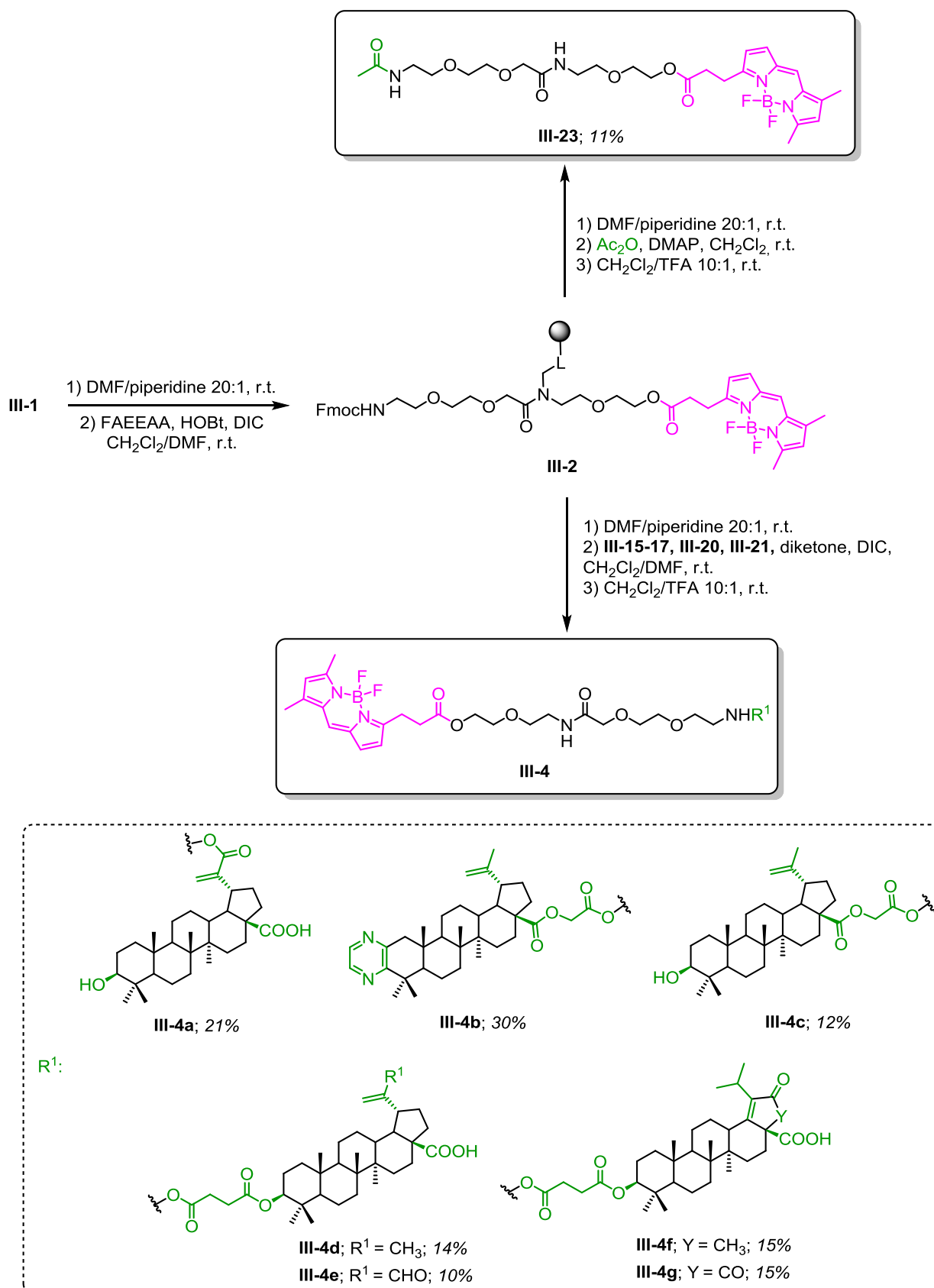


Scheme 21.

After acylation with BODIPY and deprotection of Fmoc under optimized conditions, we successfully attached FAEEAA linker to obtain preloaded resin **III-2** (Scheme 22). The following deprotection of Fmoc and DIC promoted coupling with premodified triterpenes yielded final products **III-4a-g** (Scheme 22), upon cleavage from the polymer support.

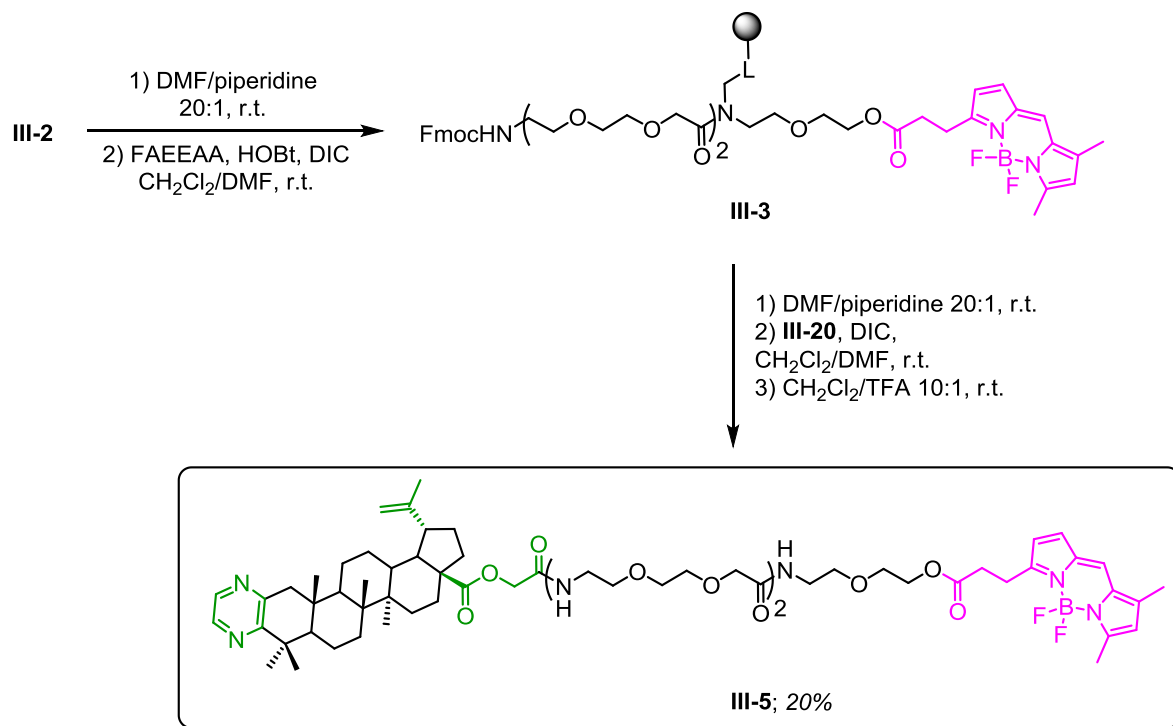
Final product **23** was prepared from **III-2** (after Fmoc deprotection) using acetic anhydride in presence of DMAP, as a negative control for biological tests (Scheme 22). The purpose of this compound was to demonstrate that the cell penetration and

targeting the organelles depended on the triterpene scaffold and not on the BODIPY core.



Scheme 22. Scheme of final conjugates.

To determine the impact of linker's length on cell targeting, elongation of the spacer **III-3** and subsequent acylation with pyrazine **III-20** (Scheme 23) to obtain final compound **III-5** was performed.



Scheme 23.

3.2.4. Photochemical measurements

All prepared final conjugates **III-4**, **III-5**, **III-23**, with amino ethoxyethanol linker, were subjected to measurements of their absorption and emission spectra and calculation of their quantum yields of fluorescence (Φ), in order to examine the impact of triterpene core on this phenomenon.

Surprisingly, we observed a quenching of fluorescence intensity by triterpene moiety, varying between 0.14 – 0.30 (Table 3), compare to BODIPY FL propanoic acid **III-14** itself ($\Phi = 0.98$). To support this theory, quantum yield of fluorescence of compound **III-23** was also calculated with value 0.71, indicating that the quenching is caused by triterpene scaffold.

| Compound | Φ | Compound | Φ |
|---------------|--------|---------------|--------|
| III-14 | 0.98 | III-4e | 0.14 |
| III-4a | 0.17 | III-4f | 0.25 |
| III-4b | 0.21 | III-4g | 0.26 |
| III-4c | 0.17 | III-5 | 0.30 |
| III-4d | 0.20 | III-23 | 0.71 |

Table 3.

Such observation could be explained by so called *static quenching* between BODIPY dye and triterpenes, presumably due to the hydrophobic effects, which was recently described in literature,^[69,70]. Noteworthy, this observation did not interfere with the subsequent fluorescent microscopy measurements.

3.3. Biology

The conjugates **III-4**, **III-5**, **III-23**, were subjected to measurements of their cytotoxic activity and to fluorescence microscopy, to investigate their distribution within cells. These measurements were provided by P. Džubák group.

Following fluorescent microscopy experiments revealed that all the tested fluorescent conjugates stain living cells and pass through the cellular membrane into the cytoplasmic compartment. In addition, we used simple BODIPY conjugate **III-23** (which has the active triterpenic scaffold replaced by acetate) as a negative control to prove, that it is the triterpenoid part that is responsible for the cellular uptake.

In case of aldehyde conjugate **III-4e**, the very reactive acrolein moiety resulted in a different staining pattern labeling cellular cytoplasm homogenously, which is presumably caused by nonspecific covalent interaction with multiple intracellular proteins. Staining is distinct when compared to other tested compounds, which labeled subtler cytoplasmic and membrane structures, likely mitochondria, endoplasmic reticulum (ER), and the nuclear membrane. Co-staining experiments are being performed to confirm this unambiguously. Such results are consistent with precedent studies on another lupane triterpenes that were found to interact with mitochondrion and ER.^[71,72]

3.4. Conclusion

We successfully optimized the route towards the fluorescently labeled preloaded resins **III-2** and **III-3**, followed by the synthesis of final compounds **III-4**, **III-5**, **III-23** with corresponding triterpenes. We also synthesized, yet commercially available but

rather expensive, BODIPY-FL propanoic acid **III-14** with modified synthesis to give better yields and suitable also for multigram scale quantities.

The prepared preloaded resins allow for routine, rapid and simple conjugation of various compounds (not necessarily triterpenes) possessing suitable functional groups to the BODIPY label through an ethylene-oxy linker of various lengths. The preloaded resin can be applied using simple laboratory equipment, common coupling reagents and conditions, and minimum *hands-on-time*. Live cell studies focused on fluorescence conjugate uptake demonstrated nonspecific labeling in aldehyde **III-4e**.

Ongoing research is now focused on a more specific determination of which organelles, proteins or protein complexes are targeted by our conjugates, and this will be the aim of further proteomic and molecular biology studies, for example, co-localization experiments.

4. Literature

- [1] G. Manning, *Science* **2002**, *298*, 1912–1934.
- [2] J.-L. Haesslein, N. Jullian, *Curr. Top. Med. Chem.* **2002**, *2*, 1037–1050.
- [3] U. Asghar, A. K. Witkiewicz, N. C. Turner, E. S. Knudsen, *Nat. Rev. Drug Discov.* **2015**, *14*, 130–146.
- [4] C. Sánchez-Martínez, L. M. Gelbert, M. J. Lallena, A. de Dios, *Bioorg. Med. Chem. Lett.* **2015**, *25*, 3420–3435.
- [5] S. Lapenna, A. Giordano, *Nat. Rev. Drug Discov.* **2009**, *8*, 547.
- [6] L. Havlíček, J. Hanuš, J. Veselý, S. Leclerc, L. Meijer, G. Shaw, M. Strnad, *J. Med. Chem.* **1997**, *40*, 408–412.
- [7] J. Cicenias, K. Kalyan, A. Sorokinas, E. Stankunas, J. Levy, I. Meskinyte, V. Stankevicius, A. Kaupinis, M. Valius, *Ann. Transl. Med.* **2015**, *3*, 135.
- [8] J. Vesely, L. Havlicek, M. Strnad, J. J. Blow, A. Donella-Deana, L. Pinna, D. S. Letham, J. Kato, L. Detivaud, S. Leclerc, et al., *Eur. J. Biochem.* **1994**, *224*, 771–786.
- [9] T. Gucký, R. Jorda, M. Zatloukal, V. Bazgier, K. Berka, E. Řezníčková, T. Béres, M. Strnad, V. Kryštof, *J. Med. Chem.* **2013**, *56*, 6234–6247.
- [10] M. Zatloukal, R. Jorda, T. Gucký, E. Řezníčková, J. Voller, T. Pospíšil, V. Malínková, H. Adamcová, V. Kryštof, M. Strnad, *Eur. J. Med. Chem.* **2013**, *61*, 61–72.
- [11] M. T. Fiorini, C. Abell, *Tetrahedron Lett.* **1998**, *39*, 1827–1830.
- [12] C. R. Coxon, E. Anscombe, S. J. Harnor, M. P. Martin, B. Carbain, B. T. Golding, I. R. Hardcastle, L. K. Harlow, S. Korolchuk, C. J. Matheson, et al., *J. Med. Chem.* **2017**, *60*, 1746–1767.
- [13] Y.-T. Chang, N. S. Gray, G. R. Rosania, D. P. Sutherlin, S. Kwon, T. C. Norman, R. Sarohia, M. Leost, L. Meijer, P. G. Schultz, *Chem. Biol.* **1999**, *6*, 361–375.
- [14] M. Legraverend, O. Ludwig, E. Bisagni, S. Leclerc, L. Meijer, N. Giocanti, R. Sadri, V. Favaudon, *Bioorg. Med. Chem.* **1999**, *7*, 1281–1293.
- [15] M. Srinivasarao, C. V. Galliford, P. S. Low, *Nat. Rev. Drug Discov.* **2015**, *14*, 203–219.
- [16] I. R. Vlahov, C. P. Leamon, *Bioconjug. Chem.* **2012**, *23*, 1357–1369.
- [17] H. Elnakat, *Adv. Drug Deliv. Rev.* **2004**, *56*, 1067–1084.
- [18] J. W. Lee, J. Y. Lu, P. S. Low, P. L. Fuchs, *Bioorg. Med. Chem.* **2002**, *10*, 2397–2414.
- [19] I. R. Vlahov, H. K. R. Santhapuram, P. J. Kleindl, S. J. Howard, K. M. Stanford, C. P. Leamon, *Bioorg. Med. Chem. Lett.* **2006**, *16*, 5093–5096.
- [20] C. P. Leamon, I. Pastan, P. S. Low, *J. Biol. Chem.* **1993**, *268*, 24847–24854.

- [21] R. Jorda, K. Paruch, V. Krystof, *Curr. Pharm. Des.* **2012**, *18*, 2974–2980.
- [22] K. Bettayeb, N. Oumata, A. Echalié, Y. Ferandin, J. A. Endicott, H. Galons, L. Meijer, *Oncogene* **2008**, *27*, 5797–5807.
- [23] C. P. Leamon, I. R. Vlahov, J. A. Reddy, M. Vetzél, H. K. R. Santhapuram, F. You, A. Bloomfield, R. Dorton, M. Nelson, P. Kleindl, et al., *Bioconjug. Chem.* **2014**, *25*, 560–568.
- [24] J. Roy, T. X. Nguyen, A. K. Kanduluru, C. Venkatesh, W. Lv, P. V. N. Reddy, P. S. Low, M. Cushman, *J. Med. Chem.* **2015**, *58*, 3094–3103.
- [25] S. Patai, Z. Rappoport, Eds., *Sulphur-Containing Functional Groups (1993)*, John Wiley & Sons, Inc., Chichester, UK, **1993**.
- [26] S. Krajčovičová, T. Gucký, D. Hendrychová, V. Kryštof, M. Soral, *J. Org. Chem.* **2017**, *82*, 13530–13541.
- [27] A. C. Lai, C. M. Crews, *Nat. Rev. Drug Discov.* **2017**, *16*, 101–114.
- [28] G. M. Burslem, C. M. Crews, *Chem. Rev.* **2017**, *117*, 11269–11301.
- [29] I. Churcher, *J. Med. Chem.* **2018**, *61*, 444–452.
- [30] G. M. Burslem, B. E. Smith, A. C. Lai, S. Jaime-Figueroa, D. C. McQuaid, D. P. Bondeson, M. Toure, H. Dong, Y. Qian, J. Wang, et al., *Cell Chem. Biol.* **2018**, *25*, 67–77.e3.
- [31] T. Ito, H. Ando, T. Suzuki, T. Ogura, K. Hotta, Y. Imamura, Y. Yamaguchi, H. Handa, *Science* **2010**, *327*, 1345–1350.
- [32] E. S. Fischer, K. Böhm, J. R. Lydeard, H. Yang, M. B. Stadler, S. Cavadini, J. Nagel, F. Serluca, V. Acker, G. M. Lingaraju, et al., *Nature* **2014**, *512*, 49–53.
- [33] J. Lu, Y. Qian, M. Altieri, H. Dong, J. Wang, K. Raina, J. Hines, J. D. Winkler, A. P. Crew, K. Coleman, et al., *Chem. Biol.* **2015**, *22*, 755–763.
- [34] G. E. Winter, D. L. Buckley, J. Paulk, J. M. Roberts, A. Souza, S. Dhe-Paganon, J. E. Bradner, *Science* **2015**, *348*, 1376–1381.
- [35] J. Lohbeck, A. K. Miller, *Bioorg. Med. Chem. Lett.* **2016**, *26*, 5260–5262.
- [36] C. M. Robb, J. I. Contreras, S. Kour, M. A. Taylor, M. Abid, Y. A. Sonawane, M. Zahid, D. J. Murry, A. Natarajan, S. Rana, *Chem. Commun.* **2017**, *53*, 7577–7580.
- [37] J. Papatzimas, E. Gorobets, D. Brownsey, R. Maity, N. Bahlis, D. Derksen, *Synlett* **2017**, *28*, 2881–2885.
- [38] R. P. Wurz, K. Dellamaggiore, H. Dou, N. Javier, M.-C. Lo, J. D. McCarter, D. Mohl, C. Sastri, J. R. Lipford, V. J. Cee, *J. Med. Chem.* **2018**, *61*, 453–461.
- [39] S. Krajcovicova, R. Jorda, D. Hendrychova, V. Krystof, M. Soral, *Chem. Commun.* **2019**, *55*, 929–932.
- [40] F. Cameron, M. Sanford, *Drugs* **2014**, *74*, 263–271.
- [41] L. D. Lavis, R. T. Raines, *ACS Chem. Biol.* **2008**, *3*, 142–155.
- [42] I. Johnson, *Histochem. J.* **1998**, *30*, 123–140.
- [43] J. Zhang, R. E. Campbell, A. Y. Ting, R. Y. Tsien, *Nat. Rev. Mol. Cell Biol.* **2002**, *3*, 906–918.
- [44] J. V. Frangioni, *Curr. Opin. Chem. Biol.* **2003**, *7*, 626–634.
- [45] J. Goddard, J. Reymond, *Curr. Opin. Biotechnol.* **2004**, *15*, 314–322.
- [46] N. Johnsson, K. Johnsson, *ACS Chem. Biol.* **2007**, *2*, 31–38.
- [47] T. Kowada, H. Maeda, K. Kikuchi, *Chem Soc Rev* **2015**, *44*, 4953–4972.
- [48] L. M. Wysocki, L. D. Lavis, *Curr. Opin. Chem. Biol.* **2011**, *15*, 752–759.
- [49] A. Loudet, K. Burgess, *Chem. Rev.* **2007**, *107*, 4891–4932.
- [50] G. Ulrich, R. Ziessel, A. Harriman, *Angew. Chem. Int. Ed.* **2008**, *47*, 1184–1201.
- [51] H. Lu, J. Mack, Y. Yang, Z. Shen, *Chem Soc Rev* **2014**, *43*, 4778–4823.

- [52] Y. Ni, J. Wu, *Org. Biomol. Chem.* **2014**, *12*, 3774.
- [53] J. Bañuelos, *Chem. Rec.* **2016**, *16*, 335–348.
- [54] J. Pollier, A. Goossens, *Phytochemistry* **2012**, *77*, 10–15.
- [55] J. S. Dahiya, *Phytochemistry* **1991**, *30*, 1235–1237.
- [56] Z. Wang, H. Zhang, W. Yuan, W. Gong, H. Tang, B. Liu, K. Krohn, L. Li, Y. Yi, W. Zhang, *Food Chem.* **2012**, *132*, 295–300.
- [57] M. Laszczyk, *Planta Med.* **2009**, *75*, 1549–1560.
- [58] J. J. Ramírez-Espinosa, M. Y. Rios, P. Paoli, V. Flores-Morales, G. Camici, V. de la Rosa-Lugo, S. Hidalgo-Figueroa, G. Navarrete-Vázquez, S. Estrada-Soto, *Eur. J. Med. Chem.* **2014**, *87*, 316–327.
- [59] R. Paduch, M. Kandefér-Szerszeń, *Mini-Rev. Org. Chem.* **2014**, *11*, 262–268.
- [60] E. A. Mireku, A. Y. Mensah, I. K. Amponsah, C. A. Danquah, D. Anokwah, M. Kwesi Baah, *Nat. Prod. Res.* **2018**, 1–4.
- [61] C.-M. Wang, H.-T. Chen, Z.-Y. Wu, Y.-L. Jhan, C.-L. Shyu, C.-H. Chou, *Molecules* **2016**, *21*, 139.
- [62] C. Beaufay, M.-F. Hérent, J. Quetin-Leclercq, J. Bero, *Malar. J.* **2017**, *16*, DOI 10.1186/s12936-017-2054-y.
- [63] J. Šarek, J. Klinot, P. Džubák, E. Klinotová, V. Nosková, V. Křeček, G. Kořínková, J. O. Thomson, A. Janošťáková, S. Wang, et al., *J. Med. Chem.* **2003**, *46*, 5402–5415.
- [64] J. Sarek, M. Kvasnica, M. Urban, J. Klinot, M. Hajduch, *Bioorg. Med. Chem. Lett.* **2005**, *15*, 4196–4200.
- [65] M. Urban, J. Sarek, M. Kvasnica, I. Tislerova, M. Hajduch, *J. Nat. Prod.* **2007**, *70*, 526–532.
- [66] L. Huo, X. Bai, Y. Wang, M. Wang, *Biomed. Pharmacother.* **2017**, *92*, 347–355.
- [67] R. Biswas, J. Chanda, A. Kar, P. K. Mukherjee, *Food Chem.* **2017**, *232*, 689–696.
- [68] M. Soural, J. Hodon, N. J. Dickinson, V. Sidova, S. Gurska, P. Dzubak, M. Hajduch, J. Sarek, M. Urban, *Bioconjug. Chem.* **2015**, *26*, 2563–2570.
- [69] C. Würth, M. Grabolle, J. Pauli, M. Spieles, U. Resch-Genger, *Nat. Protoc.* **2013**, *8*, 1535–1550.
- [70] W. Peng, F. Ding, Y.-T. Jiang, Y.-K. Peng, *J. Agric. Food Chem.* **2014**, *62*, 2271–2283.
- [71] Y. Ye, T. Zhang, H. Yuan, D. Li, H. Lou, P. Fan, *J. Med. Chem.* **2017**, *60*, 6353–6363.
- [72] S. Mitsuda, T. Yokomichi, J. Yokoigawa, T. Kataoka, *FEBS Open Bio* **2014**, *4*, 229–239.